GEOLOGICAL SURVEY OF CANADA
BULLETIN 560

BASINS AND FOLD BELTS OF PRINCE PATRICK ISLAND AND ADJACENT AREAS, CANADIAN ARCTIC ISLANDS

J.C. Harrison and T.A. Brent

2005

Natural Resources Canada
Ressources naturelles Canada

Canada

The CD-ROM accompanying this publication contains the full report, including any oversized figures and/or A-series maps, in Portable Document Format (PDF). Oversized items may be purchased separately as paper plots from any Geological Survey of Canada Bookstore location:

Geological Survey of Canada Bookstore (Ottawa)
601 Booth Street
Ottawa, Ontario
K1A 0E8
Tel.: (613) 995-4342
Tel.: (888) 252-4301 (toll-free)
Fax: (613) 943-0646
E-mail: gscbookstore@nrcan.gc.ca
Web: http://gsc.nrcan.gc.ca/bookstore/index_e.php

Geological Survey of Canada Bookstore (Calgary)
3303-33rd Street, N.W.
Calgary, Alberta
T2L 2A7
Tel.: (403) 292-7030
Fax: (403) 299-3542
E-mail: gsc_calgary@nrcan.gc.ca
Web: http://gsc.nrcan.gc.ca/org/calgary/pub/bookstore_e.php

Geological Survey of Canada Bookstore (Vancouver)
101-605 Robson Street
Vancouver, B.C.
V6B 5J3
Tel.: (604) 666-0271
Fax: (604) 666-1337
E-mail: gscvan@gsc.nrcan.gc.ca
Web: http://gsc.nrcan.gc.ca/org/vancouver/bookstore/index_e.php

Geological Survey of Canada Bookstore (Atlantic)
1 Challenger Drive
P.O. Box 1006
Dartmouth, Nova Scotia
B2Y 4A2
Tel.: (902) 426-4386
Fax: (902) 426-4848
E-mail: Jennifer.Bates@nrcan-rncan.gc.ca
Web: http://gsca.nrcan.gc.ca/pubprod/pubprod_e.php

Geological Survey of Canada Bookstore (Québec)
490, rue de la Couronne
Québec, Quebec
G1K 9A9
Tel.: (418) 654-2677
Fax: (418) 654-2660
E-mail: cgcq_librairie@rncan.gc.ca
Web: http://www.gscq.nrcan.gc.ca/bibliotheque/

Le CD-ROM qui accompagne cette publication renferme le rapport au complet, y compris les figures surdimensionnées ou les cartes de série A, en format PDF. Pour acheter des copies papier des éléments surdimensionnés, adressez-vous à la Librairie de la Commission géologique du Canada :

Librairie de la Commission géologique du Canada (Ottawa)
601, rue Booth
Ottawa (Ontario)
K1A 0E8
Tél. : (613) 995-4342
Tél. : (888) 252-4301 (sans frais)
Télécopieur : (613) 943-0646
Courriel : librairiecgc@nrcan.gc.ca
Web : http://cgc.rncan.gc.ca/librairie/index_f.php

Librairie de la Commission géologique du Canada (Calgary)
3303-33rd Street, N.W.
Calgary (Alberta)
T2L 2A7
Tél. : (403) 292-7030
Télécopieur : (403) 299-3542
Courriel : gsc_calgary@gsc.nrcan.gc.ca
Web : http://gsc.nrcan.gc.ca/org/calgary/pub/bookstore_f.php

Librairie de la Commission géologique du Canada (Vancouver)
101-605 Robson Street
Vancouver (C.-B.)
V6B 5J3
Tél. : (604) 666-0271
Télécopieur : (604) 666-1337
Courriel : gscvan@gsc.nrcan.gc.ca
Web : http://cgc.rncan.gc.ca/org/vancouver/bookstore/index_f.php

Librairie de la Commission géologique du Canada (Atlantique)
1 Challenger Drive
P.O. Box 1006
Dartmouth (Nouvelle-Écosse)
B2Y 4A2
Tél. : (902) 426-4386
Télécopieur : (902) 426-4848
Courriel : Jennifer.Bates@nrcan-rncan.gc.ca
Web : http://gsca.nrcan.gc.ca/pubprod/pubprod_f.php

Librairie de la Commission géologique du Canada (Québec)
490, rue de la Couronne
Québec (Québec) G1K 9A9
Tél. : (418) 654-2677
Télécopieur : (418) 654-2660
Courriel : cgcq_librairie@rncan.gc.ca
Web : http://www.cgcq.rncan.gc.ca/bibliotheque/

GEOLOGICAL SURVEY OF CANADA
BULLETIN 560

BASINS AND FOLD BELTS OF PRINCE PATRICK ISLAND AND ADJACENT AREAS, CANADIAN ARCTIC ISLANDS

J.C. Harrison and T.A. Brent
with contributions by
B. Beauchamp, A.F. Embry, F. Goodarzi, T. Gentzis,
Q. Goodbody, L.R. Newitt, T.P. Poulton, R. Stewart, and J.H. Wall

Paleontological contributions by
J.H. Wall, T.P. Poulton, E.H. Davies,
J.A. Jeletzky, B.S. Norford, and A.E.H. Pedder

2005

Catalogue No. M42-560E
ISBN 0-660-19008-7

Available in Canada from the Geological Survey of Canada Bookstore
(*see inside front cover for details*)

A copy of this publication is also available for reference by depository libraries across Canada through access to the Depository Services Program's Web site at http://dsp-psd.pwgsc.gc.ca

A free digital download of this publication is available from GeoPub:
http://geopub.nrcan.gc.ca/index_e.php

Cover illustration
Fault-bounded northerly trending ridge at the head of Mould Bay. The high ground is a horst block underlain by Devonian sandstone and shale. The low area to the west (left) is one of the many Middle Jurassic through Lower Cretaceous grabens in the report region, part of a 100 km wide rift zone that extends from Banks Island to northern Prince Patrick Island and provides a geological record of the early development of the Arctic Ocean basin. GSC photo HHB-R3-16-1991

Critical readers
R. Thorsteinsson
D.W. Morrow
A. van Beek
U. Mayr
B. MacLean

Authors' address
J.C. Harrison and T.A. Brent
Geological Survey of Canada
3303-33rd Street NW
Calgary, AB T2L 2A7

Original manuscript submitted: 02–07
Final version approved for publication: 04–11

CONTENTS

1 Abstract
1 Résumé
2 Summary
3 Sommaire
5 Introduction
5 Description of the study area
5 Physical and environmental features
5 Physiography
7 Climate, vegetation, and wildlife
7 History of geographical exploration
7 Prehistory
8 Franklin search expeditions
8 Mecham and M'Clintock
9 Vilhjalmur Stefansson
10 Hubert Wilkins
10 Aerial photography
10 Mould Bay Weather Station
10 Maritime transits of M'Clure Strait
11 History of geological investigations
14 Scope of present study and acknowledgments
15 Summary description of stratigraphic units
15 Stratigraphic successions
15 Summary description of map units
15 Seismic expression of Succession 1
19 Vendian (?)–Lower Devonian units of Succession 2
19 Offshore platform units
19 Units of the basinal realm
23 Devonian clastic wedge of Succession 2
25 Carboniferous and Permian strata of Succession 3
27 Mesozoic strata of Succession 3
30 Pre-rift package (Triassic–Lower Jurassic)
32 Syn-rift package (Middle Jurassic–Lower Cretaceous)
33 Post-rift package (Lower Cretaceous–Upper Cretaceous)
33 Neogene strata of Succession 4
33 Quaternary record
34 Summary description of regional structure
34 Seismic profiles and subsurface mapping
34 Surface structural elements
36 Arctic Continental Terrace Wedge
41 The Sverdrup Basin
41 Continental margin basins
41 Inter-basin highs
41 Jurassic–Cretaceous rift-related structures
42 Lower Paleozoic deformed belts
42 Subsurface structural elements
42 Mesozoic and Cenozoic features
42 Upper Paleozoic rift system
42 Devonian fold belts
46 The Arctic Platform
46 Crozier High
46 Proterozoic structure
47 Potential field anomalies
47 Gravity
47 Magnetic field

47 Fate of the Devonian fold belt west of Melville Island
47 Introduction
47 Angular unconformity above the Devonian
47 Surface evidence
51 Subsurface evidence
51 Eglinton Island
51 Prince Patrick Island
54 Folds
54 Surface evidence
56 Subsurface evidence
56 Eglinton Island
59 Western Prince Patrick Island
61 Northeastern Prince Patrick Island
63 Offshore areas
64 Thrust faults
64 Surface evidence
64 Subsurface evidence
65 Eglinton Island
66 Southwestern Prince Patrick Island
66 Central Prince Patrick Island
66 Northeastern Prince Patrick Island
67 Deep-seated thrust faults
68 Unrooted detachments in the Devonian clastic wedge
68 Detachment levels
71 Magnitudes of shortening
71 Upper Paleozoic rift and inversion tectonics in the western Sverdrup Basin
71 Introduction
73 Seismic units
73 Nature of rift-related normal faults
73 Jameson Fault-A
75 John Point Fault
77 Hemphill Fault-C
81 Hemphill Faults-A and B
81 Moore Bay faults
85 Regional implications
85 General features
86 Upper Paleozoic deformed belts
86 Serpukhovian(?)
86 Bashkirian to Kasimovian
86 Gzhelian to Sakmarian
87 Sakmarian through Kungurian
88 Melvillian Disturbance
88 Roadian and later Permian subsidence
88 Mesozoic basin evolution near the Arctic Continental margin
88 Introduction
90 Triassic to Middle Jurassic structural evolution
93 Middle Jurassic to Cretaceous extensional structure
93 Classification of structural elements
96 Eglinton Basin
96 Seismic units
97 Regional structural style
97 Faults of Eglinton Basin
101 Timing of faulting
107 Tullett Basin
107 Seismic units
107 Regional structural style

109 Green Bay Graben
113 Mould Bay Graben
116 Discovery Point Graben
116 Tullett Central Graben
118 Richards Point Graben
122 Hardinge Bay and Houghton Head grabens
125 Prince Patrick Uplift
125 Introduction
125 Manson Point Graben
125 Station Creek Graben
126 Carter Bay Graben
126 Landing Lake Graben
128 Carbonate Mounds Graben
130 Cape Cam and Causeway grabens
131 M'Clure Strait Basin
131 Sverdrup Basin
134 Summary of Mesozoic rifting events
134 Pre-rift phase
136 Rift phase
137 Post-rift phase
137 Events of the Cenozoic
137 Introduction
138 Angular unconformity below Neogene strata
138 Surface evidence
138 Subsurface evidence
138 Folds and thrust faults
138 Moore Bay Anticline
140 Elsewhere in Sverdrup Basin
140 Tullett Basin
140 Eglinton Basin
141 Uplifts
141 Prince Patrick Uplift
142 Gardiner-Intrepid High
142 Offshore gravity high
143 Neogene and Quaternary structure
143 Deformation of the Continental Terrace Wedge
143 Regional uplift
143 Faults
147 Recorded seismicity
147 Deformation of Quaternary deposits and colluvium
147 Pleistocene deformation
149 Pingos
150 Seasonal deformation in the active layer
150 Energy and mineral resources
150 Introduction
150 Thermal maturity
154 Petroleum source rocks
154 Silurian and older rocks
154 Kitson Formation
154 Blackley Formation
154 Cape de Bray Formation
154 Carboniferous and Permian formations
156 Schei Point Group
156 Grosvenor Island Formation
156 Jameson Bay Formation
156 McConnell Island and Hiccles Cove formations

160 Ringnes, Awingak, and Deer Bay formations
160 Isachsen and Christopher formations
160 Kanguk Formation
160 Hydrocarbon occurrences
162 Conceptual exploration plays
162 New opportunities on tested plays
164 New plays
166 Coal
166 Metals and minerals
167 References
Appendices
174 A Biostratigraphic determinations
190 B Magnetic compass operation at high latitudes: examples from Prince Patrick Island

Figures

6 1. Location of the report area and various geographic features cited in the text. Shown are the sledge routes of G.F. Mecham and F.L. M'Clintock (1853), and V. Stefansson (1915)
16 2. Generalized crustal-scale cross-section of the Arctic continental margin in the vicinity of Prince Patrick Island
17 3. Map of exploratory wells, location of text illustrations, and limits of Prince Patrick Platform and Crozier High; inset map illustrates the general geological features of Prince Patrick Island area
18 4. Seismic expression of Lower Devonian and older strata of southwestern Prince Patrick Island
20 5. Correlation chart for Neoproterozoic to Silurian units of Prince Patrick, Eglinton, Melville and northeast Ellesmere islands
21 6. Simplified correlation of Upper Silurian and Devonian formations of Melville and Prince Patrick islands
22 7. Seismic expression of Lower Devonian and older strata of Eglinton Island
24 8. Seismic expression of the Middle and Upper Devonian clastic wedge of southwestern Prince Patrick Island
26 9. Seismic expression of Carboniferous and Permian strata of northeastern Prince Patrick Island
27 10. Simplified correlation of Carboniferous, Permian and Lower Triassic formations of subsurface northeastern Prince Patrick Island
28 11. Seismic expression of Mesozoic strata of northeastern Prince Patrick Island
29 12. Simplified correlation of Mesozoic strata of Prince Patrick and Eglinton islands
31 13. Correlation of Boreal Jurassic biozones of Prince Patrick Uplift and the western Sverdrup Basin
35 14. Reflection seismic profiles, exploratory drillholes, structural cross-sections and location of text illustrations for the report area
37 15. Seismic expression of the downdip limit of ice-bonded permafrost
38 16. Correlation of well logs to a portion of Panarctic seismic profile 474 at the BP et al. Satellite F-68 well
39 17. Correlation of well logs to a portion of Elf seismic profile PPB32 at the Elfex et al. Wilkie Point J-51 well
40 18. Geological regions of the western Queen Elizabeth Islands and adjacent portions of the Arctic continental shelf
43 19. Geological setting of the Canadian Arctic Islands
44 20. Geological elements of the report area beneath cover of the Continental Terrace Wedge
45 21. Geological elements of the report area beneath Carboniferous and younger cover
48 22. Bouguer gravity map and earthquake epicentres for the western Queen Elizabeth Islands and adjacent portions of the Arctic continental shelf
49 23. Total magnetic field map for the western Queen Elizabeth Islands and adjacent portions of the Arctic continental shelf
50 24. Angular unconformity between flat-lying Toarcian Jameson Bay Formation and tilted Middle Devonian Weatherall Formation near Disappointment Point
52 25. Seismic expression of the angular unconformity between Jurassic and Devonian strata of central Prince Patrick Island
53 26. Indirect seismic evidence for an angular unconformity between unreflective Devonian strata and subhorizontal Carboniferous cover
54 27. Stereonet plots of poles to bedding planes for Devonian and younger strata
55 28. Anticline hinge exposed in stream bank outcrop of the Cape de Bray Formation near Walker Inlet

56	29.	Structural complications in the Cape de Bray Formation within the hinge region of a regional anticline near Walker Inlet
57	30.	Time structure contour map (two-way time) constructed on the top of the Silurian
58	31.	Named Devonian–Carboniferous structures, position of the early Paleozoic shelf-to-basin transition, seismic profiles and location of related text illustrations.
60	32.	Tectonic regions of the Devonian clastic wedge
62	33.	Near-surface minor folds and rootless minor thrusts in the Devonian clastic wedge near Dyer Bay
69	34.	Structural panels and detachment surfaces in Devonian and older strata
70	35.	Areas of compressive uplift and deep-seated thrust faulting affecting seismic units below es4 of Eglinton Island and below psЄO of Prince Patrick Island
72	36.	Regional patterns of horizontal shortening measured on the top of the Lower Devonian
74	37.	Thickness isochrons and related extensional structures for Carboniferous and pre-Roadian Permian strata of the western Arctic Islands
75	38.	Named Carboniferous–Permian normal faults, position of underlying Devonian thrust faults, and location of seismic profiles and related text figures
76	39.	Seismic expression of Jameson Fault-A and associated seismic units near the Jameson Bay C-31 well
77	40.	Mid-Carboniferous (Bashkirian) to end-Permian (Capitanian?) kinematic model for Jameson Fault-A
78	41.	Seismic expression of John Point Fault and associated seismic units on a portion of profile 467
79	42.	Mid-Carboniferous to mid-Permian kinematic model for John Point Fault based on Panarctic seismic profile 467
80	43.	Seismic expression of Hemphill Fault-C and associated seismic units on a portion of Elf profile PPA5
82	44.	Seismic expression of the Hemphill faults and associated seismic units on a portion of Panarctic profile 474
83	45.	Seismic expression of the Hemphill faults and associated seismic units on a portion of Panarctic profile 480
84	46.	Kinematic model for the Hemphill faults based on Panarctic seismic profiles 474 and 480
85	47.	Seismic expression of the Moore Bay faults and associated seismic units on a portion of BP profile T4
87	48.	Summarized tectonic and depositional history for Carboniferous and Permian faults and associated strata of northeastern Prince Patrick Island
89	49.	Thickness isochron map from the Kungurian(?) to the top of the Permian
91	50.	Thickness isochron map from the base of the Triassic to the Middle Jurassic (Aalenian)
92	51.	Preservational limits of Carboniferous through Upper Cretaceous (Turonian) strata
94	52.	Faults and thickness isochron map for Middle Jurassic (top Aalenian) through Upper Cretaceous strata
95	53.	Locations of named grabens, regional highs, seismic profiles and related text figures on the Aalenian to top Cretaceous thickness isochron map
CD-ROM	54.	Measured sections and selected well logs for Triassic through Upper Cretaceous strata (on CD-ROM)
98	55.	Seismic expression of the eastern margin of Eglinton Basin in Kellett Strait on a portion of GSI profile GM74-136
99	56.	Seismic expression of the eastern margin of Eglinton Basin in Kellett Strait on a portion of GSI profile GM74-141
100	57.	Steeply dipping minor faults displacing bentonite beds of the lower Kanguk Formation on eastern Eglinton Island
102	58.	Seismic expression of an unnamed fault on profile 462 near the Eglinton P-24 well on central Eglinton Island
103	59.	Seismic expression of half-graben structures and related listric normal faults in northern M'Clure Strait
104	60.	Seismic expression of a major half-graben structure in northern M'Clure Strait 70 km south of Cape Cam
105	61.	Seismic expression of planar normal faults in tilted Jurassic and Cretaceous strata on the western margin of Eglinton Basin in Crozier Strait
106	62.	Correlation chart for Lower Jurassic and younger tectonic, magmatic and related depositional features of Eglinton Basin and various grabens of Tullett Basin
108	63.	Generalized structural cross-section of Tullett Basin and Green Bay Uplift on western Prince Patrick Island
110	64.	Schematic structural cross-section of the named grabens in the outcrop belt of Prince Patrick Uplift
112	65.	Panorama of excavated outcrop within the uppermost part of the Hiccles Cove Formation west of the head of Green Bay
113	66.	Detail of faults in the upper Hiccles Cove Formation, west of the head of Green Bay (first example)

113	67.	Detail of faults in the upper Hiccles Cove Formation, west of the head of Green Bay (second example)
114	68.	Seismic expression of Green Bay Graben on the east side of Tullett Point Basin
115	69.	Seismic expression of Mould Bay Graben in the southern part of Tullett Point Basin
117	70.	Seismic expression of Tullett Central Graben in the central region of Tullett Point Basin
119	71.	Seismic expression of northern Richards Point Graben in the west-central part of Tullett Point Basin
120	72.	Seismic expression of central Richards Point Graben in the west-central part of Tullett Point Basin
121	73.	Seismic expression of southern Richards Point Graben
123	74.	Seismic expression of Hardinge Bay Graben and Houghton Head Graben on a portion of Elf seismic profile PPA14
124	75.	Seismic expression of Hardinge Bay Graben and Houghton Head Graben on a portion of Elf seismic profile PPB26
127	76.	Correlation chart for Lower Jurassic and younger tectonic, magmatic and related depositional features of M'Clure Strait Basin and various grabens of Prince Patrick Uplift
129	77.	Seismic expression of Landing Lake Graben
130	78.	Clast-supported, syntectonic conglomerate in the Awingak Formation of Cape Cam Graben
132	79.	Seismic expression of graben structures and related normal faults in the northern part of M'Clure Strait Basin on a portion of GSI profile GM74-142
133	80.	Seismic expression of rift-related normal faults in the northern part of M'Clure Strait Basin on a portion of GSI profile GM74-135
135	81.	Correlation chart for Lower Jurassic and younger tectonic, magmatic and related depositional features of the report area and adjacent areas of polar North America and Greenland
139	82.	Location and distribution of folds, thrust faults and uplifts of post-Cretaceous and pre-Neogene age
140	83.	Seismic expression of minor thrust anticline of probable mid-Tertiary age in Sverdrup Basin west of Satellite Bay
141	84.	Seismic expression of minor thrust folds of probable mid-Tertiary age in Tullett Basin west of Green Bay
144	85.	Thickness isochrons and spot thicknesses, seismic profiles and the location of related text illustrations for the Arctic Continental Terrace Wedge
145	86.	Aerial photographic expression of the Beaufort Formation on central Prince Patrick Island
146	87.	Schematic cross-section for the Beaufort Formation and related deposits of the Arctic Continental Terrace Wedge across central Prince Patrick Island
148	88.	Aerial view of the eastern limit of the Beaufort Formation on Prince Patrick Island
148	89.	Stratigraphic relationship between basement faults and the Beaufort Formation in outcrops west of Mould Bay
149	90.	Varved glaciolacustrine silt and mud is draped on the face of the Beaufort escarpment
149	91.	Intraformational minor folds and a related detachment surface featured in glaciolacustrine silt
150	92.	Schematic model for the origin of gravity slides in glaciolacustrine silt and mud of east-central Prince Patrick Island
151	93.	Surface gravity flows in the active layer above the Christopher Formation, Landing Lake area
152	94.	Location map of wells and resource localities mentioned in text
153	95.	Thermal maturity scales and stages of hydrocarbon evolution
154	96.	Van Krevelen-type diagram based on Rock-Eval analyses of Silurian and Lower Devonian samples
155	97.	Geographic variation in thermal maturity of Silurian and Lower Devonian strata
156	98.	Van Krevelen-type diagram based on Rock-Eval analyses of Middle and Upper Devonian samples
157	99.	Geographic variation in thermal maturity of Upper Devonian strata
158	100.	Geographic variation in thermal maturity of Carboniferous and Lower Permian strata
159	101.	Geographic variation in thermal maturity of mid- to Upper Permian strata
160	102.	Van Krevelen-type diagram based on Rock-Eval analyses of Triassic samples
161	103.	Geographic variation in thermal maturity of Upper Triassic strata
162	104.	Van Krevelen-type diagram based on Rock-Eval analyses of Jurassic samples
163	105.	Geographic variation in thermal maturity of Middle Jurassic strata
164	106.	Van Krevelen-type diagram based on Rock-Eval analyses of Cretaceous samples
165	107.	Geographic variation in thermal maturity of Cretaceous strata
166	108.	Rhodochrosite-cemented sandstone, Eglinton Member (Campanian) of Eglinton Island
190	B-1	Horizontal intensity of the magnetic field in Canada for 2001
192	B-2	Magnetic declination in 2000 for the Prince Patrick Island region

193 B-3 Secular change of declination at Mould Bay from 1966 to 1997, based on monthly mean values recorded at the Magnetic Observatory
193 B-4 Seasonal variation of declination at Mould Bay Magnetic Observatory, computed from monthly mean values for the years 1966 to 1994
194 B-5 The variability of declination from day to day, shown by plotting Mould Bay daily mean values for 1993
194 B-6 Plots of magnetic declination at Mould Bay on a magnetically quiet day (December 9, 1993), an unsettled day (June 27, 1993), and a disturbed day (March 11, 1993)
195 B-7 Magnetic declination plot at Mould Bay showing variabilities greater during the summer months due to increased magnetic disturbance during the summer
195 B-8 Daily variation of declination at Mould Bay during the winter and summer, derived from hourly mean values from the years 1966 to 1994
196 B-9 Magnetic declination plot at Mould Bay showing greater variability during the early afternoon than during the period near midnight; based on hourly range values from Mould Bay for the years 1966 to 1994

Tables

36 1. Summary interval velocity data for frozen and unfrozen stratigraphic units of the report area
36 2. Chronology of basin formation and major tectonic phases
197 B-1 Effect of common objects on a magnetic compass as measured in an ambient field of 17000 nT and scaled to 3000 nT

CD-ROM oversized sheets

Map 2026A: Bedrock geology of Prince Patrick Island, Eglinton Island and the inter-island channels, District of Franklin, Northwest Territories

Seismic transects

sheet 1 of 2: Eglinton seismic transect
Eastern Prince Patrick transect
sheet 2 of 2: Western Prince Patrick transect

Structural cross-sections

Cross-section A: Gardiner Point to Cape Nares on Eglinton Island
Cross-section B: Western Melville Island to Crozier Channel
Cross-section C: Dyer Bay to Cape Hemphill on Prince Patrick Island
Cross-section D: Bloxsome Bay to Cape Krabbé on Prince Patrick Island

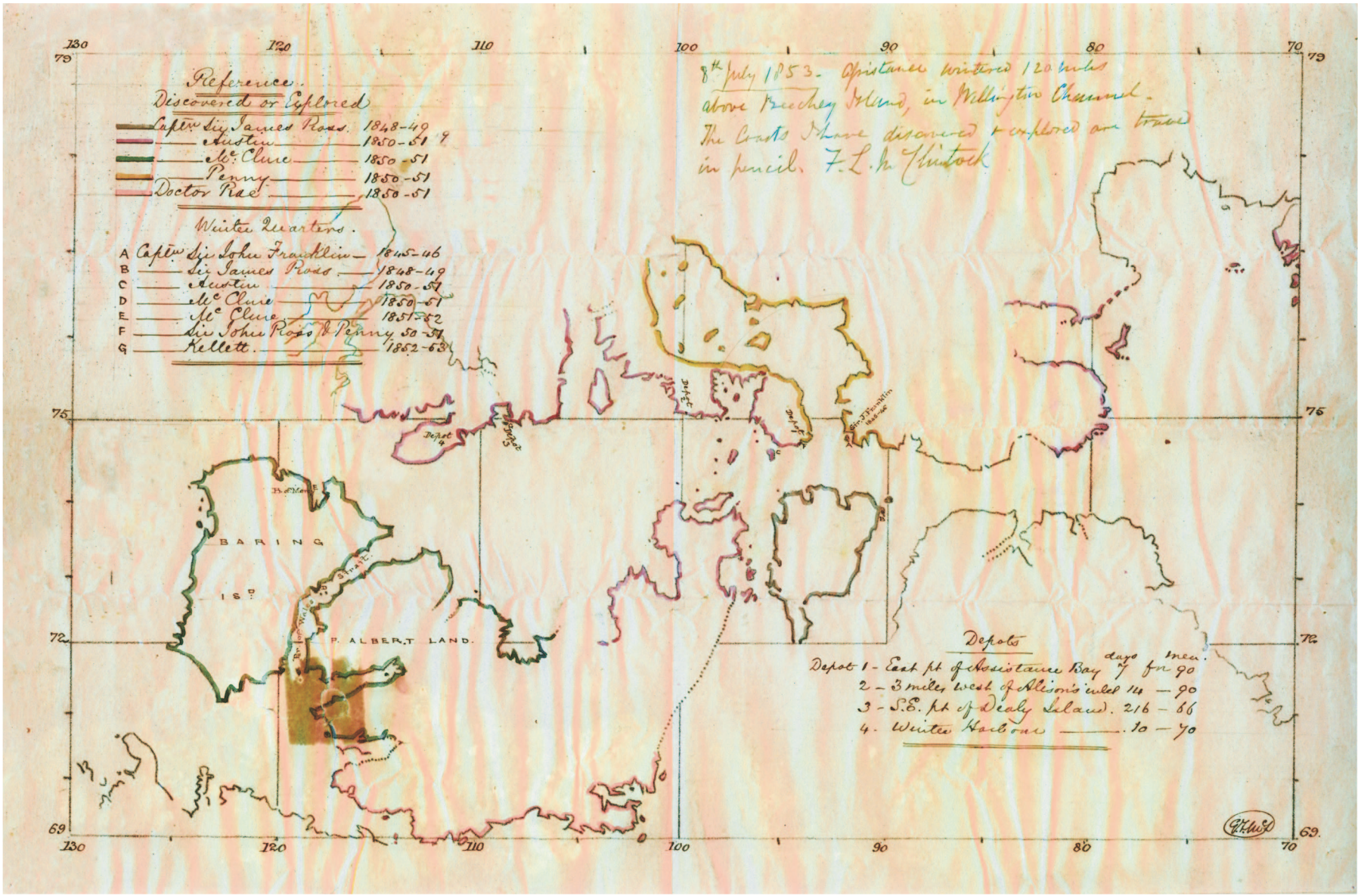

Frontispiece. *Francis Leopold M'Clintock left us the first description and the oldest known map of Prince Patrick Island and Eglinton Island following his sledge journey of nearly 1100 km in the spring of 1853. Recovered from the rock cairn at Nias Point on Melville Island in 1958 by Dr. Ray Thorsteinsson of the Geological Survey of Canada, this map was drafted in ink and watercolours by G.F. M' Dougall, Master of H.M.S. Resolute. It illustrates the shorelines of the central Arctic Islands as charted by Franklin, Austin, James Ross. M'Clure, Kellett and others down to 1853. M'Clintock has added his own new lines and his comments at upper right: "8th July 1853 - Assistance wintered 120 miles above Beechey Island in Wellington Channel. The Coasts I have discovered and explored are traced in pencil. F.L. M'Clintock". The sledge journeys of Francis M'Clintock and G.F. Mecham, and the story of this map, are described on pages 8 and 9.*

BASINS AND FOLD BELTS OF PRINCE PATRICK ISLAND AND ADJACENT AREAS, CANADIAN ARCTIC ISLANDS

Abstract

Prince Patrick and Eglinton islands have a polar desert climate and a landscape of coastal plains and dissected plateaux with limited vegetation cover. Use of a properly damped surveyor's compass is possible, however, magnetic declination changes markedly over short distances and large temporal variations are present.

Bedrock of the report area is divisible into four major successions. These include: 1) 14 to 18 km of Proterozoic(?) and/or older bedrock above the Mohorovičić Discontinuity; 2) 10 to 14 km of thermally overmature but variably tectonized ("Franklinian") strata that range from Vendian(?) at the base through Upper Devonian at the top; 3) less than 1 km grading to more than 7 km of thermally mature and immature, relatively undeformed Carboniferous through Lower Cretaceous strata of the Sverdrup Basin, including up to 2 km of Middle Jurassic through Upper Cretaceous strata preserved in four peripheral basins and numerous small grabens; and 4) 70 m to more than 600 m of unconsolidated Pliocene sand, gravel, and peat, and related seismically defined Neogene strata of the Arctic Continental Terrace Wedge. The Franklinian succession is further subdivided into siliciclastic rocks of the Devonian clastic wedge (up to 6000 m thick), subsurface Lower Devonian and older strata of the Prince Patrick Platform, and correlative seismically defined deep-water strata of Canrobert Trough.

A thrust-fold belt imaged seismically in the northeast is continuous with folds known at the surface on northwestern Melville Island, and folded Devonian strata are everywhere separated from Carboniferous and younger rocks by a profound angular unconformity. Other lower Paleozoic folds extend under southwestern Prince Patrick Island. A Carboniferous rift system located under the Sverdrup Basin margin has developed on the eroded roots of the Paleozoic fold belt. The rift formed in the Early Carboniferous (Serpukhovian), expanded to the southwest during the later Carboniferous, and was partly inverted during the Early Permian. Mid-Permian through early Middle Jurassic was a time of passive subsidence and progressive basin expansion toward the southwest. During Sverdrup Basin subsidence, four intracratonic basins, separated by Devonian "basement" highs, developed to the southwest between Middle Jurassic and Late Cretaceous time. An array of northerly trending horsts and grabens also developed during this time, part of a rift system that provides a geological record of the early development of the Arctic Ocean basin.

Potential exists for far-travelled hydrocarbons within the Permo–Carboniferous and Jurassic–Cretaceous rift systems and in stratigraphic traps on the margins of the Mesozoic basins. Subbituminous coal seams to 1.5 m occur in Lower Cretaceous strata, and deposits of manganese carbonate are widespread in Campanian sandstone of Eglinton Island.

Résumé

Les îles Prince Patrick et Eglinton ont un climat de désert polaire et un paysage composé de plaines côtières et de plateaux disséqués, avec un couvert végétal limité. Il est possible d'y utiliser une boussole d'arpenteur bien amortie, mais la déclinaison magnétique change beaucoup sur de courtes distances et varie abondamment dans le temps.

Le substratum rocheux de la région visée par le bulletin se subdivise en quatre successions principales, soit (1) de 14 à 18 km de substratum rocheux du Protérozoïque (?) ou plus vieux, au-dessus de la discontinuité de Mohorovičić; (2) de 10 à 14 km de strates thermiquement hypermatures mais diversement tectonisées («Franklinien»), dont l'âge varie du Vendien (?) à la base au Dévonien supérieur au sommet; (3) de moins de 1 km à plus de 7 km de strates relativement non déformées, thermiquement matures à immatures, du Carbonifère-Crétacé supérieur du bassin de Sverdrup, y compris jusqu'à 2 km de strates du Jurassique moyen-Crétacé supérieur conservées dans quatre bassins périphériques et de nombreux petits grabens; et (4) de 70 m à plus de 600 m de sable, de gravier et de tourbe non consolidés du Pliocène et de strates apparentées du Néogène (connues grâce à des levés sismiques) du prisme de sédiments de la terrasse continentale de l'Arctique. La succession franklinienne est elle-même subdivisée en roches silicoclastiques du biseau détritique du Dévonien (jusqu'à 6000 m d'épaisseur), en strates subsuperficielles du Dévonien inférieur et plus vieilles de la plate-forme de Prince Patrick, et en strates corrélées d'eau profonde de la cuvette de Canrobert définies à l'aide de méthodes sismiques.

Une zone de plissement et de chevauchement, reconnue par des méthodes sismiques dans le nord-est, constitue un prolongement de plis reconnus en surface dans le nord-ouest de l'île Melville. Une discordance angulaire nette sépare partout les strates plissées du Dévonien des roches du Carbonifère et plus jeunes. D'autres plis du Paléozoïque inférieur se prolongent sous la partie sud-ouest de l'île Prince Patrick. Un rift carbonifère sous la marge du bassin de Sverdrup s'est développé sur les

racines érodées de la zone de plissement du Paléozoique. Il s'est formé au Carbonifère précoce (Serpukhovien), a pris de l'expansion vers le sud-ouest au Carbonifère plus tardif et s'est inversé en partie au Permien précoce. La période du Permien moyen au début du Jurassique moyen a été une période de subsidence passive et d'expansion progressive du bassin de Sverdrup vers le sud-ouest. Pendant la subsidence du bassin, quatre bassins intracratoniques, séparés les uns des autres par des hauteurs du «socle» dévonien, se sont formés au sud-ouest entre le Jurassique moyen et le Crétacé tardif. Un réseau de horsts et de grabens de direction nord s'est également formé à cette époque. Ces structures font partie d'un rift qui témoigne d'événements géologiques survenus au début de la formation du bassin de l'océan Arctique.

Les rifts du Permo-Carbonifère et du Jurasso-Crétacé ainsi que les pièges stratigraphiques sur les marges des bassins mésozoïques pourraient contenir des hydrocarbures de provenance lointaine. Des filons de charbon subbitumineux pouvant atteindre 1,5 m d'épaisseur se rencontrent dans les strates du Crétacé inférieur, et des dépôts de carbonate de manganèse sont répandus dans les grès campaniens de l'île Eglinton.

Summary

This account deals with the onshore and offshore bedrock geology, stratigraphy, structure, tectonic evolution, and resource potential of a remote portion of Canada's westernmost Arctic Islands, situated entirely within the northern Northwest Territories north of 75 degrees North latitude.

Prince Patrick and Eglinton islands contain both coastal lowlands and dissected plateaux. Much of the northwestern half of Prince Patrick Island is part of the Arctic coastal plain, a topographically subdued and gently inclined surface underlain by Pliocene and younger unconsolidated sand and gravel. The remaining land areas feature dissected plateaux (rising to 220 m above sea level) of Devonian and Mesozoic bedrock that locally terminate in escarpments and coastal cliffs. The dissected landscape of southeastern Prince Patrick Island continues into the offshore, part of a drowned river valley system that extends to a relatively level sea floor 350 to 450 m deep in M'Clure Strait. The report area is a polar desert, with recorded January and July average temperatures of -34°C and +4°C, respectively, and annual precipitation of 93 mm. Vegetation cover is limited to lowland sedge and grass meadows, and upland lichen, saxifrage and dwarfed willow tundra.

Use of a properly damped surveyor's compass is possible within the report area. However, the magnetic declination changes markedly over short distances because there is a steep gradient near the magnetic pole, and large temporal variations are present. These variations include: 1) a secular decrease in declination, approximately 80' per year in the mid-1990s; 2) a seasonal decrease in the average declination of approximately 0.5° during the summer months; 3) a seasonal increase in the variability of declination during the summer months, up to 4° per hour; 4) a diurnal increase in the average magnetic declination of about 3.5° near local noon; and 5) a diurnal increase in the variability of declination in the early afternoon, up to about 4° per hour.

Strata of the Prince Patrick and Eglinton Island area are divisible into four major successions. These include: 1) 14 to 18 km of Proterozoic(?) and/or older bedrock above the Mohorovičić Discontinuity; 2) 10 to 14 km of thermally overmature but variably tectonized ("Franklinian") strata that range from Vendian(?) at the base through Upper Devonian at the top; 3) less than 1 km grading to more than 7 km of thermally mature and immature, relatively undeformed Carboniferous through Lower Cretaceous strata of the Sverdrup Basin, including up to 2 km of Middle Jurassic through Upper Cretaceous strata preserved in four peripheral basins and numerous small grabens; and 4) 70 m to more than 600 m of unconsolidated Pliocene sand, gravel and peat, and related, seismically defined Neogene strata of the Arctic Continental Terrace Wedge. The Franklinian succession is further subdivided into siliciclastic rocks of the Middle and Upper Devonian clastic wedge (up to 6000 m thick), subsurface Lower Devonian and older strata of the Prince Patrick Platform (the upper part known from drilling), and correlative seismically defined deep-water strata of the Canrobert Trough (also exposed on adjacent northwestern Melville Island). Strata of Prince Patrick Platform are separated from those of Canrobert Trough by Crozier High, a tectonic uplift of presumed mid-Cambrian age situated in the subsurface northwest of southern Eglinton Island.

Folded Devonian and older strata are everywhere separated from Carboniferous and younger rocks by a profound angular unconformity. A thrust-fold belt imaged seismically under northeastern Prince Patrick Island and northeastern Eglinton Island is continuous with folds known at the surface in the Canrobert Hills region of northwestern Meville Island. The subsurface fold belt has a southwesterly facing convex and arcuate geometry in map view, and a regional plunge of 0.6 to 1.3° to the northwest. Fold vergence is inconsistent. However, overall direction of tectonic transport is toward the southwest. The folds are detached in seismic Vendian(?) strata near the base of the Franklinian succession, at a mid-Cambrian level and low in the Devonian clastic wedge. Other Paleozoic folds, apparently transported from the west, extend under southwestern Prince Patrick Island.

Carboniferous and Permian strata, deposited within a rift system along the southwestern margin of the Sverdrup Basin, are understood from exploratory wells and seismic profiles of northeastern Prince Patrick Island. The rift system has developed on the eroded roots of the Paleozoic fold belt, with individual listric normal faults traceable downsection onto pre-existing thrust planes. The embryonic rift developed in seismic Serpukhovian time in the Moore Bay-Satellite Bay area, expanded to the southwest during the later Carboniferous, and was partly inverted in a transpressive tectonic regime during the Early Permian. The depositional record for strata of mid-Permian (Roadian) through lower Middle Jurassic ages is one of passive subsidence, onlap, offlap and basin marginal overstep of sequences, and progressive basin expansion toward the southwest.

The Sverdrup Basin continued to subside through the later Mesozoic. However, four new intracratonic basins, separated by Devonian "basement" highs, were formed to the southwest beginning in the Middle Jurassic: Eglinton Basin under Eglinton Island, Tullett Basin under Pliocene cover of central Prince Patrick Island, M'Clure Strait Basin in the mouth of M'Clure Strait, and Banks Basin (south of the report area) under central Banks Island. A network of northerly striking horsts and grabens also developed during this period, part of a Middle Jurassic through Cretaceous rift system at least 100 km wide and traceable from Banks Island to northern Prince Patrick Island, which provides a geological record of the early development of the Arctic Ocean basin.

Modest-scale anticlines and synclines and related thrust faults occur throughout the Cretaceous and older strata of Prince Patrick and Eglinton islands. These features are attributed to the regional effects of the late Paleocene–Eocene Eurekan Orogeny, the greater part of which accounts for the young mountainous terranes of Ellesmere and Axel Heiberg islands. Regional uplift and the development of a profound angular unconformity between tectonized Cretaceous and generally flat-lying Neogene cover is also attributed to the Eurekan Orogeny.

While discovered hydrocarbons are insignificant, the report area has received only reconnaissance seismic profiling by the exploration industry, and only the largest structures have been tested. Devonian and older rocks are thermally overmature and economically least promising. Greater potential exists for far-travelled hydrocarbons within the Permo–Carboniferious and Jurassic–Cretaceous rift systems and in stratigraphic traps on the margins of the Mesozoic basins. Coal seams are known in the Middle to Upper Devonian (to 30 cm thick), and the Middle Jurassic and Lower Cretaceous (to 1.5 m thick). Deposits of manganese carbonate are widespread in Upper Cretaceous sandstone of southern Eglinton Island.

Sommaire

Le présent bulletin décrit la géologie, la stratigraphie, la structure, l'évolution tectonique et les ressources potentielles du substratum rocheux sur terre et en mer dans une région éloignée à l'extrême ouest de l'archipel Arctique, dans la partie nord des Territoires du Nord-Ouest, au nord de 75° de latitude N.

Les îles Prince Patrick et Eglinton comportent des basses terres côtières et des plateaux disséqués. Une grande portion de la moitié nord-ouest de l'île Prince Patrick fait partie de la plaine côtière de l'Arctique, surface au relief adouci et légèrement inclinée sous laquelle on trouve des sables et des graviers non consolidés du Pliocène et plus jeunes. Le reste des étendues émergées comportent des plateaux disséqués (qui atteignent 220 m au-dessus du niveau de la mer) composés de substratum rocheux du Dévonien et du Mésozoïque qui, par endroits, se terminent par des escarpements et des falaises côtières. Le paysage disséqué du sud-est de l'île Prince Patrick se prolonge au large, partie d'un réseau de vallées et de cours d'eau submergés qui s'étend jusqu'au fond marin relativement plan à des profondeurs de 350 à 450 m dans le détroit de M'Clure. La région à l'étude est un désert polaire où les températures moyennes enregistrées en janvier et en juin sont respectivement de -34 °C et de +4 °C, et où la précipitation annuelle est de 93 mm. Le couvert végétal consiste en cariçaies et en prés de graminées dans les basses terres et en toundra à lichens, à saxifrages et à saules nains dans les hautes terres.

Il est possible d'utiliser une boussole d'arpenteur bien amortie dans la région à l'étude. Toutefois, la déclinaison magnétique change beaucoup sur de courtes distances, en raison du gradient marqué près du pôle magnétique, et varie abondamment dans le temps. Ces variations comprennent (1) une diminution séculaire de la déclinaison d'environ 80' par année au milieu des années 1990; (2) une diminution saisonnière de la déclinaison moyenne d'environ 0,5° pendant les mois d'été; (3) une augmentation saisonnière de la variabilité de la déclinaison pendant les mois d'été, soit jusqu'à 4° par heure; (4) un augmentation diurne de la déclinaison magnétique moyenne d'environ 3,5° près de midi heure locale; et (5) une augmentation diurne de la variabilité de la déclinaison au début de l'après-midi, soit jusqu'à environ 4° par heure.

Les strates de la région des îles Prince Patrick et Eglinton se subdivisent en quatre grandes successions, soit (1) de 14 à 18 km de substratum rocheux du Protérozoïque (?) ou plus vieux, au-dessus de la discontinuité de Mohorovičić; (2) de 10 à 14 km de

strates thermiquement hypermatures mais diversement tectonisées («Franklinien»), dont l'âge varie du Vendien (?) à la base au Dévonien supérieur au sommet; (3) de moins de 1 km à plus de 7 km de strates relativement non déformées, thermiquement matures et immatures, du Carbonifère-Crétacé supérieur du bassin de Sverdrup, y compris jusqu'à 2 km de strates du Jurassique moyen-Crétacé supérieur conservées dans quatre bassins périphériques et de nombreux petits grabens; et (4) de 70 m à plus de 600 m de sable, de gravier et de tourbe non consolidés du Pliocène et de strates apparentées du Néogène (connues grâce à des levés sismiques) du prisme de sédiments de la terrasse continentale de l'Arctique. La succession franklinienne est elle-même subdivisée en roches silicoclastiques du biseau détritique du Dévonien moyen-supérieur (jusqu'à 6000 m d'épaisseur), en strates subsuperficielles du Dévonien inférieur et plus vieilles de la plate-forme de Prince Patrick (la partie supérieure est connue grâce aux forages), et en couches corrélées d'eau profonde de la cuvette de Canrobert, définies à l'aide de méthodes sismiques (également exposées dans la partie nord-ouest adjacente de l'île Melville). Les strates de la plate-forme de Prince Patrick sont séparées des strates de la cuvette de Canrobert par la hauteur de Crozier, soulèvement tectonique datant vraisemblablement du Cambrien moyen et situé en subsurface au nord-ouest de la partie sud de l'île Eglington.

Une discordance angulaire nette sépare partout les strates plissées du Dévonien et plus vieilles des roches du Carbonifère et plus jeunes. Une zone de plissement et de chevauchement, reconnue par des méthodes sismiques dans le nord-est de l'île Prince Patrick et le nord-est de l'île Eglinton, est un prolongement de plis reconnus en surface dans la région des collines Canrobert, dans le nord-ouest de l'île Melville. Sur la carte, cette zone de plissement subsuperficielle présente une géométrie convexe et arquée vers le sud-ouest ainsi qu'un plongement régional de 0,6 à 1,3° vers le nord-ouest. La vergence est irrégulière. Toutefois, la direction globale de transport tectonique est vers le sud-ouest. Les plis sont détachés dans des strates sismiques du Vendien (?) près de la base de la succession franklinienne, à un niveau mi-cambrien et vers le bas du biseau détritique dévonien. D'autres plis paléozoïques, transportés semble-t-il de l'ouest, se prolongent sous la partie sud-ouest de l'île Prince Patrick.

Des strates du Carbonifère et du Permien, déposées dans un rift le long de la marge sud-ouest du bassin de Sverdrup, sont connues à partir de forages d'exploration et de profils sismiques dans le nord-est de l'île Prince Patrick. Le rift s'est développé sur les racines érodées de la zone de plissement du Paléozoïque, et on peut suivre la trace de failles normales listriques individuelles vers le bas de la coupe jusqu'à des surfaces de charriage préexistantes. Le rift embryonnaire s'est formé dans la région des baies Moore et Satellite au Serpukhovien (levés sismiques), puis a pris de l'expansion vers le sud-ouest au Carbonifère plus tardif et s'est inversé en partie au Permien précoce dans un régime tectonique de transpression. Les strates qui s'échelonnent du Permien moyen (Roadien) à base du Jurassique moyen témoignent de subsidence passive, de progradation, d'aggradation et de transgression discordante sur la marge du bassin, et de l'expansion progressive du bassin vers le sud-ouest.

La subsidence du bassin de Sverdrup s'est poursuivie au Mésozoïque plus tardif. Toutefois, quatre nouveaux bassins intracratoniques, séparés les uns des autres par des hauteurs du «socle» dévonien, se sont formés au sud-ouest à compter du Jurassique moyen, soit le bassin d'Eglinton sous l'île Eglinton, le bassin de Tullett sous la couverture pliocène dans le centre de l'île Prince Patrick, le bassin du détroit de M'Clure à l'entrée du détroit de M'Clure, et le bassin de Banks (au sud de la région à l'étude) sous le centre de l'île Banks. Un réseau de horsts et de grabens de direction nord s'est également formé à cette époque; ces structures font partie d'un rift d'au moins 100 km de largeur qui date du Jurassique moyen-Crétacé et dont on peut suivre la trace depuis l'île Banks jusque dans le nord de l'île Prince Patrick. Ce rift témoigne d'événements géologiques survenus au début de la formation du bassin de l'océan Arctique.

Des anticlinaux et synclinaux de taille modeste ainsi que des failles de chevauchement apparentées se rencontrent dans toutes les strates du Crétacé et plus vieilles des îles Prince Patrick et Eglinton. On les attribue aux effets régionaux de l'orogenèse eurékienne du Paléocène tardif-Éocène, qui est en majeure partie à l'origine des jeunes terranes montagneux des îles d'Ellesmere et Axel Heiberg. Le soulèvement régional et la formation d'une discordance angulaire nette entre la couverture crétacée tectonisée et la couverture néogène généralement plane sont également attribuées à l'orogenèse eurékienne.

Bien que les découvertes d'hydrocarbures soient négligeables, les sociétés d'exploration n'ont entrepris que des levés sismiques de reconnaissance dans la région, et seules les plus grosses structures ont été examinées. Les roches du Dévonien et plus vieilles sont thermiquement hypermatures et les moins prometteuses sur le plan économique. Il existe de meilleures possibilités pour des hydrocarbures de provenance lointaine dans les rifts du Permo-Carbonifère et du Jurasso-Crétacé et dans des pièges stratigraphiques sur les marges des bassins mésozoïques. Des filons de charbon sont connus dans les roches du Dévonien moyen-supérieur (jusqu'à 30 cm d'épaisseur) et du Jurassique moyen et du Crétacé inférieur (jusqu'à 1,5 m d'épaisseur). Des dépôts de carbonate de manganèse sont répandus dans les grès du Crétacé supérieur dans le sud de l'île Eglinton.

INTRODUCTION

Description of the study area

This account deals with the general bedrock geology, stratigraphy, structure, tectonic evolution, and resource potential of a remote portion of Canada's westernmost Arctic Islands, situated entirely within the northern Northwest Territories (Fig. 1). The bedrock geology of the report area is presented on a single map sheet at the scale of 1:250, 000 (2026A, included with this report). This map illustrates information compiled from all land and intervening offshore areas west of Melville Island within part or all of six topographic map sheets (*Eglinton Island*, NTS 88G; *Intrepid Inlet*, NTS 89B; *Satellite Bay*, NTS 89C and 99D; *Ballantyne Strait* west of 115°00' W longitude, NTS 89D; *Dyer Bay* north of 75°10'N latitude, NTS 98H; and *Hardinge Bay*, NTS 99A).

Although the land areas of Prince Patrick and Eglinton islands provide natural geographic limits to this study, the adjacent bedrock beneath M'Clure Strait and the smaller inter-island channels has also been studied. Prince Patrick Island faces the Arctic Ocean and includes the westernmost land areas of the Queen Elizabeth Islands. The island occupies an area of 15 848 km^2 and, thus, is nearly three times the size of the smallest Canadian province, Prince Edward Island (5660 km^2). Eglinton Island (551 km^2) lies to the southeast and is separated from adjacent Prince Patrick and Melville islands by Crozier Channel and Kellett Strait, respectively. These islands also face northern Banks Island to the south across M'Clure Strait. Lesser land areas featured in this report include the Polynia Islands to the northeast in Ballantyne Strait, the unnamed large island west of Walker Inlet that includes Giants Causeway, and numerous low-lying islands in Dyer Bay, Bloxsome Bay, Satellite Bay and along the Arctic coast of northwestern Prince Patrick Island.

The long dimension of Prince Patrick Island trends N45°E and is modestly oblique to both the long axis of Eglinton Island (N30°E) and the 500 m isobath (N30°E) that defines the local trend of the continental slope beneath the Arctic Ocean 200 km northwest of these islands. The southeastern coast of Prince Patrick Island includes four significant but unnamed northerly trending peninsulas. These landmasses are separated by long, estuarine bays that extend almost to the middle of the island and include, from west to east, Dyer Bay, Walker Inlet, Mould Bay, and Intrepid Inlet. A fifth unnamed peninsula lies off the northeast coast against Ballantyne Strait and is separated from the body of the island by an isthmus and two bodies of water: Moore Bay to the southeast, and Satellite Bay, which faces the Arctic Ocean.

A Canadian government weather station and geophysical observatory, occupied year round until 1997, was located on the east shore of Mould Bay at the mouth of Station Creek. An illuminated gravel airstrip, capable of handling most small, fixed-wing aircraft, was also maintained at this location. Being close to sea level and the adjacent Station Creek, the strip required careful attention to maintenance by weather station personnel, particularly during the summer period. To this end, crushed bedrock material was excavated, processed and carried by truck from a quarry located immediately north of the station. The quarried aggregate was also used to maintain the local road network.

Access to Mould Bay for the purpose of fieldwork was made in two stages. From southern Canada commercial jet aircraft (for personnel and priority cargo) made, and continue to make, regular scheduled flights into Resolute Bay located 675 km to the east on southern Cornwallis Island. Seasonal maritime shipping for fuel and other bulk cargo also exists and arrives in Resolute once each summer from Montreal. Slightly longer access routes might be utilized from other communities with routine commercial jet service from the south, including Cambridge Bay on southern Victoria Island (900 km) and Inuvik on the Mackenzie Delta (960 km). Most of Prince Patrick and Eglinton islands are accessible from these larger distant communities by means of small, fixed-wing aircraft, equipped with wheels or skis, or rotary aircraft, both capable of landing either at the weather station or on the surrounding unprepared terrain.

Physical and environmental features

Physiography

Prince Patrick and Eglinton islands contain both coastal lowlands and dissected plateaux. Lowlands are conveniently defined as low-relief areas lying below the 60 m elevation contour, but are also considered to include similar, undissected land areas as high as 125 m. The largest lowland region is the Arctic coastal plain, which embraces fully half of Prince Patrick Island northwest of a slightly sinuous line running from the head of Dyer Bay in the southwest to Cape Krabbé in the northeast. This plain, 20 to 65 km wide, slopes upward to the southeast from sea level to a maximum elevation of about 125 m. Other significant lowland areas, 2 to 10 km wide, are situated along the east shore and around the head of Intrepid Inlet, around Moore and Jameson bays, and around other intervening, unnamed bays. The north end of Eglinton Island also features a significant coastal lowland. Lowlands are generally lacking in good outcrop except locally along river banks. Braided rivers are numerous but narrow and shallow. These feed

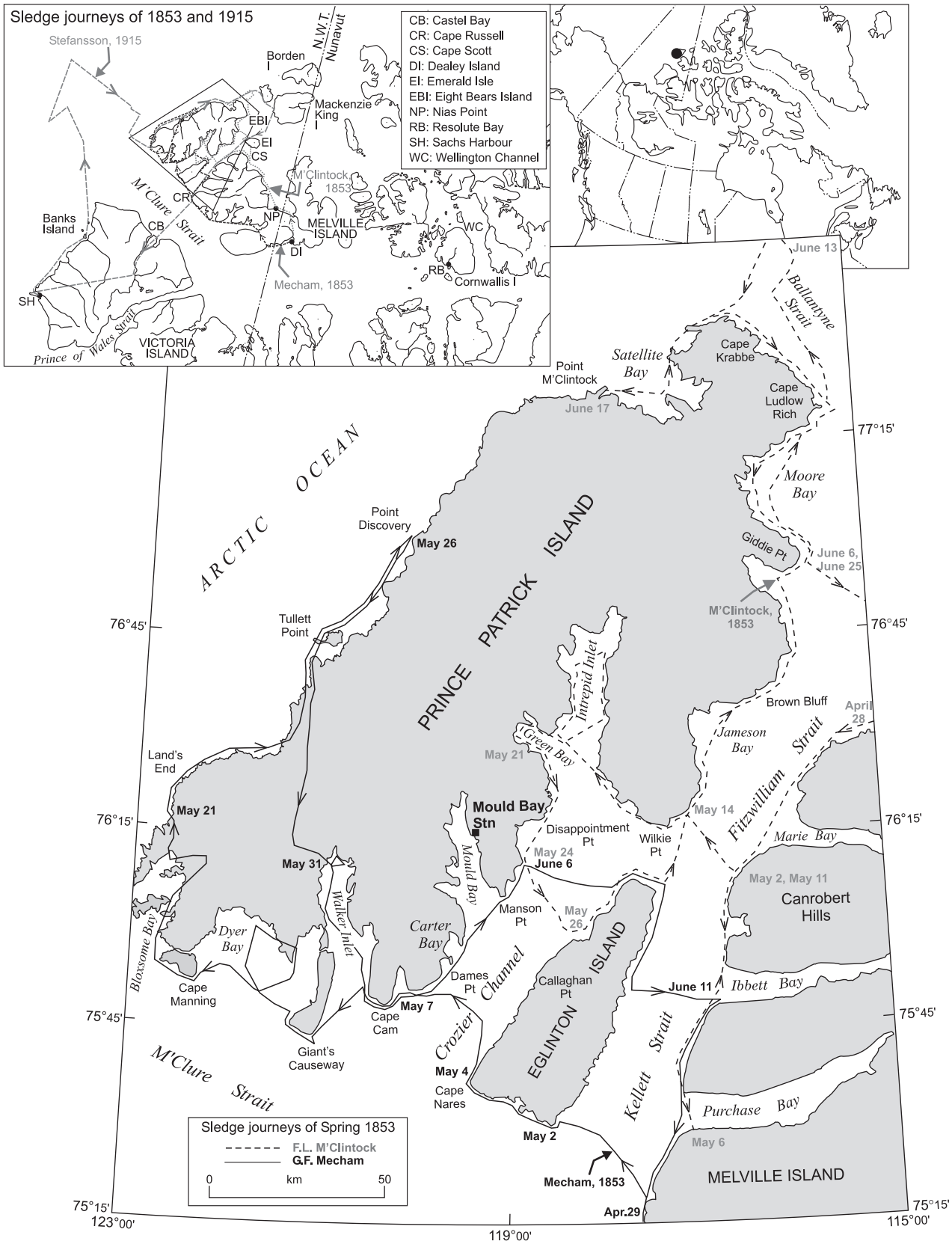

Figure 1. *Location of the report area and various geographic features cited in the text. Historic sledge routes of G.F. Mecham and F.L. M'Clintock in 1853 (British Parliamentary Papers, 1855), and of V. Stefansson in 1915 (Stefansson, 1944) are included.*

constructive lobate deltas, particularly along the northwest coast of Prince Patrick Island. Interfluvial areas have formed a plain of unconsolidated sand and mud with small lakes or ponds. The subdued topography of the coastal lowlands is continuous with extensive shallow-marine areas (<200 m deep) that lie within Bloxsome Bay, Satellite Bay, northeast of Cape Ludlow Rich, and around the Polynia Islands in Ballantyne Strait. Less is known about nearshore bathymetry northwest of Prince Patrick Island.

The remainder of Prince Patrick and Eglinton islands feature dissected plateaux. The elevation of the plateau surface is 120 m on southern Eglinton Island, 160 m east of Intrepid Inlet, and highest on the peninsula west of Mould Bay (up to 220 m). The plateau terminates in coastal cliffs around the shores of Mould Bay and Walker Inlet, but is also commonly seen as a strip of coastal lowland of variable width with rocky headlands. Examples are observed around Hiccles Cove and at Salmon Point on Intrepid Inlet, and at Cape Nares on southwesternmost Eglinton Island. Bedrock is relatively well exposed throughout the plateaux margins. Hogback ridges of modestly inclined strata present excellent sections along the east shore of Walker Inlet. More common are mesas and highly dissected escarpments of near flat-lying Devonian, Jurassic and younger strata. Southeastern Eglinton Island has the form of a single, large mesa within which the uppermost cliff-forming ledge of the mesa is defined by Upper Cretaceous sandstone selectively cemented by manganese carbonate.

A southeasterly facing escarpment, displaying the basal 30 to 50 m of the Pliocene Beaufort Formation, extends the entire length of Prince Patrick Island from Dyer Bay to Cape Krabbé. The escarpment is a highly sinuous feature and has retreated up to 10 km to the northwest at numerous locations as a consequence of fluvial dissection by southeastward-flowing drainage systems. The top of this escarpment also serves as a drainage divide separating the dissected plateaux country to the southeast from the lowlands of the Arctic coastal plain to the northwest.

Erosional remnants of the Pliocene are extremely common and form buttes and mesas, particularly on the peninsulas east of Mould Bay, east of Intrepid Inlet, and throughout the dissected plateau country northeast to Moore Bay. Buttes of Jurassic and Cretaceous erosional remnants are also common in these areas and on northern Eglinton Island, where rapid denudation of unconsolidated Cretaceous sand and the complete absence of vegetation has created a “badlands”-type of landscape reminiscent of that seen in other arid regions of the globe.

Surface materials between outcrop areas on these islands include vast expanses of sparsely vegetated frost boils, frost-shattered felsenmeer, talus, and a patchy veneer of glaciogenic sediments, Pleistocene and Recent fluvial gravels, and some raised strandline and deltaic deposits. Although there are no permanent glaciers or icecaps, small, perennial banks of ice and snow are common on some incised river banks.

The dissected landscape of southeastern Prince Patrick Island continues into the offshore. The bays, inlets and inter-island channels represent part of a drowned river valley system modified by one or more phases of glacial incision. The submerged portions of these valleys are steep sided and extend to a relatively level sea floor ranging from 300 m depth in Kellett Strait and Crozier Channel to 350 to 450 m in M'Clure Strait.

Climate, Vegetation, and Wildlife

The climate of the report area is known primarily from the weather records obtained at Mould Bay station and summarized in the Canadian Hydrographic Service (1982) and as described by Edlund and Alt (1989). Temperatures range from a January average of -34°C to an average in July of +4°C. Melting of the active layer, or uppermost part of the permafrost, begins about June 15th and persists for approximately 73 days. Mean annual total precipitation (1951–1980) is 93 mm. About half of this falls during June, July and August. This exceedingly low level of precipitation – roughly one third of that recorded annually at Kamloops, British Columbia (Aldighieri, 1996) – accounts for the “polar desert” description of the high-arctic climate.

Vegetation cover is limited to lowland sedge and grass meadows, and upland lichen, saxifrage and dwarfed willow tundra (Edlund and Alt, 1989). Floral diversity is believed to diminish progressively toward the northwest coast of Prince Patrick Island, with gradual disappearance of prostrate shrubs and sedges followed by disappearance of various woody species.

Common mammals include Peary caribou, muskox, arctic hare, arctic wolves, arctic fox, lemmings, seals in the offshore, and rare polar bears.

History of geographical exploration

Prehistory

There is no archeological evidence of prehistoric Inuit activity anywhere within the report area, although temporary summer occupation sites of Dorset, pre-Dorset and Thule cultures are known as far west as central Melville Island (Henoch, 1964; McGee, 1978). Permanent Thule culture villages are also known from Banks Island (McGee, 1978). It would appear likely that hunting expeditions might have occasionally extended as far north and west as

Eglinton and Prince Patrick islands during this period (3700 to 350 years BP). Nevertheless, throughout the prehistory period, this region appears to have been considered generally too hostile and unsuitable for either habitation or sustainable hunting practices by the native population.

Franklin search expeditions

Land west of Melville Island was unknown prior to the Franklin search expeditions of the 1850s. The eastern end of M'Clure Strait and the north coast of Banks Island had been previously sighted in 1819 by members of William Edward Parry's expedition aboard the HMS *Hecla* and *Griper* (Parry, 1821). Parry at this time had achieved the first sailing from the east of nearly the entire Northwest Passage but was thwarted from completion of this task by impenetrable pack ice south of western Melville Island.

The search for Sir John Franklin and his crew initiated an unprecedented level of exploration activity to all parts of the Arctic Islands. The existence of two potential Northwest Passage routes (the first via Amundsen Gulf, Prince of Wales Strait, and Viscount Melville Sound; the other via M'Clure Strait) was proven by Robert M'Clure's voyage aboard the HMS *Investigator* (Osborn, 1857; Armstrong, 1857). This extraordinary display of seamanship beginning in 1850 and lasting four years involved sailing from Great Britain to the Pacific via Cape Horn; the transit of Bering Strait, the north coast of Alaska and the Beaufort Sea, and, in 1851, a near circumnavigation of Banks Island. Transit of the western half of M'Clure Strait, accomplished under difficult ice conditions in September of that year, was possible only by drifting to the east and east-southeast in a narrow shore edge lead of open water that existed between the north coast of Banks Island and multi-year pack ice that filled the remainder of the strait. The low-lying coast of Prince Patrick and Eglinton islands, which lay out of sight 120 km to the north, may have been obscured by fog banks reported to have been common in the area at this time (Armstrong, 1857). HMS *Investigator* was eventually abandoned in Mercy Bay in 1853. The crew were saved by walking over the ice to Melville Island where they were rescued by search parties attached to Sir Edward Belcher's expedition of 1852–54. This represented the first complete excursion through the Northwest Passage although the portion in eastern M'Clure Strait had been undertaken on foot.

Mecham and M'Clintock

Belcher had been given orders to ascertain the fate of the Frankin expedition (1845–1848) and the whereabouts of M'Clure, Collinson and their crews who had left England in 1850. Sailing via Baffin Bay and Lancaster Sound, a western contingent of Belcher's squadron aboard HMS *Resolute* and *Intrepid* eventually reached Dealey Island on the south coast of Melville Island in autumn of 1852 (Fig. 1, inset). From there, two separate but simultaneous sledge journeys led by Leopold M'Clintock and G.F. Mecham in the spring of 1853 resulted in the discovery and charting of nearly all the coasts of Eglinton and Prince Patrick islands (British Parliamentary Papers, 1855).

The two sledge parties departed on the same day, leaving Dealey Island on the morning of April 4th, 1853. M'Clintock's party travelled overland to Hecla and Griper Bay on the north coast of Melville Island and thence northwest to Cape Scott (on the northwesternmost extremity of Melville Island), which was reached on April 28th. From this low vantage point M'Clintock first observed and named Emerald Isle. The weather was clear and relatively warm during this period. Distant land masses, normally not visible on the horizon, were seen to be raised up by the phenomenon now known as abnormal refraction (Canadian Hydrographic Service, 1982). It was by this common Arctic atmospheric condition that M'Clintock was able to "view very distant land lying beyond our next extreme of Melville Island, and stretching across to Emerald Isle". The existence of this previously unknown landmass was confirmed as M'Clintock's sledging party continued to the west on subsequent days. This was the first historically documented viewing of Prince Patrick Island, a land M'Clintock named after Queen Victoria's seventh offspring, Prince Alfred Edward Patrick, the Duke of Connaught (and future Governor General of Canada from 1911 to 1914). From the end of April to the beginning of May, M'Clintock's sledge party surveyed the western capes of Melville Island. From Blackley Haven on May 3rd, M'Clintock noted that "to the west the land is much lower and is much distorted by refraction as to appear like a group of islands". This in fact would prove to be northern Eglinton Island and the peninsulas of southern Prince Patrick Island.

Mecham's party, having departed from base on the same day as M'Clintock, proceeded on a westerly course from Dealey Island, following the south coast of Melville Island to Cape Russell on the southwesternmost part of this island, which they reached on April 29th. From the height of land Mecham made the first distant observations of Eglinton Island, this occurring several days before M'Clintock's independent discovery of the same island. On the following day (April 30), Mecham's party set out over difficult ice in Kellett Strait and made a first landfall of southeastern Eglinton Island near Pedder Point on May 2nd. His party carried on to the west surveying the south and part of the west coasts of the island before turning west again toward Prince Patrick Island, which they first identified from Cape Nares on May 4th. Their first landfall on Prince Patrick was near Cape Cam on May 7th. M'Clintock and his sledging party at this time were retracing their steps to the north in

northern Kellett Strait before turning west toward Prince Patrick Island on May 11th. His party made landfall near Wilkie Point on the 14th.

Mecham, meanwhile, had proceeded to survey the southern coasts of the island including the mouth of Walker Inlet and Dyer Bay. After the 14th, his party travelled over sea ice to the west, documenting and naming many landmarks (Bloxsome Bay, Carter Bay, Cape Cam, Dames Point, Callaghan Point) after friends at home in England. Mecham eventually crossed to the west coast of the island near Lands End on May 21st and then continued to the northeast before reaching the farthest northeast point of his journey near Discovery Point on May 26th. At this time he was compelled to turn around because of lack of carried provisions and the apparent absence of large game on the land.

M'Clintock's discoveries between the 14th and 26th of May included the charting of the shores of Intrepid Inlet and Green Bay. At Snowpatch and Disappointment points on May 21st and 24th, respectively, he left cairns and notes detailing his activities up to this time. From here he crossed over to Eglinton Island and surveyed the north coasts of this island. Another cairn with messages was constructed here before he returned to the east coast of Prince Patrick Island, passing Wilkie Point (for the second time) on May 29th. M'Clintock continued his charting of the northeast coast of Prince Patrick Island including the shores of Jameson Bay and the landmarks near Brown Bluff. On June 6th his party was rounding Giddie Point.

This same day, Mecham had come to the end of his charting work. After leaving the west coast of Prince Patrick Island late in May, his sledging party proceeded directly overland across the island taking full advantage of a strong northwesterly wind. On this route they discovered many large pieces of uncoalified wood and even logs with bark in what would later prove to be strata of Pliocene age. The party reached the head of Walker Inlet on May 31st and then proceeded to chart this entire area. Caribou hunting was successful on June 1st and, on the 3rd, the party was also able to fully restock their sledge with provisions previously cached at Cape Cam. On the following days Mecham surveyed Carter Bay and crossed the mouth of Mould Bay to Manson Point before carrying on into Intrepid Inlet. On June 6th, he was dismayed to discover the cairn and messages left by M'Clintock at Disappointment Point. Mecham's work was over. He now set off for home base by way of the east coast of Eglinton Island. His party reached Dealey Island on July 6th after a remarkable sledging journey of more than 1000 km.

After June 6th, M'Clintock's party continued the exploration and coastal charting of northeastern Prince Patrick Island. He rounded and named the Polynia Islands on June 13th. He then proceeded on a southwesterly course, and finished the crossing of Satellite Bay on the 16th. The sledging party reached Point M'Clintock on the following day. Thwarted from onward progress by high winds and driving snow, the party, now only 50 km short of Mecham's limit of exploration on this coast (at Point Discovery) were now compelled to make for home. Returning by way of Emerald Isle and Hecla and Griper Bay, M'Clintock's party left a record and map of the new discoveries in the cairn at Nias Point (on northern Melville Island, see front cover illustration). The party reached Dealey Island on July 18th, bringing to an end an equally remarkable sledge journey of nearly 1100 km.

The documents left by M'Clintock in the Nias Point cairn were recovered by Dr. Ray Thorsteinsson while undertaking survey work for the Geological Survey of Canada in 1958. Included in these documents was the chart of the new discoveries (Tozer and Thorsteinsson, 1964). This small map, drafted in ink and water colours by G.F. M'Dougall, Master of the *Resolute*, illustrates the shorelines of the central Arctic Islands as charted by Franklin, Austin, James Ross, M'Clure, Kellett, and others down to 1853. M'Clintock himself has produced our earliest known illustration of Eglinton and Prince Patrick islands by sketching in his discoveries and adding the following additional comments in front of his signature: "8th July 1853 - *Assistance* wintered 120 miles above Beechey Island in Wellington Channel. The Coasts I have discovered and explored are traced in pencil. F.L M'Clintock".

Vilhjalmur Stefansson

The completion of the charting of the unvisited 50 km stretch of northwestern Prince Patrick Island was left to Vilhjalmur Stefansson, who passed this way by dog sled in June 1915 (Stefansson, 1944). Stefansson and his party were at Sachs Harbour near the south end of Banks Island during the fall and winter of 1914–1915. During this period he received news that his expedition vessel, the *Karluk*, had been wrecked in the polar pack ice near Wrangel Island (in the Russian far east). Since departing the *Karluk* and members of his party in September, 1913, Stefansson had travelled east for over a year and was now intent on new discoveries in the Canadian Arctic. He left Sachs Harbour in April, 1915 (Fig. 1, inset) and from there traversed north along the west coast of Banks Island. After a lengthy excursion out onto the drifting pack ice west of M'Clure Strait, his party reached Prince Patrick Island near Land's End in early June. Stefansson completed the uncharted stretch of coast by the middle of June. From here he went on to discover Brock and Mackenzie King islands before returning home via Eight Bears Island, Kellett Strait, Mercy Bay, and central Banks Island.

Hubert Wilkins

A travelling companion of Stefansson during some of his excursions in the Canadian Arctic was Sir Hubert Wilkins, who was later to make many early aircraft flights in the region, including those of the search effort to discover the fate of Levanskiy's trans-polar expedition of August 1937 (Stefansson, 1944; Wilkins, 1938). The feasibility of long distance trans-ocean passenger flight was of great interest to many governments in the 1930s. Pursuant to establishing a route from Russia to North America over the pole, the Soviet government dispatched Sigismund Levanskiy and his crew to fly a wheeled, four-engine passenger aircraft from Moscow to Fairbanks, Alaska. The plane developed engine difficulties near the pole and went down in this area, never to be heard from or seen again. Having had previous Arctic flying experience, Wilkins was chosen to lead the rescue missions from the American side. Starting from a base at Coppermine, three of his many search missions to the North pole region were over the southeastern part of Prince Patrick Island. Outward bound on the second flight (on August 23rd, 1937), Wilkins landed his Canso flying boat for refueling in open water near Cape Russell off the southwest corner of Melville Island. On the return journey, poor weather in Coppermine necessitated a landing and a day's wait at anchor in Walker Inlet. Wilkins went ashore briefly but found only lemmings and the tracks of larger animals.

Aerial photography

Precise knowledge of the geography of the report area became known only with the availability of suitable air photographs. The first aerial reconnaissance missions over Prince Patrick and Eglinton islands were carried out using U.S. Air Force aircraft and the coordination of U.S. and Canadian personnel and equipment (Greenaway and Colthorpe, 1948). These long-range flights were organized from bases at Edmonton and Fairbanks and included reconnaissance missions to all parts of the Canadian Arctic. The flights over Prince Patrick and Eglinton islands in August and October, 1946 and April, 1947 were hampered by low-lying cloud and extensive snow cover. No improvements to the maps of Mecham and M'Clintock were possible at this time. Systematic aerial photography by the Canada Surveys and Mapping agency has since then been completed and includes Trimetrogon coverage obtained from 1950 to 1952 (Dunbar and Greeaway, 1956) and vertical stereoimage air photographs acquired from 1960 to 1962.

Mould Bay Weather Station

Apart from the aerial photographic surveys of 1946 and 1947, Hubert Wilkins' visit to Prince Patrick Island in 1937 was the last until the establishment of the weather station at Mould Bay by a joint U.S. and Canadian task force. Background concerning these events is provided by Johnson (1990) and unpublished reports of the Joint Canadian-United States Weather Station Programme (United States Weather Bureau, 1948; Meteorological Division, 1953). The program of weather station construction was initiated in order to provide improved weather reports and forecasting in support of increased international air transportation. Construction of the Eureka and Resolute bases was begun in early April and late August, 1947, respectively. Part of the supplies, destined for the planned Prince Patrick station, were brought to Resolute by ship in the fall of 1947. An additional 21 tons of spare parts and equipment, originating from Westover Air Force base in Massachusetts (United States Weather Bureau, 1948), were airlifted from the United States and offloaded at Resolute during the winter of early 1948.

The plan for a station on Prince Patrick Island called for a site to be located in the vicinity of Walker Inlet, or failing that, a southern coastal location between Cape Manning and Cape Cam (United States Weather Bureau, 1948). Three separate reconnaissance flights to Prince Patrick Island between March 28th and April 5th, 1948 included site selection surveys along all the coasts between Intrepid Inlet and Dyer Bay. The present site was chosen at this time. Airlift of supplies, supported by nine separate ski-equipped aircraft, was carried out from April 12th to 25th. The operation required 32 supply flights from Resolute, and involved the transport of 170 tons of supplies, 100 military and 25 civilian personnel. Seven permanent staff were eventually stationed at Mould Bay, including both Canadian and U.S. personnel. Although the weather station was situated on the sea coast, there has been no recorded attempt to reach this location by ship.

Maritime transits of M'Clure Strait

The last significant event in the geographic exploration of this region was the completion of a successful maritime transit of M'Clure Strait (Manning, 1953, 1956). This was accomplished in two seasons by motorized canoe under the command of Thomas H. Manning with assistants Andrew Macpherson (in 1952) and Capt. I.H. Sparrow (in 1953). The expedition was supported by the Defence Research Board, with the objective being to chart the coastlines and safe harbours of Banks Island. The party mobilized by RCAF Dakota aircraft from Edmonton and were set out at de Salis Bay on the southeast coast of Banks Island on May 10th, 1952. Details of the expedition rightfully belong within the history of geographic exploration of Banks Island. Suffice it to say that the voyage was accomplished by travelling clockwise around the island by following the shore-edge lead of open water. The party entered the western entrance to M'Clure Strait on August 11. Onward

progress was greatly hindered by pack ice that had drifted onshore and necessitated detours out into the main channel of up to 3 miles (5 km). On August 12th, the party climbed the height of land at Cape M'Clure and from this point were able to identify the coastline of southern Prince Patrick and Melville islands. Open water was encountered to the southeast in M'Clure Strait, resulting in better travelling. However, ice was again heavy on August 13th and progress had to be aborted for five days. On August 19, the party entered Castel Bay, where they were again left stranded by heavy ice. Caching the canoe and some supplies in this area, the party constructed an improvised sled and, on September 2nd, proceeded to walk overland more than 330 km back to Sachs Harbour near the south end of the island, which they reached on September 21st. Back in Ottawa that winter, Manning was encouraged by the Defence Research Board to complete the expedition and so, with a new assistant, he made the return trek from Sachs Harbour to northern Banks Island in the Spring of 1953, reaching the canoe and cache on July 15th. Travelling conditions for the remaining voyage through M'Clure Strait included nearshore open water in coastal inlets and bays but heavy ice around points of land, which were passable only at high tide. Problems with ice persisted within and beyond Mercy Bay and throughout August. However, the transit was accomplished on or about the 30th of that month and that same evening, Manning and Sparrow were entertained aboard the U.S. icebreaker *Burton Island*, which was surveying in Prince of Wales Strait at this time. The party safely completed their expedition at Holman Island on September 11th.

Proof of the feasibilty of navigation of M'Clure Strait by deep-draft vessels was left to the Joint Canadian-United States Beaufort Sea Expedition of 1954, as reported in press releases of the U.S. Navy and U.S. Coast Guard (respectively dated September 28th and 29th of that year) and in a newspaper report of September 4th (Navy Times, 1954). These early transits of the strait were made by the U.S. Navy icebreaker *Barter Island* commanded by Edward A. Trickey and the U.S. coast guard icebreaker *Northwind* under Capt. William L. Mahoney. The vessels departed San Diego in July, sailing to southern Banks Island via the north coast of Alaska. The *Barter Island* then proceeded through Prince of Wales Strait and arrived at the east end of M'Clure Strait in mid-August. Helicopter reconnaissance showed better than normal ice conditions to the west. This advance information then permitted the ship to pass through the middle of the strait beginning on August 11th, returning prior to August 16th by way of the northern edge of the passage where ice was found to be 8 to 10 feet (2.6–3 m) thick. The *Northwind* also used the report of favourable conditions from the *Barter Island* helicopter to effect the most difficult part of an eventual clockwise circuit of Banks Island by way of the west coast of this island and the southern edge of M'Clure Strait, where ice between August 13th and 23th was found to be 4 to 6 feet (1.3–2 m) thick. Both ships, linking up with HMCS *Labrador* on August 26th, completed the intended joint expedition work before returning to the Pacific and the home port of Seattle on September 29th. The *Labrador*, which had sailed to the north by way of eastern Canada and Baffin Bay, went on to complete another history-making event – the first circumnavigation of the North American continent in a single voyage (Pullen and Swithinbank, 1991).

Today, the largest icebreakers can probably make transits through M'Clure Strait whenever the need or desire arises. In practice, the pack ice is normally very heavy in this area and traditional maritime routes through the Northwest Passage lie either through Prince of Wales Strait east of Banks Island or through Dolphin and Union Strait between Victoria Island and the mainland (Fig. 1) (MacPhee and O'Shea, 1986).

History of geological investigations

The drawing of earliest significant conclusions concerning the geological structure of the Canadian Arctic Islands was precipitated by the availability of aerial photographs (Greenaway and Colthorpe, 1948; Dunbar and Greenaway, 1956) and direct ground observations collected by Geological Survey of Canada staff beginning in 1950 (Fortier and Thorsteinsson, 1953; Fortier et al., 1954). As part of their general survey of the geology of the Arctic Islands, Mesozoic and Cenozoic strata were found to be continuous throughout Axel Heiberg Island, the Sverdrup Islands and Prince Patrick Island. To the south, a Paleozoic folded belt was identified on Bathurst and Melville islands, which was called the “Parry Islands folded belt” (subsequently shortened to Parry Islands Fold Belt). A contact was drawn across central Melville Island and Eglinton Island between Paleozoic folded strata and flat-lying rocks of the same age located farther to the west. Concerning the western limit of the folded belt, Fortier and Thorsteinsson (1953) pointed out that: “Folded rocks occur on Prince Patrick Island, as observed by the writers both from aircraft and air photographs. However, the areas of distinctly folded rocks are restricted in extent, and there are large tracts of horizontally lying beds that, as on Melville, may represent an unconformable cover of younger strata. The trend of the folded rocks appears to be southerly, suggesting further arching of the folded belt, as on Melville Island”.

The first systematic fieldwork and geological mapping was carried out by E.T. Tozer of the Geological Survey of Canada between late April and the end of July, 1954 (Tozer, 1956). Fieldwork was facilitated by sledge and dog team traverses over the sea ice. This permitted observations on all the shorelines and peninsulas between Walker and Intrepid

inlets on Prince Patrick Island, the northwest coast of Eglinton Island between Callaghan and Gardiner points, and selected locations on western Melville Island. (Geographic place names are found on the geology map of the report area, 2026A, CD-ROM.) Numerous important structural observations were made during this time, including the documentation of two important unconformities. East and west of Mould Bay, Jurassic and Cretaceous outliers, some bound by north-striking faults, were found to unconformably overlie more than 2100 m (7300 ft.) of folded Devonian clastic rocks. The Devonian strata were found to be only modestly inclined, up to 10° with respect to the cover. Nevertheless, the concept of orogenic deformation affecting these older rocks (as on Melville Island) was not discounted. More extensive Mesozoic strata, in excess of 300 m (1030 ft.) thick, were found east of Intrepid Inlet and on Eglinton Island. A second unconformity was observed beneath an undeformed blanket of Cenozoic sand and gravel (Beaufort Formation), widespread on Prince Patrick Island.

A larger field program in the western Arctic Islands was executed by the Geological Survey of Canada in 1958. The project was supported by single-engine Piper Super-Cub aircraft equipped with large under-inflated tires that permitted numerous unscheduled landings in many remote areas of the islands. Results of the expedition were incorporated into a preliminary geological report (Thorsteinsson and Tozer, 1959) and a summary article on the structural geology of the entire archipelago (Thorsteinsson and Tozer, 1960). The final result was the first and only comprehensive geological report on the western Queen Elizabeth Islands, complete with a supporting colour geological map (Tozer and Thorsteinsson, 1964; GSC Map 1142A, now out of print). In these papers, the undeformed Mesozoic strata northeast of Green Bay (now known to include Upper Triassic limestone) were included in the Sverdrup Basin. The term Eglinton Graben was applied to the Jurassic and Cretaceous strata of Eglinton Island, and the Devonian rocks, with faulted younger outliers on southern Prince Patrick Island, were included in a new structural province called the Prince Patrick Uplift. The eastern limit of the Beaufort Formation on the Arctic coastal plain was delineated in a continuous belt extending from Cape Krabbé in the northeast to Dyer Bay in the southwest. In the last of these publications (Tozer and Thorsteinsson, 1964), the authors also chose to terminate the Parry Islands Fold Belt along the west coast of Melville Island. Concerning the folds previously described in the Devonian rocks of Prince Patrick Island, the authors were now inclined to avoid a compressive origin, preferring instead to account for the tilting by one or more phases of subsequent faulting. In a later review (Thorsteinsson and Tozer, 1970), the authors suggested that the fold belt must be offset to the north by dextral slip on one or more faults lying between Prince Patrick and Melville islands.

Important information on gross crustal structure of the western Queen Elizabeth Islands was also provided during this period by seismic refraction surveys carried out between 1959 and 1965 (Hobson, 1962, Hobson and Overton, 1967; Overton, 1970). Initial results showed 1) that the Mesozoic of the Sverdrup Basin was at least 9 to 12 km thick but thinnest beneath the Beaufort Formation on the continental margin; 2) that the Paleozoic carbonate succession of eastern Prince Patrick Island (with a velocity of about 5.6–6.2 km/s) extends from 3 km to a depth of 15 km; and 3) that the base of the crust lies variably between 30 and 40 km.

These early geological and geophysical reports inspired both Canadian and international interest in oil and gas exploration in the Arctic Islands. Stratigraphic studies and seismic reflection surveys were instigated by industrial interests on all the islands and inter-island channels of the Arctic continental margin. Exploration on Eglinton and Prince Patrick islands, including eight exploratory drill holes, was carried out between 1965 and 1976 by Elf Oil Exploration (later to become Elf-Acquitaine). Somewhat smaller exploration projects were undertaken by GSI, Panarctic Oils Limited, Triad Oil, and Gulf Canada Limited. Journal articles summarizing these efforts have been published by Bernard Plauchut and his colleagues with Elf (Plauchut, 1971, 1973; Jutard and Plauchut, 1973; Plauchut and Jutard, 1976). A related contribution was a synthesis article on the northwest margin of the Arctic Islands by Panarctic staff (Meneley et al., 1975). Seismic and drill-hole data provided these researchers with new insights into the age, depositional facies, and extent of Cretaceous and older strata beneath the Beaufort Formation and in the subsurface. An important observation was the recognition of a basin marginal uplift, and the inclination and erosional truncation of strata of the Sverdrup Basin beneath unconformable strata of the continental margin. The shelf-parallel uplift, which came to be known as the Sverdrup Rim, was found to extend from Banks Island to northern Ellesmere Island and to involve subcropping upper Paleozoic, Triassic, and younger strata.

The structural links across M'Clure Strait from Banks Island to Prince Patrick and Eglinton islands were also clarified by new stratigraphic studies and geological mapping by A.D. Miall for the Geological Survey of Canada on Banks Island in 1973 and 1974 (Miall, 1976, 1979). Miall used surface measured sections, well information, and regional gravity data to show that Eglinton Graben is continuous with the coeval Banks Basin on central Banks Island and that this shelf-parallel depocentre existed from the Middle Jurassic to the Eocene. He also showed that the west side of Banks Basin was an intermittently exposed uplift (Storkerson Uplift) and sediment source area in the Mesozoic, and postulated that this uplift may have been continuous with a similar high

located beneath the Beaufort Formation north of Dyer Bay on southwestern Prince Patrick Island. Bounding faults were placed on both the east and west sides of Banks Basin and were also interpreted to exist on either side of Eglinton Graben in Crozier Channel and Kellett Strait.

Different conclusions concerning the offshore geology south of Prince Patrick Island were provided by staff of Norlands Petroleums Limited, who synthesized reflection seismic data from M'Clure Strait, Viscount Melville Sound, and other portions of the Northwest Passage (Daae and Rutgers, 1975). Evidence was provided to indicate that upwards of 5000 m (15 000 ft.) of Mesozoic and Cenozoic sediment are present in the mouth of Lancaster Sound and that a down-to-south graben boundary fault must exist parallel and close to coastal southern Devon Island in the offshore. The similar coastal geomorphology of the islands bordering M'Clure Strait led these authors to assume that a similar graben must exist in this area. One bounding normal fault was indicated running in a west-northwesterly direction from coastal southwestern Melville Island to Cape Manning on the southernmost point of Prince Patrick Island. A second fault was indicated running along the south shore of M'Clure Strait against coastal northern Banks Island. The mouth of M'Clure Strait, (like the mouth of Lancaster Sound) was labelled an “area of foundering” and shown to transect the pre-existing northerly trend of Banks Basin-Eglinton Graben and the related peripheral uplifts.

The recognition of a graben in Lancaster Sound was later expanded by Kerr (1980, 1981) into a more speculative concept of extensional segmentation of the Arctic Islands in early Miocene or later time, following normal faults assumed to exist within the major inter-island channels. The most significant of these proposed structures, a continuous rift system running the length of the Northwest Passage from Lancaster Sound to M'Clure Strait, was paired with a similar rift in Nares Strait. Actual data in support of these extensive rift systems was not presented. A competing earlier hypothesis, (first proposed by Fortier and Morley (1956) and later expanded on by Pelletier (1966), who examined bathymetric data from the inter-island channels), attributed the channels to dissection by an antecedent drainage system of Cenozoic age, subsequently deepened and widened by Pleistocene ice streams and then flooded during the post-glacial sea-level rise. In this model the bedrock beneath the channels need not differ in any significant respect from that of the adjacent shelf areas and islands.

Additional insight into the structural geology of Eglinton and Prince Patrick islands was provided through regional-scale mapping by the Geological Survey of Canada on Melville Island between 1984 and 1987. This work also involved the re-evaluation of available reflection seismic and potential field data available up to that time (Harrison, 1991, 1995). It was shown that the bulk of the Parry Islands Fold Belt is detached above an Ordovician evaporite. Folds to the west of this evaporite were shown to be detached at a fundamentally deeper structural level, and interference patterns exist where the two fold sets intersect on central Melville Island. The term "Canrobert Hills Fold Belt" was coined to distinguish the western belt of folds from those of the salt-based Parry Islands Fold Belt. Fold axes of the Canrobert Hills Fold Belt were also shown to continue without tectonic offset from western Canrobert Hills to subsurface Eglinton Island and northeastern Prince Patrick Island beneath younger cover of Eglinton Graben and Sverdrup Basin. The fold train of the Canrobert Hills Fold Belt was shown to possess an arcuate geometry in plan view, with a convex, southwesterly facing direction. Thus, folds in the Canrobert Hills, trending westerly on northwestern Melville island and in the subsurface of Eglinton Island, were found to trend progressively more northwesterly beneath Prince Patrick Island. Mapping on western Melville Island also delineated faults potentially associated with the development of Eglinton Graben. Notable amongst these was the Comfort Cove Fault, striking parallel and close to the west coast of the island, featuring 500+ m of down-to-the-west extensional slip and up to 270 m of downthrown block-rotated Volgian graben-fill.

Interest in the structure of the islands lying on the shelf margin of the Arctic Islands has also been focussed by geophysical surveys such as those carried out in conjunction with research from the Hobson's Choice Ice Island, which was occupied by government and university research personnel during its traverse of the Canadian polar margin from northern Ellesmere Island to Prince Gustaf Adolf Sea between Ellef Ringnes and Borden islands (1984–1989). Although the results of this research are beyond the scope of this summary, important synthesis studies were carried out that summarize, for example, the nature and significance of the potential field data, heat flow and seismicity of the entire Canadian Polar margin (Forsyth et al., 1990; Sobzcak and Halpenny, 1990). Observations relevent to the present review include: 1) short, linear, high-frequency residual aeromagnetic anomalies in the mouth of M'Clure Strait that parallel both north-striking normal faults of southern Prince Patrick Island and a probable Cretaceous dyke swarm of the central Sverdrup Basin; 2) a broad, linear, residual aeromagnetic low near the transition from attenuated continental crust to oceanic crust and following the 1600 m isobath at a variable distance of 110 to 180 km west of Prince Patrick Island; and 3) a series of free-air gravity anomalies, marking the modern continental shelf edge and 500 m isobath located 80 to 110 km west of Prince Patrick Island.

Another important result arising from interest in the Canadian polar margin has been renewed attempts to

understand the fate of the Sverdrup Basin and Franklinian Mobile Belt beyond Prince Patrick Island. One theory, first suggested by Bally (in discussion with Kerr, 1982), provided for a 1000 km sinistral offset on a hypothetical strike-slip fault lying near the continent-ocean transition northwest of the Arctic Islands. It was suggested that this fault, assumed to continue south through the Richardson Mountains of northern Yukon, may have carried the continuation of the Paleozoic fold belt to the Mackenzie Delta area during southerly plate transport of northern Alaska and the formation of oceanic crust in Canada Basin. A competing theory has arisen from the oroclinal model of Carey (1957) in which northern Alaska is assumed to have rotated counterclockwise away from the Arctic Islands, implying the development of shelf-parallel extensional structures on the two conjugate trailing margins. Particularly valuable has been the attempted restoration of potentially common geological features between Prince Patrick Island and the theorized matching terrains of Point Barrow, Alaska, and the North Chukchi Basin area on the continental shelf north of Alaska (Embry, 1990; Embry and Dixon, 1994; Sherwood, 1994; Grantz et al., 1998).

Some of the key data utilized to constrain the aforementioned plate models for Canada Basin evolution were assembled in part during Geological Survey of Canada field activities on Prince Patrick and Eglinton islands from 1987 to 1992 (Harrison et al., 1988; Harrison and Brent, 1991). The nature and results of this work are described at length in the remainder of this report.

Scope of present study and acknowledgments

This report synthesizes observations obtained from air photographs, ground traverses and measured sections, exploratory well logs and cuttings, fossil collections (notably Mesozoic microfauna, microflora and Jurassic ammonites), and geophysical data, especially reflection seismic profiles. These data provide new information about the top 15 km of shallow- and mid-crustal strata representing more than 500 million years of Phanerozoic earth history.

The first fieldwork was conducted during a period of remarkably fine weather from June 28th to July 26th, 1987. This involved helicopter-supported bedrock geological mapping, foot traverses, measurement of selected stratigraphic sections and the description of numerous important but isolated outcrops. Many areas were visited, including most of the key bedrock exposures on Eglinton Island, and all of eastern Prince Patrick Island between Cape Krabbé in the north and Dyer Bay in the south. Bedrock exposures were documented for the first time in Satellite Bay and much progress was made, for example, in delineating the extent of Triassic and Early Jurassic strata around Intrepid Inlet and in subdividing and mapping the Jurassic Wilkie Point Group in all areas. This was a team effort involving the simultaneous detailed study of the Neogene continental terrace wedge sediments (J. Fyles), Quaternary geology (D. Hodgson), bedrock stratigraphy and biostratigraphy (A.F. Embry, Q. Goodbody, T.P. Poulton, J.H. Wall), and preparation of bedrock geology maps and the analysis of structure (J.C. Harrison). Capable assistance was provided by J. Timmerman and J. Devaney. Support personnel included air crew of Canadian Helicopters Limited and the cook and staff at the Mould Bay weather station.

Additional fieldwork was performed from July 4th to July 25th, 1991 by Harrison, with the assistance of R. Brady, using two Honda all terrain vehicles. As a result of extremely late snow melt, low summer temperatures, and wet ground conditions, most objectives were not fulfilled. Nevertheless, much useful detailed mapping was conducted east of the Mould Bay weather station and also to the north around the head of Mould Bay and Landing Lake.

One final week of helicopter-supported mapping and ground traversing was conducted in the area during August, 1992. This primarily involved clarification of the distribution of the upper Albian Hassel Formation on Eglinton Island and its depositional relationship to bounding shale formations.

The use of the surveyor's pocket transit (i.e., Brunton, Freiberger) or magnetic compass is a critical tool for geological and structural data gathering. However, variations in magnetic declination make such measurements prone to error and fluctuation. For this reason a paper by L.W. Newitt of the Geomagnetic Laboratory, Ottawa, is presented in Appendix B on magnetic compass operation and reliability at high latitude.

Full documentation of the stratigraphic record is beyond the scope of the present publication. In its place we provide a summary overview of mapped stratigraphic units. The depositional history is understood from detailed studies by the contributing authors including, T. de Freitas (Lower Devonian and older strata and seismic units), Q. Goodbody (measured and drilled sections of the Middle and Upper Devonian clastic wedge), B. Beauchamp (subsurface upper Paleozoic sequences), A.F. Embry (Mesozoic strata), and T.A. Brent (seismic stratigraphy). The senior author wrote the manuscript and provided supporting content from fieldwork and the interpretation of seismic profiles.

Five of the remaining sections deal with different aspects of the structural geology and tectonic history of the region. This was a co-operative effort by T.A. Brent and J.C. Harrison, with welcome contributions by B. Beauchamp on the interpretation and subsurface

correlation of the upper Paleozoic succession. Significant components of this work included reprocessing of selected industry seismic profiles (Brent), preparation of shot point maps (Brent), correlation of seismic picks with formation tops in exploratory wells (Brent) and with surface geology (Harrison), interpretation of through-going primary reflectors on all available profiles (Brent and Harrison), optimization of display parameters on all geophysical illustrations (Brent), subsurface and seafloor mapping and contouring (Brent and Harrison), drafting of illustrations (Brent and Harrison), and synthesis and write up (Harrison).

A final section on the mineral and energy resources of the report area has been developed from Rock-Eval analyses as provided by R. Stewart, and thermal maturation and related petrographic study of coal and dispersed organic matter (Goodarzi and Gentzis). These data, together with field observations and information provided by industry assessment reports, have been synthesized by the first author (Harrison).

The conclusions reached in this volume are built on a foundation of reliable biostratigraphic information. Noteworthy here are the reports, presented in Appendix 1, of T.P. Poulton (Jurassic–Cretaceous ammonites and shelly macrofauna), J.H. Wall (Jurassic–Cretaceous foraminifera from surface samples and well cuttings), E.H. Davies (Jurassic–Cretaceous dinoflagellates, spores and pollen), B.S. Norford and A.E.H. Pedder (Ordovician shelly macrofauna and Siluro–Devonian corals from the Wilkie Point J-51 well) and J.A. Jeletzky (deceased) who reported on shelly macrofauna collected from an unusual boreal limestone occurrence of Early Cretaceous age exposed west of Mould Bay.

SUMMARY DESCRIPTION OF STRATIGRAPHIC UNITS

Stratigraphic successions

Strata of the Prince Patrick and Eglinton Island area are divisible into four major successions (Fig. 2, 3). These are:

Succession 1: Approximately 14 to 18 km of undivided Proterozoic(?) and/or older bedrock (v = 5.72 km s^{-1}) above the Mohorovičić Discontinuity (v = 8.05–8.18 km s^{-1}) as constrained by refraction and reflection data acquired over southwestern Prince Patrick Island and the adjacent offshore and continental shelf (Fig. 2; Overton, 1970; Berry and Barr, 1971). Succession 1 is separated from overlying strata of Succession 2 by a seismically defined angular unconformity situated either beneath the Lower Cambrian or, more likely, in the Vendian part of the Neoproterozoic.

Succession 2: 10 to 14 km of thermally overmature but variably tectonized ("Franklinian") strata that range from Neoproterozoic(?) at the base through Upper Devonian at the top. The base is defined by a probable angular unconformity imaged on seismic profiles (below unit ps1 on Fig. 4) of southwestern Prince Patrick Island. The sub-Devonian part of this succession, known almost exclusively from seismic records, includes two distinct facies belts: an offshore platform imaged on Prince Patrick Island and a basinal belt imaged on Eglinton Island. Contrasting lower Paleozoic facies are blanketed by a common Middle and Upper Devonian foreland clastic wedge that is understood from exploratory drilling and seismic records but which also extends to surface on southeastern Prince Patrick Island (Fig. 2, 3).

Succession 3: Less than 1 km grading to more than 7 km of thermally mature and immature, relatively undeformed Carboniferous through Eocene strata of the Sverdrup Basin that extends throughout the northeastern half of Prince Patrick Island and the offshore beyond Green Bay (Fig. 2, 3). This succession also includes up to 2 km of Middle Jurassic through Upper Cretaceous strata preserved in four peripheral basins and numerous small grabens of Eglinton Island, surface and subsurface central Prince Patrick Island, and the inter-island channels including M'Clure Strait (Fig. 2, 3). The base of this succession is everywhere defined by a profound regional angular unconformity. While the youngest strata of Succession 3 are Upper Cretaceous (Campanian) in age within the report area, strata as high as the Eocene occur on Banks Island and in the eastern Arctic islands.

Succession 4: Up to 70 m of unconsolidated Pliocene sand, gravel and peat of the Beaufort Formation and related seismically defined Neogene strata (to more than 600 m; Fyles, 1990) of the Arctic Continental Terrace Wedge that extends throughout the northwestern half of Prince Patrick Island and is also exposed in outliers to the southeast (Fig. 2, 3). The base of this succession is everywhere marked by a regional angular unconformity and is also unconformably overlain by a discontinuous veneer of various Quaternary deposits.

Summary description of map units

Seismic expression of Succession 1

All map units of presumed Vendian through Lower Devonian age lie entirely in the subsurface. Several units have been penetrated by exploratory drillholes. However, those situated below the Silurian are identified and mapped on seismic profiles only. Stratigraphic features identified on reflection profiles of southwestern Prince Patrick Island include a unit of potential Proterozoic age beneath an imaged angular unconformity at and below 4.2 seconds two-way travel time (Fig. 4). The base of the Proterozoic(?) extends beyond the full length of the recorded profiles

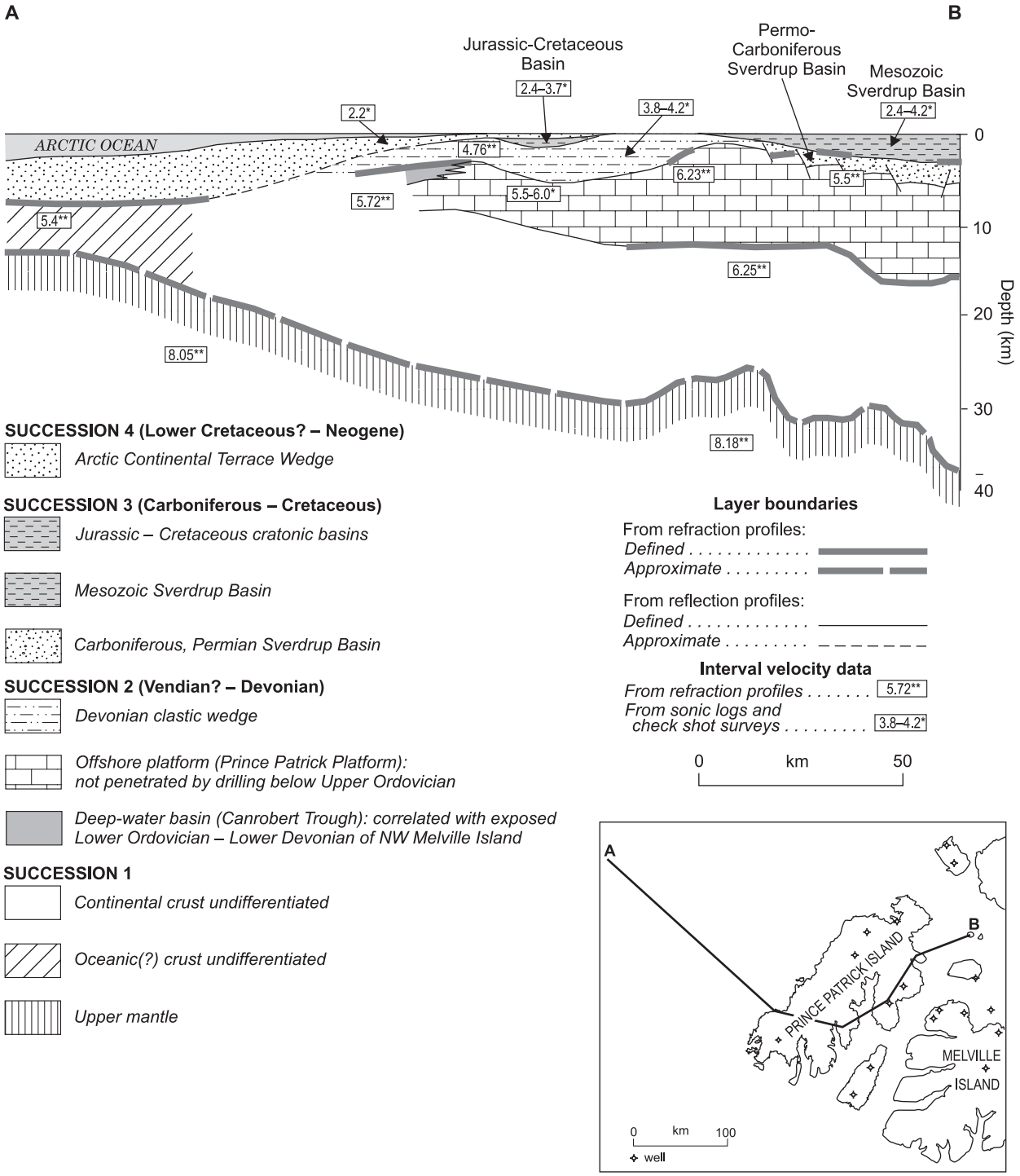

Figure 2. *Generalized crustal-scale cross-section of the Arctic continental margin in the vicinity of Prince Patrick Island, as synthesized from the refraction surveys of Overton (1970) and Berry and Barr (1972), and the interpretation of industry reflection profiles as described and illustrated in this account.*

Figure 3. *Map of exploratory wells, location of text illustrations, and limits of Prince Patrick Platform and Crozier High; inset map illustrates the general geological features of Prince Patrick Island area.*

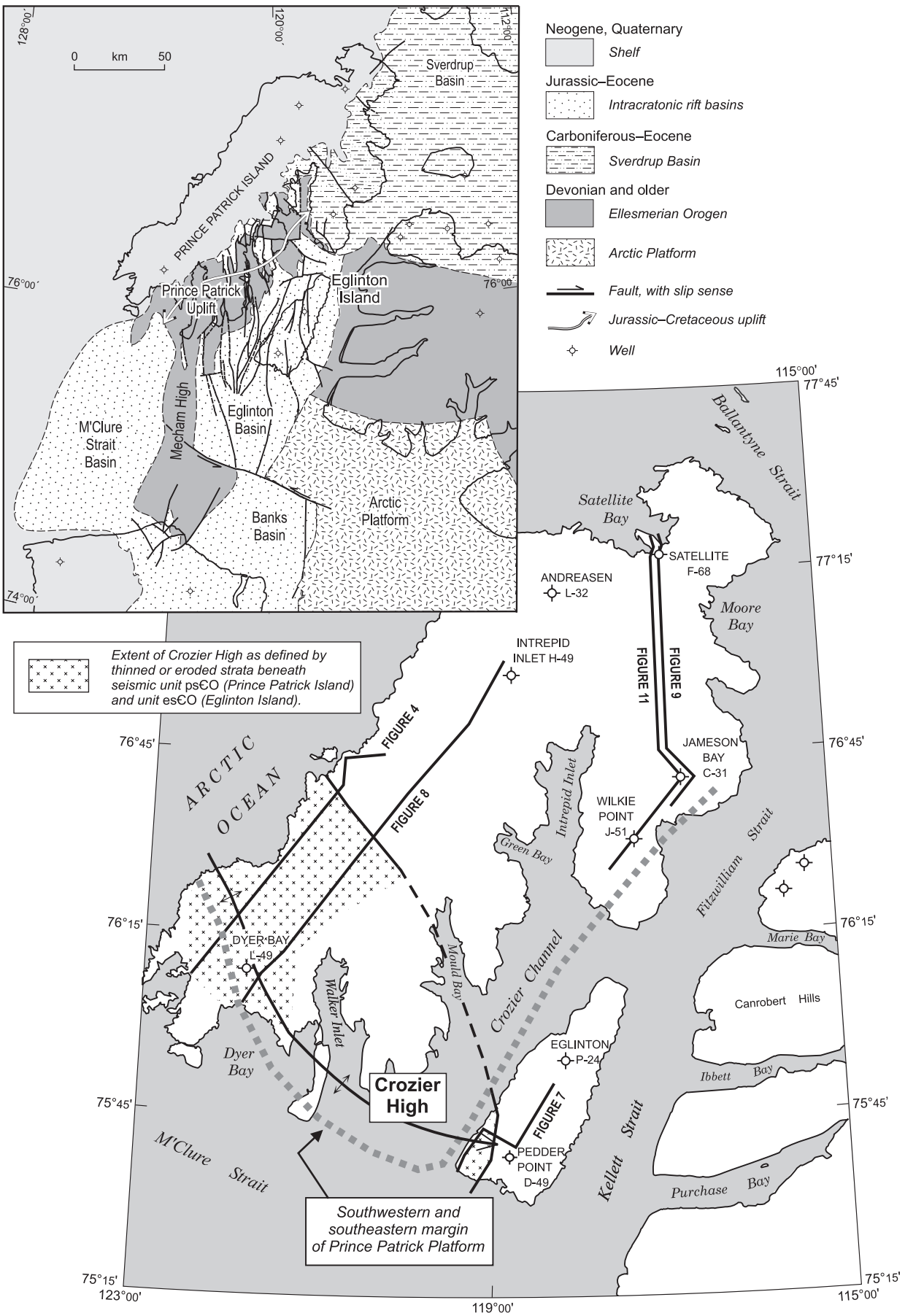
Neogene, Quaternary
Shelf
Jurassic–Eocene
Intracratonic rift basins
Carboniferous–Eocene
Sverdrup Basin
Devonian and older
Ellesmerian Orogen
Arctic Platform
Fault, with slip sense
Jurassic–Cretaceous uplift
Well
0 km 50
128°00'
120°00'
112°00'
76°00'
74°00'
Sverdrup Basin
PRINCE PATRICK ISLAND
Prince Patrick Uplift
Eglinton Island
Mecham High
Eglinton Basin
M'Clure Strait Basin
Banks Basin
Arctic Platform
115°00'
77°45'
77°15'
76°45'
76°15'
75°45'
75°15'
123°00'
119°00'
Ballantyne Strait
Satellite Bay
SATELLITE F-68
ANDREASEN L-32
Moore Bay
INTREPID INLET H-49
FIGURE 4
FIGURE 8
FIGURE 11
FIGURE 9
JAMESON BAY C-31
WILKIE POINT J-51
Intrepid Inlet
Green Bay
Fitzwilliam Strait
Marie Bay
Canrobert Hills
ARCTIC OCEAN
DYER BAY L-49
Walker Inlet
Mould Bay
Crozier Channel
Dyer Bay
Crozier High
EGLINTON P-24
Ibbett Bay
FIGURE 7
PEDDER POINT D-49
Kellett Strait
M'Clure Strait
Purchase Bay
Extent of Crozier High as defined by thinned or eroded strata beneath seismic unit psЄO (Prince Patrick Island) and unit esЄO (Eglinton Island).
Southwestern and southeastern margin of Prince Patrick Platform

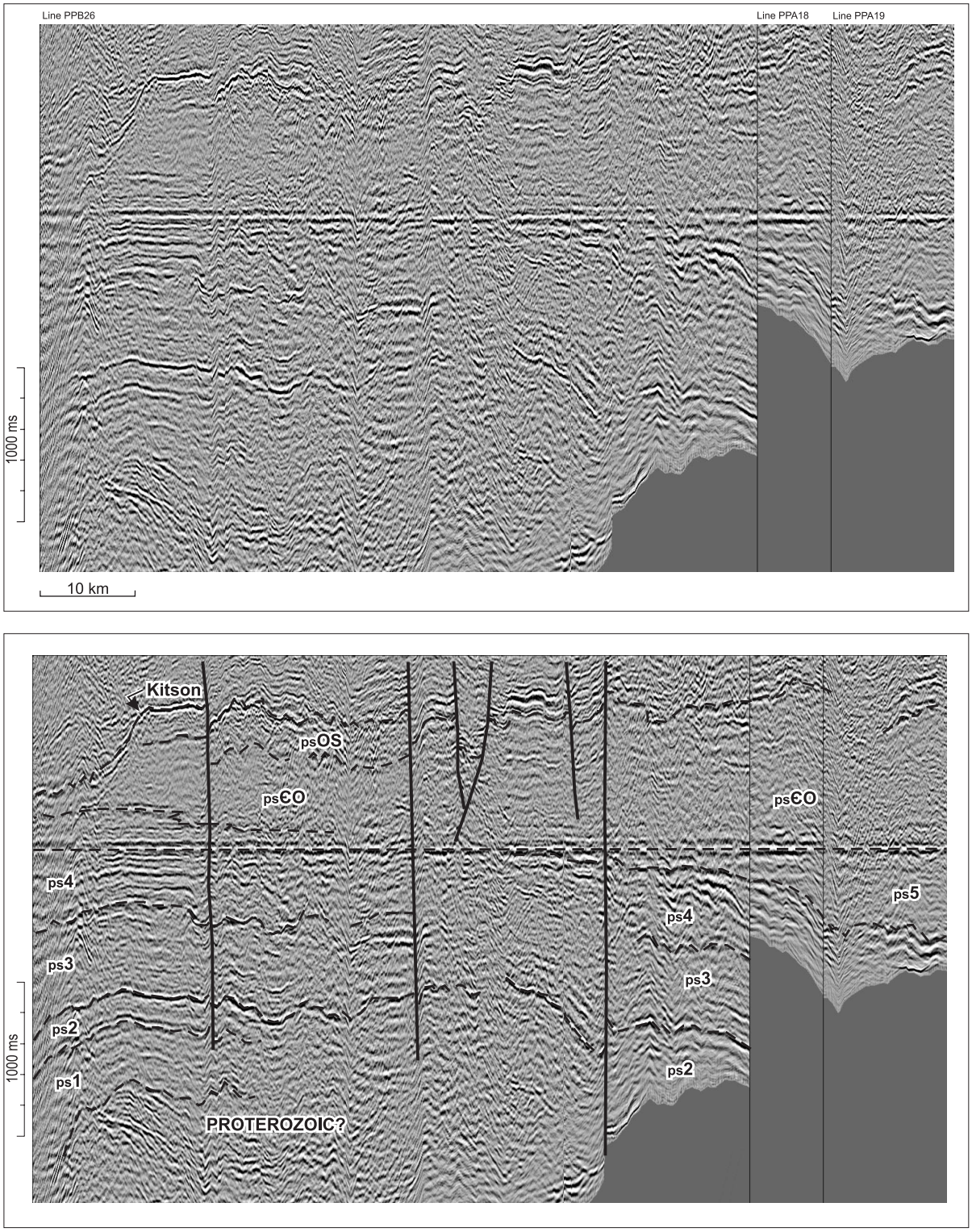

Figure 4. *Seismic expression of Lower Devonian and older strata of southwestern Prince Patrick Island on Elf profiles PPB26, PPA18, and PPA19. Section has been flattened on the base of unit* psЄO *(mid-Cambrian?). The sub-Vendian(?) angular unconformity above older Proterozoic strata lies beneath unit* ps1. *Seismic units* ps1 *and* ps2 *are tentatively correlated with the Kennedy Channel and Ella Bay formations of northeastern Ellesmere Island. Unit* ps3 *is correlated with the Ellesmere Group and the reflection below* ps4 *with the Kane Basin Formation. The unconformity below* psЄO *is equated with the base of the Cass Fjord Formation in the eastern Arctic Islands. An alternative interpretation places the sub-Lower Cambrian unconformity below* psЄO.

(maximum 8 seconds). Indicated thickness above the Mohorovicic Discontinuity is not less than 14 km.

Vendian(?)–Lower Devonian units of Succession 2

The seismic Neoproterozoic (upper Vendian?) through Lower Devonian succession of the report area occupies two contrasting geological provinces (Fig. 5). To the east is a basinal realm that underlies Eglinton Island; the upper part is thought to be continuous with the basin facies successions exposed in the Canrobert Hills region of western Melville Island. To the west, throughout much of the Prince Patrick Island area, is an offshore bank succession with an aggregate thickness of about 12 km.

Offshore platform units

There are eight seismic units on the Prince Patrick Platform (Fig. 4, 5). Each is generally tabular in shape. Individual unit thicknesses range from 200 to 700 ms or about 600 to 2100 m at 6 km/s The mapped units include: five tentatively considered to be Neoproterozoic(?) and Cambrian (ps1-ps5); one that spans the Cambro–Ordovician boundary (psЄO), one a shallow-marine carbonate package known to extend into the Upper Ordovician and Silurian (psOS); and the highest, the Kitson Formation, which in the type area on Melville Island likely spans the entire Lower Devonian and the lower part of the Eifelian in the lower Middle Devonian (Tozer and Thorsteinsson, 1964; Goodbody, 1994). Regionally significant unconformities are identified below 1) seismic unit ps1 above inclined and peneplained Proterozoic of succession 1, and 2) below seismic unit psЄO, which towards the southwest cuts out part of unit ps4 and all of unit ps5.

Although the unconformity below psЄO may coincide with the sub-Lower Cambrian unconformity, the preferred correlation is with a mid-Cambrian erosion surface that is widespread across northern Canada (Fig. 5). It follows from this that units ps1 and ps2 may correlate with seismic unit sЄ1 on Melville Island and with the Kennedy Channel and Ella Bay formations of northeastern Ellesmere Island (Kerr, 1967; Long, 1989a,b; de Freitas et al., 1997). Considered since 1989 to be trilobitic Lower Cambrian strata, new field observations by K. Dewing and others in the type area on northeastern Ellesmere Island indicate that the Kennedy Channel and Ella Bay formations are most likely post-tillite latest Vendian in age and that the base of the Cambrian is to be found in overlying shelf and slope facies siliciclastic deposits and shale of the Ellesmere Group (i.e., in the lower Archer Fiord Formation; K. Dewing, pers. comm., 2002).

On the Prince Patrick Platform, the Ellesmere Group is correlated with seismic unit ps3, and units ps4 and ps5 are equated with various younger Cambrian shelf carbonate formations below the Cass Fjord Formation (Fig. 5). Although lithology is unknown, unit psЄO is tentatively correlated with additional shelf carbonate units of the eastern Arctic Islands that range from the Upper Cambrian Cass Fjord Formation to the Upper Ordovician part of the Cornwallis Group or lower Allen Bay Formation (Trettin, 1991; de Freitas et al., 1997).

Unit psOS has been penetrated in two exploratory wells (Dyer Bay L-49 and Wilkie Point J-51). It is a finely crystalline limestone that is peloidal and variably cherty, fossiliferous and argillaceous. Intervals of calcareous and argillaceous dolostone are locally fossiliferous. Colonial and solitary rugose corals and pentamerid brachiopods collected from two cored intervals provide an Upper Silurian to Lower Devonian (possibly Eifelian) age for the upper part of the unit and an Upper Ordovician age for strata situated at 685 m below the upper contact (A.E.H. Pedder and B.S. Norford, pers. comm., 1998). These strata probably correlate with the Allen Bay Formation, the Cape Storm Formation and with the Read Bay Group of the eastern Arctic Islands. A summary description of these formations and their regional correlation across Arctic Canada and Greenland is provided by Trettin (1991), de Freitas et al. (1997), and the references contained therein.

Shelf carbonate deposits of unit psOS are gradationally overlain by the Kitson Formation (Fig. 4–6), a condensed interval of thermally overmature organic-rich black shale, black chert, and silty, calcareous, and pyritic shale that has been penetrated by two exploratory wells. The Kitson Formation in the type section in western Raglan Range of northern Melville Island contains conodonts ranging from early Lochkovian to Pragian or early Eifelian in age (Goodbody, 1994; T.T. Uyeno, *in* Harrison, 1995).

Units of the basinal realm

A distinctly different set of seismic lower Paleozoic units are encountered on profiles acquired on Eglinton Island. From the base these are labelled es1 through es6, esЄOc, esOSi and esSDi (Fig. 5, 7). The aggregate thickness is roughly 10 km with no obvious base below the lowest unit. Proximity to the basin facies exposures of the Canrobert Hills area, 20 km to the east, continuity of regional-scale structure, and arguments arising from the interpretation of unit thickness and depositional facies are invoked to suggest correlation of units esЄOc, esOSi and esSDi with the slope-facies carbonate deposits of the Early Ordovician (Arenig) Canrobert Formation, and with the graptolitic and basinal shale and deep water carbonate units of the lower and upper parts of the Ibbett Bay Formation (Llanvirn through early Eifelian; Fig. 5). A summary description of these

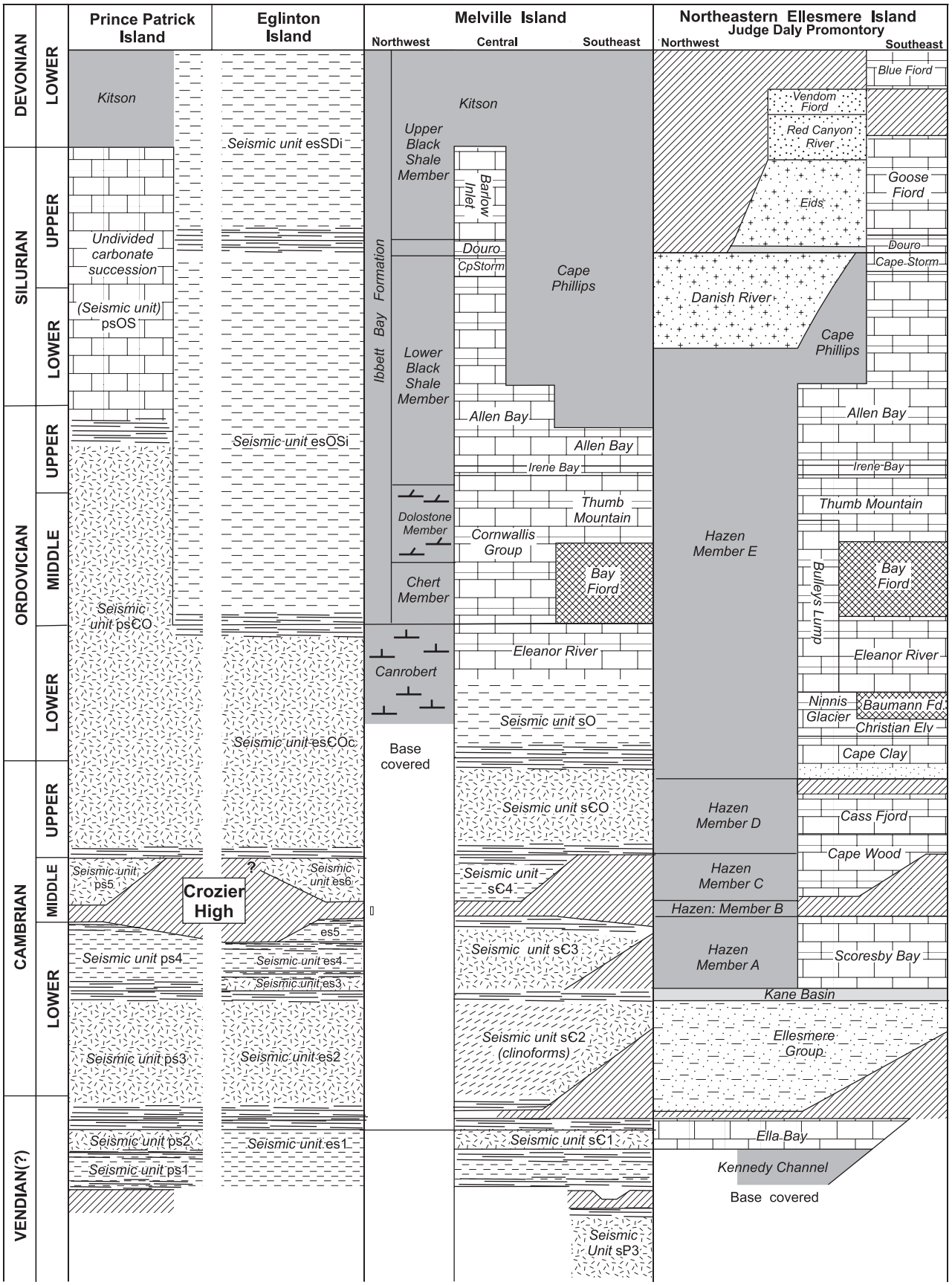

Figure 5. *Generalized correlation chart for Neoproterozoic to Silurian units of Prince Patrick and Eglinton islands, Melville Island (Harrison, 1995) and northeast Ellesmere Island (Keith Dewing, pers. comm., 2002). Explanation of patterns is provided in the legend of Figure 6.*

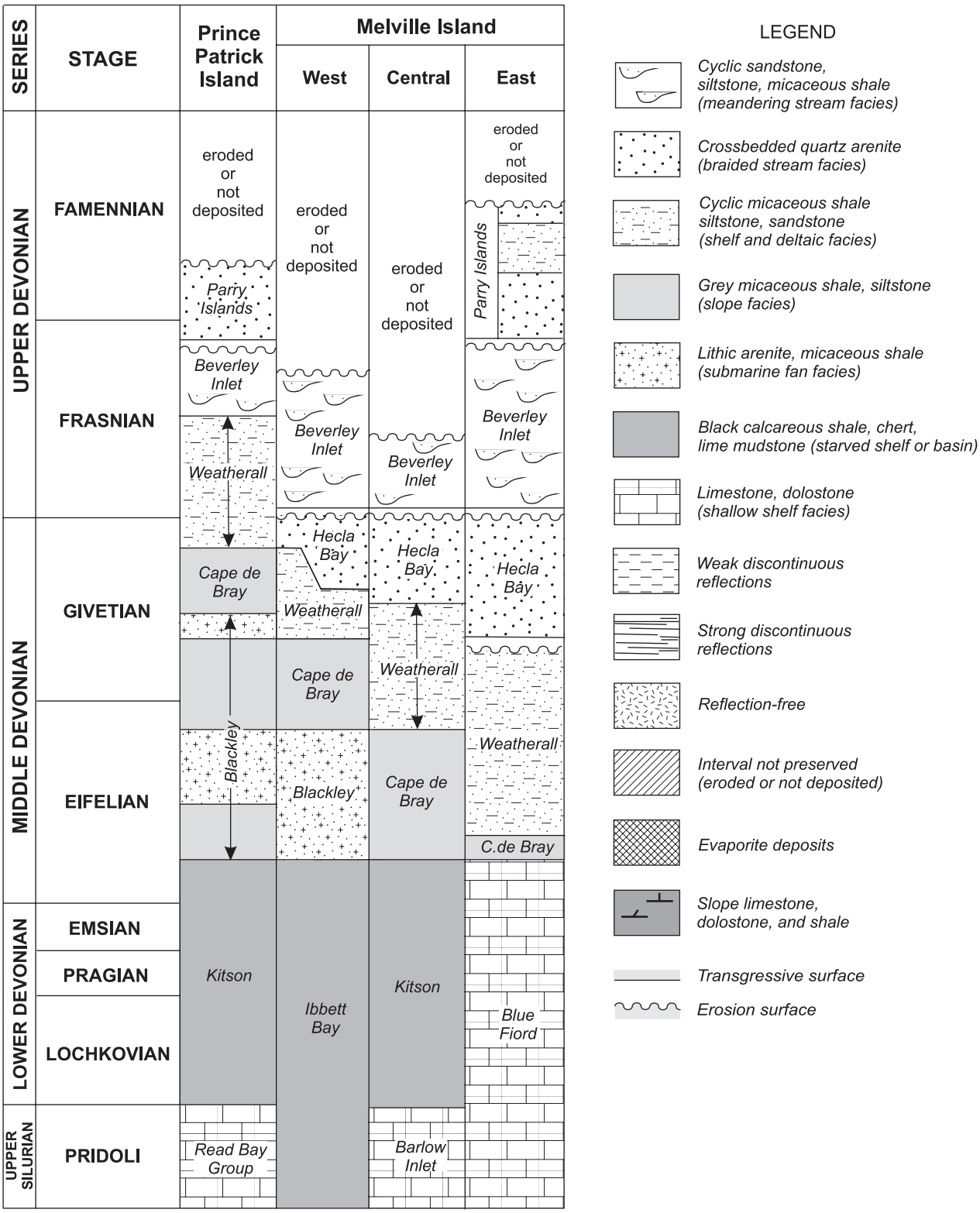

Figure 6. *Simplified correlation of Upper Silurian and Devonian formations of Melville and Prince Patrick islands. The formations of the Devonian clastic wedge include all units above the base of the Blackley Formation on Prince Patrick Island and western Melville Island, and above the base of the Cape de Bray Formation in areas farther east.*

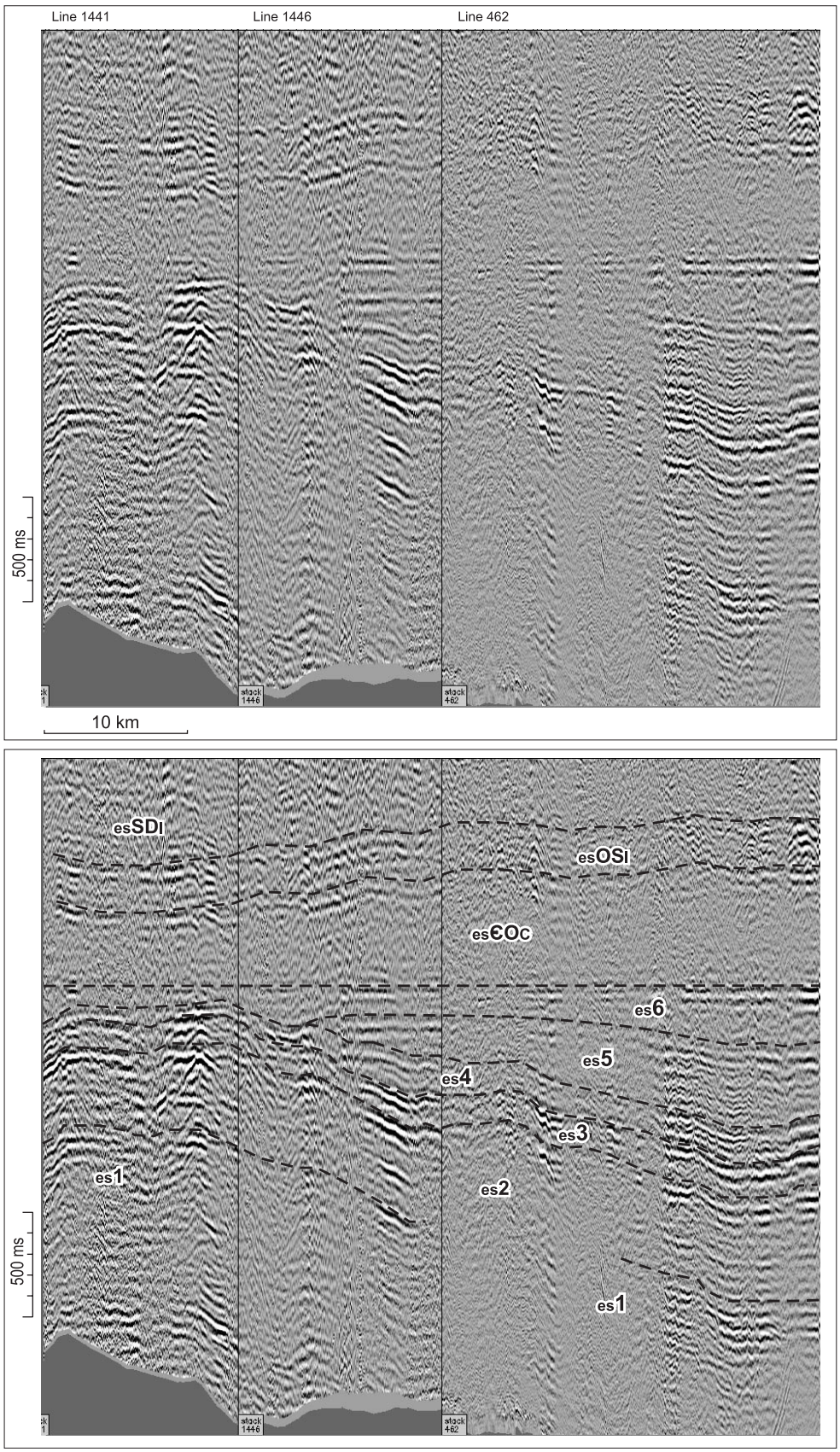

Figure 7. *Seismic expression of Lower Devonian and older strata of Eglinton Island on Panarctic profiles 1441, 462 and 1446. Section has been flattened on the base of unit* esЄOc*. Seismic units* esSDi *and* esOSi *are correlated with the Ibbett Bay Formation of northwestern Melville Island, and the upper part of* esЄOc *with the Canrobert Formation (Lower Ordovician) of the same area. Seismic units* es1 *through* es6 *are correlated with the Kennedy Channel and Ella Bay formations (upper Vendian), Ellesmere Group (Lower Cambrian), and overlying Cambrian shelf or basin facies strata of the eastern Arctic Islands.*

formations is provided by Goodbody (1994). Although the age and correlation of es1 to es6 remains unknown, it is likely that age-equivalent units include the basinal Cambrian succession of Ellesmere Island (i.e., Ellesmere Group and Hazen Formation; Fig. 5; Trettin, 1991) and the contrasting seismic units and facies of Prince Patrick Platform.

Profiles on southwestern Eglinton Island provide convincing evidence for the existence of a significant unconformity beneath unit es6 with all of unit es5 locally cut out westward beneath this surface. Thinning of units es4 and es6 is also documented in this area. These observations, together with those from the offshore platform on Prince Patrick Island, point to the existence of a buried northwest-trending high block, to which the term Crozier High is here applied (Fig. 3).

The precise location of the shelf-to-basin transition is mapped at the depositional limit of units psЄO and psOS beneath southwesternmost Prince Patrick Island (Fig. 4). It is a steep and narrowly defined facies front, which in this area has a northwesterly trend. The location of the southeastern limit of the platform is uncertain but must be situated somewhere west of both Eglinton Island and northwestern Melville Island.

The starved platform cover and basin-facies rocks of the Kitson and Ibbett Bay formations are everywhere conformably and gradationally overlain by orogen-derived sandstone and shale of the Middle and Upper Devonian clastic wedge.

Devonian clastic wedge of Succession 2

The Middle and Upper Devonian clastic wedge is a southwesterly and southerly prograded nonmarine, shelf-deltaic and slope facies complex of orogen-derived siliciclastic and shale units that were deposited across the Canadian Arctic Islands between the early Eifelian and the mid- to late(?) Famennian (Embry and Klovan, 1976; Embry, 1991b). Extensive outcrop is present on central and southern Ellesmere Island, on Grinnell Peninsula and northern Devon Island, throughout the Parry Islands to Prince Patrick Island, on northwestern Victoria Island and throughout Banks Island. Farther-travelled portions of the Devonian clastic wedge are represented by the Frasnian–Famennian Imperial Formation (shale-sandstone) in the northern Yukon and western Northwest Territories (Stott, 1991; Moore, 1993). Regionally significant depositional breaks include 1) a basal disconformity in the eastern Arctic Islands and correlative downlap surface in deep-water strata in the mid-Eifelian (Fig. 6), and disconformities 2) in the mid-Givetian (within or beneath the Hecla Bay Formation), 3) near the Frasnian–Givetian boundary (below the Beverley Inlet Formation), and 4) high in the Frasnian (beneath the Parry Islands Formation).

The Devonian clastic wedge is understood locally from a combination of surface measured sections, exploratory wells, and seismic profiles (Fig. 6, 8). Preserved thickness ranges from less than 500 m to more than 6000 m with variations attributed to regional-scale proximal (northeast) to distal thinning of the sediment wedge, local tectonic thickening by intraformational deformation and thrust stacking, and widespread erosional peneplanation of the associated Devonian thrust-folds prior to deposition of post-orogenic Carboniferous and younger cover.

There are five regionally correlated units of the Middle and Upper Devonian wedge within the report area: the Blackley, Cape de Bray, Weatherall, Beverley Inlet, and Parry Islands formations (Fig. 6). The lowermost unit, the Blackley Formation (Embry and Klovan, 1976) comprises cyclically interbedded shale and immature, calcareous sandstone and siltstone that were deposited as turbidites in a southwesterly facing submarine fan. Alternating shale- or sandstone-dominated units are recognized locally in several wells. However, two wedge-shaped units, each up to about 2000 m thick, dominate the associated seismic reflection records (Fig. 8). Minimum combined thickness of the two units below conformable cover is 846 m. Indicated age, based on contained palynomorphs, is late Eifelian to early Givetian (D.C. McGregor, pers. comm., 1995).

The overlying Cape de Bray Formation in the type area on western Melville Island is a recessive, dark brown to dark grey, micaceous silty shale (Embry and Klovan, 1976). The upper part of the formation is exposed on southern Prince Patrick Island and these strata have also been penetrated in several local wells. The overall shape of the unit is that of a narrowly tapering wedge that thins from about 1550 m north of Intrepid Inlet to a minimum of 540 m near Dyer Bay. Observations collected for this report include seismically identified clinoforms, large-scale channels, and various outcrop-scale features that indicate deposition in a basin slope setting below storm wave base. Contained palynomorphs are Givetian (Embry and Klovan, 1976; D.C. McGregor, pers. comm., 1995).

The base of the overlying Weatherall Formation is drawn below the conformable appearance of sandstone in outcrop sections throughout Melville Island (Embry and Klovan, 1976; Goodbody, 1994); commonly coinciding, more or less, with a diachronous topset truncation surface above Cape de Bray Formation clinoforms on seismic profiles (Goodbody, 1994; Harrison, 1995). Strata in the Weatherall Formation on Prince Patrick Island include cyclically interbedded shale, siltstone and variably calcareous sandstone arranged in coarsening-upward bedsets each 2 to 4 m thick. The unit is roughly tabular in shape. Thickness of

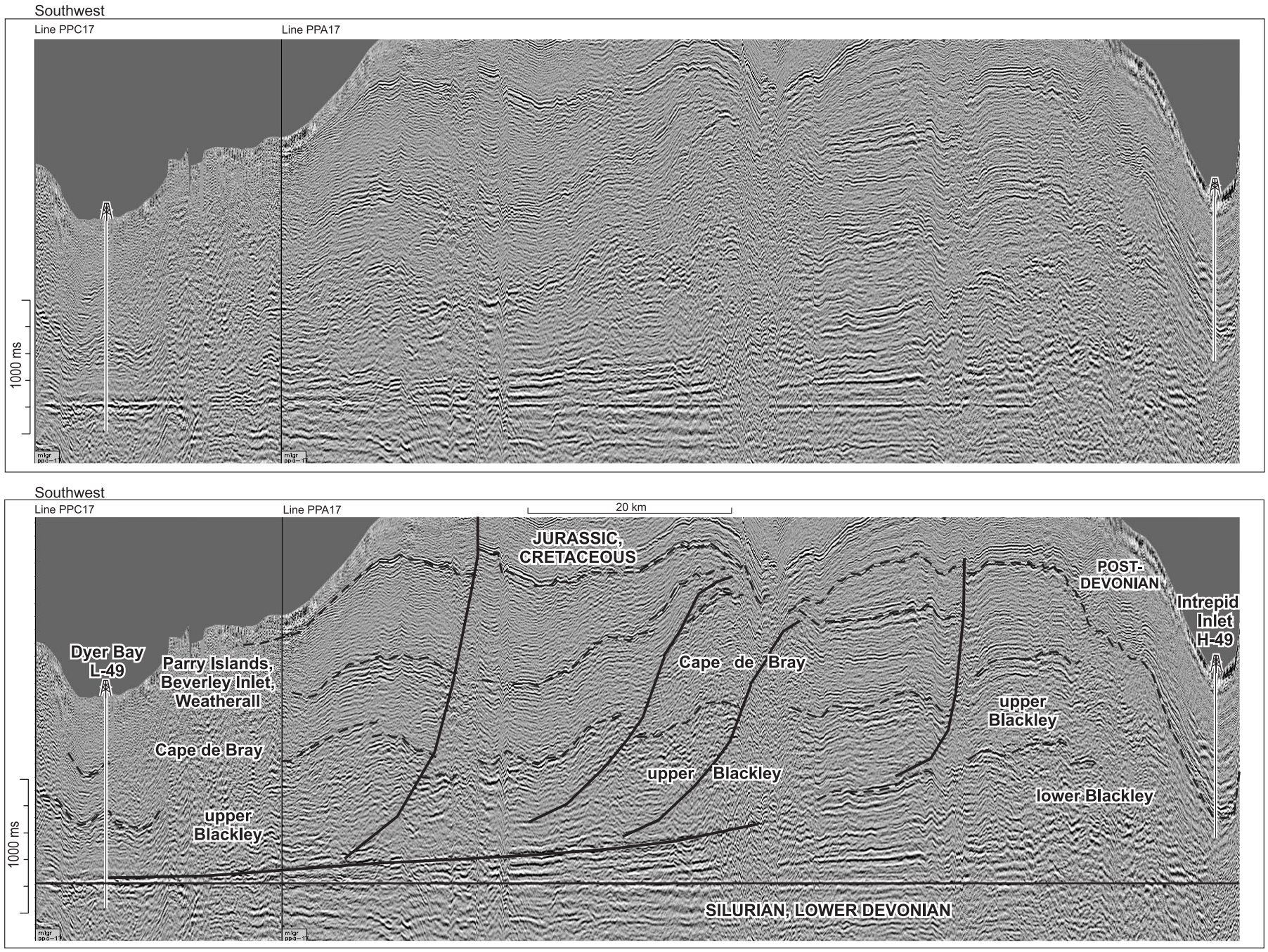
Southwest
Line PPC17
Line PPA17
1000 ms
Southwest
Line PPC17
Line PPA17
20 km
JURASSIC, CRETACEOUS
POST-DEVONIAN
Intrepid Inlet H-49
Dyer Bay L-49
Parry Islands, Beverley Inlet, Weatherall
Cape de Bray
upper Blackley
Cape de Bray
upper Blackley
upper Blackley
lower Blackley
SILURIAN, LOWER DEVONIAN
1000 ms

a section exposed along the east shore of Mould Bay is 650 m. Deposition in outer shelf to deltaic settings is indicated and palynomorph age is latest Givetian to mid-Frasnian (Chi and Hills, 1976; Embry and Klovan, 1976).

The Beverley Inlet Formation is a readily mappable unit that disconformably overlies the Hecla Bay Formation on Melville and Bathurst islands (Embry and Klovan, 1976; Goodbody, 1994). It is also now recognized locally on southern Prince Patrick Island where it is 765 m thick and conformably overlies the Weatherall Formation. Rock types typically include greenish grey fluvial sandstone, prominent in an 85 m thick bedset at the base, and inner shelf and deltaic shale and siltstone with minor, thin coal seams. The thick basal sandstone unit disappears west of Mould Bay and in these circumstances the formation as a whole appears to grade imperceptibly into the upper part of the mapped Weatherall Formation. The Weatherall and Beverley Inlet formations are also indistinguishable on seismic profiles. Palynomorph assemblages, obtained from the sampled section west of Mould Bay, are middle Frasnian (Chi and Hills, 1976; Embry and Klovan, 1976).

The Parry Islands Formation is the highest regionally mappable unit in the Devonian clastic wedge of the Arctic Islands (Embry and Klovan, 1976) and ranges at least to the Lower–Middle *crepida* Zone of the lower Famennian on eastern Melville Island (A.C. Higgins *in* Harrison, 1995). The exposures on southern Prince Patrick Island include only the lower 400 m of the formation. Typical rock types, commonly arranged in fining-upward cycles, include yellowish brown weathering, fine-grained kaolinized quartz sandstone, ripple-marked sandstone, pebbly sandstone with scattered chert clasts to several centimetres, minor chert pebble conglomerate, siltstone, shale and coal. The unit is distinguished from the underlying Beverley Inlet Formation by the common occurrence of hematitic surface staining, a higher proportion of chert in the sandstone, and the overall coarser grain size of some interbeds, especially those near the base. Depositional environments varied from fluvial braidplain to channelized floodplain and nonmarine deltaic settings. Megaspores suggest that only the late Frasnian part of the Parry Islands Formation is preserved on Prince Patrick Island (Chi and Hills, 1976; Embry and Klovan, 1976).

Carboniferous and Permian strata of Succession 3

A combination of reflection seismic and drillhole records (Fig. 9, 10) was used to elucidate the upper Paleozoic record of the report area. Total thickness of this succession ranges from a feather edge, entirely overstepped by the Triassic in the subsurface around the head of Intrepid Inlet, to more than 1350 ms (approximately 3000 m) along the northeastern edge of the report area (Beauchamp et al., 2001). Subsurface units of mostly Carboniferous age were deposited on a post-orogenic angular unconformity above folded and peneplained Devonian and older rocks of subsurface northeastern Prince Patrick Island. This is a regional geological setting not unlike that encountered in outcrop on adjacent northwestern Melville Island. Carboniferous strata are associated with syntectonic deposition in an active horst and graben system. The Permian record is more complex, but includes subsurface units deposited in various nearshore to offshore and deep-water basin post-rift, rift inversion, and inversion cover settings.

The oldest presumed Carboniferous unit is situated in the lower portion of a symmetrical northwest-trending graben in the subsurface near Satellite Bay (Fig. 9). Thickness ranges up to 1000 m (4 km/s). Preferred correlation is with the Borup Fiord Formation (Thorsteinsson, 1974; Beauchamp et al., 2001) of Lower Carboniferous (Serpukhovian) age. Inferred depostional facies include alluvial fan and braidplain conglomerate, sheetflood sandstone and minor shale. Younger Carboniferous strata (Bashkirian? to Asselian or Sakmarian) are more widely preserved in an expanded rift system that extends to the southwest in the subsurface as far as Jameson Bay and the head of Intrepid Inlet. A proximal portion of this package includes the upper part of the Canyon Fiord Formation, which was encountered near the base of the Jameson Bay C-31 well. The Canyon Fiord Formation of Ellesmere Island was named by Troelsen (1950) and described by Thorsteinsson 1974). Drill-penetrated strata on Prince Patrick Island include cyclically interbedded calcareous sandstone, red shale, siltstone, and minor arenaceous and fossiliferous limestone. Maximum thickness of the associated seismic unit is approximately 1500 m. Age-equivalent units of contrasting seismic depositional facies are tentatively assigned to the Nansen and Hare Fiord formations (Thorsteinsson, 1974). The Nansen Formation seismic interval is an estimated 1500 m thick and is assumed to comprise shelf carbonate with lesser clastic deposits (Beauchamp et al., 2001). However there are no drillhole intersections within the report area. The Hare Fiord Formation in the Satellite F-68 well is 1300 m thick (base not seen) and contains organic-rich, silty, calcareous shale, minor chert and fossiliferous limestone (Beauchamp et al., 2001).

Figure 8. *Seismic expression of the Devonian clastic wedge (Blackley through Parry Islands formations) and associated strata of southwestern Prince Patrick Island on Elf profiles PPA17 and PPC17. Section has been flattened on the downlap surface at the base of the clastic wedge.*

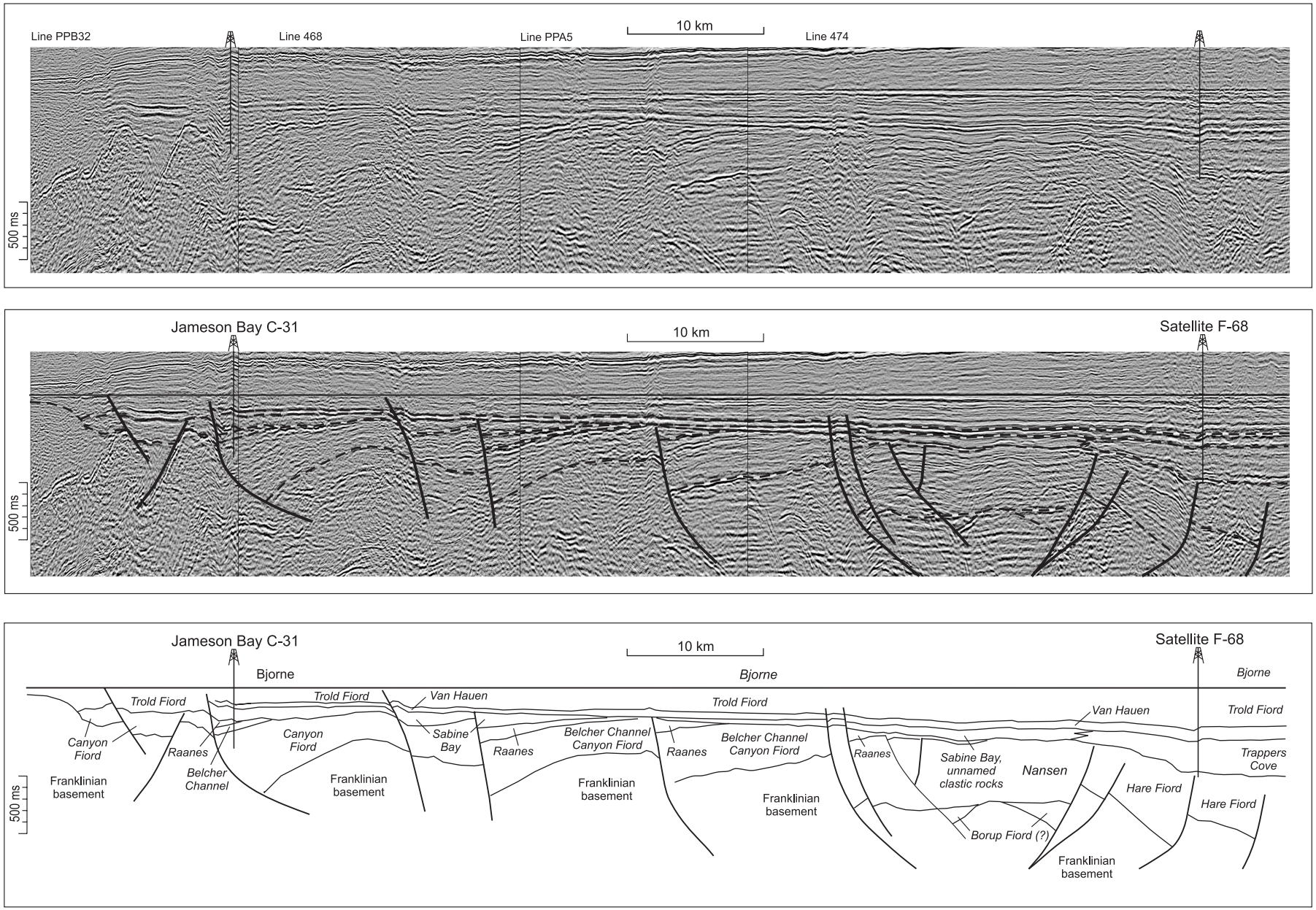

Figure 9. *Seismic expression of Carboniferous and Permian strata of northeastern Prince Patrick Island on portions of Panarctic profiles 468 and 474, and Elf profiles PPA5 and PPB32.*

The end of the rift stage in the Lower Permian is marked by the gradational replacement upsection of the Canyon Fiord Formation by the overlying Belcher Channel Formation (up to several hundred metres of cyclically interbedded arenaceous limestone, shale and marl with Sakmarian fusulinids in the Jameson Bay C-31 well), and above this the equally thin and only locally preserved Raanes Formation (up to about 300 m of shallow-water carbonate and lesser siliciclastic rocks with Sakmarian–Artinskian foraminifera in the C-31 well; Beauchamp et al., 2001). The type section Belcher Channel and Raanes formations of southwestern Ellesmere Island and Devon Island, respectively, are described by Beauchamp and Henderson (1994).

The remainder of the source-proximal Permian section is dominated by inversion- and post-inversion-related coarse and fine siliciclastic rocks variously assigned to the Sabine Bay Formation (up to 350 m of buff sandstone, conglomerate and red shale with Roadian palynomorphs in the C-31 well) and the widespread Trold Fiord Formation (which grades basinward to more than 700 m of spicular brachiopod-bearing glauconitic sandstone and intercalated chert with Late Permian palynomorphs and rare foraminifera in several local wells). The lower portion of this package includes a separately mapped interval of unnamed conglomerate, sandstone, red siltstone, and shale that might be age equivalent to limestone of the Great Bear Cape Formation (Artinskian) of the eastern Sverdrup Basin (Beauchamp et al., 2001).

The Artinskian and younger Permian slope and basin facies strata that conformably overlie the Hare Fiord Formation are confined to the Satellite Bay area and adjacent portions of subsurface Prince Patrick Island to the northeast. Units encountered in the Satellite Bay F-68 well include the Trappers Cove Formation (595 m of organic-rich pyritic shale and argillaceous siltstone) and the Van Hauen Formation (363 m of organic-rich silty shale containing Roadian and Wordian palynomorphs; lesser siltstone and argillaceous, locally fossiliferous, limestone) which is gradationally overlain by progradational Trold Fiord Formation as described above. A tongue of the Van Hauen Formation also extends to the southwest and near its preserved limit is found to disconformably overlie Roadian and older coarse siliciclastic rocks in the Jameson Bay C-31 and Andreasen L-32 wells (Beauchamp et al., 2001).

Mesozoic strata of Succession 3

Mesozoic strata are extensively exposed throughout Eglinton Island and the southeastern half of Prince Patrick Island (Fig. 3), are believed to subcrop below the Neogene of western Prince Patrick Island, and are documented seismically on the seafloor of the surrounding channels. Units mapped at the surface range from the Upper Triassic through the Upper Cretaceous. Lower and Middle Triassic strata are also encountered in exploratory wells of northeastern Prince Patrick Island. Aggregate thickness is highly variable. The most complete record is preserved in the Sverdrup Basin which, in the Satellite Bay area, has a Lower Triassic through Lower Cretaceous interval up to 3000 m thick (Fig. 11, 12). The Triassic succession is overstepped by the Lower Jurassic in the outcrop belt of

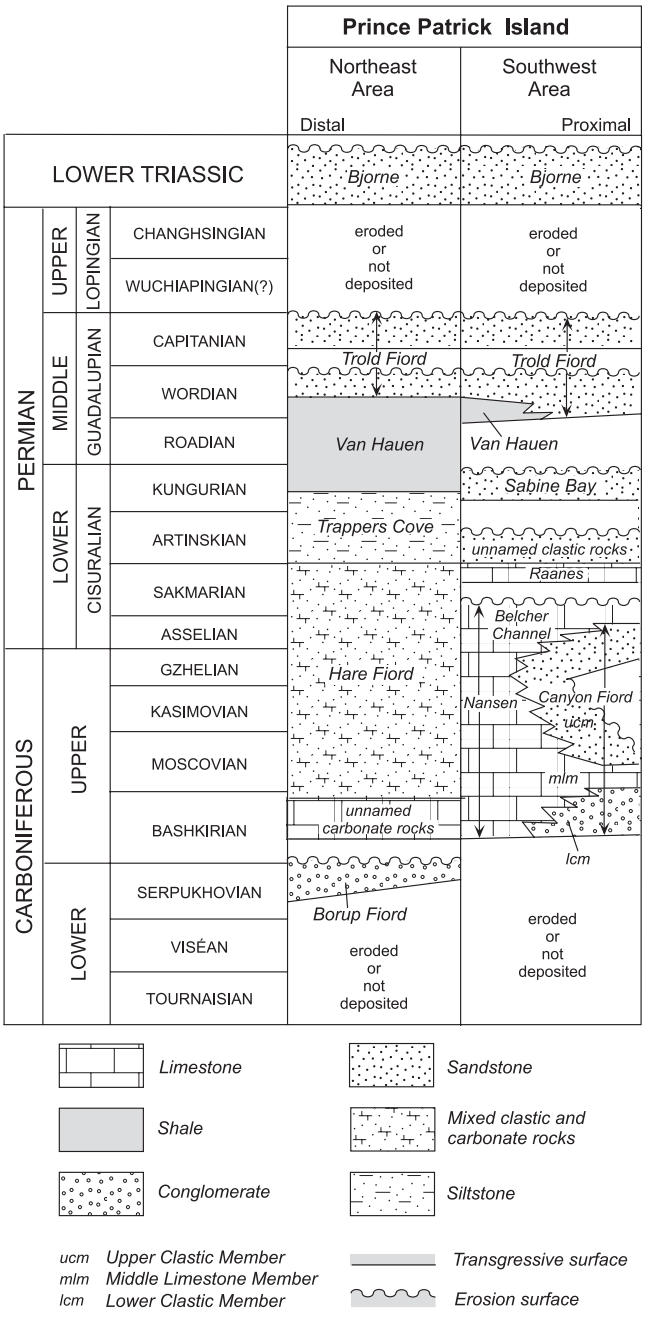

Figure 10. *Simplified correlation of Carboniferous, Permian and Lower Triassic formations of subsurface northeastern Prince Patrick Island (modified from Beauchamp et al., 2001).*

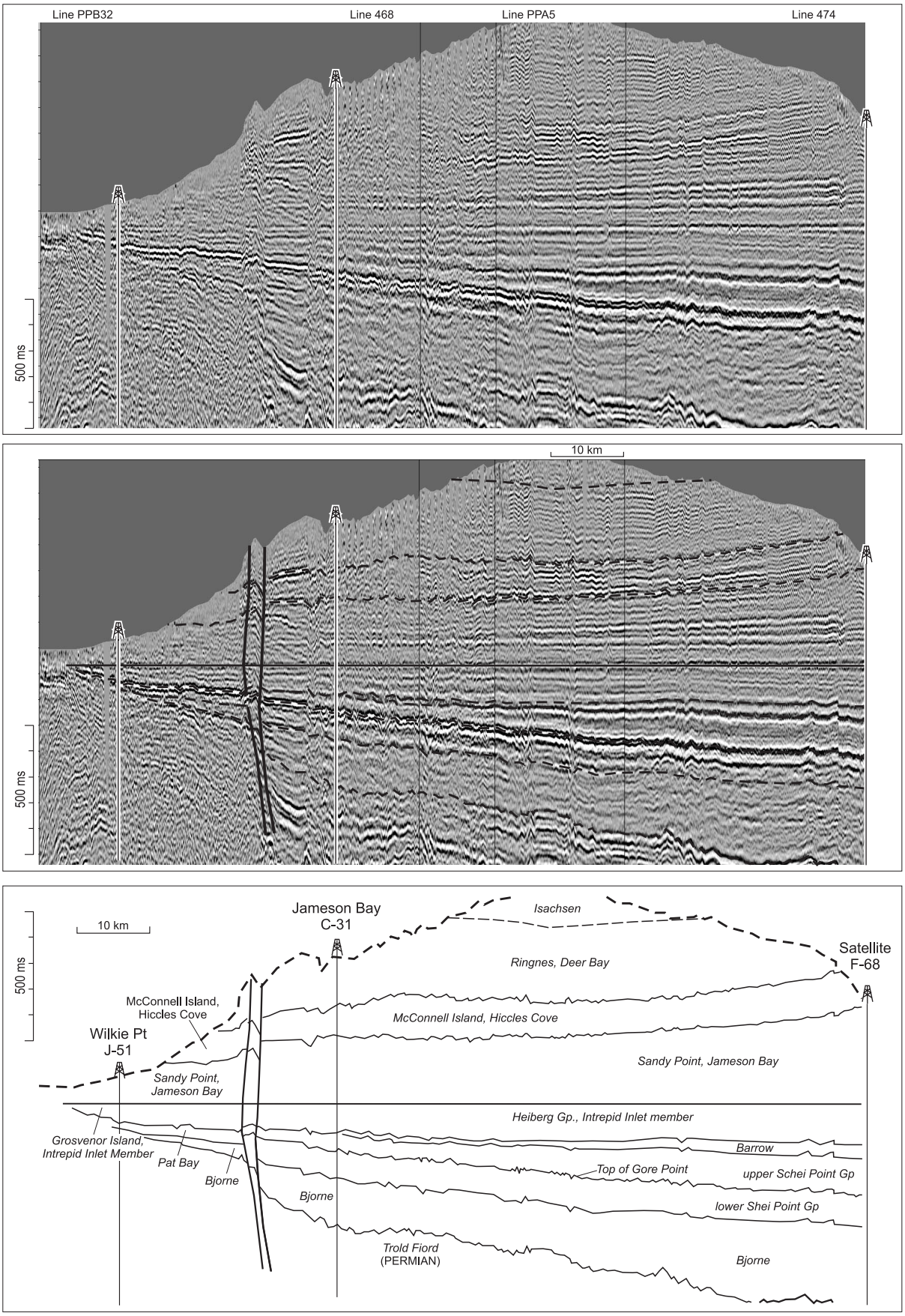

Figure 11. *Seismic expression of Mesozoic strata of northeastern Prince Patrick Island on portions of Panarctic profiles 468 and 474, and Elf profiles PPA5 and PPB32. Section has been flattened on the top of the Intrepid Inlet Member of the Jameson Bay Formation.*

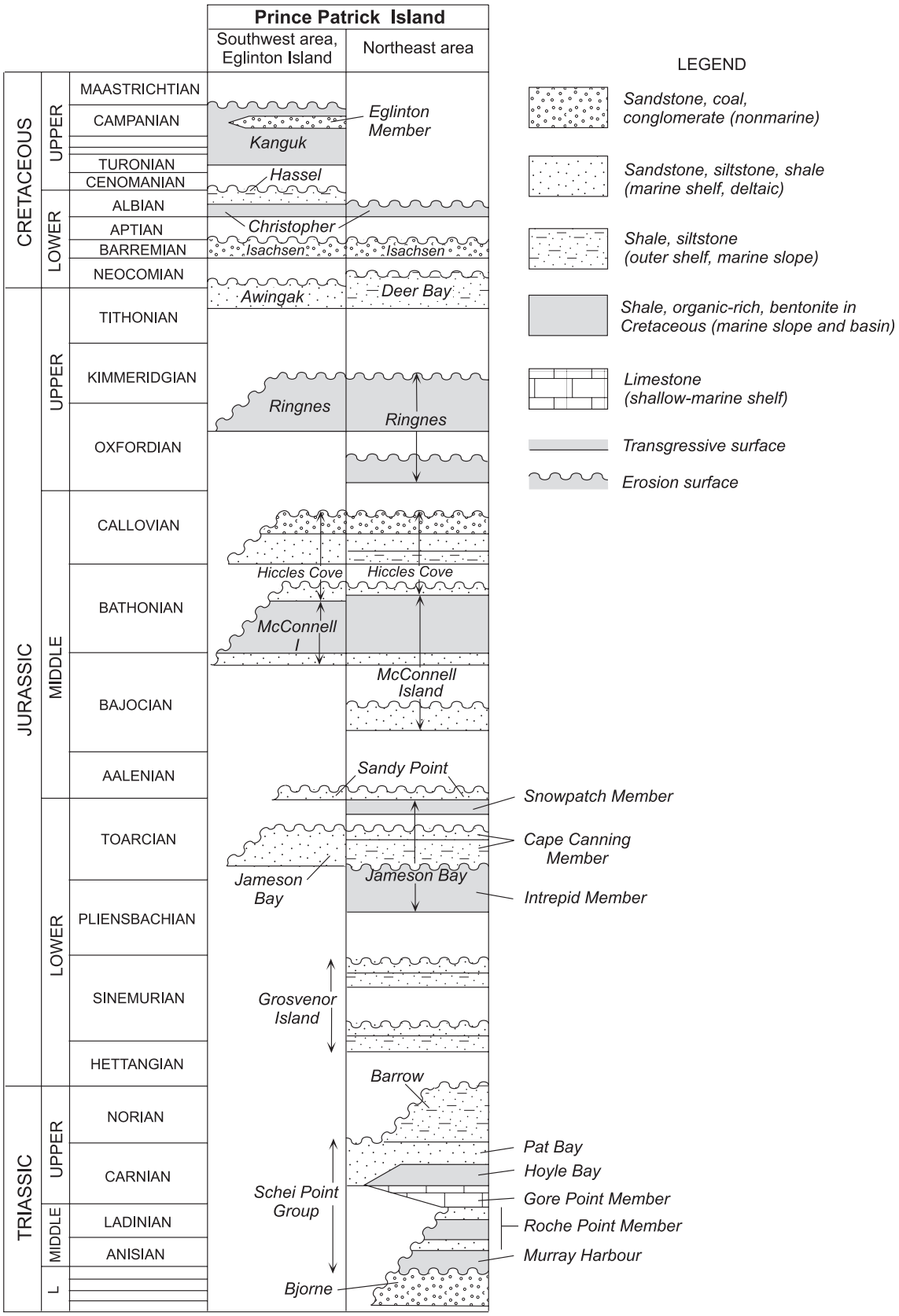

Figure 12. *Simplified correlation of Mesozoic strata of Prince Patrick and Eglinton islands.*

east-central Prince Patrick Island, and important disconformities between many of the remaining formations are characteristic of the succession documented in most areas beyond the Sverdrup Basin. The Mesozoic record is especially fragmented on southern Prince Patrick Island. In this area, up-thrown fault blocks with exposed Devonian "basement" are overlain unconformably by mid-Jurassic through Lower Cretaceous erosional remnants, some of which are preserved in north-trending half-grabens. The record of the Mesozoic is also provided on various regional seismic profiles of western Prince Patrick Island where a complex and prolonged history of Middle Jurassic and Cretaceous extension is indicated beneath widespread unconformable Neogene cover. For the purpose of simplified description, the Mesozoic record of the report area is divided into three packages: 1) a package that predates ancestral Canada Basin rifting; 2) a synrift package with a lower boundary falling beneath Middle Jurassic strata, and; 3) an Albian and younger post-rift package potentially synchronous with the drift phase of Canada Basin. While the Albian Christopher Formation and younger Cretaceous strata are tentatively considered to be post-rift units, these and all older strata were also affected by a much younger, possibly mid-Cenozoic phase of extension prior to overlap by widespread Neogene cover.

Understanding the thin sequences and tectonics within the Jurassic section has been facilitated by the locally prolific macrofauna, and particularly the studies by H. Frebold reported in Tozer and Thorsteinsson (1964). More recent studies are provided by Poulton (1994).

Pre-rift package (Triassic–Lower Jurassic)

The Lower Triassic Bjorne Formation (Tozer, 1961, 1963) disconformably overlies the Trold Fiord Formation throughout much of the subsurface of Prince Patrick Island northeast of Intrepid Inlet. Thickness ranges up to 688 m in the Satellite Bay F-68 well. The range of rock types and depositional facies are similar to those documented at the surface on northwestern Melville Island (Tozer and Thorsteinsson, 1964; Trettin and Hills, 1966) and include variegated, commonly iron oxide-stained, nonmarine quartz sandstone, conglomerate, and minor red shale. Intervals of marine shale occur in the upper part of the formation at F-68, and a separate, thin interval immediately above the Permian is likely correlated with the Blind Fiord Formation.

All of the Middle Triassic and most of the Upper Triassic strata are also confined to the subsurface, a package up to 482 m thick in the F-68 well, collectively referred to the Schei Point Group (Embry, 1984a,b; 1991b; Fig. 12). Associated units in this well include the Murray Harbour (Middle Triassic petroliferous shale and siltstone) and Roche Point (Middle Triassic sandstone) formations, the Gore Point Member (Carnian limestone), and the Hoyle Bay (Carnian petroliferous shale) and Pat Bay (Carnian sandstone) formations. Only the Pat Bay Formation extends into the outcrop belt where up to 30 m of section is preserved unconformably overlying the Middle Devonian Cape de Bray Formation east of Intrepid Inlet and in two outlier areas north of Green Bay. Typical rock types include fine- to coarse-grained calcite-cemented quartz sandstone, bioclastic quartz sandstone, and arenaceous and bioclastic limestone with *Minetrigonia, Plicatula* and *Gryphaea*.

The Pat Bay Formation is succeeded in the subsurface by the Barrow Formation (Embry, 1991b; Norian and/or Hettangian shale; max. 87 m) and above this by the Grosvenor Island Formation (late Hettangian? and Sinemurian shale and siltstone; combined max. 269 m). Only the Grosvenor Island Formation is exposed at the surface where it disconformably overlies the Pat Bay Formation east of Intrepid Inlet. The outcrop belt extends a distance of 22 km north and south of Cape Canning with the best exposures in stream cuts 4 km to the east and 6 km to the northeast of the cape. In this area the formation includes a basal bed of pebbly oolitic ironstone, 30 to 50 cm thick, overlain by 2 m of red and green claystone containing partings of fine sand and coalified plant fragments. The section from 2.5 to 15 m above base contains greenish grey shale grading up into siltstone and loosely consolidated, fine-grained sandstone. A layer containing oolitic ironstone concretions, ammonites, phosphatic nodules, selectively cemented burrows, wood fragments and leaf impressions occurs at 10 m above base. The top of the formation (from 15 to 16 m) is also marked by ammonites and numerous phosphatic concretions.

The Grosvenor Island Formation east of Intrepid Inlet contains two ammonite assemblages: the lower assemblage, collected from the basal metre of the formation, features *Badouxia*(?) sp. An Early Sinemurian (and possibly latest Hettangian) age is indicated (Fig. 13). The second ammonite assemblage collected at 10 and 16 m above base includes *Echioceras arcticum* Frebold, *Echioceras* sp., and *Gleviceras*(?) sp. of Late Sinemurian age. Associated Sinemurian (and Late Hettangian?) foraminifera, recovered from cuttings of the Jameson Bay C-31 well, include *Ammodiscus siliceus* (Terquem) and *Glomospira perplexa* Franke (J.H. Wall, pers. comm., 2000).

The Grosvenor Island Formation is overlain by the Intrepid Inlet Member of the Jameson Bay Formation (Embry, 1991b; Poulton, 1994) in outcrop areas east of Intrepid Inlet and throughout the subsurface to the northeast. The Intrepid Inlet Member (glauconitic sandstone and shale containing phosphatic nodules) is succeeded by the Cape Canning and Snowpatch members (mostly belemnitic shale with an intervening sandstone tongue located in the upper Cape Canning). The stratigraphic

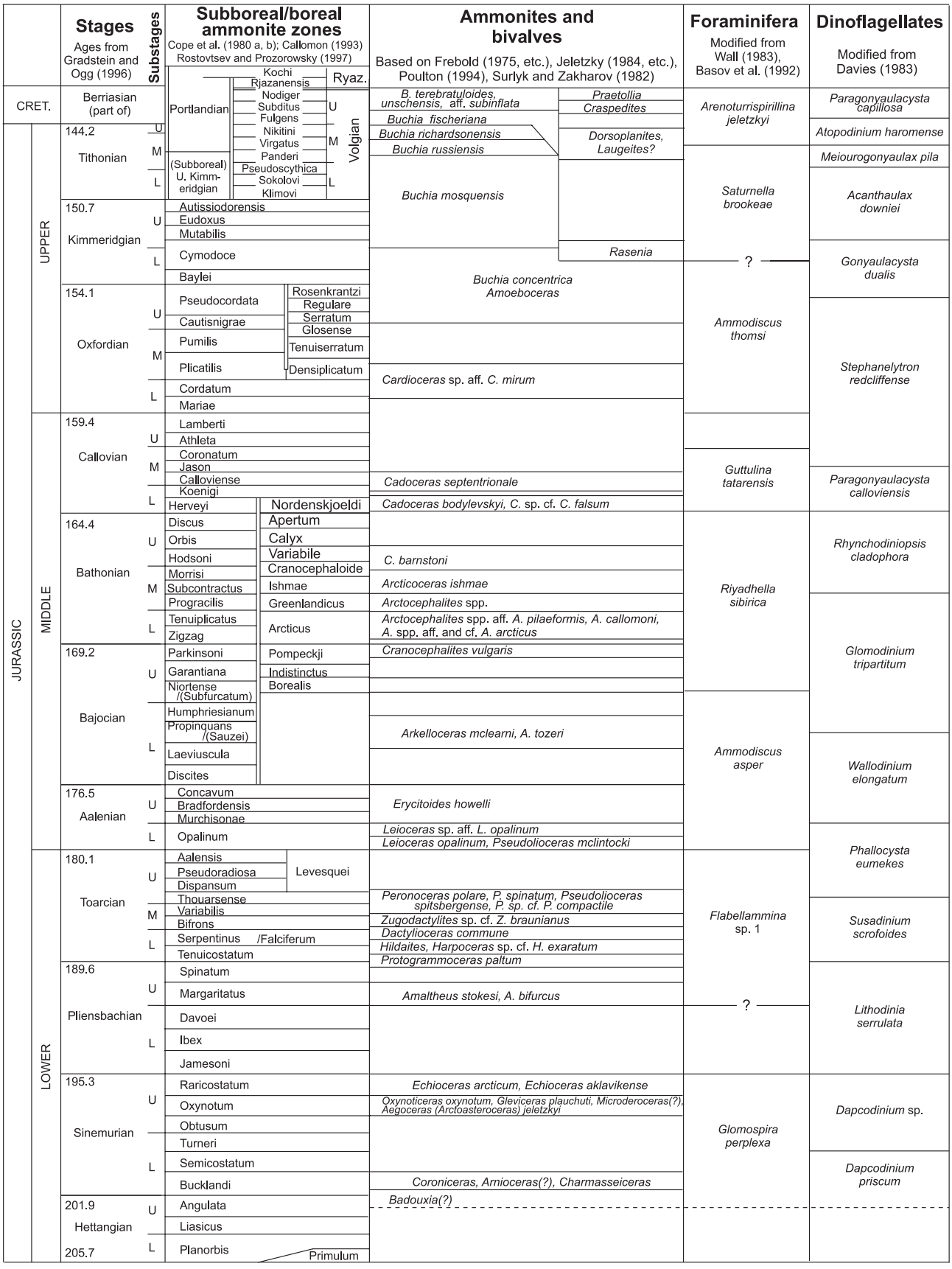

Figure 13. *Correlation of Boreal Jurassic biozones of Prince Patrick Uplift and the western Sverdrup Basin on Prince Patrick Island (reproduced from Harrison et al., 2000).*

succession is more complicated west of Intrepid Inlet. For example the Intrepid Inlet Member unconformably overlies the Pat Bay Formation along coastal Green Bay. Elsewhere, east and north of Mould Bay, the Cape Canning Member lies directly on Devonian strata. A Late Pliensbachian age for the Intrepid Inlet Member is based on the occurrence of an indeterminate form of *Amaltheus stokesi*. The Cape Canning Member is Toarcian based on the common occurrence of *Protogrammoceras, Harpoceras, Dactylioceras* sp. aff. *commune* (Simpson), *Peronoceras* sp., and *Pseudolioceras compactile* (Simpson). The maximum thickness of the Jameson Bay Formation is 135 m in the outcrop section east of Intrepid Inlet but expands to over 550 m in the subsurface around Satellite Bay.

Syn-rift package (Middle Jurassic–Lower Cretaceous)

Mesozoic strata below and including the Jameson Bay Formation generally grade to shale and thicken to the northeast toward the centre of the Sverdrup Basin. Individual sequences, bound by disconformities, display overlap relationships on the basin margin with younger units generally cutting out older strata and extending farthest from the basin centre. This relationship breaks down for strata deposited during or after the Toarcian. Seismic and outcrop evidence (presented later in this volume) indicates that the thickness and depositional facies of younger Jurassic and pre-Albian Lower Cretaceous formations were influenced by coincident slip on local faults, part of a long-lived rift zone that extends across Eglinton Island, central and western Prince Patrick Island and the adjacent channels.

The oldest of the syn-rift units (or youngest pre-rift unit) is the Sandy Point Formation (Embry, 1991b; Poulton, 1994) which, in outcrop areas east and west of Intrepid Inlet, is a 5 to 10 m thick recessive interval of uncemented quartz sandstone – not more than a marker bed at the scale of mapping. In most areas this unit disconformably overlies the Jameson Bay Formation. One exception is northeast of Green Bay where it lies directly on the Upper Triassic. The dominant ammonites are *Leioceras opalinum* (Reinecke) and *Pseudolioceras m'clintocki* (Haughton) of Early Aalenian age (Fig. 13).

The next unit of the syn-rift succession is the McConnell Island Formation (Embry, 1991b; Poulton, 1994) which includes a ledge-forming lower member of cemented ferruginous sandstone and interbedded weakly consolidated sandstone (30 m total). Characteristic Early Bajocian fauna are *Arkelloceras tozeri* Frebold, *A. mclearni* Frebold, and *Retroceramus lucifer* (Eichwald). Outcrop distribution, restricted to areas on either side of Intrepid Inlet, is similar to the Sandy Point Formation. More widespread and extending to the west as far as Landing Lake in the lower part of this formation is a latest Bajocian ammonite assemblage with *Cranocephalites vulgaris* Spath and an Early Bathonian assemblage featuring *Arctocephalites*. The upper part of the McConnell Island Formation is a yellowish brown and medium-grey weathering marine shale with common calcareous sandstone concretions. It is only distinguishable as a separately mapped unit in outcrop areas located east of Intrepid Inlet (50 m thick) and north of Green Bay.

The shale member of the McConnell Island Formation thins to the southwest and in most areas south and west of Green Bay the lower sandstone part of this formation is overlain disconformably by a similar succession of varingly cemented sandstone and fossiliferous ironstone assigned to the lower Hiccles Cove Formation (max. 40 m; Embry, 1991b; Poulton, 1994). Distinction is made on faunal grounds by the occurrence of the Late Bathonian ammonite *Arcticoceras ishmae* (Keyerserling) in the younger strata. The upper part of the Hiccles Cove Formation, most fully exposed in the tablelands east of Intrepid Inlet (ca. 110 m), is marked by a cemented sandstone bed about 1 m thick overlain by 5 m of grey, silty shale that grades upward into castellate-weathering pale grey and pale yellowish grey, highly mature quartz sandstone. The recessive uppermost part of the formation is fully exposed west of Green Bay. In this area there are 6 to 8 m of bioturbated, medium brown, fine-grained sandstone, rippled, flat-laminated and trough cross-stratified sandstone, coaly sand, and thin coal coal seams lying between the castellate sandstone unit of the Hiccles Cove (below) and disconformable Upper Jurassic shale, above. Callovian beds are indicated in the upper part of the Hiccles Cove Formation by *Cadoceras* and *Costacadoceras*.

The Upper Jurassic succession, widely exposed throughout the report area, features the Ringnes Formation (Embry, 1991b; Poulton, 1994; up to 200 m of dark grey marine shale; less than 50 m in most outcrop areas) at the base overlain in the northeast by the Deer Bay Formation (up to 500 m of marine sandstone, siltstone and shale arranged in shallowing-upward cycles) or elsewhere, to the southwest, by the Awingak Formation (up to 285 m of deltaic and marginal-marine sandstone). Characteristic of the thicker intervals of the Ringnes Formation are calcite-cemented sandstone concretions, especially common in the middle of the formation. Typical fauna include *Cardioceras* sp. (Early Oxfordian) and *Amoeboceras* sp. (Late Oxfordian to Early Kimmeridgian) east of Intrepid Inlet, and *Ammodiscus thomsi* Chamney with associated microfauna (Oxfordian–Kimmeridgian) identified by J.H. Wall from around Mould Bay and elsewhere on southern Prince Patrick Island. Bivalves in the Awingak Formation include Early to Middle Tithonian *Buchia russiensis* (Pavlow) near

Comfort Cove on southwestern Melville Island (Jeletzky *in* Harrison, 1995), and *Buchia fischieriana* (D'Orbigny) (Late Tithonian) at Cape Cam and Cape Frederick on southern Prince Patrick Island. The suite of bivalves contains some very characteristic species: *Canadarclotis rugosa* Jeletzky and Poulton, *Canadotis canadensis* Jeletzky and Poulton, *McLarenia* sp., and *Oxytoma aucla* Zakharov. The Awingak Formation grades into the Deer Bay Formation around Green Bay and therefore a similar Tithonian age appears likely. Bivalves of Valanginian age have been reported from the uppermost Deer Bay Formation north of Jameson Bay (Jeletzky *in* Tozer and Thorsteinsson, 1964).

The Deer Bay and Awingak formations are disconformably succeeded in many areas by Lower Cretaceous deltaic and nonmarine sandstone, coal, pebble conglomerate, and minor marginal-marine shale of the Isachsen Formation (Tozer and Thorsteinsson, 1964). Large thickness variations are indicated with the greatest section preserved on Eglinton Island (490 m) and on the peninsula east of Mould Bay (ca. 360 m). Age based on pollen and dinoflagellates would appear to be mostly Barremian but may also extend into the Aptian. A disconformity above the Isachsen Formation is assumed based on a locally sharp upper contact with overlying Albian shale and the apparent absence of some or most of the Aptian.

Post-rift package (Lower Cretaceous–Upper Cretaceous)

The Christopher Formation (Heywood, 1957; Tozer and Thorsteinsson, 1964) is the youngest Cretaceous unit throughout Prince Patrick Island. It occupies open synclines northeast of Jameson Bay and is the youngest unit in fault-bound outliers north and west of Mould Bay. The Christopher Formation also extends to Eglinton Island, where three members are distinguished: a lower shale with minor sandstone (70–85 m); a medial shale with large calcite-cemented sandstone concretions and minor bentonite (180 m); and an upper shale with common bentonite layers (95 m). Indicated age ranges from Early Albian at the base (*Quadrimorphina albertensis* Mellon and Wall) to Middle Albian or early Late Albian at the top based on both foraminifera (*Verneuilinoides borealis* Tappan?) and dinoflagellates (J.H. Wall, pers. comm., 1989; E.H. Davies, pers. comm., 1992). Two chemosynthetic carbonate mounds are distinct features in the lower part of the Christopher Formation exposed along a prominent north-striking fault located 14 km west of Mould Bay (Beauchamp et al., 1989c).

The remaining units of the Cretaceous are exposed only on Eglinton Island. The Hassel Formation (Heywood, 1957; Plauchut and Jutard (1976) is a thin, recessive interval of uncemented pale olive grey and yellowish grey quartz sandstone and pebbly sandstone containing detrital coal fragments and minor siltstone. A creek northeast of Cape Nares exposes a section approximately 20 m thick with a gradational lower contact. A Late Albian microflora is reported by Plauchut and Jutard (1976). The Kanguk Formation, the youngest Cretaceous unit in the report area, is readily divisible into three members on Eglinton Island (Tozer and Thorsteinsson, 1964; Plauchut and Jutard, 1976): a lower brownish black and black bituminous shale (a good oil source rock in the lower 15 m) with yellow and greyish yellow bentonite layers (230 m), a medial quartz arenite, variably medium to coarse grained, pebbly, oolitic and manganiferous (Eglinton Member, 50 m); and an upper brownish black and black shale, like the lower member, also containing bentonite layers (40 m+). The age of the formation ranges from Cenomanian or Turonian near the base to early Campanian at the top.

Neogene strata of Succession 4

A profound angular unconformity separates faulted and tilted Cretaceous and older strata, below, from generally undeformed Neogene strata above. The unconformity extends throughout Prince Patrick Island from Ballantyne Strait in the northeast to Dyer Bay in the southwest (Fig. 3). While the Neogene includes both Miocene and Pliocene beds on Banks Island, the exposed section on Prince Patrick Island is represented by the Beaufort Formation *sensu lato* (Fyles, 1990), now considered to be exclusively Pliocene in age based on diagnostic fauna collected from Meighen Island and elsewhere. Representative rock types of the Beaufort Formation within the report area, described by Devaney (1991), are tabular and trough cross-stratified sand, rippled sand, uncoalified wood and plant debris, minor gravel, and mud. The formation is up to 70 m thick in surface exposures. Additional intervals of undivided Neogene strata occur in four exploratory wells (maximum 175 m) and seismic profiles indicate a thickness in excess of 600 m beneath the northwest coast of Prince Patrick Island.

Quaternary record

Quaternary deposits within the report area are extremely poorly preserved. Meltwater channels and glaciofluvial deposits are identified on some air photographs of the Arctic coastal plain, especially north of the head of Mould Bay and northwest of Green Bay. Related gravel and peat are commonly exposed in river banks in this region but are not easily mapped separately from incised Pliocene deposits. Glacial erratics have been identified throughout the report area (Fyles, 1990) but it is uncertain as to whether these have been transported by ice sheets or by iceberg rafting during periods of pre-Late Quaternary highstand. Nevertheless, glacial striations on Devonian bedrock have

been identified by one of us (JCH) on the upland surface and cliff tops around the head of Mould Bay. Channel-fill deposits of probable Quaternary age are also identified on marine seismic records on the floor of Dyer Bay, Intrepid Inlet, Crozier Channel and eastern Kellet Strait. The Late Quaternary and Holocene sea-level history for the region is described by Hodgson et al. (1994). Raised strandline deposits are rare. The southeast coast has emerged up to 24 m since 11 ka. The northwest coast is relatively stable (eustatic sea-level rise is balanced by regional uplift) and the southwest coast is currently subsiding.

SUMMARY DESCRIPTION OF REGIONAL STRUCTURE

Seismic profiles and subsurface mapping

The industry reflection seismic data set utilized for this report includes mostly unmigrated paper copies of the original 4 to 6 second stacks obtained from the assessment reports presently held by the National Energy Board (formerly by the Canadian Oil and Gas Lands Administration). Important new insights into shallow- and mid-crustal structure were also obtained from the reprocessing of reflection profiles. The extent and distribution of all these kinds of seismic data are illustrated on Figure 14.

The advantages of seismic reprocessing include the migration of previously unmigrated data, display of the entire recorded section (mostly to 6 seconds), elimination of some types of linear coherent noise by filtering and deconvolution, digital merging of intersecting stacks to obtain a more regional view of subsurface structure, and the optimization of display parameters for publication. The benefits of the migration step are substantial and include collapsing of diffractions from laterally terminated reflectors and point diffractors, resolution of the shape and location of deep focus synclines by eradication of "bowties", and the displacement of dipping reflection segments to their correct subsurface locations.

In spite of these attempts to create a reliable display of subsurface structure, interpretive pitfalls remain in the data. These pitfalls include 1) the loss of signal strength with increasing distance and time beginning with the high-frequency information (spherical divergence); 2) lateral variations in primary signal response as a result of field acquisition problems or complex subsurface structure; 3) overmigration hyperbolae; 4) residual diffractions; 5) pull-up or sag due to lateral velocity variations higher in the section; 6) multiples; 7) variations in vertical exaggeration from top to bottom in the profiles as a result of changes in interval velocity as a function of depth of burial, rock porosity and density; and 8) reflector mismatch and polarity reversals between profiles.

The effects of permafrost are apparently small. Sonic log and downhole checkshot survey data indicate that frozen, ice-saturated Jurassic and younger sands have interval velocities in the range of 3.4 to 3.8 km s^{-1} while equivalent unfrozen sands are 2.2 to 3.2 km s^{-1} (Table 1). Velocity contrast is less between frozen and unfrozen shale or cemented sand. In some porous sandstone units it is possible to correlate a base of permafrost reflection (Fig. 15). In other units having interlayered porous and impermeable layers, it is possible to detect the downdip limit of frozen porous layers (Brent and Harrison, 1998). Strong impedance contrasts are created between frozen, ice-filled layers and relatively dry and impermeable lenses. The base of the permafrost can in these instances be drawn downdip where the impedance contrast generated by the interstitial ice is no longer present.

Vertical exaggeration on most page-size illustrated profiles in this report ranges from approximately 0.6 for Cambrian to Silurian rocks with interval velocities of 6.0 km s^{-1} to 1.6 at 2.2 km s^{-1}, for the youngest unfrozen and unconsolidated sediments. The bulk of the Middle Devonian through Cretaceous rocks possesses interval velocities in the range of 3.5±1.0 km s^{-1}. Vertical exaggeration of the corresponding seismic intervals is 1.0±0.3.

Seismic profiles have been converted from time to depth, using interval velocities as obtained from the sonic logs and check-shot surveys of exploratory wells. These logs, used in combination with downhole checkshot surveys, density logs and calculated synthetic seismograms also permit the correlation of drilled formations to seismic units. Examples of this technique applied to the BP et al. Satellite F-68 and Elfex et al. Wilkie Point J-51 well are illustrated in Figures 16 and 17. Additional interval velocity data for Silurian and older units, presumed to exist below the deepest well penetrations, have been obtained from well logs of equivalent strata of Melville Island and from the refraction seismic profiles of Overton (1970). Interval velocities of selected near-surface stratigraphic units have also been obtained from the normal moveout (NMO) correction during seismic data processing as provided by the Dix equation (Dix, 1955).

Surface structural elements

Geological regions of the western Arctic Islands region are illustrated in Figure 18 and include the lower Paleozoic Arctic Platform, three deformed belts of the lower Paleozoic Franklinian Mobile Belt, the Sverdrup Basin, four rift-

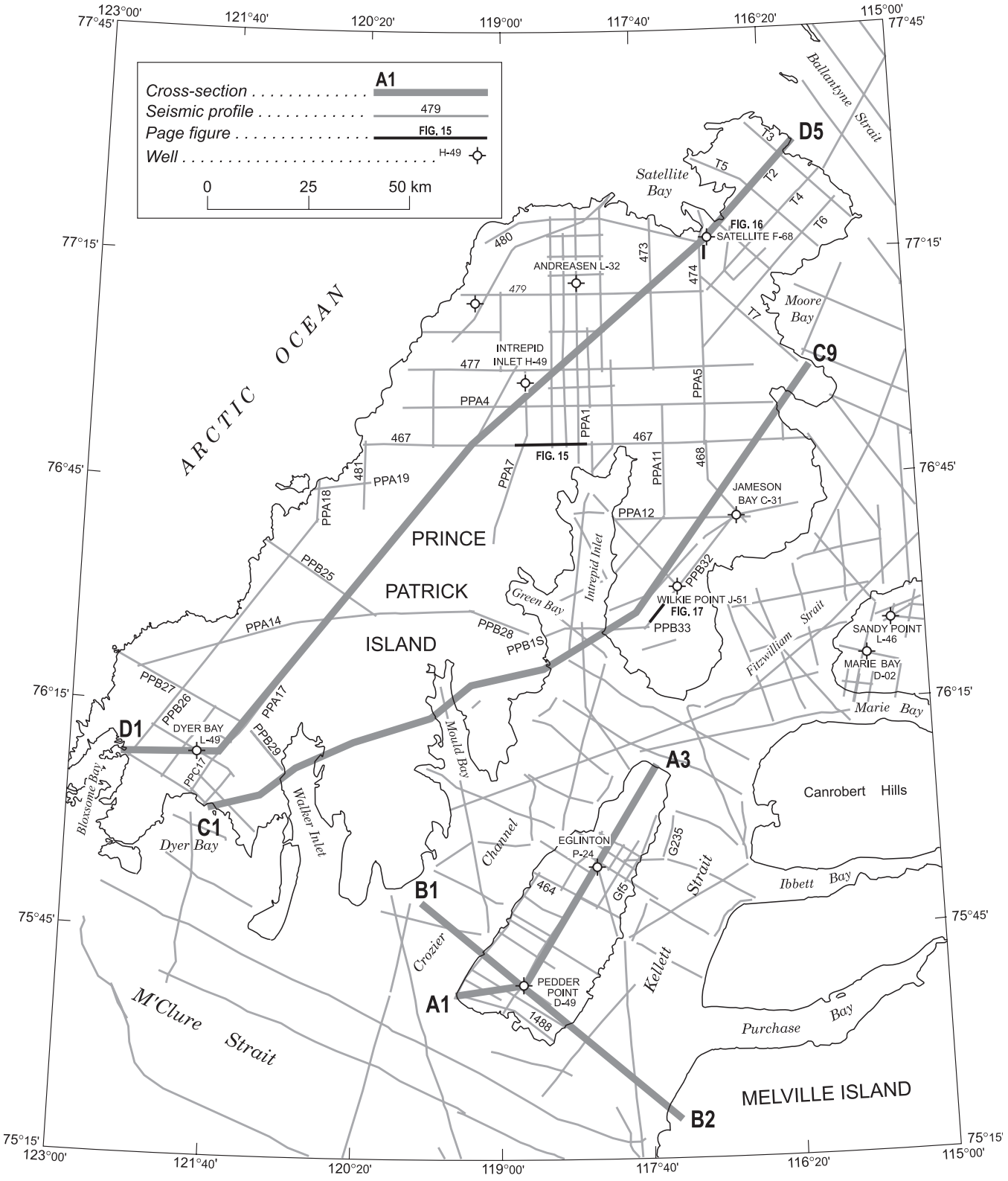

Figure 14. *Reflection seismic profiles, exploratory drillholes, structural cross-sections and location of text illustrations of Prince Patrick and Eglinton islands, including the adjacent offshore areas.*

Table 1
Summary interval velocity data for frozen and unfrozen stratigraphic units of the report area

Unit or Layer	Interval velocity (km s-1)
Sea water	1.45
Beaufort Formation	
frozen	3.8
unfrozen	2.2
Kanguk Formation	
frozen	2.7
unfrozen	2.4?
Christopher Formation	
frozen	2.7
unfrozen	2.6
Awingak, Deer Bay formations	
frozen	3.7
unfrozen	2.6–3.2
Isachsen Formation	
frozen	3.5
unfrozen	2.4–3.2
Ringes Formation	
frozen	2.8?
unfrozen	2.8
Hiccles Cove, McConnell Island formations	
frozen	3.8
unfrozen	3.0–3.7
Sandy Point, Jameson Bay formations	
frozen	3.4
unfrozen	2.6–3.0
Heiberg Group	3.0
Schei Point Group	
upper part	3.0–3.2
lower part	3.8–4.2
Bjorne and Blind formations	3.6–4.2
Permian	
clastic rocks, undivided	3.8–4.1
carbonate rocks, undivided	4.6–5.3
Van Hauen Formation	4.0–4.8
Canyon Fiord Formation	4.4–5.0
Hare Fiord Formation	3.9–4.7
Weatherall Formation	3.9–4.2
Cape de Bray Formation	
Blackley Formation	3.9–4.2
Kitson and Ibbett Bay formations	4.6–4.8
Silurian carbonate rocks	6.0
Vendian? to Ordovician, undivided	5.5

related continental margin basins of Jurassic through Paleogene age, three inter-basin highs, and the Arctic Continental Terrace Wedge. Chronology of basin formation and tectonic activity is provided in Table 2.

Arctic Continental Terrace Wedge

The Arctic Continental Terrace Wedge forms a continuous blanket of Pliocene and younger strata across the western half of Prince Patrick Island and is continuous with similar

Table 2
Chronology of basin formation and major tectonic phases in the western Arctic Islands region

Age	Tectonic activity
Erosion surface	
Neogene (late Pliocene–Recent)	Glaciotectonics and neotectonics
Regional unconformity	
Neogene (mid-Miocene–mid-Pliocene)	Subsidence of Canada Basin and its margins
Erosion surface	
Paleogene and Neogene (Oligocene–mid-Miocene)	Canada Basin subsidence and extension
Angular unconformity	
Paleogene (mid-Paleocene–late Eocene)	Eurekan and Beaufort thrust-fold belts
Downlap surface	
Early Cretaceous–Paleogene (Aptian–mid-Paleocene)	Subsidence of Canada Basin and its margins
Flooding surface	
Middle Jurassic–Early Cretaceous (Aalenian–Aptian)	Rifting within and marginal to Canada Basin
Regional unconformity	
Mid-Permian–Lower Jurassic (Roadian–Toarcian)	Subsidence of ancestral Sverdrup Basin
Regional unconformity	
Early Carboniferous–Mid-Permian (Viséan–Roadian)	Basin margin inversions: rifting of ancestral Sverdrup Basin
Angular unconformity	
Latest Devonian–Early Carboniferous (Famennian–Viséan)	Formation of thrust-fold belts in the Franklinian foreland
Erosion Surface	
Middle–Late Devonian (Eifelian–Famennian)	Foredeep and foreland clastic wedge
Downlap surface	
Early Devonian (Lochkovian–Eifelian)	Drowning of Prince Patrick Bank (Kitson Formation)
Flooding surface	
Vendian?–Silurian	Canrobert Trough, Crozier High and Prince Patrick bank formed
Angular unconformity	
Proterozoic?	extension phase(s)

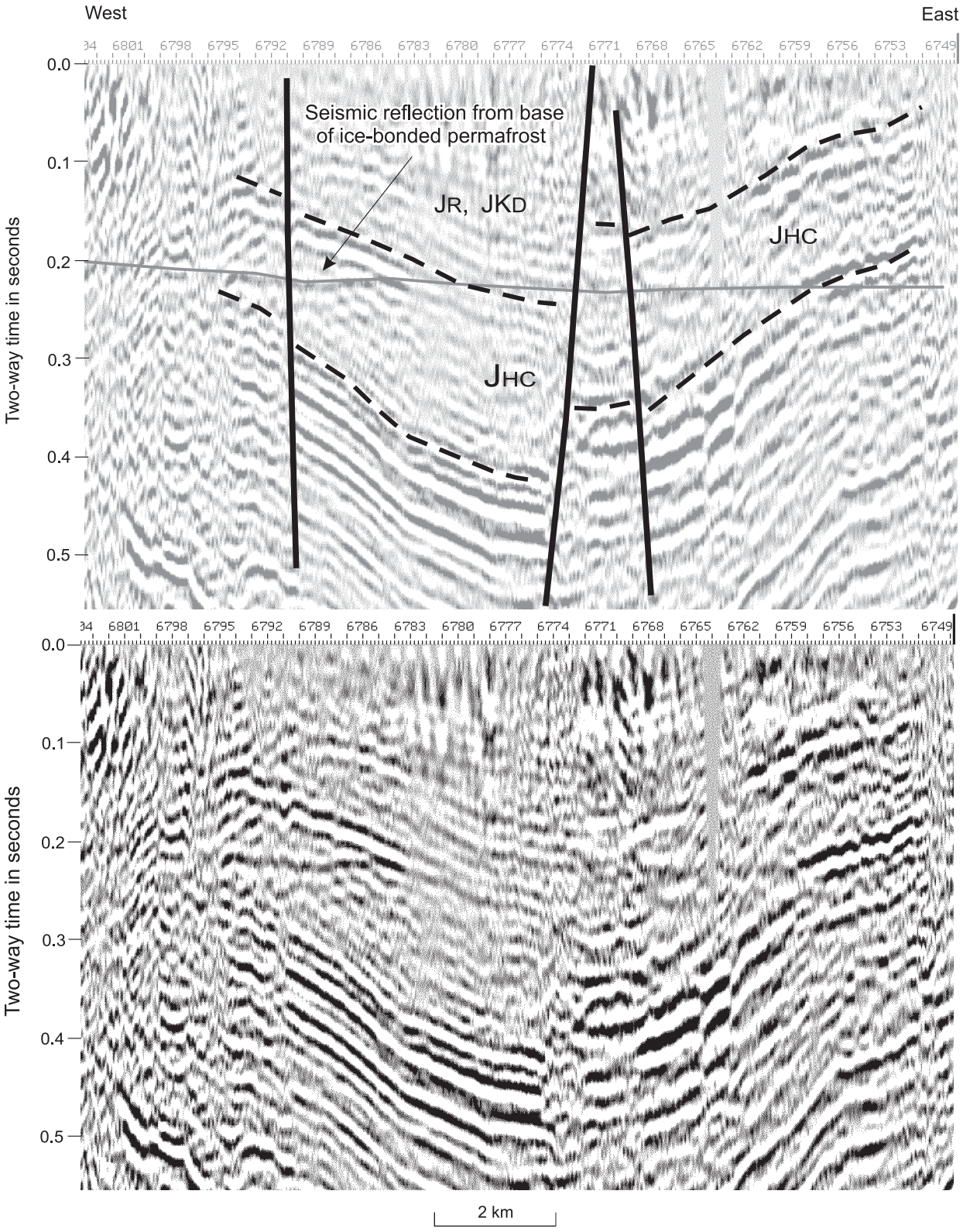

Figure 15. *Seismic expression of the downdip limit of ice-bonded permafrost and a base of permafrost reflection in Middle Jurassic sandstone (*JHC*: Hiccles Cove Formation) of central Prince Patrick Island on a portion of Panarctic seismic profile P467. The 35% reduction in interval time-thickness of the Hiccles Cove Formation above 200 ms is attributed to the higher velocity of the ice-bonded sand. Note also the abupt change in amplitude of primary reflectors passing through the base of permafrost. Profile is located on Figure 14.*

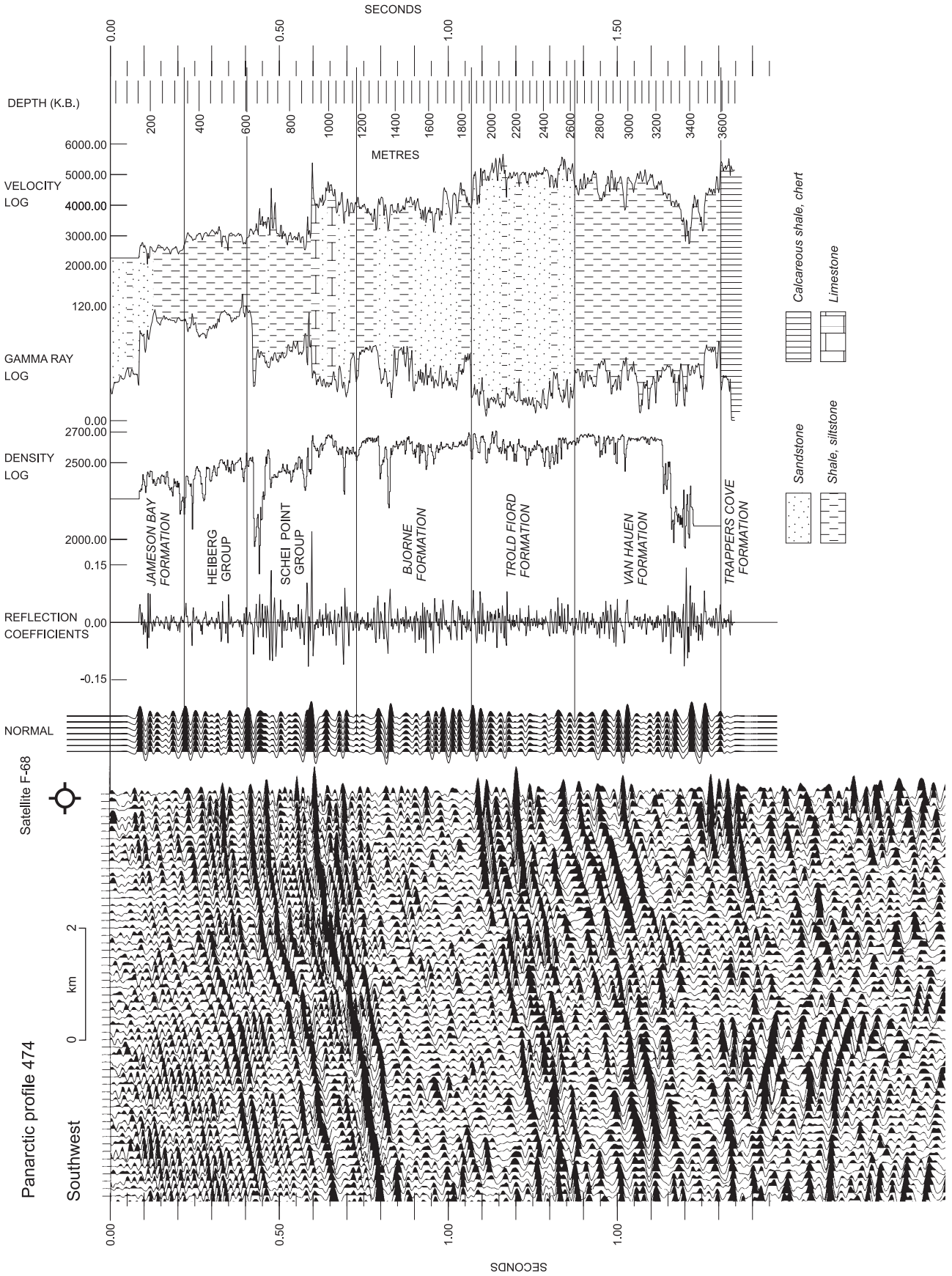

Figure 16. *Correlation of well logs to a portion of Panarctic seismic profile 474 for the BP et al. Satellite F-68 well, northeastern Prince Patrick Island (see Fig. 14 for location). Quality of correlation is very high in contrast to that observed elsewhere.*

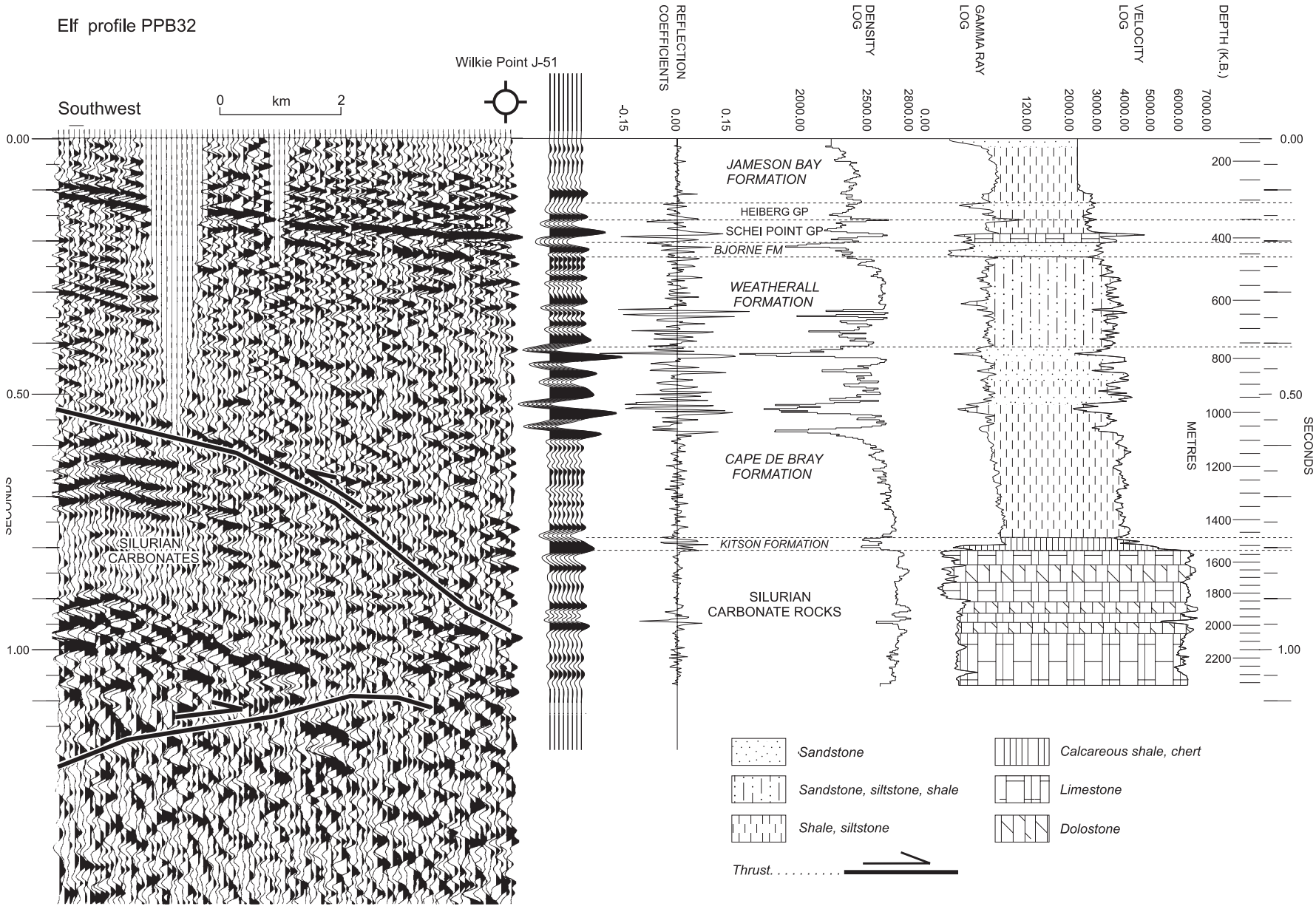

Figure 17. *Correlation of well logs to a portion of Elf seismic profile PPB32 for the Elfex et al. Wilkie Point J-51 well, east-central Prince Patrick Island. Poor quality of correlation may be attributed to inadequate redundancy of trace gathers on profile PPB32, local deformation and perhaps brecciation in Devonian and older strata below the Bjorne Formation.*

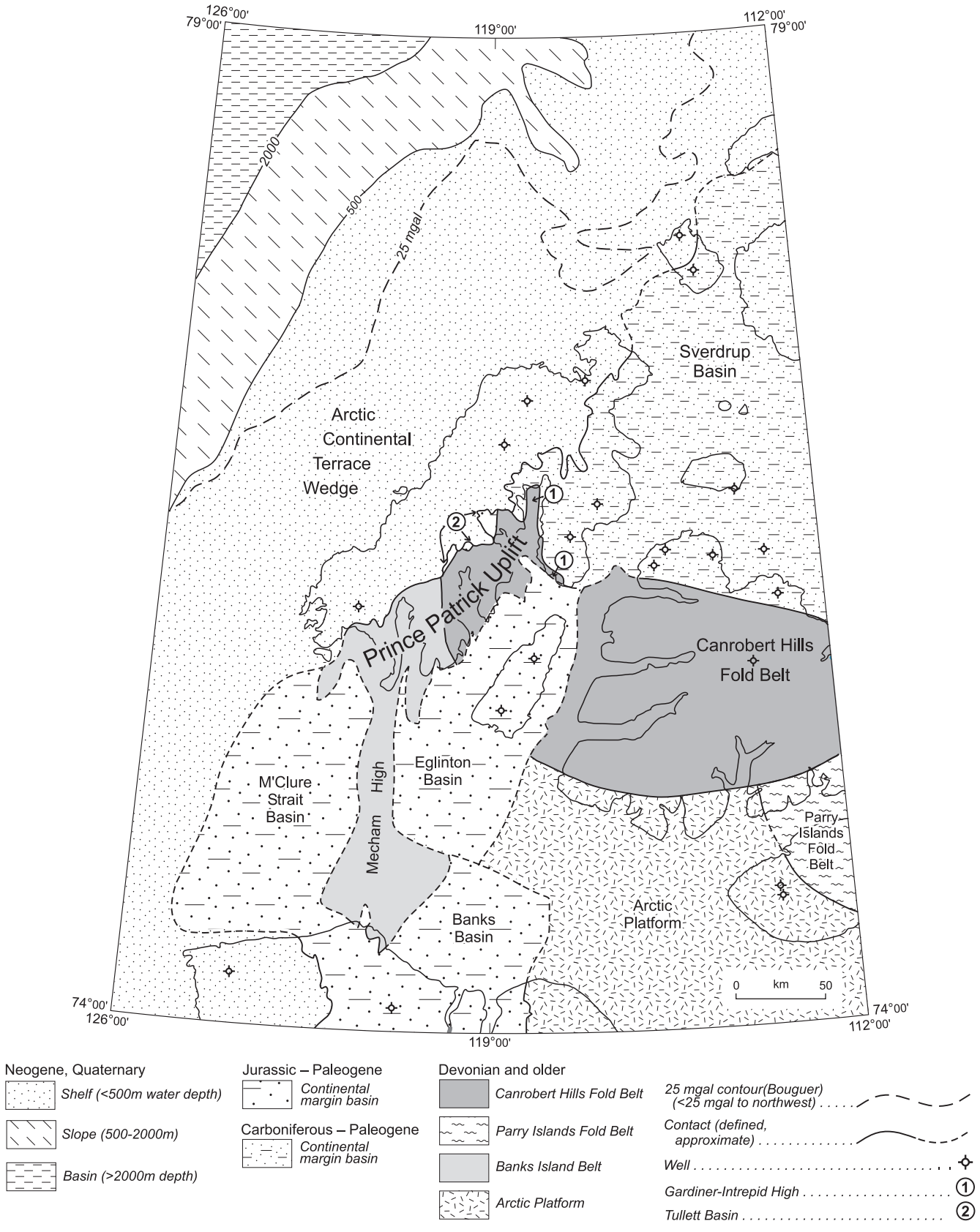

Figure 18. *Geological regions of the western Queen Elizabeth Islands and adjacent portions of the Arctic continental shelf. Thick development of the Arctic Continental Terrace Wedge is assumed to exist on the shelf outboard of the -25 mgal Bouguer gravity contour.*

deposits exposed on northwestern Brock, Borden and Banks islands. The wedge is assumed to continue out to the present continental shelf edge, defined by the 500 m isobath some 80 to 120 km northwest of the island. The continental slope extends from 500 m to about 2000 m water depth and is 53 to 65 km wide. A refraction profile from Mould Bay to the basin floor 200 km west of Houghton Head shows that the crust thins from 28±4 km under the island to 15±9 km under the basin (Berry and Barr, 1971). The continental crust is also assumed to be substantially thinned in those areas of the shelf where the Bouguer anomaly exceeds +25 mgal. The lower contact of the terrace wedge, widely exposed on the east side of Prince Patrick Island, is a sinuous and fluvially dissected southeast-facing escarpment of unconsolidated sand and gravel lying with pronounced angular unconformity on variably deformed strata of Late Devonian through Early Cretaceous age.

The Sverdrup Basin

Strata of Late Triassic through Early Cretaceous age, assigned to the Sverdrup Basin, are exposed southeast of the Arctic Continental Terrace Wedge. Exposures are situated north of Salmon Point on the west side of Intrepid Inlet, and on all land areas and unnamed peninsulas from Cape Canning (on the east side of Intrepid Inlet) to near Cape Krabbé on the north coast of the island. Strata of the Sverdrup Basin also subcrop on the seafloor of Ballantyne Strait (southwest of Brock Island) and Fitzwilliam Strait. The Sverdrup Basin, which contains more than 6500 m of section within the report area, also includes subsurface Carboniferous and Permian strata.

Continental margin basins

Eglinton Graben, hereafter referred to as Eglinton Basin, is up to 73 km wide, has a northerly trending long dimension of 165 km, and contains up to 2000 m of Middle Jurassic through Upper Cretaceous strata. The term "Eglinton Graben", widely used in the literature since the 1950s, has been abandoned in the present account because this structure lacks classic graben characteristics. The old term is also abandoned to avoid confusion over the distinction between this large, complexly faulted basin-shaped structure and smaller half-grabens, of which there are many within the report area. Strata of Eglinton Basin are everywhere exposed on Eglinton Island. The preserved limits have also been mapped to the east on the floor of Kellett Strait, where Jurassic strata lie unconformably on open folded Devonian strata of the Franklinian Mobile Belt or on relatively undeformed strata of the Arctic Platform. The west side of Eglinton Basin lies in a broad zone of intense faulting that runs the length of Crozier Channel.

M'Clure Strait Basin, with more than 600 m of Cretaceous(?) and/or younger section, lies entirely offshore in the mouth of M'Clure Strait and is imaged on marine seismic profles in Dyer Bay and south of Cape Manning. Gravity data suggest that the basin underlies an area of at least 12 000 sq km. M'Clure Strait and Eglinton basins are both indirectly connected with Banks Basin, which Miall (1979) has shown to contain more than 1800 m of Lower Cretaceous through Eocene strata on northern Banks Island

Tullett Basin, with up to 1600 m of Lower Jurassic through Cretaceous strata and erosional remnants of older Mesozoic section, is almost entirely covered by the Arctic Continental Terrace Wedge of western Prince Patrick Island. Related exposures of the basin margin occur west of Green Bay and at the head of Mould Bay.

Inter-basin highs

The term Prince Patrick Uplift is retained for a broad, high-standing block that was elevated at various times in the later Jurassic, Cretaceous and Paleogene. The exposed portion of the uplift lies between Eglinton Basin and the Arctic Continental Terrace Wedge sediments of southeastern Prince Patrick Island. The "basement" section within the uplift features exposures of Devonian strata on both sides of Intrepid Inlet as well as similar more extensive exposures that extend to the south as far as Dyer Bay. The north end of Eglinton Basin is separated from the southern margin of the Sverdrup Basin by the southeasterly plunging Gardiner-Intrepid High situated in the offshore south of Wilkie Point. This structure extends to the north beneath Intrepid Inlet and into the subsurface where it is a prominent north- and northwest-trending raised block within the western margin of the Sverdrup Basin. This high also marks the approximate eastern limit of Jura-Cretaceous horst and graben tectonics associated with Eglinton and Tullett basins and Prince Patrick Uplift.

A third high block lies almost entirely in the offshore. Eglinton and Banks basins are separated from M'Clure Strait Basin to the west by the 180 km long, northerly-trending Mecham High. Defined by gravity and some seismic data, the high is believed to extend across M'Clure Strait to an inlier of Devonian strata on the north coast of Banks Island.

Jurassic-Cretaceous rift-related structures

Extending throughout the Prince Patrick Uplift are a series of eight, small, northerly-trending, named grabens and half-grabens, and many other fault blocks and unnamed erosional remnants of Jurassic and Cretaceous strata. Some

of these structures and the associated bounding faults also continue to the south into Crozier Channel, where they have been mapped within the western flank of Eglinton Basin.

Lower Paleozoic deformed belts

Compressively deformed elements of the Franklinian Mobile Belt of the Canadian Arctic Islands are illustrated in Figures 18 and 19, and in the report area include 1) the salt-based Parry Islands Fold Belt, which terminates on central Melville Island; 2) the northwest-trending Canrobert Hills Fold Belt with an intensely deformed inner subdomain and a broadly folded outer subdomain (Harrison, 1995); and 3) the Banks Island Belt. The latter is a northerly trending belt of tilted, broadly folded and otherwise compressively deformed and peneplained Devonian and older strata that underlies extensive, near-flat-lying Jurassic and Cretaceous cover of western and northern Banks Island, M'Clure Strait and parts of the report area (Harrison and Brent, 1991; Harrison, 1995).

Maps provided with the present report also show that the exposed Devonian section within Prince Patrick Uplift is broadly folded, locally thrust faulted, and everywhere peneplained at surface beneath either flat-lying or gently inclined Mesozoic strata. Northwest-trending folds in the northeast part of the uplift are included in the Canrobert Hills Fold Belt whereas other folds, to the southwest around Dyer Bay, are included in the Banks Island Belt. Sandwiched between these two folded belts is a broad, flat-bottomed synclinorium potentially linked to the northern extremity of the Arctic Platform.

Subsurface structural elements

Mesozoic and Cenozoic features

Considered here are additional geological features of regional significance that have been revealed by subsurface mapping utilizing reflection profiles from the Continental Terrace Wedge of western Prince Patrick Island. Features illustrated on Figure 20 include those shown on Figure 18 as well as others projected to surface through cover of the Pliocene Beaufort Formation. In the northeast, the Sverdrup Basin is seen to extend beneath cover to the north coast of the island to the limits of data along the north coast. Sverdrup Basin strata also extend beneath the Beaufort Formation in Ballantyne Strait. The subcrop of Devonian strata beneath the Beaufort Formation is more limited in extent. A small area of subcropping Devonian strata is likely west of Green Bay. However, in most areas, the west side of Prince Patrick Uplift, defined by the limit of continuous unconformable cover of Jurassic and Cretaceous on the Devonian, is also close to the southeastern erosional limit of the Beaufort Formation. Nevertheless subsurface mapping reveals that the Devonian is much more extensive directly beneath the Pliocene in most onshore areas of southwestern Prince Patrick Island and the Prince Patrick Uplift must turn to the north in the subsurface north of Dyer Bay. The northern and western limits of this uplift are unknown as there have been no seismic surveys conducted anywhere on the westernmost peninulas of the island, in Bloxsome Bay, in western M'Clure Strait, or on the continental shelf.

The most significant new feature defined by sub-Beaufort mapping is the onland extent of Tullett Basin. It is similar in shape and geological character to the Eglinton Basin located on the opposite side of the Prince Patrick Uplift and underlies an area of at least 5500 km^2. Three of the smaller half-graben basins mapped at the surface within the uplift probably also extend to the north into Tullett Basin. Other grabens and half-grabens lying within Tullett Basin, four of which have been named in this account, are entirely covered by Continental Terrace Wedge strata. The eastern subsurface limit of Jura-Cretaceous horsts and grabens within and peripheral to Tullett Basin is partly defined by the subsurface continuation of the Gardiner-Intrepid High.

Upper Paleozoic rift system

Reflection profiles and five exploratory wells indicate that an upper Paleozoic rift system, partly exposed at the base of the Sverdrup Basin in the eastern and central Arctic Islands, extends to the west from northern Melville Island to subsurface northeastern Prince Patrick Island (Beauchamp et al., 2001). The extent of this belt is defined by the southwestern limit of Permian and Carboniferous strata beneath conformable Triassic cover (Fig. 21). The rift belt features 1) an inner system of grabens and horsts blocks to the northeast that contain Lower Carboniferous (Serpukhovian) through Lower Permian rift-fill and overlying post-rift deep shelf and basin facies strata; and 2) an outer portion to the southwest featuring Upper Carboniferous rift-fill partly inverted and covered by shallow-shelf sediments during the Early Permian. The upper Paleozoic rift system has been constructed on the eroded roots of the Canrobert Hills Fold Belt.

Devonian fold belts

The belt of tight plunging folds representative of the inner portion of the Canrobert Hills Fold Belt on western Melville Island (Harrison, 1995) is also continuous beneath Jurassic and Cretaceous cover of Eglinton Basin, beneath Carboniferous and younger Sverdrup Basin sediments, and within and beneath intensely deformed Devonian shale of

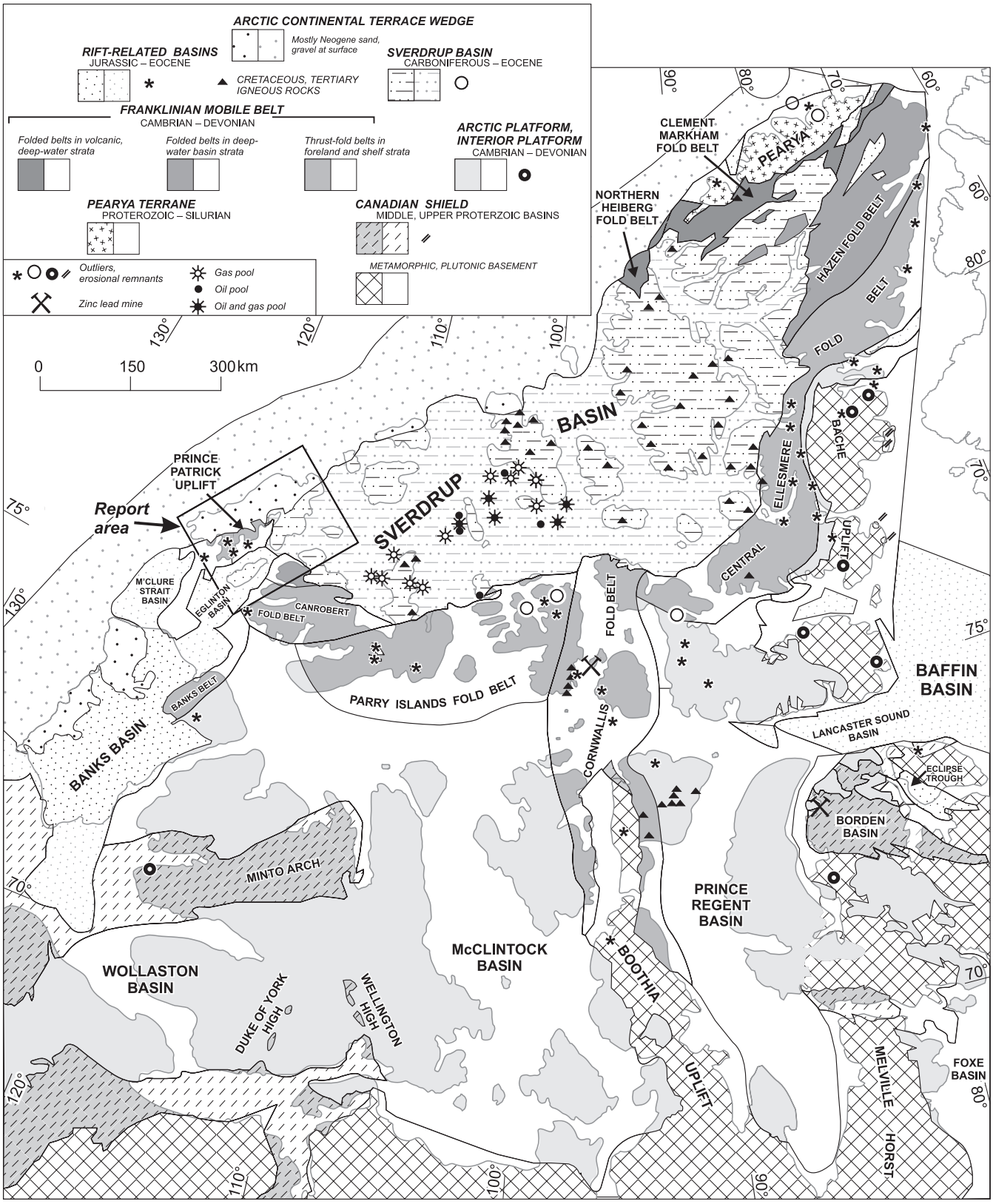

Figure 19. *Geological setting of the Canadian Arctic Islands.*

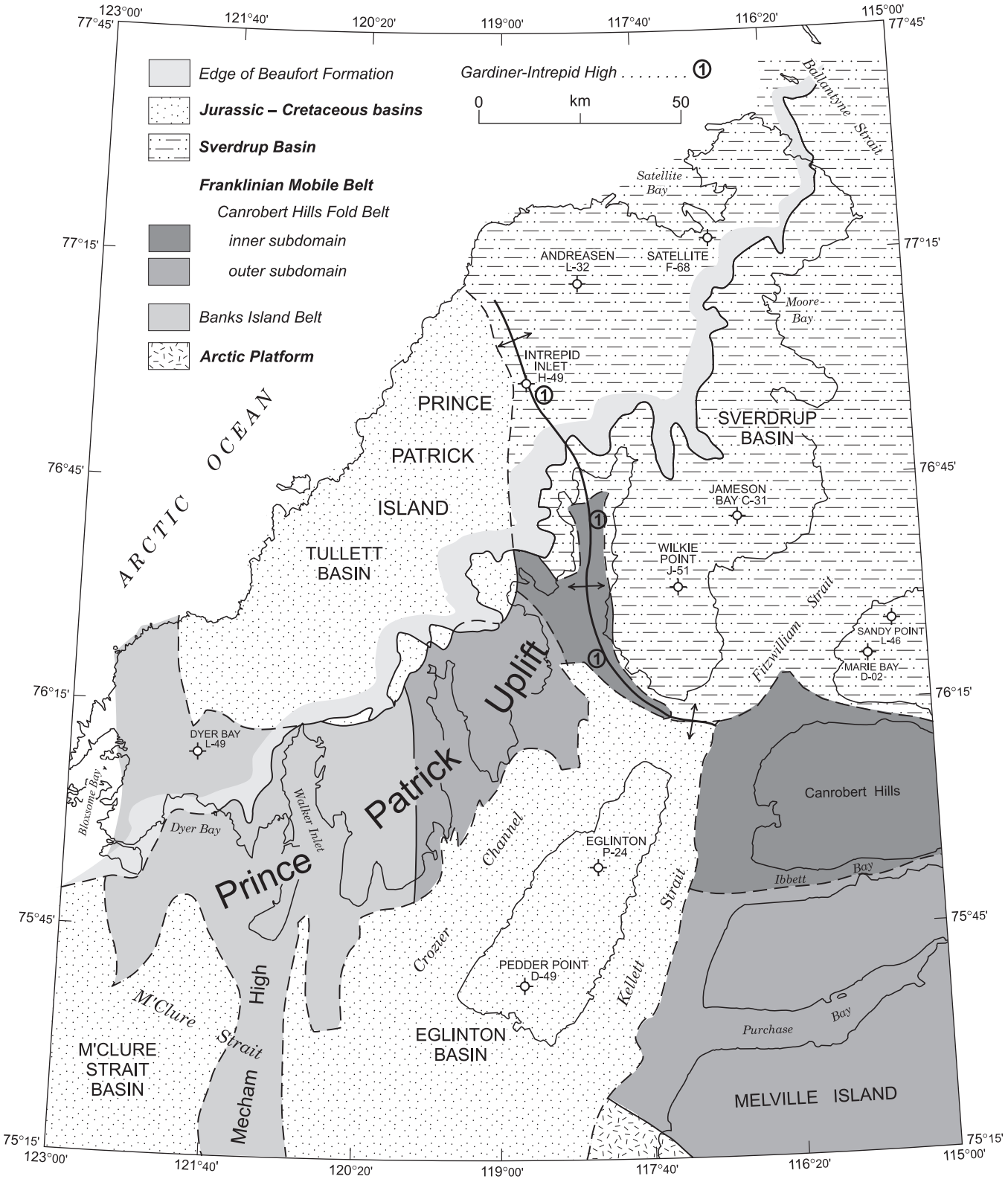

Figure 20. *Geological elements of the report area beneath cover of the Continental Terrace Wedge. In this view, the Pliocene Beaufort Formation and associated Neogene strata have been stripped off.*

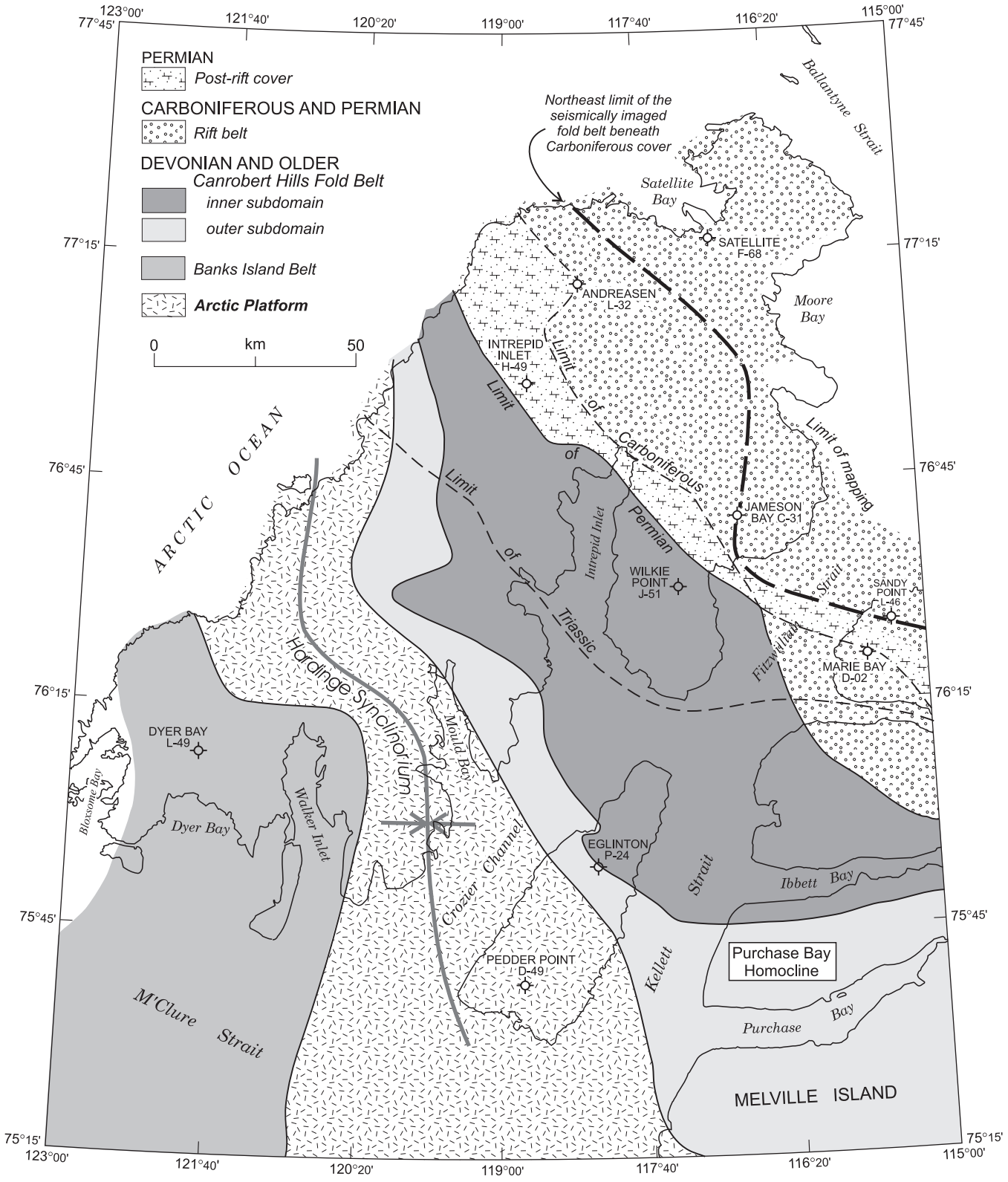

Figure 21. *Geological elements of the report area beneath Carboniferous and younger cover, fold belts, and other major features of the Franklinian Mobile Belt. Also shown are preservational limits for unconformable Carboniferous, Permian, and Triassic strata that lie to the northeast.*

northern Prince Patrick Uplift on Prince Patrick Island. Although lateral variations in lower Paleozoic depositional facies are apparent between these areas within Canrobert Hills Fold Belt, all of these regions would appear to share a common pattern of tight folding, continuity of arcuate structural trend, extensive and deep erosion of Middle and Upper Devonian strata, and superimposed Carboniferous and Permian extensional structures associated with the embryonic development of the Sverdrup Basin. These portions of the inner subdomain of Canrobert Hills Fold Belt are flanked to the southeast by the southerly facing, systematically and gradationally varying, to southwesterly facing, Purchase Bay Homocline (Harrison, 1995). Folds and thrusts also are found within the homocline. However, the scale and intensity of shortening is greatly reduced from that seen farther north and for this reason the homoclinal flexure is included in an outer subdomain of Canrobert Hills Fold Belt.

Regional subsurface mapping reveals that compressive deformation features (anticlines, synclines, thrusts) of pre-Mesozoic but post-Frasnian Upper Devonian age are also present throughout westernmost Prince Patrick Uplift. These features, here included in the Banks Island Belt, are also documented in the subsurface of M'Clure Strait and continue across and throughout the subsurface of western Banks Island (Harrison and Brent, 1991; Harrison, 1995). The nature of the compressive deformation on Banks Island and the specific kinematic links between this area and southern Prince Patrick Island have not been investigated.

The Arctic Platform

Lower Paleozoic fold belts of the western Arctic Islands are flanked to the south and to the east by age-equivalent undeformed strata of the Arctic Platform, which encompasses the flat-lying lower Paleozoic cover on the North American craton. Contacts with the deformed belts are gradational. The Arctic Platform structural province is also believed to extend under southern Eglinton Basin, possibly as far as central Prince Patrick Island beneath Hardinge Synclinorium (Fig. 21). Craton cover in these areas exceeds 10 km in thickness, includes outer-shelf and deep-water realms in the pre-Middle Devonian lower Paleozoic, and foreland siliciclastic units in the later Devonian.

Crozier High

Seismic basin facies realms are believed to exist under Eglinton Island (within the Canrobert Trough of Harrison, 1995) and under southwesternmost Prince Patrick Island. The remainder of Prince Patrick Island to the northeastern limit of seismic resolution within the inner domain of Canrobert Hills Fold Belt is interpreted as an isolated offshore bank referred to as the Prince Patrick Platform. The bank is generally defined by reflection seismic character and is therefore composed of a largely unknown lithofacies assemblage. A platformal carbonate succession of Upper Ordovician and Silurian age has been intersected by two exploration wells in the uppermost part of the offshore bank. The location of the Prince Patrick Platform has been influenced by the pre-existence of Crozier High; a southeasterly trending high block that extends from southwestern Prince Patrick Island to the subsurface of Crozier Channel west of southern Eglinton Island (Fig. 4–6). The high is defined by Lower to mid-Cambrian seismic units ps4 and ps5, which are thinned and overstepped, respectively, by later Cambrian strata (unit ps$\in$O). Crozier High is also defined by southwesterly thinning of seismic units es4 and es6, and possible overstep of seismic unit es5 in Canrobert Trough beneath southwestern Eglinton Island (Fig. 5 and 7).

Proterozoic structure

Refraction seismic data from Berry and Barr (1971) indicate that the Mohorovičić discontinuity and depth to base of crust is 28±4 km under southern Prince Patrick Island. Depth-converted seismic reflection data feature a potential angular unconformity beneath Neoproterozoic (Vendian?) in this same area that lies at 10.7 to 12.4 km depth (cross-section D, attached, and supportive seismic profiles). Elsewhere the Vendian and lower Paleozoic record is thicker and this unconformity surface lies beyond the limit of seismic resolution at 11 to more than 14 km. This implies a thickness of sub-Vendian Proterozoic and older crust that may be as little as 14 to 18 km thick. Normal thicknesses of continental crust in cratonized Archean and Proterozoic shield and thin platform cover areas elsewhere in North America range from 35 to 55 km (Mooney and Braile, 1989).

Interpreted seismic profiles from Melville Island indicate that the Proterozoic was deformed prior to a major pre-Early Cambrian peneplaining event. (In light of recent observations from northeastern Ellesmere Island on the reassigned late Vendian age for the Kennedy Channel and Ella Bay formations, the peneplaining event of subsurface Melville Island would be pre-late Vendian; K. Dewing, pers. comm., 2002). This would account for erosively truncated reflections in the seismic Proterozoic. The extreme attenuation of the Precambrian crust of Prince Patrick Island, to 25 to 50% of normal thickness, has apparently not affected the terminal Vendian(?), Cambrian and younger cover. This appears to support a suggestion that crustal thinning has been accomplished by one or more phases of crustal extension during pre-late Vendian time.

Potential field anomalies

Gravity

A regional Bouguer gravity anomaly map for the islands and offshore is illustrated in Figure 22. General features of the Arctic gravity field are described and interpreted in Sobczak and Halpenny (1990) and Sobczak et al. (1991). Anomalies have been corrected to sea level using a replacement density of 2.67 mg/m^3. Anomaly range is mostly -25 to +25 mgal except on the outer shelf where anomalies range up to +65 mgal, and in deep water (greater than 500 m) of the Arctic Ocean, where anomalies range up to +175 mgal. These latter anomalies are partly attributed to thinned continental crust and the presence of higher density oceanic crust and lithosphere at and/or closer to the surface. Negative anomalies in and between the islands are partly attributed to Jurassic–Paleogene sedimentary basins, as is the case for the gravity lows over central Prince Patrick Island, southern Eglinton Island, and north-central Banks Island. The anomaly in the mouth of M'Clure Strait is also probably accounted for in this way. Some of these negative anomalies and others (for example, the two anomalies over southwestern Melville Island) may be accounted for by excessive thickness of Devonian foreland clastic deposits.

The Emerald Isle area and the inter-island channels east of Prince Patrick Island in the Sverdrup Islands also feature a broad regional gravity low corresponding to the depocentre of the Sverdrup Basin. The gravity low would be even more pronounced and similar to the -15 mgal anomaly over Emerald Isle if a lower, more realistic, replacement density (i.e., 2.2 mg/m^3) were applied to basin areas below sea level.

Gravity highs (-5 to +10 mgal) over the islands and inter-island channels are associated with young uplifts, including those of southeastern Prince Patrick Island lying along the axis of Prince Patrick Uplift, the Cape Mecham Uplift in M'Clure Strait, the Gardiner-Intrepid High, and the Canrobert Hills region of northwestern Melville Island.

Magnetic field

An aeromagnetic map of the islands and adjacent offshore is illustrated in Figure 23 and has been described by Forsyth et al. (1990) and Coles (1991). Anomaly range is -220 to +500 nT. Most areas of western Melville, Eglinton, Prince Patrick and the western Sverdrup Islands including the inter-island channels and M'Clure Strait feature low, long-wavelength, negative, semi-circular to elliptical-shaped anomalies (-100 to -200 nT). Northward-trending, higher amplitude negative anomalies are featured in the mouth of M'Clure Strait (-100 to -220 nT) and on Melville Island (see also Harrison, 1995). Semi-elliptical and kidney-shaped, high-amplitude positive anomalies are scattered across the Arctic continental shelf west and north of Prince Patrick Island.

The large area of long-wavelength negative magnetic response is attributed to the great depth to magnetic basement and thick cover of low-susceptibility sediments. Linear anomalies on Melville Island are linked to exposed and unroofed gabbro dykes of Lower Cretaceous(?) age (Harrison, 1995; Balkwill and Fox, 1982). A similar explanation has been postulated for the linear anomalies in the mouth of M'Clure Strait (Forsyth et al., 1990) although the highs do not exceed -100 nT, suggesting a great thickness of sedimentary cover on the proposed dykes. The kidney-shaped aeromagnetic highs on the continental shelf are probably attributable to magnetically susceptible mafic intrusives or volcanic centres either on the seafloor or beneath the Neogene terrace wedge.

FATE OF THE DEVONIAN FOLD BELT WEST OF MELVILLE ISLAND

Introduction

The fate of the Devonian fold belt west of Melville Island has been determined by a combination of field observations, bedrock mapping with the aid of stereoscopic pairs of air photographs, and subsurface evidence as provided by reflection seismic profiles calibrated into local exploratory wells. The evidence includes 1) a regional angular unconformity and thermal break above the eroded roots of deformed Devonian strata, 2) surface and subsurface map- and outcrop-scale folds, and 3) surface and subsurface thrusts and bedding-plane detachments. These and other features of the Devonian orogenic belt have been synthesized from three regional seismic transects, three structural cross-sections, and a structure contour map drawn on the prominent reflector that marks the upper surface of the Silurian carbonate bank succession on Prince Patrick Island and the correlative level within basin facies strata of Eglinton Island.

Angular unconformity above the Devonian

Surface evidence

This section describes the field evidence for an angular unconformity between the Devonian clastic wedge and various post-tectonic formations of Late Triassic and younger age.

1. On Salmon Point, situated on the west side of Intrepid Inlet, subhorizontal Pat Bay Formation (Carnian) rests with modest angular unconformity on the Cape de Bray Formation; the latter with a measured attitude of N50°W/5°SW. One outcrop of the Cape de Bray

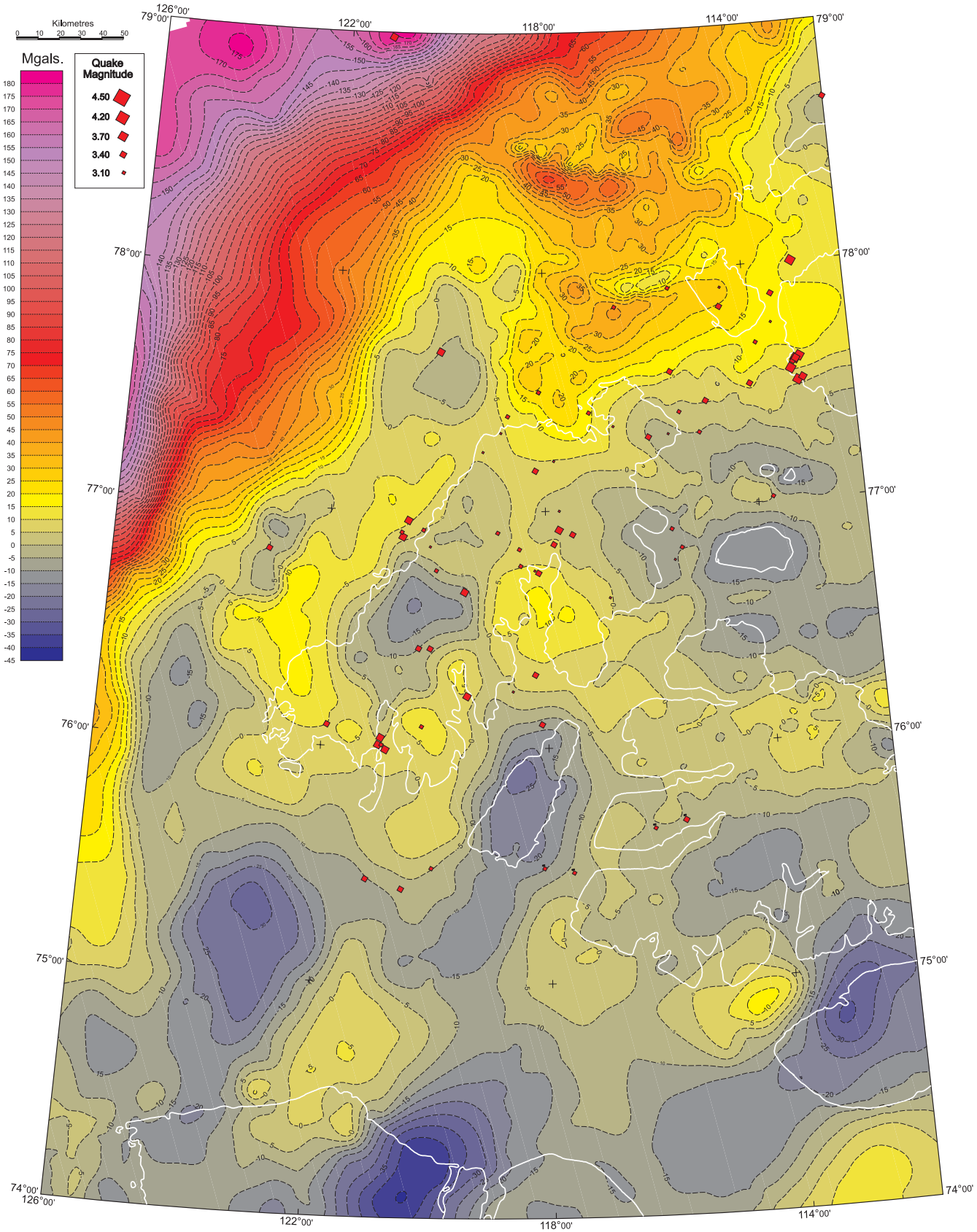

Figure 22. *Bouguer gravity map and earthquake epicentres for the western Queen Elizabeth Islands and adjacent portions of the Arctic continental shelf. Gravity lows centred on Eglinton Island, west-central Prince Patrick Island and northern Banks Island coincide with separate Jurassic–Cretaceous age saucer-shaped basins. The gravity low in the mouth of M'Clure Strait is assumed to be another similar basin (M'Clure Strait Basin) part of which has been imaged on marine seismic profiles south of Prince Patrick Island.*

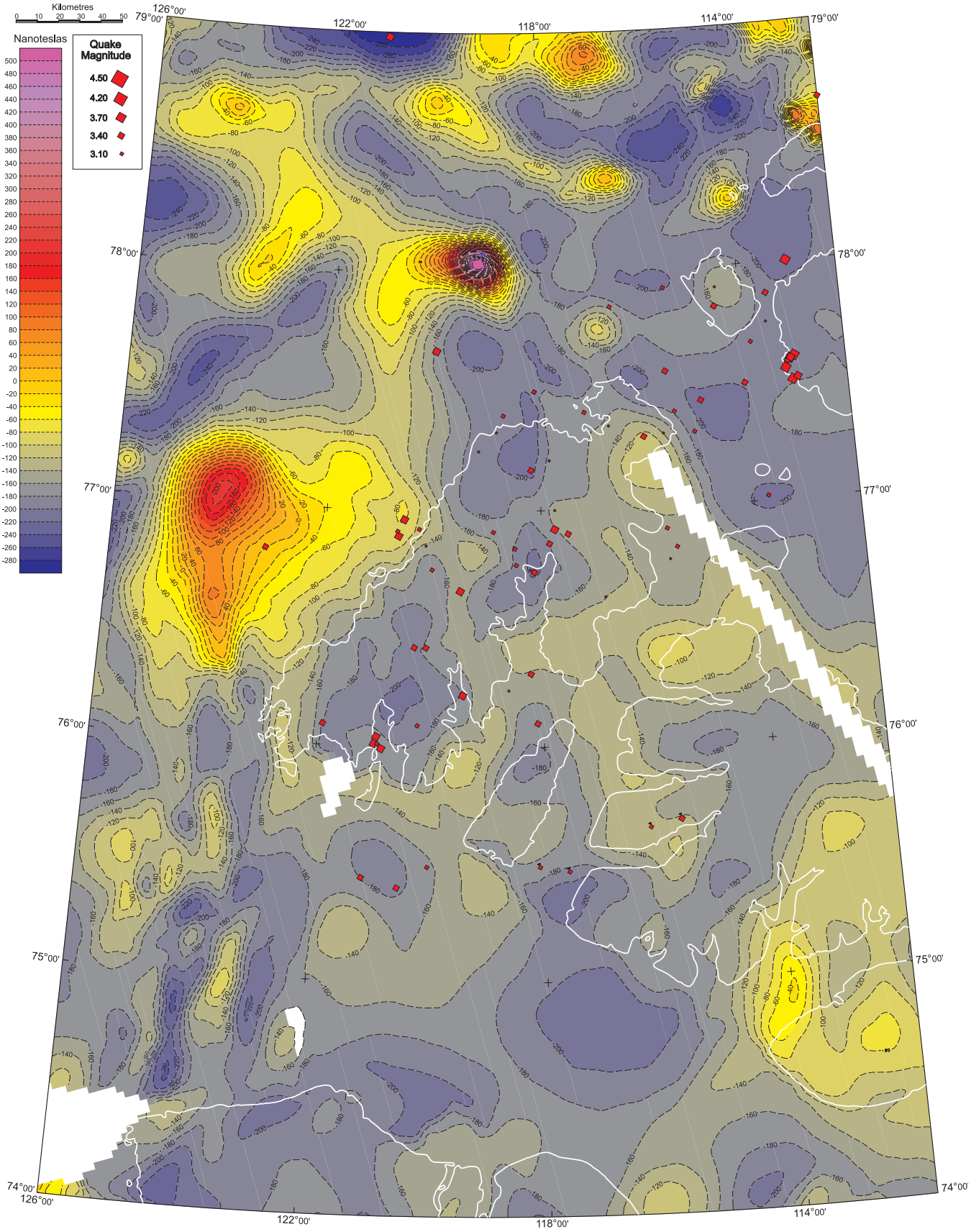

Figure 23. *Total magnetic field map for the western Queen Elizabeth Islands and adjacent portions of the Arctic continental shelf. Elliptical magnetic highs on the shelf are assumed to be either mafic volcanics or intrusives situated at a shallow depth below the Neogene Continental Terrace Wedge. Lower amplitude, north-trending, linear magnetic anomalies in the mouth of M'Clure strait have been interpreted by Forsyth et al. (1990) to be part of a Cretaceous mafic dyke swarm.*

Formation in this area features tight to isoclinal and recumbent minor folds and incipient cleavage development in thin-bedded shale and siltstone. The folds have westerly trending axial planes and are overturned to the south.

2. Five km east of the Mould Bay weather station are exposures of Devonian strata in the upthrown footwall of the Station Creek Fault. Bedding attitudes in the Weatherall and Beverley Inlet formations (Frasnian) include N80°E/10°S and N85°E/16°S. The Devonian here is overlain with pronounced angular unconformity by Toarcian strata of the Jameson Bay Formation, which strikes northerly and dips to the east at about 5°. Elsewhere, 6 km west of Disappointment Point, an angular unconformity separates flat-lying Toarcian beds from Devonian rocks with apparent dips of 12° (Fig. 24). A similar angular relationship, between the Devonian Weatherall Formation and the Jurassic cover, exists in two areas east of the head of Mould Bay, where the Devonian strikes easterly and the cover strikes to the north. Measured angularity on the unconformity ranges from 11 to 43°.

3. In contrast, the Devonian and Jurassic strata exposed in the hills immediately behind the weather station possess northwesterly strike directions. Dip of cover is northeasterly at 5°. The erosionally truncated Beverley Inlet Formation dips to the southwest at 6 to 42°.

4. Similarly, Devonian Weatherall Formation, exposed in fault blocks north of the head of Mould Bay, dips either easterly or southerly at 11 to 31°. Dip of Jura-Cretaceous cover is variably to the east and north at 4° or less.

5. Outliers of flat-lying Ringnes Formation, situated west of Mould Bay and near the south end of Landing Lake Graben (see Map 2026A), overlie Parry Islands Formation, which is locally inclined to the northeast at 70°. An outlier of flat-lying Ringnes and Awingak formations 5.5 km west of Cape Frederick, overlies Beverley Inlet Formation dipping southerly at 83°. These two examples are unusual and extreme instances of tilted pre-Jurassic strata. In most areas west of Mould Bay, dips in the Devonian strata range from horizontal to about 20° below and between exposures

Figure 24. *Angular unconformity between flat-lying Toarcian Jameson Bay Formation and tilted Middle Devonian Weatherall Formation exposed 6 km west of Disappointment Point. View is to the east with Devonian inclined to the northeast. Site is located on Figure 31(GSCC photo 3820-5).*

of cover. In contrast, bedding in the Jurassic and Cretaceous ranges from horizontal up to about 7°.

Subsurface evidence

Reflection seismic data, considered together with exploratory well information, provides evidence for major tectonic disturbance and peneplaining erosion between the deposition of the youngest preserved Devonian strata and the subsequent overlap by upper Paleozoic and younger beds. This angular unconformity has been imaged in nearly all areas of Prince Patrick and Eglinton islands. Exceptions exist only where data quality is compromised by either the extreme depth of the unconformity (northeast of the Satellite F-68 well) or in most offshore areas, where signal penetration is generally poor and reflectivity of the Devonian clastic formations is weak.

Both direct and indirect evidence for an angular unconformity is provided by the available seismic profiles. Direct evidence includes those areas where inclined seismic reflections in the Devonian succession are truncated by subhorizontal or oppositely inclined reflections from post-Devonian cover (Fig. 25). Less direct evidence for an angular unconformity is provided where subhorizontal post-tectonic cover overlies unreflective Devonian, which in turn overlies oppositely inclined deeper reflections from Silurian and older strata (Fig. 26). In the absence of any contrary evidence, the Devonian is assumed to be deformed in a fashion similar to that observed in the older strata.

Data in the following examples have been assembled from measurements and geometric calculations performed on thickness isochron maps of the Devonian clastic wedge (100 ms contours) and similar data sets of the cover succession.

Eglinton Island

Although Devonian strata are entirely hidden by continuous cover of Jurassic and Cretaceous strata of Eglinton Island, seismic and well data indicate the widespread existence of a pronounced pre-Jurassic tectonic and erosion cycle affecting Devonian and older strata. The critical evidence follows.

1. Toarcian and younger strata (Ro up to 0.65), penetrated by the Eglinton P-24 well, dip to the southwest at 0.9°. These beds lie with moderate angular unconformity on the Weatherall Formation which has yielded Givetian spores (TAI 3+ to 4-; Ro 1.3+). Attitudes of these Devonian beds within a 6 km radius of the well range from N18–56°W and dip to the southwest at 9 to 16°. Minimum thickness of erosively truncated section is 600 m within 5 km of the well.

2. Middle Jurassic strata are also nearly flat lying in the Pedder Point D-49 well (dip 1.2 to 2.0°S). These beds rest with modest angular unconformity on Devonian strata that yield late Givetian to Frasnian spores. The Devonian rocks strike approximately N60°W and dip to the south-southwest at 5.5°. The magnitude of minimum eroded section is small in this local area. However, regional subsurface mapping suggests that more than 4200 m of section have been removed by pre-Jurassic erosion on Purchase Bay Homocline over a distance of 65 km between northern and southern subsurface Eglinton Island (see cross-section A).

Prince Patrick Island

1. Seismic data acquired in the vicinity of Cape Canning on the east side of Intrepid Inlet indicate that the exposed Devonian Cape de Bray Formation in this area strikes N50°W and dips to the northeast at 8°. The post-tectonic Pat Bay Formation dips to the northeast at 0.5 to 1.0°.

2. Lower Triassic Bjorne Formation, and Middle and Upper Triassic Schei Point Group (Ro of 0.6 +- 0.1), in the Wilkie Point J-51 well, rest with profound unconformity on the lower part of the Blackley Formation yielding mid-Eifelian to early Givetian spores (TAI 3+ to 4-; Ro on dispersed organic matter of 2.2+). Thickness of eroded Devonian between the well and Cape de Bray Formation outcrops at Cape Canning is approximately 1230 m over a distance of 18 kms.

3. Cuttings collected from the Intrepid Inlet H-49 well indicate that Permian strata, yielding Wordian palynomorphs (TAI 2; Ro 0.6) rest unconformably on Devonian clastic deposits that have provided early Eifelian to late Givetian spores with TAI 3+ to 4-. Calculated bedding attitudes in the Devonian, within a 10 km radius of the Intrepid Inlet H-49 well, range from N31–39°W and dip to the northeast at 20 to 25°. Local minimum thickness of inclined Devonian section, erosionally truncated by Permian cover (dip 0.5°N) is approximately 2900 m (1.5 seconds at 3.9 km s^{-1}).

4. Similarly, deformed Devonian clastic rocks are also interpreted to exist beneath seismically imaged Carboniferous and younger cover farther north. A Permian portion of this succession was penetrated by the Andreasen L-32 well (Ro 0.7 or less). Attitude of Devonian strata below the subhorizontal cover is N43W/20°SW.

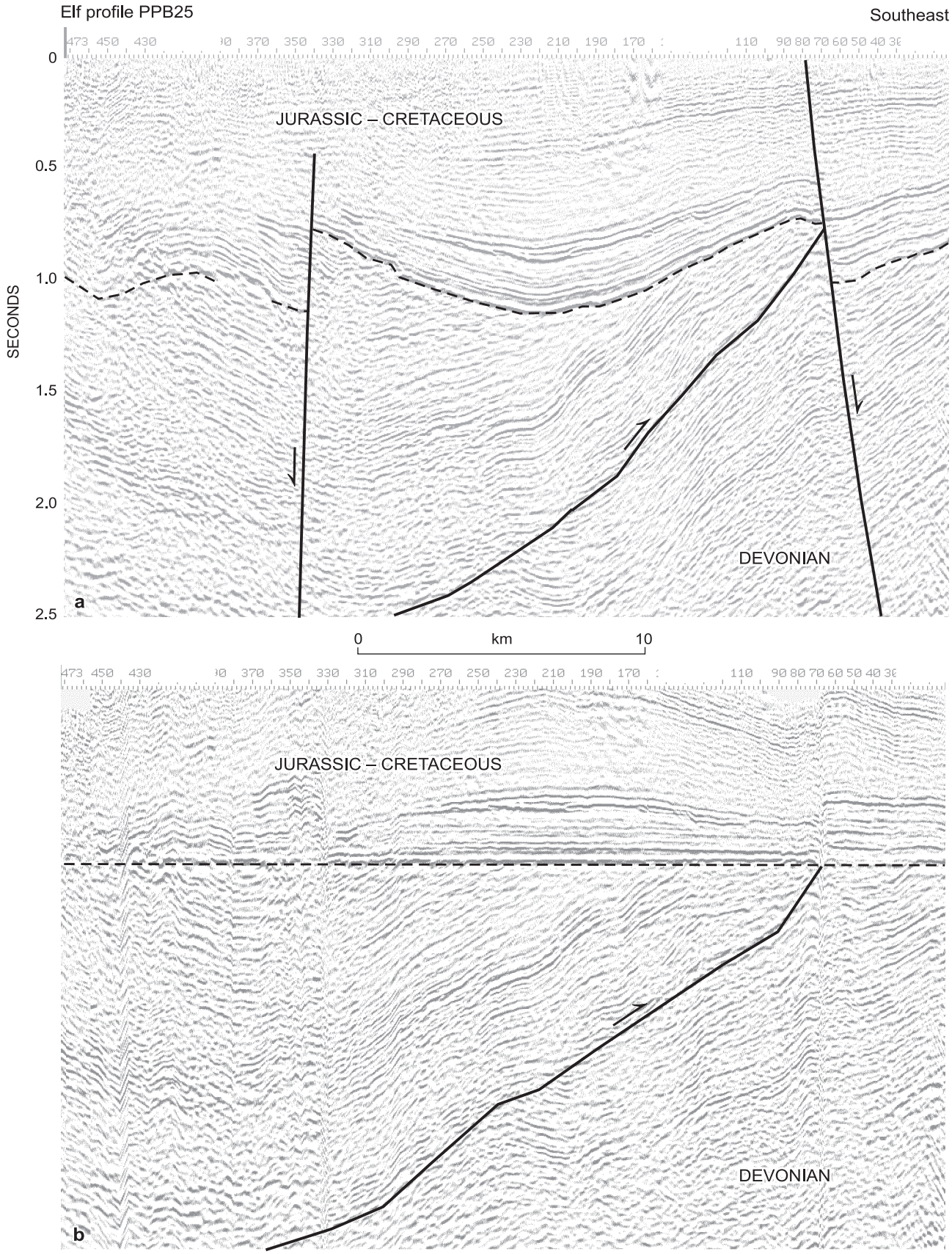

Figure 25. *a) Seismic expression of the angular unconformity between Jurassic and Devonian strata of central Prince Patrick Island. b) A southeasterly vergent thrust of pre-Jurassic age, and synclines in the footwall and hanging wall, are identifiable in the Devonian clastic wedge after flattening on the sub-Jurassic unconformity. Profile is located on Figure 31.*

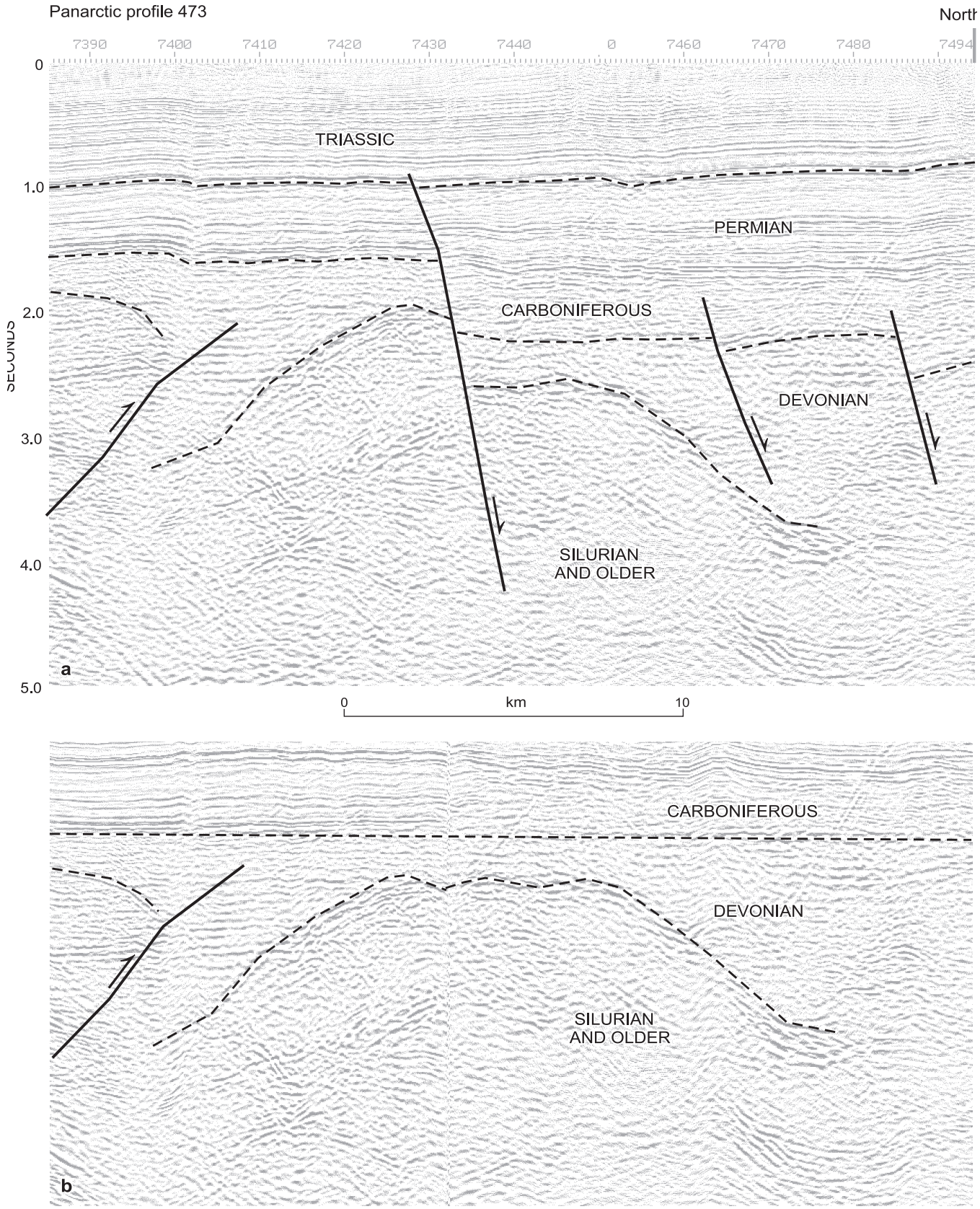

Figure 26. *a) Part of Panarctic seismic profile 473 illustrating some indirect evidence for an angular unconformity between unreflective Devonian strata and subhorizontal Carboniferous cover. b) The anticlinal hinge, imaged above the Silurian in the restored profile, is assumed to extend into the Devonian and to be reduced to a peneplain on the sub-Carboniferous erosion surface. Primaries are partly obscured by horizontal multiples below 1500 ms. Profile is located on Figure 31.*

5. The Beaufort Formation dips to the northwest at 0.8 to 1.4° in the vicinity of the Dyer Bay L-49 well. Mesozoic strata are missing in this area and the Devonian Weatherall Formation directly below the Beaufort, strikes variably N13–22°W and dips southwest at 7 to 16°. Thickness of locally eroded Devonian section is 600 m within 8 km of the well.

6. The most pronounced sub-Jurassic erosion of tectonized Devonian occurs on the southwesterly facing flank of Wilkie Point Anticlinorium. Cross-section D illustrates this significant stratigraphic truncation between 20 and 45 km southwest of the Intrepid Inlet H-49 well. Thickness of eroded section is approximately 4200 m within a radius of 25 km.

Folds

Surface evidence

Poles to measured bedding planes for all stations on Prince Patrick and Eglinton islands are plotted on lower hemisphere equal area stereonet diagrams (Fig. 27). The entire data set for the Devonian of Prince Patrick Island is displayed in Figure 27a. Bedding forms a fairly tight cluster with most dips less than 30° and dip directions ranging from northeast, to east, southeast, south and southwest. Poles to bedding in the Devonian reveal more pronounced trends when split into two geographically separated populations. Bedding poles from Devonian exposures located east of Mould Bay lie on a great circle girdle with an implied, shallow, southeasterly plunging ß-pole trending toward 132/8 (Fig. 27b). In contrast, Devonian exposures located west of Mould Bay possess clustered poles to bedding on a girdle with a more southerly near-horizontally plunging ß-pole trending toward 178/1 (Fig. 27c).

Air photo interpretation and bedrock mapping also reveal a series of fourteen regional-scale folds. These include six regional synclines and eight anticlines affecting only the Devonian succession. Axial trace lengths range from three up to 46 km, the distance being profoundly constrained by the extensive cover of Beaufort Formation and outliers of Jurassic and Cretaceous strata. Trend directions of axial traces fall into two groups: 1) a set trending N27–49°W, plunge toward southeast and northwest; and 2) a set trending N12°W to N18°E, plunge northerly and southerly. The two sets of folds are not geographically separated. Rather there is a mixed distribution of fold trends. Southerly

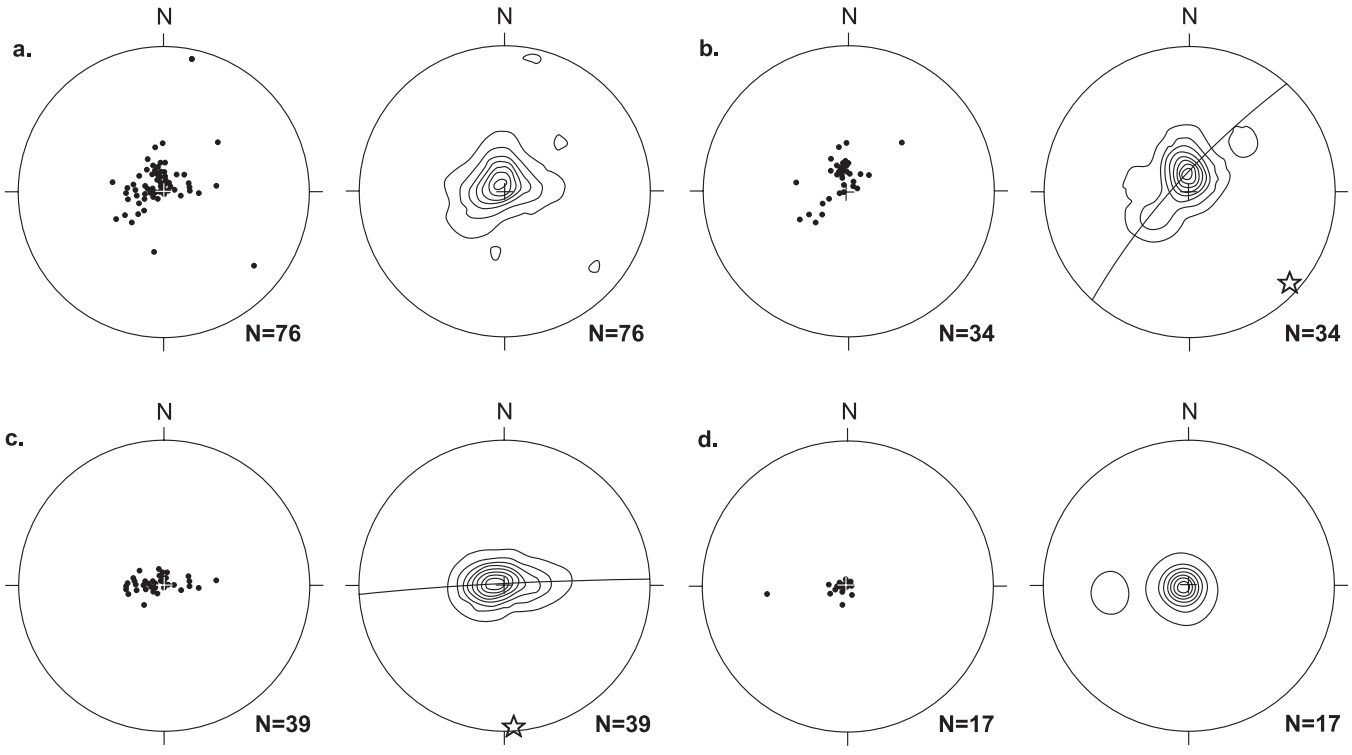

Figure 27. *Lower hemisphere equal area stereonet plots of poles to bedding planes for a) Devonian strata, all sources; b) Devonian strata west of Mould Bay; c) Devonian strata east of Mould Bay; and d) Triassic and younger strata, all sources, including Eglinton Island.*

and southeasterly plunging folds outnumber northerly and northwesterly ones by about two to one. There is uncertainty concerning plunge direction on six. Fold half wavelengths range from less than 2 km to a maximum of 19.5 with an average of 8.9. Axial planes are nearly upright (three folds) or inclined to not less than 80°. For the inclined folds, eight display a westerly to southwesterly asymmetry, two face to the east and the facing direction of one is unknown. Three hanging wall anticlines are also associated with northeasterly and easterly dipping thrusts: a closely spaced pair at the head of Mould Bay (Landing Lake Anticline); the other near Domville Point on the east shore of Dyer Bay (Hardinge Mountains Anticline). Three of the other regionally significant folds are described in more detail below.

A regional syncline occupies nearly the entire Devonian outcrop belt of Weatherall Formation on the eastern half of the peninsula east of Mould Bay. The curvilinear axial trace plunges toward N49°W. The northeastern limb is at least 19.5 km wide and extends as far as Cape de Bray Formation exposures on Salmon Point. The western limb is mostly obscured by post-tectonic Mesozoic cover but may extend 17.5 km to the thrust anticlines at the head of Mould Bay. Thickness of the exposed section erosively truncated by folding and peneplanation is 2800 m.

The largest Paleozoic fold at surface is a syncline exposed on the peninsula west of Mould Bay. It is traceable from Landing Lake in the north to Cape Frederick area in the south. It features a sinuous axial trace trending variably toward S11°E in a northern segment, toward N27°E and toward N13°W over an outcrop length of 46 km. A plunge depression occurs at approximately 76°11'N. The folded and peneplained stratigraphic section at surface is about 1800 m thick and includes Weatherall, Beverley Inlet and Parry Islands formations. The syncline is greatly disrupted by postorogenic cover and by northerly striking faults often oblique to bedding attitudes in the Devonian. The southern end of the syncline dies out in an area that includes two, short-wavelength anticline-syncline pairs.

The regional syncline has a half wavelength of 18 km and extends to the west as far as the axial trace of Walker Inlet Anticline exposed near the northeast shore of Walker Inlet. Plunge on the anticline appears to be toward N09°E. However, structural relationships in the north are obscured by Beaufort Formation and to the south the fold trace extends into Walker Inlet. The anticline faces west with a steep, easterly dipping axial plane. However, locally contrary asymmetry is indicated by a unique hinge area outcrop. The Cape de Bray Formation in this outcrop is locally inclined to 90° on the east-facing limb (Fig. 28),

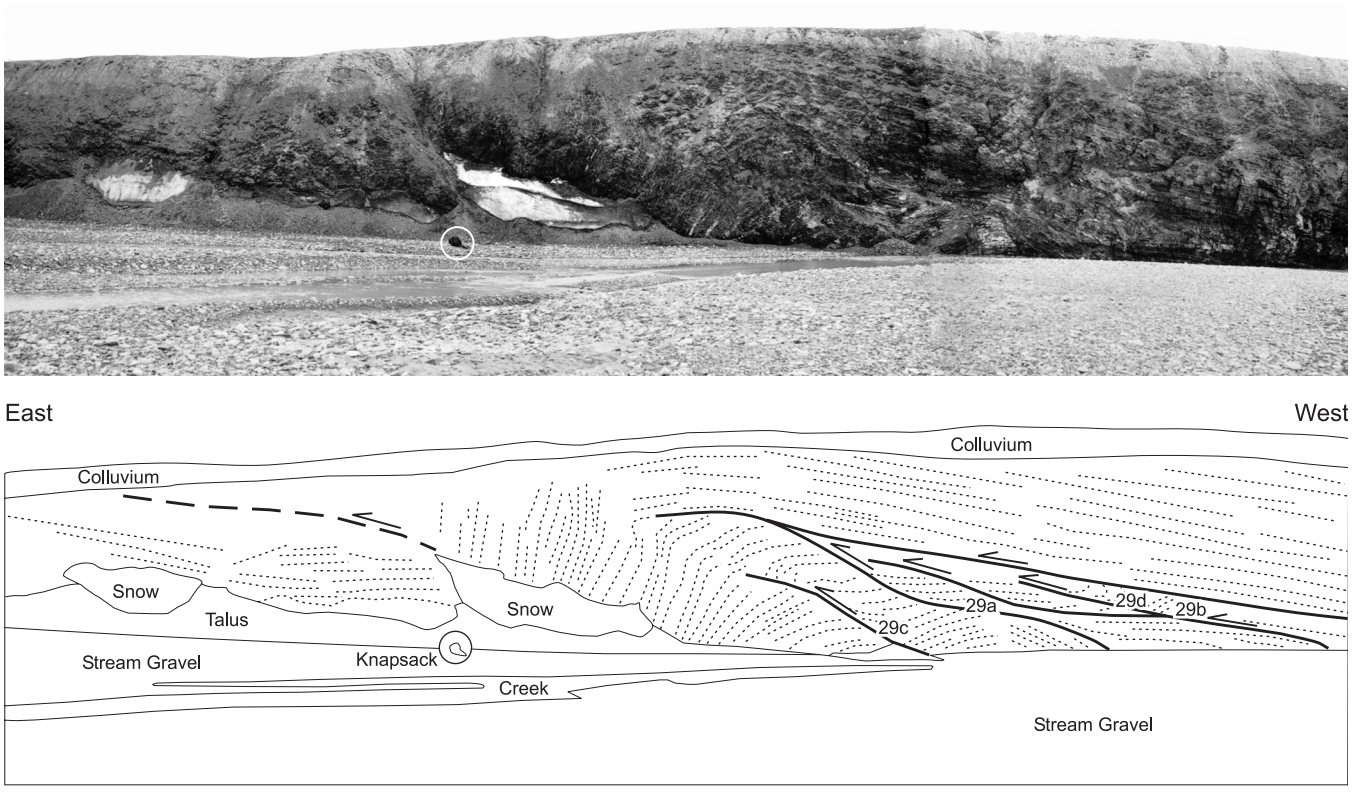

Figure 28. *Anticline hinge exposed in stream bank outcrop of the Cape de Bray Formation, 1.5 km east of the closest part of Walker Inlet (see Fig. 31 for location). Illustrated minor thrusts and this local fold hinge are east vergent although the larger structure displays a west-vergent asymmetry (see also cross-section B, CD-ROM) (GSC photos 3820-89,90,91).*

whereas the west limb dips at not more than 15 to 32°. An extremely tight radius of curvature and incipient cleavage development are key features of the fold hinge. Structural complications within the hinge also provide important supportive evidence for east- and west-directed compressive slip on various minor thrusts (Fig. 29).

Subsurface evidence

Evidence for folding of Upper Devonian and older rocks prior to overlap by Carboniferous and younger strata is also provided by regional seismic profiles and derivative cross-sections (attached). Data are compiled on a time-structure contour map drawn on a widespread reflection near the top of the Silurian (Fig. 30). This map also displays the axial traces of subsurface folds and the linkage of these folds to those mapped at surface on southern Prince Patrick and western Melville islands. The subsurface folds in each case are defined by: 1) the pattern of erosional truncation of dipping reflectors below post-orogenic cover; 2) by the sinusoidal pattern of throughgoing reflectors within the Devonian and older section, most notably the reflection near the top of the Silurian carbonate succession, and; 3) time-structure isochrons on the base of the Devonian clastic wedge (Fig. 30).

Eglinton Island

Regional subsurface folds of Eglinton Island are defined below Jurassic and younger cover. The most obvious of these, underlying the northeast part of the island, are included in the inner subdomain of the Canrobert Hills Fold Belt.

General features of the lower Paleozoic succession of Eglinton Island are described elsewhere in this volume. The Devonian clastic wedge, up to 2700 ms thick, is characterized by numerous, short, subparallel reflection

Figure 29. *Structural complications in the Cape de Bray Formation within the hinge region of a regional anticline near Walker Inlet, same locality as in Figure 28. Minor thrusts are transporting hanging wall section toward the east (left) [GSC photos 3820-82 (a), 3820-3 (b), 3820-8 (c), 3820-1 (d)].*

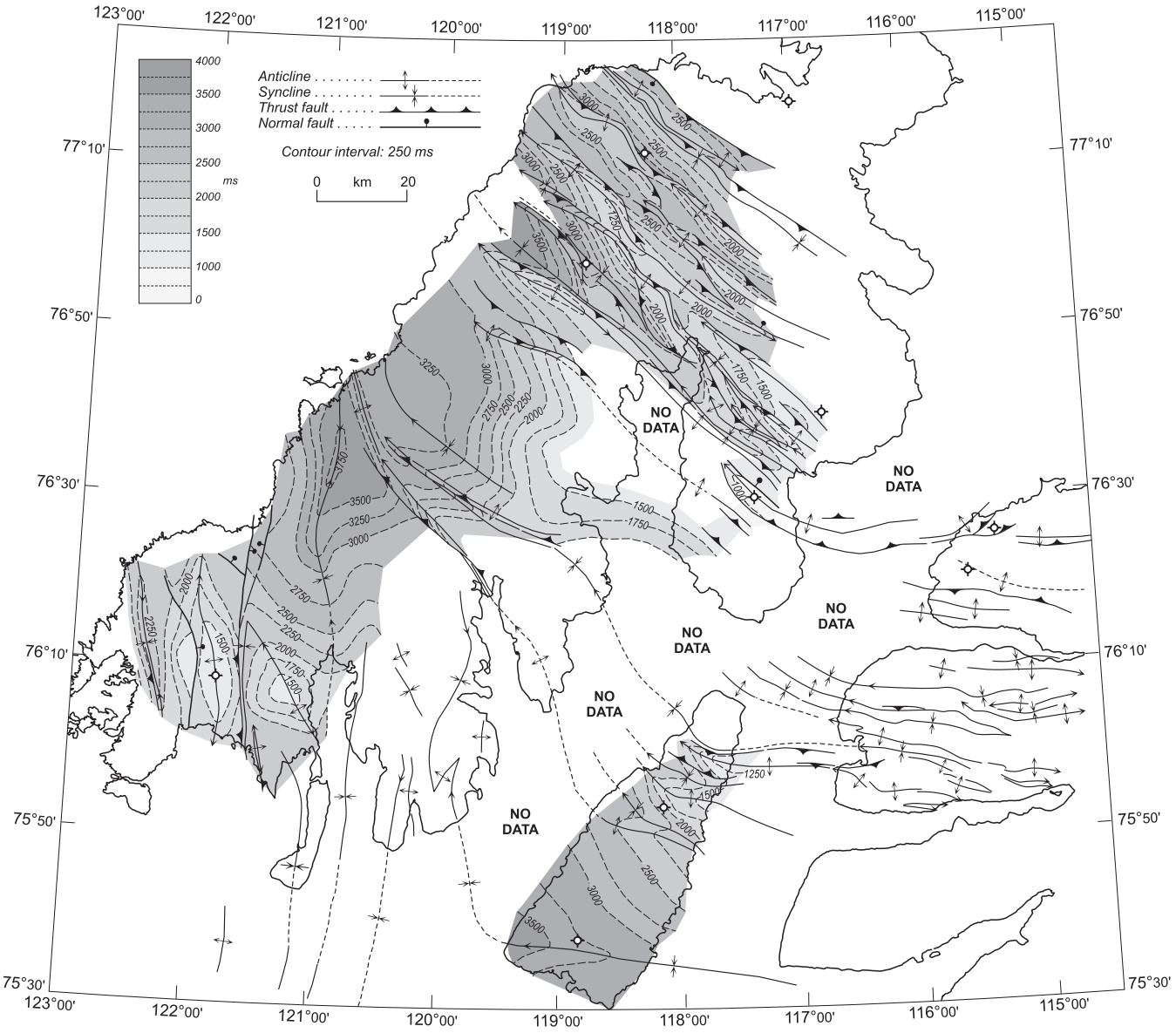

Figure 30. *Time structure contour map (two-way time) constructed on the top of the Silurian together with fold axes and thrust faults of probable Late Devonian to Early Carboniferous age. Fold axes of southern Prince Patrick Island and western Melville Island are compiled from Maps 2026A (included with this volume) and 1844A (Harrison, 1995).*

segments that defy internal subdivision. Seismic response is better in the underlying package of presumed Lower Devonian and older units that range up to at least 2700 ms in thickness (7300 m at 5.4 km s^{-1}). Through-going reflections of variable amplitude, character and spacing permit ready distinction and correlation of seismic units es1 through es6, Canrobert and Ibbett Bay formations (see legend of Map 2026A and cross-section A, attached). Primary signal extends to depths of at least 5.3 seconds. Contrary to expectation, quality of seismic response from the Lower Devonian and older strata is best in the areas of most intense folding and is not as good in the south where the same strata are essentially flat lying but the thickness of the Devonian clastic wedge is greater.

Two regional anticlines and part of a third have been mapped on seismic profiles under the northeastern part of the island with fold crests at 3.9, 18.8 and perhaps 26 km northeast of the Eglinton P-24 well (Fig. 31, cross-section A). The southwesternmost limb of Eglinton Anticline marks the local limit of obvious compressive deformation within Devonian and older strata. Thickness of section involved in folding amounts to at least 1800 ms (3600 m) of Devonian clastic strata and at least 2700 ms (7400 m) of older section. The southwestern limit of deformation is gradational and difficult to define as strata above seismic unit es4 display a regional shallow dip of 3.5° to the southwest (and away from the anticlinal crest) over a fold half-wavelength of up to 40 km. The explanation for this gradational deformation

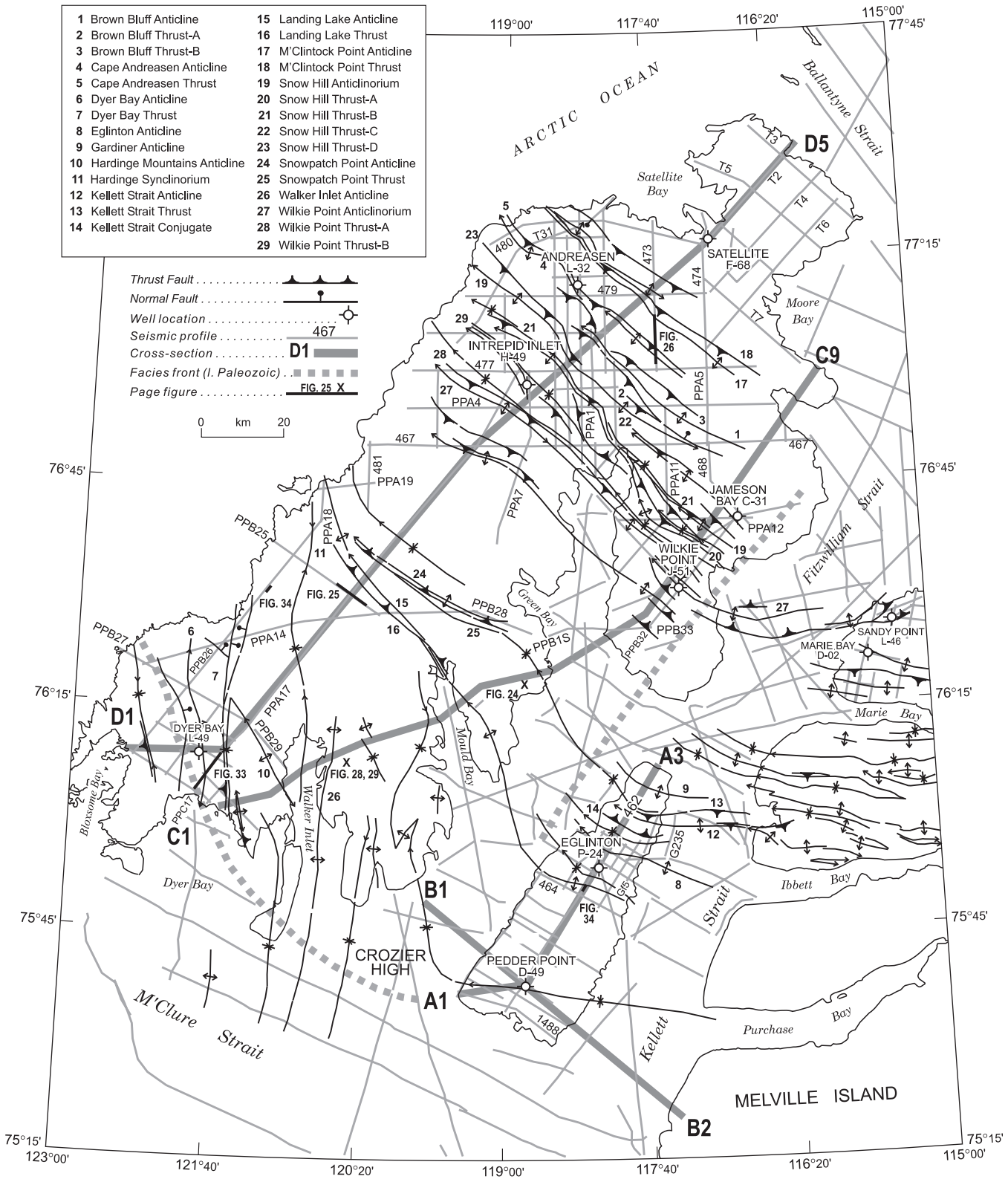

Figure 31. *Named Devonian-Carboniferous structures, position of the early Paleozoic shelf-to-basin transition, seismic profiles and location of related text illustrations.*

limit is offered on cross-section A. Shallow-dipping, southwesterly vergent thrusts are interpreted to exist in the stratigraphic interval between the base of unit es3 and the top of es4. Horizontal shortening has produced a southwesterly tapering duplex within the es3 and es4 interval and an equally wide southwesterly inclination of all overlying strata.

Dips range up to 18° on the southwest limb of Eglinton Anticline and up to 13° on the opposite limb, which indicates a steep northeasterly dipping axial plane and an implied southwesterly direction of tectonic transport. The axial trace of Eglinton Anticline, interpreted on five seismic profiles, is convex and southwest facing, and plunges variably toward N85°W near the east coast of the island to N45°W near the west coast. Thickness of Devonian clastic strata over the fold crest is least near the east coast (550 ms). Axial plunge, defined by time-structure contours on the base of the Devonian clastic wedge, is 560 ms over a distance of 16.5 km or about 4° toward the west and northwest. The favoured model for development of Eglinton Anticline is by transport of section on two oppositely and inwardly dipping thrust ramps that link a deep detachment high in unit es1 to mid-level detachments at the base of unit es3 and near the top of unit es4.

Less is known about Kellett Strait Anticline as it is only imaged in its entirety on two seismic profiles, including Gf5 with cross-section A (attached), and one unmigrated offshore survey (G235 on Fig. 31). Limb dips are up to 21° on the southwest side but may locally range up to 60° or more on the opposite, northeast-facing limb. Thrust faults are interpreted to displace the Ibbett Bay and Canrobert formations on both fold limbs and emerge into the lower part of the Devonian clastic wedge in the unnamed synclines north and south of Kellett Strait Anticline. Post-orogenic erosion has brought the Silurian to within 400 ms of the sub-Jurassic unconformity over the fold crest and to within 1000 and 1100 ms of the unconformity above the adjacent synclines.

Even less is known concerning the nature of Gardiner Point Anticline. The existence of this structure is implied by a southwesterly-facing stratigraphic panel at the northeastern end of seismic profile Gf5, potentially part of a fold limb, and by the geometric necessity of equating deep-seated shortening below unit es3 on this profile with comparable shortening assumed to exist in younger strata off the north end of the same profile.

Western Prince Patrick Island

Broad structural features of western subsurface Prince Patrick Island are provided by a widely spaced grid of high-quality five- and six-second regional seismic profiles (many reprocessed and migrated; Fig. 31 and examples with regional cross-sections C and D, attached). This region includes portions of Purchase Bay Homocline and Hardinge Synclinorium (Fig. 32) as well as large folds north of Dyer Bay that mark the western limit of the synclinorium. The Devonian clastic wedge in this area features five locally mappable seismic units, all readily correlated into adjacent wells and exposed bedrock. The underlying succession, believed to range from at least late Vendian to Early Devonian in age, includes six regionally mappable seismic units and the Kitson Formation (labelled ps1 through psOS and Dk on the legend of Map 2026A and cross-section D). The seismic profiles in the Dyer Bay area, mostly recorded to six seconds, feature all known units down to the sub-Vendian(?) unconformity below four seconds. Below this are potential sequences of previously deformed and peneplained Proterozoic(?) units that extend beyond six seconds. There are fewer profiles on west-central Prince Patrick Island and some of these have only been recorded to five seconds (i.e., profile PPA17). The top of the Lower Devonian is also deeper in this area. Nevertheless, signal penetration is excellent. Some through-going reflectors, such as those from the top of unit ps2 (seismic Kane Basin Formation?; see Fig. 5), extend beyond the base of the profiles.

Potential linkage of five surface folds to equivalent seismically imaged structures is illustrated on Figures 30 and 31.

1. The N49°W-plunging unnamed syncline underlying the peninsula west of Green Bay projects into a syncline axial trace imaged near SP 350 on seismic profile PPA14 and near SP 775 on profile PPA17 (cross-section D). The mapped base of the Weatherall Formation is about two seconds above the seismically defined top of the Lower Devonian where profiles cross the exposed northeast limb of this syncline near Green Bay.

2. The N36°W-trending, southwest-vergent and thrust-faulted Landing Lake Anticline mapped at the head of Mould Bay is also imaged near SP 980 on PPA17 (Fig. 31; cross-section D). Seismic data indicate that folding has affected all lower Paleozoic strata above the middle of unit ps5 (above base of seismic Cass Fjord Formation?; see Fig. 5).

3. A S61°E-plunging syncline on the peninsula west of Mould Bay probably extends into Hardinge Synclinorium, which is imaged on four seismic profiles including PPA17 at SP 1360 (cross-section D).

4. the S42°E-plunging Hardinge Mountains Anticline, exposed in the narrow Devonian outcrop belt on the west side of Walker Inlet, is probably continuous with

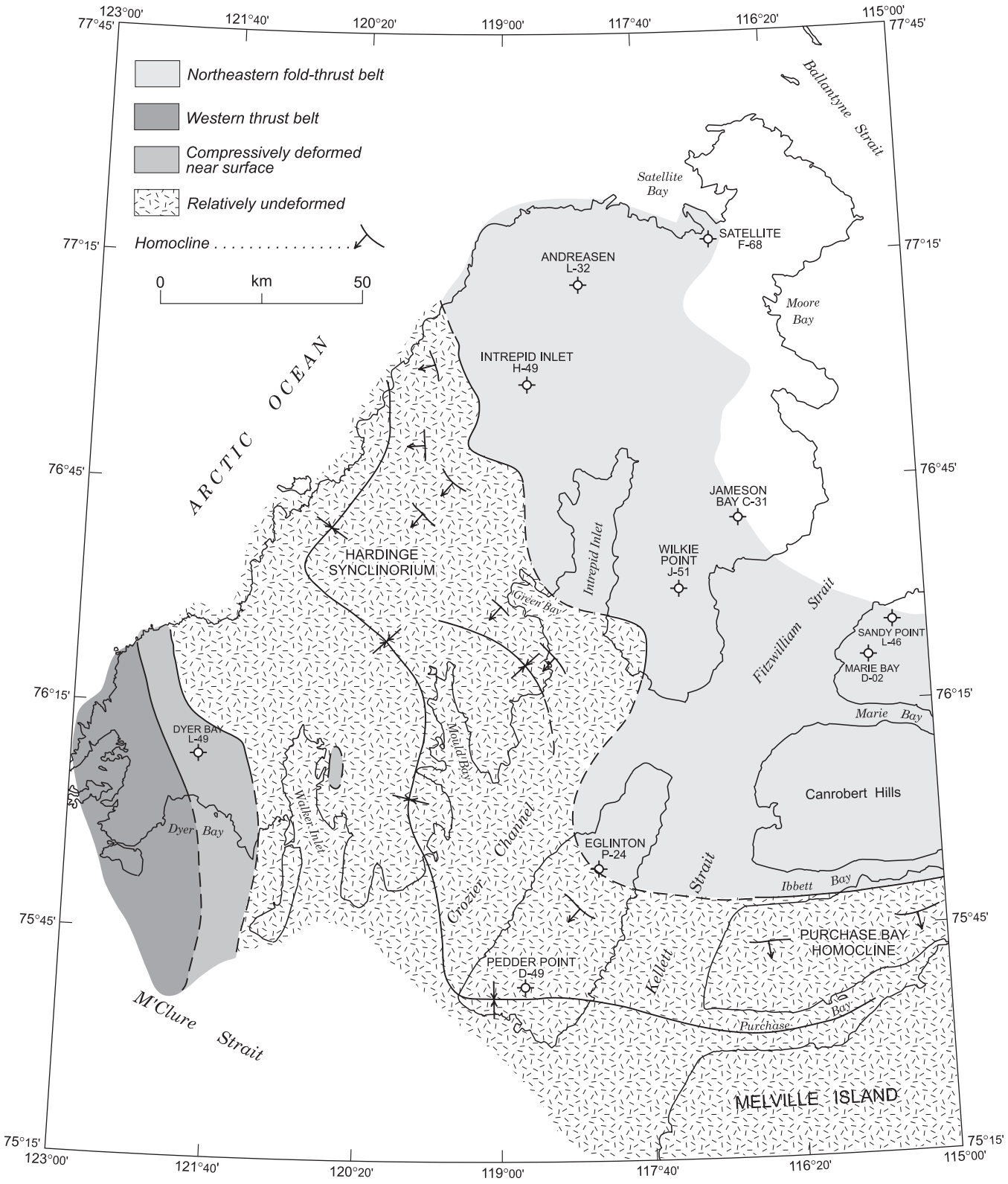

Figure 32. *Tectonic regions of the Devonian clastic wedge. The relatively undeformed region features regional-scale folds and minor thrusts in the clastic wedge. On seismic profiles, this region is distinguished from more intensely deformed areas to the northeast and southwest by the existence of a coherent Middle and Upper Devonian seismic stratigraphy. Areas compressively deformed near the surface lie structurally above these coherent seismic units.*

the anticline imaged near SP70 on PPC17 (cross-section D). An intervening culmination is inferred in the subsurface of the Hardinge Mountains. Folding has affected all lower Paleozoic strata including part of unit ps1 (seismic Kennedy Channel Formation?; upper Vendian; see Fig. 5).

5. The southerly plunging syncline axial trace on Cape Mecham and beneath Wooley Bay is aligned with a narrow and faulted syncline located on six seismic profiles north of Domville Point and east of the Dyer Bay L-49 well (near SP 140, PPC17; cross-section D).

The largest structure in this part of Prince Patrick Island is entirely covered by the Beaufort Formation. This is the Dyer Bay Anticline (cross-section D). The culmination has been drilled at the Dyer Bay L-49 well and the hinge and limbs imaged on a small grid of seven seismic profiles. The entire stratigraphic section from the Vendian to the Devonian has been folded. Fold amplitude is up to 1185 ms (2370 m) measured on thickness of preserved Devonian clastic deposits from the culmination to the axial line of the syncline on the west side. Wavelength is 21 to 23 km measured between axial traces on two bounding synclines to east and west. Anticline plunge to the north of the well is 66 m km^{-1} or about 3.8°. Plunge is more gentle to the south. An east-vergent thrust fault is mapped on the east-facing limb. This is also the direction of transport implied by axial plane asymmetry.

Smaller structures displayed on profile PPC17, and on the west ends of PPB26 and PPB27 include moderate wavelength folds stratigraphically restricted to the Devonian clastic wedge above the limbs of the Dyer Bay Anticline (Fig. 33).

Northeastern Prince Patrick Island

The majority of the mapped folds beneath cover on northeastern Prince Patrick Island have no surface expression, neither can they be traced laterally into known folds mapped at the surface. Most notable is a complex belt of thrust-faulted anticlinoria and synclinoria lying under post-orogenic cover of the Sverdrup Basin. This belt is imaged on seismic profiles located throughout the peninsula east of Intrepid Inlet and in most areas of the island northeast of Green Bay (Fig. 30, 31; cross-sections C and D). The belt is at least 75 km wide and has been imaged over a tectonic strike length of 94 km. It is bound by Hardinge Synclinorium to the southwest, which on profile PPB26 preserves up to 3165 ms (6200 m) of Devonian clastic strata. The limit of the fold-thrust belt to the northeast has not been imaged as a result of the excessive thickness of Sverdrup Basin cover in these areas. Particularly poor is the signal response from the deformed Devonian and older section located east of the Jameson Bay C-31 well. Cover in this area ranges from 2000 to more than 2500 ms. Signal from the pre-Carboniferous is also mostly lost on the single-fold seismic profiles located east and northeast of the Satellite F-68 well where the post-orogenic cover everywhere exceeds 2500 ms in thickness. In these areas, indication of deformation is provided by inclined and erosively truncated reflections beneath seismic Carboniferous. Entirely lacking, however, is a coherent seismic stratigraphic succession.

Reduced quality of seismic response throughout the fold-thrust belt of northeastern Prince Patrick Island is typical. This is a result of shallow structural complications in the cover, low fold shot gathers, steeply dipping strata, and the rarity of seismic profiles acquired in directions perpendicular to regional tectonic trends. East-west profiles lie at 40 to 55° to tectonic strike; north-south profiles at 35 to 50°. These geometries have greatly hindered the ability to collapse diffractions and to properly restore primary reflections during seismic migration processing. Nevertheless, a common feature throughout this belt is a strong throughgoing reflection assumed to correspond to the top of the Silurian carbonate bank succession above unit psOS (profiles with cross-sections C and D; Fig. 26). This level has also been intersected in the Dyer Bay L-49 and Wilkie Point J-51 wells (Fig. 17). Nearly as strong and continuous is the reflection from the top of seismic unit ps5 variably located 750 to 1000 ms below the top Silurian reflector. The upper part of unit ps5 may also feature a 200 to 300 ms thick bundle of discontinous parallel reflections. This is commonly the stratigraphically lowest primary signal from within the fold belt. Locally, however, there are windows into deeper primary data; for example, the reflector assumed to mark the top of seismic unit ps3 (seismic Kane Basin Formation?), and the footwall cutoff of Cambrian(?) seismic units beneath Wilkie Point Forethrust near Cape Canning and the Wilkie Point J-51 well (profile PPB33, cross-section C).

The fold-thrust belt is remarkable for its uniformity of tectonic trend. The trend direction of nine axial trace segments, defined by two or more seismic profiles, narrowly range between N35°W and N50°W. Structure contouring defines at least six distinct anticlinoria, up to five of which might be crossed on any single regional perpendicular transect. Those illustrated and named on Figures 30, 31 and cross-sections C and D are more aptly described as forethrust (or backthrust) duplex anticlines with multiple levels of detachment in the Silurian and older parts of the section.

Wavelengths of anticlinoria, measured crest to crest, range from 5.3 to 17.2 km. Five out of eight of these are more than 11.0 km. The remaining short-wavelength folds are featured on profiles near the Wilkie Point J-51 well

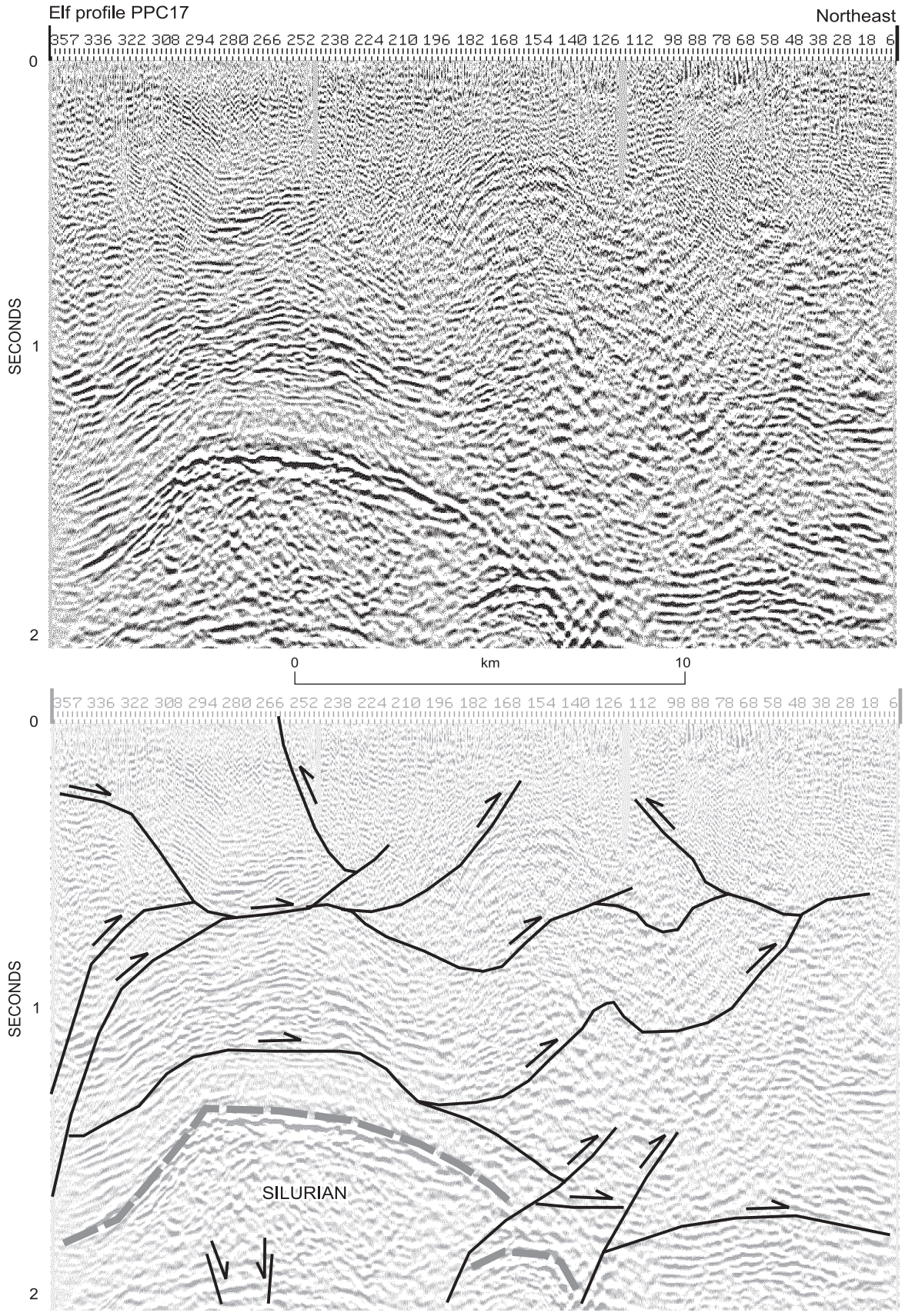

Figure 33. *Near-surface minor folds and rootless minor thrusts in the Devonian clastic wedge near Dyer Bay on a portion of seismic profile PPC17. Note that a coherent seismic stratigraphy in the Devonian to the northeast extends to the southwest beneath these structures.*

(profile PPB32, cross-section C). Plunge directions toward the northwest outnumber those to the southeast by thirteen to two, and the fold belt as a whole plunges toward the northwest throughout the imaged strike length of 94 km.

The magnitude of fold belt plunge is provided by variation in thickness of the Devonian clastic deposits preserved over fold crests. Profiles in the Wilkie Point J-51 and Jameson Bay C-31 area display local crestal minima (listed from southwest to northeast) of 775, 50, less than 45, and less than 105 ms (average less than 245 ms). In contrast, folds along strike to the northwest in the Intrepid Inlet H-49 and Andresen L-32 area have thickness minima of 940, 365, 190, 600, 675 and 420 ms (average 532 ms). Regional fold-belt plunge is also indicated by preserved Devonian clastic deposits as maximally preserved in faulted synclines: 1160, 1085 and 1355 ms (average 1200 ms) at the southeast end of the belt; 1405, 2365, 1625, 2285 and 1825 ms (average 1900 ms) within synclines in the northwest. These data translate into a regional fold-belt plunge to the northwest of 10 m km^{-1} or 0.6° measured over anticlinal crests and 23 m km^{-1} or 1.3° measured within synclines using an interval velocity of 4.0 km s^{-1}. These values reflect the configuration of the fold belt beneath Carboniferous and younger cover; in other words, the fold belt as it appeared in the Early Carboniferous following the post-orogenic erosion cycle but prior to subsequent mid-Carboniferous rifting and younger tectonic events.

The steeper plunge of synclines with respect to anticlines also implies an increase in fold amplitude along strike to the northwest. Crest-to-trough amplitudes in the Wilkie Point J-51 and Jameson Bay C-31 area range from 165 to 730 ms (average 415 ms) or 330 to 1460 m at 4 km s^{-1} (average 830 m). In contrast, amplitudes in the Intrepid Inlet L-32 and Andreasen H-49 area range from 495 to 1775 ms (average 1165 ms) or 990 to 3550 m at 4 km s^{-1} (average 2330 m).

The subsurface thrust-fold belt as a whole is also uplifted with respect to the less deformed areas of central Prince Patrick Island (cross-sections C and D). The magnitude of regional uplift is obtained by comparison of the thickness of Devonian strata in synclines within the thrust-fold belt (average thickness maxima increasing along strike from 1200 ms in the Wilkie-Jameson area to 1900 ms in the Intrepid-Andreasen area) with preserved maxima to the southwest in Hardinge Synclinorium (circa 3000 ms). Implied regional uplift of the entire thrust-fold belt with respect to its southwestern para-autochthonous foreland is 1800 ms (3600 m at 4 km s^{-1}) decreasing northwest to 1100 ms (2200 m).

Offshore areas

Quality of data displayed on the offshore profiles is everywhere inferior to that of the onland data. Profiles from Kellett Strait, Crozier Channel, and southern Fitzwilliam Strait display recognizable primary reflections from Jurassic and Cretaceous cover (as on Eglinton Island). However the lower Paleozoic is either acoustically unresponsive or features short, characterless, and uncorrelatable reflection segments, mostly from the Devonian clastic wedge succession. Profile G235, lying offshore east of Eglinton Island, displays seismic units esOS and esЄO (as on profiles Gf5 and 462, cross-section A) and the eastward continuation of Kellett Strait Anticline. Characterless dipping reflection segments are observed on other profiles in Kellett Strait. These data point to continuity of Kellett Strait Anticline with the southernmost onshore anticline of the Canrobert Hills on coastal northwestern Melville Island. Likewise, Eglinton Anticline also extends into Kellett Strait and appears to possess an axial trace that is aligned with the mouth of Ibbett Bay. The south-facing limb of Eglinton Anticline is aligned with the south-facing Purchase Bay Homocline south of Ibbett Bay. A southerly dipping, possible top Lower Devonian reflection correlated on a regional profile extending from Catherine Point area on Eglinton Island to the mouth of Ibbett Bay indicates that the combined thickness of Cape de Bray and Blackley formations south of Ibbett Bay is about 1200 ms (2400 m at 4 km s^{-1}). An unnamed regional syncline on southern Eglinton Island (Fig. 30) also extends under Kellett Strait to the east and appears to comprise more than 2300 ms (4600 m) of sub-Jurassic section above the Lower Devonian. The axial trace of this structure is aligned with the mouth of Purchase Bay on western Melville Island and may be continuous with the Blue Hills Syncline located still farther to the east (GSC Map 1844A in Harrison, 1995).

Regional correlations also favour the linkage of Blue Hills Syncline and the syncline in southern Kellett Strait and southern Eglinton Island with the syncline occupied by Parry Islands Formation west of Mould Bay and ultimately with Hardinge Synclinorium under west-central Prince Patrick, which features a depositional maximum of 3165 ms for the Devonian clastic wedge on profile PPB26 (Fig. 31). Nevertheless, the interpretation of the nature of Devonian structure beneath Crozier Channel is inhibited by the absence of primary signal from the sub-Jurassic interval on offshore seismic profiles in this area. This situation is only modestly improved on widely spaced profiles in northern M'Clure Strait. Characterless dipping reflections point to the southerly continuation of Walker Inlet Anticline, two unamed synclines and an unnamed anticline to at least 20 km south of Cape Mecham.

Uncorrelated reflections have also helped to define a series of anticlines and synclines on profiles in northern Crozier Channel and southern Fitzwilliam Strait. These modest indications lend additional support to the proposal that the Canrobert Hills Fold Belt of Melville Island must continue without substantial offset into subsurface northeastern Prince Patrick Island.

Thrust faults

Surface evidence

Only meagre evidence exists for past thrust faulting exclusively in Devonian and older surface exposures of Prince Patrick Island. These occurrences have already been introduced in the previous discussion of the surface evidence for mid-Paleozoic folding. Two anticlines mapped in the narrow outcrop belt of Weatherall Formation situated north of the head of Mould Bay are also associated with two probable thrust faults. The surface traces of these faults both trend N36°W and also parallel the axial traces of the folds. One of the anticlines lies in a hanging wall position with respect to one of the fault traces. The faults themselves are covered by rubble and talus, and can only be identified by offset of bounding strata. Steep dips on both faults are assumed based on lack of sinuosity. Direction of dip, toward the northeast, is based on the assumption that the strata in the more topographically elevated block to the northeast must also occupy the fault hanging wall. There is additional subsurface evidence in support of this dip direction. These thrust-anticlines are also associated with fault-trace-parallel slickensides in cemented sandstone with dip directions to northeast and southwest at 65 to 87°, and northwest-plunging, oblique-slip fault-plane lineations (with unidentified senses of slip).

The two thrust faults have apparently experienced two separate phases of slip. The more southwesterly fault trace is overlain with pronounced angular unconformity by the Awingak Formation and therefore must have experienced its last phase of slip prior to the Late Jurassic. In contrast, the fault lying more to the northeast may be responsible for both an early phase of displacement and tilting of Devonian strata and a later phase of shortening causing uplift and probable offset of the Awingak Formation.

The only other unequivocal example of thrust faulting in Devonian strata lies in an exposed hinge of Walker Inlet Anticline in two stream bank outcrops situated 1.2 and 1.3 km east of an unnamed bay on the east shore of Walker Inlet. The more easterly outcrop lies on the north bank within the east-facing fold limb and features an internally folded imbricate stack of three, minor, west-directed intraformational thrusts in incipiently cleaved Cape de Bray shale and siltstone. Dip of bedding increases upsection across the faults from 22 to 56°. Measured bedding-parallel fault surfaces dip at 45 to 56° to the east-northeast. The second key outcrop lies about 100 m to the west and downstream on the opposite (south) bank (Fig. 28, 29). Four minor thrusts lie within similar thin-bedded siltstone and shale of the upper Cape de Bray Formation. Three of these thrusts dip to the west at 20 to 44° and both ramp upsection and converge on a common bedding plane detachment in the outcrop. A fourth thrust, situated downsection to the east in the same outcrop, is inferred through cover and by the association of vertical-dipping beds in apparent tectonic contact with near-horizontal footwall strata. Transport of hanging wall strata to the east is implied by the asymmetry of hanging wall and footwall parasitic folds and by the east-facing asymmetry of the outcrop anticline (Fig. 28). The narrow radius of curvature of this anticline and the shallow to moderate dip of the two sets of seven inwardly vergent intraformational thrusts in both outcrops implies that all of the faults are probably restricted to the Cape de Bray Formation and arise from a bedding plane detachment within the same formation. Nevertheless, the anticline as a whole (cross-section C) is a large structure and can only likely be explained by compressive slip on and above a more deep-seated basal decoupling surface.

Other Paleozoic thrust faults may exist on southern Prince Patrick Island. However, data are presently insufficient to distinguish these from the many faults that could equally be interpreted as extensional in origin, or initially compressional and later reactivated in extension. The true nature and extent of Paleozoic thrust faulting and the ultimate depth to detachment beneath the structures mapped at surface is exclusively provided by adjacent seismic profiles.

Subsurface evidence

There is no direct evidence for thrust duplication of stratigraphic section in any of the drill holes of Prince Patrick and Eglinton islands. Indirect evidence for subsurface thrusting is provided through the interpretation of regional seismic profiles and includes: 1) velocity pull-up of primary reflectors caused by tectonic duplication of high-velocity strata in a shallower part of the section; 2) stacked repetition of seismic units; and 3) reflections from fault planes. Bedding plane detachments can also be recognized by divergence of reflections and folds that die out up- or down-section. Care must be exercised to distinguish tectonic divergence of reflectors from divergences of depositional origin such as sigmoidal or hummocky bedding, and mounded depositional facies.

For the seismic data of Eglinton and Prince Patrick islands, thrust faults in the lower Paleozoic usually occupy one of three stratigraphic positions: 1) lying entirely within

the Devonian clastic wedge; 2) emerging into the Devonian clastic wedge but demonstrably offsetting the more rigid tectonic units of Lower Devonian and older age; or 3) lying between detachments entirely within the Vendian(?) to Lower Devonian part of the section. For the latter faults, compressive deformation may be entirely absorbed upsection by folding and strain partitioning. Alternatively the slip may be transferred laterally on bedding plane detachments and carried upsection on shallower thrust faults.

Faults of the second type are most notable for their regional significance and mappability. Thirteen can be correlated between two or more seismic profiles. Whereas the foreland side of the deformed belt is believed to lie under southern Eglinton and central Prince Patrick islands, with the bulk of the orogen lying to the northeast, it would be expected that thrust transport would be directed toward the southwest and away from this deformed belt. However, eleven of the fifteen major faults arising from the sub-Devonian section dip to the southwest and, together with the asymmetry of hanging wall anticlines, indicate a northeasterly sense of vergence away from the foreland. This situation is balanced in part by minor thrusts (that can only be mapped on a single seismic profile) which are dominantly southwest vergent, and by deep-seated thrust faults of the third type, described above, which are believed to possess foreland-directed transport.

Eglinton Island

The high quality of the seismic data from northern Eglinton Island permits the identification of thrust faults and detachment surfaces spanning nearly the entire seismic stratigraphic interval below the Jurassic (profiles P462 and Gf5, cross-section A). There are two thrust faults of map-scale significance that have been interpreted to displace the Lower Devonian and older section, and to extend upsection into the Middle and Upper Devonian clastic wedge. The northeasterly vergent Kellett Strait Thrust is featured on two parallel seismic profiles of Kellett Strait Anticline (Gf5, and G235 located offshore to the east). The upper part of the Canrobert Formation has been tectonically emplaced over the upper part of the Ibbett Bay Formation. Indicated stratigraphic separation is about 540 ms below SP501 on profile Gf5. Displacement of the contact above the Canrobert, parallel to the line of profile and cross-section A, is 600 to 1100 m and is assumed to decrease upsection as a consequence of increased shortening by folding in the footwall and hanging wall. The kinematically related, southwesterly vergent Kellett Strait Conjugate is interpreted on two land-based profiles. Upper Canrobert Formation is emplaced over basal Ibbett Bay Formation with 140 ms of stratigraphic separation below SP519 on profile Gf5.

In addition to the mappable thrust faults in the upper part of the section below the top of the Lower Devonian, there are also a number of locally developed forethrust and backthrust ramps in this interval. Slip on these latter faults is linked to the growth of a small group of parasitic hanging wall anticlines. Examples include two near the crest of Eglinton Anticline below SP 128 and 123 on profile Gf5 with local detachments in the lower Ibbett Bay Formation and in the lower part of the Devonian clastic wedge; one with a crest situated in the regional syncline north of Eglinton Anticline below SP 5918 on profile 462, detached in the upper Canrobert Formation; and one on the south-facing limb of Kellett Strait Anticline below SP 515 on Gf5, detached in esOSi and upper es$\in$O.

However, the gross-scale geometry of Eglinton and Kellett Strait anticlines is related to deep-seated slip and thrust ramp development on Kellett Strait and Gardiner Point thrusts. Northeasterly directed slip is indicated on these faults found between detachments in seismic unit es1 and low in es3. The most significant thrust fault beneath Eglinton Island is the southwesterly directed Eglinton Forethrust. Stratigraphic separation ranges up to 1030 ms below SP127 on profile Gf5 where unit es1 is emplaced over es2. Compressive slip in the direction of transport is at least 13 km for the basal beds of unit es1 in the thrust hanging wall. The northern limit of this fault and of the duplicated interval (es1 to basal es3) lies beyond the north end of the Eglinton Island seismic grid. The southern limit of the es1 décollement is marked by a frontal ramp below SP5944 on profile 462, where slip is transferred upsection from unit es1 to the base of es3. Additional slip is carried upsection on the Kellett Strait and Gardiner Point thrusts. Thickening of units es3 and es4 south of SP5944 is attributed to tectonic stacking of imbricates in this interval between detachments at the base of es3 and at the top of es4. The thickened interval tapers to a potential subsurface deformation limit about 11 km northeast of the Pedder Point D-49 well.

Only equivocal evidence exists for restricting compressive slip exclusively to the Devonian clastic wedge. Hummocky reflectors of possible tectonic origin are common throughout the clastic wedge but have been most notably imaged on the south-facing limb of Eglinton Anticline (profile 462, SP5955 to 5995) and in the regional syncline to the north (profile 462, SP5914). The lowest hummocks and lowest underlying indicated intraformational slip surface lies immediately above the Ibbett Bay Formation, which is gently inclined but otherwise undeformed at the scale of the seismic profile. Other slip surfaces in the clastic wedge appear likely but cannot be mapped individually. A depositional origin for these hummocks is also possible.

Southwestern Prince Patrick Island

Major thrust faults detected in the Devonian clastic wedge and rooted in the middle part of the Silurian and older carbonate bank succession are associated with each of the major anticlines and anticlinoria of subsurface Prince Patrick Island (Fig. 30, 31; seismic profiles, cross-sections C and D). Ten of the thirteen major thrusts of this type occur in the fold-thrust belt of northeastern Prince Patrick Island. All but three of these are northeasterly vergent. This style of thrust faulting is also assumed to exist beneath the surface anticlines exposed between Dyer Bay and Intrepid Inlet. However the geometry, magnitude of transport, and depth to detachment for these assumed subsurface structures remains speculative.

The easterly vergent Dyer Bay Thrust has been mapped on five seismic profiles over the east limb of Dyer Bay Anticline. Stratigraphic separation is 240 ms below SP 193 of profile PPC17 where medial unit psЄO (seismic Cass Fjord Formation) has been placed over the lower part of unit psOS (seismic Allen Bay Formation). The thrust hanging wall includes all seismic units above the base of the Vendian. A basal décollement below unit ps2 (in seismic Kennedy Channel Formation) is assumed for the structural cross-sections.

Central Prince Patrick Island

The southwesterly vergent Landing Lake Thrust is mapped on two seismic profiles of central Prince Patrick Island (cross-section D). Medial psЄO has been placed over lower psOS and displays 265 ms of stratigraphic separation beneath SP993 of profile PPA17. Thrust transport decreases to the northeast. A close association is indicated between the thrust and the Landing Lake Anticline, which lies in the fault hanging wall. The thrust appears to be rooted on a décollement beneath ps5 1350 ms (4300 m) below the top of the Lower Devonian. The thrust also flattens upsection into a detachment in the lower part of the Cape de Bray Formation approximately 1300 ms (2600 m) above the Lower Devonian.

In the same area is the Snowpatch Point Thrust associated with a lesser understood anticline believed to exist in the subsurface east of Green Bay. A similar level of detachment low in ps5 is assumed and although this structure is insignificant below SP897 on profile PPA17, magnitude of slip and the related amplitude and wavelength of the hanging wall anticline all increase to the southeast onto profile PPA14 (cross-section C).

Northeastern Prince Patrick Island

There are two northeast-vergent and regionally mappable thrusts associated with Wilkie Point Anticlinorium (seismic profiles with cross-sections C and D). Wilkie Point Thrust-A is mappable on two, possibly three, profiles. Medial psЄO has been placed over lower psOS on PPA 17. Maximum stratigraphic separation is uncertain. Wilkie Point Thrust-B is interpreted on five profiles. Maximum stratigraphic separation of 955 ms is displayed where ps5 (seismic mid-Cambrian) appears to have been emplaced over the undivided lower part of the Devonian clastic wedge on profile PPA 4 (Fig. 31). Indicated depth to detachment for Wilkie Point Thrust-B on this profile is 470 ms (1300 m) below the top of unit ps5 and about 1300 ms (3600 m) below the top of the Lower Devonian. Up to six northeasterly vergent minor thrusts can be inferred in the uppermost part of the sub-Lower Devonian interval between SP120 and 350 on PPA17. Signal response is mediocre and depth to detachment is uncertain. Similarly, at least four other southeast vergent thrusts of uncertain regional significance are interpreted on profiles PPB32 and PPC33 near and southwest of the Wilkie Point J-51 well. In this area, the minimum thickness of thrust-faulted strata is 1350 ms measured from the top of the Lower Devonian on these profiles, which is also close to the thickness of the succession above the Wilkie Point Thrust-B detachment on profile PPA4. However, the ultimate depth to detachment on the peninsula east of Intrepid Inlet lies above a throughgoing reflector at 4400 ms below Cape Canning area deepening to more than 5500 ms near the Wilkie Point J-51 well.

Snow Hill Anticlinorium is associated with at least four mappable thrusts, all northeasterly vergent, all associated with hanging wall anticlines detached in ps5, and each traceable across two to four seismic profiles. These faults have been labelled from top to bottom in the imbricated section that includes ps5 through to the preserved lower part of the undivided Devonian clastic wedge. Snow Hill Thrust-A lies beneath a parasitic anticline on the southwest-facing limb of Snow Hill Anticlinorium. It is the structurally highest thrust in this group and situated farthest to the southwest, but is lower than the Wilkie Point thrusts, which are detached at the same level. Snow Hill thrusts labelled B, C and D are all found on the northeast-facing limb of Snow Hill Anticlinorium and, in map view, are arranged in an approximate en echelon pattern such that the northwestern thrust tip of Thrust-B does not extend as far to the northwest as Thrust-C, which fails to reach as far to the northwest as Thrust-D. Typical stratigraphic separations range from 400 ms on Thrust-C (profile PPA4) to a maximum of 1080 ms

on Thrust-D (profile 479). Some of the evidence for a common depth to one mid-level detachment include tectonically divergent reflections at 1) 460 ms below the top of ps5 and 1340 ms below the top of the Lower Devonian, Snow Hill Thrust-A (profile PPA4); 2) 485 ms below the top of ps5 and 1310 ms below the top of the Lower Devonian, Snow Hill Thrust-B (profile PPA12); and 3) 340 ms below the top of ps5 and 1215 ms below the top of the Lower Devonian, Snow Hill Thrust-D (profile 479).

Brown Bluff Anticline lies in the subsurface 15 to 19 km north of the head of Intrepid Inlet. This structure has also been projected onto cross-section D. The anticline is associated with two inwardly dipping and oppositely vergent thrusts, both emergent from the top of seismic unit psOS on each fold limb and imaged on two parallel seismic profiles. Displacment and statigraphic separation is greater on the northeast vergent Brown Bluff Thrust-B (485 ms on profile 477 increasing to 1010 ms on PPA4) than on Thrust-A, which terminates downsection against Thrust-B. Like the Wilkie Point and Snow Hill thrusts, Brown Bluff Thrust-B is believed to flatten downsection into unit ps5. Depth to detachment, implied by divergent reflections, is 285 ms below the top of ps5 and 1175 ms below the top of the Lower Devonian (SP 7973 on profile 477).

Cape Andreasen and M'Clintock Point anticlines are each associated with a single major northeast-vergent thrust. The Cape Andreasen Thrust is traceable across eight seismic profiles for an imaged strike length of 55 km. Stratigraphic separation ranges up to 665 ms on profile 479 where unit psЄO has been emplaced over the lower part of the Devonian clastic wedge. Thickness of strata below the top of the Lower Devonian and implied minimum depth to detachment on profile 477 is about 1300 ms, which is comparable to that for other major thrusts of northeastern Prince Patrick Island.

The very similar but structurally lower M'Clintock Point Thrust has been imaged on at least seven profiles for a minimum strike length of 61 km. This thrust emerges into the Devonian clastic wedge on the northeast-facing limb of M'Clintock Point Anticline and has up to 700 ms of stratigraphic separation where the lower part of unit psЄO has been emplaced over the lower part of the clastic wedge on profile 479. Separation decreases to the limit of the seismic records on profile 480. Minimum section involved in deformation includes at least 1270 ms of strata below the top of the Lower Devonian.

Deep-seated thrust faults

Compelling and relatively direct seismic evidence has now been collected to indicate the existence of thrust faults in the lower Paleozoic above a widespread detachment in unit ps5 (seismic mid-Cambrian) throughout northeastern Prince Patrick Island. There are also lines of indirect evidence to indicate that at least three additional thrust faults must exist in this same part of Prince Patrick Island entirely beneath the ps5 detachment. First and most significantly, local and regional structural relief exists on the ps5 detachment. In other words, this surface has been folded and these long-wavelength folds can be accounted for by slip on thrust ramps found deeper in the section. Second, faults and horizontal shortening located and measured above the ps5 detachment must be rooted and accounted for by shortening at depth. These faults might be situated either on the lines of section or off the sections to the northeast or southwest. Since the Arctic Platform and the craton of North America lie under the southern Arctic Islands, the fold-thrust belt of northeastern Prince Patrick Island is more likely rooted under and northeast of this belt. Third, deep-seated thrust faults have been imaged within an adjacent part of this belt under northeastern Eglinton Island. Fourth, evidence is provided for a potential northeasterly facing thrust-plane reflection above unit ps2 on profiles PPB32 and PPB33 (with cross-section C), southeast of the Wilkie Point J-51 well.

The structural model illustrated on cross-sections C and D provides a basal décollement within or above unit ps1 (in seismic upper Vendian Kennedy Channel Formation) and undivided unit ps throughout the northeastern part of the island. A minimum of three deep-seated thrust faults can account for the geometry of the folded ps5 detachment under northeastern Prince Patrick Island. The first, a shallow-dipping thrust ramp on Wilkie Point Forethrust, links the top ps1 décollement to the detachment in ps5. This thrust ramp accounts for much of the regional southwest dip on Purchase Bay Homocline and the extreme stratigraphic relief on the southwest-facing limb of Wilkie Point Anticlinorium. Foreland-directed shortening on the Wilkie Point Forethrust is balanced by thrust faulting and folding within Landing Lake and Snowpatch Point anticlines and by hinterland-directed slip within the shallow parts of the Wilkie Point and Snowpatch thrust-anticlinoria. The second involved two phases of compressive slip for Snow Hill Forethrust-A as indicated on cross-section D. An earlier phase has carried slip from the top ps1 décollement to the ps5 detachment, which was then carried upsection elsewhere on thrust ramps above ps5. The later slip on Snow Hill Forethrust-A was carried through the ps5 detachment to the Devonian clastic wedge such that Forethrust-A also offsets one or more Wilkie Point thrusts. The later phase of compressive slip may also have occurred near cross-section C. However, the situation is complicated by younger extension. The third deep-seated thrust fault is Snow Hill Forethrust-B, which lies in the footwall of Forethrust-A on the cross-sections. Forethrust-B is

constructed to balance additional compressive slip documented upsection within Brown Bluff, Cape Andreasen, and M'Clintock Point anticlines, and to satisfy the geometry of the folded ps5 detachment within Snow Hill Anticlinorium.

Unrooted detachments in the Devonian clastic wedge

Evidence for slip surfaces produced by horizontal compression in the Devonian clastic wedge has already been described for Eglinton Island. Many of the thrust faults rooted in the Vendian(?) to Lower Devonian section also flatten upsection into the clastic wedge in the subsurface of Prince Patrick Island. Examples include Landing Lake and Snowpatch Point thrusts on profile PPA17 (cross-section D). There are other examples of detachment faults in the clastic wedge that cannot be related to specific thrust ramps at depth. This is particularly true of extensional faults that also offset the Cretaceous and older cover rocks.

Less common are bedding-parallel slip surfaces produced in compression for which a link to depth is not identified. One example is provided by a parasitic anticline in the Cape de Bray Formation near the crest of Landing Lake Anticline below SP880 to 960 on PPA17. The parasitic structure dies out downsection and appears to have been detached at about 320 ms above the base of the Cape de Bray Formation. Other compressional bedding-plane slip surfaces are recognized by divergent seismic reflectors over the flanks of Wilkie Point Anticlinorium, notably 390 and 550 ms above the base of the Lower Devonian on profile PPA7, and 500 to 600 ms above the Lower Devonian between SP50 and 195 on PPA17. Other examples may exist within the northeastern fold-thrust belt of Prince Patrick Island but are only ambiguously distinguished from topset truncations on depositional clinoforms or geophysical artifacts created in part by reflection multiples from shallow primary signal. Understanding the tectonic character of the Devonian clastic wedge in the northeast is also hindered by a lack of coherent seismic stratigraphy and the extreme depth of pre-Carboniferous erosion.

The largest area of apparently rootless detachment surfaces in the Devonian clastic wedge occurs above and west of the crest of Dyer Bay Anticline (Fig. 33). Examples occur on parts of at least four regional seismic profiles. The surfaces are recognized by divergent and convergent reflections providing evidence of mesoscale folding that is not apparent at and below the top of the Silurian. Implied direction of transport is both to the east and to the west on individual slip surfaces. However, transport of detached stratigraphic panels is more predominantly to the east and the basal slip surface, located 160 to 320 ms above the Silurian in the clastic wedge, also climbs progressively eastward on four seismic profiles (PPA14, PPC17, PPB26 and PPB27; Fig. 33). The various shallow thrust faults in the Devonian clastic wedge are assumed to root in deformed Vendian(?) to Lower Devonian strata situated farther to the west under M'Clure Strait.

Detachment levels

A regional assessment of major and minor detachment levels in sub-Carboniferous strata for Prince Patrick and Eglinton islands is provided on Figure 34. Major detachments lie above unit ps1 (seismic Kennedy Channel Formation) and within ps5 (seismic mid-Cambrian) on the seismic profiles of Prince Patrick Island. Minor detachments have also been identified at various levels in a décollement zone 160 to 600 ms above the top of the Silurian in either the Blackley Formation or in the Devonian clastic wedge undivided. A local detachment is also identified at 300 ms above the base of the Cape de Bray Formation.

For Eglinton Island, major detachment surfaces are correlated in seismic unit es1 (seismic upper Vendian, undivided), at the base of es3 (seismic Kane Basin Formation) and at the top of es4. Local detachments are recognized in the upper part of the Canrobert Formation and at three levels in the Ibbett Bay Formation. Slip surfaces are also common in a detachment zone 50 to 300 ms above the top of the Ibbett Bay Formation in the Devonian clastic wedge, undivided.

A major correlation barrier is presented by an inability to carry various Silurian and underlying seismic units across the Crozier High. Structural constraints relating to this problem are illustrated on Figure 35. Thrust faults mapped on Figure 35 include only those arising from the basal décollement located below the upper part of es1 on Eglinton Island and below ps2 on Prince Patrick Island. Shaded hanging wall panels include units es1 and es2 beneath northeastern Eglinton Island and units above ps1 throughout northeastern and parts of western Prince Patrick Island. In contrast, hanging wall panels are only deformed above the base of es3 under southwest Eglinton Island and above the base of ps5 under central and parts of western Prince Patrick Island. Fundamental structural linkages (entertained in Fig. 34, 35) include continuity of Wilkie Point Forethrust with the Eglinton Forethrust and continuation of Snow Hill Forethrust onto Sproule Peninsula of northwesternmost Melville Island without substantial offset across the Crozier High. If true, then unit ps1 and the lower part of es1 everywhere lie together in a common autochthonous footwall section beneath the mappable thrusts, and that upper es1, es2, and ps2 through ps4 all lie together in a second higher structural panel between two laterally linked basal and mid-level décollements. Similarly, units es3

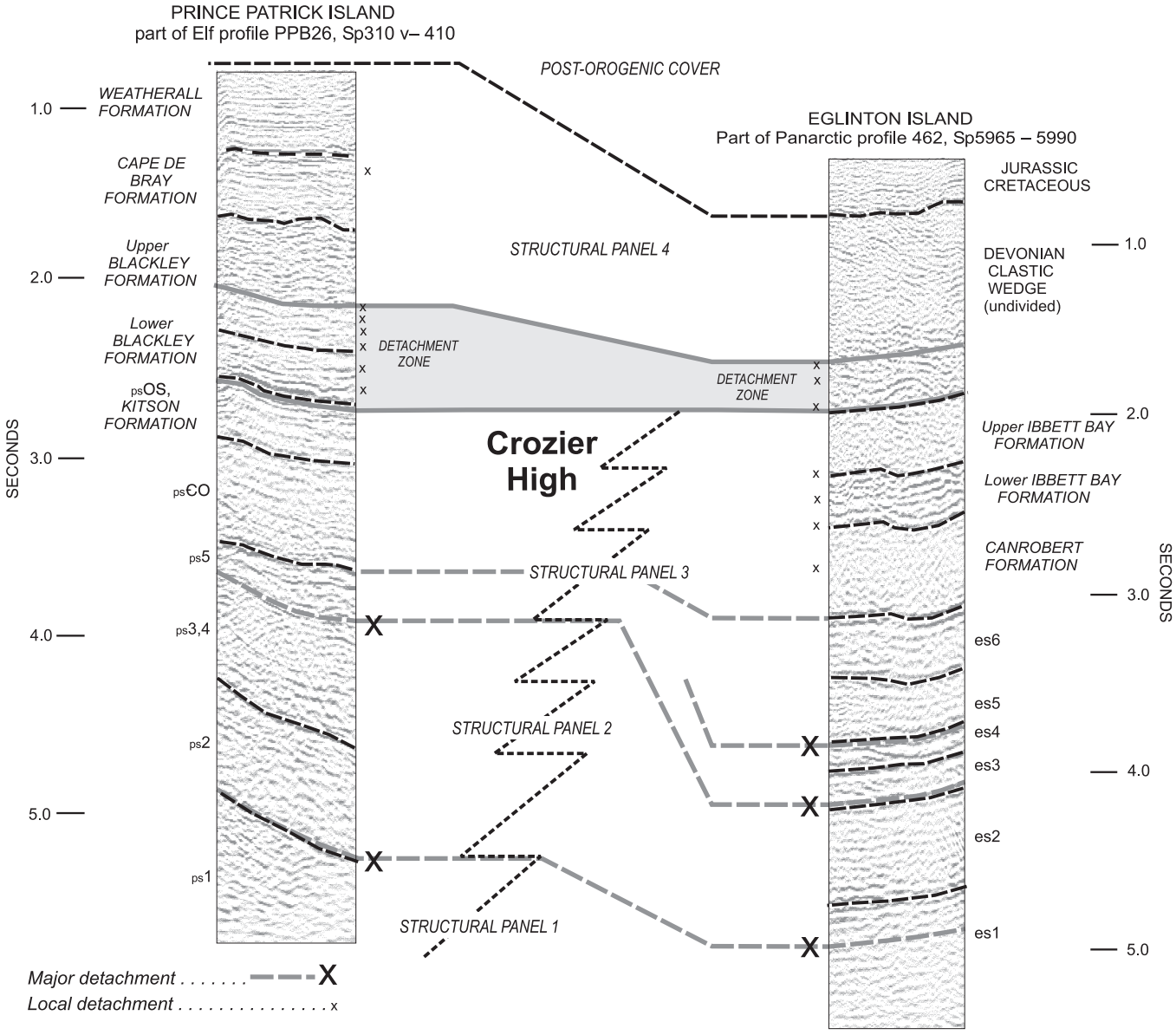

Figure 34. *Structural panels and stratigraphic distribution of major (X) and minor (x) detachment surfaces in Devonian and older strata of subsurface Eglinton and Prince Patrick islands. The Crozier High marks the approximate location of a long-lived shelf-to-basin transition in Silurian and older strata. Units* es5 *and* es6 *are also cut out against the high by unconformable Canrobert Formation. Nevertheless, major throughgoing detachments that separate the four recognized structural panels provide tentative links between age-equivalent strata on either side of the high. The seismic examples are located on Figure 31.*

through the Ibbett Bay Formation, and ps5 through to the Kitson Formation lie together in a third structural panel above the lowest major mid-level detachment. The top of this third panel is defined by the décollement zone situated in the lower part of the Devonian clastic wedge of both Eglinton and Prince Patrick islands. The remaining younger Devonian units, all within the clastic wedge, are lumped together in a fourth and highest structural panel, part of which has been removed by erosion prior to post-orogenic overlap.

In summary, potential structural links have been shown to exist within the Lower Devonian and older strata between Eglinton and Prince Patrick islands. Major transitions in depositional facies exist between these two areas across the Crozier High, and tectonic activity on the margins of the high would also have been likely during deposition of the contrasting stratigraphic units preserved on either side. However, the linkage of major detachments and four structural panels across the high would appear to negate the possiblilty of significant motion on the Crozier High during

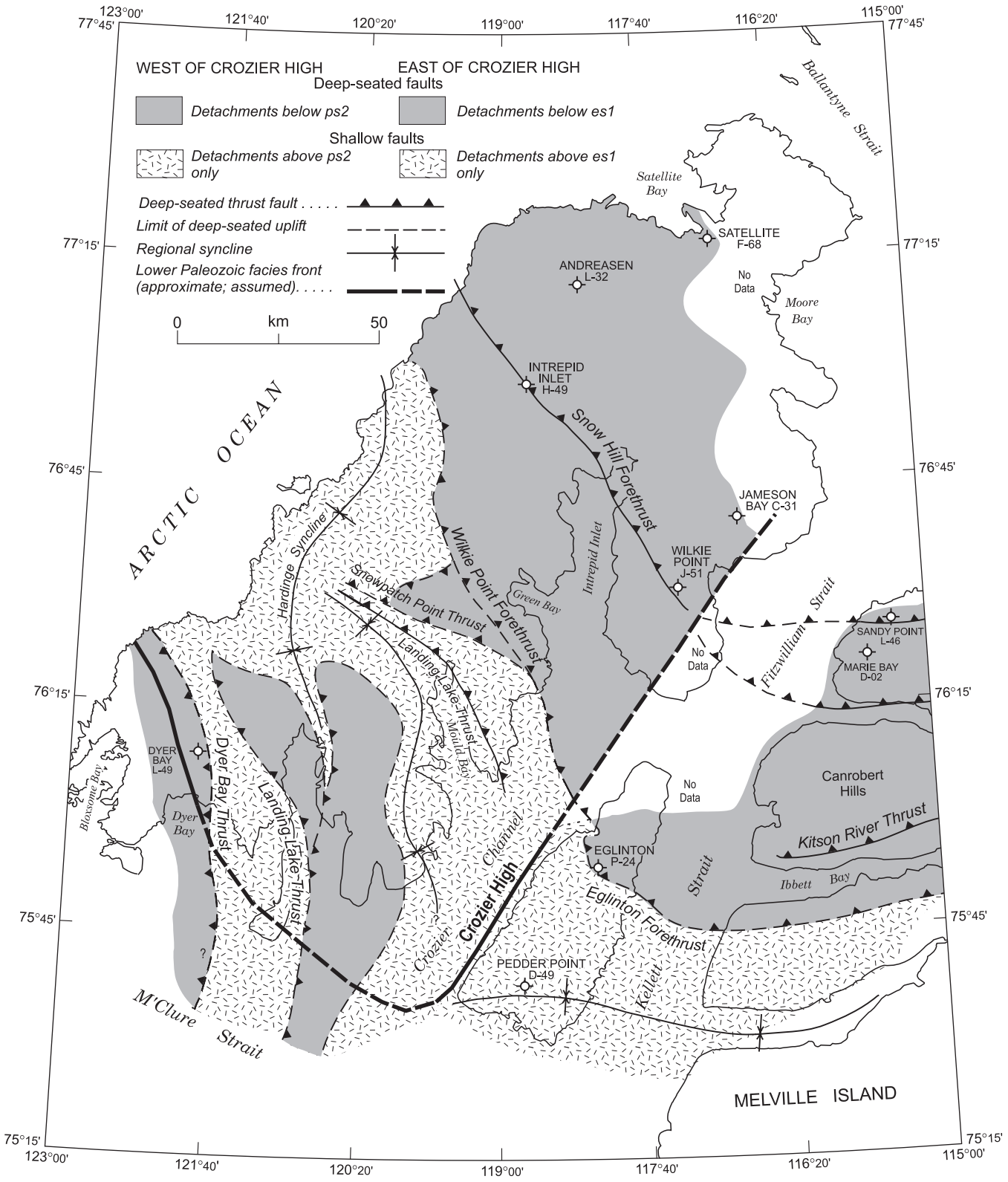

Figure 35. *Areas of compressive uplift and deep-seated thrust faulting affecting seismic units below* es4 *of Eglinton Island and below* psЄO *of Prince Patrick Island. Eglinton Forethrust within sub-Canrobert Formation strata of Canrobert Trough is continuous with Wilkie Point Forethrust in shelf-related lower Paleozoic strata of Prince Patrick Island. Similarly, Snowhill Forethrust is continuous with similar major structures of Sproule Peninsula.*

the main phase(s) of pre-Carboniferous compressive deformation.

Magnitudes of shortening

The cumulative horizontal shortening of Silurian and Lower Devonian strata has been measured at appropriate intervals along structural cross-section A of Eglinton Island and along sections C and D of Prince Patrick Island. Results are compiled in Figure 36 together with similar shortening values from Ordovician strata of western Melville Island (Harrison, 1995). Certain assumptions have been made in order to obtain the values inherent in the contoured data. First, Dyer Bay, Hardinge Mountains and Walker Inlet anticlines are assumed to have been transported from the west and the associated thrust faults are rooted beneath a larger thrust belt (Banks Island Belt) also presumably located to the west under M'Clure Strait. Second, the foreland limit of deformation for the Canrobert Hills Fold Belt on Prince Patrick Island is assumed to lie in the hanging wall of the Landing Lake Thrust located near SP1020 on PPA17 of cross-section D and in the vicinity of Mould Bay station on cross-section C. The limit of deformation is also placed on the south side of Eglinton Anticline south of the Eglinton P-24 well. This zero isoshortening contour is assumed to be continuous with the same contour that marks the boundary between the Arctic Platform and the Canrobert Hills Fold Belt under southwestern Melville Island (see Fig. 98 of Harrison, 1995).

Results indicate that total accumulated southwest-directed shortening is 13.1 km measured to the footwall of the Gardiner Point Thrust located somewhere below the northeast end of Eglinton Island on cross-section A; 30.7 km measured to the footwall of Snow Hill Thrust-C at the limit of imaged data below the Jameson Bay C-31 well on cross-section C; and 35.2 km measured to the footwall of the M'Clintock Point Thrust northeast of the Andreasen L-32 well on cross-section D. At the west end of Prince Patrick Island, more than 10 km of east-directed shortening is indicated on cross-section C. Three of the anticlines on this section die away to the north. Thus, cumulative east-directed shortening is only 3.0 km at the west end of cross-section D.

Arcuation of Canrobert Hills Fold Belt, with convex side facing to the southwest, is observed in both the contours (Fig. 36) and fold axial traces (Fig. 19, 30). The nose of this salient lies along the depocentral line of Canrobert Trough. Two reentrants are indicated by the fold axial traces and isoshortening contours: one under southwestern Melville Island and the other under and to the west of Prince Patrick Island. Both these areas are believed to be underlain by relatively rigid, carbonate-dominated strata similar to those encountered in the lower part of the Dyer Bay L-49 well. In earlier discussion of the folds of subsurface northeastern Prince Patrick Island it was suggested that the regional fold plunge to the northwest, and the overall reduction in fold belt amplitude (in the same direction) with respect to the foreland, may be due to decreased shortening. This suggestion is supported by the compiled data on Figure 36. Accumulated shortening measured from the foreland to the crest of Wilkie Point Anticlinorium decreases systematically from about 23 km near the Wilkie Point J-51 well to about 12 km northwest of the Intrepid Inlet H-49 well. A similar pattern is indicated for the Snow Hill Anticlinorium and other structures in this region.

UPPER PALEOZOIC RIFT AND INVERSION TECTONICS IN THE WESTERN SVERDRUP BASIN

Introduction

Data presented in the previous chapter demonstrated the existence of compressive deformation structures of post-Devonian age throughout Prince Patrick and Eglinton islands. Beauchamp et al. (2001) described the nature of the Carboniferous and Permian post-orogenic cover of northeastern Prince Patrick Island. The present contribution summarizes the mostly rift-related structure of the upper Paleozoic succession, and the spatial and kinematic relationship between rifting and the previous orogenic activity (Table 2).

As Permian and Carboniferous strata are entirely covered by Triassic and younger beds in this part of the Arctic Islands, and direct subsurface information is limited to five exploratory wells, much of the following description is provided by interpretation of reflection seismic profiles and comparison with rift-related structures in the upper Paleozoic of adjacent islands. The exposed strata and subsurface seismic expression of the Permian and Carboniferous of Melville Island was provided by Harrison (1995). Similar structures have also been described from Cameron Island (Davies and Nassichuk, 1991), Bathurst Island (Harrison et al., 1993), Grinnell Peninsula on western Devon Island (Beauchamp et al., 1998) and western and northern Ellesmere Island (Beauchamp, 1987; Thériault et al, 1995). The belt of upper Paleozoic rift-related structures of northwestern Melville and northeastern Prince Patrick Island is parallel to, and lies entirely within and above the inner subdomain of the Canrobert Hills Fold Belt (Fig. 21). This report will show that individual rift-related normal faults are spatially and kinematically linked to specific pre-existing structures in the underlying thrust-fold belt.

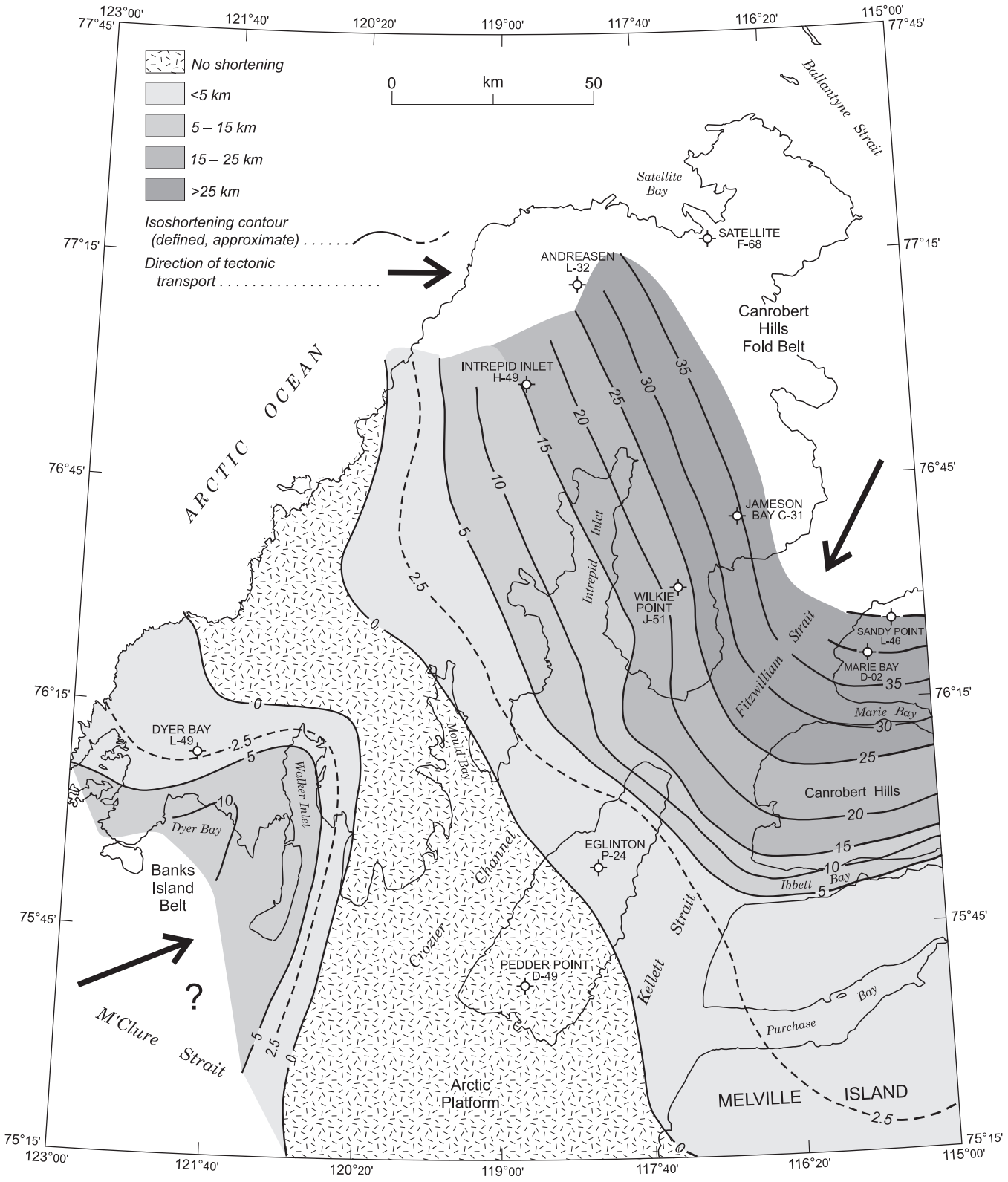

Figure 36. *Regional patterns of horizontal shortening measured on the top of the Lower Devonian. Data for western Melville Island has been obtained from Section J and Figure 98 of Harrison (1995). Careful comparison with Figure 30 (this paper) reveals that these contours are oblique to mapped structures, which implies a regional decrease in accumulated shortening along tectonic strike toward the northwest.*

Seismic units

Seismically defined Carboniferous and Lower Permian strata are common in a large region that extends from Jameson Bay to Moore Bay and Satellite Bay (Fig. 21). The best seismic images were acquired in the vicinity of the Jameson Bay C-31 well. Lack of well control, and minimal impedance contrast between the Carboniferous and the pre-orogenic Devonian causes difficulty in picking the base of the Carboniferous. This stratigraphic level is progressively more uncertain to the north where it lies at less than 1.3 seconds near Jameson Bay but occurs below 3.0 seconds in most areas north of Moore Bay and northeast of Satellite Bay.

Beauchamp et al. (2001) identified seven depositional sequences in the Prince Patrick Island area. From the top down these include:

6, 7. Trold Fiord and Van Hauen formations (Roadian and younger; two sequences): a widespread package of continuous, moderate-amplitude reflectors that diverge and thicken progressively toward the northeast and that lies unconformably on sequence 5.

5. Sabine Bay Formation and correlative slope deposits (Kungurian): a thin but fairly extensive low-amplitude reflection package of locally variable thickness lying with profound unconformity on sequence 4.

4. Raanes Formation and correlative deep-water deposits (Sakmarian, Artinskian): high-amplitude, continuous reflectors preserved as erosional remnants in some grabens, disconformably overlying sequence 3.

3. Seismic upper Hare Fiord, upper Nansen, upper Canyon Fiord formations and Belcher Channel Formation (Gzhelian to Sakmarian): a widespread succession of locally variable thickness featuring divergent, high-amplitude, semicontinuous reflection segments.

2. Seismic lower Hare Fiord, lower Nansen, and lower Canyon Fiord formations (Bashkirian to Kasimovian): a widespread succession of mostly parallel reflection segments, commonly block rotated with divergent reflections locally preserved in the upper part; the sequence unconformably overlies Devonian 'basement' or sequence 1.

1. Seismic Borup Fiord Formation (Serpukhovian?): a very locally developed succession featuring block-rotated reflections unconformably overlying Devonian and older 'basement' rocks.

It should be emphasized that between drill holes the designation of formation names, depositional facies, and ages is based on extremely tenuous information. Biostratigraphic reports from the report area wells contain no proven palynomorphs or microfossils older than Artinskian or younger than Wordian. There is no proven Kungurian assemblage. Identified material is commonly caved, recycled, long ranging, and open to multiple interpretations. Therefore assignment of ages to sequence boundaries, particularly in Carboniferous strata or post-Wordian Permian strata, should be considered educated guessing and not proof.

Nature of rift-related normal faults

The distribution of syndepositional normal faults together with the contoured time-thickness of graben-fill Carboniferous and Permian strata is illustrated in Figure 37. At least thirteen faults have been defined within the report area by the available seismic profiles. Nine of these appear on two or more profiles each, and are named and located on Figure 38 and on cross-sections C and D. The strike direction of these faults falls in a relatively narrow range between N40°W and N70°W. Eight of the faults and all but three of the major faults feature down-to-the-northeast senses of slip. The remaining five faults, with down-to-the southwest slip, all lie near the limit of coherent data in the Satellite Bay-Moore Bay area. All of the major and minor faults, south of latitude 77°00'N, disappear along tectonic strike to the northwest and die away in a sinistral en echelon pattern at about longitude 117°20'W. In contrast, the imaged normal faults in the north are traceable across the entire set of onland seismic profiles.

The remainder of this part of the chapter, dealing with upper Paleozoic structure, is devoted to an examination of deformation history and associated sediment accumulation related to each of the major faults. Important variations are noted in the nature of the footwall and hanging wall graben-fill successions for each fault, and information is provided for relative dating of the various phases of faulting. Description starts with faults in the southwest and finishes with those in the northeast: from rift margin toward rift axis.

Jameson Fault-A

Jameson Fault-A and the related graben-fill succession are best imaged on profiles PPA12 and 468 (Fig. 39). Together with profile PPB-32, the minimum strike length is less than six kilometres. Actual strike length, however, is probably in excess of 30 km because the horizontal separation on the base of the Carboniferous is up to 2.5 km in this area and the stratigraphic separation ranges up to 865 ms. The fault merges with the smaller Jameson Fault-B to the south and together both die away to the northwest short of profiles PPA11 and 467 (Fig. 38). A low-angle listric shape for Jameson Fault-A is implied by the rotation of the Permo-

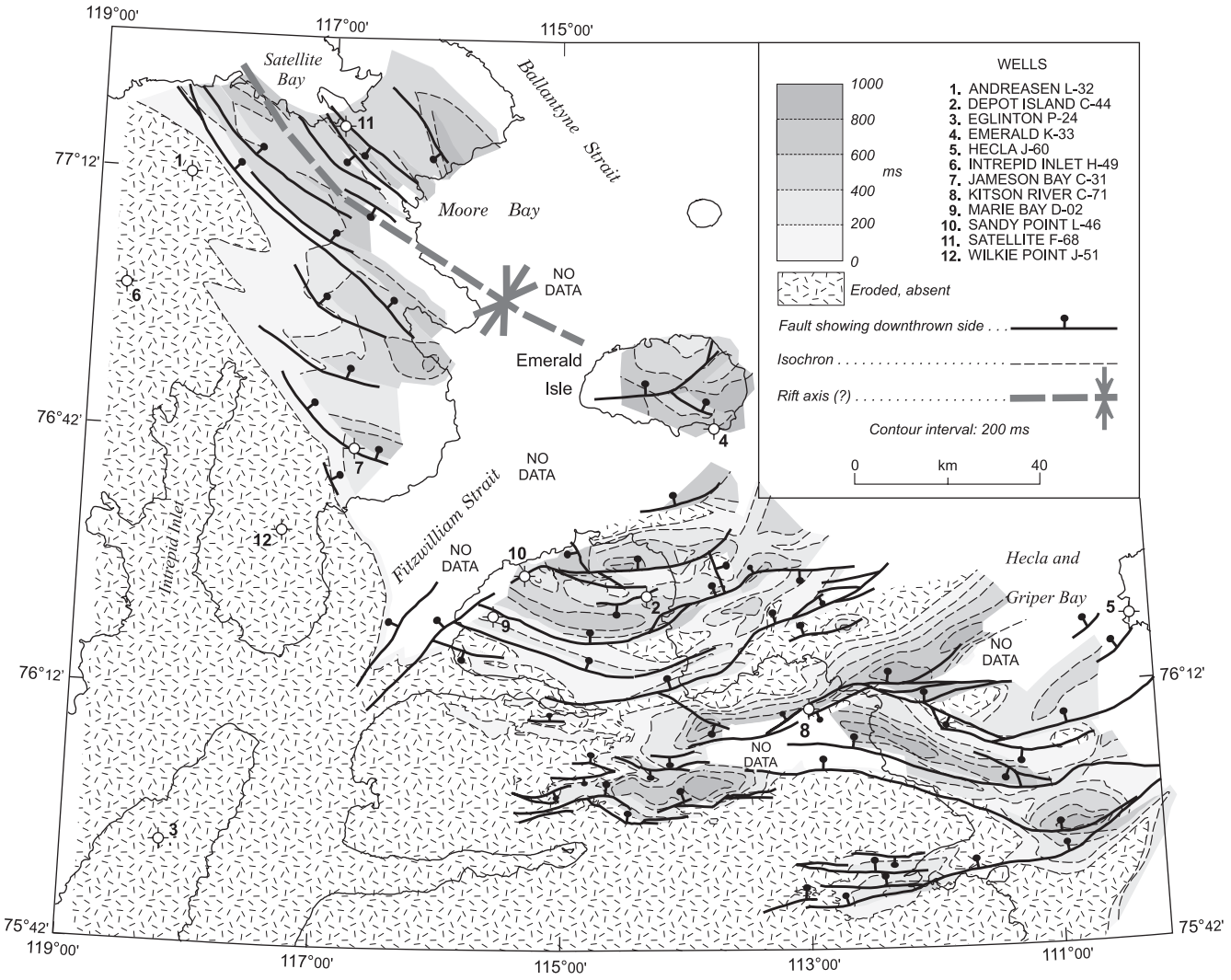

Figure 37. *Thickness isochrons and related extensional structures for Carboniferous and pre-Roadian Permian strata of the western Arctic Islands. Areas where these strata are either eroded or absent define horst blocks that have been mapped on the sub-mid-Permian unconformity. The possible rift axis on this figure is parallel to, but does not coincide with, the axis of the Sverdrup Basin, which lies northeast of Prince Patrick Island roughly along the midline of Ballantyne Strait.*

Carboniferous hanging wall succession, which ranges up to 1015 ms thick measured perpendicular to bedding and close to the assumed fault trace. This thickness is much greater than that which might be encountered in any one vertical drill hole: drilled wells which would intersect either an incomplete section above the footwall fault or a depositionally thinned interval in the graben but at some distance from the same fault. The inferred level of detachment for Jameson Fault-A lies in the panel of Ordovician(?) and older units inclined to the northeast on the thrust ramp lying above Snow Hill Forethrust-A. Upsection, the fault appears to bifurcate and die out in high Permian strata in the hinge of a regional low-amplitude anticline. On other profiles the fault has displaced units as high as the Jurassic.

Detailed stratigraphic features relating to the upper Paleozoic history of Jameson Fault-A are summarized below.

1. The Bashkirian–Kasimovian sequence everywhere rests on an angular unconformity above various inclined and peneplained Ordovician to Devonian seismic units.

2. The Bashkirian–Kasimovian sequence has a uniform thickness in the downthrown succession and appears to be onlapped from the south by the Gzhelian–Sakmarian sequence. Bashkirian–Kasimovian strata are thinner in the upthrown block.

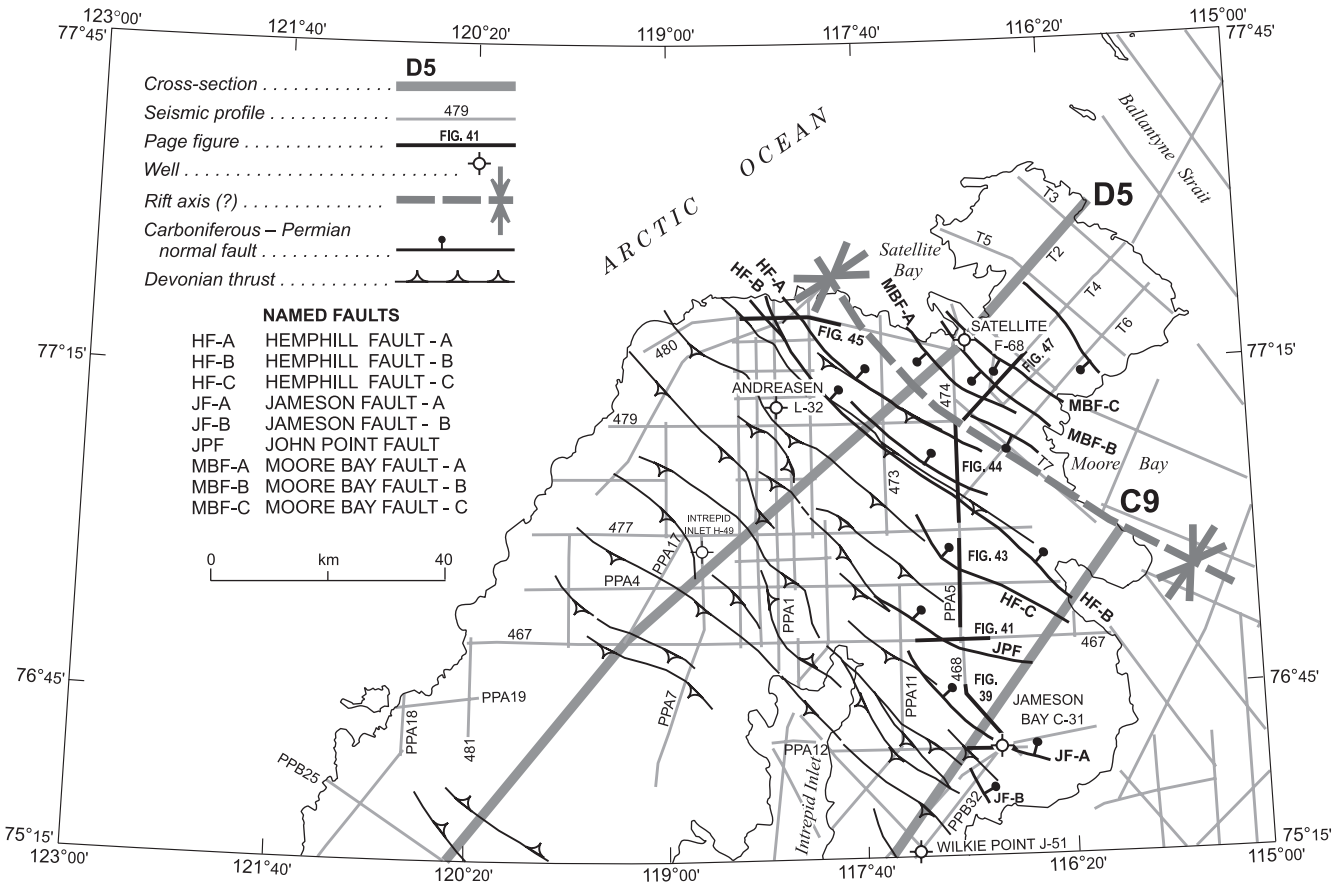

Figure 38. *Named Carboniferous–Permian normal faults, position of underlying Devonian thrust faults, and location of seismic profiles and related text figures. Orientation of the younger structures has been influenced by the anisotropy associated with the parallel attitude of the older faults.*

3. The Gzhelian–Sakmarian sequence, the principal unit of graben-fill, has divergent internal reflections. The unit thickens southward toward Jameson Fault-A. The sequence is much thinner to the southwest on the upthrown footwall block.

4. The Sakmarian–Artinskian sequence is thickest and apparently conformable with Gzhelian–Kasimovian strata on the downthrown side of Jameson Fault-A. The sequence is absent in the footwall.

5. The Kungurian sequence, preserved only in the fault hanging wall, rests with angular unconformity on rotated and peneplained strata of the Sakmarian–Artinskian and Gzhelian–Sakmarian sequences.

6. Roadian–Wordian and younger Permian strata overstep the Kungurian sequence toward the southeast and toward the northwest. The thickest section of these sequences is preserved above the updip limit of Jameson Fault-A.

7. Roadian and younger Permian sequences, and all overlying Triassic and Jurassic units, have been compressively folded such that a broad anticline is now developed over the updip limit of Jameson Fault-A.

A conceptual sketch of the Carboniferous and Permian tectonic history of Jameson Fault-A and associated structures is illustrated in Figure 40.

John Point Fault

The John Point Fault is imaged on four profiles east of the head of Intrepid Inlet (467, 468, PPA5 and unmigrated profile PPA11; Fig. 38). Minimum strike length is 13 kms with 600 m of horizontal separation and up to 635 ms of stratigraphic throw on profile 467 (Fig. 37, 38, 41). Subsurface mapping indicates that John Point Fault extends to depth into Silurian and older seismic units, that the fault is parallel to the axial trace of Brown Bluff Anticline, and that it is coplanar and potentially continuous with the northeasterly dipping Brown Bluff Thrust-A (Fig. 30, 38).

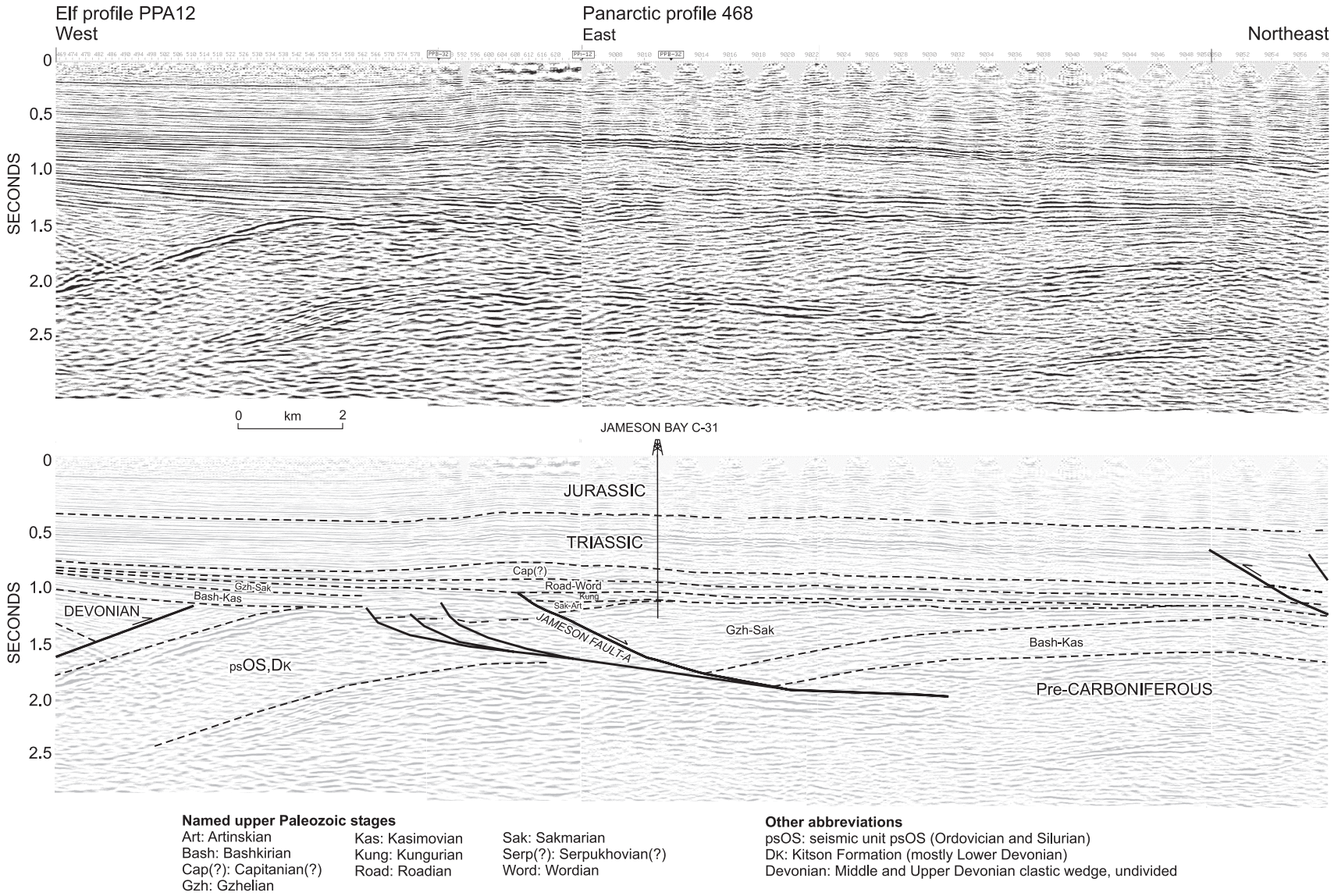

Figure 39. *Seismic expression of Jameson Fault-A and associated seismic units on portions of Panarctic profile 468 and Elf profile PPA12 near the Jameson Bay C-31 well. Syntectonic sedimentation is associated with the Bashkirian through Artinskian interval. A major unconformity occurs below the Kungurian(?) sequence and a low-amplitude inversion anticline occurs in Jurassic and older strata above Jameson Fault-A.*

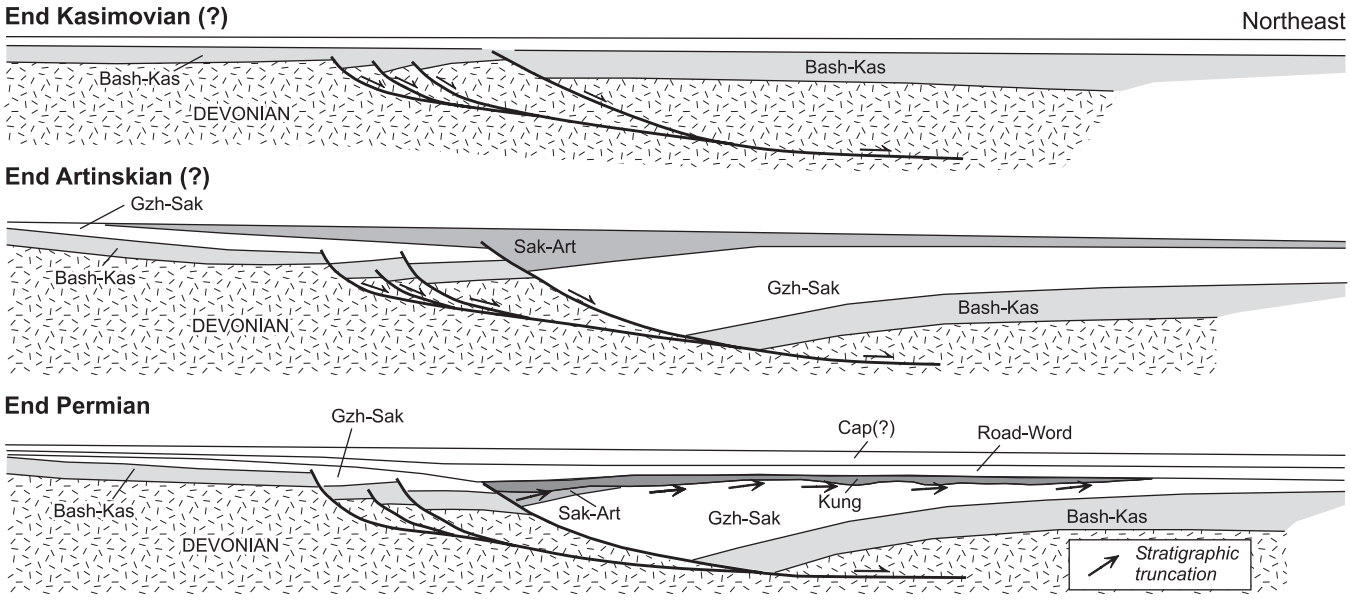

Figure 40. *Mid-Carboniferous (Bashkirian) to end-Permian (Capitanian?) kinematic model for Jameson Fault-A based on Elf seismic profile PPA12 (Fig. 39).The inversion anticline, evident in the higher strata of Figure 39 but not shown in this model, is believed to be Paleogene in age. See Figure 39 for explanation of abbreviations.*

Seismic expression of John Point Fault on profile 467 is illustrated in Figure 41. Specific seismic depositional features relating to upper Paleozoic deformation history are summarized below.

1. The Bashkirian–Kasimovian sequence in the footwall block rests on an angular unconformity above modestly inclined and peneplained Devonian strata near the prominent top-Silurian reflection. Position of the unconformity in the hanging wall is less obvious.

2. The Bashkirian–Kasimovian sequence in the fault footwall and the lower part of the same sequence in the hanging wall appears to be of uniform thickness. The upper part of the hanging wall sequence has divergent internal reflection segments.

3. The Gzhelian–Sakmarian sequence is noticeably thicker in the hanging wall of the John Point Fault than in the footwall. Internal reflections in the downthrown succession are modestly divergent, and dip away from the fault trace.

4. Sakmarian–Artinskian strata, which display local thickness variations in the downthrown succession, thin toward the bounding fault and are entirely missing in the footwall block.

5. The upper Paleozoic succession, which includes sequences as high as the Artinskian in the graben, has been flexed into an open upright anticline-syncline pair. The anticline hinge, 7 km east of the fault (as measured along the illustrated profile), has about 100 ms of maximum structural relief. Hanging wall strata dip away from John Point Fault and toward the syncline hinge, which is situated 3.8 km east of the fault in the Artinskian part of the section.

6. John Point Fault is terminated upsection below the Kungurian, and the open folds developed in Artinskian and underlying strata have been peneplained prior to unconformable overlap by the Kungurian sequence.

7. The base of the Kungurian onlaps the unconformity above the Artinskian in a westerly direction. Although the Kungurian has a relatively uniform thickness, it is thicker to the east and on profile 467 (Fig. 41), and is locally thickest above the buried graben-fill and related hanging wall syncline. The local thickness maximum of the Kungurian is developed only in the lower part of the unit.

The upper Paleozoic tectonic history of John Point Fault and the affected strata is illustrated in Figure 42.

Hemphill Fault-C

The arcuate Hemphill Fault-C is best displayed on profile PPA5 (Fig. 43). It may also extend to the southeast where it crosses the east end of profile PPA4. To the northwest the fault appears to be imaged near its strike limit on profile 477. Minimum strike length is 25 km, limit undefined to the southeast. Stratigraphic throw on profile PPA5 is about 500

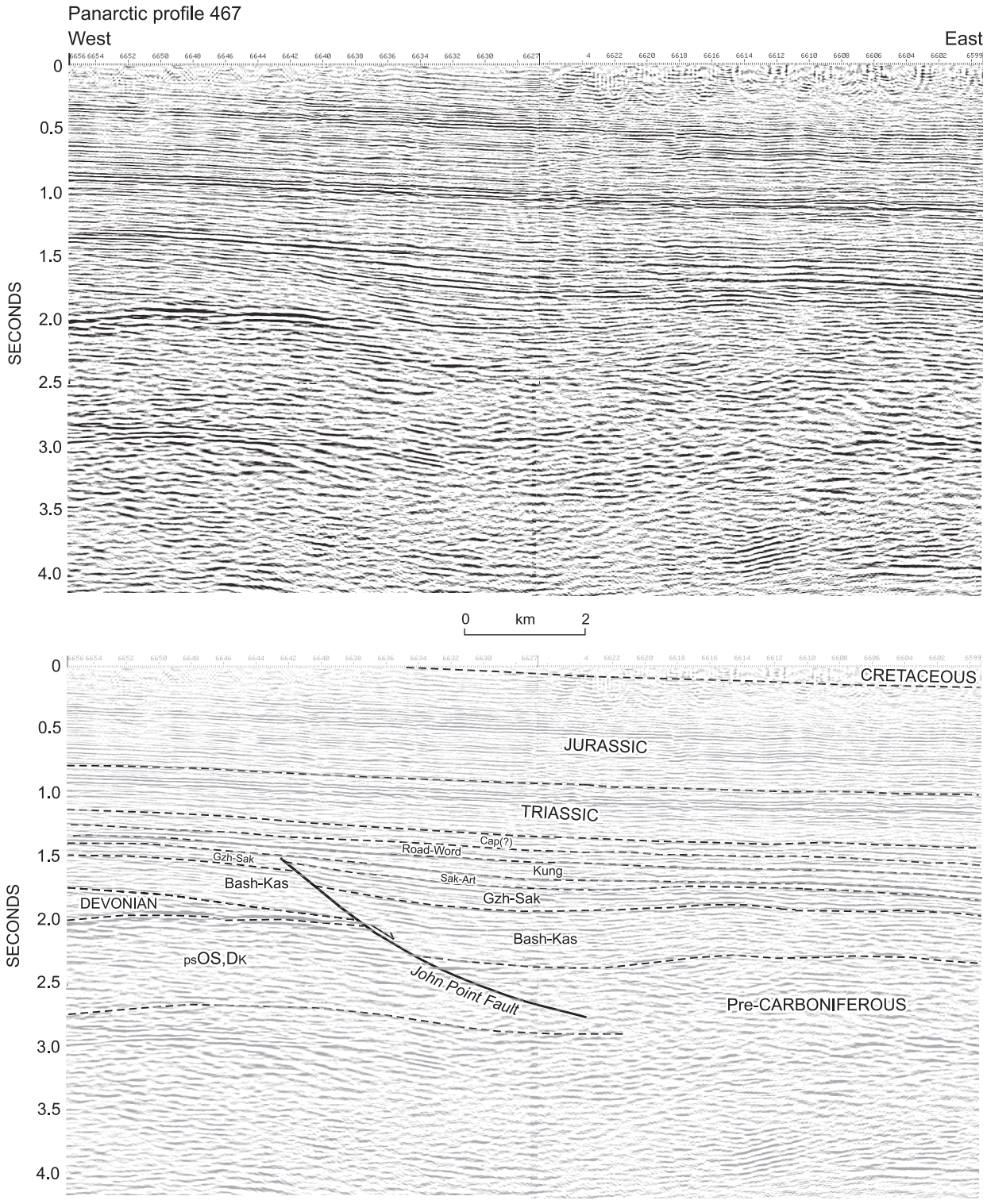

Figure 41. *Seismic expression of John Point Fault and associated seismic units on a portion of profile 467. A low-amplitude, long-wavelength anticline (with hinge below SP6614) affects Gzhelian and underlying strata, and is truncated by an angular unconformity at the base of the Sakmarian–Artinskian(?) sequence. Downthrown in the hanging wall of the John Point Fault and thickest in an adjacent syncline (with hinge below SP 6627), Sakmarian–Artinskian strata are missing below the Kungurian(?) in the upthrown footwall succession. See Figure 39 for explanation of abbreviations.*

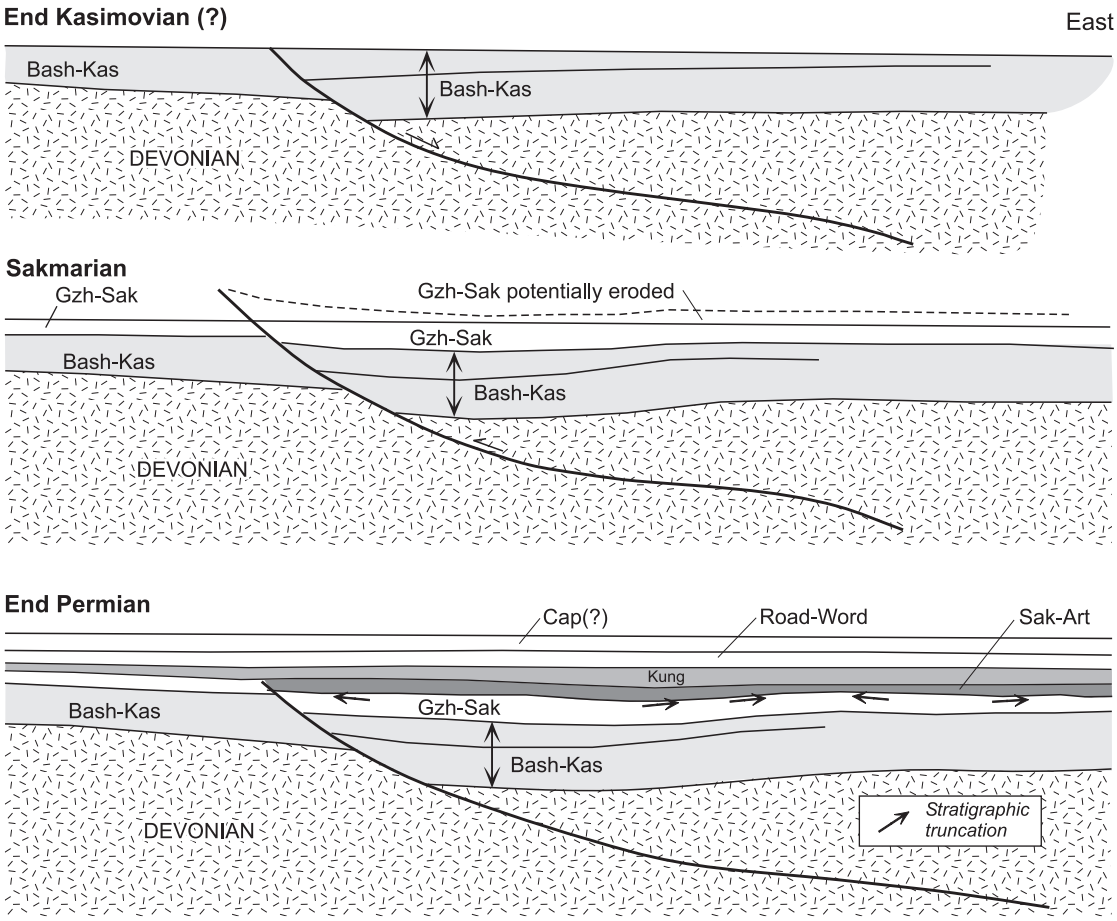

Figure 42. *Mid-Carboniferous to mid-Permian kinematic model for John Point Fault based on Panarctic seismic profile 467 (Fig. 41). Thickness of Gzhelian-Sakmarian strata, deposited prior to inversion during the Melvillian Disturbance, is drawn schematically. Local thickening of Roadian and younger Permian strata above the buried graben might be attributed to differential compaction. See Figure 39 for explanation of abbreviations.*

ms measured on the base of the Carboniferous, decreasing to less than 100 ms on the base of the Triassic (Fig. 43). Maximum horizontal separation is 950 m. The fault has a listric profile and a local detachment assumed to be near the top of the Lower Devonian, possibly on the northeast-dipping back limb of Andreasen Anticline. Hemphill Fault-C splays upsection into two separate strands on profile PPA5 (Fig. 43). One strand features a young phase of extensional slip that is traceable as high as the Triassic Schei Point Group. Related tilting of cover affects strata as high as the Middle Jurassic. The second, more northerly fault strand displays a young phase of compressive slip that extends as high as the Lower Jurassic. Specific seismic features relating to upper Paleozoic deformation history are listed below.

1. A regional angular unconformity can be correlated below the Bashkirian–Kasimovian sequence in both the footwall and hanging wall.

2. The Bashkirian–Kasimovian sequence in the downthrown block has a uniform thickness and subparallel internal reflection segments. The unit is thinner in the upthrown block and thinnest close to the trace of Hemphill Fault-C where it appears to be partly cut out by the overlying Gzhelian–Sakmarian sequence.

3. Onlapping reflection segments are indicated at the base of the Gzhelian–Sakmarian sequence in the graben. Onlap is to the north. This unit and the overlying Sakmarian–Artinskian sequence thicken and diverge toward Hemphill Fault-C in the graben and away from the fault in the upthrown block to the south.

4. The Kungurian sequence is either too thin to be resolved or is absent in both the graben and footwall close to the fault.

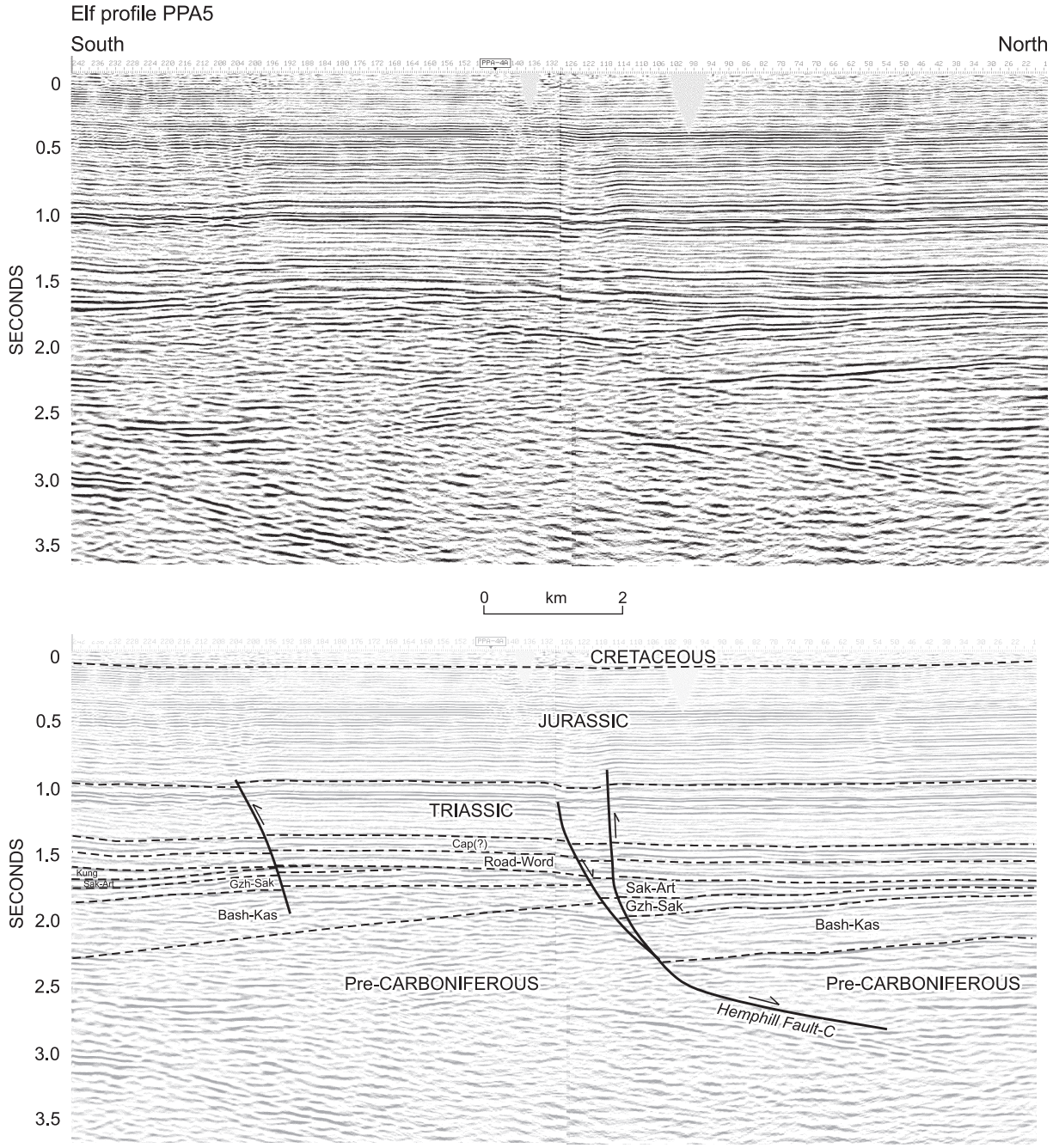

Figure 43. *Seismic expression of Hemphill Fault-C and associated seismic units on a portion of Elf profile PPA5. Significant phases of slip on this fault occurred prior to overlap by Roadian strata. The later normal faulting may be Jurassic or later in age. The compressive inversion features, evident on both Fault-C and an unnamed reverse fault below SP 200, may be Cenozoic. See Figure 39 for explanation of abbreviations.*

5. The base of the Roadian and younger Permian succession is an important unconformity surface that cuts down to the Gzhelian–Sakmarian sequence in the footwall and the top truncates inclined pre-Roadian reflectors in the graben.

6. There is no indication of faulting during deposition of Roadian and younger Permian sequences. This package has a tabular geometry with a very modest indication of progressive thickening to the north.

Hemphill Faults-A and -B

Hemphill Faults-A and -B are the longest and most fully imaged Permo-Carboniferous structures of Prince Patrick Island. They are each imaged on five or more migrated seismic profiles over minimum strike lengths of 36 and 47 km for Faults A and B, respectively (Fig. 37). Maximum stratigraphic throw ranges up to 780 ms measured on the base of the graben-fill near profile 479 for Hemphill Fault-B and up to 225 ms for Fault-A near profile 480. Maximum horizontal separation in the same areas for these structures is 2000 m and 500 m for Faults B and A, respectively. Magnitude of displacement decreases upsection within the upper Paleozoic but is observed to die away entirely at different stratigraphic levels. On profiles P474 and P480 (Fig. 44, 45) Fault-A dies out within or below the Sakmarian–Artinskian sequence. In contrast, Fault-B extends into the lower part of the Roadian–Wordian sequence on one profile but on the other it clearly displaces reflectors in the Jurassic. Small inversion structures evident in the Permian part of the section affect strata as high as the Middle Triassic in the hanging wall of both Hemphill faults on Figure 44.

Hemphill Faults-A and -B have a common strike direction, and are parallel to the axial trace of the underlying and adjacent lower Paleozoic M'Clintock Anticline and M'Clintock Point Thrust. Faults-A and -B also have a listric, concave-up profile and a common level of detachment above the northeast-dipping forelimb of M'Clintock Anticline in the lower part of the Devonian clastic wedge (cross-section D, Fig. 44, 45). Additional extensional slip is indicated within units psOS through Dk on profile 480. The seismic example in Figure 45 features a high-amplitude reflection interpreted as a primary signal response from a deep-seated, southwesterly dipping, low-angle normal fault.

Seismic depositional features specifically relating to the upper Paleozoic history of Hemphill Faults-A and -B are listed below.

1. The unconformity below the Carboniferous is drawn on a discontinuous reflector with locally moderate amplitude.

2. The Serpukhovian(?) Sequence is locally preserved on the downthrown side of Hemphill Fault-A.

3. The three sequences between the Bashkirian and the Artinskian display thickening across Hemphill Fault-B into the hanging wall succession although the pattern of thickening is inconsistent between seismic profiles (Fig. 44, 45).

4. Hemphill Fault-A appears to be detached at an intermediate level in the lower part of the Bashkirian–Kasimovian sequence on profile P474 (Fig. 44).

5. The Kungurian and younger Permian succession features a continuous, moderate amplitude reflector at the base that is apparently conformable with the Artinskian at the scale of the seismic profiles. There is no clear evidence for syntectonic sediment accumulation across Hemphill Fault-B in the lower part of this succession (Fig. 44). The Kungurian and younger Permian package is tabular in form and has a uniform thickness. Gradual thickening toward the north and east is associated with both onlapping reflection segments above the base and divergence of internal reflectors in the upper part.

A schematic deformation history of Hemphill Faults-A and -B is displayed on Figure 46.

Moore Bay faults

The dominant structure in the Satellite Bay and Moore Bay area is the pre-Pliocene Moore Bay Anticline, which involves the entire Carboniferous through Lower Cretaceous section as illustrated on Figure 47. Constraints on Permian stratigraphy are provided by the Satellite F-68 well as described by Beauchamp et al. (2001).

There are three, named, upper Paleozoic faults of regional significance in the Moore Bay and southern Satellite Bay areas. These have been identified on a portion of profile T4 (Fig. 47) and are also mapped on adjacent profiles including 474, 480, T2 and T6 (Fig. 38). The T2, T4 and T6 profiles are old single-fold surveys but do provide some constraints on upper Paleozoic geology. Several other unnamed faults are interpreted on a single seismic profile each. All of these share a common down-to-the-southwest sense of extensional slip, a listric profile and a block-rotated hanging wall half-graben succession. Minimum strike length of the named faults ranges from 20 to 25 km. Estimates of stratigraphic throw, measured on the base of the Carboniferous, range up to at least 500 ms for Moore Bay Fault-A; probably less than 250 ms for the others. Combined horizontal separation is about four km. Level of detachment is uncertain. A prominent, southwesterly dipping, seismically defined fabric is typical of the pre-Carboniferous beneath the grabens on profiles T4 and 474. There is some indication that the Moore Bay faults may root in the reactivated, low-angle, southwest-dipping thrust fault noted on seismic profile 480 (Fig. 45 and cross-section D). Stratigraphic features relevant to structural history are listed below.

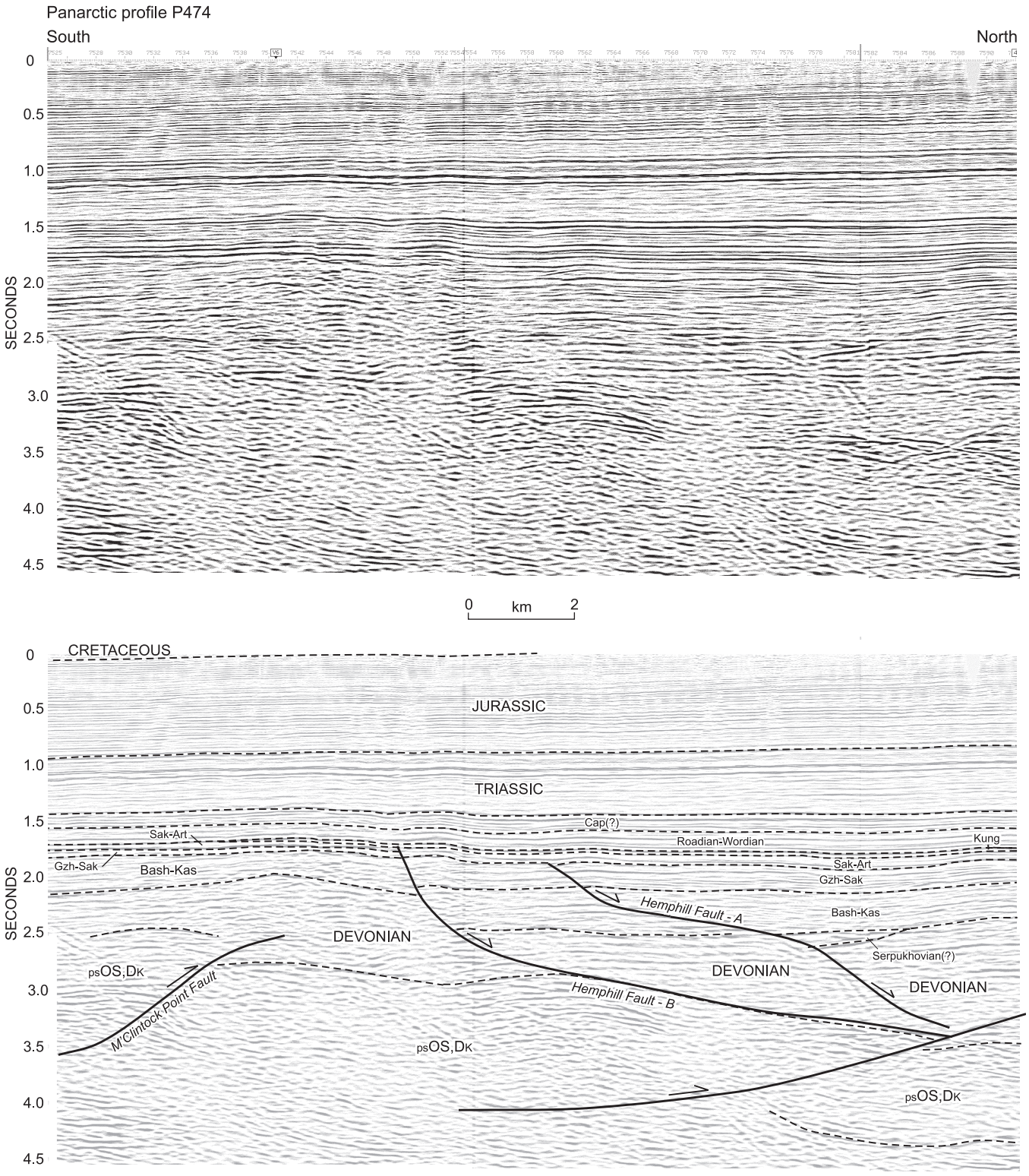

Figure 44. *Seismic expression of Hemphill Faults-A and -B and associated seismic units on a portion of Panarctic profile 474. The flattening of Fault-A in the middle of the Bashkirian-Kasimovian is attributed to sliding on a local detachment, possibly evaporite deposits that are age-equivalent to the Otto Fiord Formation (Bashkirian). Fault-B is detached near the top of the Silurian on the forelimb of a pre-existent thrust-anticline. The last phase of slip on Fault-B is compressive and appears to affect strata as high as the Carnian carbonate reflector in the Upper Triassic. See Figure 39 for explanation of abbreviations.*

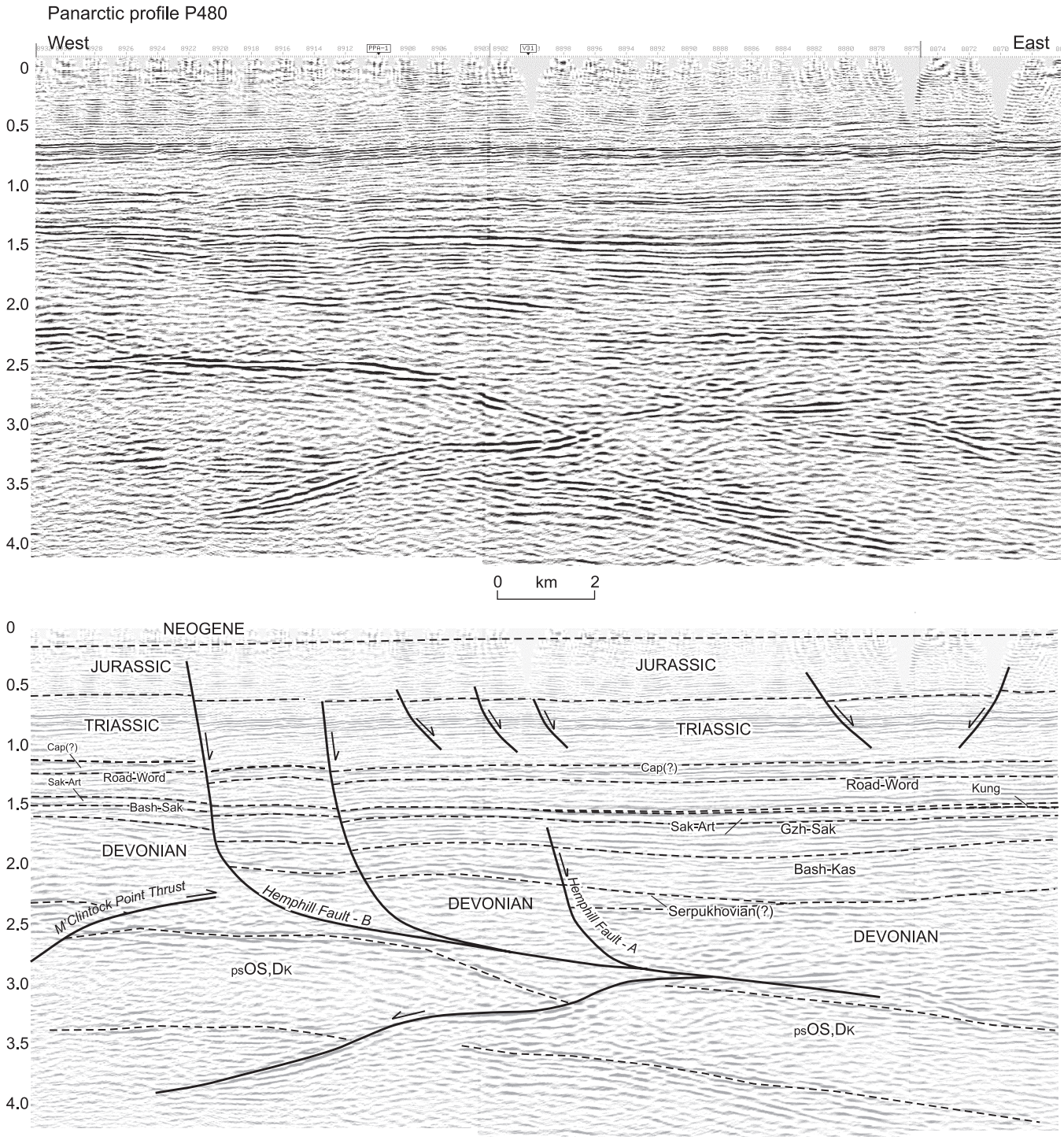

Figure 45. *Seismic expression of Hemphill Faults-A and -B and associated seismic units on a portion of Panarctic profile 480. Fault-B, as in profile 474 (Fig. 44), is detached on a pre-existent, northeast-facing fold limb. Extensional slip is also carried downsection on a pre-existent, southwesterly dipping thrust that is parallel to, and underlies, M'Clintock Point Thrust. The array of small, late stage, normal faults above 1.0 second are believed to be post-Middle Jurassic in age. See Figure 39 for explanation of abbreviations.*

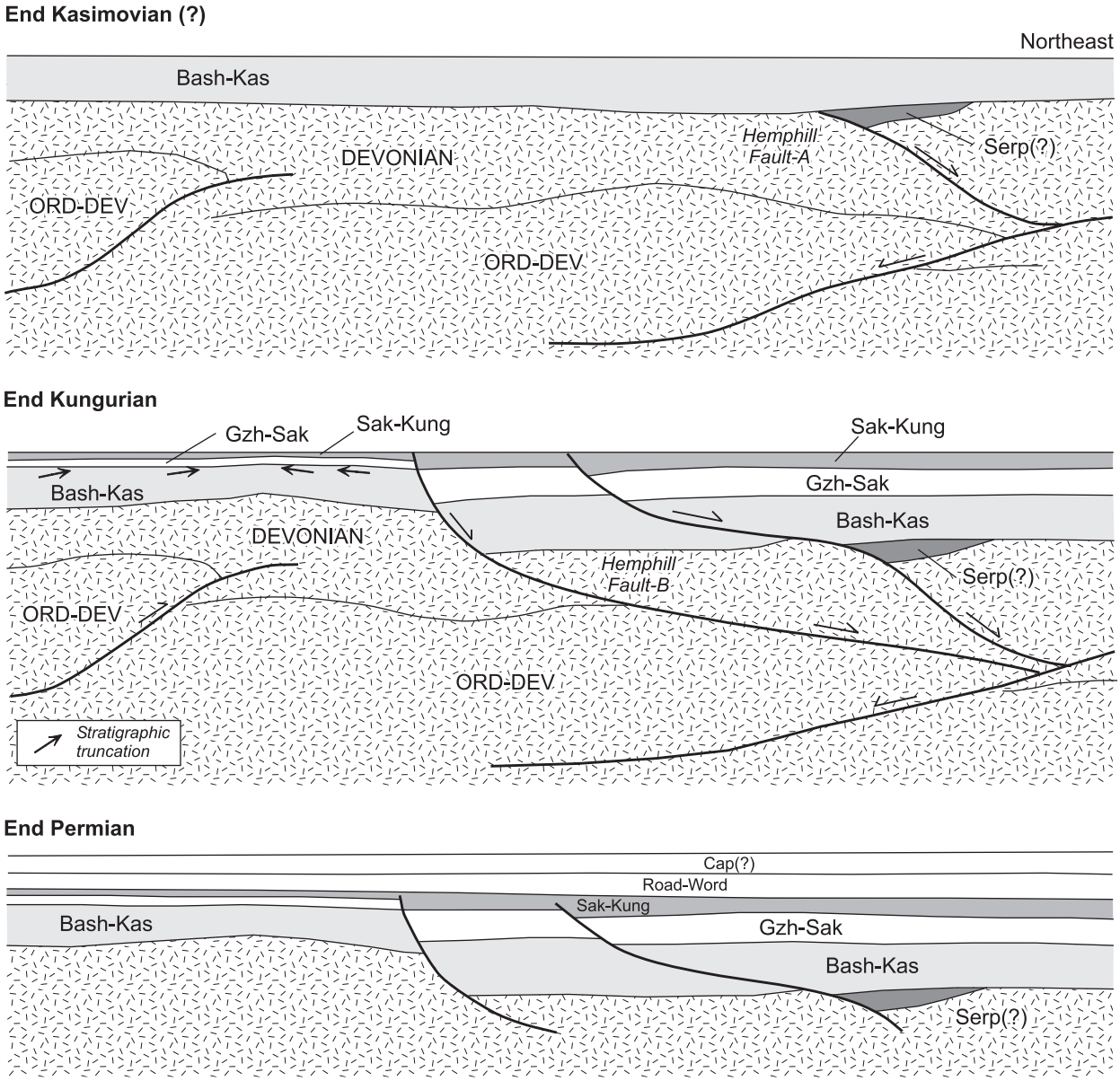

Figure 46. *Kinematic model for Hemphill Faults-A and -B based on Panarctic seismic profiles 474 (Fig. 44) and 480 (Fig. 45). The extensional slip that develops in the mid-Carboniferous and Permian is restored into a Devonian(?) thrust anticline that must have existed in the Early Carboniferous. Compressive slip on M'Clintock Point thrust is interpreted to have been rejuvenated in the Early Permian because a long-wavelength anticline expressed in the Bashkirian–Kasimovian sequence is peneplained below undeformed Gzhelian(?) and younger strata. See Figure 39 for explanation of abbreviations.*

1. Serpukhovian(?) strata have been interpreted in the hanging wall only of Moore Bay Fault-A.

2. Internally divergent reflections near the base of the Gzhelian–Sakmarian unit are especially well defined in the hanging wall half-graben above Moore Bay Fault-C on T4 (Fig. 47). Part of the structure in this graben has been modified by a later, northeast-vergent, minor thrust that appears to be detached near the base of the Gzhelian–Sakmarian sequence. Divergence of reflectors also occurs in this sequence in the half-grabens above Moore Bay Faults-A and -B, and divergent reflection segments are indicated through the Gzhelian to Artinskian interval north of Fault-C. The Kungurian and younger Permian succession is a roughly tabular set of units with internal and bounding reflections that progressively diverge toward the northeast.

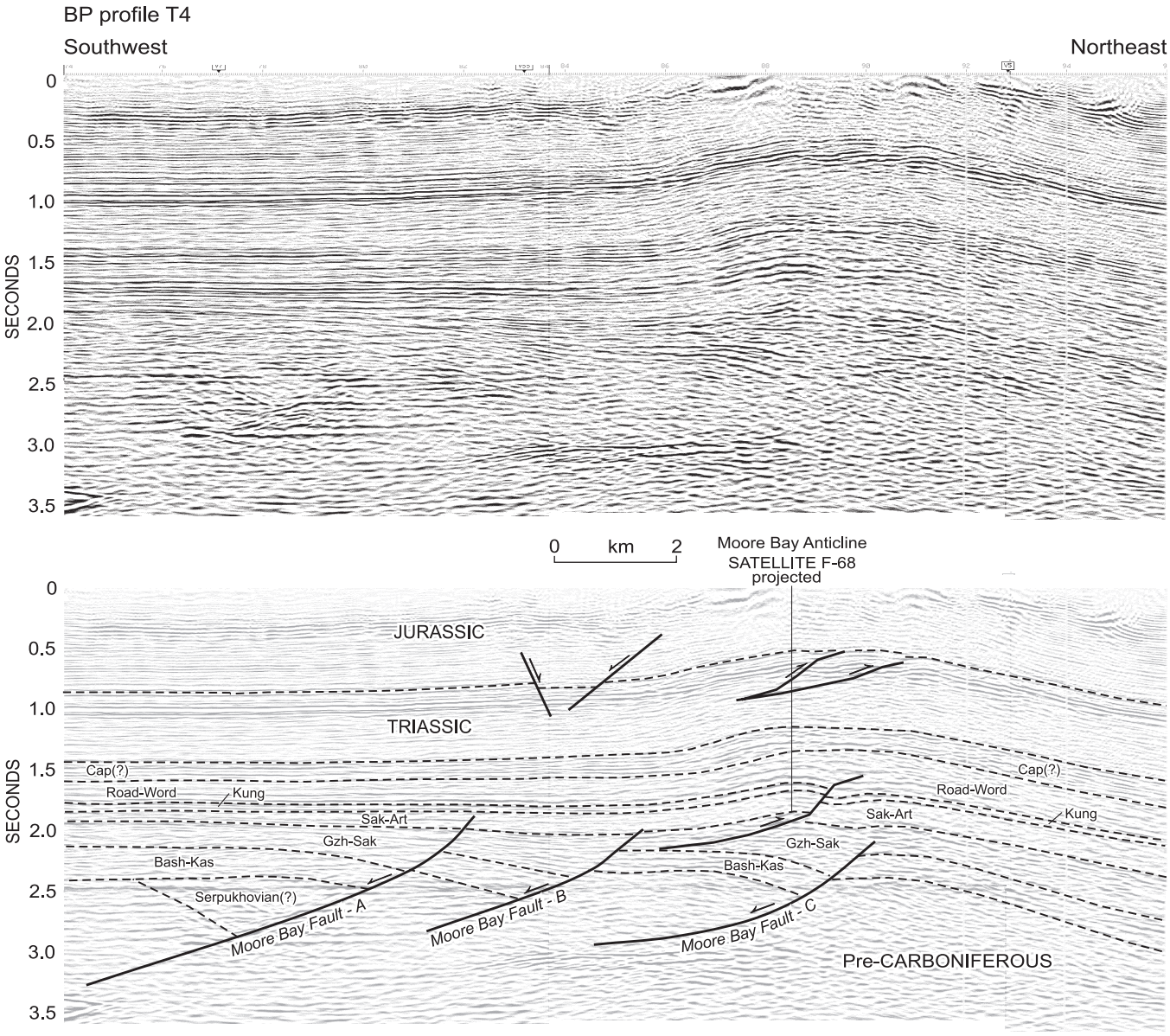

Figure 47. *Seismic expression of Moore Bay Faults -A, -B and -C, and associated seismic units on a portion of BP profile T4. Late Paleozoic slip on these faults is extensional in character and occurred in two phases: Pre-Bashkirian (Serpukhovian?) and Gzhelian–Sakmarian. The normal faults above 1.0 second are Middle Jurassic or younger. The Moore Bay Anticline and associated small thrust faults in the hinge area are probably Paleogene structures. Primary signal below 2.0 seconds is partly obscured by horizontal multiples. See Figure 39 for explanation of abbreviations.*

Regional implications

General features

The seismic profiles of Prince Patrick Island reveal that the Carboniferous and Permian rift belt of northern Melville Island and adjacent areas of the Sverdrup Basin also continues to the west (Fig. 37). A close spatial and kinematic relationship exists between pre-existing Franklinian structure and the distribution of extensional structures in the upper Paleozoic. In map view, this is manifested by the coincident location of the rift belt over the internal subdomain of Canrobert Hills Fold Belt and by the parallel development of specific graben-boundary faults and specific underlying folds and thrusts (Fig. 38). The convex, southwestward-facing, arcuate shape of folds and thrusts in the Franklinian belt is matched by the convex southwestward-facing arcuate pattern of normal faults and grabens in the rift belt of the embryonic Sverdrup Basin.

This spatial association of younger and older structures is readily explained by a linked kinematic history. The pre-existence of dipping planes of weakness parallel to bedding in the lower Paleozoic has provided suitable surfaces for slip reactivation during subsequent extension (Fig. 46). Key surfaces include shale units in the lower part of the Devonian clastic wedge and the detachment in the upper part of seismic unit ps5. Northeastward-dipping planes in the Devonian and older section of the thrust-fold belt have been especially vulnerable to reactivation. This accounts for the predominance of down-to-the-northeast extension faults in the upper Paleozoic. Some of the normal faults are rooted on pre-existent thrusts. Therefore, restoration of the upper Paleozoic extension provides for an equivalent amount of additional shortening in the older, underlying thrust belt; approximately 12 km of horizontal separation measured on the sub-Carboniferous unconformity surface.

It has also been shown that thrust-folds in the Canrobert Hills Fold Belt tend to plunge and die away to the west. The form of termination is right-hand en echelon, a pattern that necessitates the existence of unrecognized elements of dextral strain between the thrust-fold belt and a rigid block to the west under Prince Patrick Island. Similarly, graben-boundary normal faults extend farther to the south on western Melville Island than on Prince Patrick Island and die away to the west in an en echelon arrangement that matches the arrangement in the underlying thrust-fold belt. Assuming a stationary block in the west and south, the mobile components of the rift zone would have slid to the north, necessitating approximately 4.5 km of sinistral strain within the region of terminating extension faults situated between westernmost Melville Island and northwestern Prince Patrick Island.

Upper Paleozoic deformed belts

The deformation history of the various faults that are mapped and illustrated on Figures 38 through 47 is summarized on a simplified tectonic correlation chart (Fig. 48). Specific faults named and located in columns on this diagram are arranged geographically from southwest at left to northeast at right. There are two geographically and tectonically distinct regions: 1) a northeastern region, that includes the three Moore Bay faults, Hemphill Fault-A and the hanging wall of Hemphill Fault-B, which has a multi-phase extension history followed by passive subsidence beginning in Sakmarian or Artinskian time; and 2) a region, embracing the footwall of Hemphill Fault-B and all areas to the southwest, that has a history of Carboniferous extension followed by a mostly Permian interval of interwoven inversion and extension that persisted until passive subsidence set in before the Roadian.

Serpukhovian(?)

Seismic interpretation indicates that rifting began with deposition in a narrow belt of block-rotated strata now preserved in the hanging wall of Moore Bay Fault-A and Hemphill Fault-A of the subsurface Satellite Bay area. While Beauchamp et al. (2001) has suggested a correlation of this sequence with the conglomerate and redbed deposits of the Serpukhovian Borup Fiord, there is no age control. Alternative correlation might be with younger Carboniferous redbed units, such as the Canyon Fiord Formation, with older, graben-related, Carboniferous strata such as the fluvial and lacustrine Emma Fiord Formation (late Viséan), or with some other package of upper Devonian to lower Carboniferous (mid-Famennian through mid-Viséan) strata not yet encountered in the Canadian Arctic Islands.

Bashkirian to Kasimovian

The belt of Carboniferous strata expanded far to the southwest beginning in the Bashkirian and is believed to be associated with accumulation of terrestrial redbed deposits and shallow-marine strata of the lower Canyon Formation Formation (Beauchamp et al., 2001). The restored (pre-deformed) Bashkirian–Kasimovian seismic sequence is a gradually tapering wedge that thickens to the northeast across most of subsurface northeastern Prince Patrick Island. Synsedimentary deformation of Bashkirian age is apparently restricted to extensional slip on Jameson Fault-A. In contrast, extension on John Point Fault does not become apparent until later in the deposition of this sequence (Moscovian time, perhaps). Again there is no age control on any of these observations. However, transgressive Bashkirian and Moscovian strata are widespread in the upper Paleozoic rift belt of northern Melville Island (Riediger and Harrison, 1994).

Gzhelian to Sakmarian

This interval is associated with deposition of the Belcher Channel and Nansen formations of the shelf and the Hare Fiord Formation of the deeper water realm (Beauchamp et al., 2001). Erosion and possible compressive buckling of the Bashkirian–Kasimovian sequence is evident in the footwall of Hemphill Fault-B prior to deposition of the Gzhelian–Sakmarian sequence (Fig. 44, 46). However, widespread synsedimentary extension faulting is more generally typical of tectonic activity during deposition of the younger sequence. This activity includes rejuvenated slip on Moore Bay Fault-A and the first obvious phase of syndepositional slip on Hemphill Faults-B and -C, and Moore Bay Faults-B

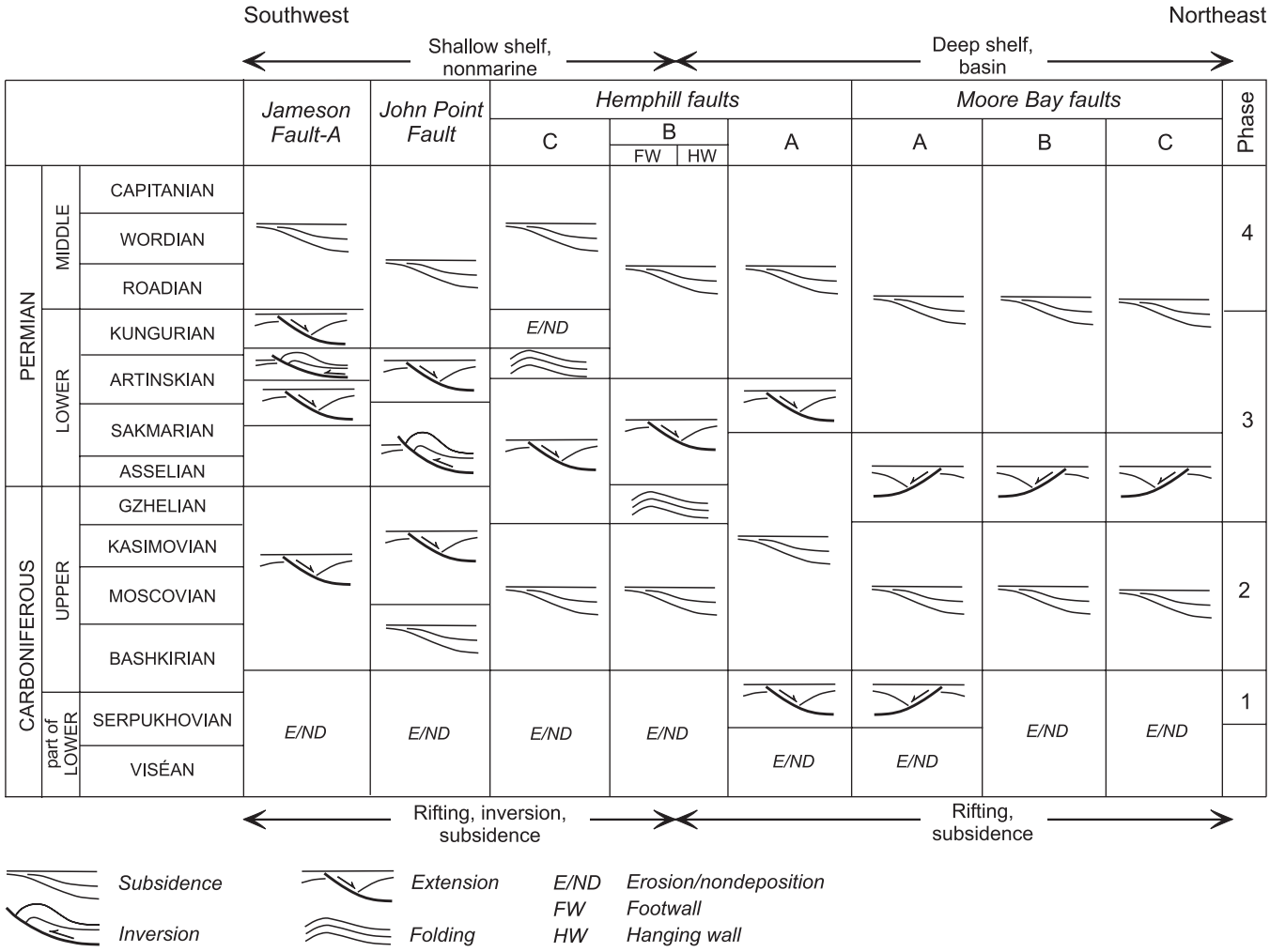

Figure 48. *Summarized tectonic and depositional history for Carboniferous and Permian faults and associated strata of subsurface northeastern Prince Patrick Island. The Carboniferous rift belt appeared first in the Serpukhovian(?) in the northeast and expanded to its full extent during the Bashkirian. Inversion structures occur only southwest of Hemphill Fault-B. However, stages of inversion and extension appear to be unconstrained temporally within the Lower Permian. For example, folds have developed in the Permian section at three different times adjacent to four different faults, and syndepositional extension occurred subsequent to peneplaining of these folds at three different times on three of the four same faults.*

and -C. Westerly directed open folding of the Gzhelian–Sakmarian and underlying sequences in the hanging wall of John Point Fault, and the development of an angular unconformity below the Kungurian sequence invites several interpretations. However, discussion of this topic is deferred to a general presentation of the regional tectonic setting as it existed prior to the Roadian (see under "Melvillian Disturbance" below).

Sakmarian through Kungurian

This time interval spans the period of deposition of the Raanes and Sabine Bay formations of the shelf and the upper Hare Fiord and Trappers Cove formations of the basin slope. Syndepositional extension terminated prior to overlap of these basin facies deposits above the Moore Bay faults (Fig. 47). However, slip appears to have continued during the Sakmarian to Artinskian interval on all the Permo-Carboniferous faults of the shelf region to the southwest (Fig. 48). The Kungurian appears to be conformable on the Artinskian at the scale of the seismic profiles in the hanging wall graben fill of Hemphill Faults-A and -B and John Point Fault. However, the Kungurian and overlying Permian sequences are separated from the Sakmarian–Artinskian by a seismically defined disconformity in the hanging wall of Jameson Fault-A and Hemphill Fault-C. A final interval of extensional faulting is indicated on Jameson Fault-A during the Kungurian prior to conformable overlap by Roadian and younger strata.

Melvillian Disturbance

The Melvillian Disturbance was named by Thorsteinsson and Tozer (1970) for compressive deformation features, typically represented on northwestern Melville Island, that affect the Carboniferous Canyon Fiord Formation but not the unconformable cover of near-flat-lying Trold Fiord Formation (Wordian). Evidence for Early Permian tectonics elsewhere in the Arctic region was also summarized by Thorsteinsson and Tozer (1970). Many new field and subsurface observations, having both local and regional significance, are provided by Beauchamp et al. (1989a, b, 2001) and Beauchamp (1987). Harrison (1995) described various structures specifically associated with the Melvillian Disturbance in the Canrobert Hills region of Melville Island and suggested that sandstone and pebble conglomerate of the mid-Permian Sabine Bay Formation represent detritus shed from the exposed region of Melvillian deformation. After additional consideration of the Prince Patrick Island seismic data, Beauchamp et al. (2001) suggested that the definition of the Melvillian Disturbance should be expanded to include all structures formed in compression between the Gzhelian and the end of the early Permian (Kungurian). Beauchamp et al. (2001) indicated three potential phases for the Melvillian deformation: the Gzhelian–Asselian, Sakmarian, and Kungurian.

The tectonic setting proposed for the Melvillian Disturbance on northwestern Melville Island is consistent with overall strike-slip deformation (Harrison, 1995). This setting explains the occurrence in that area (the Canrobert Hills region) of dextral offsets on easterly striking vertical faults, graben-fill inversion folds with easterly to northeasterly striking axial planes, and secondary directions of tectonic transport consistent with extension on northwesterly striking faults. Beauchamp et al. (2001) pointed out that this analysis of the strain elements affecting Carboniferous strata of northwestern Melville Island can be equally applied to the mapped structures within Lower Permian and Carboniferous strata of subsurface Prince Patrick Island. The present analysis supports these conclusions. However, it is also worth pointing out that each of the mapped faults on Prince Patrick Island has a distinct and characteristic slip history (Fig. 48). Stages of inversion and extension appear to be unconstrained temporally within the Early Permian. For example, folds have developed in the Permian section at three different times adjacent to four different faults, and syndepositional extension occurred subsequent to peneplaining of these folds at three different times on three of the four same faults. While separate phases or stages of Melvillian deformation can be counted, based on the number of intervening depositional sequences, data are presently insufficient to prove that overall regional style of deformation has changed in any way between the Gzhelian and the end of the Kungurian. A simpler model would be to consider the Melvillian Disturbance a protracted interval of localized transpressive and transtensive crustal deformation superimposed on the evolving pattern of Lower Permian sediment accumulation and related eustatic events.

While Lower Permian folds, minor thrusts and extension faults are spatially constrained to the southwestern basin-marginal region, coeval deformation affecting deeper water strata to the northeast is exclusively extensional in character. This paleogeographic arrangement of contrasting deformed belts was also described from the southwestern basin margin (Canrobert Hills) and deeper water (Sabine Peninsula) areas of Melville Island (Harrison, 1995). On both Prince Patrick and Melville islands, Permian inversion structures are only found within the pre-existing shallow-marine and nonmarine Upper Carboniferous rift belt. The Sabine Bay Formation (Kungurian) remains the only proven succession of recycled siliciclastic detritus shed from subaerially exposed Melvillian highlands. Barring the probability of a major eustatic sea-level drop at this time, the climax and termination of the Melvillian Disturbance appears to have immediately preceded or been synchronous with deposition of the Kungurian clastic wedge.

Roadian and later Permian subsidence

The deposition of the Kungurian sequence marks the end of significant faulting in the upper Paleozoic of Prince Patrick Island. Subsequent patterns of sediment accumulation in the later Permian were influenced by the rift architecture of the embryonic Sverdrup Basin in so far as thickness isochrons are parallel to the regional trends of the underlying rift zone (Fig. 37, 38, 49). However, the dominant influences on basin evolution during this time, and continuing down to the Middle Jurassic, were eustasy, sediment supply, paleoclimate, and rates of regional basin subsidence (Beauchamp et al., 2001). An important related observation is that the post-rift Permian, Triassic, and younger strata continue to thicken to the northeast beyond Prince Patrick Island. The Carboniferous rift axis noted between Moore Bay Fault-A and Hemphill Fault-A does not appear to have had a sustained influence on the subsequent alignment of the Sverdrup Basin depocentre.

MESOZOIC BASIN EVOLUTION NEAR THE ARCTIC CONTINENTAL MARGIN

Introduction

The Mesozoic history of the report area is informally divisible into three phases, each having a distinct pattern of basin formation and related deformation. The first phase is marked by the ongoing subsidence of the Sverdrup Basin,

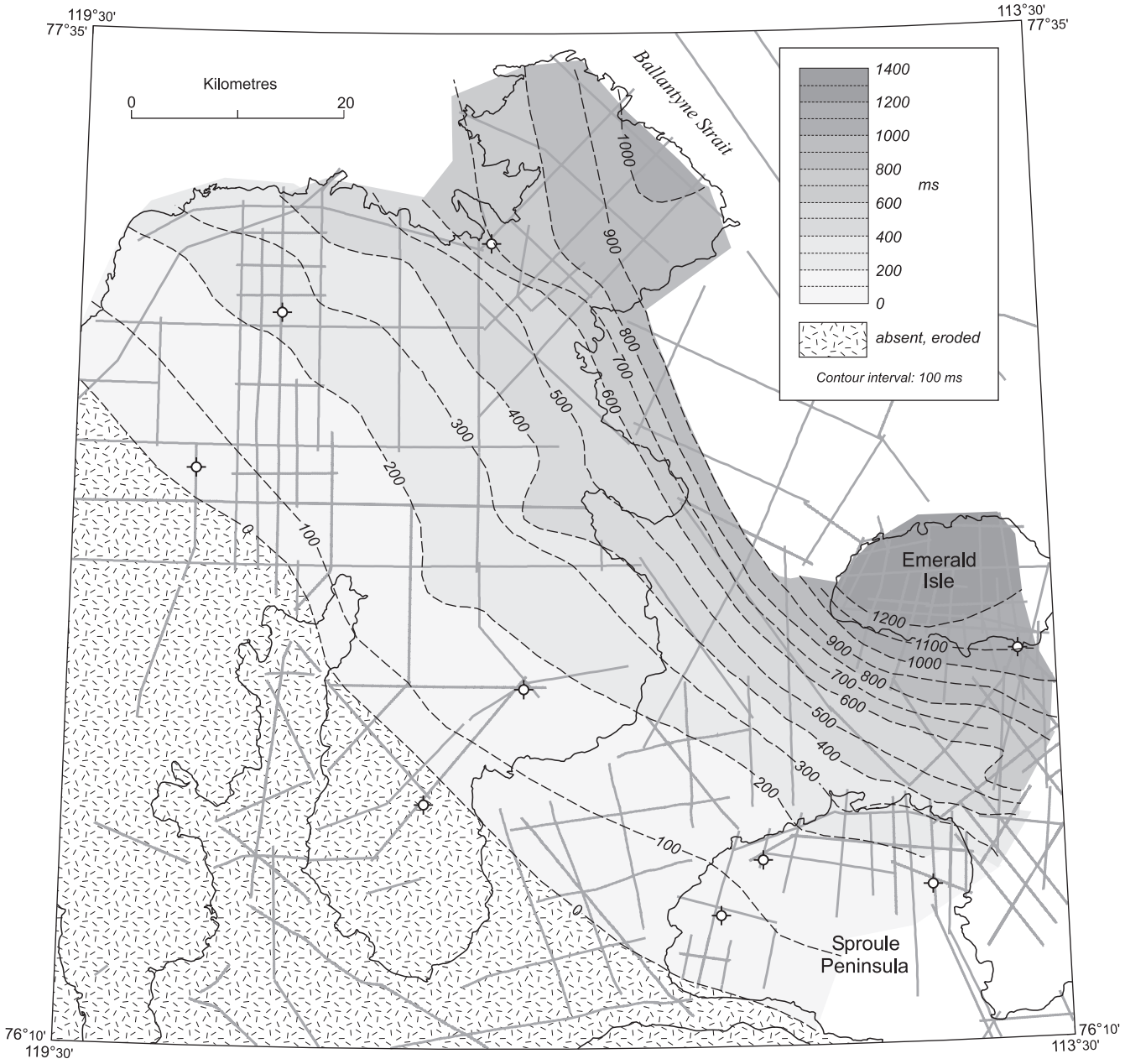

Figure 49. *Thickness isochron map from the base of the Sabine Bay Formation (Kungurian?) to the top of the Trold Fiord Formation (top of Permian), northeastern Prince Patrick Island, Emerald Isle, and Sproule Peninsula on northwest Melville Island. Contours are broadly parallel to the rift-related normal faults shown on Figure 37. However the maximum thickness isochron for later Permian strata lies northwest of the underlying Carboniferous rift axis (compare with Fig. 37).*

which began in the mid-Permian and continued at least to the beginning of the Middle Jurassic. The second phase, starting in approximately Aalenian time, is marked by the additional development of four cratonic basins southwest of the Sverdrup Basin, and the propagation from Banks Island to northern Prince Patrick Island of a northerly trending Jurassic–Lower Cretaceous rift system parallel to the Arctic continental margin. The third phase of Mesozoic basin development is represented by the early Albian burial of the pre-existing rift system, and the growth of a continental-margin sedimentary prism during and subsequent to sea floor spreading in the Arctic Ocean basin.

Triassic to Middle Jurassic structural evolution

The previous discussion of the structural geology of the Carboniferous and Permian succession of Prince Patrick Island has established, from seismic evidence, several phases of rifting in the western Sverdrup Basin and a transition to passive subsidence following an episode of Early Permian graben inversion (Table 2). The regional subsidence patterns for the early history of the western Sverdrup Basin are illustrated on a structure isochron map for the mid-Permian (approximately Roadian) to top Permian seismic interval (Fig. 49). The pattern for the later Permian continued from the Early Triassic to approximately the base of the Middle Jurassic (Fig. 50). General features of the preserved Mesozoic depositional record include unconformity-bound transgressive-regressive sequences dominated by deltaic and shelf-proximal quartz-rich sandstone deposits in the southwest (with an interval of variably siliciclastic limestone in the Upper Triassic) and offshore mudrock to the northeast. Numerous faults and some folds have been mapped that offset or otherwise deform these strata. However, there is very little evidence to indicate that any of these structures actually existed or influenced the patterns of deposition prior to the Middle Jurassic. Evolution of subsidence and basin filling from the Early Triassic to the end of the Early Jurassic was primarily influenced by external factors including eustasy, climate and sediment supply. However, insights into subtle shifts in the locus and trend of basin margin uplift and subsidence are provided by the preserved limits of the mapped sequences (Fig. 51). Data on this map are compiled from measured sections, wells and seismic profiles. The map illustrates the sequence preservation limits prior to widespread regional uplift events of the post-Cretaceous and pre-Pliocene period. In most instances the lines on this figure do not correspond to depositional limits because the nonmarine and proximal marine facies belts, potentially many tens or even hundreds of kilometres wide, have been removed during intervals of erosion that preceded overlap of subsequent transgressive deposits.

The Carboniferous limit on Figure 51 defines the erosional edge of the Bashkirian to Sakmarian Canyon Fiord Formation and related shelf carbonate units. The preserved limit of these strata defines the approximate southwestern extent of rift-related normal faulting associated with the embryonic development of the Sverdrup Basin. A modest realignment and southerly shift is evident in the northwestern segment of the basin margin and hinge of basin subsidence for the Roadian and overlying Permian on Prince Patrick Island, which includes the Van Hauen and Trold Fiord formations.

The limit for the Lower Triassic (Bjorne Formation) is slightly to the southwest of the Permian limit. However, there is no indication of a shift in local tectonic setting and no change in basin-margin trend. A significant southwesterly expansion of the subsiding basin margin is also indicated for the Lower to Upper Triassic depositional interval without a corresponding shift in tectonic setting or basin-margin realignment. The limit for the subsurface Middle Triassic is believed to follow closely that of the Upper Triassic. The Carnian part of the Upper Triassic, however, extends into the outcrop belt. This relationship is expressed in exposures of the Pat Bay Formation in outcrop sections both east and west of Intrepid Inlet. The limit for the Sinemurian is similar to that for the Upper Triassic. The modest basinward shift of the Sinemurian zero edge is reflected by the overstep of the Grosvenor Island Formation by the Intrepid Inlet Member of the Jameson Bay Formation between the east and west sides of Intrepid Inlet. The Toarcian limit, which lies in the Jameson Bay Formation, is the latest zero edge for which a persistent northwesterly trend is apparent for the basin margin. The southwesterly shift of the basin margin in the Toarcian is expressed by numerous sections east of Mould Bay and around Landing Lake, and by the limit of the correlative seismic unit on Eglinton Island and western Prince Patrick Island. This zero edge projects to the southeast toward west-central Melville Island. However, the Toarcian and all younger strata (as high as the Volgian) have been entirely stripped from above the Devonian on all parts of southwestern Melville Island.

Evidence provided by surface sections and seismic profiles in the Green Bay area suggests that a significant adjustment in patterns of sediment accumulation and related structural style was initiated during an interval of basin margin exposure between the late Toarcian and the early Aalenian. This is expressed on Figure 51 by local relief on the post-Toarcian unconformity surface below overstepping Aalenian strata. The result of the pre-early Aalenian tectonic adjustment is also expressed by the preserved limit for Bajocian and Bathonian strata below disconformable cover of Callovian and Oxfordian to Kimmeridgian strata. Jurassic sediments through this period occupied a trough aligned with Eglinton Island and the axial line of the embryonic Eglinton Basin. The basin is bound to the west by the ancestral Prince Patrick Uplift. The ancestral uplift was most extensive in the Middle Jurassic prior to the Bajocian, it persisted throughout the Middle and Late Jurassic and still existed farther to the west (north of Dyer Bay) in the Volgian. An uplift of comparable Middle Jurassic age also existed east of Eglinton Basin on southwestern Melville Island. Amidst these Jurassic paleogeographic highs and the intervening basin is a complex array of seismically defined half-grabens and

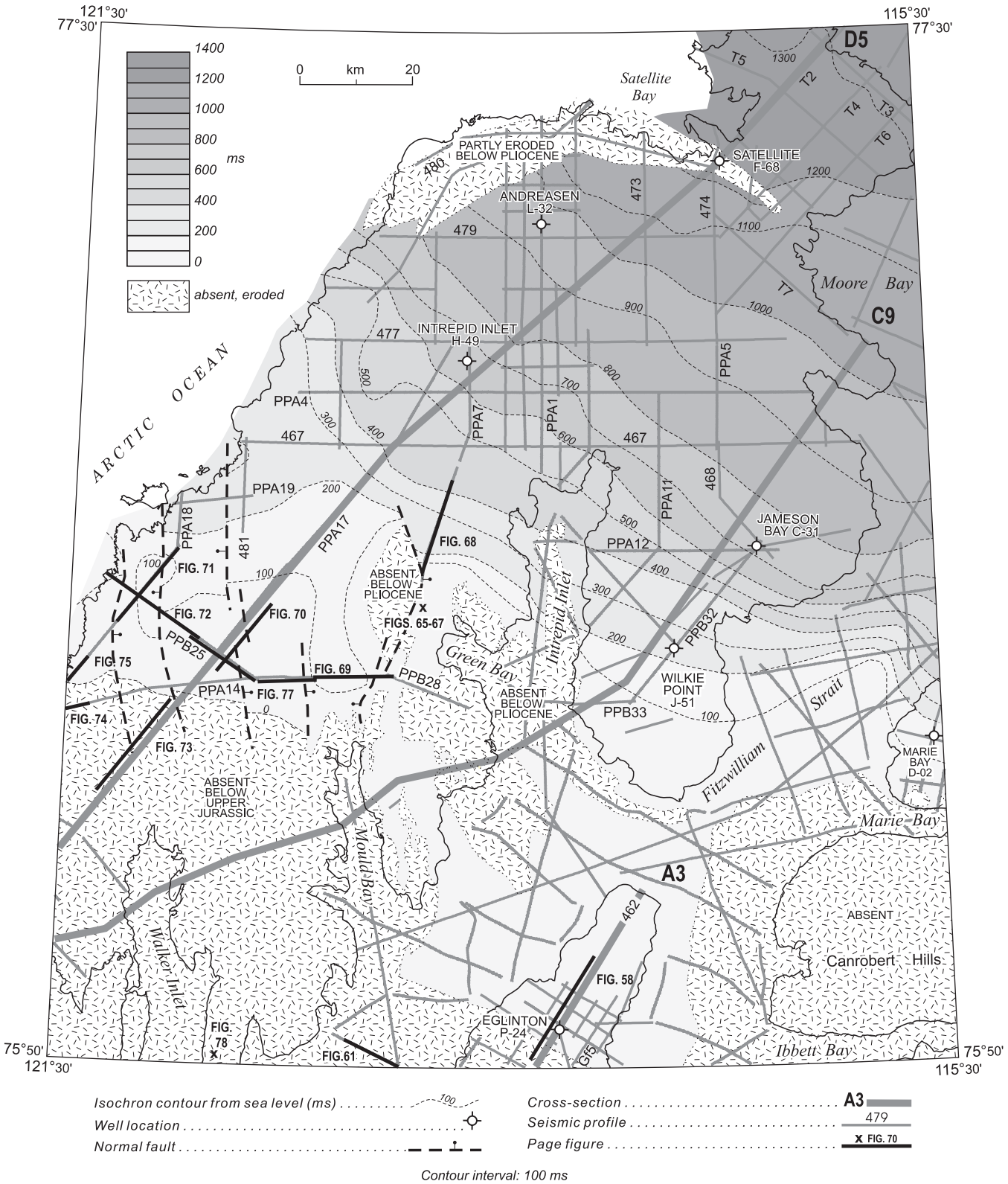

Figure 50. *Thickness isochron map from the base of the Lower Triassic Bjorne Formation through to the top of the Middle Jurassic (Aalenian) Sandy Point Formation of Prince Patrick and Eglinton islands. Areas of local absence or erosion of these strata around Satellite Bay, Green Bay and Intrepid Inlet, and on Melville Island south of Marie Bay also correspond to positive Bouguer anomalies (Fig. 22). Folding and local uplift in the mid-Tertiary is assumed.*

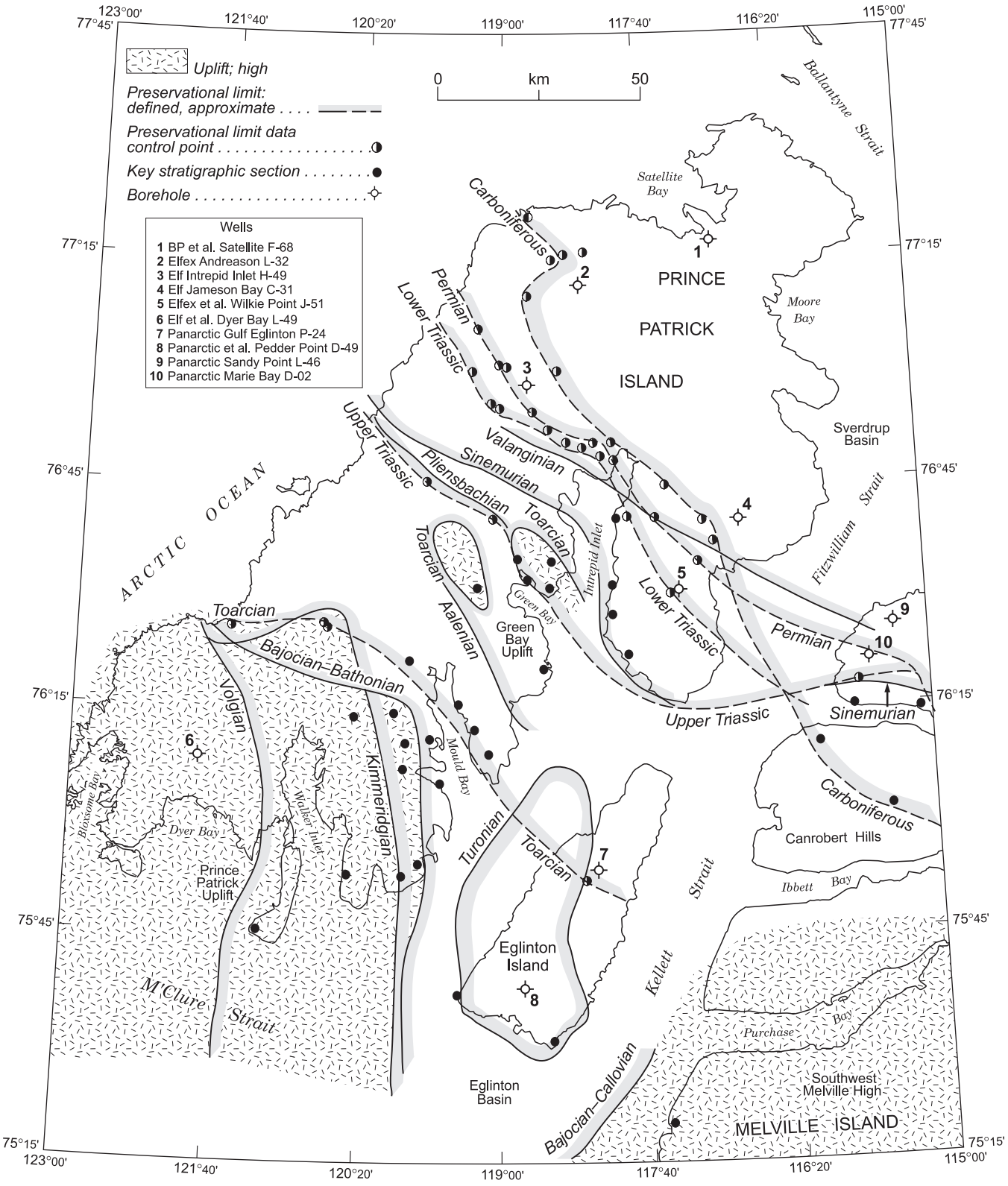

Figure 51. *Preservational limits of Carboniferous through Upper Cretaceous (Turonian) strata of Prince Patrick and Eglinton islands. Dominant northwest trends are related to patterns of Sverdrup Basin subsidence. The basin expanded progressively to the southwest through time. Local erosion of Toarcian strata around Green Bay is related to a significant phase of uplift and tectonic readjustment prior to the Aalenian. The locus of sedimentation is believed to have shifted into Eglinton Basin at this time.*

paired horst blocks, each displaying a characteristic history of subsidence and uplift. These features are described in the following pages.

Middle Jurassic to Cretaceous extensional structure

Classification of structural elements

The range of structural styles affecting Cretaceous and older strata in the Eglinton and Prince Patrick islands region necessitates some introductory remarks concerning the definition of terms and the approach taken in the description of structural elements.

The largest structural feature of the region is the Sverdrup Basin (Fig. 18, 20). The Carboniferous and Permian rifting phases and mid-Permian through Jurassic period of subsidence have already been described. The preserved stratigraphic record for the mid-Triassic to Lower Jurassic of the Sverdrup Basin has also been shown to extend as far southwest as central Eglinton Island and Mould Bay area on Prince Patrick Island (Fig. 51). Likewise the Sverdrup Basin continued to subside throughout the subsequent Jurassic and Cretaceous period. However, additional basins evolved in the Middle Jurassic: Eglinton Basin (the term “Eglinton Graben” has been abandoned in this account); M'Clure Strait Basin situated to the west in the mouth of M'Clure Strait; Tullett Basin, under the continental terrace wedge of western Prince Patrick Island; and Banks Basin, outside the report area to the south (Fig. 18, 52, 53). Common features of these basins include saucer-shaped profiles with gently inward-dipping strata on all sides, flat-lying strata in each basin centre, and semicircular to elliptical shapes in map view. The stratigraphic record of basin subsidence within the report area ranges from the Middle or Upper Jurassic to the Upper Cretaceous (Campanian). The thermal maturity of Cretaceous coal on Eglinton Island also indicates the pre-existence of a significant interval of younger strata, potentially comparable to the more than 1200 m of Paleocene and Eocene Eureka Sound Group still preserved in northern Banks Basin (Miall, 1979).

Part of the preserved record in the northern part of Eglinton Basin retains erosional remnants of the Sverdrup Basin-margin wedge, notably the Toarcian part of the Jameson Bay Formation. Likewise, the northern part of Tullett Basin includes Sverdrup Basin-margin strata extending back to the Lower Triassic.

The Sverdrup Basin and the three Jura-Cretaceous basins within the report area are each separated by high-standing blocks of open-folded and peneplained Devonian strata that can be considered tectonic "basement" with respect to the Mesozoic record of sediment deposition and deformation. The longest and widest of these highs is the Prince Patrick Uplift (Fig. 18, 53) which separates Eglinton Basin from Tullett Basin to the west and also separates Tullett Basin from the offshore M'Clure Strait Basin. A similar but narrower structure, the Gardiner-Intrepid High, provides a suitable structural definition for the present boundary between the Sverdrup Basin and the northern limits of Eglinton Basin and Tullett Basin. (This is strictly a structural definition for the Sverdrup Basin margin because the full depositional extent of the Sverdrup Basin lay well to the southwest in earlier times). Likewise, two small, northward-trending uplifted blocks (including Mecham High) lie between and east of the basins in M'Clure Strait. A unifying feature of all these high blocks is the parallel alignment of the axial crest or mid-line of each high with the strike of beds preserved on the basin flanks. Flanking Mesozoic strata also tend to dip away from the axial line of each high. This pattern of basement uplift has been influenced by various phases of faulting.

The strike directions for some faults are parallel and close to the axial alignment of the basement highs. The northeasterly trending portion of the Prince Patrick Uplift is a significant exception. The axis of this high is parallel to the western edge of Eglinton Basin and the northern and southern limits of M'Clure Strait and Tullett basins, respectively. However, there is also a prominent array of normal faults and small half-grabens, widely exposed on southern Prince Patrick Island, that strike northward, extend obliquely across the uplift, and provide direct structural links between the northern and southern basins.

Smaller Jurassic and Cretaceous structures have also developed within and between the larger Jurassic–Cretaceous basins. These include grabens and half-grabens, horst blocks each bound by outward-dipping normal faults, and syndepositional normal faults (Fig. 52, 53). The shape and width of half-grabens in the outcrop belt on southern Prince Patrick Island have also been influenced by westerly striking tear faults, each with a limited strike length. Direct and indirect evidence for the timing of syndepositional slip on the various bounding faults is approximately Toarcian or Aalenian to Albian. Seismic profiles indicate different phases of slip for different faults. All of these structures are part of a rift zone that is at least 100 km wide and may extend from the eastern Mackenzie Delta via Banks Basin on central Banks Island to the continental shelf north of Prince Patrick Island (Dixon and Dietrich, 1990). The full width is unknown. However, north-trending linear aeromagnetic anomalies described earlier (Fig. 23) and by Forsyth et al. (1990) are present in the mouth of M'Clure Strait and may provide for a rift zone more than 210 km wide.

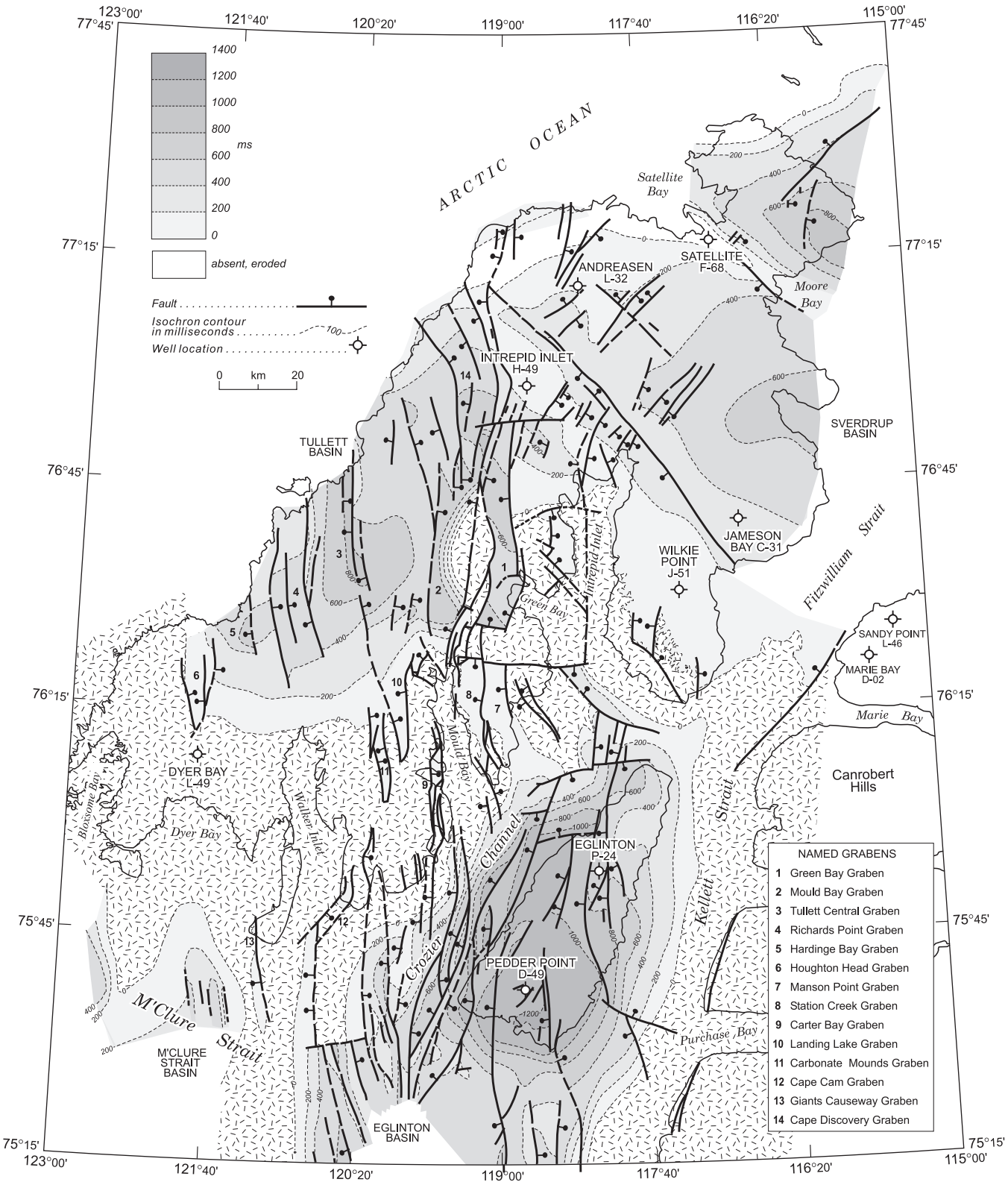

Figure 52. *Faults and thickness isochron map for Middle Jurassic (top Aalenian) through Upper Cretaceous strata of Prince Patrick and Eglinton islands including intervening offshore areas. Eglinton and Tullett basins are elliptical, saucer-shaped structures transected by a complex array of normal faults that are mostly oblique to thickness isochrons.*

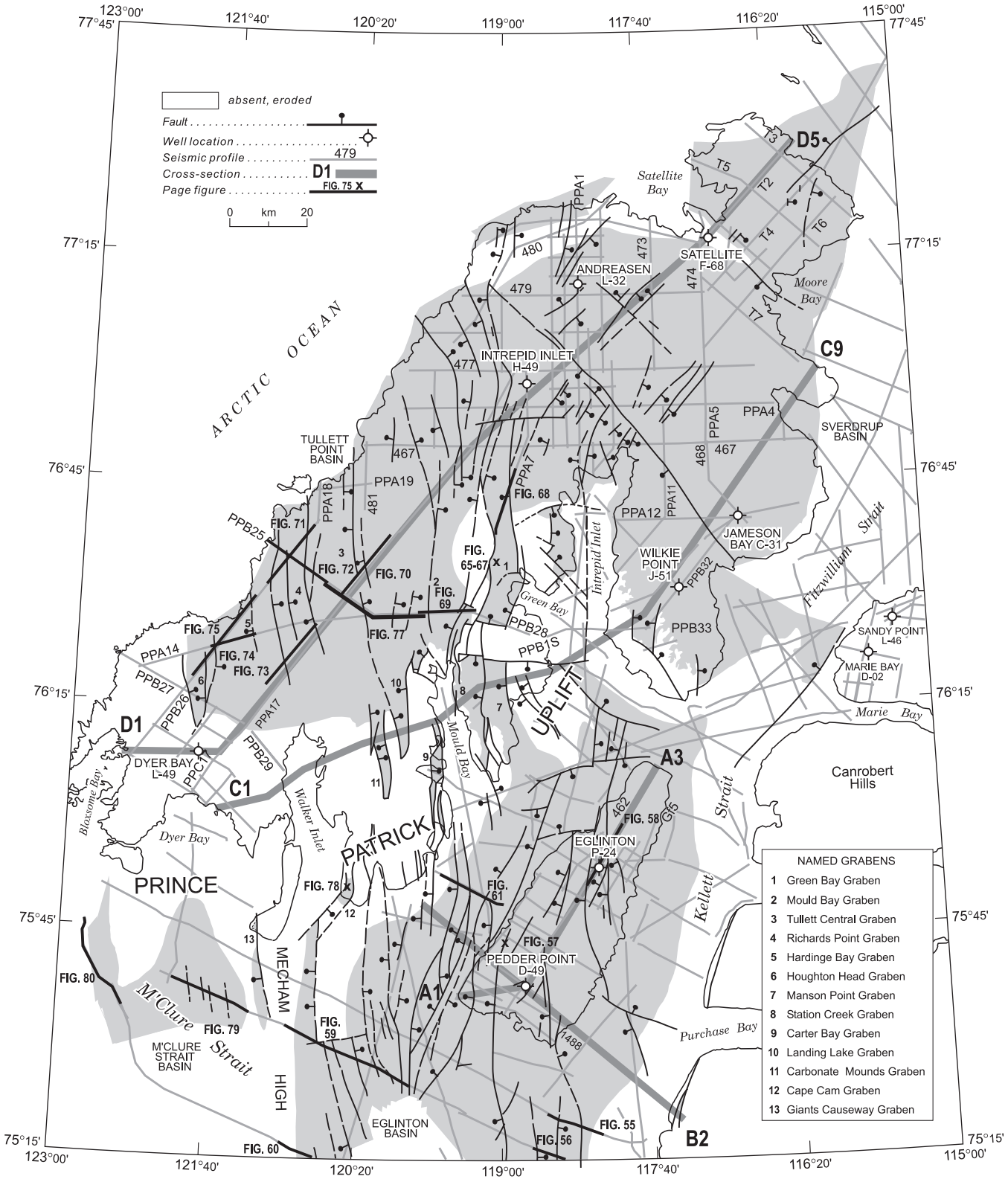

Figure 53. *Locations of named grabens, regional highs, seismic profiles and related text figures on the Aalenian to top Cretaceous thickness isochron map for Prince Patrick and Eglinton islands. The Gardiner-Intrepid High (not shown) lying east of the mouth of Marie Bay and north of Eglinton Island, extends to the north and west via Intrepid Inlet to beyond the Intrepid H-49 well. This structure may be, in part, compressive in origin and mid-Tertiary in age (see Fig. 82).*

The larger grabens within the report area have been named after local topographic features and each bounding master extension fault is usually named after the adjacent graben. Named grabens are located on Figures 52 and 53 and on the regional geology map (2026A). There are eight significant half-graben type structures situated in the outcrop belt and within the Prince Patrick Uplift between Intrepid Inlet and Dyer Bay on southern Prince Patrick Island. The largest is the Green Bay Graben west of Green Bay. It extends to the north into Tullett Basin, mostly beneath Beaufort Formation, and has an imaged strike length of 50 km. Farther north is Discovery Point Graben, which appears to continue beyond the north coast of the island. Four other named grabens are found to the west within Tullett Basin. Numerous smaller unnamed grabens and normal-faulted structures are noted within Eglinton Basin and several others are imaged in northern M'Clure Strait Basin.

Numerous normal faults are found in Crozier Channel but are also scattered throughout the project area. These structures commonly display dip-slip displacement and elements of differential rotation with respect to upthrown footwall blocks. However, for many, the timing of displacement, as interpreted from offshore seismic profiles, is apparently younger than the age of the rotated Jurassic and Cretaceous strata. These faults must therefore represent a distinctly younger phase of extension faulting – younger than the youngest rotated strata which for the faults under Crozier Channel include beds as high as the Kanguk Formation (Turonian to lower Campanian). The problem of fault timing is especially difficult for the onland faults within the Prince Patrick Uplift. Evidence for syndepositional slip on these structures is indirect and includes the style of deformation in footwall and hanging wall, and the comparative stratigraphy and sedimentology of graben-fill and graben cover. For the faults within Tullett Basin, there is unequivical reflection seismic evidence for faulting during or between phases of sediment accumulation in many grabens. Firm dating of the graben fill is hindered by lack of outcrop and well data.

Also younger than the extension phases of the Jurassic and Cretaceous but older than the Beaufort Formation are various compressional structures, anticlines, synclines, and thrust faults. The largest structure of this type is the west northwesterly trending Moore Bay Anticline, which has been mapped from west of Emerald Isle to Satellite Bay. Smaller folds are found in outcrops east and west of Intrepid Inlet and within the Cretaceous on Eglinton Island. Similarly, minor thrust-anticlines and inversion structures are seen on seismic profiles throughout Prince Patrick Island.

Eglinton Basin

Seismic units

The stratigraphy of Eglinton Basin has been compiled from surface geology, well logs and cuttings as illustrated in Figure 54 (columns 12, 20–22 CD-ROM). Maximum thickness of section is 1900 m measured from the top of the Devonian to the top of the Upper Cretaceous as preserved on land near the Pedder Point D-49 well.

The oldest post-Devonian strata of Eglinton Basin are assigned to the Jameson Bay and Sandy Point formations. Both units are thin (less than 100 ms) and unsubdivided on seismic proflies 462 and G(f)5 (see seismic transect and cross-section A of Eglinton Island). Seismic expression is one of moderate amplitude, subparallel, continuous bounding reflections. Modest relief on the basal surface is attributed to erosional paleotopography on the pre-Jurassic peneplain surface.

The McConnell Island and Hiccles Cove formations together range in thickness from 95 ms in the north to 77 ms in the south. Moderate amplitude, parallel, continuous reflections occur at the base and top of these formations and together they form a single seismic unit. Strength of the bounding reflections weakens southward, presumably as a consequence of thinning of the shale in the McConnell Island Formation and a corresponding thinning of the Ringnes Formation shale in the lower part of the overlying seismic unit. This has produced sand-on-sand stratigraphic relationships in the south that have inhibited reflectivity. The internal seismic character of the Hiccles Cove-McConnell Island seismic unit includes a number of very short and widely scattered hummocky reflection segments.

The Ringnes and Awingak formations together form a single seismic unit ranging from 276 ms at Eglinton P-24, to 220 ms at Pedder Point D-49. Short, horizontal but widely scattered reflection segments occur throughout. Compared to underlying and overlying units, the Ringnes-Awingak unit is nearly reflection free. The Isachsen Formation (277 to 344 ms) features numerous, high-amplitude, slightly hummocky or subparallel reflection segments. Its lower seismic contact is drawn below the lowest of these discontinous reflections. The Christopher Formation is only fully represented in the Pedder Point D-49 well (261 ms). The lower contact is gradational. Internal character is generally reflection-free. The Hassel Formation is a marker unit, expressed as a strong, semicontinuous reflector near the top of Pedder Point D-49. The Kanguk Formation is again a more unreflective unit lying only within the top 200 ms of the seismic data.

Regional structural style

Eglinton Island. The greater part of Eglinton Basin is exposed on Eglinton Island. Offshore seismic profiles, however, provide reliable determination of the location and geometry of the basin limits under the surrounding channels. Onland and seafloor geology is illustrated on the regional geological map (2026A). Thickness isochrons for Middle Jurassic through Upper Cretaceous strata and related subsurface structure are shown on Figure 52. These data indicate a maximum basin width of 73 km measured parallel and close to the south coast of the island. The long dimension of the basin coincides with the long axis of the island and extends from south of Wilkie Point in Fitzwilliam Strait 165 km southwest to central M'Clure Strait (Fig. 18). A single seismic profile, which crosses the strait to Castel Bay on northern Banks Island, reveals that Jurassic and Cretaceous units of Eglinton Basin are continuous and readily correlated with similar units in Banks Basin.

The surface strata on Eglinton Island are very nearly flat lying. Observed and measured bedding attitudes range from horizontal to 6°. Geometric calculations indicate local dips of up to 13° (near Cape Nares, for example). Local variation in bedding attitude is particularly evident on the mapped base of the Eglinton Member of the Kanguk Formation, which is both faulted and gently warped about various, upright N20°W- to N40°E-striking axial planes. However, the overall onland structure for Eglinton Basin is one featuring a regional synclinorium with an axial plunge that varies from S12°W at 0.9° in the north to S20 to S25°E at 0.8° in the vicinity of the Pedder Point D-49 well. The axial line of the synclinorium parallels and bisects the long axis of the island in the south. Farther north the regional fold hinge curves more to the north and extends into the offshore of northern Crozier Channel. Marine seismic profiles indicate that the synclinorium of central Eglinton Island is continuous with the axial line of Manson Point Graben on southern Prince Patrick Island.

Kellett Strait. The eastern extent of Eglinton Basin is imaged on each of eleven seismic profiles in Kellett Strait. The Jurassic and Cretaceous is featured as a series of subparallel, moderate-amplitude reflections and the base, above peneplained Devonian, is drawn below the lowest of these reflectors (Fig. 55, 56). The Devonian is acoustically transparent on many profiles; although weak, unidentifiable, and uncorrelatable dipping reflection segments can be observed locally. Strike directions for basin-fill units under Kellett Strait range from N27°W opposite Pedder Point, to N16°W near Catherine Point, to N07°W east of Gardiner Point. The basin margin under Kellett Strait dips gently to the west and the unconformity between the Devonian and the Jurassic intersects the seafloor in mid-channel. The eastern half of Kellett Strait is underlain by the Devonian clastic wedge. Taking into account the local variation in seafloor bathymetry, which ranges to 330 m, dip on the sub-Jurassic unconformity has been determined in three locations in Kellett Strait. The dip east of Pedder Point averages 2.4°W but appears to increase to as much as 11° at the eastern limit of subcropping Jurassic. The dip east of Catherine Point is also 2.4°W, and the dip of strata in the north end of Kellett Strait is 1.9°W.

While the east side of Eglinton Basin is not marked by a mappable fault on any of the seismic profiles, the acoustic transparency of the offshore Devonian does not rule out the possiblity of a major Jurassic–Cretaceous-age normal fault within these rocks. The most convincing argument for the existence of an undetected offshore fault in eastern Kellett Strait is the presence of faulted outliers of the Awingak Formation near Comfort Cove on southwestern Melville Island (Fig. 51). Several of the mapped faults are parallel to the western coast of the island and could be considered subsidiary to a potentially larger parallel fault in the immediate offshore.

Crozier Channel. Eglinton Basin is bound to the west by a southeastward-dipping panel of seismic units greatly dissected by an array of subparallel, mostly down-to-the-west normal faults that run the length of Crozier Channel. Correlation between onshore and offshore seismic stratigraphies reveals that no substantial difference is indicated in thickness or style of deposition for any single unit within the Middle Jurassic to Upper Cretaceous basin-fill. Calculated bedding attitudes mostly range from 10 to 13° but may range up to 21° for individual faulted panels. Strike direction of bedding is N17–24°E west of Cape Nares ranging to N30–38°E west of Callaghan Point as the basin narrows to the north and closes about a northwest-trending basement high under the channel north of Gardiner Point.

Faults of Eglinton Basin

Onland faults. There are 21 mapped faults at the surface on Eglinton Island. Most of these occur in the southwestern part of the island where displacements of the cliff-forming Eglinton Member of the Kanguk Formation are readily identified on air photographs. There are two distinct strike directions for these faults: a set that strikes N08–20°E, and a set of shorter fault segments that strike N45–70°E. The geometry of two small cross-faults, situated near the middle of the island, suggests a wrench tectonic link between two of the larger, northward-striking faults. The longest faults and all those with more than 200 m of stratigraphic throw belong to the northerly striking set and feature strata consistently downthrown to the west. Faults with downthrown beds to the north and west also outnumber

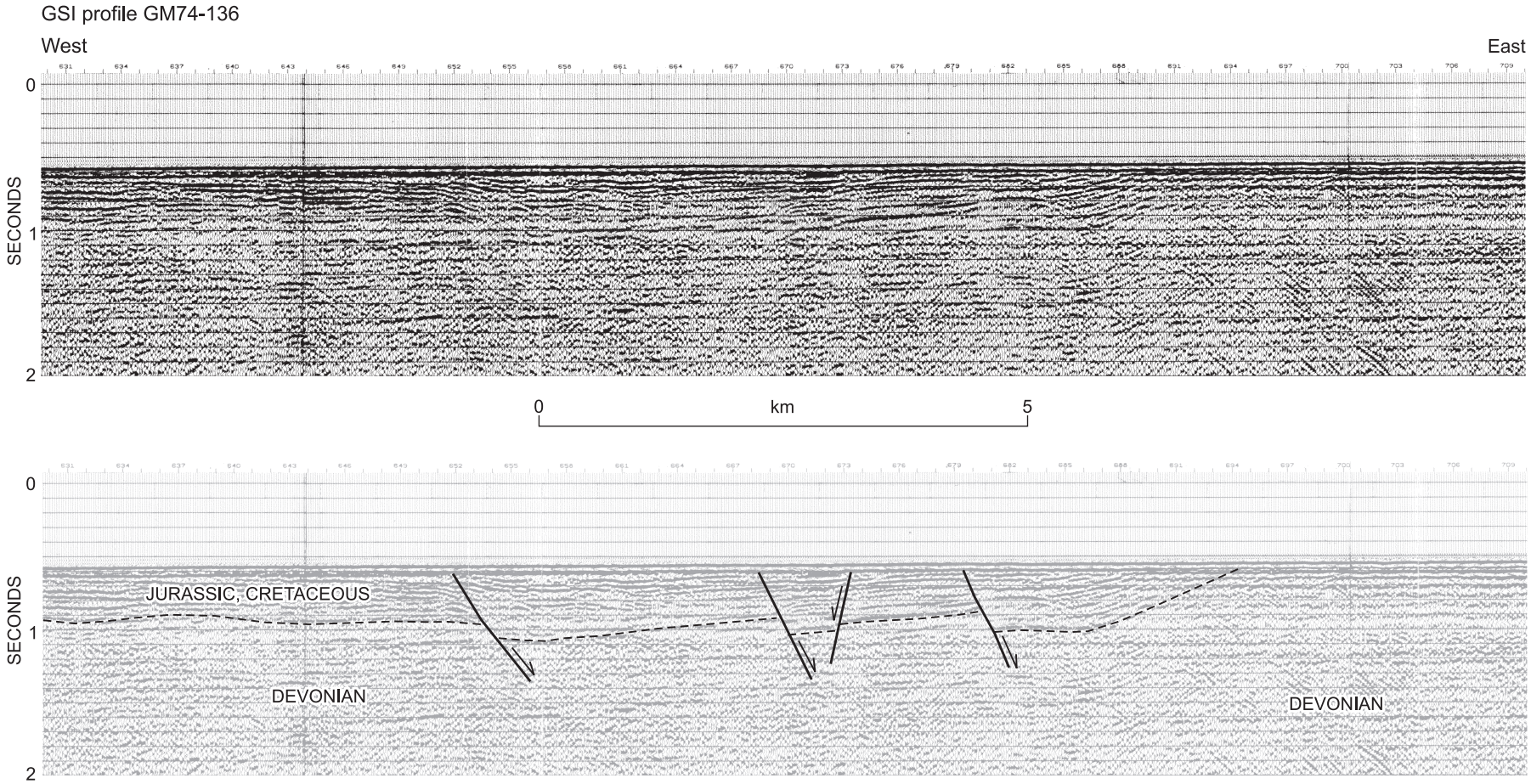

Figure 55. *Seismic expression of the eastern margin of Eglinton Basin in Kellett Strait on a portion of GSI profile GM74-136. Mesozoic units are believed to include McConnell Island Formation at the base through Christopher Formation at the top. Profile is located on Figure 53.*

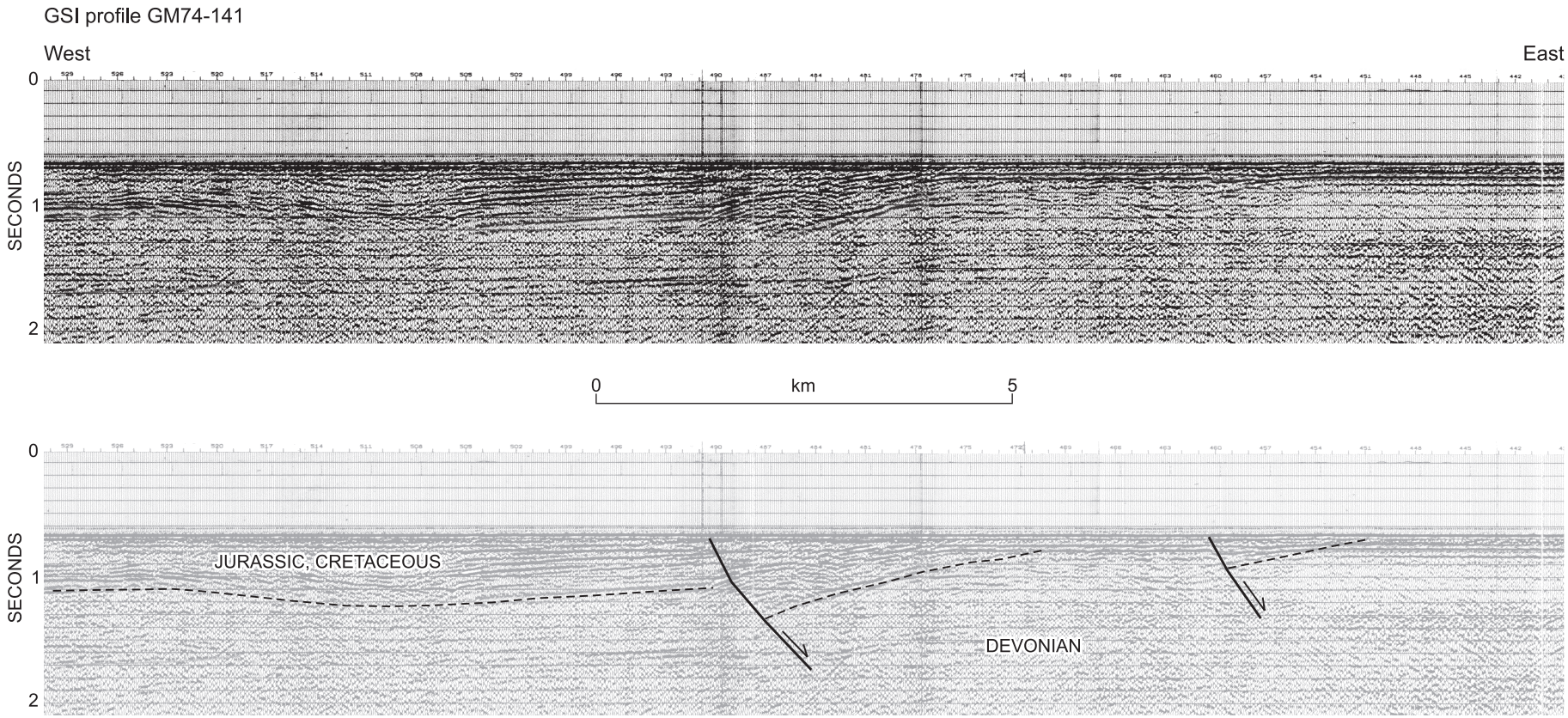

Figure 56. *Seismic expression of the eastern margin of Eglinton Basin in Kellett Strait on a portion of GSI profile GM74-141. Mesozoic units are believed to include McConnell Island Formation at the base through Christopher Formation at the top. Profile is located on Figure 53.*

those downthrown to the south and east by a factor of two to one.

The Catherine Point Fault, which strikes N17°W, has a maximum down-to-west stratigraphic throw of about 250 m where medial Christopher Formation is in tectonic contact with the medial part of the unnamed lower member of the Kanguk Formation. Two other unnamed, northward-striking faults each have up to 290 m of stratigraphic throw (as measured at 16.5 km west-northwest of Catherine Point, and at 9.5 km east of Callaghan Point) where upper Christopher Formation abuts against the downthrown Eglinton Member of the Kanguk Formation. A seismic profile over the latter fault displays a comparable 250 ms of throw (350 m at 2.8 km s^{-1}) measured on the displaced base of the Jurassic. Two other faults each have about 250 m of throw at the surface in the Cretaceous: one near the west coast of the island 5.7 km northeast of Callaghan Point; the other, the Cape Nares Fault in the southwest, which places Hassel Formation against the downthrown Eglinton Member.

Uncertainty exists as to the degree to which the observed low-amplitude buckling in the Cretaceous might have been generated through horizontal compressive deformation and the extent to which the adjacent faults may have experienced phases of compressive reverse slip. Nevertheless, reflection seismic profiles clearly reveal that most of the onland faults of Eglinton Basin that are large enough to be imaged, also possess a dip direction compatible with a principal origin in extension. Although the distribution of faults mapped on seismic profiles is comparable to that seen at the surface, many individual faults may not be recognizable at surface either because of inadequate outcrop or upward splaying and dying out of faults in near-surface units. An example of this is illustrated in Figure 57. Indeed, the largest subsurface onland fault, imaged on profile 462 at SP5929 (Fig. 58), has no surface expression at all. This is attributed to colluvium, sedge growth, and related ground cover on the lower Isachsen Formation over the expected fault trace 4.5 km northeast of the Eglinton P-24 well. Offset on the base of the Jameson Bay Formation at this location is 220 ms (310 m at 2.8 km s^{-1}).

One other significant seismic fault is situated 14 km east-northeast of Callaghan Point. The fault has 170 ms (240 m at 2.8 km s^{-1}) of displacement on the base of the Jurassic but is unrecognized at the surface in the Christopher Formation. Numerous other subsurface onland faults are illustrated on Figure 51. Most have stratigraphic throw maxima between 30 and 115 ms (40–160 m at 2.8 km s^{-1}). A characteristic feature of all these structures is the widespread occurrence of flat-lying or very gently warped strata between faults,

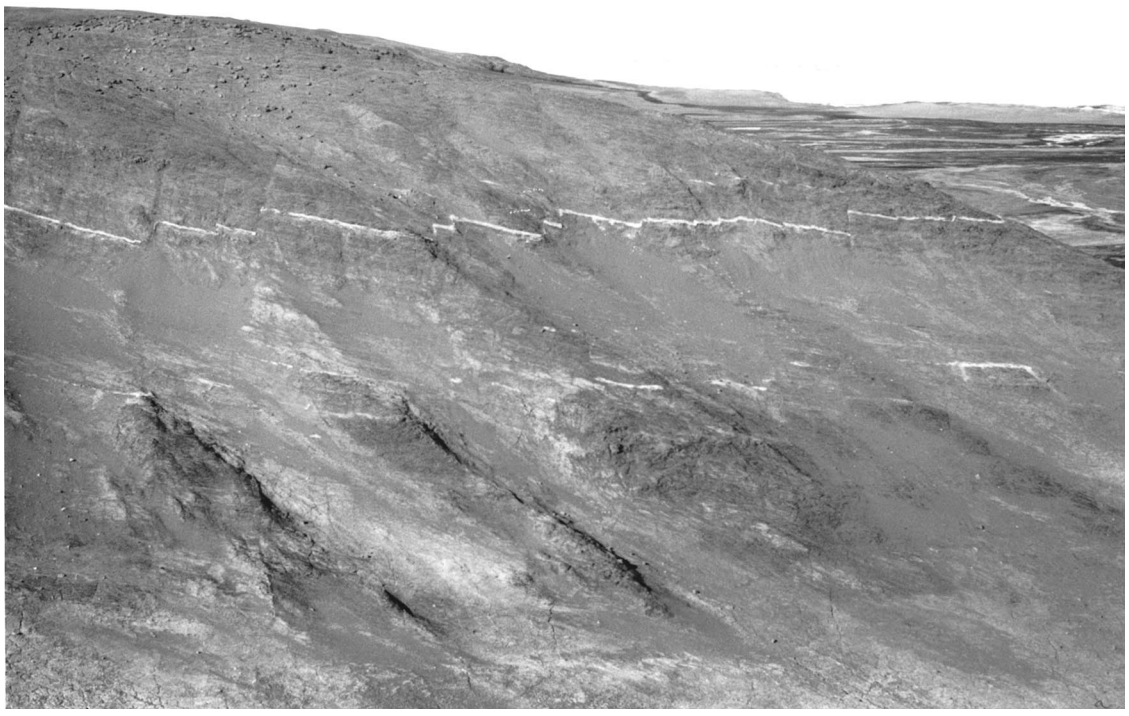

Figure 57. *Steeply dipping minor faults displacing bentonite beds of the lower Kanguk Formation on eastern Eglinton Island. View is to the south with strata generally downthrown to the east. Foreground relief is about 75 m. See Figure 53 for location (GSCC photo 3820-61).*

and the general absence of any significant block rotation or inclination of upthrown or downthrown strata against the same faults. Subtle tilting is noted, as in Figure 58, but is everywhere comparable to that observed at the surface.

Seismically defined normal faults of onland Eglinton Basin are detached in the lower part of the Devonian clastic wedge or, less commonly, in the Ibbett Bay or Canrobert formations (cross-section A). Many faults cannot be traced downsection through the clastic wedge and thus have an unknown level of décollement. Influence of Franklinian structure on the location of these later normal faults appears unlikely, as the two structural trends are nearly perpendicular.

Offshore faults. Faults are rare on seismic profiles of Kellett Strait. In contrast, more than twenty faults have been mapped beneath Crozier Channel and northern M'Clure Strait. Strike directions for these structures are similar to the major faults on land and range from N08°W to N34°E. Most display down-to-the-west senses of displacement. Faults down-thrown to the east are more common in northern M'Clure Strait. Several of the longest faults, also featuring the largest stratigraphic throw, have been named. They are: Crozier Channel Fault (72 km long, up to 425 ms or 600 m of throw at 2.8 km s^{-1}); the Dames Point faults, with east and west strands (53 km+ long, up to 600 m of throw); and Callaghan Point Fault lying immediately off the west coast of Eglinton Island (360 m of throw). Nares Strait Fault is also imaged an additional 25 km to the south of the island.

Callaghan Point and Crozier Channel faults are aligned with Manson Point Graben on Prince Patrick Island, although mapping indicates that the faults terminate in the offshore. The Dames Point faults are aligned with and may continue to the north under Mould Bay. However, seismic profiles collected within the bay have failed to image faults in probable Devonian strata of seafloor bedrock. Small unnamed faults imaged southwest of Mould Bay are aligned with Carter Bay Graben. The upthrown footwalls of the various offshore grabens in the mouth of Mould Bay have significant submarine relief that mimics the exposed topographic relief east and west of Mould Bay, where high-standing horst blocks of resistant Devonian sandstone lie between low-relief grabens underlain by recessive Jurassic and Cretaceous strata.

Offshore faults with the greatest throw are situated in the westernmost portion of Eglinton Basin (Fig. 59, 60). Faults in this part of Eglinton Basin strike N10°E to N15°W and are aligned with Walker Inlet. Several may extend onshore at Cape Cam. Stratigraphic throw ranges up to the 650 ms (900 m, west side down) for the one illustrated in Figure 60, about 70 km south of Cape Cam. Kanguk Formation is believed to be downthrown against flat-lying lower Isachsen Formation on this structure. The downthrown units display clear evidence of fault-related tilt to the east at 18° into the plane of the fault. Normal drag is also apparent in the immediate hanging wall. Several other faults in this northern part of M'Clure Strait also demonstrate evidence of inclination and differential rotation of downthrown strata; features characteristic of listric faults that flatten at a relatively shallow depth in the Devonian basement under each hanging wall graben.

In contrast, most of the faults south of Eglinton Island in northern M'Clure Strait and in Crozier Channel have a planar geometry, at least within the imaged upper 1.5 seconds of the seismic records (Fig. 61). As discussed previously, inclination of strata to the east (at up to 20°) is featured throughout this western margin of Eglinton Basin. Each of the Nares Point, Dames Point, Crozier Channel and Callaghan Point faults have displaced the inclined basin-margin strata and produced down-to-the-west senses of slip. However, the regional inclination of the basin margin need not be kinematically related to motion on these faults.

Faults in Crozier Channel, as on Eglinton Island, also appear to be spatially and kinematically unrelated to folding and thrusting in the lower Paleozoic (compare Fig. 31 and 52). Alternatively, the young faults parallel to the long axis of the channel are rooted in mid-Cambrian or older basement faults that define the southeast margin of the lower Paleozoic Prince Patrick Platform (compare Fig. 35 and 52).

Timing of faulting

Evidence concerning the timing of faulting in Eglinton Basin is summarized on Figure 62. Regional mapping and seismic interpretation has shown that the Jameson Bay-Sandy Point and the McConnell Island-Hiccles Cove units of Eglinton Island are preserved only in a narrow belt that extends into the far southwestern part of Eglinton Basin (Fig. 51). However, there is no convincing indication that any of the mapped faults offshore were active during these depositional intervals or prior to overlap by the Ringnes Formation.

The unnamed fault northeast of the Eglinton P-24 well (Fig. 58) provides one of the few convincing examples of a phase of faulting affecting the thickness of the Ringnes-Awingak sequence prior to overlap by the Isachsen Formation. Thinning of the Ringnes-Awingak sequence over the upthrown northeastern footwall block is attributed to prolonged exposure and erosion of the footwall region as a consequence of post-Volgian, and pre-Barremian or pre-Hauterivian faulting.

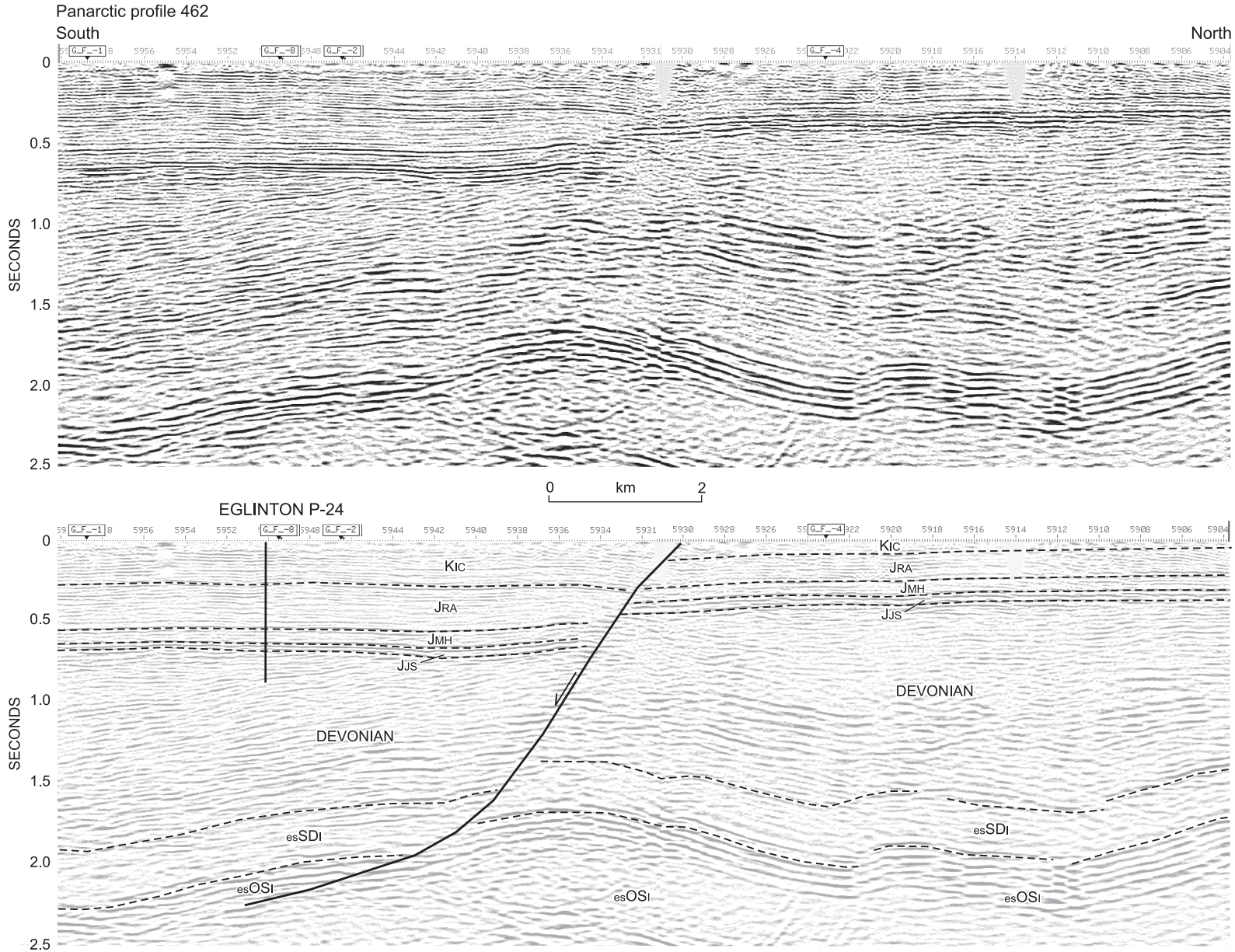

Figure 58. *Seismic expression of an unnamed fault on profile 462 near the Eglinton P-24 well on central Eglinton Island.* esOSI, esSDI*: lower and upper parts of the Ibbett Bay Formation (Ordovician to Lower Devonian); Devonian: Middle and Upper Devonian clastic wedge;* JJS*: Jameson Bay and Sandy Point formations;* JMH*: McConnell Island and Hiccles Cove formations;* JRA*: Ringnes and Awingak formations;* KIC*: Isachsen and Christopher formations. Base of the Isachsen in the upthrown footwall is constrained by surface geology. Southward syntectonic thickening of the Ringnes and Awingak formations is indicated. Profile is located on Figures 50 and 53.*

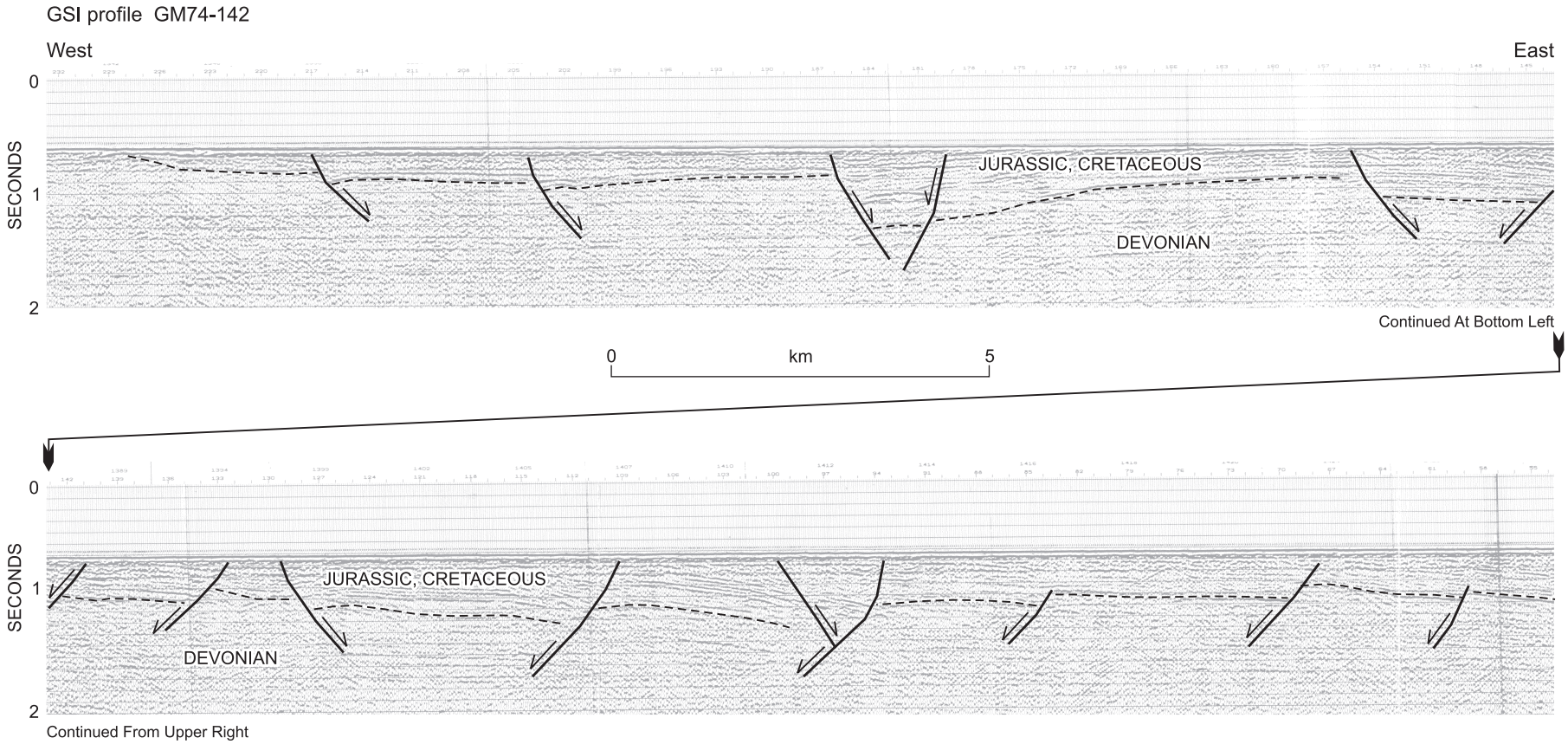

Figure 59. *Seismic expression of half-graben structures and related listric normal faults in northern M'Clure Strait 40 km south of Cape Cam on a portion of GSI profile GM74-142. Part of Mecham High is located at top left. Profile is located on Figure 53.*

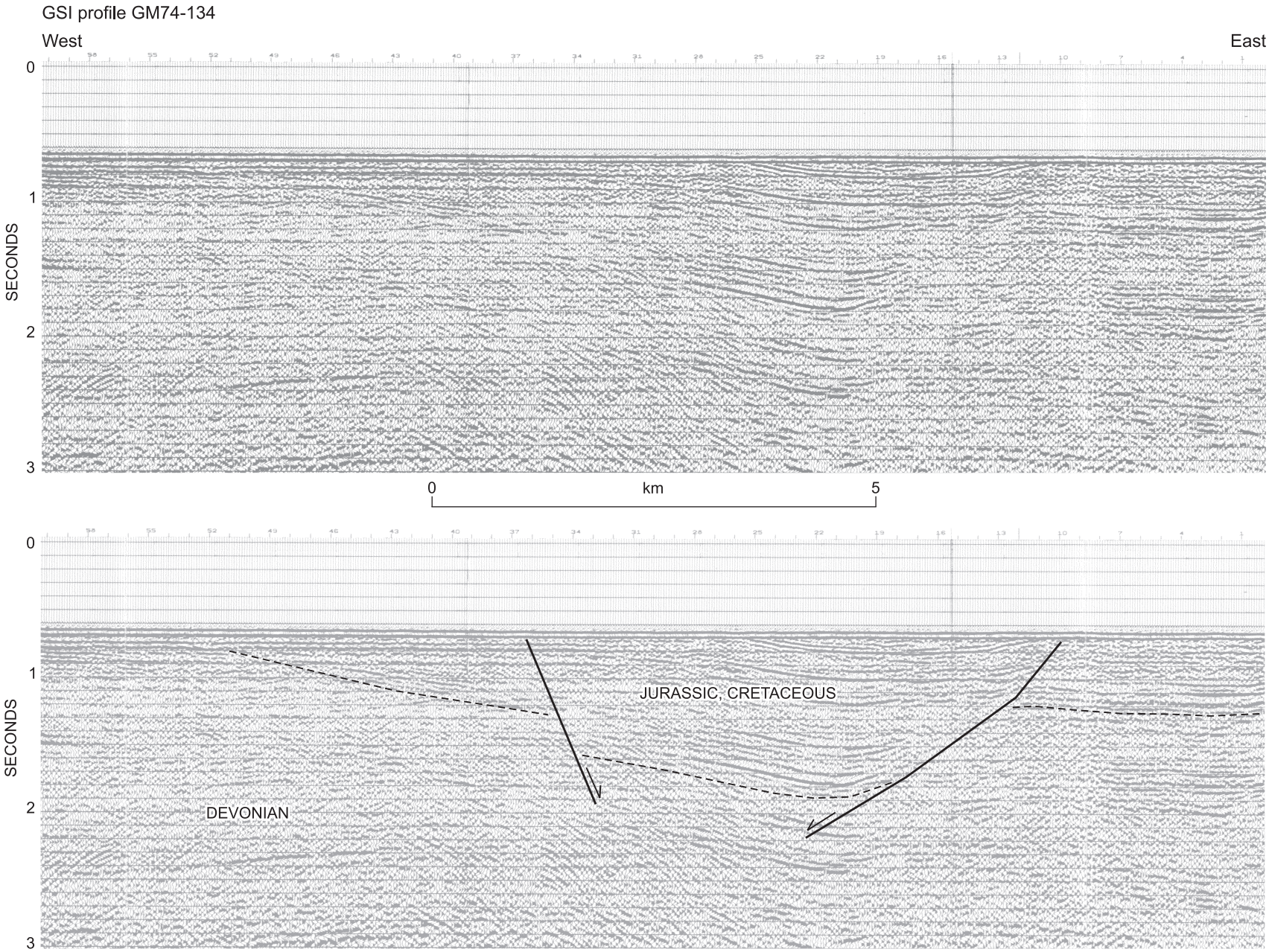

Figure 60. *Seismic expression of a major half-graben structure in northern M'Clure Strait 70 km south of Cape Cam on a portion of GSI profile GM74-134. Profile is located on Figure 53.*

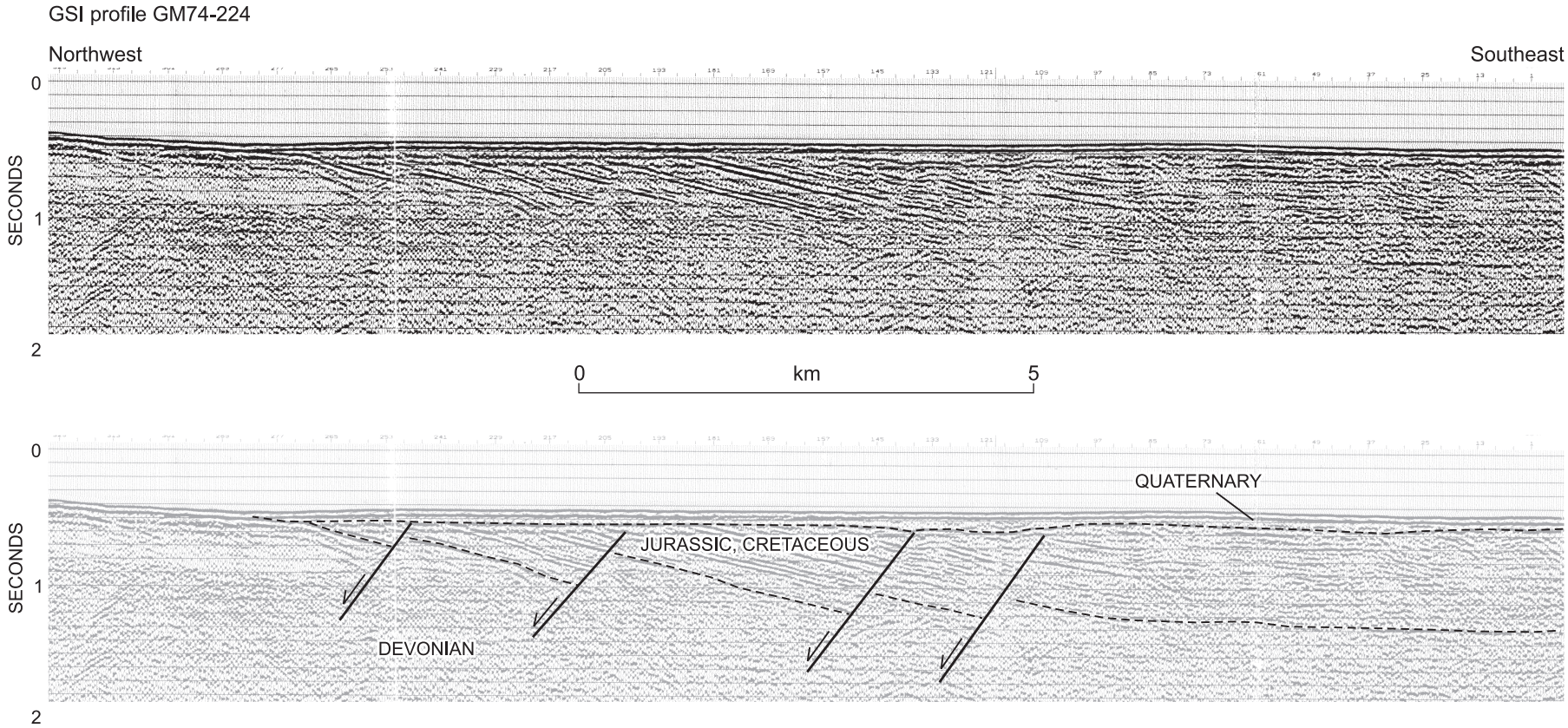

Figure 61. *Seismic expression of planar-normal faults in tilted Jurassic and Cretaceous strata on the western margin of Eglinton Basin in Crozier Strait on part of GSI profile GM74-224. Part of Prince Patrick Uplift is located at far left. Profile is located on Figures 50 and 53.*

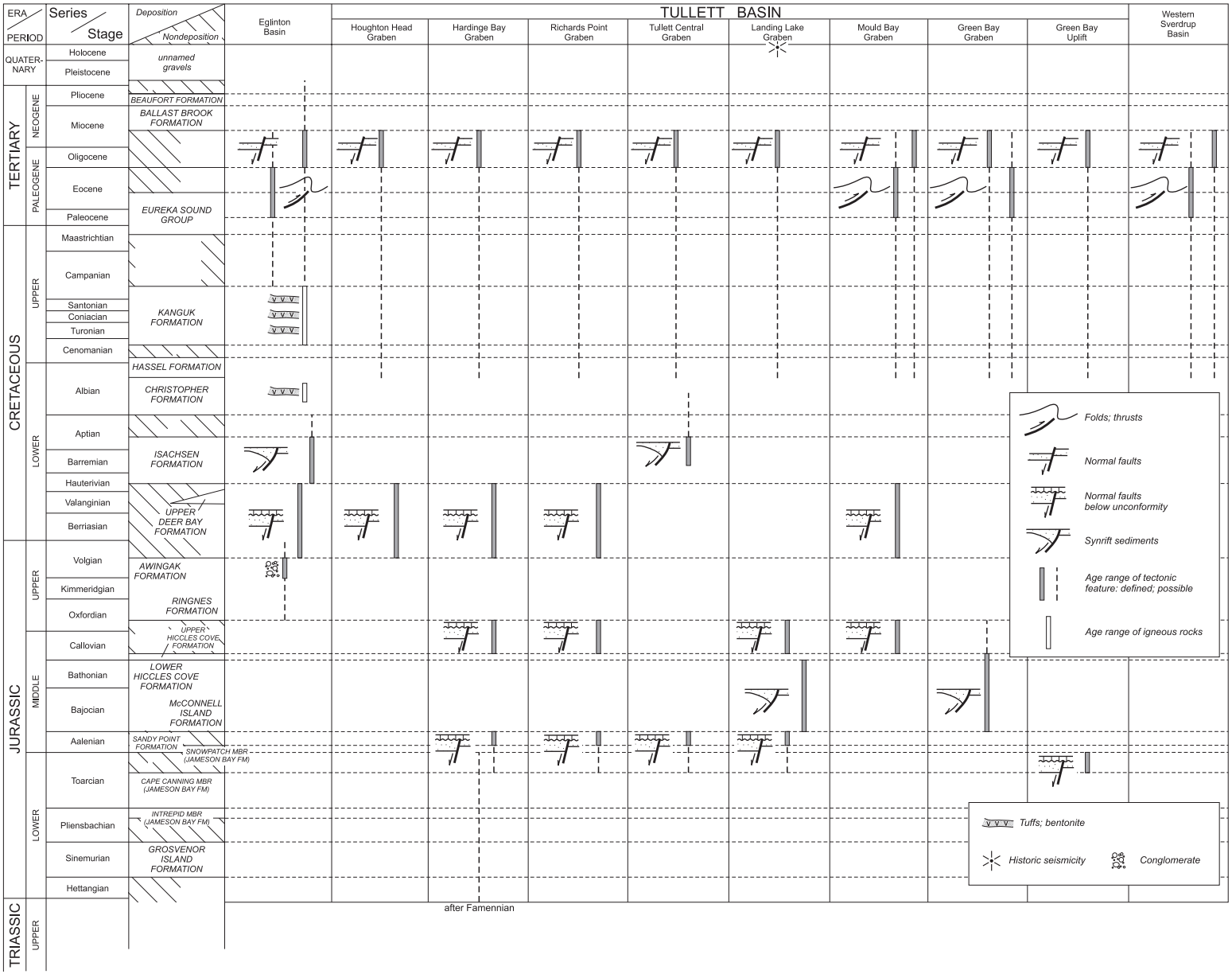

Figure 62. *Correlation chart for Lower Jurassic and younger tectonic, magmatic and related depositional features of Eglinton Basin and various grabens of Tullett Basin. The Ballast Brook Formation is widespread on Banks Island (Fyles, 1994) and is presumably also present in the lower part of the Arctic Continental Terrace Wedge in the subsurface of western Prince Patrick Island. The main phase of rift-related extension mostly ranges from the Aalenian to Aptian for Tullett Basin, and from Volgian to Aptian for Eglinton Basin. Ages of late-stage faults and folds are based on regional considerations (see also Fig. 81).*

Greater preserved thicknesses for the Ringnes and Awingak formations are also indicated within Eglinton Basin relative to that now found in adjacent areas of southern Prince Patrick Island (Fig. 54). Similarly, the southwestern region of Melville Island was tectonically elevated during the Volgian – it was an active source region for Devonian sandstone clasts preserved in nearshore marine conglomerates of the Awingak Formation in Comfort Cove Graben. Southeastern and central Melville Island appear to have been entirely stripped of Jurassic and older post-Devonian strata prior to overlap by the Isachsen Formation.

Faulting during sediment deposition in Eglinton Basin is suggested, but not proven, by large lateral variations in thickness of the Lower Cretaceous Isachsen Formation. The Isachsen Formation ranges up to 561 m thick in the Pedder Point D-49 well. In contrast, the Isachsen is mostly less than 300 m thick in the grabens on Prince Patrick Uplift and is only 65 m thick on the high block at the head of Mould Bay. Much of central and southern Melville Island was also relatively high standing at this time as the formation thickness in outcrop below the Christopher Formation ranges from less than 200 m on the margin of the Sverdrup Basin to 23 m in the southeastern part of the island (Goodarzi et al., 1994).

Mapping clearly indicates that the final phase of extension faulting has affected strata as high as the upper member of the Kanguk Formation, which is dated as Maastrichtian on the basis of dinoflaggelates and palynomorphs (Plauchut and Jutard, 1976) and as no younger than early Campanian based on the foraminiferal assemblage (sample C-156057, in appendix, this volume) and inoceramids (Tozer and Thorsteinsson, 1964). Faulting on northern Banks Basin has affected strata as young as middle Eocene age (Miall, 1979).

Tullett Basin

Seismic units

Lack of outcrop and a complete absence of drillhole data in critical areas has created problems in correlating surface strata to seismic units of subsurface western Prince Patrick Island. The Andreasen L-32 and Intrepid Inlet H-49 wells, located east of Tullett Basin, were spudded below the top of the Middle Jurassic and therefore do not provide a means of correlation and dating of Upper Jurassic and Cretaceous strata believed to be common in areas to the southwest. Likewise the Dyer Bay L-49 well intersected, exclusively Devonian and older strata below the Beaufort Formation.

Two major assumptions have been required to provide a reasonable stratigraphic framework and to assign tentative ages to the post-Devonian seismic units of Tullett Basin. The first assumption is that the Jurassic and Cretaceous units observed in the outcrop belt in the southern part of the island (Fig. 54) are the same as those imaged in the subsurface to the north, and that overstep relationships are also similar.

The second major assumption is that the seismic characteristics of the Jurassic and Cretaceous sequences, imaged on Eglinton Island and intersected in the Eglinton P-24 and Pedder Point D-02 wells, are equally valid for sequence correlation on the seismic profiles of western Prince Patrick Island. Results of these assumed correlations are summarized on Figure 63 and cross-section D.

Regional structural style

The greater part of Tullett Basin underlies continuous cover of Beaufort Formation throughout west-central Prince Patrick Island (Fig. 20). The southern fringe of the basin extends into the southern outcrop belt of Jurassic and Cretaceous exposures northeast of the head of Walker Inlet, north of the head of Mould Bay, and west of Green Bay. The basin has an imaged maximum length of 122 km measured parallel to a N36°E- to N26°E-trending long axis and a width of at least 47 km. The full width of the basin must extend northwest into the offshore. However, Bouguer gravity anomalies (Fig. 22) and thickness isochron contours drawn on the base of the Middle Jurassic (Fig. 52) indicate that a basin axial depression lies onshore and that a basin rim (or intra-basin high) probably exists a short distance offshore. Maximum thickness of basin fill, obtained by summing the thickness isochrons of Figures 50 and 52, is in the northern part of Green Bay Graben (Fig. 53, 63) with up to 1500 ms of Triassic to Cretaceous section. Maximum thickness of Middle Jurassic through Cretaceous strata, deposited synchronously with horst and graben development, is 800 ms or about 1120 m at 2.8 km s^{-1}. The preserved basin margin is marked by the unconformable and inward-dipping contact below Jurassic or Cretaceous strata deposited above the Devonian peneplain. Magnitude of dip is 1.8 to 2.3° N on the southern margin, 2.9 to 6.4° NW calculated at different places on the southern margin, 2.1° S at the northern end of the basin, and 2.8 and 3.8° SE and E measured on the northwest and west margins, respectively.

Northerly striking extension faults are common throughout Tullett Basin. There are approximately 30 faults mapped on seismic profiles in this area. Fifteen are mapped on two or more profiles and four faults can be correlated from seismic profile to outcrop. Fault strike directions mostly range from N5°E to N20°W. Thus, there is an approximate 30 to 45° orientation difference in map view between the northeast-trending basin axis and the strike direction of the rift-related normal faults. Exceptions

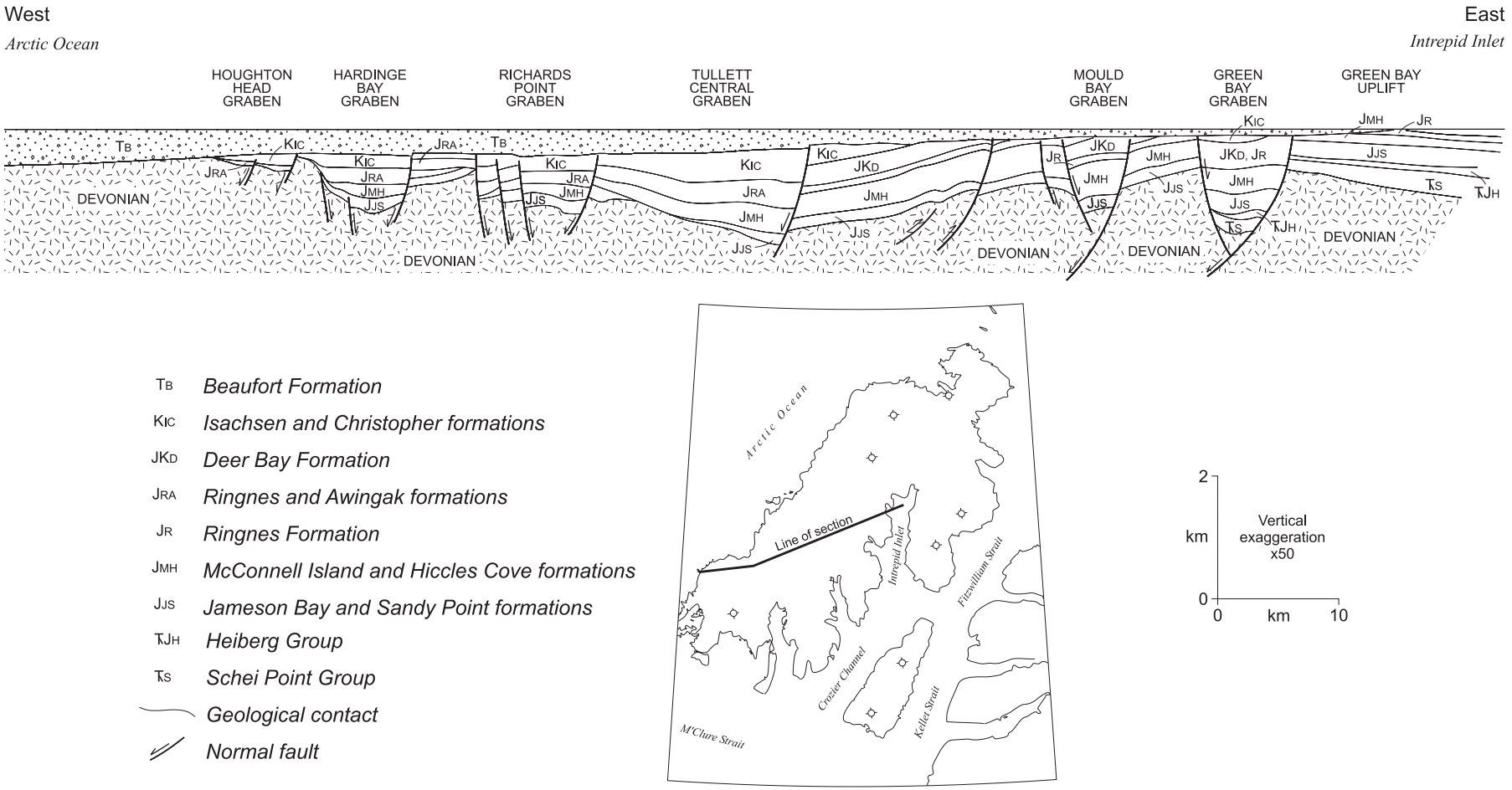

Figure 63. *Generalized structural cross-section of Tullett Basin and Green Bay Uplift on western Prince Patrick Island. The line of section runs from Houghton Head on the southwest coast to the north end of Intrepid Inlet. There have been no wells drilled into the basin.*

include normal faults at the head of Mould Bay that strike N25°E, and four others at the north end of the basin that strike N18°W to N35°W.

Eastward-dipping faults (18) outnumber those dipping to the west (12) by a factor of three to two. Eastward-dipping faults have also had a more significant influence on the direction of block rotation in downthrown strata. In other words, the eastward-dipping set of faults are more likely to display a downward-flattening, listric profile with hanging wall strata that dip toward the fault plane. In contrast, westward-dipping faults have a greater tendency to feature downthrown strata that dip away from each fault plane. There are at least six exceptions, not least of which is the Green Bay Fault, which defines the eastern limit of the Green Bay Graben and is a local eastern boundary of Tullett Basin. There is no geographical preference for east- and west-dipping faults. Instead, the basin appears to have been divided into a series of seven, major half-grabens and many other small, rotated blocks. Characteristic features for each of the major half-grabens within Tullett Basin are provided below.

All of the Tullett Basin faults are rooted within or below the Devonian clastic wedge. Nevertheless the tectonic fabric of folds and thrusts of the Franklinian Mobile Belt are highly oblique to that of rift trends in the younger basin and therefore appear to have had little or no influence on the kinematic development of the basin (compare Fig. 30 and 52).

Green Bay Graben

Surface geology. The Green Bay Graben is the largest and easternmost rift-related structure within Tullett Basin. Present understanding of this structure is based on bedrock exposures and measured sections in the south (Fig. 54, 64), and seismic data in the north (Fig. 63). The southern part of the graben, including the bounding Green Bay and Mould Bay faults, and the upthrown footwall blocks to east and west, respectively, have been mapped west of the head of Green Bay on east-central Prince Patrick. The principal inward-dipping graben-boundary faults strike N25°E varying to N10°W farther north. The graben is up to 9 km wide in the outcrop belt, but terminates abruptly to the south against a N79°W-striking tear fault. Throw on each of the bounding faults is at least 400 m where Lower Cretaceous Isachsen Formation in the hanging wall is placed in tectonic contact with Devonian Cape de Bray Formation in the footwall. Identification of the master fault, using direction of block rotation, is obscured by structural complication in the graben-fill and by ambiguous structural characteristics of the bounding upthrown blocks. The graben-fill has been deformed into open folds with axial trends of N20°W varying to N42°W; trends that are noticeably oblique to the northward-striking boundary faults. Likewise, the upthrown blocks to east and west have Mesozoic cover that dips outward from the graben and thus provides only limited insight into the kinematics of graben formation.

Phases of fault movement are provided by comparison of footwall and hanging wall stratigraphic sections (columns 13 to 16, Fig. 54). Columns 13 and 14 were measured within the graben west of the head of Green Bay and along the coast, respectively. Column 15 includes only the older strata exposed in the eastern upthrown footwall block (Green Bay Uplift) north of Salmon Point. Column 16 was measured farther to the northeast off the hinge of the uplift. At the lowest levels above the post-Devonian peneplain, arenaceous limestone of the Pat Bay Formation (Carnian) is traceable from Column 15 on the uplift to column 14 on the west side of the Green Bay Fault in the eastern part of the graben. However, Triassic strata are absent farther west in the graben below the Toarcian part of the Jameson Bay Formation in column 13. This relationship is attributed to the pattern of transgression, regression, exposure, erosion, and subsequent marine onlap that repeatedly affected the ancestral Sverdrup Basin margin prior to graben formation.

Evidence for the first phase of differential movement between Green Bay Uplift and the adjacent graben is provided by differences in the overlying strata above the Pat Bay Formation in columns 14 and 15 and above the Devonian in column 13. The oldest Jurassic strata are preserved in the graben and include the Intrepid Inlet Member (containing Pliensbachian ammonites; sample C-133909, in appendix) of the Jameson Bay Formation in column 14 and the Cape Canning Member of the same formation (with middle to late Toarcian ammonites, C-163563, in appendix) in column 13. In contrast the entire Jameson Bay Formation is absent below 6 m of Sandy Point Formation in column 15 over the hinge of Green Bay Uplift. The Pliensbachian and Toarcian strata, preserved in the graben, are dominated by offshore marine shale with lesser marine sandstone. The implication of these sections is that the Pliensbachian and Toarcian beds were also probably deposited in similar offshore marine depositional settings on the site of the future uplift to the east but were removed as a consequence of a phase of uplift and erosion related to slip on Green Bay Fault that did not result in subaerial exposure of the graben-fill. The end of the first phase of uplift and slip on Green Bay Fault must predate the early Aalenian phase of marine overlap onto the uplift.

There is neither stratigraphic nor sedimentological evidence for additional slip in either the later Jurassic or the Cretaceous. However, all the graben-boundary faults have displaced and tilted Isachsen Formation strata in the graben, and these faults and inclined graben strata are overlain with pronounced angular unconformity by the Beaufort Formation. Less obvious are the kinematics of slip on the

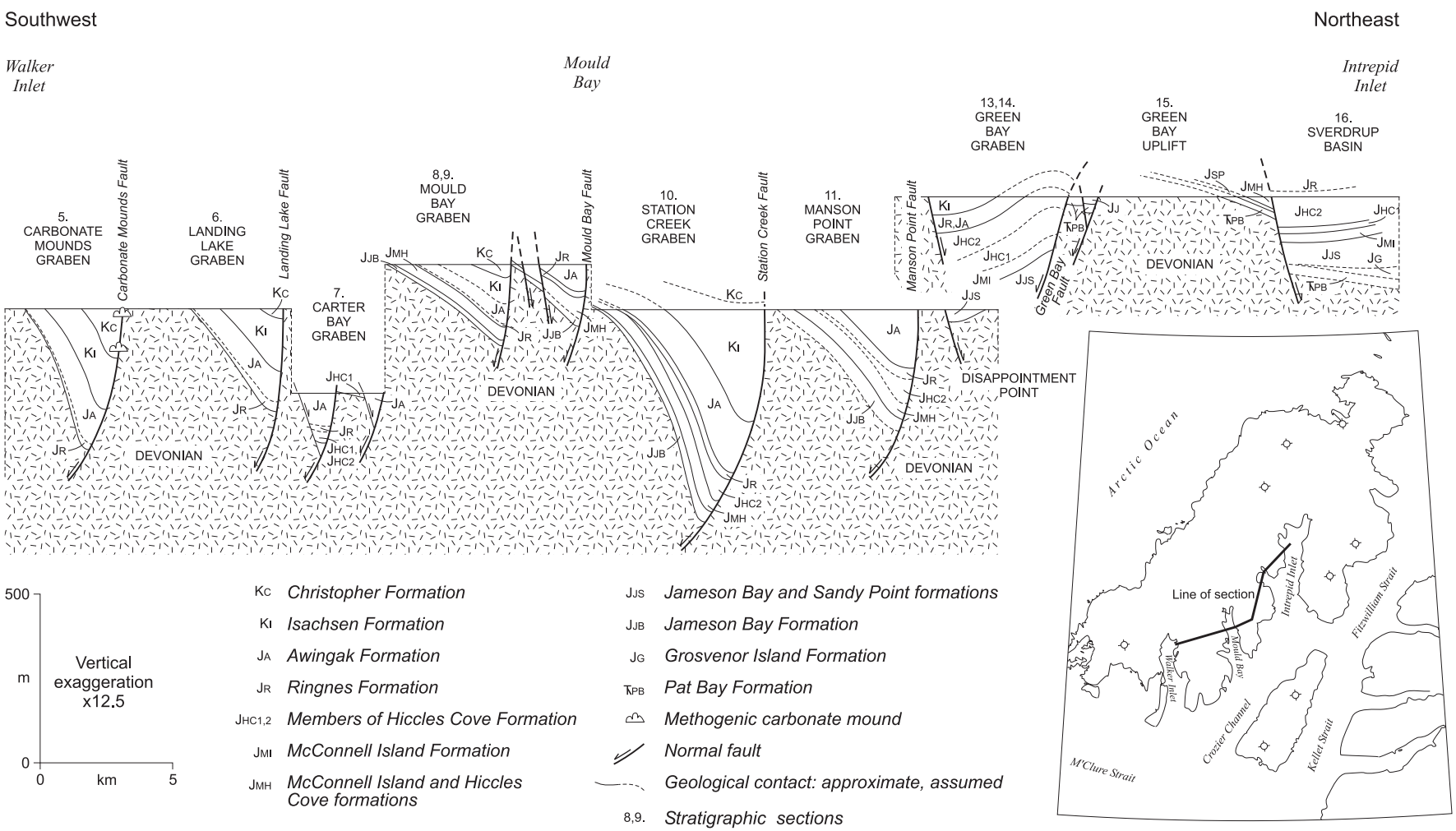

Figure 64. *Schematic structural cross-section of the named grabens in the outcrop belt of Prince Patrick Uplift between Walker Inlet and Intrepid Inlet based on outcrop data, geological mapping and the measured sections illustrated in Figure 54. Different datums have been adopted for structures projected onto the line of section either from the north (at top) or from the south (below).*

faults that offset the Cretaceous since there was probably also a slip phase coincident with the compressive buckling of the graben-fill.

Green Bay region has failed to yield any useful outcrop information concerning the dip direction, dip angle or slip sense for the map-scale faults. However, an excavated outcrop within the highest beds of the Hiccles Cove Formation in a stream bank section 3.1 km west of the northernmost part of Green Bay provides convincing evidence for the existence of postdepositional planar and listric normal faults in Middle Jurassic (Callovian) strata (Fig. 65, 67). The faulted strata consist of uncemented, fine-grained, white quartz sand; flat-laminated, very fine-grained, brown sand; thin coal seams; thin shale layers, and shale partings. Primary depositional features also include depositional clinoforms, cut-and-fill structures, and root casts. There are eleven clearly defined faults in the panoramic view of this outcrop (Fig. 65). Net displacement is 2.1 m down to the southeast accomodated on five, southeast-dipping faults. Excavation of one fault plane has provided an attitude of N35°E, dip 72°SE with strata also downthrown to the southeast. Four faults are near vertical with several tens of cms of throw down to the northwest, and two display a reverse sense of slip (Fig. 67). The faults in sectional view are irregular, braided, upward bifurcating and anastomosing (Fig. 66, 67). Fault planes are delineated by fine white sand. Displacement on one of the larger faults lies within a comminuted and presumably sheared interval 10 cms wide. Several faults flatten downsection.

Subsurface geology. A subsurface portion of Green Bay Graben and Green Bay Uplift, including the Mould Bay and Green Bay faults, is imaged west of Intrepid Inlet on seismic profile 467 and, in a highly oblique survey, on profile PPA7 (Fig. 68). The axial line of the graben continues to the north but terminates near 76°52'N about 8 km south of the Intrepid Inlet H-49 well.

Thickness of graben-fill increases progressively to the north from the outcrop belt as far as the north end of Green Bay Fault at about 76°50N. Graben-fill, for example, is up to 1100 ms on PPA7 (Fig. 68), and reaches a maximum of 1450 ms on profile 467. Similarly, cover on the Devonian increases to the north over the footwall Green Bay Uplift from a zero edge on Salmon Point in the south to 450 ms at SP 334 on PPA7, to 660 ms at SP 6898 on profile 467 in the north. The thickness of Lower Jurassic and older strata continues to increase within the graben and over the adjacent uplift in areas north of latitude 76°50N. However, the depth of pre-Pliocene erosion also increases to the north so that only Middle Jurassic and older strata are preserved below the Beaufort Formation across the northern part of the graben.

Correlation of seismic units lying in the immediate subsurface beneath the Beaufort Formation is constrained by outcrop exposed in incised river valleys east of profile PPA7, and by easy correlation of reflections from the Intrepid Inlet H-49 well to the Green Bay Uplift. These data sources indicate the presence of Hiccles Cove Formation on the sub-Beaufort surface over the Green Bay Uplift on profile PPA7 west of the head of Intrepid Inlet, and either Isachsen or Christopher Formation near the surface in the graben. The deepest reflective unit above the Devonian on the uplift is correlated with the Schei Point Group. This unit carries on into the graben as does the Jameson Bay Formation, which oversteps the Triassic to the west within the basal part of the graben fill succession. Subdivision of the remaining graben fill is based on an assumed correlation of a high-amplitude continuous reflector at 400 to 500 ms with the base of the Ringnes Formation. The top of the Deer Bay Formation is drawn on a low-amplitude continuous reflector below reflection-free Isachsen Formation. This assumed contact provides for a combined Ringnes and Deer Bay seismic unit that is 265 ms thick and similar to the 235 to 270 ms thickness encountered on most profiles of the Sverdrup Basin north of the Jameson Bay C-31 well on northeastern Prince Patrick Island. The principal implication of these correlations is that the Hiccles Cove and McConnell Island seismic unit (225 to 280 ms) is 25 to 55% thicker in the Green Bay Graben than in most areas of the Sverdrup Basin immediately east of the graben where the thickness range is 125 to 165 ms.

Seismic profile PPA7 (Fig. 68) also provides significant structural information, albeit on an oblique survey, of Green Bay Graben and the adjacent uplifts. The eastern boundary fault (Green Bay Fault) displays 650 ms of throw on PPA7 decreasing northward to 430 ms on profile 467 as measured on the base of the Triassic. This fault has a concave profile that flattens downsection to the west onto a bedding-parallel detachment 450 ms above the base of the Devonian clastic wedge on PPA7. Regional dip of strata is to the east on the Green Bay Uplift. Hanging wall strata in the graben dip more steeply to the east and appear to have been rotated during slip on the Green Bay Fault. Regional attitude of graben-fill varies from eastward-dipping in the south on profile PPA7 to westward dipping on profile 467. Thus, the Green Bay Fault appears to be the master bounding structure in the southern half of the graben and the Mould Bay Fault has played a subsidiary or conjugate role. In the north, the graben is more symmetrical with equal displacement on the bounding normal faults.

Open regional folds, similar to those mapped at the surface in the southern part of the Green Bay Graben, have also played a part in the structural style of the graben fill (Fig. 68). These folds are described in the chapter dealing with the Cenozoic(?) compressive deformation of the report area.

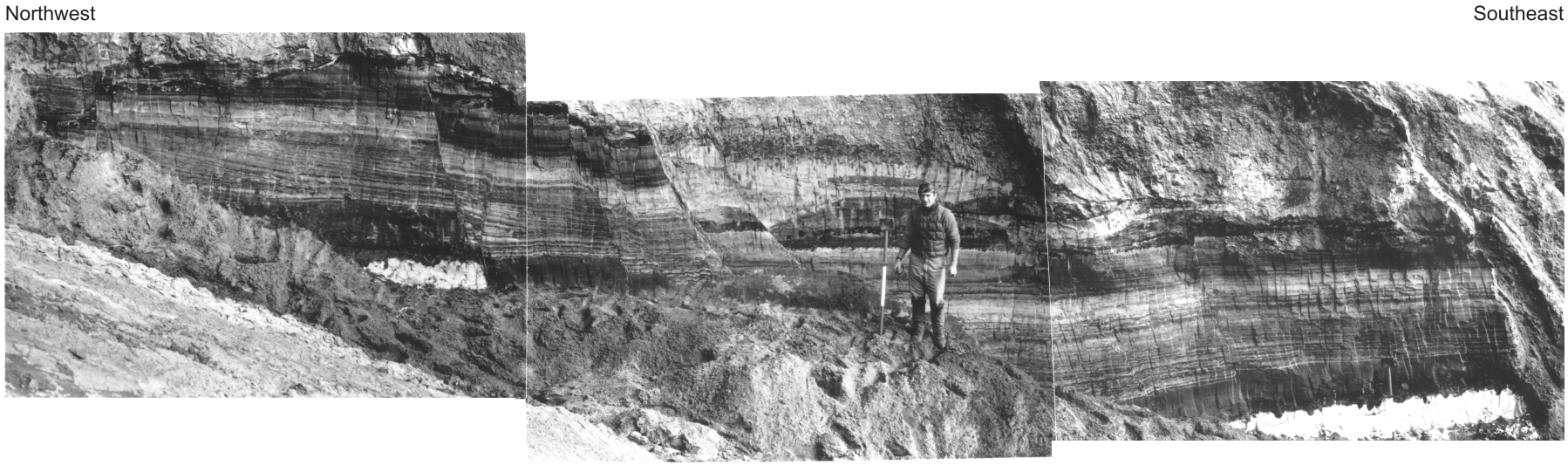

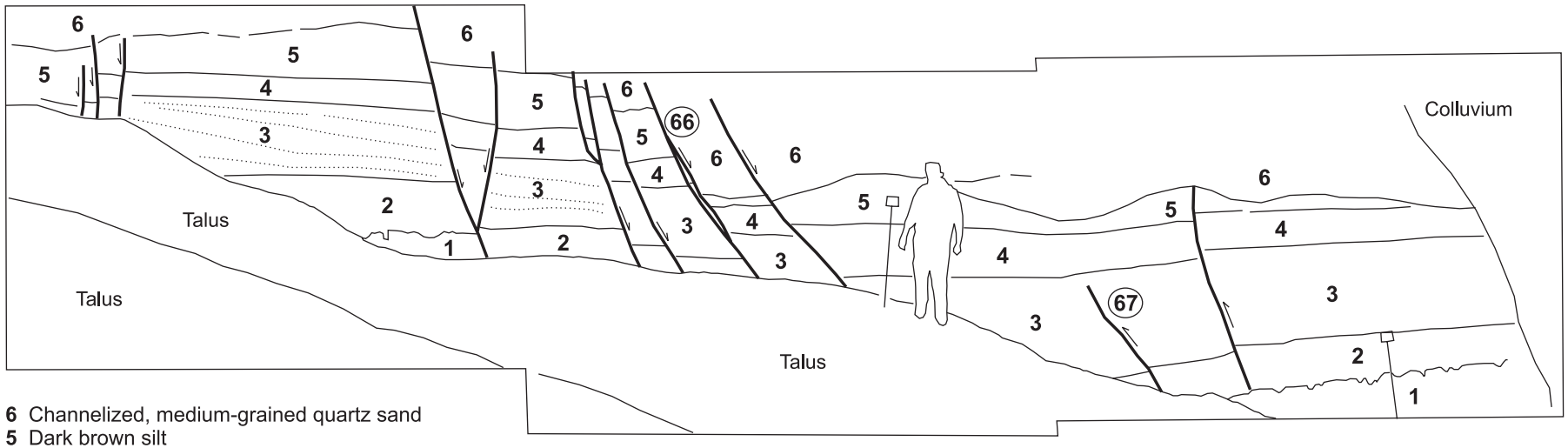

6 Channelized, medium-grained quartz sand
5 Dark brown silt
4 Parallel laminated, fine-grained sand
3 Clinoformed, fine-grained sand
2 Dark brown silt
1 White, medium-grained quartz sand

(66) Location of photographs in Figures 66,67

Figure 65. *Panorama of excavated outcrop within the uppermost part of the Hiccles Cove Formation west of the head of Green Bay. There are two obvious unconformities and an intervening unit of clinoformed sand. The listric normal faults, mostly downthrown to the east, are believed to be characteristic of those mapped elsewhere at surface and identified on seismic profiles throughout western Prince Patrick Island. See Figures 50 and 53 for location (GSCC photos 3820-16, 26, 27).*

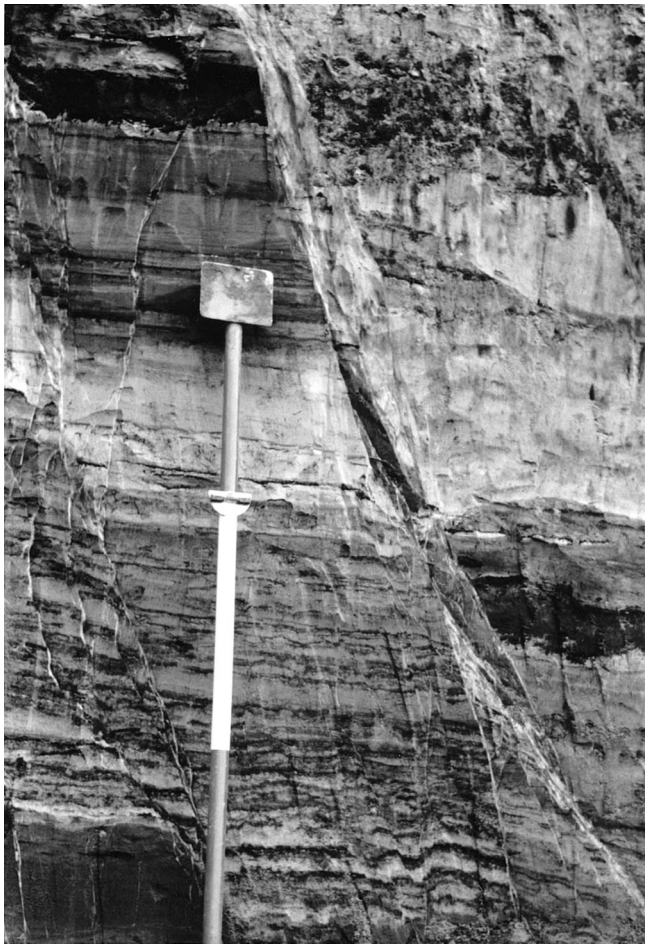

Figure 66. *Detail of faults in the upper Hiccles Cove Formation, west of the head of Green Bay. The faults defined by offset bedding and finely comminuted white sand are complex, anastamosing structures that appear to be progressively flattened downsection (GSCC photo 3820-22).*

Figure 67. *Detail of faults in the upper Hiccles Cove Formation, west of the head of Green Bay. Some minor faults display a reverse sense of slip. The upthrown block (to right) has been displaced compressively toward the west (GSCC photo 3820-23).*

Mould Bay Graben

Mould Bay Graben lies within the southern portion of Tullett Basin, north of the head of Mould Bay, and is almost entirely obscured by Beaufort Formation. The northward-striking fault array associated with the southern termination of Mould Bay Graben has been mapped in the narrow outcrop belt north of the head of the bay. However, the thickness of Jurassic and Cretaceous strata is only 220 m in this area (column 9 on Fig. 54) and would appear to have accumulated south of the actively subsided portion of the graben.

The Mould Bay Graben has been imaged on profiles PPA14 (Fig. 69) and PPA17. The east side of the graben is defined by a large, uplifted block of Devonian basement rocks (Cape de Bray and Weatherall formations) a greater part of which is exposed at the head of Mould Bay and in an inlier, situated in the footwall of the east-dipping Mould Bay Fault, west of Green Bay. The basement inlier plunges to the north into Tullett Basin and throw on the related boundary faults also dies away to the north. The graben itself merges with the larger Green Bay Graben in the vicinity of profile 467. Graben fill, and the Devonian below it, is broadly buckled, particularly along the faulted west side of the basement uplift on PPA14 (Fig. 69). A single master fault defines the west boundary of Mould Bay Graben with similar properties on both PPA17 (at SP530) and PPA14 (at SP453). This is an east-dipping normal fault with 500 ms of stratigraphic throw measured across the base of the Jurassic on PPA14, and 285 ms of throw on PPA17. The fault has a listric profile and a probable detachment level in the lower part of the Devonian clastic wedge. West-dipping graben-fill strata characterize the downthrown hanging wall section. Part of the inclination of strata on PPA14, and perhaps all of the tilt on PPA17, appear to have

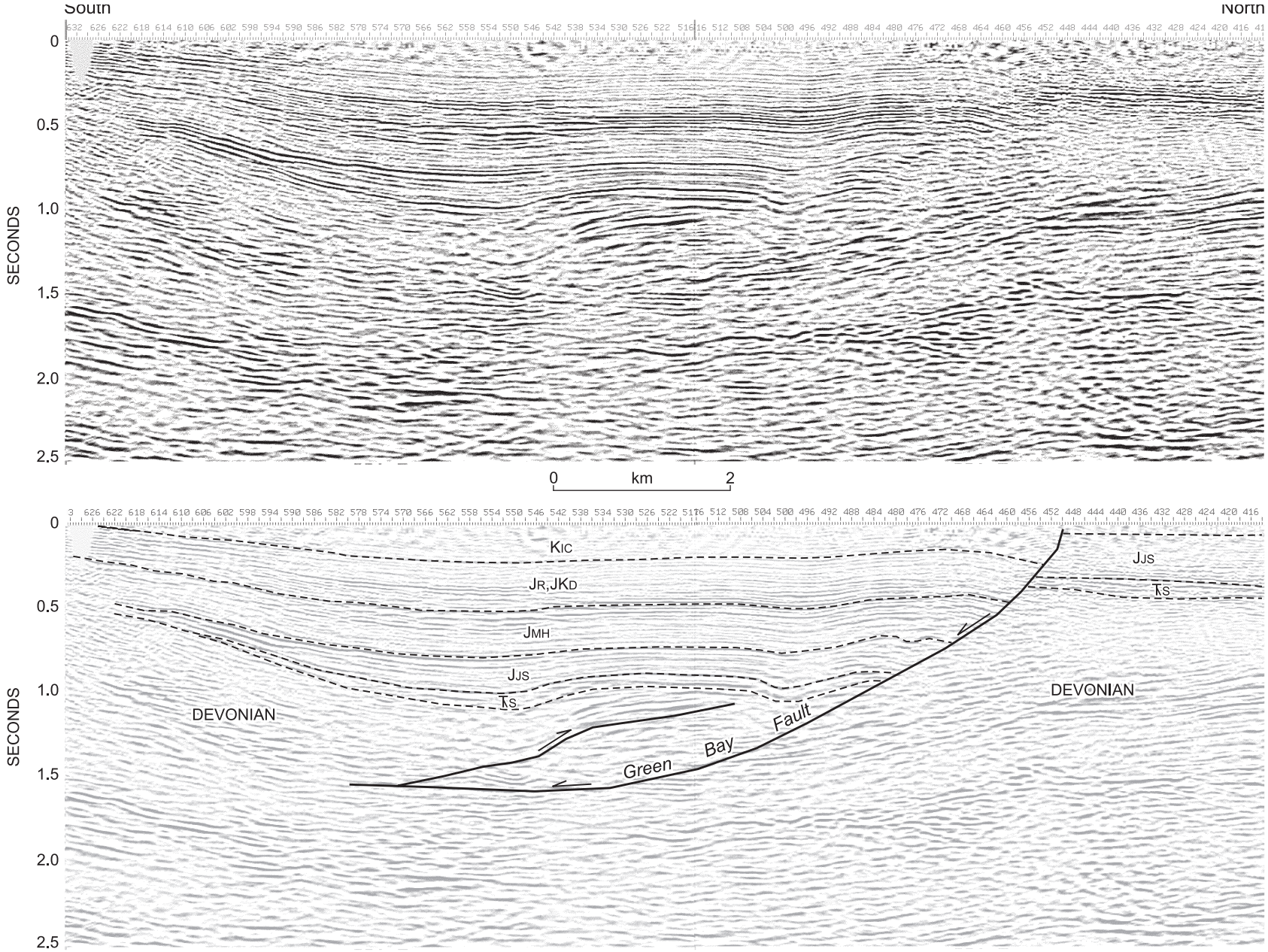

Figure 68. *Seismic expression of Green Bay Graben on the east side of Tullett Point Basin, and Green Bay Uplift on a portion of Elf seismic profile PPA7.* TS*: Schei Point Group;* JJS*: Jameson Bay and Sandy Point formations;* JMH*: McConnell Island and Hiccles Cove formations;* JR*: Ringnes Formation;* JKD*: Deer*

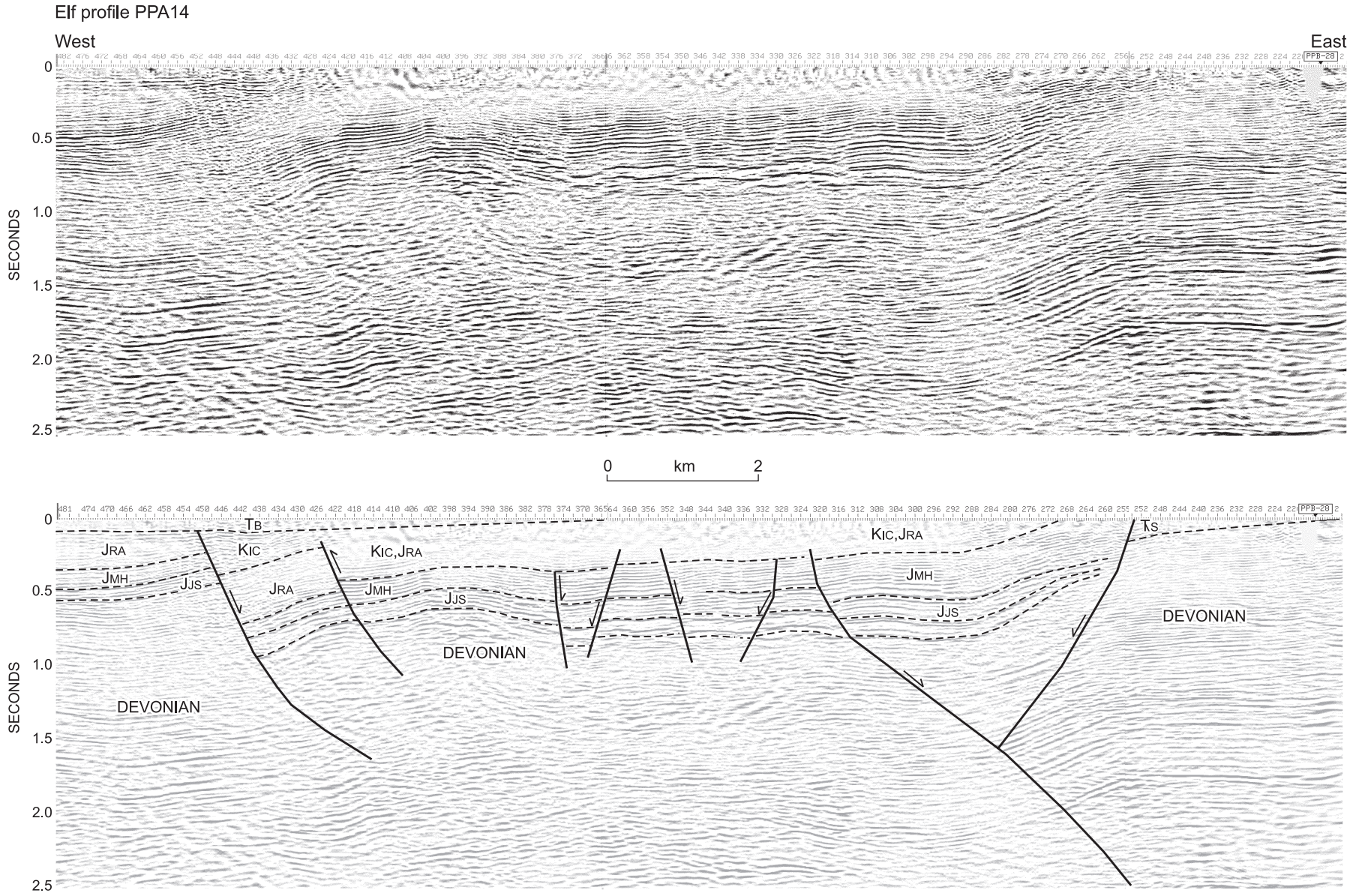

Figure 69. *Seismic expression of Mould Bay Graben in the southern part of Tullett Point Basin on a portion of Elf seismic profile PPA14.* TS*: Schei Point Group;* JJS*: Jameson Bay and Sandy Point formations;* JMH*: McConnell Island and Hiccles Cove formations;* JRA*: Ringnes and Awingak formations;* KIC*: Isachsen and Christopher formations;* TB*: Beaufort Formation and related strata of the Arctic continental terrace wedge. Profile is located on Figures 50 and 53.*

been generated by rotation during normal slip on the adjacent and underlying listric fault. The structure on PPA14 is modified by a minor thrust-anticline (at SP 421) apparently related to inversion of a pre-existing normal fault.

Data relating to the tectonic history of Mould Bay Graben and other named grabens of Tullett Basin are summarized in Figure 62. Unlike Green Bay Graben to the east, no good case can be made for syndepostional slip on any single fault during sediment accumulation in Mould Bay Graben. Nevertheless, Christopher Formation is known at the surface near the line of profile within the graben in the vicinity of SP295 on PPA14 (11 kms north of the head of Mould Bay) and the preserved thickness of Mesozoic section must increase from 220 m measured below the eroded top of the Christopher Formation in column 9 measured 5 km north of Mould Bay (Fig. 54), to 825 ms (or 1155 m at 2.8 km s^{-1}) only 6 km to the north at SP 295 on the line of profile. Correlation of formations to seismic units on the profile is uncertain. However, there is no obvious reflector that might be equivalent to the Schei Point limestone and, thus, there is no reason to believe that there are strata older than the Jameson Bay Formation in the graben. The preferred interpretation is a correlation of the near-surface reflection-free unit on PPA14 with the Awingak Formation and the top of the underlying reflective succession with the Ringnes Formation. Since the Christopher Formation underlies the sub-Beaufort surface in the graben near SP295, then the reflection-free unit, 250 ms thick in this area, must include all of the Ringnes, Awingak and Isachsen formations, and part of the Christopher Formation in unknown proportions. Nevertheless, the combined thickness of these four formations must dramatically increase northward, from 185 m in column 9 to a maximum of 575 ms (approx. 800 m) on the west side of the graben on profile PPA14. Similarly, the Jameson Bay to top Hiccles succession, which is only 40 m thick in column 9, has expanded to a maximum of 560 ms (approx. 780 m) at SP 290 on PPA14 in the axial area of the graben. The rapidity of lateral thickening is greater than would be expected from a passively subsiding basin in which associated extension faults are all younger than the associated strata. A more likely scenario is that one or more of the graben-boundary faults has experienced episodic extensional slip during the period of punctuated Middle Jurassic to Lower Cretaceous sediment accumulation, and that only the last phase of normal faulting postdates the Christopher Formation, but predates overlap by the Beaufort Formation.

Discovery Point Graben

The southern extent of Discovery Point Graben lies mostly to the west and north of Mould Bay Graben. The down-to-the-west bounding normal fault, lying on the east side of Discovery Point Graben, is situated 20 km west of the Intrepid H-49 well and has a strike length of at least 40 kilometres. The graben is imaged on profile P467 and three other regional profiles to the north (Fig. 53). Throw on the eastern boundary fault is greatest on P467 (about 420 ms) and preserved post-Devonian strata range up to about 1500 ms. Preserved section in the graben includes Middle to Upper Triassic Schei Point Group through probable Lower Cretaceous Isachsen and Christopher formations in the south, and also includes Permian and Lower Triassic in the north. The poor quality of seismic data in this part of Tullett Basin, particularly in the Jurassic interval, precludes any meaningful interpretation of the timing of faulting and history of graben formation.

Tullett Central Graben

Tullett Central Graben, as its name implies, lies in the central region of the Tullett Basin (Fig. 63). The onland portion of this half-graben is entirely obscured by Beaufort Formation and related Neogene cover. The axial line of the half-graben trends northward, and the eastern boundary faults have a minimum strike length of at least 24 km measured from SP 937 on PPA17 (Fig. 70) to SP69 on PPA19. The bounding faults on these profiles have listric profiles with downsection flattening to the west, and a basal detachment in the medial part of the Blackley Formation (cross-section D). A regional dip to the east is readily apparent in the hanging wall section on PPA17 (Fig. 70). A very shallow-limbed hanging wall syncline has also formed immediately adjacent to the eastern boundary fault with shallow dips to the west in the highest beds of the graben-fill. Stratigraphic throw on this fault is modest in the south (160 ms at the base of the Jurassic on PPA17) but increases northward to 330 ms on PPA19.

The seismic stratigraphy of Tullett Basin is best developed on the portion of PPA17 illustrated in Figure 70. Angular truncation of reflectors in the Devonian clearly marks the base of the graben fill at 900 to 1400 ms in the half-graben and at 950 to 1200 ms in the footwall block. Jameson Bay and Sandy Point formations at the base are overstepped to the west by a modestly reflective McConnell Island and Hiccles Cove sequence that includes a continuous, moderate-amplitude basal reflector. The Ringnes Formation, also featuring a high-amplitude reflection at the base, is gradational with the reflection-free Awingak Formation. The Isachsen and Christopher formations are again moderately reflective but not obviously distinguishable. On PPA17 (Fig. 70), the base of the Beaufort Formation is drawn on the profile at about 200 ms. This level corresponds to the gradational base of a correlative unreflective seismic unit below which there is at least local evidence of tectonic displacement of primary reflections in the seismic Lower Cretaceous.

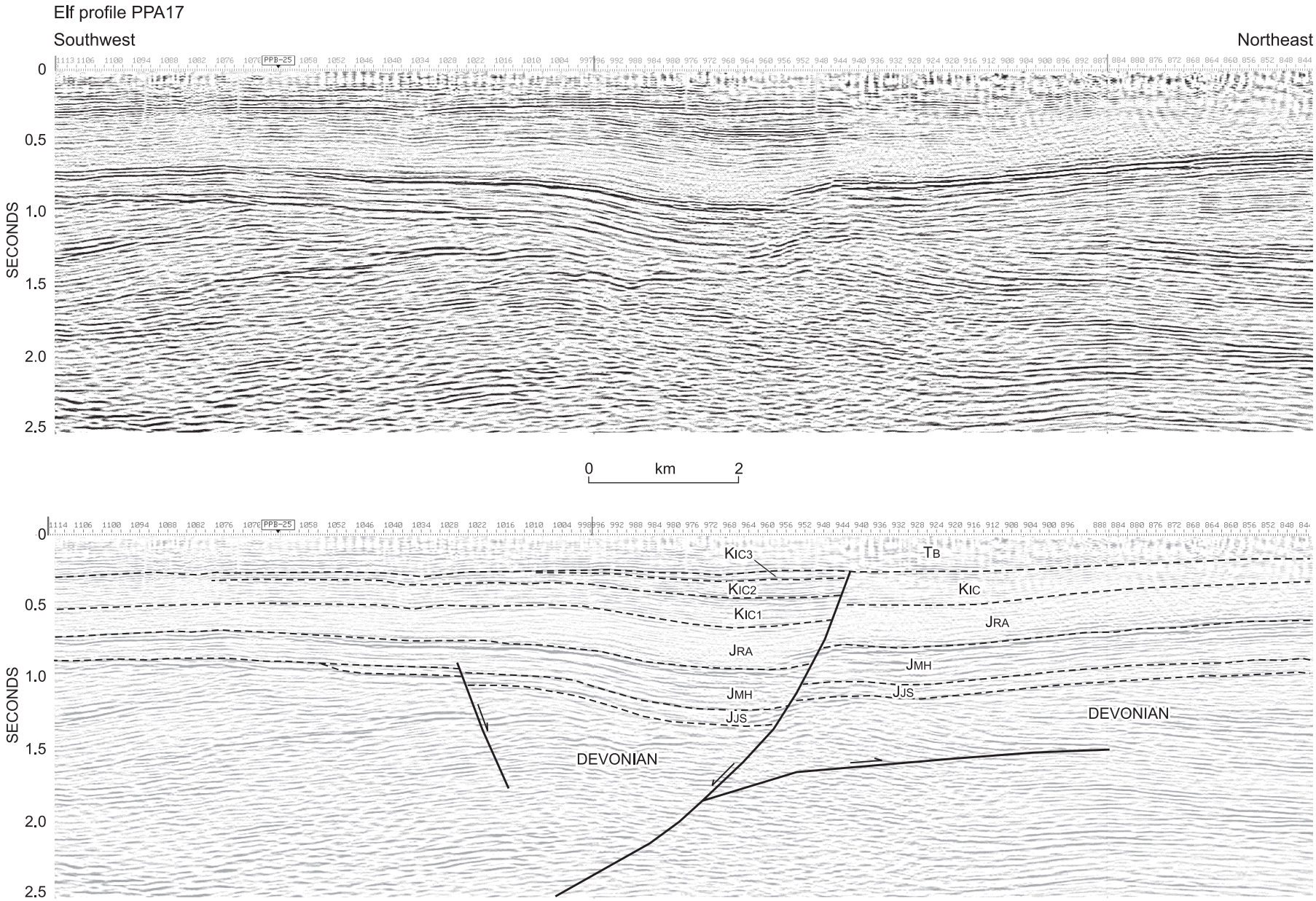

Figure 70. *Seismic expression of Tullett Central Graben in the central region of Tullett Point Basin on a portion of Elf seismic profile PPA17.* JJS*: Jameson Bay and Sandy Point formations;* JMH*: McConnell Island and Hiccles Cove formations;* JRA*: Ringnes and Awingak formations;* KIC1-3*: local seismic units of the Isachsen and Christopher formations;* TB*: Beaufort Formation and related strata of the Arctic Continental Terrace Wedge. Profile is located on Figures 50 and 53.*

There are three indicated phases of extensional displacement on the eastern boundary fault for Tullett Central Graben on PPA17 (Fig. 62). The earliest phase of slip accounts for thickness variation in the undivided Hiccles Cove-McConnell Island unit, which may have occurred either during deposition of this package or prior to channel development in the basal Ringnes Formation.

Syntectonic deposition can also be inferred for the seismic unit embracing the undivided Isachsen and Christopher formations in the half-graben. This package is locally divisible into three informal members between SP 940 and 1030 on PPA17 (Fig. 70). Divergence of reflectors and thickening into the graben is indicated for the medial informal member, which might correlate with either the upper Isachsen or lower Christopher formations.

The graben boundary fault itself cuts all units as high as the Beaufort Formation, which implies either a continuation of the second phase of slip or a third and distinctly younger phase of post-Early Cretaceous and pre-Pliocene faulting.

Richards Point Graben

Richards Point Graben lies in the west-central part of Tullett Basin beneath continuous cover of Beaufort Formation and related strata of the continental terrace wedge. Richards Point itself lies above an unnamed horst block west of the axial line of the graben. Geology of Richards Point Graben is provided by Figure 63 and profiles PPB25 and PPB26 (Fig. 71, 72). The graben also extends onto PPA14 and PPA17 (Fig. 73) for a total imaged north-south length of 26 km. The bounding faults are up to 7 km apart in the north, where maximum stratigraphic throw on the base of the Jurassic is 280 ms. These faults diverge to the south, and although the graben is 10 km wide in the vicinity of profile PPA17, the associated faults each have less than 100 ms of throw.

The base of graben fill is defined by a pronounced angular discordance and topset truncation of dipping reflectors in Devonian basement against more gently inclined Jurassic units. Rotational inclination of graben fill is best developed against one or more east-dipping faults within and along the west side of the graben. Other vertical or west-dipping faults appear to have had no influence on bedding attitudes (Fig. 71, 72). Some of the faults appear to flatten downsection. The basal décollement is interpreted to be above 1600 ms in the upper part of the preserved Devonian clastic wedge as there is generally no evidence for extensional offset of primary reflection energy below the base of the Weatherall Formation.

Thickness of graben-fill increases to the north from local maxima of 460 ms on PPA17 to 760 ms on PPB26. Seismic stratigraphic units are similar to those encountered elsewhere in Tullett Basin. The undivided Jameson Bay and Sandy Point unit ranges up to local thickness maxima of about 180 ms in the examples on Figures 71 and 72. The unit thins to the south onto PPA17. Lateral thickness variations are also characteristic and attributed to partial or complete topset (erosional) truncation of reflections beneath the sub-McConnell Island reflector. One example of this is near SP310 on PPB25 (Fig. 72).

The undivided McConnell Island and Hiccles Cove seismic sequence has local thickness maxima of 280 ms in the north of the graben and 135 ms in the south. The unit, however, is laterally more continuous than the older strata of the graben fill and much of the thickness variation is related to a regional westward-thinning trend. Bounding reflections are continuous but over short distances, vary from low- to very high-amplitude. Internal reflections are subparallel, semicontinuous and low to moderate in amplitude. Reflections, onlapping to the west, are noted at the base in areas east of the graben and SP325 on PPB25 (Fig. 72). Fine examples of channeling also occur in the same area in the upper part of the sequence. Local thickness variation is related to postdepositional faulting and topset truncation of internal reflection segments. A good example of a sub-Ringnes angular unconformity above tilted Hiccles Cove and older Jurassic strata occurs at SP295 to 325 on PPB26 (Fig. 71). Channels below the Ringnes and apparent topset truncation of underlying reflectors east of SP270 on PPB25 (Fig. 72) could be interpreted as evidence of an erosion surface, a marine flooding surface, or both. The undivided Ringnes-Awingak sequence, as elsewhere, is reflection free and weak, but laterally continuous reflectors mark the base and, locally, also the top of the sequence. Apart from several notable exceptions, this sequence has a fairly uniform thickness of about 230 ms in the northern part of the graben. Westward thinning is more obvious in the southern part of the graben on PPA17 (Fig. 73), from a local maximum of 150 ms to less than 65 ms over the upthrown western footwall block. The undivided Isachsen and Christopher formations are also believed to be widespread in the area. However, measurement of the thickness of the sequence is hampered, particularly in the northern part of the graben, by uncertainty in picking and correlating the base of the Beaufort Formation and related Neogene strata.

There is evidence for four phases of faulting within Richards Point Graben (Fig. 62). The first phase of slip on the unnamed east-dipping fault at SP200 on PPB26 (Fig. 71) occurred during or subsequent to deposition of the Jameson Bay-Sandy Point sequence, which thickens abruptly across the fault from 120 ms on the upthrown side to 150 ms on the low side. Similarly, there is an abrupt lateral limit for the Jameson Bay-Sandy Point sequence observed against the western graben-boundary fault on

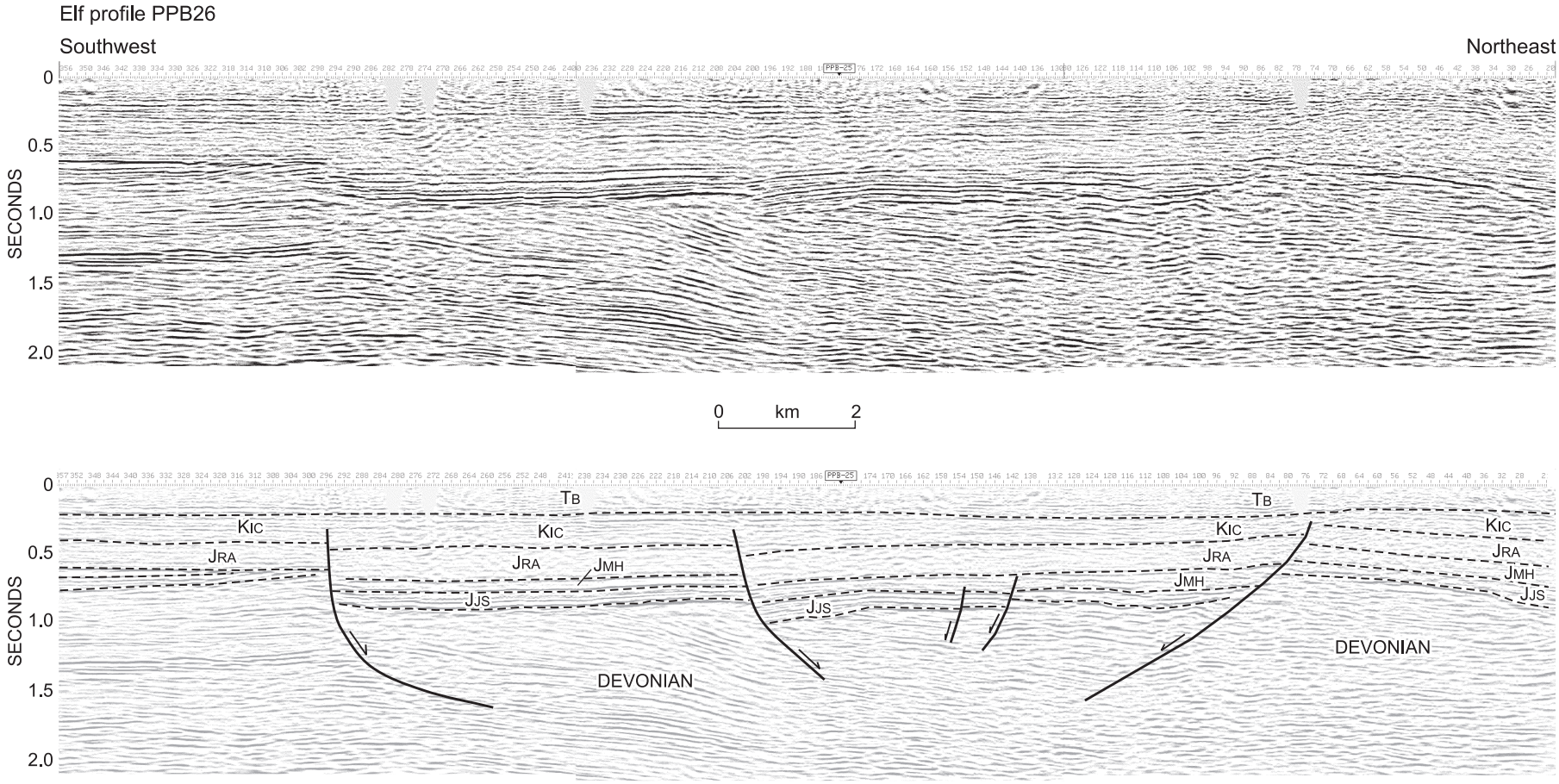

Figure 71. *Seismic expression of northern Richards Point Graben in the west-central part of Tullett Point Basin on a portion of Elf seismic profile PPB26.* JJS: *Jameson Bay and Sandy Point formations;* JMH: *McConnell Island and Hiccles Cove formations;* JRA: *Ringnes and Awingak formations;* KIC: *Isachsen and Christopher formations;* TB: *Beaufort Formation and related strata of the Arctic Continental Terrace Wedge. Profile is located on Figures 50 and 53.*

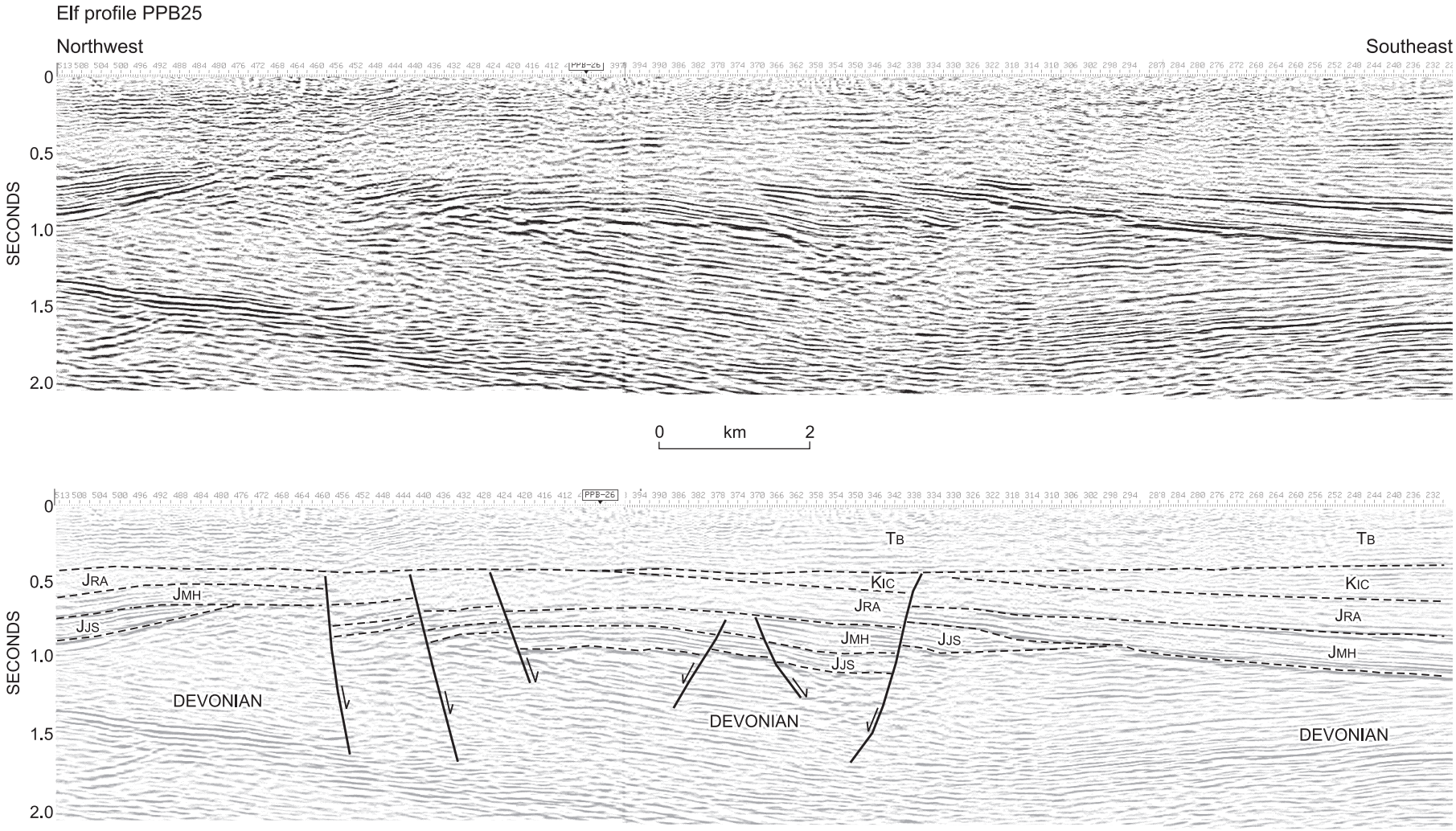

Figure 72. *Seismic expression of central Richards Point Graben in the west-central part of Tullett Point Basin on a portion of Elf seismic profile PPB25.* JJS: *Jameson Bay and Sandy Point formations;* JMH: *McConnell Island and Hiccles Cove formations;* JRA: *Ringnes and Awingak formations;* KIC: *Isachsen and Christopher formations;* TB: *Beaufort Formation and related strata of the Arctic Continental Terrace Wedge. Profile is located on Figures 50 and 53.*

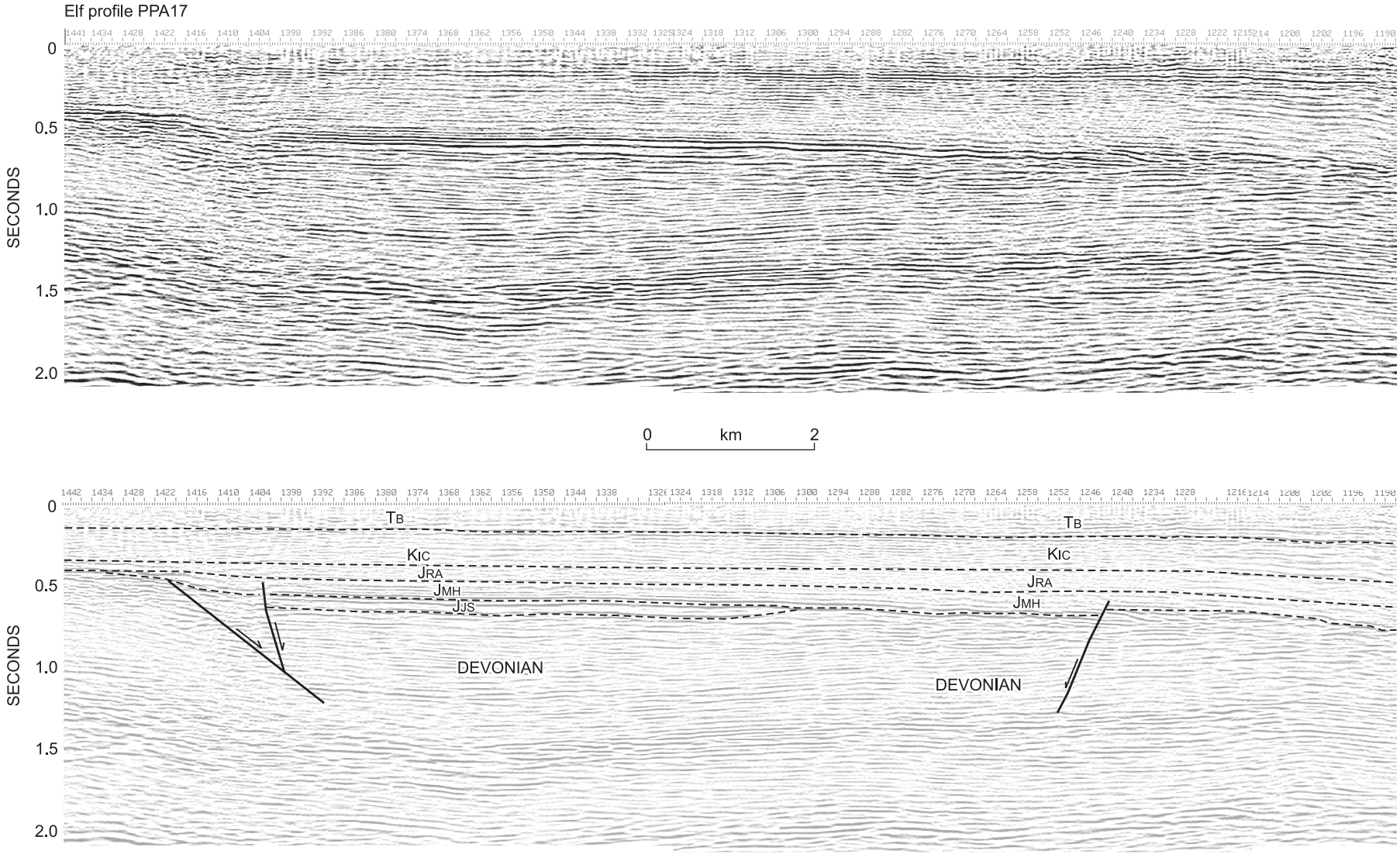

Figure 73. *Seismic expression of southern Richards Point Graben on a portion of Elf seismic profile PPA17.* JJS: *Jameson Bay and Sandy Point formations;* JMH: *McConnell Island and Hiccles Cove formations;* JRA: *Ringnes and Awingak formations;* KIC: *Isachsen and Christopher formations;* TB: *Beaufort Formation and related strata of the Arctic Continental Terrace Wedge. Profile is located on Figures 50 and 53.*

PPA17, and the same fault appears to be overstepped without offset by the McConnell Island-Hiccles Cove sequence (Fig. 73). Erosional truncation of this sequence by the sub-McConnell Island reflection occurs on PPA17 (Fig. 73) and at two places on PPB25 (Fig. 72) which supports one view that the first phase of extensional tectonics postdated at least the earlier period of Jameson Bay deposition in this area and preceded overlap by the McConnell Island.

For the east-dipping fault at SP200 on PPB26, for the east-dipping boundary faults near SP 1400 on PPA17 (Fig. 73) and for the main west-dipping boundary faults at SP330 on PPB26, abrupt thickening of the McConnell Island-Hiccles Cove sequence across and into the downthrown succession is attributed to the second phase of faulting. The McConnell Island-Hiccles Cove sequence displays parallel internal reflections and the timing of faulting would again appear to postdate the earlier period of sediment accumulation but precede overlap of the top-truncated reflections that have produced a local angular unconformity below the overstepping Ringnes Formation. This relationship is documented over the upthrown side of the steep, down-to-the-east faults at SP300 on PPB26 (Fig. 71) and at SP1415 on PPA17 (Fig. 73).

The third phase of faulting is related to thickness variation of the Ringnes-Awingak sequence across faults at SP210 and SP300 on PPB26, and at SP1415 on PPA17. This deformation phase could have been either coeval with sediment accumulation in the Late Jurassic or could have preceded overlap by the Isachsen Formation.

The fourth and final phase accounts for tilt and offset of the Isachsen and Christopher sequence as, for example, on the eastern graben-boundary fault at SP330, PPB25 and at SP70, PPB26. Late-stage slip is also indicated for the western boundary faults on PPB25.

Hardinge Bay and Houghton Head grabens

Key seismic profiles for the present understanding of the two, small, subsurface grabens at the far west end of Tullett Basin include PPA14 (Fig. 74), PPB26 (Fig. 75) and PPB27. In spite of their limited size, the Hardinge Bay and Houghton Head grabens provide some of the most compelling evidence for multiple phases of rifting within Tullett Basin. Structural style and seismic stratigraphy of the graben fill and cover on adjacent high blocks is similar to that described for Richards Point Graben and will not be repeated.

The bounding faults for Hardinge Bay Graben are unusual in that they can be interpreted downsection where they offset shelf carbonate and related units in the lower Paleozoic through the base of unit psЄO for the east-dipping fault below SP575 on PPB26 (Fig. 75). Useful for understanding the magnitude of stratigraphic throw in the Devonian clastic wedge is the throughgoing reflector at the base of the Weatherall Formation. For many of the faults illustrated on Figures 74 and 75, the throw on the base of the Weatherall Formation is significantly greater than that at the base of the Jurassic. For example, the eastern boundary fault for Hardinge Bay Graben at SP410 on PPB26 displays 335 ms of throw on the base of Weatherall, but only 90 ms of throw on the base of the Jameson Bay Formation. Similarly, the western boundary fault for the same graben at SP1145 on PPA14 and at SP570 on PPB26 features about 310 ms of throw on the base of the Weatherall but less than 100 ms on the base of the Jurassic. For the eastern footwall uplift of Hardinge Bay Graben there has been 260 ms of throw on the fault and an equivalent thickness of Devonian section stripped from the upthrown block prior to overlap by the McConnell Island Formation.

For the high block west of Hardinge Bay Graben, 315 ms of throw on the east-dipping boundary fault has resulted in erosional stripping of an equivalent thickness of Devonian over the uplift prior to overlap by the Ringnes-Awingak and Isachsen-Christopher sequences. In contrast, the eastern boundary fault of Houghton Head Graben (SP1180 on PPA14 and SP630 of PPB26) does not appear to have existed prior to deposition of the Ringnes-Awingak sequence because the thickness of Devonian above the base of the Weatherall Formation and beneath the Upper Jurassic is the same over the high as it is beneath the graben.

Another early phase of fault motion is indicated for the east-dipping planar normal fault at SP500 on PPB26 (Fig. 75). Fifty to 70 ms of offset are shown on the base of the Weatherall and for the base of the Sandy Point-Jameson Bay sequence. The fault dies out in the medial part of this latter sequence, implying that the one and only phase of slip must have preceded deposition of the higher beds within the Sandy Point-Jameson Bay sequence. This evidence infers an Aalenian phase of faulting.

The subsequent tectonic history of these two grabens follows a pattern similar to that established for other grabens of Tullett Basin. An early phase of block rotation on the west side of Hardinge Bay Graben has produced an angular unconformity below the Ringnes Formation. Faulting during or subsequent to deposition of the upper McConnell Island-Hiccles Cove sequence is indicated for the west-dipping boundary faults of Hardinge Bay Graben at SP 410, PPB26 and SP1050, PPA14. The basal Ringnes reflection also oversteps the older Jurassic units and lies directly on the Devonian over the east side high of Hardinge Bay Graben at SP960 to 1000 on PPA14. Similar overstep relationships exist on the high block between Hardinge Bay and Houghton Head grabens at SP560 to 600 on PPB26.

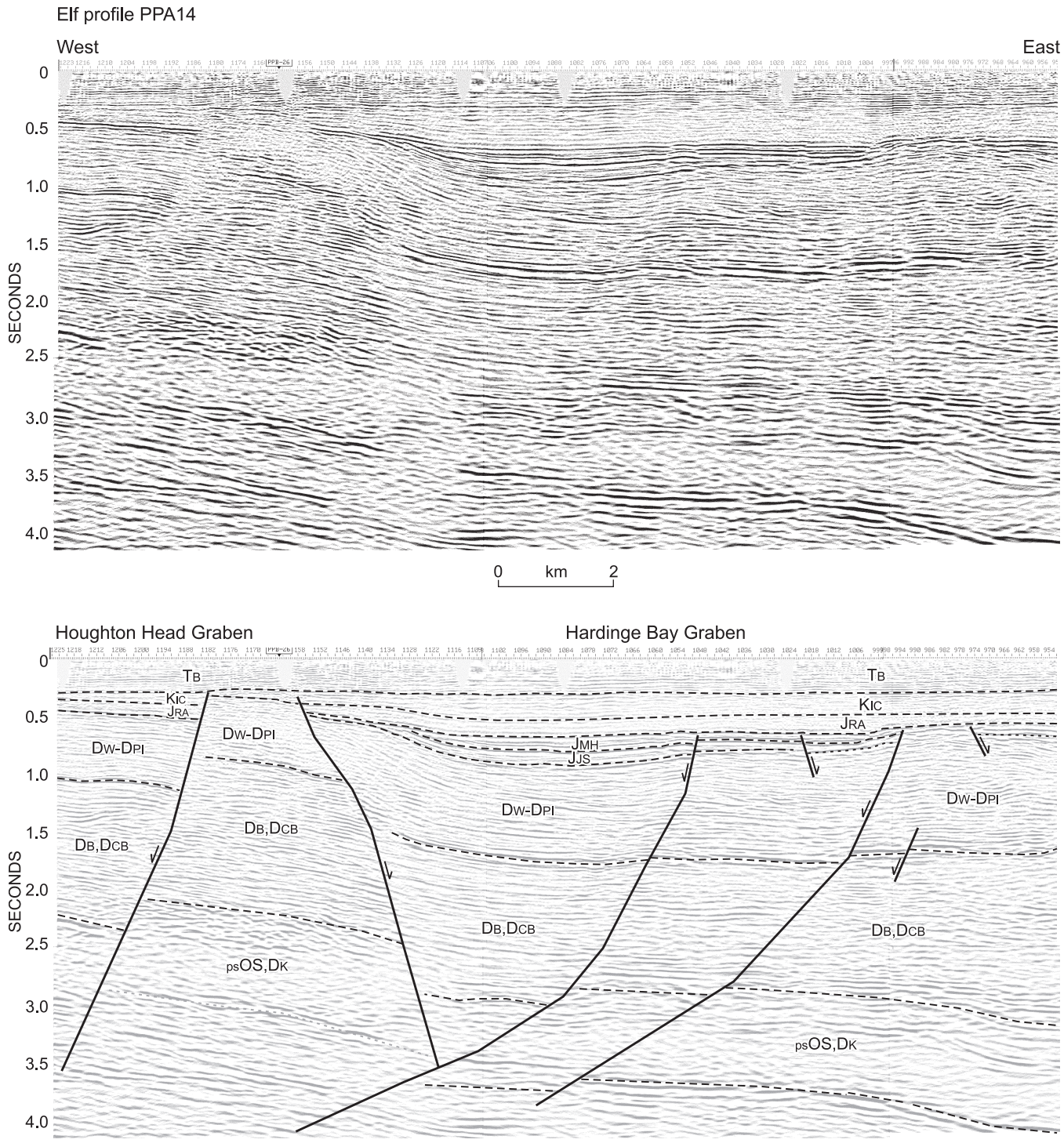

Figure 74. *Seismic expression of Hardinge Bay Graben and Houghton Head Graben on a portion of Elf seismic profile PPA14.* psOS: *Ordovician and Silurian shelf units;* DK: *Kitson Formation;* DB: *Blackley Formation;* DCB: *Cape de Bray Formation;* DW-DPI: *Weatherall, Beverley Inlet and Parry Islands formations;* JJS: *Jameson Bay and Sandy Point formations;* JMH: *McConnell Island and Hiccles Cove formations;* JRA: *Ringnes and Awingak formations;* KIC: *Isachsen and Christopher formations;* TB: *Beaufort Formation and related strata of the Arctic Continental Terrace Wedge. Profile is located on Figure 53.*

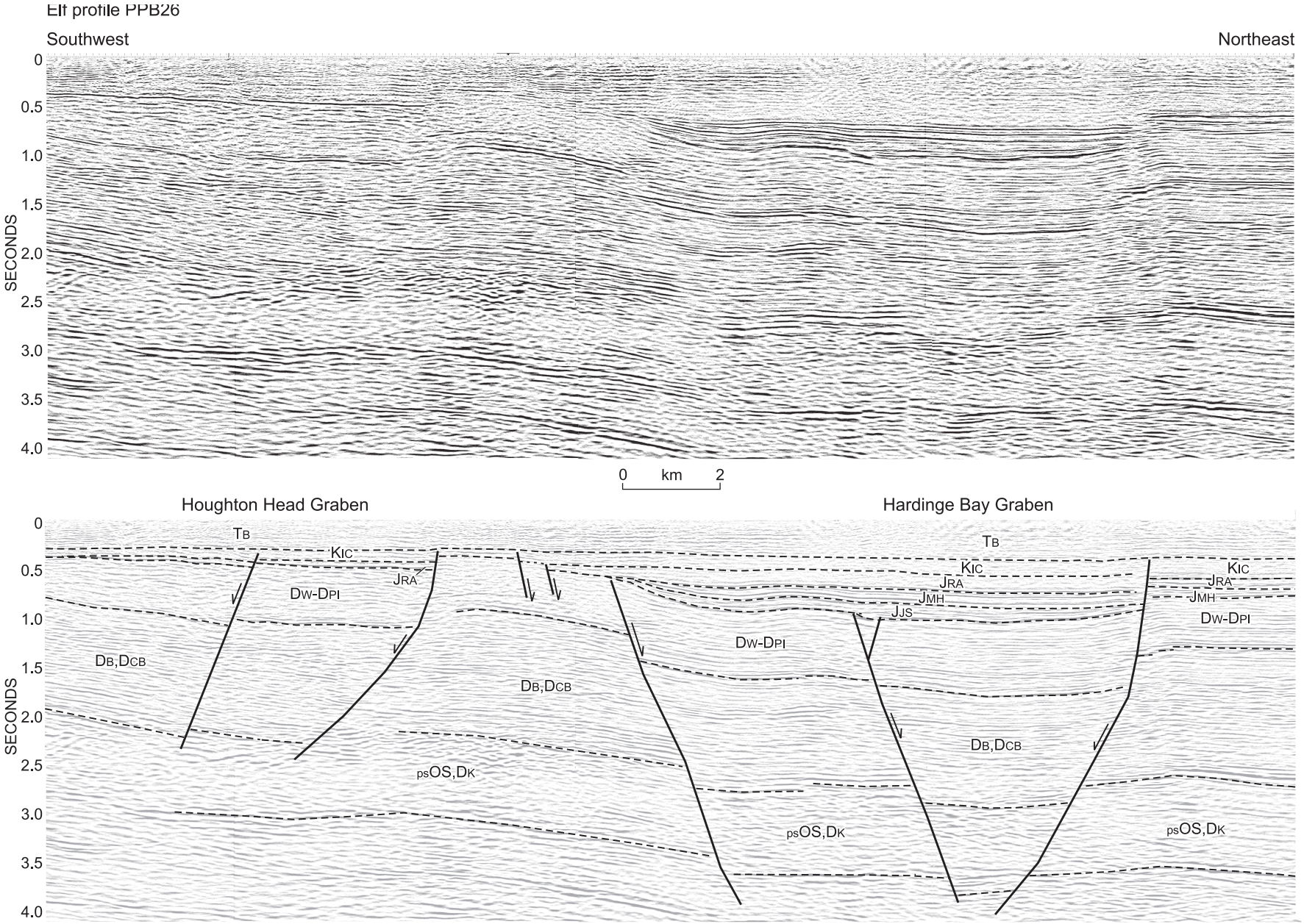

Figure 75. *Seismic expression of Hardinge Bay Graben and Houghton Head Graben on a portion of Elf seismic profile PPB26. Seismic units are the same as those identified in the caption of Figure 74. Profile is located on Figures 50 and 53.*

This block continued to remain high until after the Jurassic because the Isachsen Formation has overstepped the Ringnes-Awingak sequence and lies directly on the Devonian on the west side of the uplift in the immediate footwall of the eastern boundary fault of Houghton Head Graben. Late stages of slip affecting the Isachsen-Christopher sequence but not the Beaufort Formation and related cover are indicated for the two west-side-down faults marking the eastern boundary of both grabens. These examples occur at SP 1180, PPA14 and SP630, PPB26 for the Houghton Head Graben and at SP410 for Hardinge Bay Graben.

Prince Patrick Uplift

Introduction

The previous description of Tullett Basin has provided compelling evidence for multiple phases of extension faulting during basin development. The temporal correlation of these events is supported to a limited extent by measured stratigraphic sections in the southern Green Bay Graben and Green Bay Uplift to the east. Seven other graben structures lie almost entirely in the outcrop belt of the Prince Patrick Uplift (Fig. 64). Evidence for faulting during the Middle Jurassic to Lower Cretaceous interval of sediment accumulation in these outcrop belt grabens is, however, relatively circumstantial. The following descriptions for individual grabens provide the lines of evidence for extensional tectonics and various rifting phases within the Prince Patrick Uplift, bearing in mind the previous observations and conclusions drawn from the seismic profiles of Tullett Basin.

Manson Point Graben

Manson Point Graben, actually more appropriately described as a half-graben, lies on the peninsula west of Intrepid Inlet and extends 26 km northward from the east side of Manson Point. Graben fill includes strata of the Jameson Bay, Sandy Point, McConnell Island, Hiccles Cove, and Ringnes formations and the lower part of the Awingak Formation (Fig. 64; column 11 on Fig. 54). The uplifted west side of the half-graben includes Devonian basement strata lying in the footwall of the adjacent Station Creek Fault. The axial trend of the graben is aligned with that of Green Bay Graben, to the north, but is separated from it by a fault-bound high block of Devonian stata. The two high block boundary faults to north and south, respectively trend N77°W and N86°W, and are essentially perpendicular to Green Bay (N21°E) and Manson Point (N01°W) faults on the east side of the two aligned grabens. Strata in Manson Point Graben possess a regional eastward dip of 2.5 to 3.5° based on a minimum thickness of graben fill and width of the outcrop belt. This dip is consistent with a listric down-to-the-west profile for Manson Point Fault (as for Green Bay Fault) and a block-rotation origin for hanging wall structure during extensional slip on the same fault. Eastward-shallowing of dip also occurs within graben fill into a hanging wall syncline with a sinuous axial line about one kilometre west of Manson Point Fault. An origin for the syncline by west-directed horizontal compression is possible. However, limb dips are less than 5°. An alternative interpretation is that graben-fill units have a divergent and eastward-thickening profile as a consequence of syndepositional slip on Manson Point Fault. The east limb of the syncline has then been modified by normal drag during block rotation and/or by partial compressive inversion of the graben during a subsequent phase of reverse slip on the boundary fault.

Station Creek Graben

Station Creek Graben, situated east of Mould Bay, is parallel to and lies immediately to the west of Manson Point Graben (Fig. 53, 64). Station Creek Graben has a northward-trending axial line, a length of 37 km and a width of up to 9 km. Graben fill units are the same as in Manson Point Graben but also include a significant erosional remnant of the Isachsen Formation. Measured dips range from 6 to 11°. However, regional dip of graben fill is to the east at 3.1 to 4.2° based on outcrop width and a 230 m thickness for Jurassic strata below the Isachsen. Thinning of section to the south and to the west is apparent at three stratigraphic levels within the graben. The Jameson Bay Formation thins from 42 m over the high east of Station Creek Fault to as little as 3 to 5 m in the vicinity of Mould Bay weather station. Westward thinning of the preserved Toarcian, accompanied by an increase in the occurrence of proximal marine (foreshore) conglomerate, is attributed to regional subsidence patterns of the Sverdrup Basin prior to rifting.

Southward and westward thinning of the Hiccles Cove Formation is also evident within the graben from at least 50 m in the section 4 km north of the weather station, to a minimum of about 25 m at 1.7 km south of the station. Thinning is attributed to overstep and erosional truncation of the Callovian upper sandstone member of the Hiccles Cove Formation by the Ringnes Formation, an observation consistent with the widespread evidence for a major unconformity at the base of the Ringnes Formation on seismic profiles of Tullett Basin (Fig. 74, 75). The rapid local thinning of the Hiccles Cove Formation is also consistent with a coeval phase of pre-Oxfordian late Middle Jurassic (late Callovian?) slip on Mould Bay Fault (Fig. 62) and hanging wall block rotation, although there is no evidence that this faulting was coincident with deposition of any of the preserved Middle Jurassic strata. In the same

area, the Ringnes Formation thins from 15 m east of the station to only 30 cm in the section located 1.7 km south of the station. A thicker Ringnes Formation appears again in other grabens to the west. Therefore, the local thinning pattern can be safely attributed to marine onlap in the Oxfordian of the differentially uplifted west side of the half-graben subsequent to the Callovian(?) phase of rifting.

Fault movements in the Lower Cretaceous are also inferred from local thickness variation in the Isachsen Formation (Fig. 76). Reliable estimation of the thickness of Isachsen Formation in Station Creek Graben is hampered by structural complication and inadequate exposure. Complexities include intraformational faults, locally steeper bedding attitudes (to 11°) and regional eastward-striking bedding in the northern part of the graben. Although the top is not seen below the Beaufort Formation, reasonable estimates of preserved section range from 205 m to more than 430 m. In contrast, the near flat-lying Isachsen Formation at the head of Mould Bay (columns 8 and 9, Fig. 54) is only 65 m thick below the Christopher Formation. This dramatic local thinning is attributed to extensional block rotation on Mould Bay Fault and differential erosional truncation on an unconformity below the Christopher Formation. Timing of deformation and erosion is provided by local biostratigraphic constraints. Shale partings collected from pebble conglomerate in the highest preserved beds of the Isachsen Formation in Station Creek Graben (column 10, Fig. 54) yield a Barremian to Aptian palynomorph assemblage (C-198964, in appendix). In contrast, the Christopher Formation, at about 20 m above the Isachsen Formation at the head of Mould Bay (column 9, Fig. 54), contains foraminifera and palynomorphs of Early to Middle Albian age (C-198997, in appendix). These data imply a probable phase of deformation in the Aptian. Supporting this conclusion is the seismic evidence for a potential upper Isachsen or lower Christopher phase of faulting suggested for Tullett Central Graben (Fig. 70).

A final faulting phase of probable extensional character has displaced the Isachsen and older formations in the graben. Outliers of the Beaufort Formation blanket, without offset, the surface trace of Mould Bay Fault and others in the same area at 2.5 to 8.5 km east of the head of Mould Bay. These relationships provide an Aptian to pre-Pliocene window for the time of last fault displacement.

Carter Bay Graben

Carter Bay Graben is a narrow erosional remanent of Middle and Upper Jurassic strata lying along the west side of Mould Bay and extending 27.5 km southward to Carter Bay. The graben is fault-bounded on both sides and is also bisected in the south by a central horst block. The narrower north end of the graben has several N25°E- to N35°E-striking fault segments that connect the longer north–south set. Jurassic strata vary from flat lying to modest dip to the west implying at least some rotation on the down-to-the-east boundary fault lying along the west side of the graben. The axial line of Carter Bay Graben is aligned with the subsurface Mould Bay Graben north of a Devonian high block (the Mould Bay High) situated near and around the head of Mould Bay.

Preserved strata in the graben include Hiccles Cove, Ringnes, and Awingak formations (column 7, Fig. 54). Jameson Bay Formation is overstepped to the east such that the basal beds in Carter Bay Graben contain a late Middle to Late Bathonian shelly macrofaunal assemblage (including ammonites, bivalves and belemnites; C-163558, in appendix) at 4 m above the Devonian. Nevertheless, the Hiccles Cove Formation includes the white, castellate-weathering quartz sandstone member characteristic of the Callovian upper part of the formation. The same member is overstepped to the east in Station Creek Graben. From this it can be concluded that the horst block between the two grabens, mostly covered at present by the waters of Mould Bay, was tectonically elevated in the latest(?) Callovian, and that differential preservation of the Callovian sand in Carter Bay Graben can be accounted for by down-to-the-west extensional slip on the eastern boundary fault prior to overlap by the Ringnes Formation in the Oxfordian (Fig. 76). Likewise the marine shale facies of the Ringnes Formation also accumulated to a greater thickness (of 8 to 10 m) and may have persisted longer in Carter Bay Graben than over the high to the east where it is as little as 30 cm thick in the section 1.7 km south of the weather station.

Landing Lake Graben

Landing Lake Graben, situated on the peninsula west of Mould Bay (Fig. 52; Map 2026A and inset), is up to 4.5 km wide and has a north–south length in outcrop of 32 km. The graben continues into Tullett Basin as far north as seismic profiles PPA14 and PPB25 (for a full length of 38 km) where it projects onto the unnamed high east of Tullett Central Graben.

Landing Lake Graben is faulted, mostly against Devonian, over its full length on the east side (Landing Lake Fault) and is also locally faulted to the west. Post-Devonian strata preserved in the southern exposed part of the graben range from the Ringnes Formation at the base to the Christopher Formation (Fig. 64; column 6, Fig. 54). Regional dip is to the east at about 4.5° in this area and is attributed to down-to-the-west slip and block rotation on Landing Lake Fault.

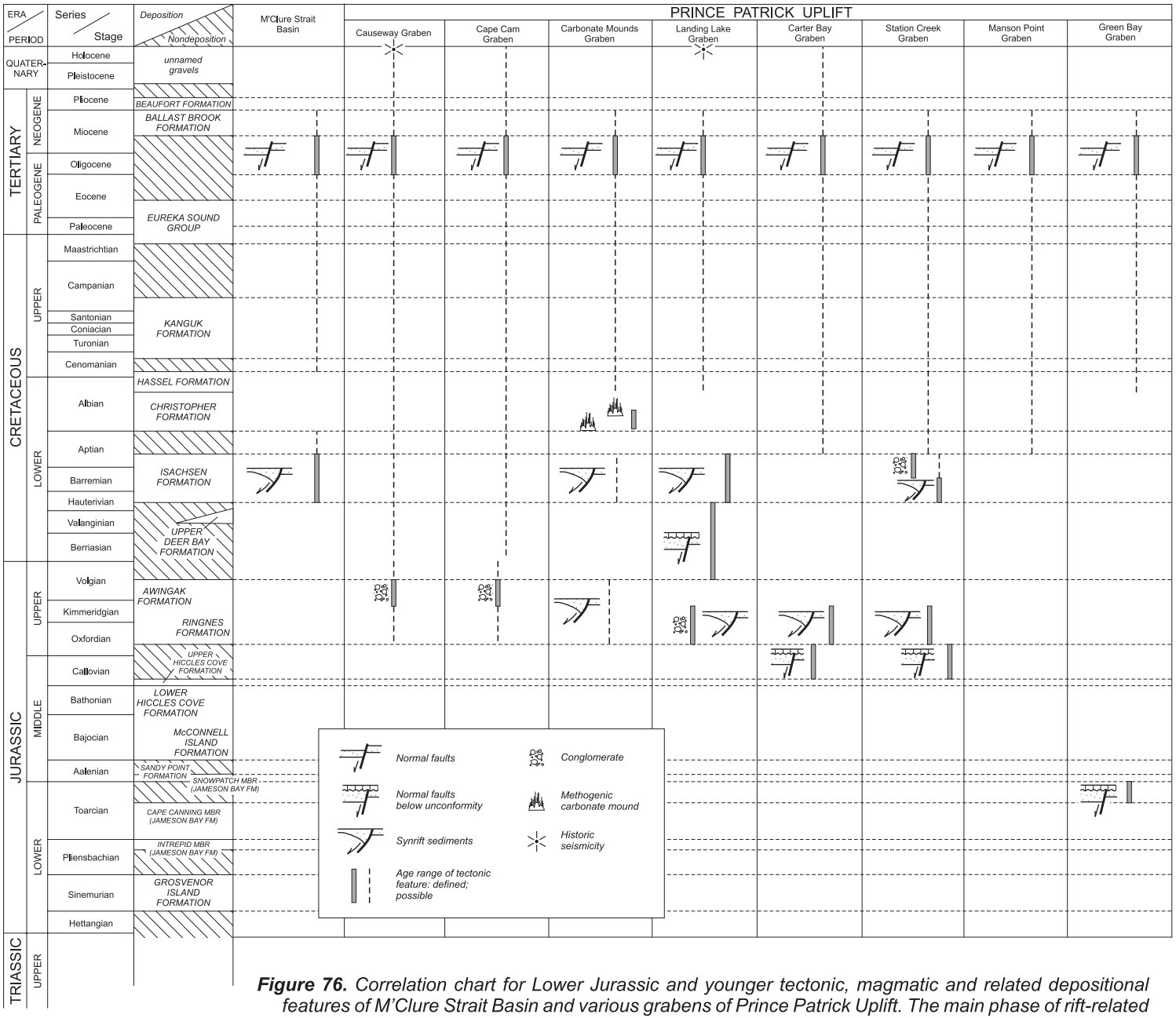

Figure 76. *Correlation chart for Lower Jurassic and younger tectonic, magmatic and related depositional features of M'Clure Strait Basin and various grabens of Prince Patrick Uplift. The main phase of rift-related extension mostly ranges from the Callovian to Aptian for the grabens on the uplift. A Barremian–Aptian phase of extension is indicated for M'Clure Strait Basin, however, little is known about the structure of this region.*

Timing of tectonic activity on this fault, summarized on Figure 76, is provided by map relations and comparison of column 6 in the graben with column 8, which was measured over Mould Bay High to the northeast. Extension faulting does not appear to have influenced the southern graben prior to the Oxfordian. Jameson Bay, McConnell Island and Hiccles Cove formations are all present around the high near Landing Lake and are also thought to lie within the northern part of the graben. However, these units are overstepped southward by the Ringnes Formation. The Ringnes is 5 m thick over the high but ranges up to 22 m near Landing Lake Fault along the axial line of the southern graben. Syndepositional evidence for local faulting is also provided by beds of sandstone (in column 6) that are in part conglomeratic, and interstratified with shale in the graben section of the Ringnes Formation. The conglomeratic sandstone contains rounded clasts of cemented sandstone up to 20 cm in diameter, believed to be derived from local and regional exposures of the Devonian clastic wedge. The shale at zero to 2 m above the base of the Ringnes Formation in column 6 contains early to middle Kimmeridgian dinoflagellates and Oxfordian to Kimmeridgian foraminifera (sample C-133985, in appendix). Sandstone at 5 to 5.8 m above the base of the Ringnes contains latest(?) Volgian bivalves (sample C-133984, in appendix).

Evidence for a second phase of slip on the eastern boundary fault is provided by comparison of preserved Awingak Formation in the southern part of the graben (80 to 100 m near column 6) with that preserved below the Isachsen Formation over the Mould Bay High (about 35 m at column 8). These contrasts are attributed to a phase of slip and differential uplift affecting the upthrown footwall of Landing Lake Fault after deposition of the Awingak (after the Volgian) but prior to overlap by the Isachsen Formation. The upper age limit for this deformation is provided by an assemblage of Barremian to Aptian pollen collected at 22 m above the base of the Isachsen Formation near Landing Lake (sample C-199006, in appendix).

The thickness differential for the Isachsen in the graben (115–150 m) compared with that over the high to the east (65 m) provides the evidence for a third phase of differential uplift and erosion possibly coinciding with an Aptian depositional break preceding overlap by the Christopher Formation.

A fourth and final phase of fault motion has occurred on Landing Lake Fault subsequent to offset of the Christopher Formation but prior to overlap by the Beaufort Formation.

Seismic expression of Landing Lake Graben on portions of PPA14 and PPB25 is provided on Figure 77. The graben is subdivisible into eastern and western portions bound by east-dipping normal faults that extend down into the Devonian clastic wedge. The structure of the graben on the seismic profile differs fundamentally from the outcrop portion in so far as the tilt of graben-fill in the south is to the east as a consequence of rotation on the underlying west-dipping Landing Lake Fault. In contrast, dip direction of strata is to the west on the seismic profiles and is related to down-to-the-east rotation on two different faults on the opposite side of the graben. Seismic units above the Devonian are similar to those in other grabens of central and western Tullett Basin. The undivided Jameson Bay and Sandy Point unit is the oldest sequence interpreted within the graben but has been cut out across the western boundary fault as a consequence of an extensional deformation phase preceding overlap by the McConnell Island-Hiccles Cove sequence. Onlapping reflection patterns at the base of the McConnell Island testify to transgressive encroachment of the McConnell Island shale toward the east. The McConnell Island-Hiccles Cove sequence is characterized by a modestly divergent internal reflection pattern with unit thickening to the west in the graben and thickening west of the footwall high at SP75, PPB25. A subtle thickness maximum of 240 ms for the Hiccles -McConnell Island sequence is observed in the graben hanging wall at SP60 on PPB25. Part of the gradual thinning to the east in the graben and rapid thinning to the west across the adjacent fault is attributed to postdepositional truncation of the upper Hiccles Cove by pre-Ringnes subaerial erosion and channelling as identified at SP100-145, PPB25. The implication of these observations is that slip on the western graben-boundary fault could have occurred both during deposition of the McConnell Island-Hiccles Cove sequence in the Bathonian and Callovian, and also during a period of widespread nondeposition prior to overlap by the Ringnes in the Oxfordian or Kimmeridgian (Fig. 62).

There is no seismic evidence for extension faulting during deposition of the Ringnes-Awingak or Isachsen-Christopher sequences. However, fault-related rotation and peneplaining of graben fill apparently predates a seismically imaged reflection from the base of the continental terrace wedge sequence variously located at 120 to 230 ms from SP520 on PPA14 to SP60 on PPB25 in the seismic example (Fig. 77). The boundary fault at SP70, PPB25, also extends into and displaces the terrace wedge sequence.

Carbonate Mounds Graben

The Carbonate Mounds Graben is situated 2.2 to 3.2 km west of Landing Lake Graben on the opposite side of an intervening horst block of Devonian basement strata. Strata exposed in the graben are illustrated on Figure 64 and in column 5, Figure 54. Measured regional dip is to the east at 10° in the Awingak Formation, decreasing upsection and eastward to 7° in the Isachsen Formation, to 3° in the Christopher Formation. The dip direction implies modest rotation on the eastern graben-boundary fault. The upsection decrease in dip angle could reflect a similar

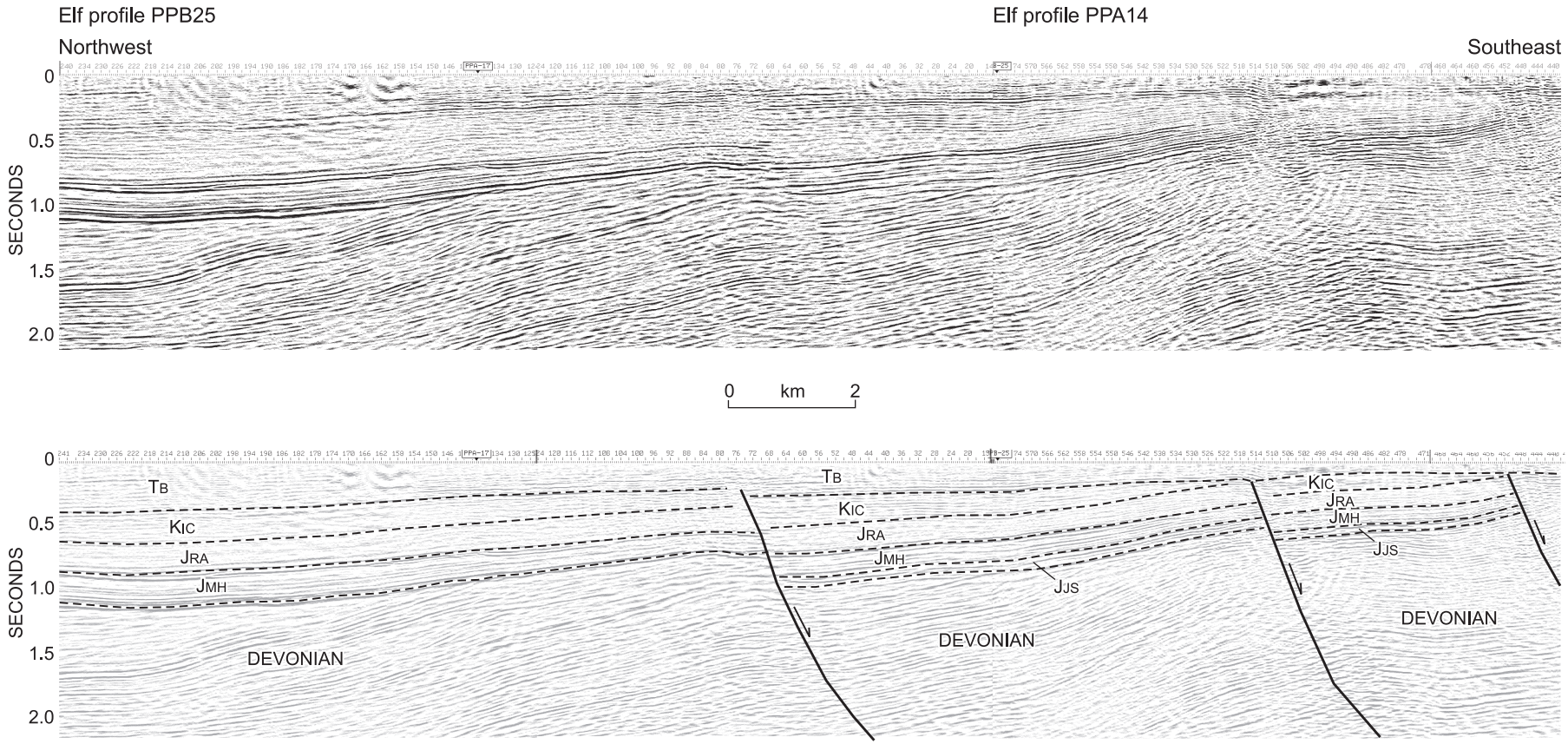

Figure 77. *Seismic expression of Landing Lake Graben on portions of seismic profiles PPA14 and PPB25.* JJS: *Jameson Bay and Sandy Point formations;* JMH: *McConnell Island and Hiccles Cove formations;* JRA: *Ringnes and Awingak formations;* KIC: *Isachsen and Christopher formations;* TB: *Beaufort Formation and related strata of the Arctic Continental Terrace Wedge. Profile is located on Figures 50 and 53.*

structural variation on the base of the Jurassic. A reasonable alternative is that the 10° dip angle for Jurassic strata extends under the Cretaceous and that the upsection decrease in dip angle reflects stratal divergence and eastward thickening of the Ringnes to top-Isachsen interval as a result of syndepositional slip on the eastern boundary fault.

Unrelated evidence for a younger syndepositional phase of fault-related activity is provided by the coincident occurrence of two methogenic carbonate mounds in the Christopher Formation situated directly on the trace of the eastern boundary fault. The geology and significance of these limestone mounds is described by Beauchamp and Savard (1992). From the perspective of regional structure, the localization of these mounds, 8.5 km apart but situated over the same fault trace, is evidence that methane gas, gas hydrates (clathrates) and related basinal fluids have migrated into the fault during accumulation of the Christopher Formation and that the fault, therefore, must have already been in existence prior to this time. Shale, collected at 30 m above the base of the Christopher Formation in the immediate substrate of the stratigraphically lower mound, contains forams of the *Q. albertensis* assemblage (Early Albian; C-133991, in appendix). A second carbonate mound, at 125 m above the Isachsen Formation, contains a long-ranging Early Cretaceous shelly macrofauna (C-133992, in appendix).

Cape Cam and Causeway grabens

Two fault-bound outliers of the Awingak Formation are found near Cape Cam east of Walker Inlet and on the south end of the Giants Causeway island. Stratigraphy of the outliers is provided in columns 1 and 2 of Figure 54. Awingak Formation is the only post-Devonian unit recognized at the surface in these outliers although a covered interval at the base may include several metres of Ringnes Formation shale. The Awingak Formation dips to the east in Causeway Graben and is offset by a probable down-to-the-west normal fault on the east side. Marine seismic profiles indicate continuity with an erosional remnant of the graben in the offshore to the south. The faults in Cape Cam Graben lie both to the east and west. However graben fill dips to the south and the relative importance of the two boundary faults is ambiguous.

As well as the typical, shallow-marine sandstone of the Awingak Formation, there are also intervals of conglomerate situated at about 100 m above the Devonian in Cape Cam Graben (Fig. 78) and at 6 m above the Devonian on Giants Causeway. The proximal character of these coarse clastic deposits is considered indirect evidence for syndepositional uplift and possible extensional slip on adjacent graben boundary faults. The coarse facies deposit at Cape Cam is a clast-supported polymictic conglomerate

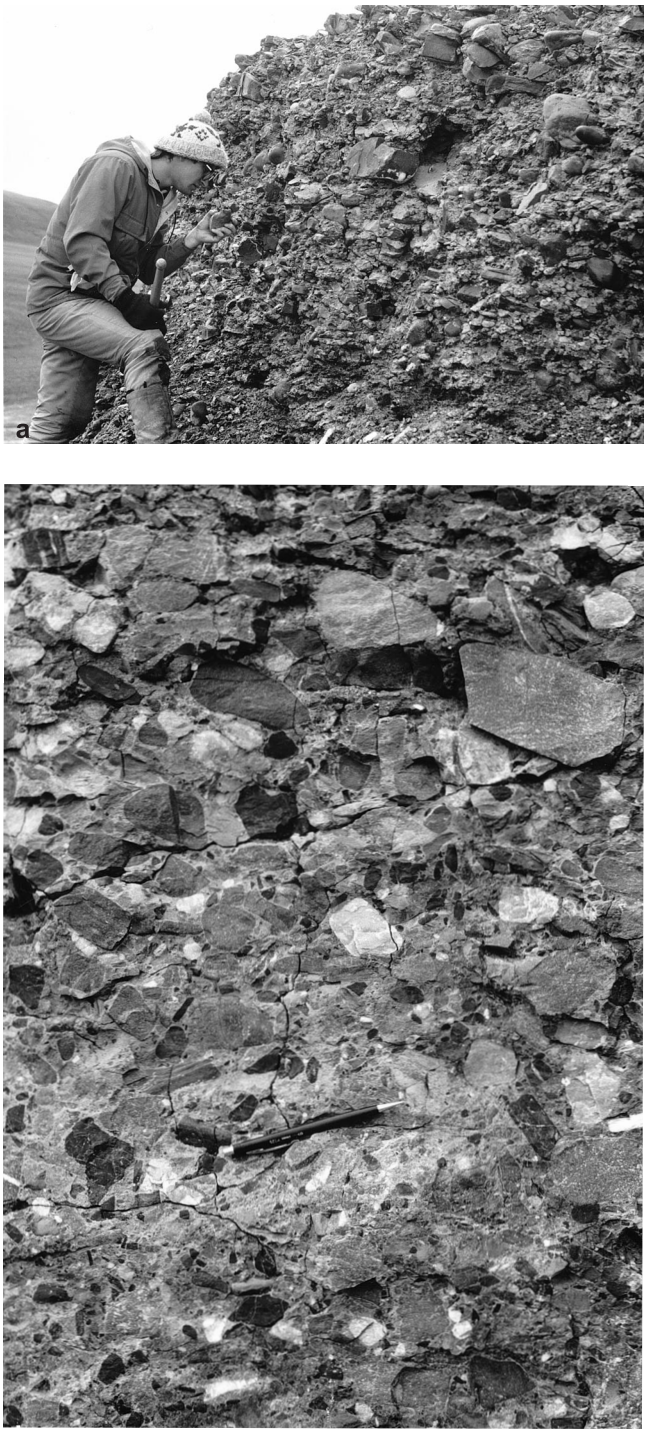

Figure 78. *Clast-supported, syntectonic conglomerate in the Awingak Formation of Cape Cam Graben (see Fig. 53 for location). Clasts, ranging from moderately rounded to highly angular, are compositionally similar to sandstones found in nearby outcrops of the Devonian Weatherall and Parry Islands formations [GSCC photos 3820-10 (a), 3820-13 (b)].*

containing a variety of green, grey, black and white, variably flat-laminated, micaceous and quartz-rich sandstone clasts up to 30 cm (Fig. 78). There are also clasts of orthoquartzite, fissile shale, and siltstone. All these lithologies are typical of those found in the Devonian clastic wedge. Clasts of well-rounded chert are considered to be reworked from Frasnian-age pebbly sandstone of the Beverley Inlet Formation. Clasts, in general, vary from well rounded to highly angular (Fig. 78) and testify to a local, tectonically active source area. Shelly macrofauna collected at about 10 m above the base of the Awingak Formation in the Cape Cam section are considered to be of probable Volgian age (C-163555, in appendix).

The Giants Causeway section includes clast-supported boulder conglomerate (clasts to 50 cm) in the lower part, grading upward into matrix-supported conglomerate featuring pebbles and small cobbles in a greenish grey silt matrix. The highest beds are dominated by silt with scattered angular pebbles. Clast compositions are similar to those encountered in the nearby exposures of the Devonian clastic wedge. The shale above the conglomerate beds at Giants Causeway contains early to middle Kimmeridgian dinoflagellates (C-163556, in appendix).

M'Clure Strait Basin

The west side of Eglinton Basin is defined on seismic profiles by the Cape Mecham High (Fig. 18, 52, 53), a raised block of Devonian and older basement rocks that extends southward from Cape Mecham over a distance of at least 50 km into northern M'Clure Strait. The width of the high ranges from 12 km at 75°30'N to 23.5 km at 75°15'N and is in part defined by a relative Bouguer gravity high (actually a wide, low-amplitude negative anomaly) that covers southern Prince Patrick Island including Cape Mecham, part of M'Clure Strait and part of coastal northernmost Banks Island (Fig. 22). These relationships also indicate probable continuity of the Mecham High with Devonian inliers at Cape Crozier on Banks Island (Fig. 18; Miall, 1979).

The west side of Mecham High is defined by the unconformity mapped on the seafloor between the Devonian and the Cretaceous cover of M'Clure Strait Basin, which lies entirely in M'Clure Strait west of longitude 121°30W. The basin is imaged on five marine seismic profiles. The northern end of the basin bifurcates around a local, southerly plunging, high block of Devonian basement strata that subcrops on the seafloor south of Cape Manning. The various merged components of the basin widen to at least 50 km at about 75°25'N. The centre of the basin, however, is believed to coincide with a -25 mgal Bouguer gravity anomaly in central M'Clure Strait (Fig. 22). Thickness of Mesozoic cover in the imaged northern part of the basin is mostly less than 360 ms (470 m at 2.6 km s^{-1}) but ranges up to 450 ms (590 m) in several small half grabens, and up to 525 ms (680 m at 2.6 km s^{-1}) in the westernmost arm of the basin. Thickness of strata in the basin centre may be comparable to that under southern Eglinton Island judging by the similarity in scale of the associated gravity lows. Faults associated with graben development in M'Clure Strait Basin are observed only on two, widely separated seismic profiles. Therefore, northerly strike directions (indicated for these structures on map 2026A and on Fig. 52, 53), which parallel the trend of the basin margin and of sediment thickness isochrons, are highly interpretive.

Seismic stratigraphy of M'Clure Strait Basin remains unknown. The preferred interpretation is that Isachsen Formation overlies the Devonian and that the uppermost strata could include Christopher Formation. This interpretation follows from that of onland seismic data in Tullett Basin where Isachsen Formation is believed to overstep the Awingak Formation in the subsurface northwest of Walker Inlet. An alternative is that Christopher Formation lies on the Devonian as is the case throughout subsurface western Banks Island (Miall, 1979). Bedding is flat lying or very gently inclined toward the east or west from the basin margins (Fig. 79, 80). Variation of bedding attitude is more pronounced in areas of faulting. One early phase of faulting in M'Clure Stait basin is believed to coincide with deposition of the oldest graben fill (Isachsen Formation?) which, in at least two places, displays divergent bounding reflections between local boundary faults (Fig. 76; SP 362, 385, Fig. 79). Mapped faults also extend to the seafloor as a consequence of later extensional slip on the same slip planes. The last phase of fault-related inclination of graben fill strata predates Quaternary cover and the peneplaining event associated with the development of the seafloor surface.

Sverdrup Basin

The fault system associated with the development of Eglinton, Tullett, and M'Clure Strait basins is also known in various parts of Sverdrup Basin on northeastern Prince Patrick Island (2026A; Fig. 52, 53). Four faults of extensional origin are mapped at the surface on the peninsula north of Wilkie Point. Strike directions are similar to others mapped in offshore Eglinton Basin and in the Green Bay area to the west. Maximum stratigraphic throw is about 140 m and occurs where medial Jameson Bay Formation is in tectonic contact with upper Hiccles Cove Formation.

Other northerly striking normal faults are mapped displacing strata as high as the Christopher Formation east of the Jameson Bay C-31 well. These faults have a modest to obvious arcuate shape in map view that, in one case, has produced block rotation and parasitic faulting in

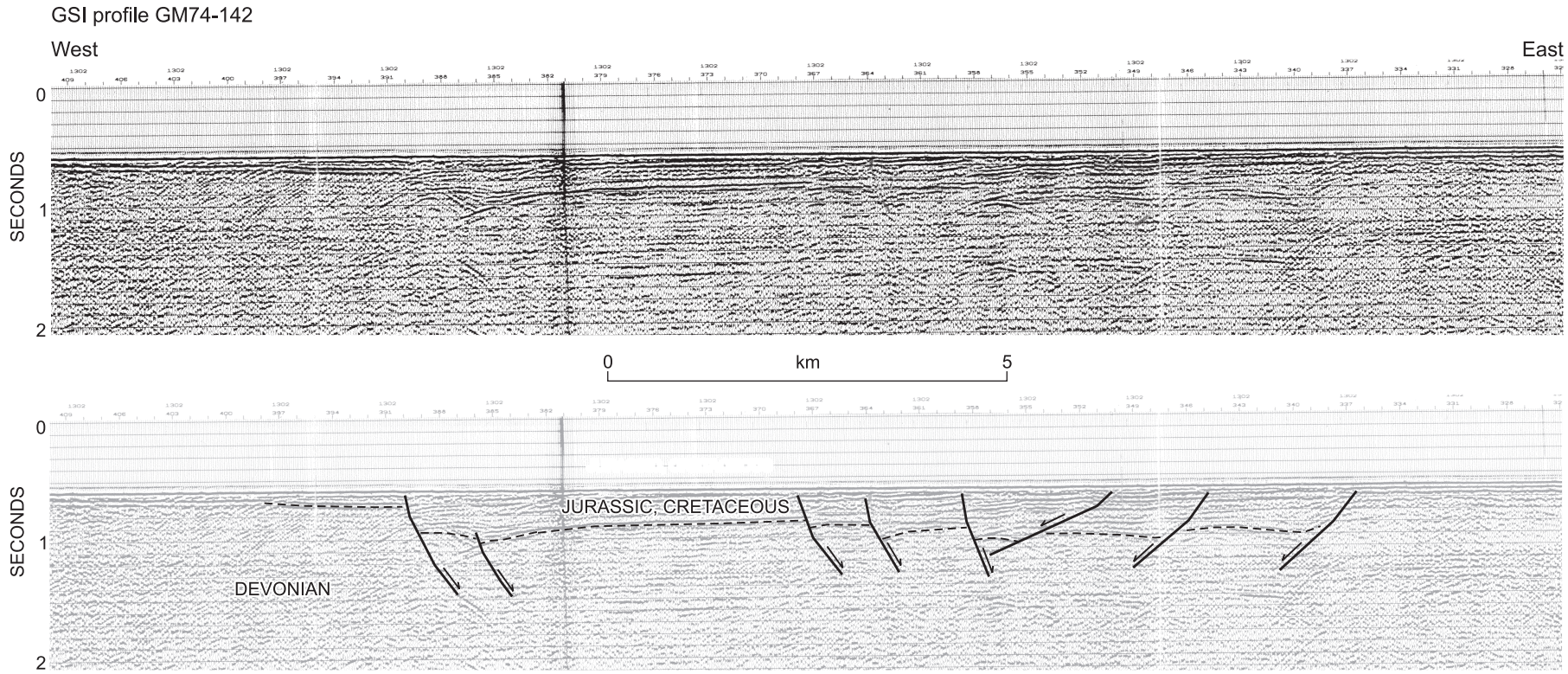

Figure 79. *Seismic expression of graben structures and related normal faults in the northern part of M'Clure Strait Basin on a portion of GSI profile GM74-142. Existence of Jurassic strata in these grabens is doubtful. Cretaceous strata may only include Isachsen and Christopher formations. Profile is located on Figure 53.*

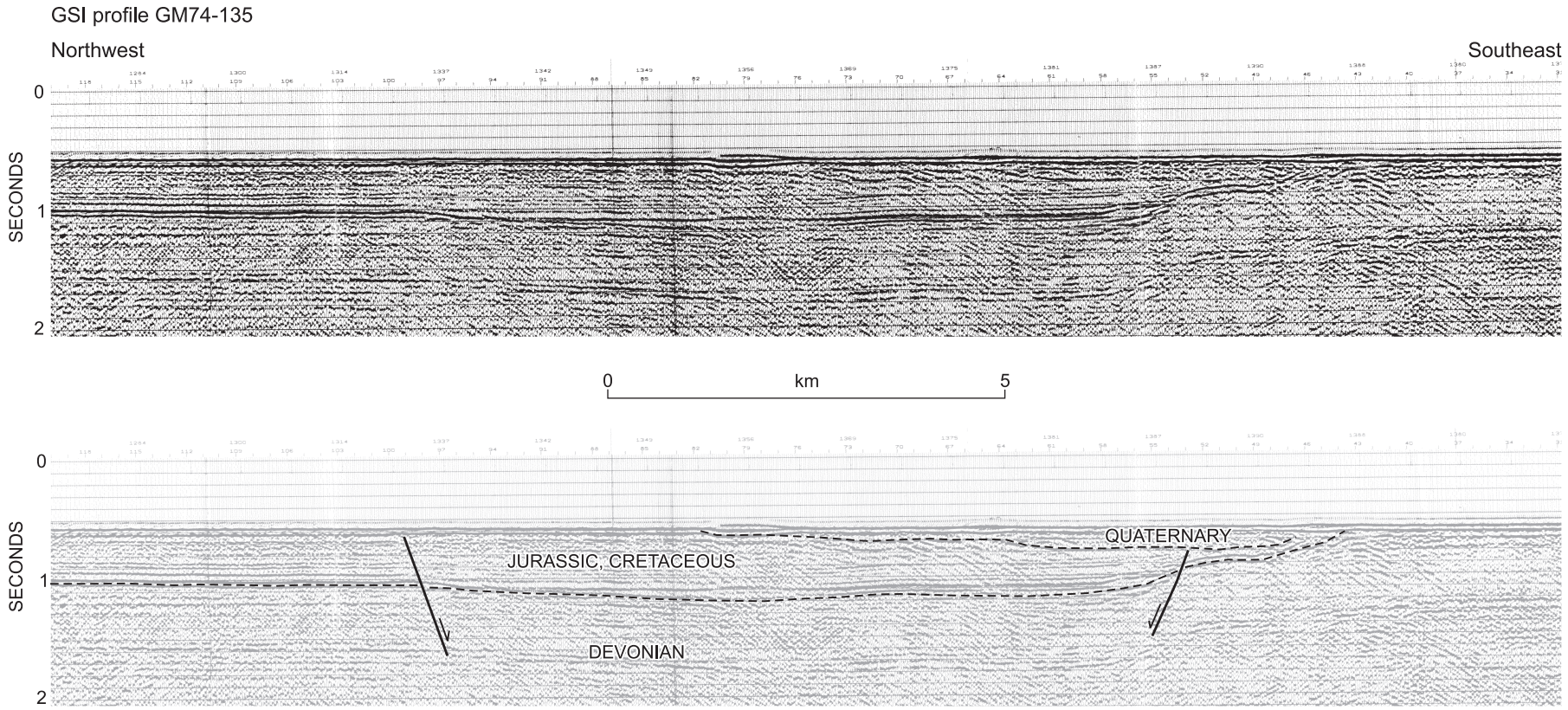

Figure 80. *Seismic expression of rift-related normal faults in the northern part of M'Clure Strait Basin on a portion of GSI profile GM74-135. Existence of Jurassic strata in this basin is doubtful. Cretaceous strata may only include Isachsen and Christopher formations. Profile is located on Figure 53.*

downthrown Isachsen Formation. Actual strike directions for these faults range from N20°W to N27°E. The more northeasterly striking faults are matched in orientation by two other planar normal faults in this part of the Sverdrup Basin. One is mapped onland near Cape Krabbé where Isachsen Formation is downfaulted against Deer Bay Formation along a fault that strikes N43°E. Although this fault has limited displacement, it has also been mapped offshore in Ballanytne Strait and has a minimum strike length of 35 km. A second planar fault, striking N32-40°E, lies in Fitzwilliam Strait just offshore Sproule Peninsula northwest of Melville Island. This structure is identified seismically in the lower Paleozoic but probably offsets strata as high as the Deer Bay or Isachsen Formation. Faults of this same orientation have been mapped onshore on Sproule Peninsula.

Linear, northeasterly striking, in part northerly striking, faults are the dominant fault type in the Cretaceous and older strata beneath the Beaufort Formation throughout northern Prince Patrick Island. In each case, stratigraphic throw is less than less than 150 m and strike length does not exceed 15 km. Kinematics of faulting remain uncertain. The faults are steeply inclined, with dip directions consistent with either orthogonal or oblique extension. In some cases, individual fault strands appear to be rooted downsection on pre-existing upper Paleozoic graben boundary normal faults, as in the case of Hemphill Fault-B (Fig. 45). Comparison of Figures 52 and 37 reveals, however, that the two fault systems are highly oblique to each other.

Summary of Mesozoic rifting events

Evidence for deformation since the Triassic in the Prince Patrick and Eglinton islands region, and adjacent portions of the Canadian Arctic and Greenland, is summarized on Figure 81. Plate tectonic activity associated with this time interval includes the rifting and spreading history of Canada Basin, extension in Baffin Bay and Labrador Sea and compressive deformation in the ancestral Brooks Range. The principal observations to be drawn from the account to this point are 1) the structural and depositional history from the mid-Permian to the mid-Jurassic is associated with an enduring subsidence phase for the Sverdrup Basin; 2) small, elliptical basins and associated northeast-striking normal faults documented within the report area are part of a major rift zone that can be traced from the northern Yukon through Banks Island to northern Prince Patrick Island; and 3) this rift zone preserves a protracted extensional history, knowledge of which places useful constraints on tectonic models for the age and origin of Canada Basin. There are three phases of tectonism (Table 2): a pre-rift phase (Early Triassic to end Early Jurassic); a rifting phase (Middle Jurassic to Early Cretaceous) and a post-rift subsidence phase (Early Cretaceous through Late Cretaceous).

Pre-rift Phase

The pre-rift phase within the report area includes sediment accumulation associated with the subsurface Bjorne and Blind Fiord formations (Lower Triassic); the mostly subsurface Middle and Upper Triassic Schei Point Group, which includes exposures of the Pat Bay Formation (Carnian) east and west of Intrepid Inlet; the mostly subsurface Heiberg Group; and the Lower Jurassic Jameson Bay Formation, which is widespread on southern Prince Patrick Island. Association of these strata with the subsidence phase of the Sverdrup Basin is indicated by the uniform northwesterly trend of thickness isochrons (Fig. 50) and unit preservational limits (Fig. 51), all of which mimic thickness isochrons in the Permian (Fig. 49) and graben-boundary normal faults in the Carboniferous (Fig. 37, 38). The younger units of the pre-rift succession are featured in northwesterly striking exposures of the Grosvenor Island Formation east of Intrepid Inlet. Characteristic greenish grey shale contains a late Sinemurian ammonite assemblage that includes *Echioceras arcticum* Frebold, *Echioceras* sp., *Cenoceras* sp., and *Gleviceras*(?) sp. (C-163533, C-163556, in appendix). Northwestly striking beds are also characteristic of glauconitic sandstone and phosphatic shale in the Intrepid Inlet Member of the Jameson Bay Formation, which contains a Pliensbachian macrofauna including *Amaltheus* sp. and an indeterminate species resembling *A. stokesi* (C-133908, C-163544, in appendix). The highest beds of the pre-rift succession are shale, with minor cemented sandstone and pebble conglomerate of the Cape Canning Member of the Jameson Bay Formation. The southeastern preservational limit passes just south of the Eglinton P-24 well on central Eglinton Island and is defined in outcrop along the east side of Mould Bay, where early Toarcian ammonites are common, including *Pseudolioceras* sp. aff. *compactile* (Simpson) and *Dactylioceras* sp. aff. *commune* (Simpson) (samples 24641,2, C-163560, C-134000, in appendix).

Figure 81. *Correlation chart for Lower Jurassic and younger tectonic, magmatic and related depositional features of the report area and adjacent areas of polar North America and Greenland. The late Toarcian/Aalenian through early Aptian phase of extension indicated by data provided in this report for the western Arctic Islands provides constraints on the timing of similar rift-related structures of the Beaufort Basin, Blow Trough in northern Yukon, and Dinkum Graben on the Alaska North Slope. Extension in the Labrador Sea, Baffin Bay and on south-central Ellesmere is later (late Aptian to early Paleocene). Late-stage folds in the Prince Patrick Island area are believed to be the same age as late Paleocene to late Eocene compressive structures documented in the western Beaufort Basin and on Ellesmere Island. Late-stage normal faults may be coeval with Oligocene to early Miocene extension in the eastern Beaufort Basin.*

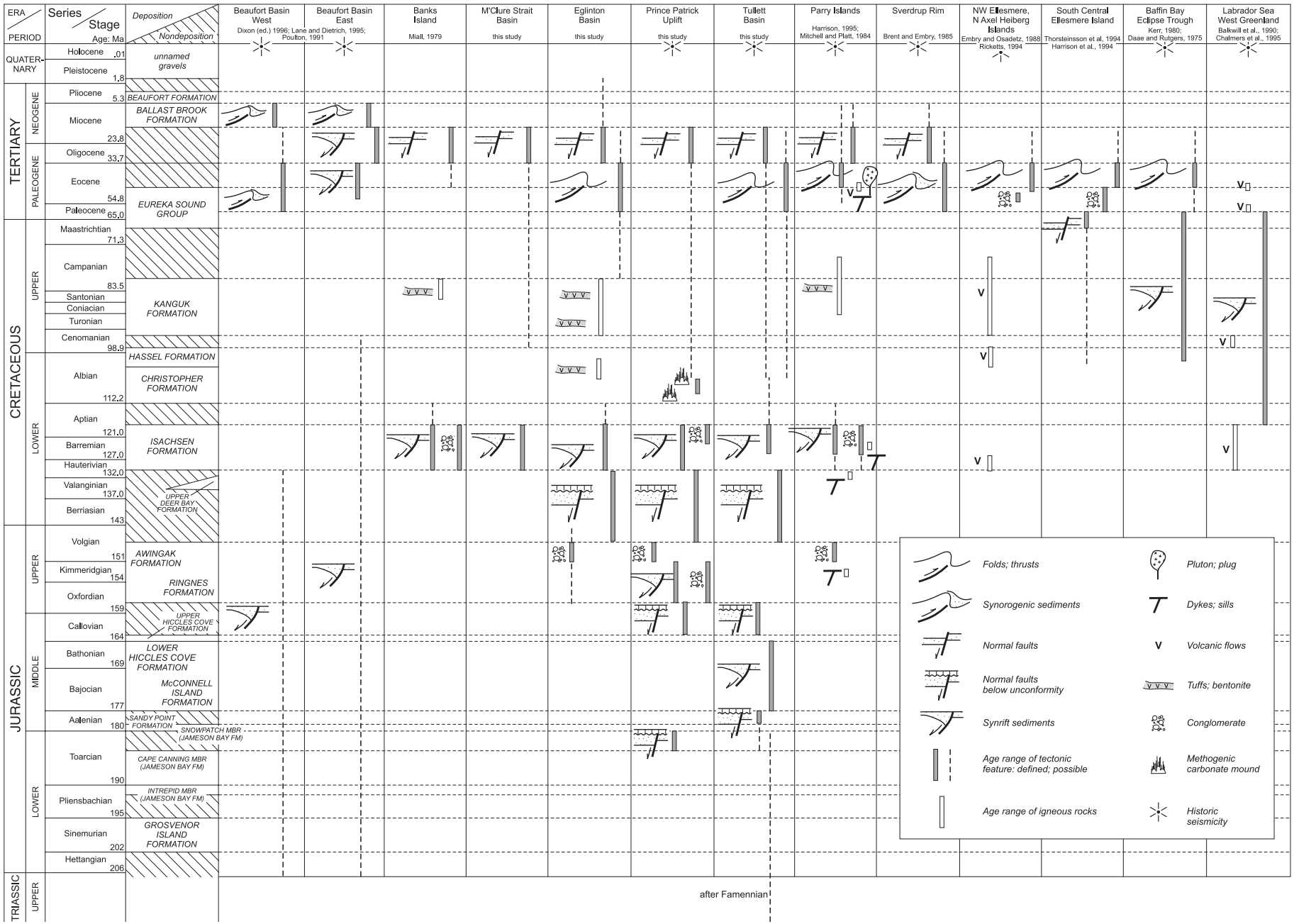
ERA
PERIOD
Series
Stage
Age: Ma
Deposition
Nondeposition
Beaufort Basin West
Dixon (ed.) 1996; Lane and Dietrich, 1995; Poulton, 1991
Beaufort Basin East
Banks Island
Miall, 1979
M'Clure Strait Basin
this study
Eglinton Basin
this study
Prince Patrick Uplift
this study
Tullett Basin
this study
Parry Islands
Harrison, 1995; Mitchell and Platt, 1984
Sverdrup Rim
Brent and Embry, 1985
NW Ellesmere, N Axel Heiberg Islands
Embry and Osadetz, 1988; Ricketts, 1994
South Central Ellesmere Island
Thorsteinsson et al, 1994 Harrison et al., 1994
Baffin Bay Eclipse Trough
Kerr, 1980; Daae and Rutgers, 1975
Labrador Sea West Greenland
Balkwill et al., 1990; Chalmers et al., 1995
QUATERNARY
Holocene .01
Pleistocene 1.8
unnamed gravels
TERTIARY
NEOGENE
Pliocene 5.3
BEAUFORT FORMATION
Miocene 23.8
BALLAST BROOK FORMATION
PALEOGENE
Oligocene 33.7
Eocene 54.8
Paleocene 65.0
EUREKA SOUND GROUP
CRETACEOUS
UPPER
Maastrichtian 71.3
Campanian 83.5
Santonian
Coniacian
Turonian
Cenomanian 98.9
KANGUK FORMATION
LOWER
HASSEL FORMATION
Albian 112.2
CHRISTOPHER FORMATION
Aptian 121.0
Barremian 127.0
Hauterivian 132.0
ISACHSEN FORMATION
Valanginian 137.0
Berriasian 143
UPPER DEER BAY FORMATION
JURASSIC
UPPER
Volgian 151
Kimmeridgian 154
Oxfordian 159
AWINGAK FORMATION
RINGNES FORMATION
MIDDLE
Callovian 164
UPPER HICCLES COVE FORMATION
Bathonian 169
Bajocian 177
Aalenian 180
LOWER HICCLES COVE FORMATION
McCONNELL ISLAND FORMATION
SANDY POINT FORMATION
SNOWPATCH MBR (JAMESON BAY FM)
LOWER
Toarcian 190
CAPE CANNING MBR (JAMESON BAY FM)
Pliensbachian 195
INTREPID MBR (JAMESON BAY FM)
Sinemurian 202
GROSVENOR ISLAND FORMATION
Hettangian 206
TRIASSIC
UPPER
after Famennian
Folds; thrusts
Synorogenic sediments
Normal faults
Normal faults below unconformity
Synrift sediments
Age range of tectonic feature: defined; possible
Age range of igneous rocks
Pluton; plug
Dykes; sills
Volcanic flows
Tuffs; bentonite
Conglomerate
Methogenic carbonate mound
Historic seismicity

Rift phase

The oldest structural disturbance potentially associated with the onset of the Jurassic rift phase along the Canadian Arctic continental margin is manifested by uplift of the Jameson Bay Formation beneath overlapping Sandy Point Formation on Green Bay High (Fig. 51, 54, 62). The termination of local uplift is provided by Aalenian macrofauna in the overlap sequence. Diagnostic fauna in the Sandy Point Formation on southern Prince Patrick Island include *Leioceras opalinum* (Reinecke) of early Aalenian age (samples 24658, C-163510,1, in appendix). Geophysical evidence for Aalenian or older normal faulting is also provided by seismic profiles of Hardinge Bay Graben in western Tullett Basin (Fig. 75).

Geophysical profiles indicate widespread development of normal faults throughout Tullett Basin in the early Middle Jurassic (mid- to late Aalenian). This has resulted in differential preservation of the Sandy Point-Jameson Bay sequence in the downthrown hanging wall of normal faults associated with Tullett Central, Richards Point, Hardinge Bay, and Landing Lake grabens (Fig. 62, 70–77, 81). This faulting appears to predate overlap by the McConnell Island-Hiccles Cove sequence which, on Prince Patrick Uplift, contains an early Bajocian macrofaunal assemblage at the base (columns 13–17 on Fig. 54) including *Arkelloceras tozeri* Frebold, *Arkelloceras* sp., *Retroceramus* sp. and *Camptonectes* sp. (samples 24661, 35324, C-164503, C-164513,4, in appendix). Stratal divergence of the McConnell Island-Hiccles Cove sequence is also featured on seismic profiles across Landing Lake Graben (Fig. 77) implying rift-related faulting during Bajocian to early Callovian sediment accumulation.

Evidence for tectonism prior to overlap by the Ringnes Formation is widespread throughout both Tullett Basin and Prince Patrick Uplift. Related features include erosive overstep of the upper member of the Hiccles Cove in Station Creek Graben, differential preservation of the same beds below Ringnes Formation in Carter Bay Graben (Fig. 64; 2026A), sub-Ringnes channeling, and local angular unconformity above the McConnell Island-Hiccles Cove sequence on seismic profiles of Tullett Central, Richards Point, Hardinge Bay and Landing Lake grabens (Fig. 70–77). Duration of this deformation interval (approximately mid-Callovian to Oxfordian) is constrained by the occurrence of early Callovian *Cadoceras* cf. *C. bodylevski* Frebold and *Cadoceras* sp. in the upper Hiccles Cove Formation near Hiccles Cove (column 17, Fig. 54; samples 70405-8, in appendix) and by Callovian foraminifera (C-198995, C-156037, in appendix), and Callovian dinoflagellates and other microflora of Oppel zones H1 to H2 in the same strata near the head of Mould Bay (column 9, Fig. 54; C-198996, in appendix). Age of the oldest post-tectonic strata is provided by the occurrence of *Ammodiscus thomsi* Chamney and associated foraminifera (Oxfordian–Kimmeridgian) and by Oppel zone H3 dinoflagellates (late Oxfordian) at 5.0 m below the top of the Ringnes Formation at the head of Mould Bay (column 9, Fig. 54; C-199004, in appendix).

There is also widespread evidence for syntectonic sedimentation during accumulation of the Ringnes and Awingak formations in Tullett Basin, on Prince Patrick Uplift, and along the southeastern margin of Eglinton Basin on southwest Melville Island. Evidence includes syntectonic conglomerate in the Ringnes Formation of Landing Lake Graben (column 6, Fig. 54; Oxfordian–Kimmeridgian foraminifera; early to middle Kimmeridgian Oppel Zone I dinoflagellates; C-133985, in appendix), and in the Awingak Formation of Cape Cam Graben (column 2, Fig. 54; Fig. 78; Volgian bivalves, C-163555, in appendix), Causeway Graben (column 1, Fig. 54; early to middle Kimmeridgian microflora, C-163556, in appendix), and in Comfort Cove Graben on southwesternmost Melville Island (which contains a diverse assemblage of macrofauna including Early Volgian bivalves of the *Buchia russiensis* Zone as described by Jeletzky and Poulton, in appendix 4 of Harrison, 1995).

Differential preservation of the Ringnes-Awingak sequence below unconformable cover of Isachsen Formation also provides supportive proof for rift-related fault motion during the late Volgian to approximately mid-Hauterivian depositional hiatus. This evidence has been acquired from seismic profiles of Eglinton Basin (Fig. 58), from surface sections of Landing Lake and Carter Bay grabens on Prince Patrick Uplift (compare columns 6 to 8, Fig. 54), and from profiles of Richards Point, Hardinge Bay, and Houghton Head grabens in Tullett Basin (Fig. 71, 73–75).

The highest widespread occurrence of rift-related faulting and associated depositional features occurs in the Isachsen Formation. Features include differential preservation of Isachsen siliciclastic rocks and equivalent seismic intervals in the hanging wall of normal faults of Eglinton Basin (column 12, Fig. 54), M'Clure Strait Basin (Fig. 79), Station Creek, Landing Lake and Carbonate Mounds grabens on Prince Patrick Uplift (columns 5–10, Fig. 54, and Mould Bay, Tullett Central, Richards Point, Hardinge Bay and Houghton Head grabens in Tullett Basin (Fig. 69–72, 74, 75). Age of these strata is provided by Barremian dinoflagellates and other microflora collected at 25 m and about 300 m above the base of the formation at localities at the head of Mould Bay and in Station Creek graben (columns 9, 10, Fig. 54; C-198967, C-198965, in appendix). Syntectonic gravels also occur in the uppermost preserved part of the Isachsen Formation in Station Creek Graben, where microflora are Barremian to Aptian age (column 10; C-198964, in appendix). Similar syntectonic conglomerate and differentially preserved Isachsen Formation strata have been documented from northern

Banks Basin (Miall, 1979) and on southeastern Melville Island (Goodarzi et al., 1994).

Post-rift phase

The end of the rifting phase within the report area and in the surrounding region is provided by the overstep of the Isachsen Formation by marine shale of the Christopher Formation. This has been documented on northern Banks Island where the Christopher Formation oversteps the Isachsen Formation preserved in Banks Basin and lies directly on Devonian strata of Storkerson Uplift (western Banks Island) and on Proterozoic strata of Cape Lambton Uplift (southern Banks Island). Similar overstep relationships have been documented throughout southeastern Melville Island. Within the report area the base of the Christopher Formation is marked by erosional truncation of the upper Isachsen Formation and a preservational hiatus that includes some or all of the Aptian as constrained by the occurrence of Barremian microflora in the uppermost Isachsen Formation at the head of Mould Bay (column 10, Fig. 54), by the occurrence of *Quadrimorphina albertensis* assemblage foraminifera (early Albian) at 30 m above the base of the Christopher Formation in Carbonate Mounds Graben, and by *Vesperopsis mayii* Zone (early to middle Albian) dinoflagellates in the lower part of the same unit at the head of Mould Bay (columns 5, 9, Fig. 54; C-133991, C-198997, in appendix).

The post-rift phase is associated with widespread deep-water marine conditions as characterized by the shales of the Christopher and Kanguk formations. Two methogenic carbonate mounds, situated astride the trace of Carbonate Mounds Fault in the lower Christopher Formation (column 5, Fig. 54; Fig. 64), provide evidence for diagenesis-related degassing during sediment accumulation. The derivative gases have clearly utilized channelways on or near the pre-existing graben-boundary fault. The fault-controlled location of the mounds, however, neither indicates nor requires synchronous fault motion.

Distant volcanic activity during the post-rift phase is indicated by bentonite beds in the medial to upper Christopher Formation (mid-Albian) and throughout the Kanguk Formation of Eglinton Island (columns 20–22, Fig. 54). Ages of local Kanguk Formation bentonites, provided by microfossil assemblages from intervening shale layers, range from Cenomanian to Turonian (dinoflagellates of the *Isabelidinium magnum* Zone; C-198984, in appendix) at 50 cm above the base to early Campanian at the top based on the occurrence of *Trochammina ribstonensis* of the *Dorothia smokyensis* foraminiferal assemblage (C-156070, in appendix). Bentonites are common throughout the Kanguk Formation of the Sverdrup Basin, where they range into the upper Campanian on Sabine Peninsula of northern Melville Island, and also occur in the Santonian–lower Campanian part of the formation in Banks Basin (Miall, 1979). On northern Ellesmere Island, Embry and Osadetz (1988) have documented tholeiitic basalt flows in the lower Isachsen Formation (Hauterivian), Hassel Formation (Upper Albian) and through most of the Upper Cretaceous.

The favoured plate tectonic setting for the post-rift phase of the report area is one in which rifting has succeeded throughout the adjacent Canada Basin, a process that led to active seafloor spreading. The volcanic flows and bentonites in mid-Albian to upper Campanian post-rift strata provide some of the supportive evidence for the interval of plate spreading. Much discussion exists in the literature as to the timing of onset of the spreading phase in Canada Basin. The mid-Hauterivian is often quoted as a likely time for onset (Embry and Dixon, 1994; Grantz et al., 1994). However, it is clear from the geological record in the western Arctic Islands that high blocks shedding proximal detritus and fault-bounding half-grabens preserving conglomerate and sandstone were still in existence throughout the deposition of the Isachsen Formation (mid-Hauterivian through early? Aptian) on Banks, Prince Patrick and Melville islands (Miall, 1979; Goodarzi et al., 1994).

Although the post-rift phase within the report area lacks definitive evidence for syndepositional faulting, many Jurassic to Early Cretaceous normal faults have experienced one additional phase of extensional slip prior to overlap by Neogene strata of the Arctic Continental Terrace Wedge. Motion of these faults in the mid- to Late Cretaceous, as indicated in Figure 81, is potentially synchronous with widespread rifting in Baffin Bay and Labrador Sea (Kerr, 1980; Balkwill et al., 1990). More likely is a phase of extension, subsequent to the Paleocene–Eocene Eurekan Orogeny, that would coincide with Oligocene–early Miocene normal faulting in Banks Basin and eastern Beaufort Sea (Miall, 1979; Lane and Dietrich, 1995).

EVENTS OF THE CENOZOIC

Introduction

Modest-scale anticlines and synclines and related thrust faults occur throughout the Cretaceous and older strata of Prince Patrick and Eglinton islands. These features are attributed to the regional effects of the Eurekan Orogeny, the greater part of which accounts for the young mountainous terranes of Ellesmere and Axel Heiberg islands (Okulitch and Trettin, 1991). In the western Arctic Islands, the topography is subdued. Nevertheless, regional uplift and the development of a profound angular unconformity between tectonized Cretaceous and generally

flat-lying Neogene cover can also be attributed to the Eurekan Orogeny (Table 2).

Angular unconconformity below Neogene strata

Surface evidence

The surface evidence for a regional sub-Neogene angular unconformity is provided by the contact between the Beaufort Formation and various open-folded and faulted units of Early Cretaceous and older ages in the outcrop belt running from Dyer Bay northeast to Cape Krabbé. Attitudes in Cretaceous and older strata have already been described. Most bedding strikes variously northwestward in the Sverdrup Basin to northward in the horsts and grabens of Prince Patrick Uplift. Dips range from less than 1° in many areas of the Sverdrup Basin to a common maximum of about 11° in areas of inclined graben-fill east and west of Mould Bay (Fig. 27d). In contrast, the base of the Beaufort Formation mostly strikes northeastward and dips to the northwest at less than 1° (structure of these younger strata is deferred to later in the chapter). Thus the magnitude of the sub-Neogene angular unconformity ranges up to about 10° of dip.

In the Sverdrup Basin region, generally defined as those areas lying northeast of Green Bay, the Beaufort Formation commonly lies on the Isachsen and Deer Bay formations. In smaller regions, notably west of Moore Bay and east and west of Intrepid Inlet, the Beaufort Formation lies unconformably on beds as old as the Jameson Bay Formation. Over the Green Bay Uplift, near Salmon Point, and in all areas to the southwest as far as Dyer Bay, the Beaufort Formation rests on strata as young as the Christopher Formation and as old as the Cape de Bray Formation (Map 2026A, attached).

Subsurface evidence

Recognition of the base of the Beaufort Formation and related Neogene strata in the subsurface is based on selected well picks and by isolated examples of a presumed sub-Neogene angular unconformity on reflection seismic profiles (Fig. 77). Nevertheless, the sub-Neogene surface is either acoustically transparent on seismic profiles or is subparallel to underlying Cretaceous strata in many areas of Tullett Basin; the existence and location of an angular tectonic relationship between the continental terrace wedge and Cretaceous and older strata is inferred. The favoured interpretation of the depth to this surface ranges from about 100 ms above sea level on profiles north of the head of Intrepid Inlet to a maximum of 500 ms below sea level near the southwestern coast of the island. The geology on the sub-Neogene unconformity is displayed on the regional geology map (2026A). Undivided Devonian and undivided Lower Cretaceous (Isachsen and Christopher formations) are common map units throughout the subsurface of western Tullett Basin and Prince Patrick Uplift north of Dyer Bay. Nevertheless, the magnitude of post-Lower Cretaceous, pre-Neogene uplift need not be significant because there is little or no paleothermal or structural evidence to indicate the prior existence of thick pre-Neogene cover on the Cretaceous or Devonian.

In contrast, regional uplift has been much greater in the northeastern part of Tullett Basin and in the Sverdrup Basin from the Intrepid Inlet H-49 well to Ballantyne Strait. Indeed, the depth of erosion expressed on the pre-Neogene peneplain increases progressively to the north and in many local areas, around Satellite Bay and in Ballantyne Strait, the Sandy Point and Jameson Bay formations, undivided, lie below the sub-Neogene unconformity. In these areas the minimum pre-Neogene uplift is about 1200 m measured against the thickness preserved in adjacent areas to the south underlain by the Isachsen Formation. The N65°E to N75°E axes of uplift and southward tilting of eastern Tullett Basin and adjacent parts of the Sverdrup Basin are highly oblique, almost orthogonal, to the axial trace of anticlines and synclines attributed to the Eurekan Orogeny (N28–52°W). This suggests that the two sets of structural features were temporally and kinematically unrelated. Less clear is the relative timing of folding with respect to basin margin uplift.

Folds and thrust faults

Moore Bay Anticline

The Moore Bay Anticline is the highest amplitude and longest wavelength compressive deformation feature of the western Sverdrup Basin (Fig. 47, 82). The hinge of the southeast-plunging anticline and a related southwest-vergent thrust trace have been mapped at surface west of Moore Bay. Seismic profiles show that the hinge extends to the west in the subsurface to the southern coastal region of Satellite Bay (Fig. 47). The fold hinge coincides with a positive Bouguer gravity anomaly that narrows and plunges to the southeast like the fold itself (Fig. 22). The oldest exposed strata in the hinge are believed to include the Sandy Point Formation, although the oldest fossils are early Bajocian (or older) bivalves from the lower part of the Hiccles Cove Formation. Older hinge-region strata are assigned to the Jameson Bay Formation where intersected under post-tectonic Neogene cover in the Sallelite F-68 well. The anticline is flanked to northeast and southwest by syncline axial traces in the Isachsen and Christopher formations, all of which can be traced southeastward on marine seismic profiles almost to Emerald Isle. Fold wavelength, measured between synclinal traces, ranges

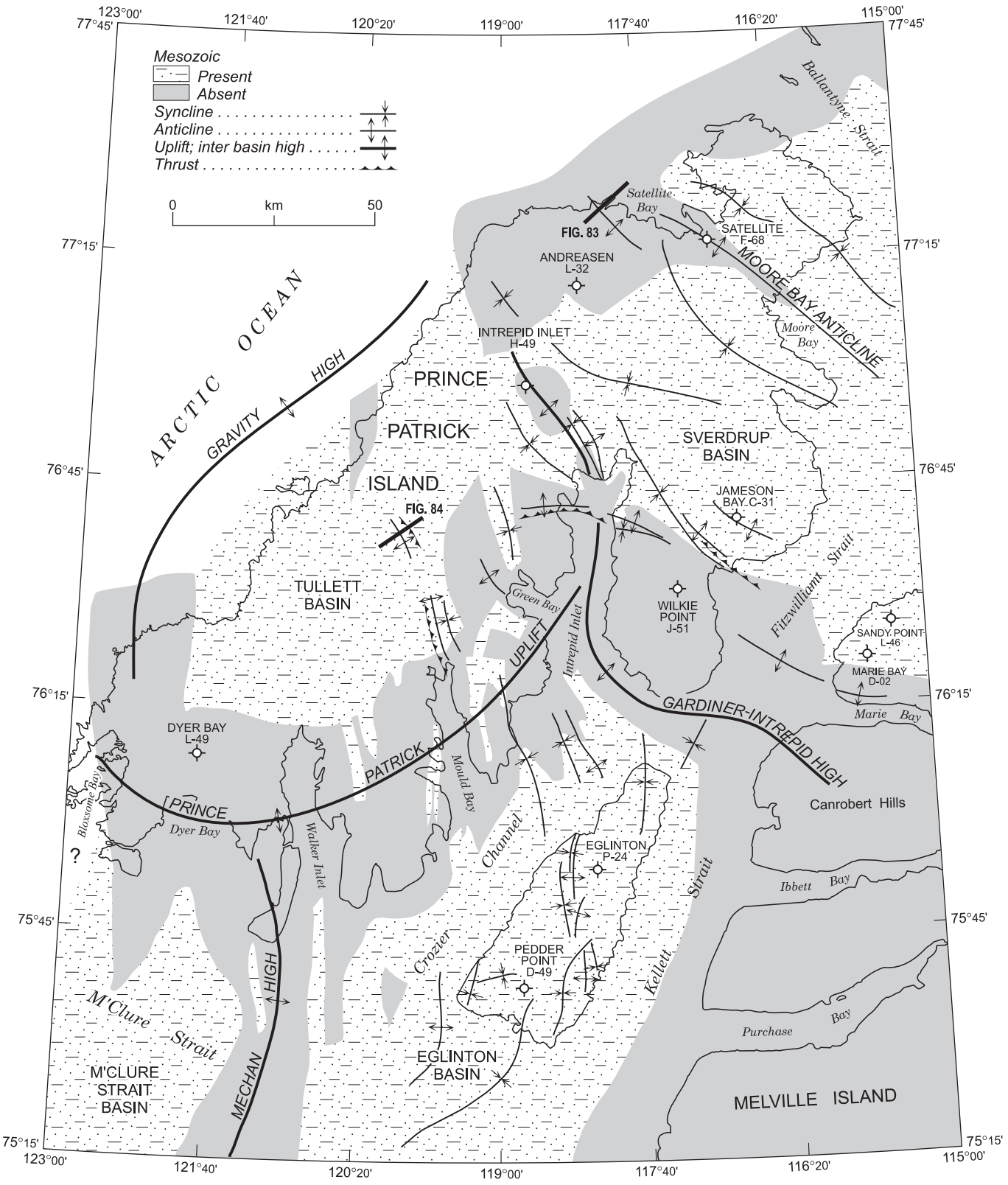

Figure 82. *Location and distribution of folds, thrust faults and uplifts of post-Cretaceous and pre-Neogene age. Structures formed through horizontal compressive deformation are attributed to the mid-Tertiary Eurekan Orogeny as provided by regional constraints illustrated in Figure 81.*

from 23 to 38 km; its amplitude up to about 1200 m. Mapping has shown that an inlier of Ringnes Formation is exposed near the shoreline and on islands in Satellite Bay. This was initally assumed to be evidence to indicate that the hinge of the Moore Bay Anticline was located here and that the anticline was also reactivated subsequent to deposition of the Beaufort Formation. Interpretation of seismic profiles, however, indicates that the principal fold crest lies 4.3 to 7.0 km to the southwest. Therefore, the existence of the inlier, perhaps mostly a product of deep valley incision prior to flooding of Satellite Bay, could also be attributed to subtle predepositional paleotopographic relief on the sub-Neogene surface or postdepositional structural relief that also affected Neogene cover.

Thrust faults in Moore Bay Anticline do not displace the Beaufort Formation. Mapping shows the thrust fault in the outcrop belt to have propagated through the pre-existing southwest-facing fold limb such that the hanging wall anticline Hiccles Cove and McConnell Island formations are now in tectonic contact with footwall syncline Deer Bay and Ringnes formations. Maximum statigraphic throw on the fault is about 225 m. A single-fold seismic profile over this part of the anticline reveals a local detachment in the Van Hauen Formation. Minor thrusts, none of which reach the surface, are also found in the medial Triassic Schei Point Group. The favoured interpretation is that the Moore Bay Anticline has been constructed above thrust-reactivated Permo-Carboniferous graben-boundary normal faults, rooted in the lower Paleozoic. One viable alternate model places the anticline above one or more blind thrusts that rise off a décollement within and above the updip limit of Otto Fiord Formation evaporite deposits. At least one parasitic thrust anticline in this area is detached at this level in the upper Paleozoic graben-fill (Fig. 47).

Elsewhere in Sverdrup Basin

All other major, compressive deformation features of probable mid-Cenozoic age are illustrated on Figure 82 and on the bedrock geology map (2026A). The most notable of these are found within the Sverdrup Basin region. Anticline axial traces are mapped within the outcrop belt including two west of Intrepid Inlet, three north of the head of Intrepid Inlet and two on the peninsula east of Intrepid Inlet. The folds at the head of the inlet are continuous with a subsurface structural culmination located at the Intrepid Inlet H-49 well.

Minor thrust inversion structures are associated with pre-existing upper Paleozoic normal faults. Some of these have been described and illustrated previously. Examples include an inversion anticline with about 50 ms of relief on the medial Schei Point Group above Jameson Fault-A (Fig. 39), a minor anticline and thrust splay off Hemphill Fault-C (Fig. 43), and a minor inversion anticline attributed to reverse slip on Hemphill Fault-B (Fig. 44). One unnamed parasitic thrust-anticline in Figure 44 appears to be locally detached in the lower part of the upper Paleozoic graben fill. Other minor thrust anticlines are detached in the Carboniferous but do not appear to have had a history of slip prior to the mid-Cenozoic (Fig. 83).

Tullett Basin

Structures originating through compressive deformation are also known within Tullett Basin. Notable examples include folds, some in the southern outcrop belt, of Green Bay Graben (Fig. 68) and throughout Mould Bay Graben north of the head of Mould Bay (Fig. 69). Two other examples, apparently unrelated to reactivation of older structure are situated near the centre of the basin east of Tullett Central Graben (Fig. 84).

Eglinton Basin

Gentle undulations of Upper Cretaceous strata are typical of the Kanguk Formation, especially within the Eglinton Member, on Eglinton Island. Range of bedding attitudes is horizontal up to about 6°, occasionally to 13°. Much of this

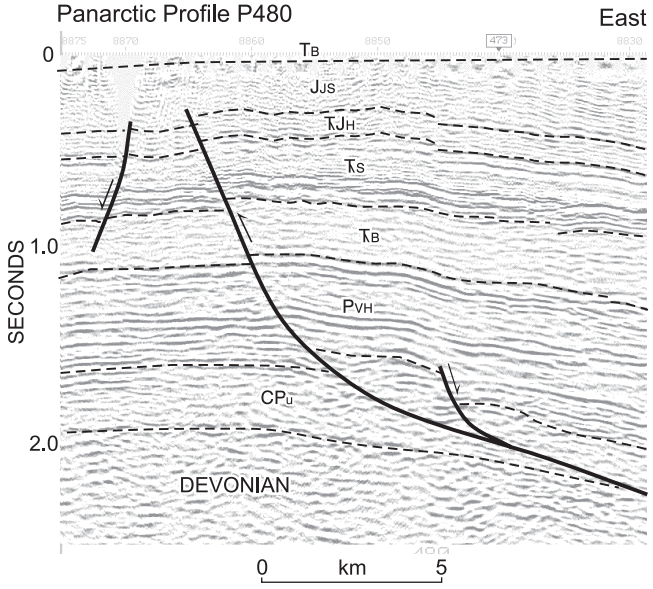

Figure 83. *Seismic expression of minor thrust anticline of probable mid-Tertiary age in Sverdrup Basin west of Satellite Bay on a portion of Panarctic profile P480.* CPu: *Carboniferous and Lower Permian strata;* PVH: *Van Hauen Formation;* TB: *Blind Fiord and Bjorne formations;* TS: *Schei Point Group;* TJH: *Heiberg Group;* JJS: *Jameson Bay and Sandy Point formations;* TB: *Beaufort Formation and related Neogene strata. Profile is located on Figure 82.*

warped bedding is probably related to drag associated with normal faulting. However, three anticlines mapped across the centre of the island, from 9.5 km east of Callaghan Point in the north to 14 km west of Catherine Point in the south (Fig. 82), are distributed in upthrown strata east of several, major, northward-striking faults. The anticlines are matched by a syncline in the downthrown section to the west. The arrangement of the folds is consistent with at least one phase of westerly directed horizontal compressive deformation.

Uplifts

Prince Patrick Uplift

The Prince Patrick Uplift has already been discussed in some detail with regards to the nature and significance of Jurassic and Cretaceous graben fill. Early uplift history is recognized by thinning of units onto the margins of the high from the adjacent basins. From the Sverdrup Basin side there is thinning and overstepping documented southwestward onto the high in all units from the Permian to the end of the Lower Jurassic (Toarcian). For Tullett Basin the contained strata thin to the south and to the southeast, and range from the Middle Jurassic to at least the end of the Upper Jurassic. Strata of the Lower Cretaceous are also overstepped by the Beaufort Formation toward the basin margins, although thinning of Lower Cretaceous units toward the basin margin is less certain. For Eglinton Basin, Middle Jurassic through to end Lower Cretaceous (Albian) strata thin to the northwest and north onto the Prince Patrick Uplift.

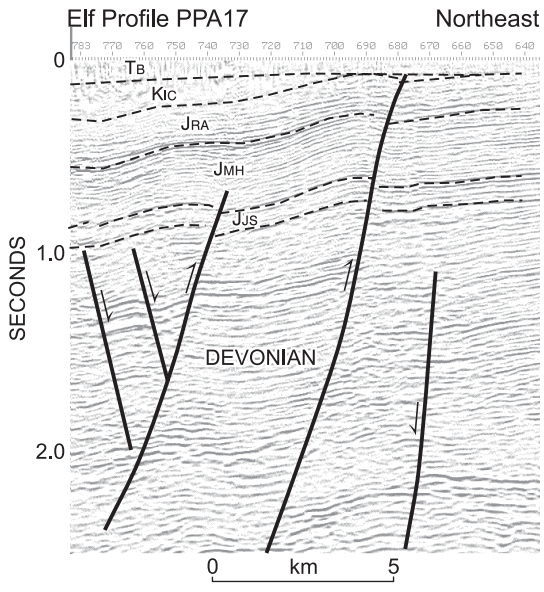

Figure 84. *Seismic expression of minor thrust folds of probable mid-Tertiary age in Tullett Basin west of Green Bay on a portion of Elf profile PPA17.* JJS: *Jameson Bay and Sandy Point formations;* JMH: *McConnell Island and Hiccles Cove formations;* JRA: *Ringnes and Awingak formations;* KIC: *Isachsen and Christopher formations;* TB: *Beaufort Formation and related Neogene strata. Profile is located on Figure 82.*

In spite of these relationships, there is every indication that the uplift was probably entirely covered by Cretaceous, and in many areas also Jurassic, strata prior to the phase of uplift that preceded burial by the Beaufort Formation. The evidence for this lies with the generally far-travelled nature of the clastic sediments within most Jurassic and Cretaceous units of the grabens preserved on the uplift. This suggests that the upthrown sides of the grabens were topographically subdued features, incapable of providing proximal coarse-clastic debris to the adjacent grabens. It is unlikely that the Prince Patrick Uplift was substantially elevated at any time in the Late Cretaceous because strata in this age range, presently preserved in Eglinton Basin, are also generally far travelled in character. The coarsest grade material, which occurs in the Campanian–Maastrichtian Eglinton Member, contains only nearshore, pebble-grade quartz sandstone. The depositional facies supports the interpretation of a nearby strandline, potentially coinciding with the margins of the uplift. The high degree of rounding and sorting in these sands, however, points to transport over distances of hundreds of kilometres and the uplift, at this time, would appear to have been only a periodically emergent, low-relief feature.

These conclusions neccessitate the last pre-Neogene phase of uplift to have been in the earlier Cenozoic. This is consistent with Miall's (1979) interpretation of the Eureka Sound Group on Banks Island. Miall's sedimentological and provenance studies indicated that sand was derived from an eastern and southeastern landmass (in the vicinity of present day Victoria Island) for the Paleocene part of this package. In contrast, sand of Eocene age in the Castel Bay area on the north coast of Banks Island is interpreted to have been transported from Prince Patrick Uplift. A major phase of uplift at this time would also coincide with the compressive deformation associated with the Eurekan Orogeny elsewhere in the Arctic Islands (mid-Paleocene through Eocene; Fig. 81; Okulitch and Trettin, 1991; de Paor et al., 1989; Ricketts, 1994) and in the Beaufort Fold Belt of Beaufort Basin (mid Paleocene to terminal Eocene; Dixon, 1996; Lane and Dietrich, 1995). This then introduces the proposal that the Prince Patrick Uplift, as it is currently expressed, is primarily the product of compressive deformation and should be temporally and kinematically linked to Moore Bay Anticline and other smaller inversion structures of the western Arctic Islands. The remaining paragraphs under the present subtitle present the existing

evidence for a post-Cretaceous phase of compressive deformation on Prince Patrick Uplift.

Folds have been documented throughout the Devonian clastic wedge and older strata on the Prince Patrick Uplift. Considered together with available seismic profiles, the majority of this compressive deformation is reasonably considered to be linked to the origin and evolution of the Early Carboniferous and older Ellesmerian Orogeny and the Franklinian Mobile Belt. However, rejuvenated deformation on specific folds and thrusts cannot be ruled out. For example, there are two northwest-striking thrust faults mapped in the Devonian at the head of Mould Bay. One of these is terminated below the base of the Jurassic. However, the other thrust fault appears to continue to the northwest under the Beaufort Formation and is identified as a thrust-anticline in Isachsen, Christopher, and older formations of southern Mould Bay Graben (Fig. 69).

The tilt of graben fill in Manson Point, Station Creek, Landing Lake and other half-grabens of Prince Patrick Uplift has been attributed to block rotation of fill during extensional slip on the bounding normal faults. However, fold-axial traces within some of these grabens could be interpreted as evidence of partial inversion. A S15°E-trending syncline axial trace lies in the eastern part of Manson Point Graben. The fold plunges and widens southward into northern Eglinton Basin. Other folds, plunging toward S25–30°E, occur within Jurassic and Devonian strata and, locally, define the contact between Prince Patrick Uplift and Eglinton Basin in the offshore southeast of Disappointment Point. The trend of these folds is consistent with a phase of tectonic rejuvenation influenced by pre-existing lower Paleozoic structures as expressed by the onland syncline in the Devonian northwest of Disappointment Point. A short, syncline axial trace trending N30°W lies in central Station Creek Graben. It is aligned with a similar northwest-striking segment of Station Creek Fault and a culmination in the upthrown footwall. These features, considered together, are consistent with transpressive partial inversion of the graben fill produced in a regional, southwesterly directed horizontal compressive stress field.

Thickness of preserved graben fill in successive half grabens of Prince Patrick Uplift (Fig. 54, 63) is primarily a response to differential subsidence during rifting. However, the widths of the half-grabens generally narrow to the west on the uplift from Station Creek Graben, and the widths of intervening highs also increase in the same direction at the expense of graben fill. The tiny erosional remnants of Jurassic around Walker Inlet and the complete absence of Mesozoic under the Beaufort Formation north of Dyer Bay are also believed to be indications of greater mid-Cenozoic uplift in these areas with respect to the coeval uplift around Mould Bay and Green Bay.

The principal conclusions to be drawn from the above observations is that the major features of the Prince Patrick Uplift, (including the widespread occurrence of Devonian at the surface and under the sub-Beaufort unconformity, and the angular unconformity or profound disconformity between Jura-Cretaceous strata and Neogene cover), are due to a mid-Paleocene through Eocene phase of compressive deformation. The orientation of folds and some minor thrusts in Cretaceous and older strata in the eastern part of the uplift is consistent with a southwesterly directed horizontal compressive stress during deformation influenced by the pre-existence of optimally oriented lower Paleozoic and Jurassic–Cretaceous structures. The relative magnitude of uplift also increases to the southwest to a maximum in the Dyer Bay area where the trend of the uplift is perpendicular to the presumed direction of maximum horizontal compressive stress. The locations of fold axial traces are consistent with reverse slip on some pre-existing graben-boundary normal faults and partial inversion of graben fill (in the case of Station Creek and Manson Point grabens) in a manner similar to that already documented for Green Bay and Mould Bay grabens.

Gardiner-Intrepid High

Other structures potentially attributable to mid-Cenozoic compressive deformation are illustrated on Figure 82 and on map 2026A(attached). The most notable of these features is the Gardiner-Intrepid High, situated in the offshore north of Eglinton Island. Limb dips are relatively subtle: 3.6 to 6.9°SW on the south-facing limb in the offshore north of Eglinton Island and only 0.5 to 0.9°NE on the opposite limb north of Wilkie Point. Nevertheless, elements of compressive deformation are indicated by map patterns and the parallel alignment of this structure with other fold-axial traces in the same region. Mapping and positive Bouguer gravity anomalies (Fig. 22) indicate that this same mid-Cenozoic high continues to the east into the Canrobert Hills region on northwestern Melville Island. This is a large area that has has also been stripped of all Permian to Middle Jurassic proximal-marine strata of the Sverdrup Basin margin.

Offshore gravity high

The western limit of Tullett Basin under the continental terrace wedge is assumed to correspond to a northeast-trending gravity high located on the continental shelf west of Prince Patrick Island (Fig. 22, 82). The full extent of this high, mostly defined by a 0 to 15 mgal positive-amplitude Bouguer anomaly, extends from offshore Houghton Head 120 km northeast to beyond Discovery Point. This high may also provide a link between the southern end of Prince Patrick Uplift and the uplifted margin of the Sverdrup Basin

around Satellite Bay. Less clear is the extent to which this hypothetical high is the product of compressive deformation. The axis of the gravity anomaly is parallel to portions of Prince Patrick Uplift. However, the offshore anomaly, like the region of inclined Sverdrup Basin strata in the Satellite Bay area, would appear to be unrelated to the obvious compressive deformation structures including Moore Bay Anticline and other southwest-plunging folds. An alternate explanation is that the nearshore gravity high and the Satellite Bay-area uplift of the Sverdrup Basin reflect a regional-scale thermal or tectonic response to rifting and seafloor spreading in the Arctic Ocean basin. A dyke swarm and submarine volcanic complex, potentially related to late-stage thermal uplift of the continental margin, may be responsible for linear magnetic anomalies in western M'Clure Strait and two large, elliptical, magnetic highs on the continental shelf northwest of Prince Patrick Island (Fig. 23).

Neogene and Quaternary structure

Deformation of the Continental Terrace Wedge

Regional uplift

Most of the present understanding of the geometry and deformation of the Arctic Continental Terrace Wedge on Prince Patrick Island, including the Beaufort Formation, has been compiled from the fieldwork and related studies of Fyles (1990). The Neogene successsion has a northwesterly thickening, wedge-shaped profile (Fig. 85). The basal surface, defined by the pre-Neogene angular unconformity and peneplain above Cretaceous and older strata extends from nearly 200 m above sea level in the east to locally more than 600 m below sea level on the Arctic coast (Fig. 85). Strata within the wedge generally strike N40°E to N50°E. Calculated dip in the outcrop belt of the Beaufort Formation is toward the northwest at between 0.2° and 0.7°. Farther to the west, in the subsurface, the basal surface dips more steeply to the northwest at up to about 1.1°. One notable departure from this pattern occurs in and around Satellite Bay, where the base of the Beaufort Formation, situated near sea level, strikes N49°W and wraps around a linear inlier of Ringnes Formation (Map 2026A, attached).

V-shaped drainage patterns on the Beaufort erosion surface identified on air photographs (Fig. 86) are assumed to have developed in Neogene beds that dip to the northwest at a gentle angle steeper than the present, west-facing topographic surface. These attitudes are plotted on Map 2026A.

The internal stratigraphy of the wedge is known from measured sections, drillholes and reflection seismic profiles. Details are provided by Fyles (1990). In many areas, the terrace wedge is entirely above sea level and/or too thin to have a distinct seismic expression. In the southwestern part of the island, where the wedge ranges to more than 500 ms, geophysical records reveal a reflection-free upper part that is gradational with a variably stratified lower part (Fig. 73, 74). Onlapping reflections mark the base on some profiles (Fig. 77).

A schematic cross-section of the Continental Terrace Wedge profile is illustrated in Figure 87. The older parts of the wedge lie to the west in the subsurface on Prince Patrick Island. The strata exposed along the eastern edge of the deposit represent only the most proximal components deposited during the terminal stages of a major marine transgressive event and subsequent Pliocene sea-level highstand. Sea-level retreat and deposition of the younger pre-Pleistocene components of the terrace wedge were accompanied by continued subsidence in the west and differential uplift in the east varying from 0 to almost 200 m over the strike length of these deposits.

Faults

The erosional limit of the Beaufort Formation on the east side of Prince Patrick Island is represented by a prominent escarpment and high-standing, ridge-crest outliers of unconsolidated sand and gravel (Fig. 88). Bedrock Beaufort Formation is only locally exposed in stream-dissected embankments. More common is a veneer of Quaternary gravel and colluvium that drapes the escarpment face and the contact between the Beaufort Formation and low-standing Cretaceous and older bedrock. Nevertheless, mapping has provided numerous examples where faults in basement have failed to displace the sub-Beaufort unconformity. Also common is the development of modest relief on the peneplain with drape or channeling of Neogene sand over this paleotopography.

Significant paleotopographic relief is indicated along the trace of Landing Lake Fault (Fig. 89). The base of the Beaufort Formation lies at 90 to 120 m above sea level, where it overlies the Isachsen and Christopher formations in Landing Lake Graben. In contrast, the top of the Devonian peneplain in the upthrown footwall east of Landing Lake Fault is 150 to 210 m above sea level. Nevertheless, the base of the Beaufort Formation drapes over the fault trace in many places and shows no evidence of tectonic offset. The principal conclusion is that the Beaufort Formation was deposited on topography with 30 to 120 m of local relief and that relief was generated by differential erosion of the younger, more unconsolidated formations of the Cretaceous relative to the more resistant Devonian. Indeed, some of the present differences in relief on the plateaux (between the low-standing Cretaceous in the grabens and the high-standing Devonian basement horst blocks) may reflect the

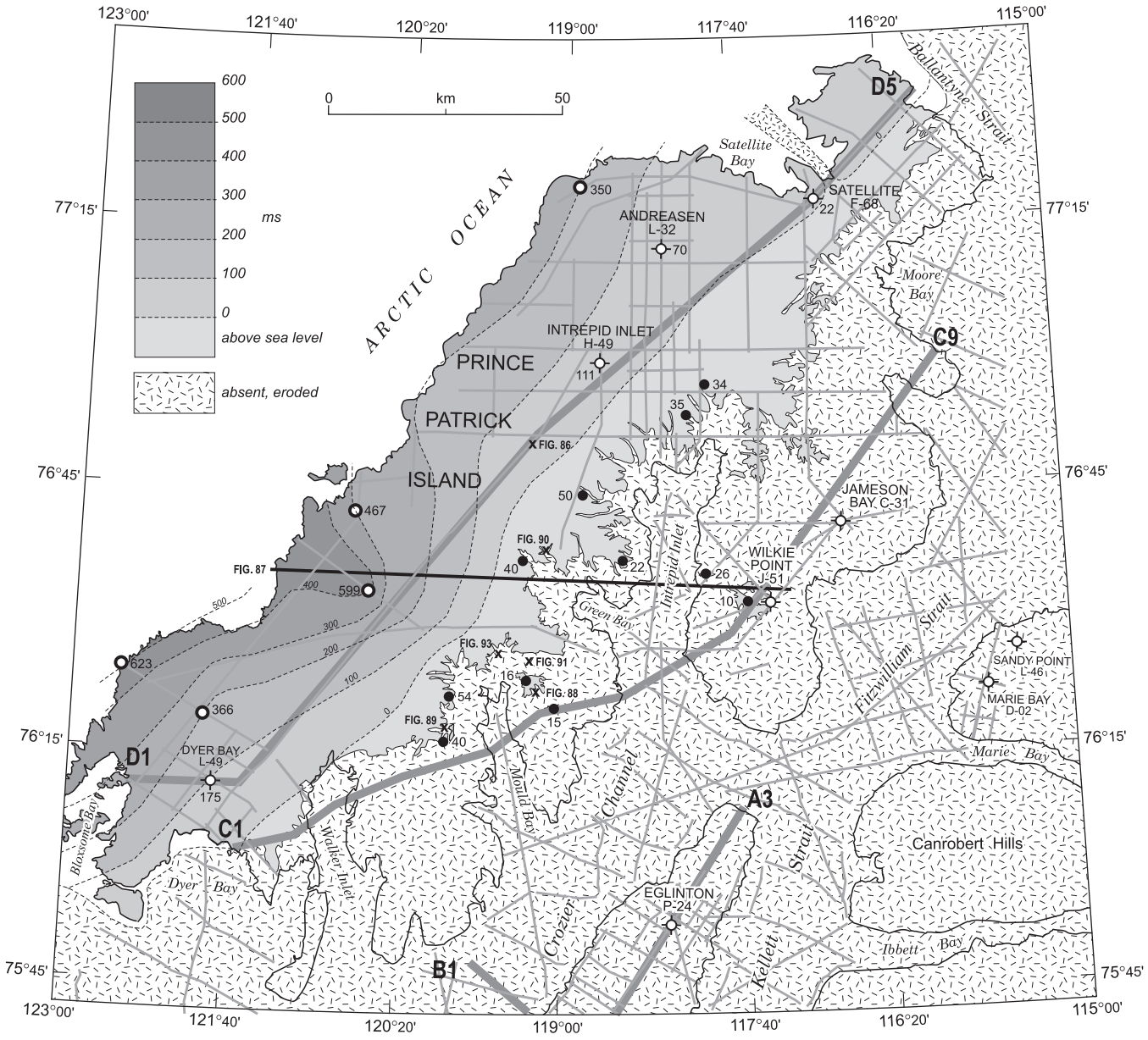

Figure 85. *Thickness isochrons and spot thicknesses (in metres), seismic profiles and the location of related text illustrations for the Arctic Continental Terrace Wedge (including the Beaufort Formation), on Prince Patrick Island.*

relief of the unroofed peneplain surface and the topography of Prince Patrick Island as it existed in pre-Beaufort time. The principal modification of this surface was caused by the regional uplift of basement and of the Beaufort Formation along its eastern margin (as described above), and various processes causing valley incision and fiord formation on southern Prince Patrick Island.

Although the exposed Beaufort Formation appears to be undeformed on eastern Prince Patrick Island, other data indicate that faults have been active within and below the Arctic Continental Terrace Wedge since deposition of these strata. There are three lines of evidence: mappable faults at surface, reflection seismic evidence of faulted terrace-wedge strata, and historical seismicity.

The distribution of known and suspected faults and tectonic lineaments in the Beaufort Formation of central and western Prince Patrick Island is illustrated in black on the bedrock geology map Map 2026A (included with this

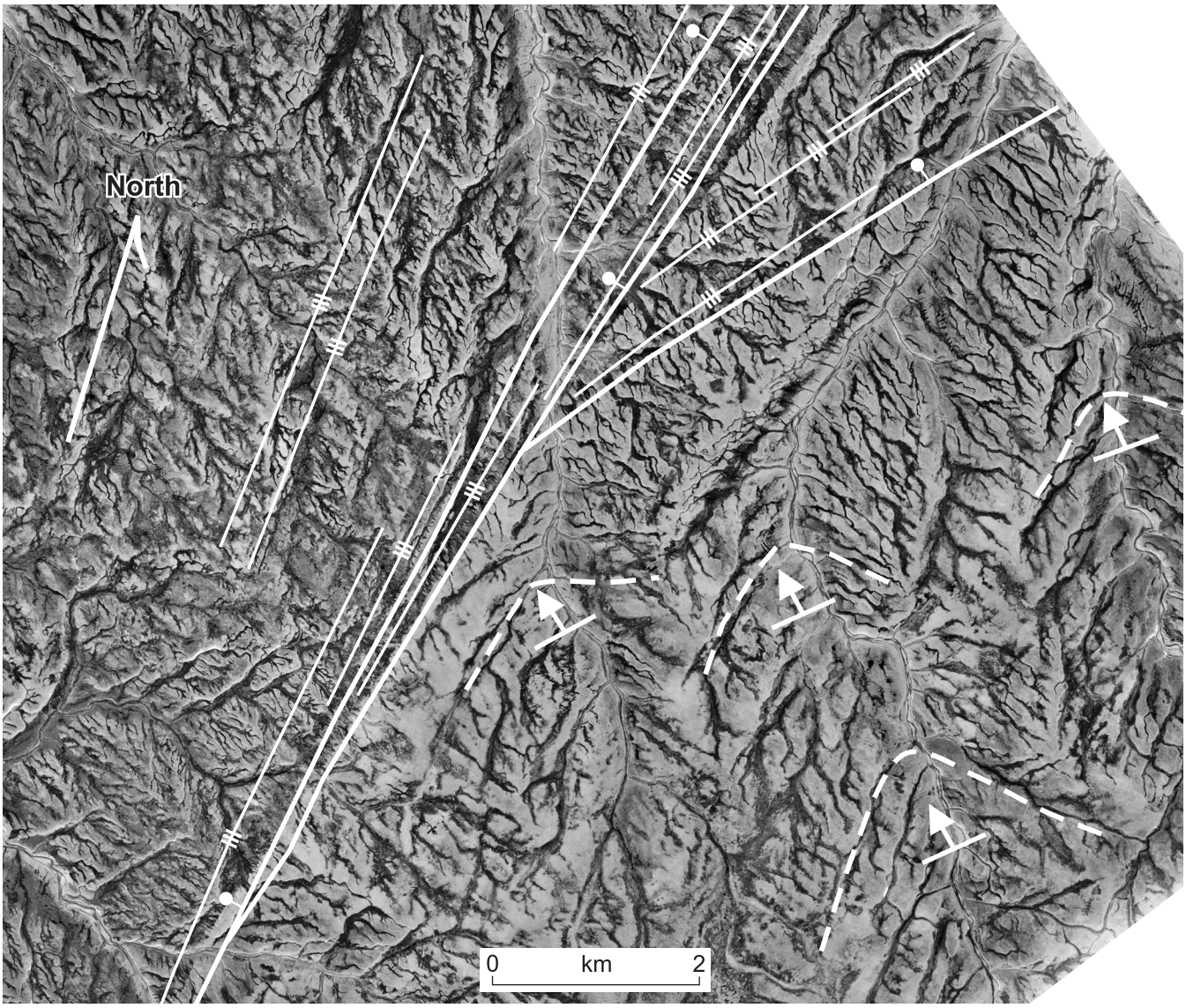

***Figure 86**. Aerial photographic expression of the Beaufort Formation and related strata of the Arctic Continental Terrace Wedge on central Prince Patrick Island. Major features include faults, lineaments and stream dissection into very gently inclined bedding. Area of photograph is located on Figure 85 (NAPL photo A17451-100). Bedding inclination for the Beaufort Formation is provided by the "rule of V's" and related V-shaped erosional features.*

report). Lineaments are identified on air photographs by a preferred alignment of gravel ridges, vegetation growth, drainage elements, ponds and similar features (Fig. 86). Faults are recognized by similar linear elements but are distinguished from lineaments by evidence of stratigraphic throw. The main throw indicator is a contrast in relief on either side of the fault trace. The upthrown side is identified by better drained, higher relief, less vegetated, light coloured sands. In contrast, the downthrown side is a more heavily vegetated, darker and poorly drained region with ponds and sedge meadow covering large areas of bedrock surface.

Faults and lineaments are especially common between longitude 119°25'W and 120°35'W, beginning 16 km north of the head of Mould Bay and extending north to the northwest coast. These northward-trending structures are parallel to, and lie directly above, Landing Lake, Mould Bay, and Tullett Central grabens. Downthrown strata lie variously to east or west on different fault strands, as is also the case for the subsurface faults. Indeed, the eastern boundary-normal fault of Tullett Central Graben exactly coincides with a fault of greater known length mapped at the surface in the Beaufort Formation, and consistent indication of throw, down-to-the-west, is provided both at surface and on seismic profiles. However, the majority of the basement faults do not extend into the Beaufort Formation.

A second set of faults and lineaments occurs in the Beaufort Formation. This array trends N30°E to N45°E and is featured, most notably, between the Intrepid Inlet H-49 and Andreasen L-32 wells. The longest of these faults is 67 km. All are downthrown to the northwest. There are many, short, normal faults with these orientations scattered throughout the Cretacous and older strata in this part of the Sverdrup Basin. There is only local coincidence of surface and subsurface structure. Indeed many major sub-Beaufort features, such as the northwest-striking faults and smaller fold-axial traces associated with the Gardiner-Intrepid High, are nearly perpendicular to the trace of structural elements in the Beaufort Formation.

Peripheral effects of faulting on the attitude of the Beaufort Formation appear to be mostly insignificant as these strata are nearly universally less than 1° or flat lying. J.R. Devaney (*in* Harrison et al., 1988) observed one streambank outcrop of Beaufort Formation on central Prince Patrick Island, where strata are locally inclined to 15°. However, this may be due to local, near-surface buckling asociated with periglacial processes and the recent growth of pingos in the exposed Beaufort Formation.

The vast majority of the surface faults and lineaments have no seismic expression of offset. There are, in fact, only two known examples of a seismically defined fault offset of the Beaufort Formation, and correlation into the faults mapped at surface is indicated for only one of these. The latter structure occurs within Landing Lake Graben on

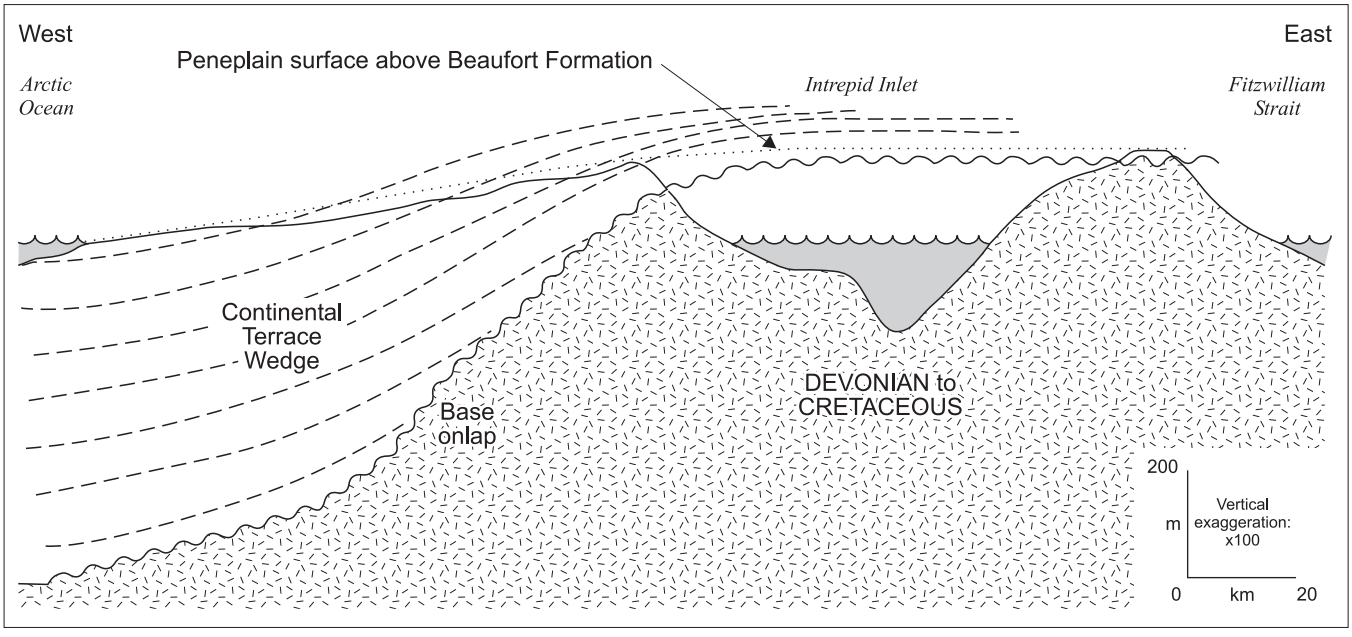

Figure 87. *Schematic cross-section for the Beaufort Formation and related deposits of the Arctic Continental Terrace Wedge across central Prince Patrick Island, modified from illustrations in Fyles (1990). Line of section is indicated on Figure 85. Surface dissection of inclined strata is implied by V-shaped erosional features on air photos (see Fig. 86). Base onlap is indicated on selected seismic profiles (see Fig. 70, 77).*

intersecting portions of seismic profiles PPA14 and PPB25 (Fig. 77). Two significant normal faults are evident on these profiles. The base reflections of the terrace wedge are uncertainly affected by the eastern fault. However, there is clear evidence of displacement of the terrace-wedge strata by the western fault (with about 50 ms of throw) and the fault may continue upsection toward the surface.

The above observations suggest that either the faults mapped at the surface in the Beaufort Formation have only a few metres of normal offset or that the sense of slip is primarily left or right lateral but too small to produce a seismic expression of offset. For example, strike-slip displacements of a few tens or hundreds of metres on any one of the various surface and basement rocks would probably not be noticed on the available seismic records. A less plausible explanation is that the lineaments, and possibly some of the "faults", may represent some other phenomenon such as drape or differential compaction of the Beaufort Formation over unfaulted, linear paleotopographic features on the sub-Beaufort surface.

Recorded seismicity

The most convincing proof that faulting has occurred in this region since deposition of the Beaufort Formation is provided by the existence of historic seismicity. Recorded earthquake epicentres are shown on the regional Bouguer anomaly and magnetic maps (Fig. 22, 23). Uncertainty in positions mostly range from 20 to 40 km. A total of 76 seismic events greater than magnitude 3.0 (excluding most aftershocks) have been recorded within the greater report area between January 1963, the last event in November 1993. The majority of epicentres are scattered across Prince Patrick Island and Ballantyne Strait as far as Mackenzie King Island. In contrast, western Melville Island, M'Clure Strait, northern Banks Island and the continental shelf region has witnessed much less seismic activity. These data include 12 events of magnitude 4.0 to 4.5 of which six, recorded between January 20 and February 23rd 1984, occurred with at least 25 aftershocks under the channel east of Brock Island. Earthquake foci (source depths) and fault plane solutions have not been calculated.

Deformation of Quaternary deposits and colluvium

Pleistocene deformation

The earlier Quaternary stratigraphic record includes a wide variety of Pleistocene glaciofluvial gravel, ice-marginal gravel mounds, erratics, ice-rafted debris, varved glaciomarine mud, and peat. The gravel includes rounded granite clasts and other far-travelled material, likely transported from a provenance area in the Canadian shield. The offshore channels also feature incised valley-fill deposits of probable Quaternary age with many fine examples provided on seismic profiles of Crozier Channel (Fig. 61), Intrepid Inlet, eastern Kellett Strait, northern M'Clure Channel (Fig. 80) and Dyer Bay.

Related evidence for the prior existence of major ice streams on eastern Prince Patrick Island includes bedrock glacial striations at elevations of up to 200 m. These features are locally well developed within cemented Devonian sandstone on various plateau surfaces around the head of Mould Bay. Measurements indicate ice-flow directions subparallel to the length of the bay. These data also support the view that Mould Bay was filled with, and in part excavated by, a tongue of the Laurentide Ice Sheet on at least one occasion during the Pleistocene. Studies on Banks and Melville islands suggest that the Laurentide Ice Sheet probably did not extend across M'Clure Strait at any time in the Late Pleistocene. Rather M'Clure Strait was probably occupied by an ice shelf from the main Laurentide ice mass to the east and south (Vincent, 1989; Hodgson et al., 1994). Of the two older glaciations described by Vincent (1989), the earlier, more extensive ice sheet of the Banks Glaciation, before 0.73 Ma in the Early Pleistocene, is the one most likely to have reached Prince Patrick Island. This suggests that the Mould Bay ice tongue and the far-travelled glacial gravel elsewhere on Prince Patrick Island were also Early Pleistocene in age.

Pleistocene deposits are scattered throughout the island and in many cases are preserved in close and complex association with the Beaufort Formation. Large, gravel-filled glaciofluvial channels, for example, have been identified on air photographs on the Beaufort plain in many areas northwest of Green Bay. In many cases, Pleistocene sediments form a veneer that has been draped over the east-facing escarpment and related outliers of the Beaufort Formation (Fig. 88, 90). One area, 16.5 km northwest of Green Bay, provides many useful examples of this. Draping sediments in this area include a distinctive, varved, glaciolacustrine mud deposit (Fig. 90). The contact between the Beaufort Formation and the Pleistocene mud occurs on the lower and middle slopes of the sinuous escarpment face. The base of the mud layer is very sharp at this location and is almost certainly a major disconformity surface. When excavated, the unconformity was found to coincide with the sloping surface, showing that the escarpment existed and had been fluvially dissected prior to deposition of the varved mud. The mud also contains intraformational ductile folds and sliding surfaces identifiable both from the air and on the ground (Fig. 91a, b).

The geological origin of the escarpment and of the overlying deformed mud is schematically illustrated in Figure 92. The escarpment was dissected by fluvial downcutting in the late Pliocene or Early Pleistocene

Figure 88. *The eastern edge of the Beaufort Formation on Prince Patrick Island is represented by a sinuous stream dissected escarpment. Photo taken from low-flying aircraft north of the head of Mould Bay (GSCC photo 3820-7).*

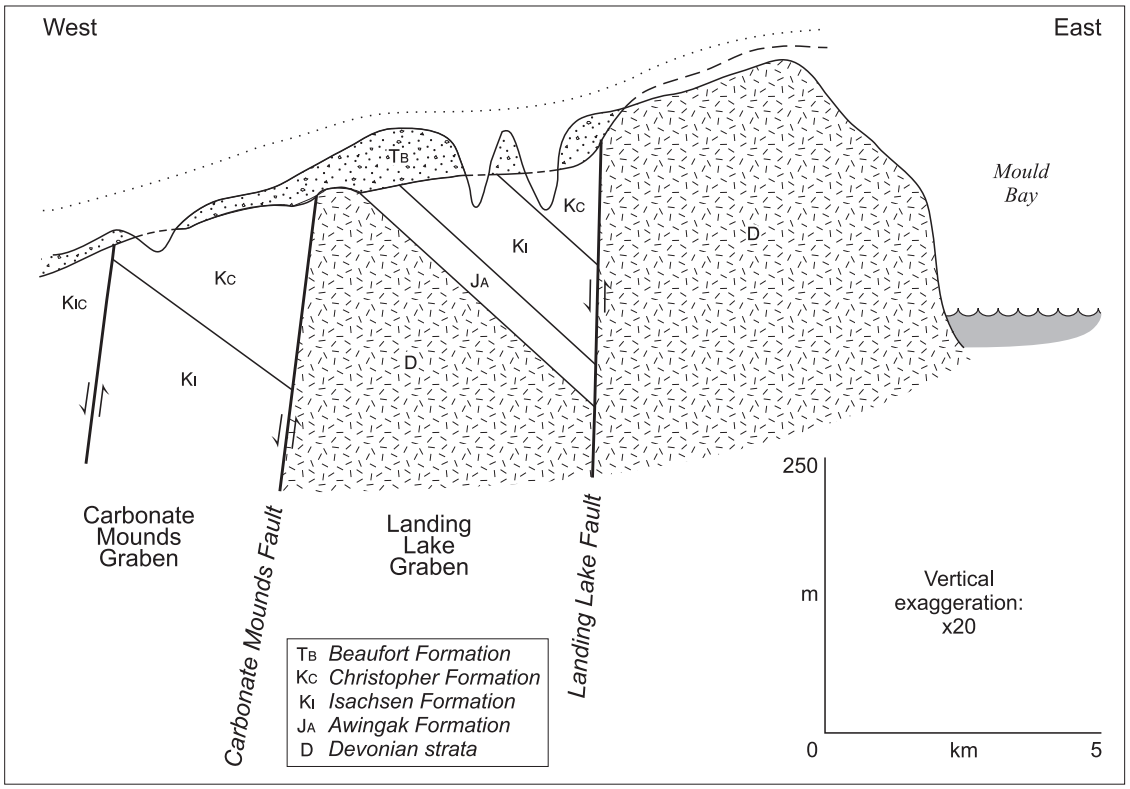

Figure 89. *Stratigraphic relationship between basement faults and the Beaufort Formation in outcrops west of Mould Bay. The base of the Beaufort Formation is 100 m higher east of the fault than it is above Cretaceous strata in the graben. There is, however, no indication of fault offset of these strata. Paleotopographic relief is indicated on the sub-Beaufort unconformity. Section is located on Figure 85.*

(Fig. 92a). A tongue of the Laurentide ice sheet then advanced to the north and occupied the Intrepid Inlet and Green Bay areas in Early to mid-Pleistocene time. The ice front came to rest, at least temporarily, below and east of the Beaufort escarpment. This terminal position allowed for the creation of a local meltwater lake, dammed on one side by the ice front and on the other by the face of the escarpment (Fig. 92b). Retreat of the ice front to the south led to the eventual collapse of the ice dam and the draining of the ice-front lake. Left unsupported by the ice front, the glaciolacustrine muds then slid down the face of the Beaufort escarpment facilitated by natural sliding surfaces within and below the mud (Fig. 92c).

Pingos

Pingos of Prince Patrick Island have been mapped and described by Pissart (1967). Although such features are only peripherally associated with the structural geology of the report area, they are mentioned here because of the tendency for pingo growth to induce local faulting and to create local tilting (to about 30°) and deformation of colluvium and near-surface bedrock. Mapped pingos, ranging from 3 m high and a few tens of metres in diameter each to 13 m high and several hundreds of metres in length for coalesced pingo complexes, are most abundantly developed in the Beaufort Formation west of Intrepid Inlet (where the Pliocene is locally inclined to 15°) and east of Satellite Bay. Other localities are documented by Pissart (1967) north of Landing Lake Graben, also in the Beaufort Formation. One of us (JCH) has observed a stream-dissected pingo in southern Landing Lake Graben that has formed in and deformed Isachsen Formation bedrock and grass-covered colluvium cover. Pissart (1967) also provides field evidence for a pingo complex in the Devonian west of Mould Bay. These features and occurrences indicate that, although the process can occur in a wide range and age of

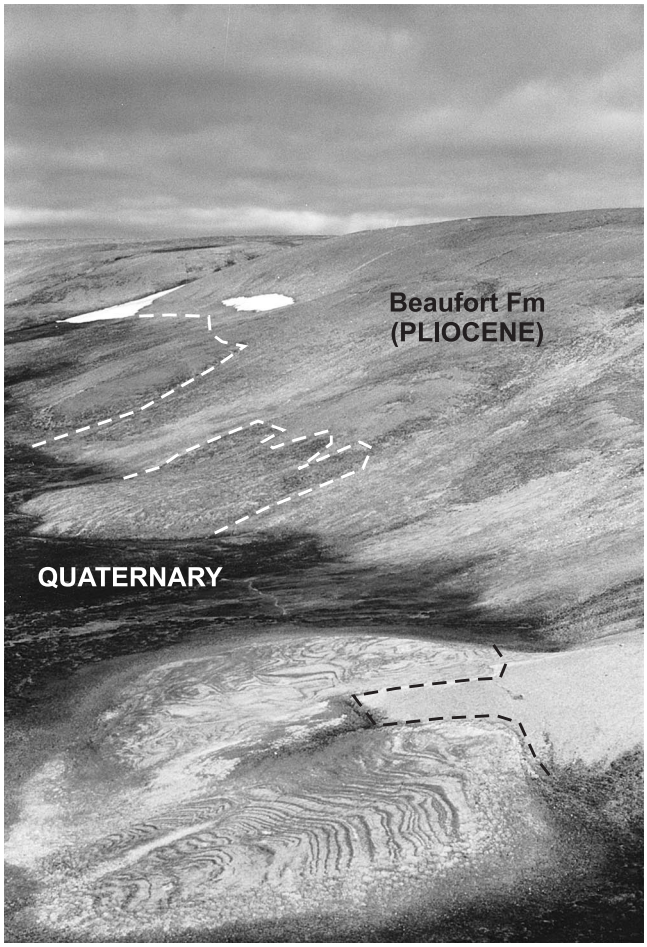

Figure 90. *Varved glaciolacustrine silt and mud is draped on the face of the Beaufort escarpment and has slid on the scarp face to produce intraformational minor folds. Photo taken 16.5 km west of Green Bay. Scarp height is about 40 m. The implication is that the escarpment formed prior to at least one glaciation (GSCC photo 3820-80).*

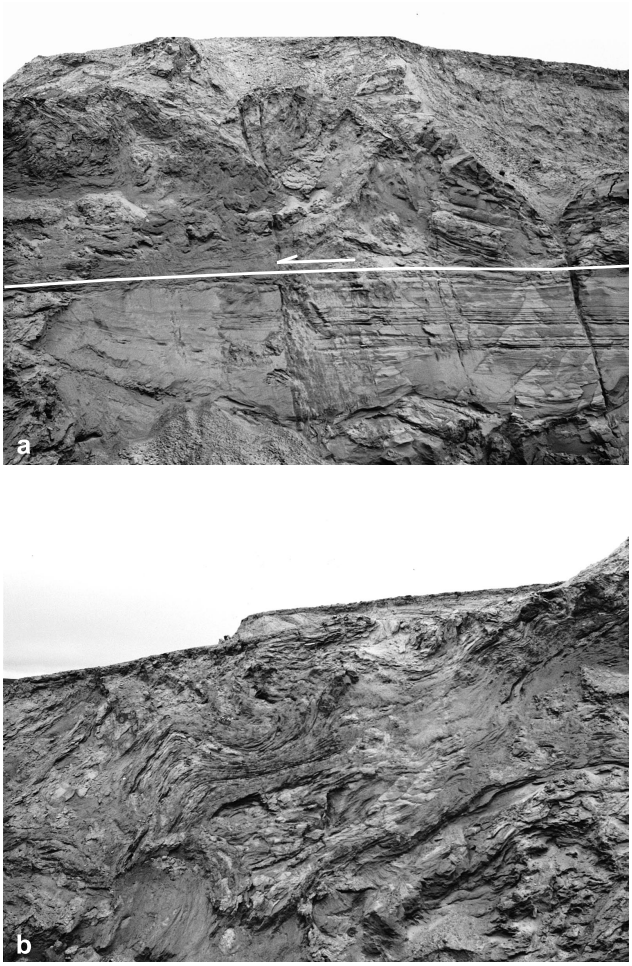

Figure 91. *Intraformational minor folds and a related detachment surface featured in glaciolacustrine silt at a site located north of the head of Mould Bay. Height of exposure is about 3 m [GSCC photo 3820-85 (a), 3820-84 (b)].*

rocks lying within the active layer, the age of pingo formation is recent.

Seasonal deformation in the active layer

Holocene deposits include beach ridges, stream gravels, deltaic and floodplain sands, active-layer felsenmeer and related colluvium. The most obvious deformation occurs within the active layer. Seasonally active mass-flow deposits, often a few tens of metres long and a few metres wide at the toe, are especially common on steeper slopes and on valley sides in water-saturated mud and colluvium. Active-layer gravity slides can also be much larger (Fig. 93). For example, sliding has occurred within about 50 cm of the surface, on a very gently inclined, and fully vegetated slope underlain by Christopher Formation at a locality 7 km north of the head of Mould Bay. Slope failure has exposed the black shale bedrock in the area of upslope calving. Gravity flows extend downslope for approximately 1000 m in several separate lobes. The longest of these (Fig. 93) terminates near river level in a region of tightly folded bedrock shale, water-saturated mud, and vegetated ground cover along a 100 m-wide front.

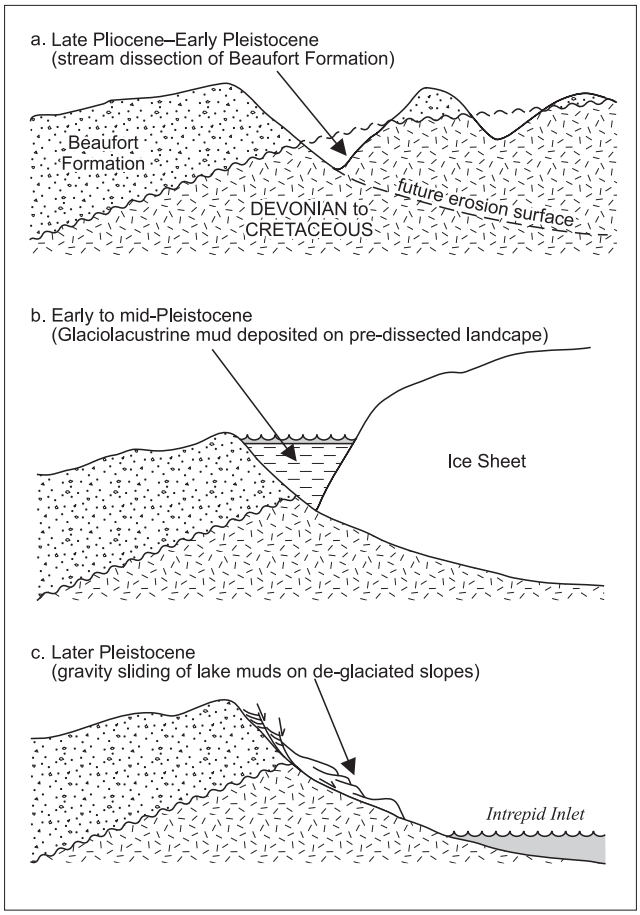

Figure 92. *Schematic model for the origin of gravity slides in glaciolacustrine silt and mud of east-central Prince Patrick Island. The implication of this model is that the escarpment of the Beaufort Formation may be the product of late Pliocene to Early Pleistocene fluvial dissection.*

ENERGY AND MINERAL RESOURCES

Introduction

Oil and gas exploration on Eglinton and Prince Patrick islands was carried out between 1965 and 1976 by Elf Oil Exploration (later to become Elf-Acquitaine) and to a lesser extent by GSI, Panarctic Oils Limited, Triad Oil, and Gulf Canada Limited. Preliminary work included strategic mapping, stratigraphic studies, gravity surveys, marine (over sea ice) and onshore reflection seismic profiling. This work led to the delineation and testing of eight structural targets: five within and beneath the Sverdrup Basin on northeastern Prince Patrick Island, two in Jurassic–Cretaceous strata of Eglinton Island and one on the Silurian shelf edge of Dyer Bay Anticline north of Dyer Bay. While discovered hydrocarbons are insignificant, the report area has received only reconnaissance-scale exploration by industry, and only the largest structures have been drilled (Fig. 94).

Bituminous and subbituminous grade coals were reported by Tozer and Thorsteinsson (1964) from Devonian, Jurassic and Lower Cretaceous strata. Metal sulphides are unknown within the report area. However, manganese cements (mostly rhodochrosite) are widespread in the Eglinton Member of the Kanguk Formation on Eglinton Island (Tozer and Thorsteinsson, 1964).

Thermal maturity

Thermal maturity has been assessed from core and cuttings samples collected from the eight area wells, and from measured surface sections and isolated outcrops. Thermal maturity estimates have been obtained from 1) quantitative measurements of vitrinite reflectance ($\%Ro_{VIT}$); 2) measurements of reflectance of bitumen ($\%Ro_{BIT}$); 3) T_{MAX} values obtained through the Rock-Eval pyrolysis procedure; 4) the qualitative assessment of the colour of palynomorphs in transmitted light with reference to the thermal alteration index (TAI scale) of Correia (1969) and Hunt (1979); 5) mean maximum reflectances measured on graptolites (Gro_{max}) as provided by the scale of Goodarzi and Norford (1985); and 6) the colour of conodonts in transmitted light using the conodont alteration index (CAI) as developed by Epstein et al. (1991). Correlation of these various scales is illustrated in Figure 95.

Thermal maturation data in the form of vitinite reflectances are available for most intervals in the Satellite

Figure 93. *Surface gravity flows in the active layer above the Christopher Formation, Landing Lake area. This one flow approximately 1 km long by 100 m wide extends upslope to the low skyline hill at upper right. View is to the east. Site is located on Figure 85 (GSCC Photo 3820-49).*

F-68 well with the exception of the Bjorne Formation, which lacks organic matter. The top of the oil window (%Ro_{VIT} = 0.5) occurs in the upper part of the Grosvenor Island Formation, the interval of peak oil generation (i.e., %Ro_{VIT} = 0.7–1.0) is inferred to lie in the upper Bjorne Formation, and the transition to wet gas generation, at Ro 1.3, occurs in the Trappers Cove Formation.

For the Andreasen L-32 well the thermal maturation gradient is poorly constrained in the Lower Triassic and above the lower part of the Jameson Bay Formation. The top of the oil window is inferred to lie in the Barrow Formation (Upper Triassic) while the mid-Permian, at 2050 m below surface lies in the interval of peak oil generation (i.e., %Ro_{VIT} = 0.75).

Vitrinite paleotemperature data for the Jameson Bay C-31 well are clearly defined for the Permian and Middle Jurassic. There is also much data for the Middle Triassic, although there is wide scatter in the results. Top of the oil window lies in the Hiccles Cove Formation and peak oil generation temperatures (%Ro_{VIT} = 0.7–0.9) were attained through the Permian and most of the Lower Triassic interval.

Most vitinite reflectance data in the Intrepid Inlet H-49 well was collected for the Schei Point Group, augmented with several data points in the Devonian, Permian, and Middle Jurassic. The strata above the top of the Schei Point Group are immature, and the oldest strata above the post-Devonian unconformity lie within the lower part of the oil window. Vitrinite reflectance values from the Devonian are highly variable, presumably as a result of a combination of older Devonian material being recycled into younger Devonian strata, and caving of the sidewall down the hole during drilling. Nevertheless, this part of the Devonian clastic wedge would not appear to have experienced temperatures above the level of peak oil generation.

Material suited to thermal maturation analysis is scarce above the Devonian unconformity in the Wilkie Point J-51 well. Based on additional samples collected from adjacent outcrops, the top of the oil window lies in the Jameson Bay Formation. Older strata above the Devonian (such as the Schei Point Group) are only marginally mature (%Ro_{VIT} = 0.5–0.7). Vitrinite reflectance values from the Blackley Formation, and bitumen reflectance values from the Lower Devonian, and from all older strata, are entirely overmature. The thickness of unroofed pre-Triassic strata implied by the thermal maturity gradient in the extant Silurian and Devonian may exceed 8 km.

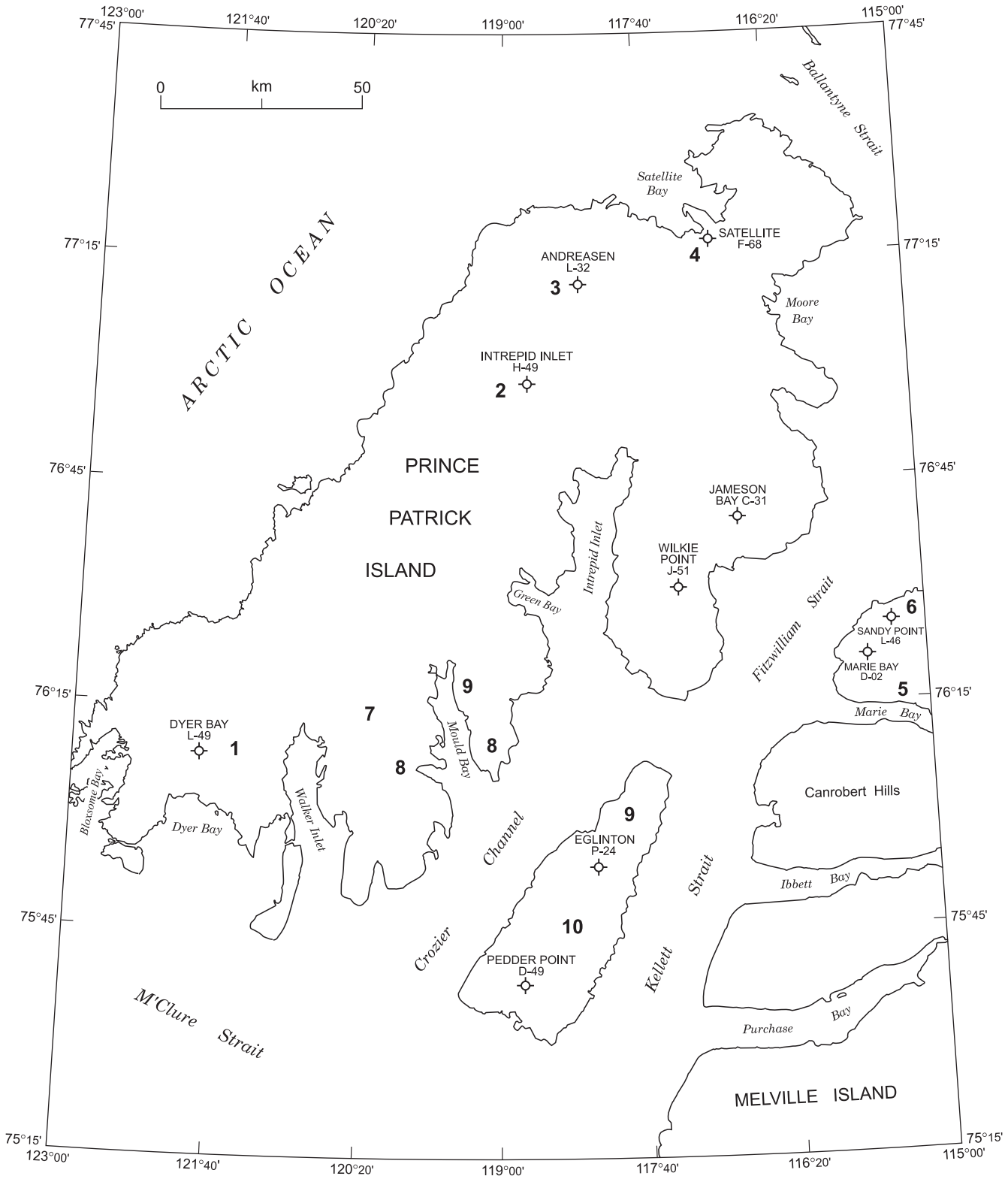

1 *Pyrobitumen in Silurian carbonate rocks, Lower Devonian Kitson Fm and in Middle Devonian Blackley Fm; Dyer Bay L-49 well*

2 *Oil staining in medial Trold Fiord Formation (mid-Permian); Intrepid Inlet H-49 well*

3 *Logged gas detected in Trold Fiord Formation; oil staining and logged gas shows in Middle Triassic and Upper Triassic of Andreasen L-32 well*

4 *Gas detected in Middle and Upper Triassic Schei Point Group; bitumen and logged gas in upper Bjorne Formation; Satellite F-68 well*

5 *Bitumen deposits (10) in Lower Triassic Bjorne Formation on Sproule Peninsula (Trettin and Hills, 1966)*

6 *Live oil in Lower Cretaceous Isachsen Formation of Sproule Peninsula*

7 *Methogenic carbonate mounds (2) on fault trace in Lower Cretaceous (Albian) Christopher Formation*

8 *Coal seams in Parry Islands Formation east and west of Mould Bay*

9 *Coal seams in the Lower Cretaceous Isachen Formation of northern Eglinton Island and west of Mould Bay*

10 *Manganese deposits and occurrences in the Eglinton Member of the Kanguk Formation (Campanian) throughout southern Eglinton Island*

Figure 94. *Location map of wells and resource localities mentioned in text.*

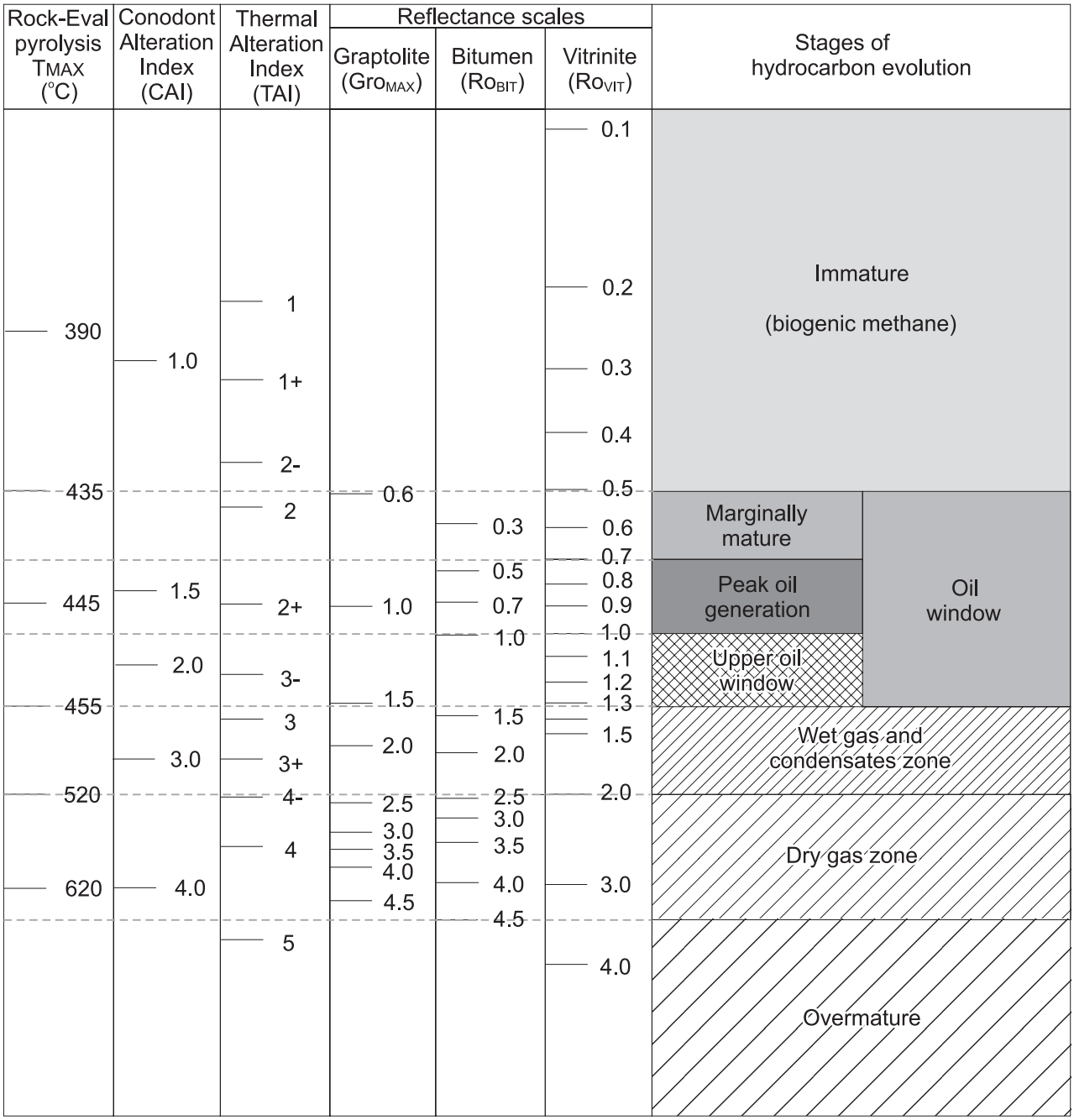

Figure 95. *Thermal maturity scales and stages of hydrocarbon evolution, compiled from related illustrations in Utting et al. (1989) and Gentzis et al. (1996).*

Middle Jurassic through Upper Cretaceous strata, preserved in the two wells on Eglinton Island, lie entirely in the upper part of the oil window (%Ro_{VIT} = 0.5–0.7). Devonian strata in the Eglinton P-24 well are overmature, whereas a sample from the Devonian at the base of the Pedder Point D-49 well lies within the oil window. Implied differential thickness of strata removed between the two wells prior to overlap by the Middle Jurassic is about 900 m. This is close to the thickness of locally eroded section determined from reflection seismic profiles acquired over this part of Eglinton Island. The thickness of eroded section removed above the preserved Devonian section at Pedder Point D-49, prior to overlap by the Jurassic, may exceed 3000 m.

Thermal maturity of Silurian through Middle Devonian strata penetrated in the Dyer Bay L-49 well, provided by a small number of widely separated samples, lies within the dry gas range.

Petroleum source rocks

Silurian and older rocks

The Silurian rocks intersected in the Dyer Bay L-49 and Wilkie Point J-51 wells are part of a carbonate bank succession that underlies much of southern Prince Patrick Island. The intervals intersected in the wells have low hydrocarbon yields (TOC <1%) and hydrogen indices (HI) less than 40 mg HC/g Corg (Fig. 96). Petrographic studies indicate that the organic carbon exists mostly as granular and nongranular bitumen with minimum reflectances ranging from 2.0 (1.6% Ro_{VIT}) in J-51 to 2.7 (2.1% Ro_{VIT}) in L-49 . The Silurian carbonate facies is believed to grade southward and eastward into seismically defined slope and basin facies shale and fine-grained carbonate strata equivalent to the medial part of the Ibbett Bay Formation on western Melville Island. Although such strata may have intervals of high residual organic carbon, all such rocks are believed to be currently overmature and only potentially capable of yielding dry gas (Fig. 97).

Kitson Formation

The Kitson Formation is a 50 to 75 m thick condensed interval of black shale and argillaceous limestone that spans the entire Lower Devonian. In the Dyer Bay L-49 and Wilkie Point J-51 wells, it is characterized by high residual total organic carbon (2.6–4.4% TOC). Although HI is mostly low, one analysis produced 90 mg HC/g Corg (Fig. 96). Petrographic studies indicate that organic carbon resides in granular and nongranular bitumen and as intercrystalline and particulate coatings. There are two or more reflectance populations in most samples that range from a minimum $\%Ro_{BIT}$ of 2.0 (1.6% Ro_{VIT}) in the J-51 well (wet gas) to a maximum $\%Ro_{BIT}$ of 3.3 (2.5% Ro_{VIT}) in the L-49 well (dry gas). Although likely to have been an important Type II petroleum source rock in the past, these strata are now probably overmature throughout the report area (Fig. 97).

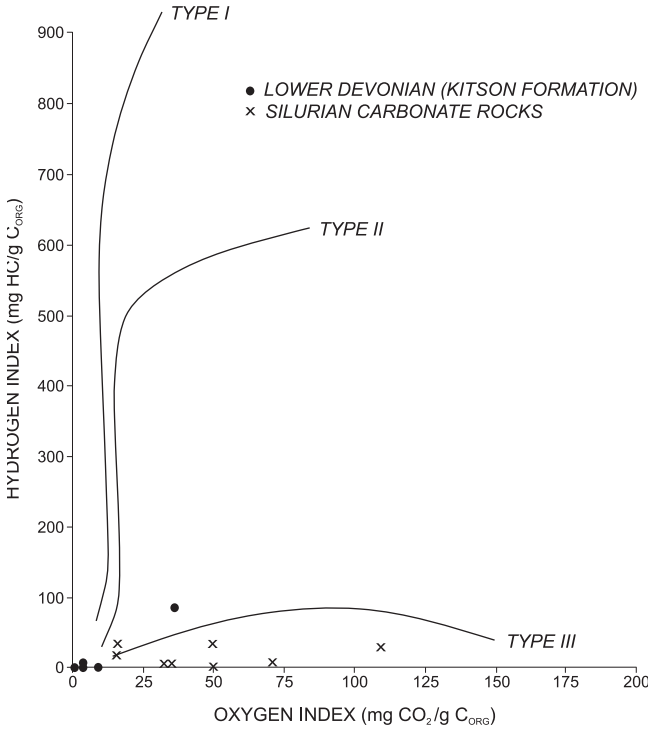

Figure 96. *Van Krevelen-type diagram based on Rock-Eval analyses of Silurian and Lower Devonian samples from the report area exploration wells.*

Blackley Formation

The Blackley Formation is a widespread succession of interbedded siliceous turbidite deposits and shale that underlies much of Prince Patrick, Eglinton and western Melville islands. The unit has a wedge-shaped profile that ranges from a minimum of 900 m in Dyer Bay L-49 to more than 3000 m in the subsurface of Green Bay area. Organic matter exists mostly as carbonized pollen grains and related terrestrial plant remains. Rock-Eval analyses have low HI values and show Type III characteristics (Fig. 98). TOC is uniformly low in the representative cuttings samples collected from Dyer Bay L-49 (0.1 to 0.2%) and Wilkie Point J-51 (0.5%), and the formation is everywhere overmature.

Cape de Bray Formation

The Cape de Bray Formation is a widespread and relatively homogeneous slope-and-basin facies silty shale unit that is Eifelian and Givetian in age west of Melville Island. Average thickness is about 900 m with local variation due to internal deformation. HI values are up to 50 mg HC/g Corg, and organic matter is Type III (Fig. 98) in the form of coalified plant remains, carbonized palynomorphs and solid bitumen. Total organic carbon has a uniform and narrow range of 0.2 to 0.3% in the Dyer Bay L-49 well and similar low values have been encountered in the Melville Island wells studied by Powell (1978). The formation lies within the wet gas range on western Melville Island and ranges to dry gas range on Prince Patrick Island. Younger formations of the Devonian clastic wedge are poor oil source rocks but lie within the oil window over a large area (Fig. 99).

Carboniferous and Permian formations

Beauchamp et al. (2001) summarized the oil-source potential of the local upper Paleozoic succession. Favourable-looking Carboniferous shale units, such as the

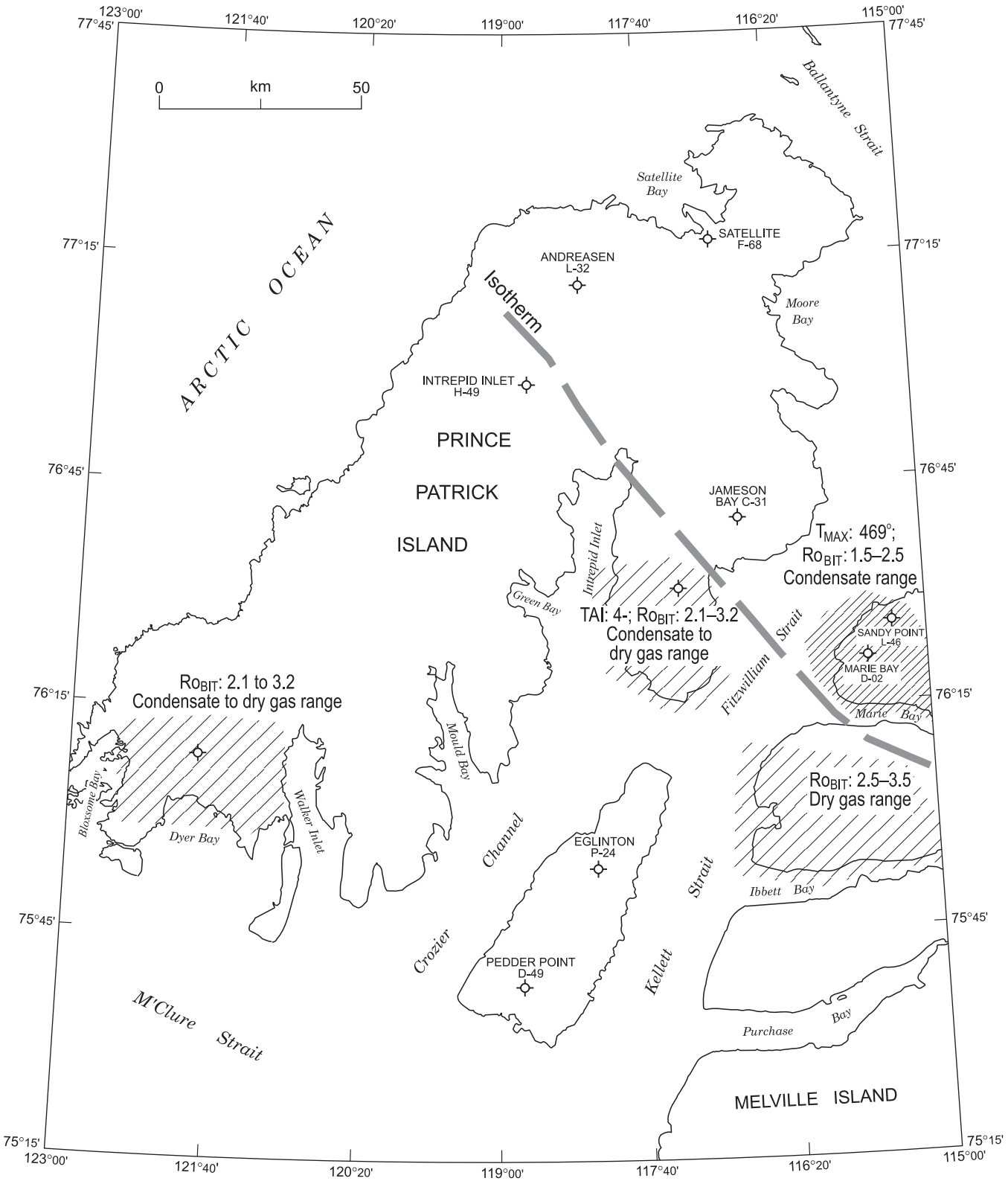

Figure 97. *Geographic variation in thermal maturity of Silurian and Lower Devonian strata (abbreviations and patterns as for Fig. 95).*

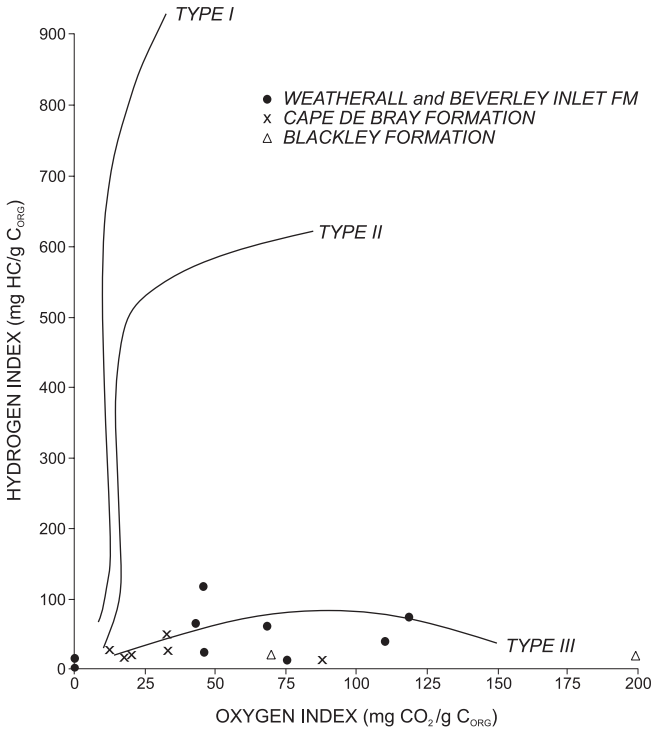

Figure 98. *Van Krevelen-type diagram based on Rock-Eval analyses of Middle and Upper Devonian samples from the area wells.*

Hare Fiord Formation, are thermally overmature where intersected in the Satellite F-68 well (Fig. 100). Permian shale and chert, including that of the Van Hauen and Trappers Cove formations, lie within the oil window (Fig. 101) but have generally low residual TOC values. The Trold Fiord Formation in the Intrepid Inlet H-49, Andreasen L-32, and Satellite F-68 wells contains a thin (0.5 m) and apparently widespread interval of coaly shale with TOC values ranging to 57%. These shales in the Andreasen L-32 and Intrepid Inlet M-49 wells are rich in terrestrial liptinite and as such could be a potential Type I hydrocarbon source. Similar facies are known from the Canyon Fiord, Belcher Channel and Sabine Bay formations elsewhere in the Arctic Islands but have not been analyzed within the report area.

Schei Point Group

Characterization and source potential of the Schei Point Group has been considered in some detail by Goodarzi et al. (1989). The thickest and most important organic-rich shale unit in the Schei Point Group on the southwestern margin of the Sverdrup Basin is found in Carnian shale units of the subsurface Hoyle Bay Formation. Source rock intervals range from 12 m thick at Wilkie Point J-51 to 100 m at Satellite F-68. TOC values range from 2.2% at Wilkie Point J-51 to more than 11% in Intrepid Inlet H-49. Samples studied by Powell (1978) showed a distribution of hydrocarbons typical of marine organic matter and excellent potential for the generation of heavy oils from suitably mature material. Petrographic studies by Goodarzi et al. (1989) indicate that the organic fraction is retained in liptinite-rich organic matter including phytoplankton (*Tasmanales* algae), dinoflagellate cysts, and alginite films. Amorphous bituminite is common in the matrix. Rock-Eval analyses indicate HI values up to 700 mg HC/g Corg. Bulk and hand-picked samples plot in the fields of Type II and even Type I kerogen (Fig. 102).The Schei Point Group is marginally mature in most subsurface areas (Fig. 103).

Grosvenor Island Formation

Hettangian(?) and Sinemurian beds are exposed east of Intrepid Inlet and occur throughout the subsurface of northeastern Prince Patrick Island to a maximum thickness of 250 m in the Satellite F-68 well. Powell (1978) found an average of about 1% TOC in this interval. Organic matter in the laterally equivalent sandstone of the Heiberg group, elsewhere in the Sverdrup Basin, occurs mostly in the form of terrestrial plant matter and thin coal stringers. These strata are mostly gas prone.

Jameson Bay Formation

The Jameson Bay Formation is a widespread Lower Jurassic marine shale that extends from a preservational limit near Mould Bay and in the subsurface of central Eglinton Island eastward to a thickness maximum of more than 300 m at Satellite F-68. In this well Powell (1978) found that organic-rich intervals are best developed in the lower part of the formation (to 3%) and the unit as a whole contains over 1% TOC. Elsewhere, to the southwest within the report area, the formation has a normal TOC range of 0.5 to 1.0%. Petrographic study shows that the organic fraction resides in recycled coal particles with some alginite. Rock-eval pyrolysis has Type III characteristics with an HI scatter between 70 and 150 mg HC/g Corg (Fig. 104).

McConnell Island and Hiccles Cove formations

The McConnell Island Formation (maximum 60 to 80 m) is the principal marine sandstone-shale unit of the Middle Jurassic and, within the report area, grades southwestward into marginal marine and deltaic quartz sandstone of the Hiccles Cove Formation (maximum 150 m). Powell (1978) found a highly variable pattern of total organic carbon in these formations, mostly less than 1% with peaks of over 2% in the Jameson Bay C-31 well, for example. Rock-eval pyrolysis of McConnell Island shale from the Intrepid Inlet H-49 well has Type III features (Fig. 104). Surface samples of the Bathonian part of the McConnell Island Formation and of the Callovian shale in the medial Hiccles Cove Formation possess strong Type III features with oxygen

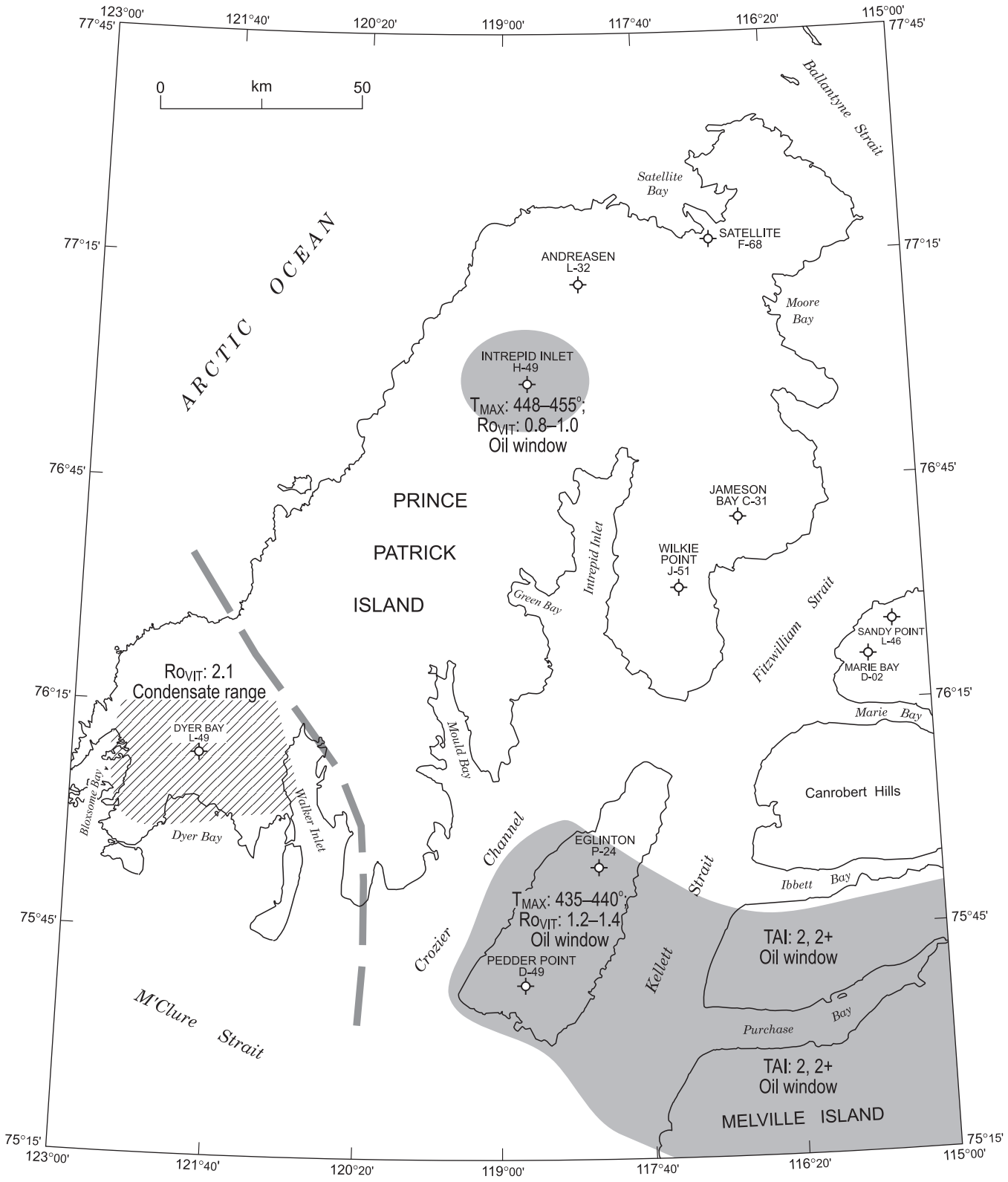

Figure 99. *Geographic variation in thermal maturity of Upper Devonian strata (abbreviations and patterns as for Fig. 95).*

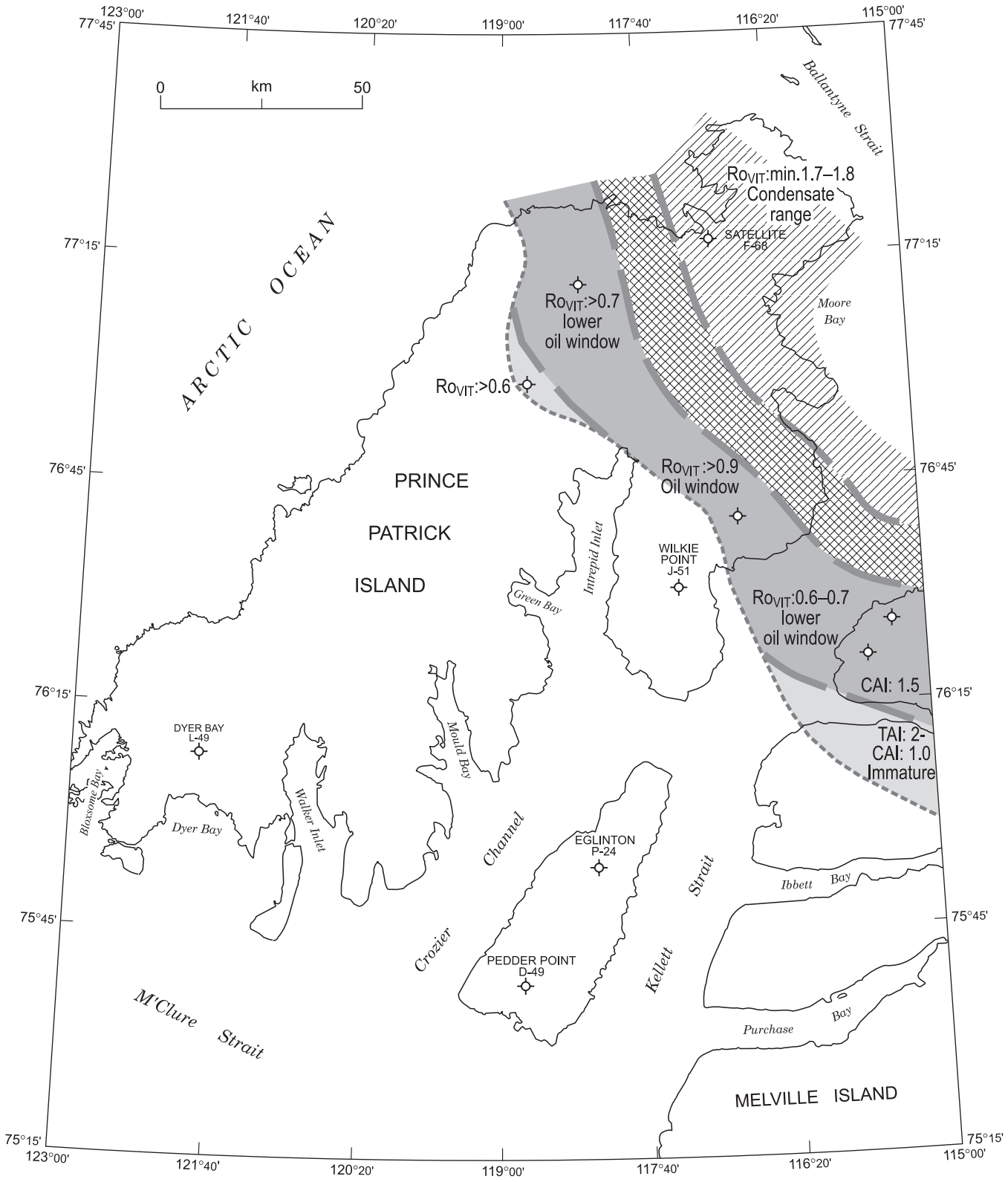

Figure 100. *Geographic variation in thermal maturity of Carboniferous and Lower Permian strata (abbreviations and patterns as for Fig. 95).*

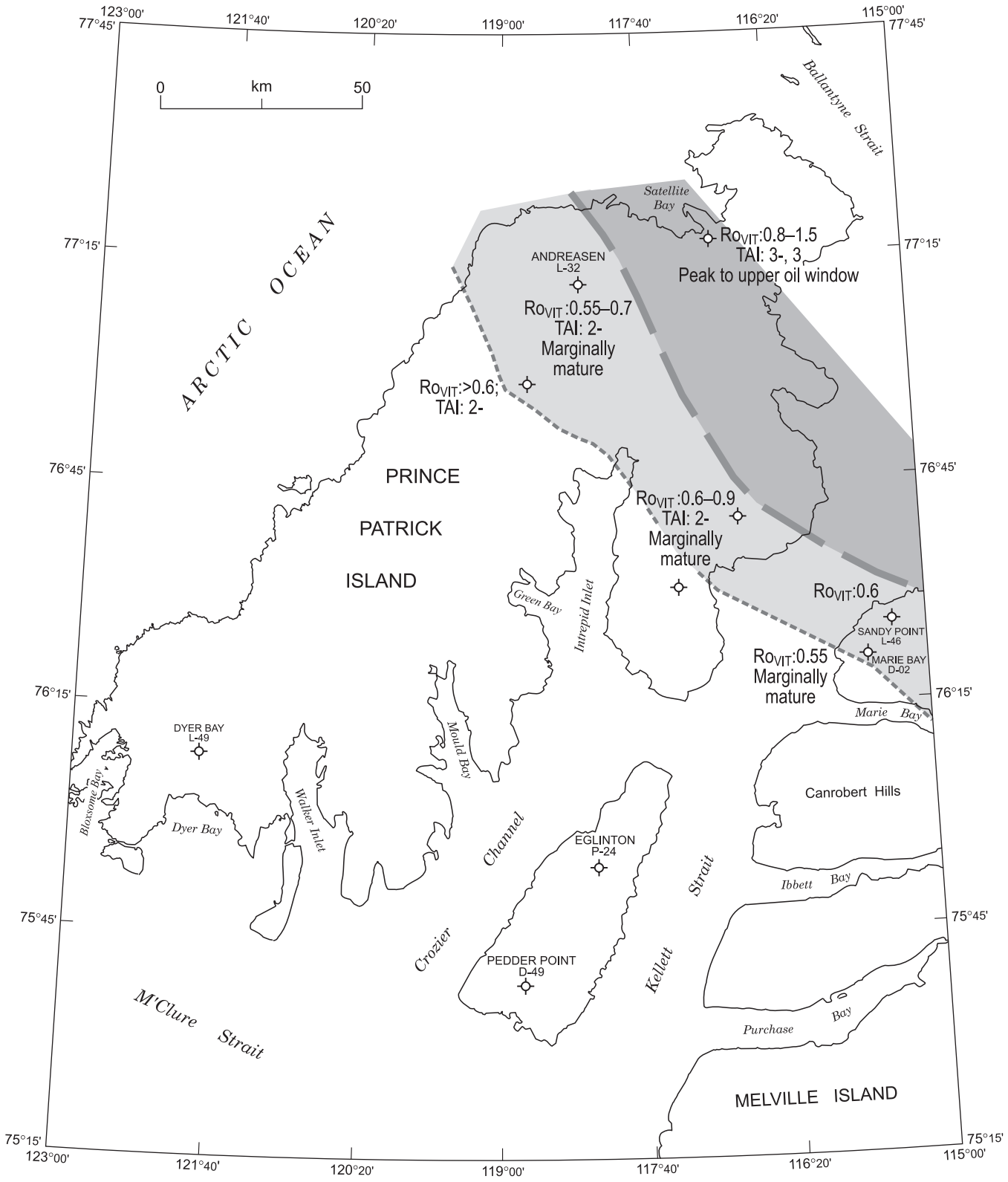

Figure 101. *Geographic variation in thermal maturity of mid- to Upper Permian strata (abbreviations and patterns as for Fig. 95).*

indices up to 318 and mostly less than 1.1% TOC. One sample, collected north of the head of Mould Bay, contained 8.4% TOC. In contrast shale intervals in the Hiccles Cove Formation in Pedder Point D-49 are oil prone with classic Type II features, HI up to 300 mg HC/g Corg and up to 5.3% TOC. These strata are immature in most areas but range to marginally mature on Eglinton Island and northeastern Prince Patrick Island (Fig. 105).

Ringnes, Awingak, and Deer Bay formations

The Ringnes Formation is a thin but widespread, marine, black shale unit of Oxfordian–Kimmeridgian age ranging from only a few metres in thickness west of Mould Bay, to more than 200 m in the Jameson Bay C-31 well. TOC profiles and sample extracts provided by Powell (1978) reveal consistent values of over 3% (some over 5%) in the lower part of the formation in the C-31 and in Emerald K-33 (on nearby southern Emerald Isle), and concentrations consistently above 1% for the formation as a whole. TOC values are 1.0 to 1.6% in Pedder Point D-49 and 1.5 to 3.3% in Eglinton P-24. Rock-eval analyses feature a mixture of Type II and Type III organic matter (Fig. 104) with HI up to 160 mg HC/g Corg. Surface samples collected around Green Bay and to the north as far as Satellite Bay contain 2.2 to 4.0% TOC. In contrast, shale interbeds in the Awingak and Deer Bay formations, and thinner intervals of the Ringnes Formation encountered in sections around and west of Mould Bay contain less than 1% TOC. All surface samples

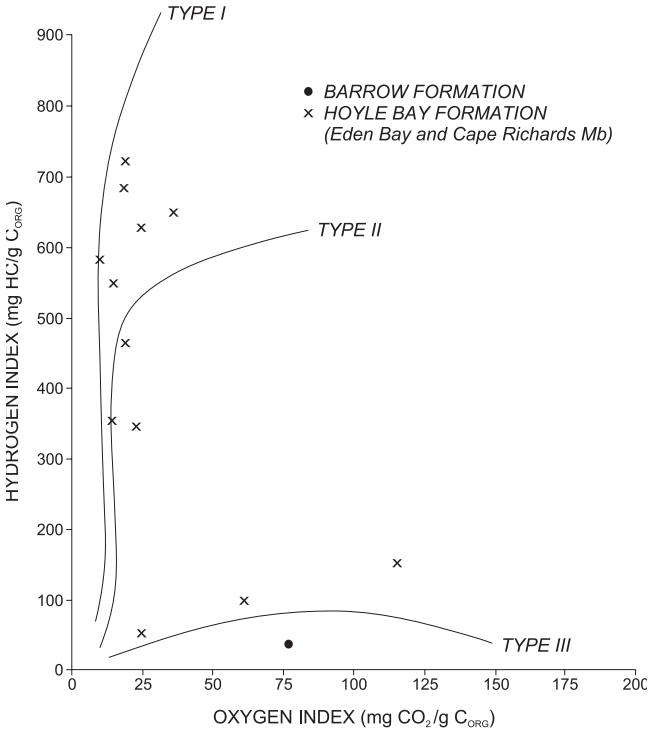

Figure 102. *Van Krevelen-type diagram based on Rock-Eval analyses of Triassic samples from the area wells.*

tend to have a pronounced Type III character with HI mostly less the 30.

Isachsen and Christopher formations

The Isachsen Formation is mostly a Barremian and Aptian quartz sandstone with intercalations of coal and minor silty shale. Coal cuttings examined from the Pedder Point D-49 well contain humodetrinite and abundant phlobaphinite. Rock-Eval analyses reveal a mixture of Type III and Type II organic matter with HI between 80 and 310 (Fig. 106). Although somewhat gas prone, overall TOC for the formation is low.

The Albian Christopher Formation is widely preserved throughout the report area but has been intersected only in the Pedder Point D-49 and Eglinton P-24 wells on Eglinton Island. Surface samples collected from the lower 100 m of the formation around Mould Bay and north of Jameson Bay contain 3.3 to 5.8% TOC. Likewise, TOC values in the area wells are highest in the lower part of the formation (3.0 to 4.9% over 50 m) and are also consistently elevated in the upper part of the formation (2.1 to 3.0% over 270 m). Similar results are reported by Powell (1978) from wells on northeastern Melville Island. Rock-Eval pyrolysis indicates typical Type III organic matter with a narrow HI range of less than 60 and gas-prone characteristics for both surface samples and subsurface cuttings (Fig. 106). Collected material is thermally immature on Prince Patrick Island and ranges to marginally mature on Eglinton Island (Fig. 107).

Kanguk Formation

Organic-rich marine shale and bentonite of the Upper Cretaceous (Cenomanian–Campanian) Kanguk Formation are preserved only on Eglinton Island and in the surrounding offshore. These strata have been intersected in the Pedder Point D-49 well. TOC is highest in the lower part (7.9 to 12.1% over 15.5 m as obtained from surface samples) but is also consistently elevated through the remainder of the formation (1.0 to 3.7% TOC over 240 m measured on well cuttings). Rock-Eval analyses have Type II features (Fig. 106). HI range is 50 to 470 mg HC/g Corg. The Kanguk Formation has good oil-source potential but is undermature on Eglinton Island.

Hydrocarbon occurrences

There was no significant flow of hydrocarbons in any of the exploration wells drilled within the report area (Fig. 94). Visible pyrobitumen occurs locally in the Silurian carbonate deposits in Wilkie Point J-51, in the Lower Devonian Kitson Formation, and in the lowest part of the overlying Blackley Formation in Dyer Bay L-49. In the Intrepid Inlet H-49

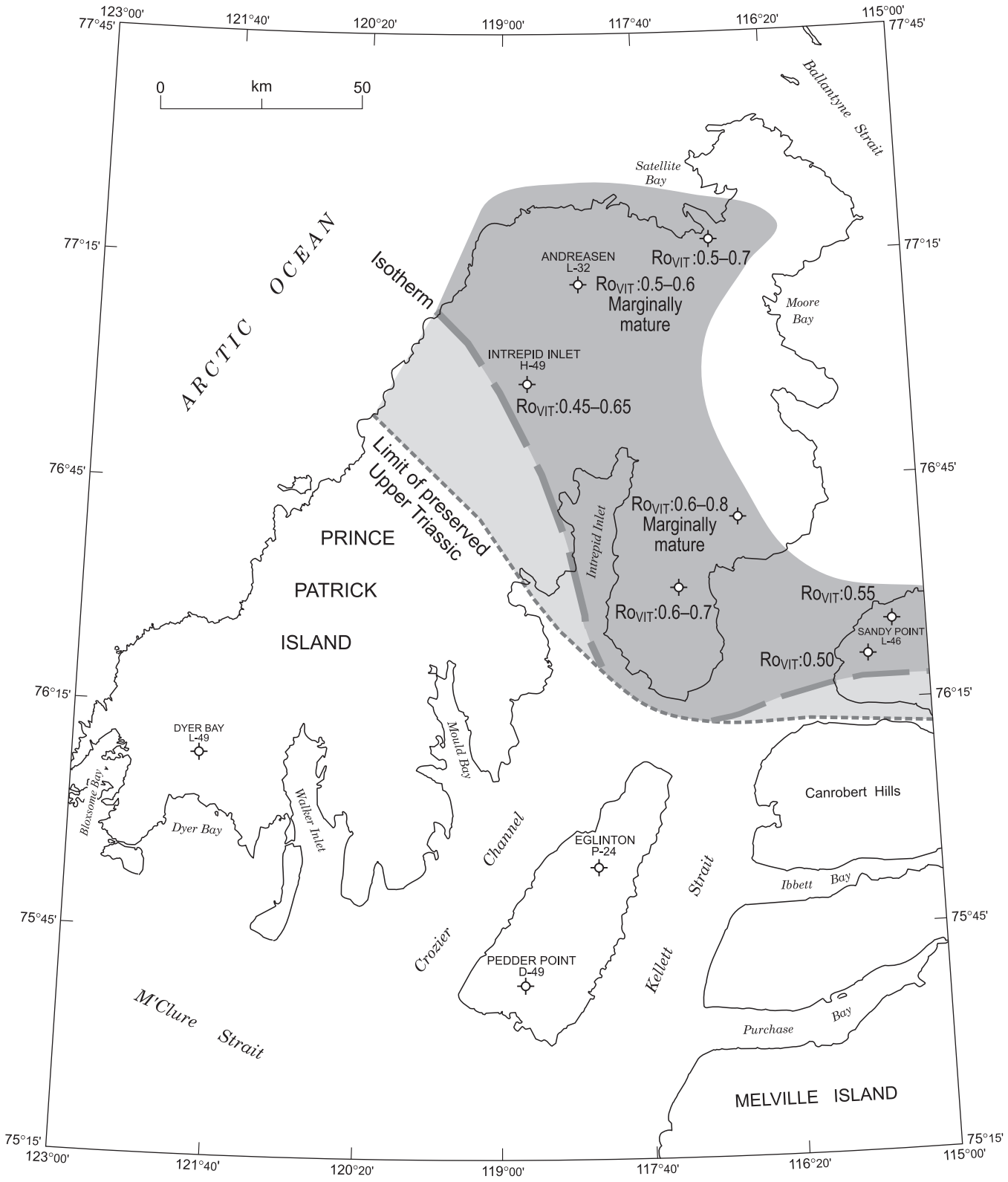

Figure 103. *Geographic variation in thermal maturity of Upper Triassic strata (abbreviations and patterns as for Fig. 95).*

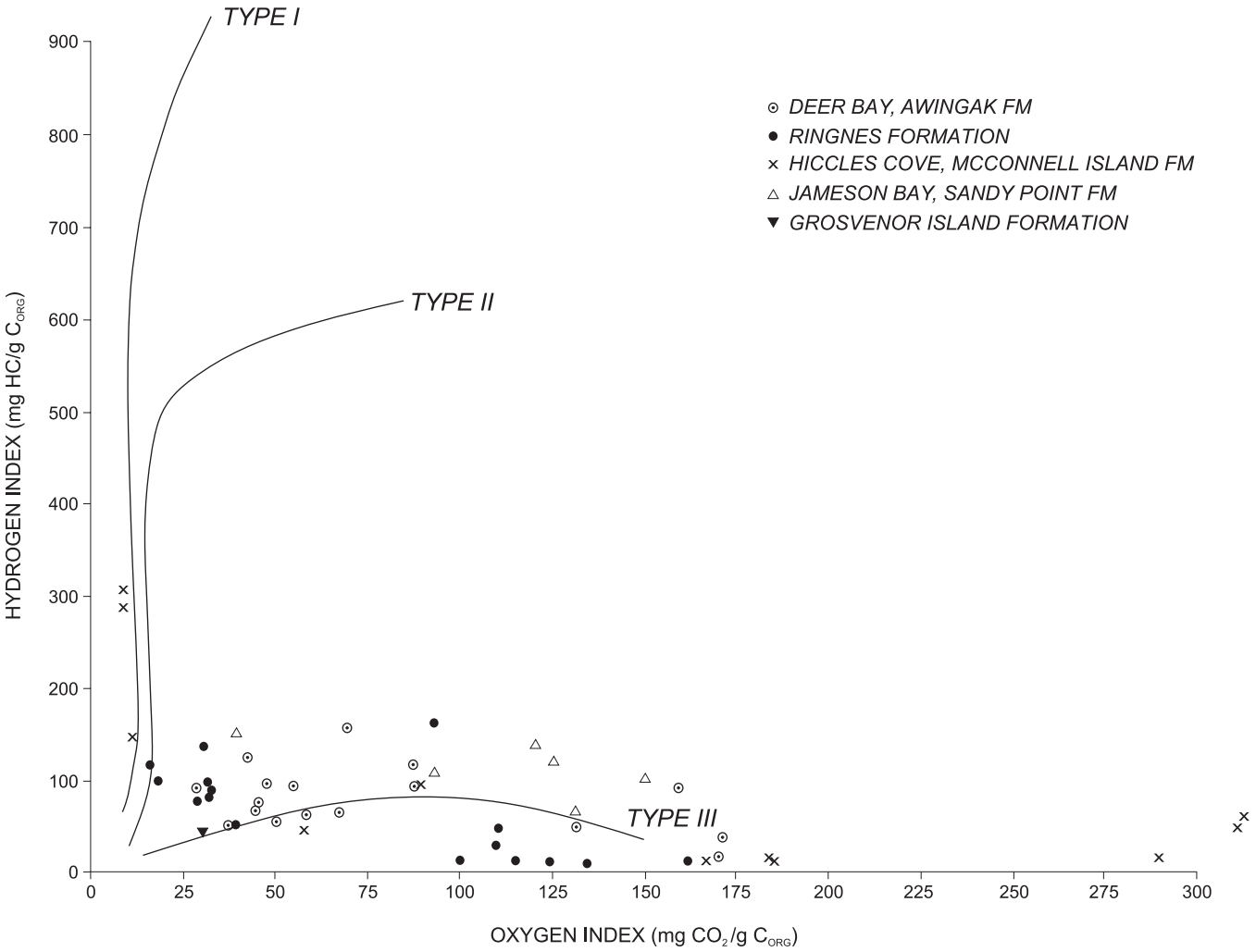

Figure 104. *Van Krevelen-type diagram based on Rock-Eval analyses of Jurassic samples from the area wells.*

well, oil staining is well developed in the medial Trold Fiord Formation (mid-Permian), and in the Andreasen L-32 well staining occurs in sandstone intervals of the Murray Harbour Formation (Middle Triassic) and in the Gore Point Member limestone (Upper Triassic). Bitumen occupies modest matrix porosity in the upper part of the Bjorne Formation (Lower Triassic) beneath a Murray Harbour Formation seal in the Satellite F-68 well. Outside the report area on nearby northwestern Melville Island, ten significant bitumen deposits occur in the Bjorne Formation near the updip limit of this formation on the Sverdrup Basin margin of southern Sproule Peninsula (Trettin and Hills, 1966). Live oil also occurs in exposures of the Isachsen Formation (Lower Cretaceous) on northern Sproule Peninsula (Harrison, 1995).

Gas, detected during mud logging, was most productive from the top of the Bjorne Formation and generally from the Schei Point Group (Middle and Upper Triassic) in Satellite F-68, from the Gore Point Member and Hoyle Bay Formation in Andreasen L-32 and, to a lesser extent, from the top of the Trold Fiord Formation also in L-32.

Indirect evidence of former discharge of natural gas from Lower Cretaceous strata is provided by the occurrence, in two places, of syndepositional methogenic carbonate mounds and fossilized serpulid-bivalve cold seep communities in the Lower Albian part of the Christopher Formation (Beauchamp et al., 1989a, b). Both mounds are situated along the surface trace of the Carbonate Mounds Fault west of Mould Bay. Although the specific methane source rock is unknown, the fault roots in gas-prone Devonian foreland clastic deposits and carries gas-prone Ringnes, Awingak, Isachsen ,and Christopher formations in the hanging wall.

Conceptual exploration plays

New opportunities on tested plays

A carbonate shelf edge situated on an anticlinal culmination in the lower Paleozoic was probably part of the motivation for drilling the Dyer Bay L-49 well (cross-section D; Fig. 30, 31, 35). While favourable Lower Devonian

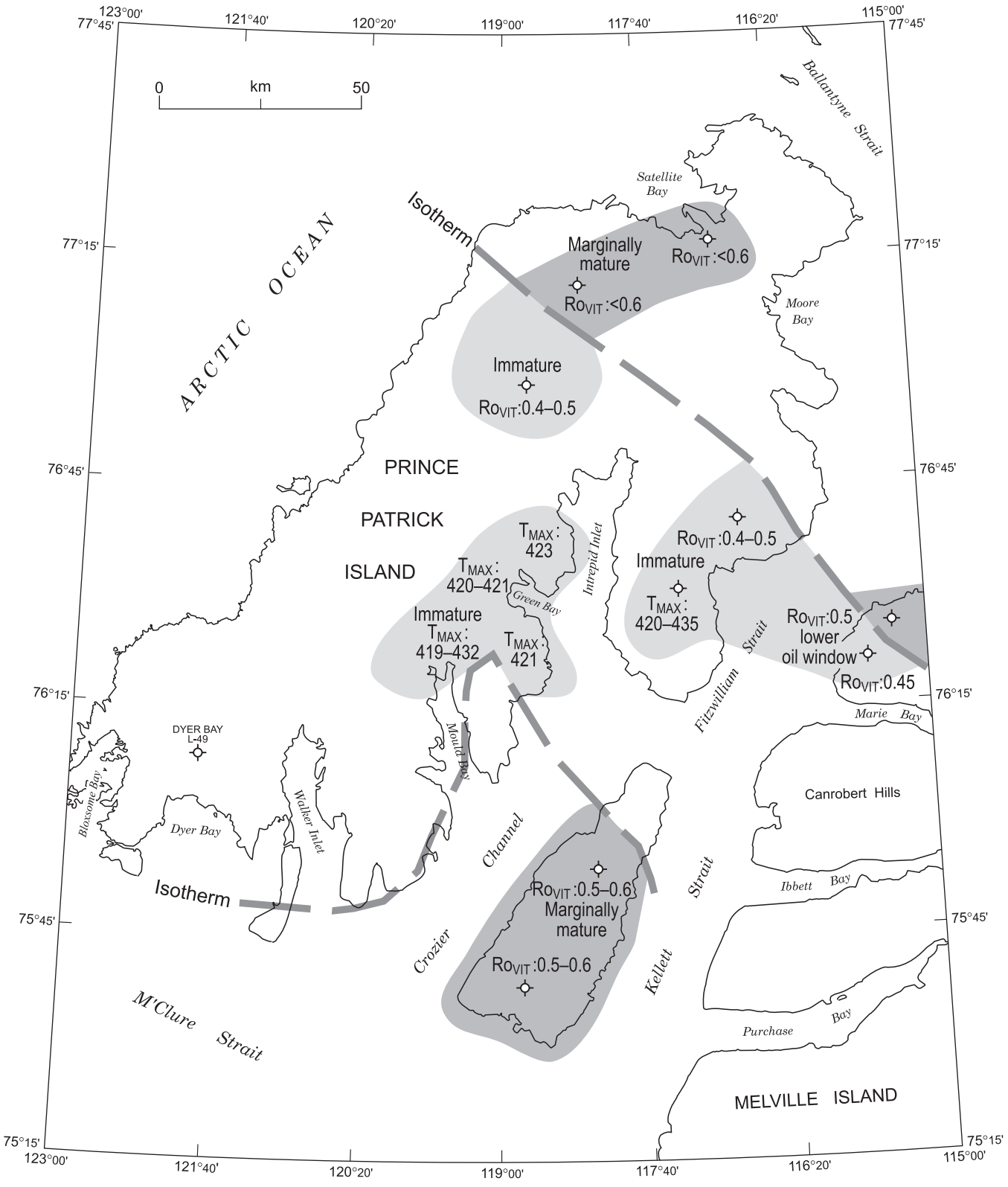

Figure 105. *Geographic variation in thermal maturity of Middle Jurassic strata (abbreviations and patterns as for Fig. 95).*

carbonate deposits may have been hoped for, as at Bent Horn (on Cameron Island), drilling found overmature conditions and Silurian carbonate units with low porosity. A structural high was also penetrated at the Wilkie Point J-31 well (cross-section C; Fig. 30, 31). There is no indication, however, that this well was intentionally drilled on a lower Paleozoic structural target and there is nothing to indicate that closure may exist at this location below the sub-Triassic angular unconformity. Remaining to be tested in the lower Paleozoic succession are at least eight other anticlinal culminations (Fig. 30). All but one of these lie in the subsurface fold-thrust belt northeast of Intrepid Inlet. Infill seismic profiles would probably reveal others.

Anticlinal closure was also clearly the structural target for the Satellite F-68 and Intrepid Inlet H-49 wells (cross-section D; Fig. 47, 82). Both structures are believed to be associated with southwesterly directed, compressive, Cenozoic deformation. For the Moore Bay Anticline at the Satellite F-68 well, there is no indication of a specific stratigraphic target in the structure, and the location of the apex of the culmination remains ill-defined as there is insufficient seismic control to the northwest. The culmination at Intrepid Inlet H-49 is better defined although the structure is complicated by many small faults of uncertain strike direction. The well is situated close to the Sverdrup Basin margin where stratigraphic traps are likely at the updip limit of various Triassic reservoir sands. The Jameson Bay C-31 well was drilled on a modestly inverted rollover anticline expressed in Triassic and Jurassic strata above a buried Carboniferous graben (Fig. 39). The principal stratigraphic target was probably favourable

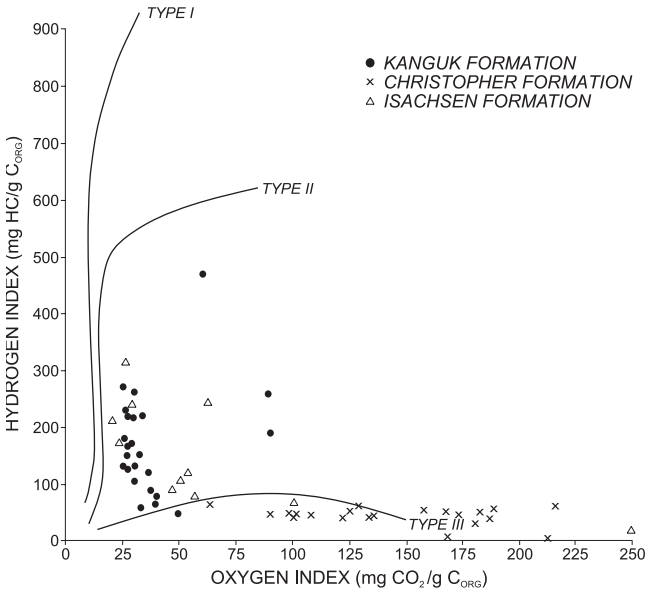

Figure 106. *Van Krevelen-type diagram based on Rock-Eval analyses of Cretaceous samples from the area wells.*

reservoir sands in the Triassic and Lower Jurassic. Other anticlines of probable Cenozoic age are illustrated on Figure 82. Although most are smaller than the structures at F-68 and H-49, the magnitude of closure for each remains poorly defined on the existing set of early-vintage low-fold and single-fold seismic profiles.

Subtle structural closure may have been detected in Jurassic strata at the Wilkie Point J-51 well. However, the principal intent was probably to test for trapped hydrocarbons at the updip limit of the Lower Triassic Bjorne Formation (cross-section C; Fig. 17, 51). The play is sealed by overstepping younger shale, as is the case for bitumen deposits on Sproule Peninsula (Trettin and Hills, 1966). Unconformity-related stratigraphic targets remain a highly promising setting for future exploration on Prince Patrick Island. The most favourable area is a 25 km wide and more than 125 km long belt situated northeast of Green Bay and on Wilkie Point at the updip preservation limit of various Lower through Upper Triassic and Lower Jurassic reservoir sands (Fig. 51).

New plays

While much of the lower Paleozoic, including the favourable source rock of the Lower Devonian, is presently overmature, there is no question that the known source beds passed through the oil window and in so doing must have generated a significant quantity of Type II hydrocarbon. Preservation of Lower Devonian-sourced oils would be most likely to have occurred in Upper Devonian reservoir sands, strata still widely preserved in the regional-scale synclines of central Prince Patrick Island. Specific targets could be identified with infill reflection seismic profiling.

Favourable thermal conditions exist for the production, migration, entrapment and preservation of gas and potentially some oil in the Carboniferous and Lower Permian succession. Stratigraphic targets to be considered include sandstone and conglomerate ranging from Serpukhovian(?) to Kungurian in age that are sealed by either Hare Fiord Formation or Van Hauen Formation in syndepositional grabens or graben inversion structures that may have formed structural traps on northeastern Prince Patrick Island (see Fig. 37 for location of grabens). Improved definition of these structures would be provided by a northeast-trending grid of higher-fold seismic profiles.

The most attractive plays in the Triassic and Lower Jurassic are basin-margin unconformity-related stratigraphic targets as previously described. Above this level, successful exploration of Middle Jurassic and younger strata will rely on definition of plays that assume long-distance migration of hydrocarbons from either mature source rocks of Lower Jurassic and older age of the

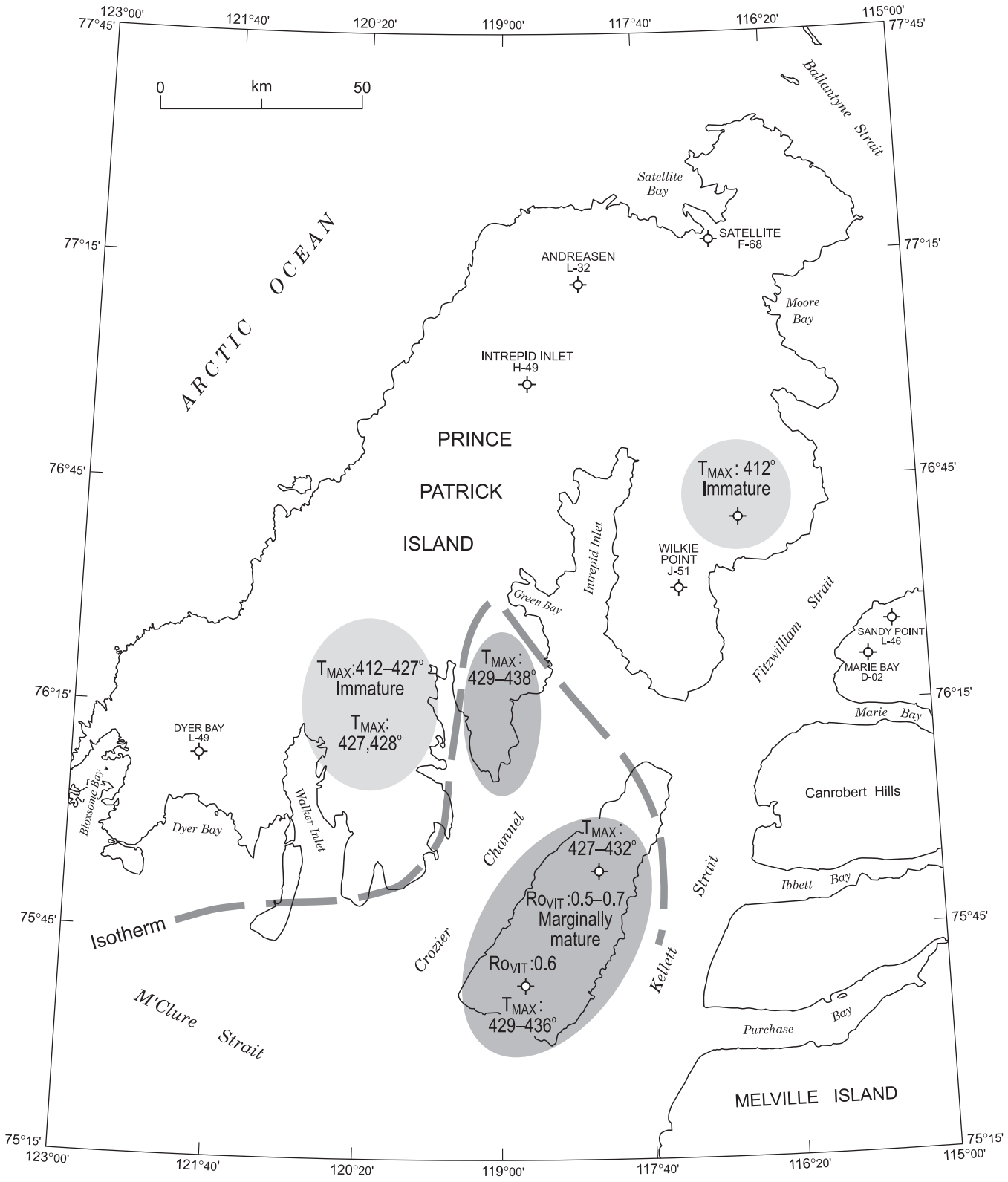

Figure 107. *Geographic variation in thermal maturity of Cretaceous strata (abbreviations and patterns as for Fig. 95).*

Sverdrup Basin, or from younger mature source rocks (i.e., Kanguk Formation) presumed to exist on the Arctic continental shelf. The most promising reservoirs include various clean quartz sands such as the Callovian part of the Hiccles Cove Formation, the Awingak, Isachsen, and Hassel formations. Suitable seals include various widespread shale units, most notably the Ringnes, Christopher, and Kanguk formations. Favourable traps, apart from Cenozoic anticlinal closures, probably exist in various Middle Jurassic through Lower Cretaceous horst-and-graben structures (Fig. 52); settings similar to those that host the Atkinson Point oil field and the Parsons gas discovery, both situated in Lower Cretaceous sandstone in the eastern Beaufort Basin (Morrell, 1996a, b).

Coal

Thin, bituminous-grade coal seams, nowhere found to exceed 30 cm in thickness, and coaly shale beds occur in the Weatherall, Beverley Inlet, and Parry Islands formations throughout the outcrop belt east and west of Mould Bay (Fig. 94).

Subbituminous grade coal also occurs in the Isachsen Formation. The thickest surface seams, reported by Tozer and Thorsteinsson (1964), occur in the Isachsen Formation 10 km northeast of Mould Bay Station (to 1.5 m thick) and in flat-lying exposures of the same formation on northern Eglinton Island (to 1 m thick). Coaly shale is also common in many Isachsen Formation sections including those east of the Mould Bay weather station. In the subsurface, Isachsen Formation coal seams are encountered in the Pedder Point D-49 and Eglinton P-24 wells. Detailed petrographic studies reveal a predominance of huminite group macerals with humotelinite (22.3 to 70.7%) in excess of humocollinite (14.0 to 34.0%). Corpohuminite and humodetrinite comprise the remaining macerals in this group. Sporinite and cutinite are the common liptinite macerals (1.3 to 17.9%). Total inertinite ranges from < 2.0 to 44.4%, with semifusinite dominant over fusinite.

Elsewhere in the subsurface, seams of liptinitic coal and coaly shale in intervals to 1 m thick occur in the Trold Fiord Formation in the Andreasen L-32 and Intrepid Inlet H-49 wells (Beauchamp et al., 2001).

We have not been able to confirm the report by Tozer and Thorsteinsson (1964) of a 3 ft. (1 m) thick seam of subbituminous B grade coal in Wilkie Point strata 7 km north of Salmon Point on the west side of Intrepid Inlet. However, thin coal seams (10 cm) and coaly shale beds are a frequent occurrence in the mostly nonmarine Callovian part of the Hiccles Cove Formation. It is these beds that are the likely host for locally thicker seams.

Metals and minerals

Beds and nodules of earthy to submetallic grey pisolitic rhodochrosite ($MnCO_3$) are a common occurrence in the Eglinton Member of the Kanguk Formation on Eglinton Island (Fig. 94). Manganese oxides and manganese carbonates are also a common matrix cement, and ubiquitous surface or fracture stain in this sandstone. Bedsets of manganese-rich sandstone occur in intervals up to several metres thick, with individual grab samples containing up to 65% manganese carbonate (Fig. 108). The lateral continuity and economic significance of these manganese occurrences has not been established.

Figure 108. *Gun-metal grey rhodochrosite-cemented sandstone, Eglinton Member of the Kanguk Formation of southern Eglinton Island. The rock hammer is 30 cm in length and the height of the outcrop is 2.4 m. Grab samples contain up to 65% MnCO3 (GSC photo HBB-R5-10-1991).*

REFERENCES

Aldighieri, A.M. (ed.)
1996: Canadian Almanac and Directory; Toronto, C.A. and D. Publishing Co. Ltd.

Armstrong, Sir Alexander
1857: A personal narrative of the discovery of the Northwest Passage; London, Hurst and Blackett, 616 p.

Balkwill, H.R. and Fox, F.G.
1982: Incipient rift zone, western Sverdrup Basin; *in* Arctic Geology and Geophysics, (ed.) A.F. Embry and H.R. Balkwill; Canadian Society of Petroleum Geologists, Alberta, p. 171–187.

Balkwill, H.R., McMillan, N.J., MacLean, B., Williams, G.L., and Srivastava, S.P.
1990: Geology of the Labrador Shelf, Baffin Bay, and Davis Strait; Chapter 7 *in* Geology of the Continental Margin of Eastern Canada, (ed.) M.J. Keen and G.L. Williams; Geological Survey of Canada, Geology of Canada, No. 2, p. 293–348.

Banerjee, I. and Davies, E.H.
1986: An integrated lithostratigraphic and palynostratigraphic study of the Ostracode Zone and adjacent strata in the Edmonton Embayment, central Alberta; *in* Sequences, stratigraphy, sedimentology: surface and subsurface, (ed.) D.P. James and D.A. Leckie; Canadian Society of Petroleum Geologists, Memoir 15, p. 261–274.

Basov, V.A., Wall., J.H., Sokolov, A.R., Yakovlev, S.P., Poulton, T.P., and Embry A.F.
1992: The *Riyadhella sibirica* foraminiferal zone in the Middle Jurassic of northern Russia and Canada; Abstracts, International Conference on Arctic Margins, Anchorage, Alaska, p. 63.

Beauchamp, B.
1987: Stratigraphy and facies analysis of the Upper Carboniferous to Lower Permian Canyon Fiord, Belcher Channel and Nansen formations, southwestern Ellesmere Island; Ph.D. thesis, University of Calgary, 370 p.

Beauchamp, B. and Henderson, C.M.
1994: The Lower Permian (Artinskian) Raanes, Great Bear Cape, and Trappers Cove formations: three new stratigraphic units of the Sverdrup Basin, Canadian Arctic; Bulletin of Canadian Petroleum Geology, v. 42, p. 562–597.

Beauchamp, B. and Savard, M.
1992: Cretaceous chemosynthetic mounds in the Canadian Arctic; Palaios, v. 7, p. 434–450.

Beauchamp, B., Harrison, J.C., and Henderson, C.M.
1989a: Upper Paleozoic stratigraphy and basin analysis of the Sverdrup Basin, Canadian Arctic Archipelago: 1 - time frame and tectonic evolution; *in* Current Research, Part G; Geological Survey of Canada, Paper 89-1G, p. 105–113.

1989b: Upper Paleozoic stratigraphy and basin analysis of the Sverdrup Basin, Canadian Arctic Archipelago: 2 - transgressive-regressive sequences; *in* Current Research, Part G; Geological Survey of Canada, Paper 89-1G, p. 115–124.

Beauchamp, B., Harrison, J.C., Nassichuk, W.W., and Eliuk, L.S.
1989c: Lower Cretaceous (Albian) serpulid-bivalve carbonate "mounds" related to hydrocarbon seeps, Canadian Arctic Archipelago; *in* Reefs - Canada and Adjacent Areas, (ed.) H.J. Geldsetzer, N.P. James, G.E. Tebbutt, and D.J. Glass; Canadian Society of Petroleum Geologists, Memoir 13, p. 706–712.

Beauchamp, B., Harrison, J.C., Utting, J., Brent, T.A., and Pinard, S.
2001: Carboniferous and Permian subsurface stratigraphy, Prince Patrick Island, Canadian Arctic; Geological Survey of Canada, Bulletin 565, 93 p.

Beauchamp, B., Krouse, H.R., Harrison, J.C., Nassichuk, W.W. and Eliuk, L.S.
1989d: Cretaceous cold seep “life oases” and methane- derived carbonates in the Canadian Arctic; Science, v. 244, p. 53–56.

Beauchamp, B., Theriault, P., Henderson, C.M., Lin, R., and Pinard, S.
1998: Carboniferous to Triassic formations of the Sverdrup Basin; *in* The Geology of Devon Island north of 76°, Canadian Arctic Archipelago; Geological Survey of Canada, Bulletin 526, p. 195–233.

Berry, M.J. and Barr, K.G.
1971: A seismic refraction profile across the polar continental shelf of the Queen Elizabeth Islands; Canadian Journal of Earth Sciences, v. 8, p. 347–360.

Brent, T.A. and Harrison, J.C.
1998: Characterization and mapping of the permafrost zone on land based seismic reflection data, Canadian Arctic Islands; Proceedings of the 7th International Conference on Permafrost, Yellowknife, N.W.T.

British Parliamentary Papers
1855: Further papers relative to the recent Arctic Expeditions in search of Sir John Franklin and the crews of H.M.S. *Eerebus* and *Terror*; London, Eyre and Spottiswoode, for H.M. Stationery Office, 958 p.

Callomon, J.H.
1993: Jurassic ammonite biochronology of Greenland and the Arctic; Geological Society of Denmark Bulletin, v. 41, p. 128–137.

Canadian Hydrographic Service
1982: Sailing Directions - Arctic Canada, (Third edition) vol. 1; Ottawa, Deptartment of Fisheries and Oceans, 284 p.

Carey, S.W.
1957: A tectonic approach to continental drift; *in* Proceedings of a Symposium on Continental Drift; University of Tasmania, p. 177–355.

Chalmers, J.A., Dahl-Jensen, T., Bate, K.J., and Whittaker, R.C.
1995: Geology and petroleum prospectivity of the region offshore southern West Greenland - a summary; *in* Rapport, Gronlands Geologiske Undersogelse, v. 165, p. 13–21.

Chi, B.I and Hills, L.V.
1976: Biostratigraphy and taxonomy of Devonian megaspores; Bulletin of Canadian Petroleum Geology, v. 24, p. 640–818.

Coles, R.L.
1991: Aeromagnetic field; Chapter 5 *in* Innuitian Orogen and Arctic Platform of Canada and Greenland, (ed.) H.P. Trettin; Geological Survey of Canada, Geology of Canada No. 3 (*also*, The Geology of North America, Geological Society of America, v. E, p. 84–88).

Cope, J.C.W., Getty, T.A., Howarth, M.K., Morton, N., and Torrens, H.S.
1980a: A correlation of Jurassic rocks in the British Isles, Part 1, Introduction and Lower Jurassic; Geological Society of London, Special Report, 14, 73 p.

Cope, J.C.W., Duff, K.L., Parsons, C.F., Torrens, H.S., Wimbledon, W.A., and Wright J.K.
1980b: A correlation of Jurassic rocks in the British Isles, Part 2, Middle and Upper Jurassic; Geological Society of London, Special Report, 15, 109 p.

Correia, M.
1969: Contribution à la recherche des zones favorables à la genèse du pétrole par l'observation microscopique de la matière organique figurée; Revue de l'Institute français du pétrole, v. 24, p. 1417–1454.

Daae, H.D. and Rutgers, A.T.C.
1975: Geological history of the Northwest Passage; Bulletin of Canadian Petroleum Geology, v. 23, p. 84–108.

Davies, E.H.
1983: The dinoflagellate Oppel-zonation of the Jurassic-Lower Cretaceous sequence in the Sverdrup Basin, Arctic Canada; Geological Survey of Canada, Bulletin 359, 59 p.

Davies, G.R. and Nassichuk, W.W.
1991: Carboniferous to Permian geology of the Sverdrup Basin, Canadian Arctic Archipelago; *in* Innuitian Orogen and Arctic Platform: Canada and Greenland, (ed.) H.P. Trettin; Geological Survey of Canada, Geology of Canada No. 3 (*also*, The Geology of North America, Geological Society of America, v. E, p. 343–367).

Dawson, E. and Newitt, L.R.
1984: Magnetic declination in Canada from 1750 to 1980; The Canadian Surveyor, v. 38, p. 35–40.

de Paor, D.G., Bradley, D.C., Eisenstadt, G., and Phillips, S.M.
1989: The Arctic Eurekan orogen: A most unusual fold-and-thrust belt; Geological Association of America, Bulletin, v. 101, p. 952–967.

de Freitas, T., Mayr, U., and Harrison, J.C.
1997: Sequence stratigraphic correlation charts of the lower Paleozoic Franklinian succession, Canadian Arctic and parts of North Greenland; Geological Survey of Canada, Open File 3410, 3 charts.

Devaney, J.R.
1991: Clastic sedimentology of the Beaufort Formation, Prince Patrick Island, Canadian Arctic islands; late Tertiary sandy braided river deposits with woody detritus beds; Arctic, v. 44, no. 3, p. 206–216.

Dix, C.H.
1955: Seismic velocities from surface measurements; Geophysics, v. 20, p. 68–86.

Dixon, J. (ed.)
1996: Geological atlas of the Beaufort - Mackenzie area; Geological Survey of Canada, Miscellaneous Report 59, 173 p.

Dixon, J. and Dietrich, J.R.
1990: Canadian Beaufort Sea and adjacent land areas; *in* The Arctic Ocean Region, (ed.) A. Grantz, L. Johnson, and J.F. Sweeney; The Geology of North America, Geological Society of America, v. L, p. 239–256.

Dunbar, M. and Greenaway, K.R.
1956: Arctic Canada from the Air; Canada, Defence Research Board, Queen's Printer, Ottawa, 541 p.

Edlund, S.A. and Alt, B.T.
1989: Regional congruence of vegetation and summer climate patterns in the Queen Elizabeth Islands, Northwest Territories, Canada; Arctic, v. 42, p. 3–23.

Embry, A.F.
1984a: The Schei Point and Blaa Mountain groups (Middle-Upper Triassic) Sverdrup Basin, Canadian Arctic Archipelago; *in* Current Research, Part B; Geological Survey of Canada, Paper 84-1B, p. 327–336.

1984b: Stratigraphic subdivision of the Roche Point, Hoyle Bay and Barrow formations (Schei Point Group), western Sverdrup Basin, Arctic islands; *in* Current Research, Part B; Geological Survey of Canada, Paper 84-1B, p. 327–336.

1990: Geological and geophysical evidence in support of the hypothesis of anticlockwise rotation of northern Alaska; Marine Geology, v. 93, p. 317–330.

1991a: Mesozoic history of the Arctic Islands; Chapter 14 *in* Innuitian Orogen and Arctic Platform: Canada and Greenland, (ed.) H.P. Trettin; Geological Survey of Canada, Geology of Canada No. 3 (*also*, The Geology of North America, Geological Society of America, v. E, p. 369–433).

1991b: Middle-Upper Devonian clastic wedge of the Arctic Islands; Chapter 10 *in* Innuitian Orogen and Arctic Platform: Canada and Greenland, (ed.) H.P. Trettin; Geological Survey of Canada, Geology of Canada No. 3 (also, The Geology of North America, Geological Society of America, v. E, p. 261–279).

Embry, A.F. and Dixon, J.
1994: Age of the Amerasia Basin; *in* 1992 Proceedings, International Conference on Arctic Margins, (ed.) D.K. Thurston and K. Fujita; U.S. Department of the Interior, Minerals Management Service, Anchorage, Alaska, p. 289–294.

Embry, A.F. and Klovan, J.E.
1976: The Middle-Upper Devonian clastic wedge of the Franklinian Geosyncline; Bulletin of Canadian Petroleum Geology, v. 24, p. 485–639.

Embry, A.F. and Osadetz, K.G.
1988: Stratigraphy and tectonic significance of Cretaceous volcanism in the Queen Elizabeth Islands; Canadian Journal of Earth Sciences, v. 25, p. 1209–1219.

Epstein, A.G., Epstein, J.B., and Harris, L.D.
1991: Conondont color alteration - an index to organic metamorphism; United States Geological Survey Professional Paper 995, 27 p.

Forsyth, D.A., Broome, J., Embry, A.F., and Halpenny, J.F.
1990: Features of the Canadian Polar Margin; Marine Geology, v. 93, p. 147–177.

Fortier, Y.O. and Morley, L.W.
1956: Geological unity of the Arctic Islands; *in* Proceedings of a symposium on the Ocean Floors of Canada, Transactions of the Royal Society of Canada, v. 50, ser. 3 p. 3–12.

Fortier, Y.O. and Thorsteinsson, R.
1953: The Parry Islands Fold Belt in the Canadian Arctic Archipelago; American Journal of Science, v. 251, p. 259–267.

Fortier, Y.O., McNair, A.H., and Thorsteinsson, R.
1954: Geology and Petroleum Possibilities in Canadian Arctic islands; American Association of Petroleum Geologists, Bulletin, v. 38, no. 10, p. 2075–2109.

Frebold, H.
1957: The Jurassic Fernie Group in the Canadian Rocky Mountains and Foothills; Geological Survey of Canada, Memoir 287, 197 p.

1958: Stratigraphy and correlation of the Jurassic in the Canadian Rocky Mountains and Foothills; *in* Jurassic and Carboniferous of Western Canada, (ed.) A.J. Goodman; John Andrew Allan Memorial Volume, American Association of Petroleum Geologicsts, p. 10–26.

1960: The Jurassic faunas of the Canadian Arctic; Lower Jurassic and lowermost Middle Jurassic ammonites; Geological Survey of Canada, Bulletin 59, 63 p.

1961: The Jurassic faunas of the Canadian Arctic, Middle and Upper Jurassic ammonites; Geological Survey of Canada, Bulletin 74, 43 p.

1975: The Jurassic faunas of the Canadian Arctic, Lower Jurassic ammonites, biostratigraphy and correlations; Geological Survey of Canada, Bulletin 243, 35 p.

Fyles, J.G.
1990: Beaufort Formation (Late Tertiary) as seen from Prince Patrick Island, Arctic Canada; Arctic, v. 43, no. 4, p. 393–403.

Fyles, J.G., Hills, L.V., Matthews, J.V., Jr., Barendregt, R., Baker, J., Irving, E., and Jetté, H.
1994: Ballast Brook and Beafort formations (Late Tertiary) on northern Banks Island, Arctic Canada; Quaternary International, v. 22/23, p. 141–171.

Gentzis, T., de Freitas, T., Goodarzi, F., Melchin, M., and Lenz, A.
1996: Thermal maturity of lower Paleozoic sedimentary successions in Arctic Canada; American Association of Petroleum Geologists, Bulletin, v. 80, no. 7, p. 1065–1084.

Goodarzi, F. and Norford, B.S.
1985: Graptolites as indicators of the temperature histories of rocks; Journal of the Geological Society of London, v. 142, part 6, p. 1089–1099.

Goodarzi, F., Brooks, P.W., and Embry, A.F.
1989: Regional maturity as determined by organic petrology and geochemistry of the Schei Point Group (Triassic) in Western Sverdrup Basin, Canadian Archipelago; Marine Petroleum Geology, v. 6, p. 290–302.

Goodarzi, F., Harrison, J.C., and Wall, J.H.
1994: Stratigraphy and petrology of Lower Cretaceous coal, southeastern Melville Island, District of Franklin, Arctic Canada; *in* The Geology of Melville Island, (ed.) R.L. Christie and N.J. MacMillan; Geological Survey of Canada, Bulletin 450, p. 229–245.

Goodbody, Q. H.
1994: Lower and Middle Paleozoic stratigraphy of Melville Island; *in* The Geology of Melville Island, Arctic Canada, (ed.) R.L. Christie and N.J. McMillan; Geological Survey of Canada, Bulletin 450, p. 23–103.

Gradstein, F.M. and Ogg, J.
1995: A Phanerozoic time scale; Episodes, v. 19, p. 3–5, 26 (chart).

Grantz, A, May, S.D., and Hart, P.E.
1994: Geology of the Arctic continental margin of Alaska; *in* The Geology of Alaska, (ed.) G. Plafker and H.C. Berg; Geological Society of America, The Geology of North America, v. G-1, p. 17–48.

Grantz, A., Clark, D.L., Phillips, R.L., Srivastava, S.P., Blome, C.D., Gray, L.B., Haga, H., Mamet, B.L. McIntyre, D.J., McNeil, D.H., Mickey, M.B., Mullen, M.W., Murchey, B.L., Ross, C.A., Stevens, C.H., Silberling, N.J., Wall, J.H., and Willard, D.A.
1998: Phanerozoic stratigraphy of Northwind Ridge, magnetic anomalies in the Canada Basin, and the geometry and timing of rifting in the Amerasia Basin, Arctic Ocean; Geological Society of America, Bulletin, v. 110, no. 6, p. 801–820.

Greenaway, K.R. and Colthorpe, S.E.
1948: An Aerial Reconnaissance of Arctic North America; Ottawa, Joint Intelligence Bureau, 294 p.

Haines, G.V. and Newitt., L.R.
1997: The Canadian Geomagnetic Reference Field 1995; Journal of Geomagnetism and Geoelectricity, v. 49, p. 317–336.

Harrison, J.C.
1991: Geology, seismic profiles and structural cross-sections, Melville Island, N.W.T.; Geological Survey of Canada, Open File 2335 (13 oversized sheets).

1995: Melville Island's salt-based fold belt, Arctic Canada; Geological Survey of Canada, Bulletin 472, 331 p.

Harrison, J.C. and Brent, T.
1991: Late Devonian - Early Carboniferous deformation, Prince Patrick and Banks islands; Chapter 12H; *in* Innuitian Orogen and Arctic Platform: Canada and Greenland; Geological Survey of Canada, Geology of Canada, No. 3 (*also* Geological Society of America, The Geology of North America, v. E), p. 334–336.

1996: Geology and resource potential of Prince Patrick and Eglinton islands region, Canadian Arctic Islands; *in* Proceedings of the Oil and Gas Forum '95, (ed.) J.S. Bell, T.D. Bird, T.L. Hillier and P.L. Greener; Geological Survey of Canada, Open File 3058, p. 193–197.

Harrison, J.C., de Freitas, T.A., and Thorsteinsson, R.
1993: New field observations on the geology of Bathurst Island, Arctic Canada: Part B, structure and tectonic history; *in* Current Research, Part B; Geological Survey of Canada, Paper 93-1B, p. 11–21.

Harrison, J.C., Embry, A.F., and Poulton, P.
1988: Field observations of the structural and depositional history of Prince Patrick Island and adjacent areas, Canadian Arctic Islands; *in* Current Research, Part D, Geological Survey of Canada, Paper 88-1A, p. 41–50.

Harrison, J.C., Thorsteinsson, R., and de Freitas, T.A.
1994: Phanerozoic geology of Strathcona Fiord map-area (NTS 49E and part of 39F), District of Franklin, Northwest Territories; Geological Survey of Canada, Open File 2881, scale 1:125, 000.

Harrison, J.C., Wall, J.H., Brent, T.A., Poulton, T.P., and Davies, E.H.
2000: A Jurassic rift system in the Canadian Arctic Islands; *in* Advances in Jurassic Research 2000, (ed.) R.L. Hall and P.L. Smith; GeoResearch Forum, v. 6, p. 427–436.

Henoch, W.E.S.
1964: Preliminary geomorphological study of a newly discovered Dorset Culture site on Melville Island; Arctic, v. 17, no. 2, p. 119–125.

Heywood, W.W.
1957: Isachsen area, Ellef Ringnes Island, District of Franklin, Northwest Territories; Geological Survey of Canada, Paper 56-8, 36 p.

Hobson, G.D.
1962: Seismic exploration in the Canadian Arctic Islands; Geophysics, v. 27, p. 253–273.

Hobson, G.D. and Overton, A.
1967: A seismic section of the Sverdrup Basin, Canadian Arctic islands; *in* Seismic Refraction Prospecting, (ed.) A.W. Musgrave; Society of Exploration Geophysicists, Tulsa, Oklahoma, p. 550–562.

Hodgson, D.A., Taylor, R.B., and Fyles, J.G.
1994: Episodic ice streams and ice shelves during retreat of the northwesternmost sector of the late Wisconsinian Laurentide Ice Sheet over the central Canadian Arctic Archipelago; Boreas, v. 23, p. 14–28.

Hunt, J.M.
1979: Petroleum Geochemistry and Geology; Freeman and Company, San Francisco, 617 p.

Jeletzky, J.A.
1966: Upper Volgian (latest Jurassic) ammonites and buchias of Arctic Canada; Geological Survey of Canada, Bulletin 128, 51 p.

1973: Biochronology of the marine boreal latest Jurassic Berriasian and Valanginian in Canada; *in* The Boreal Lower Cretaceous, (ed.) R. Casey and P.F. Rawson; Geological Journal, Special Issue, 5, p. 41–80.

1984: Jurassic-Cretaceous boundary beds of western and Arctic Canada and the problem of the Tithonian-Berriasian stages in the Boreal Realm; in Jurassic-Cretaceous biochronology and paleogeography of North America, (ed.) G.E.G. Westermann; Geological Association of Canada, Special Paper 27, p. 175–255.

Johnson, J.P., Jr.
1990: The establishment of Alert, N.W.T., Canada; Arctic, v. 43, p. 21–34.

Jutard, G. and Plauchut, B.P.
1973: Cretaceous and Tertiary stratigraphy, northern Banks Island; *in* Proceedings, Symposium on the Geology of the Canadian Arctic, (ed.) J.D. Aitken, and D.J Glass; Canadian Society of Petroleum Geologists, Geological Association of Canada, p. 203–219.

Kerr, J.W.
1967: Stratigraphy of central and eastern Ellesmere Island, Arctic Canada. Part I. Proterozoic and Cambrian; Geological Survey of Canada, Paper 67-27, 63 p.

1980: Structural framework of Lancaster Aulacogen, Arctic Canada; Geological Survey of Canada, Bulletin 319, 24 p.

Kerr, J.W. (cont.)
1981: Evolution of the Canadian Arctic Islands: a transition between the Atlantic and Arctic Oceans. The Ocean Basins and Margins; New York, Plenum Press, v. 5, p. 105–199.

1982: Evolution of sedimentary basins in the Canadian Arctic; Philosophical Transactions of the Royal Society, v. 305, p. 193–205.

Lane, L.S. and Dietrich, J.R.
1995: Tertiary structural evolution of the Beaufort Sea - Mackenzie Delta region, Arctic Canada; Bulletin of Canadian Petroleum Geology, v. 43, p. 293–314.

Long, D.G.F.
1989a: Kennedy Channel Formation: key to the early history of the Franklinian continental margin, central eastern Ellesmere Island, Arctic Canada; Canadian Journal of Earth Science, v. 26, p. 1147–1159.

1989b: Ella Bay Formation: Early Cambrian shelf differentiation in the Franklinian basin, central eastern Ellesmere Island, Arctic Canada; Canadian Journal of Earth Science, v. 26, p. 2621–2635.

Loomer, E.I.
1979: The effect of changes in the interplanetary magnetic field on the reduction of magnetic survey data from the polar cap; Geomagnetic Series, v. 17, Earth Physics Branch, Ottawa.

Loomer, E.I. and Whitham K.
1963: On certain characteristics of irregular magnetic activity observed at Canadian magnetic observatories during 1960; Publications of the Dominion Observatory, v. 27, no. 2, Ottawa.

Loomer, E.I. and Jansen van Beek, G.
1969: The effect of the solar cycle on magnetic activity at high latitudes; Publications of the Dominion Observatory, v. 37, No. 6, Ottawa.

MacPhee, S. and O'Shea, J.
1986: Charting of safe deep draught shipping routes in Canadian Arctic waters; Proceedings of the International Polar Transportation Conference, v. 2, p. 820–828.

Mandea, M., MacMillan, S., Bondar, T., Golovkov, V., Langlais, B., Lowes, F., Olsen, N., Quinn, J., and Sabaka, T.
2000: International Geomagnetic Reference Field – 2000; Physics of the Earth and Planetary Interiors, v. 120, p. 39–42.

Manning, T.H.
1953: Narrative of an unsuccessful attempt to circumnavigate Banks Island by canoe in 1952; Arctic, v. 6, p. 170–197.

Manning, T.H.
1956: Narrative of a second Defence Research Board expedition to Banks Island, with notes on the country and its history; Arctic, v. 9, p. 3–77.

McGhee, R.
1978: Canadian Arctic Prehistory; Van Nostrand Reinhold Ltd., Toronto, for the National Museum of Man, 128 p.

Meneley, R.A., Henao, D., and Merritt, R.
1975: The northwest margin of the Sverdrup Basin; *in* Canada's continental margins and offshore petroleum exploration, (ed.) C.J. Yorath, E.R. Parker and D.J. Glass; Canadian Society of Petroleum Geologists, Memoir 4, p. 531–544.

Meterological Division
1953: A review of the establishment and operation of the joint Arctic weather stations at Eureka, Resolute, Isachsen, Mould Bay, and Alert and a summary of the scientific activities at these stations, 1946-1951; Meteorological Division, Department of Transport, Canada and U.S. Weather Bureau, Department of Commerce, United States, 147 p.

Miall, A.D.
1976: Proterozoic and Paleozoic geology of Banks Island, Arctic Canada; Geological Survey of Canada, Bulletin 258, 77 p.

1979: Mesozoic and Tertiary geology of Banks Island, Arctic Canada; Geological Survey of Canada, Memoir 387, 235 p.

Mitchell, R.H. and Platt, R.G.
1984: The Freemans Cove volcanic suite: field relations, petrochemistry, and tectonic setting of nephelinite - basanite volcanism associated with rifting in the Canadian Arctic Archipelago; Canadian Journal of Earth Sciences, v. 21, p. 428–436.

Mooney, W.D. and Braile, L.W.
1989: The seismic structure of the continental crust and upper mantle of North America; *in* The Geology of North America - an overview, (ed.) A.W. Bally and A.R. Palmer; Geological Society of America, The Geology of North America, v. A, p. 39–52.

Moore, P.F.
1993: Devonian; Subchapter 4D; *in* Sedimentary Cover of the North American Craton, (ed.) D.F. Stott and J.D. Aitken; Geological Survey of Canada, Geology of Canada No. 5, p. 150–201 (also, Geological Society of America, The Geology of North America, v. D-1).

Morrell, G.R.
1996a: Atkinson Point Oil Discovery; *in* Geological Atlas of the Beaufort-Mackenzie area, (ed.) J. Dixon; Geological Survey of Canada, Miscellaneous Report 59, p. 150–151.

1996b: Parsons Gas Discovery; *in* Geological Atlas of the Beaufort-Mackenzie area, (ed.) J. Dixon; Geological Survey of Canada, Miscellaneous Report 59, p. 152–153.

Navy Times
1954: Icebreakers write history in Arctic; Anonymous article in the Navy Times newspaper of Sept. 4, 1954, p. 10.

Newitt, L.R.
1991: The effect of changing magnetic declination on the compass; Geological Survey of Canada Miscellaneous Report No. 52.

2000: Magnetic declination chart for Canada 2000.0; Natural Resources Canada, Geological Survey of Canada, Geomagnetic Laboratory.

Newitt, L.R. and Barton, C.E.
1996: The position of the north magnetic dip pole in 1994; Journal of Geomagnetism and Geoelectricity, v. 48, p. 221–232.

Newitt, L.R. and Dawson, E.
1980: Kingston Harbour magnetic anomaly; The Canadian Surveyor, v. 34, p. 397–405.

Newitt, L.R. and Walker, J.K.
1986: Correction of high latitude magnetic repeat station observations for disturbances; Earth Physics Branch, Open File 86-12, Ottawa.

1990: Removing magnetic activity from high latitude magnetic repeat station observations. Journal of Geomagnetism and Geoelectricity, v. 42, p. 937–949.

Okulitch, A.V. and Trettin, H.P.
1991: Late Cretaceous - Early Tertiary deformation, Arctic Islands; Chapter 17 *in* Innuitian Orogen and Arctic Platform: Canada and Greenland, (ed.) H.P. Trettin; Geological Survey of Canada, Geology of Canada No. 3 (*also*, The Geology of North America, Geological Society of America, v. E, p. 469–489).

Osborn, S. (ed.)
1857: The discovery of the North-west Passage by H.M.S. *Investigator*, from the logs and journals of Capt. Robert M'Clure, 1850, 1851, 1852, 1853, 1854 (Second edition); London, Longmans Green, 463 p.

Overton, A.
1970: Seismic refraction surveys, western Queen Elizabeth Islands and Polar continental margin; Canadian Journal of Earth Sciences, v. 7, p. 346–365.

Parry, Sir William Edward
1821: Journal of a voyage for the discovery of a north-west passage from the Atlantic to the Pacific performed in the years 1819-1820 in H.M.S. *Hecla* and *Griper*; London, John Murray.

Pelletier, B.R.
1966: Development of submarine physiography in the Canadian Arctic and its relation to crustal movements ; *in* Continental Drift, (ed.) G.D. Garland; The Royal Society of Canada, Special Publication no. 9, p. 77–101.

Pissart, A.
1967: The pingos of Prince Patrick Island (76°N - 120°W); Geographical Bulletin, v. 9, p. 189– 217.

Plauchut, B.P.
1971: Geology of the Sverdrup Basin; Bulletin of Canadian Petroleum Geology, v. 19, no. 3, p. 659–679.

1973: Géologie de l'Archipel Arctique Canadien; Revu Associations Techniciens Pétrole, no. 216, p. 23–51.

Plauchut, B.P. and Jutard, G.G.
1976: Cretaceous and Tertiary stratigraphy, Banks and Eglinton islands and Anderson Plain (N.W.T.); Bulletin of Canadian Petroleum Geology, v. 24, no. 3, p. 321–371.

Potter, A.W. and Blodgett, R.B.
1988: Paleogeographic relations and paleogeographic significance of late Ordovician brachiopods from Alaska; Geological Society of America, Abstracts with Programs, p. A339.

Poulton, T.P.
1991: Hettangian through Aalenian (Jurassic) guide fossils and biostratigraphy, northern Yukon and adjacent Northwest Territories; Geological Survey of Canada, Bulletin 410, 95 p.

1994: Jurassic stratigraphy and fossil occurrences - Melville, Prince Patrick, and Borden islands; *in* Geology of Melville Island, (ed.) R.L. Christie and N.J. McMillan; Geological Survey of Canada, Bulletin 450, p. 161–193.

Powell, T.G.
1978: An assessment of the hydrocarbon potential of the Canadian Arctic Islands; Geological Survey of Canada, Paper 78-12, 82 p.

Pullen, T.C. and Swithinbanke, C.
1991: Transits of the Northwest Passage, 1906-90; Polar Record, v. 27, p. 365–367.

Ricketts, B.D.
1994: Basin analysis, Eureka Sound Group, Axel Heiberg and Ellesmere islands, Canadian Arctic Archipelago; Geological Survey of Canada, Memoir 439, 119 p.

Riediger, C.L. and Harrison, J.C.
1994: Stratigraphy and sedimentology of the Canyon Fiord Formation, Melville Island; *in* Geology of Melville Island, (ed.) R.L. Christie and N.J. McMillan; Geological Survey of Canada, Bulletin 450, p. 121–138.

Rostovtsev, K.O. and Prozorowsky, V.A.
1997: Information on resolutions of standing commissions of the Interdepartmental Stratigraphic Committee (ISC) on the Jurassic and Cretaceous systems; International Subcommission on Jurassic Stratigraphy, Newsletter, v. 24, p. 48–49.

Sherwood, K.W.
1994: Stratigraphy, structure and origin of the Franklinian, northeast Chukchi Basin, Arctic Alaska plate; *in* 1992 Proceedings, International Conference on Arctic Margins, (ed.) D.K. Thurston and K. Fujita; U.S. Department of the Interior, Minerals Management Service, Anchorage, Alaska, p. 245–250.

Sliter, W.V.
1981: Albian foraminifera from the Lower Cretaceous Christopher Formation of the Canadian Arctic Islands; *in* Contributions to Canadian Paleontology, Geological Survey of Canada, Bulletin 300, p. 41–70.

Sobzcak, L.W. and Halpenny, J.F.
1990: Gravity anomaly maps of the Arctic; Marine Geology, v. 93, p. 15–41.

Sobczak, L.W., Forsyth, D.A., Overton, A., and Asudeh, I.
1991: Crustal structure from seismic and gravity studies; *in* Chapter 5 of Innuitian Orogen and Arctic Platform: Canada and Greenland, (ed.) H.P. Trettin; Geological Survey of Canada, Geology of Canada No. 3 (*also*, The Geology of North America, Geological Society of America, v. E, p. 71–100).

Stefansson, V.
1944: The Friendly Arctic, the story of five years in polar regions; New York, Macmillan Company, 784 p.

Stott, D.F. (comp.)
1991: Geotectonic correlation chart, Sheet 1, Northwest Territories and Yukon; *in* Sedimentary Cover of the North American Craton, (ed.) D.F. Stott and J.D. Aitken; Geological Survey of Canada, Geology of Canada No. 5 (*also*, Geological Society of America, The Geology of North America, v. D-1.).

Surlyk, F. And Zakharov, V.A.
1982: Buchiid bivalces from the Upper Jurassic and Lower Cretaceous of East Greenland; Paleontology, v. 25, p. 727–753.

Thériault, P., Beauchamp, B., Harrison, J.C., Mayr, U., and Steel, R.
1995: Serpukhovian and Bashkirian (Carboniferous) stratigraphy (Borup Fiord and Otto Fiord formations; Unit C1), Hvitland Peninsula and adjacent areas, northwestern Ellesmere Island, Arctic Canada; Geological Survey of Canada, Current Research 1995-B, p. 29–36.

Thorsteinsson, R.
1974: Carboniferous and Permian stratigraphy of Axel Heiberg Island and western Ellesmere Island, Canadian Arctic Archipelago; Geological Survey of Canada, Bulletin 224, 115 p.

Thorsteinsson, R. and Tozer, E.T.
1959: Western Queen Elizabeth Islands, District of Franklin, Northwest Territories; Geological Survey of Canada, Paper 59-1, 7 p.

1960: Summary account of structural history of the Canadian Arctic Archipelago since Precambrian time; Geological Survey of Canada, Paper 60-7, 25 p.

1970: Geology of the Arctic Archipelago; *in* Geology and Economic Minerals of Canada, (ed.) R.J.W. Douglas; Geological Survey of Canada, Economic Geology Report no. 1, p. 547–590.

Thorsteinsson, R., Harrison, J.C. , and de Freitas, T.A.
1994: Phanerozoic geology of Vendom Fiord map-area (NTS 49D), District of Franklin, Northwest Territories; Geological Survey of Canada, Open File 2882, scale 1:125, 000.

Tozer, E.T.
1956: Geological reconnaissance, Prince Patrick, Eglinton, and western Melville Islands, Arctic Archipelago, Northwest Territories; Geological Survey of Canada, Paper 55-5, 32 p.

1961: Triassic stratigraphy and faunas, Queen Elizabeth Islands, Arctic Archipelago; Geological Survey of Canada, Memoir 316, 184 p.

1963: Mesozoic and Tertiary stratigraphy; *in* Geology of the north-central part of the Arctic Archipelago, Northwest Territories (Operation Franklin); Geological Survey of Canada, Memoir 320, p. 74–95.

Tozer, E.T. and Thorsteinsson, R.
1964: Western Queen Elizabeth Islands, Arctic Archipelago; Geological Survey of Canada, Memoir 332, 242 p.

Trettin, H.P. (ed.)
1991: Geology of the Innuitian Orogen and Arctic Platform of Canada and Greenland; Geological Survey of Canada, Geology of Canada, No. 3 (*also*, Geological Society of America, The Geology of North America, v. E, 569 p.).

Trettin, H.P. and Hills, L.V.
1966: Lower Triassic tar sands of northwestern Melville Island; Geological Survey of Canada, Paper 66-34, 122 p.

Troelsen, J.C.
1950: Contributions to the geology of northwest Greenland, Ellesmere, and Axel Heiberg Islands; Meddelelser om Grønland, v. 147, no. 7, 86 p.

Turner, R.F.
1994: Biostratigraphy; *in* Geological, geochemical and operational summary, Aurora well, OCS Y-0943-1, Beaufort Sea, Alaska, (ed.) L.E. Paul; OCS Minerals Management Service, Report 94-0001, p. 15–25.

United States Weather Bureau
1948: Plans for installation of joint Canadian - U.S. satellite meteorological stations at Isachsen Land and Prince Patrick Island, N.W.T.; Canada in co-operation with the U.S Air Force, 45 p.

Utting, J., Goodarzi, F., Dougherty, B.J., and Henderson, C.M.
1989: Thermal maturity of Carboniferous and Permian rocks of the Sverdrup Basin, Canadian Arctic Archipelago; Geological Survey of Canada, Paper 89-19, 20 p.

Vincent, J-S.
1989: Quaternary geology of the northern Interior Plains; *in* Chapter 2 of Quaternary Geology of Canada and Greenland, (ed.) R.J. Fulton; Geological Survey of Canada, Geology of Canada, No.1 (*also*, Geological Society of America, The Geology of North America, v. K-1, p. 100–137).

Wall, J.H.
1983: Jurassic and Cretaceous foraminiferal biostratigraphy in the eastern Sverdrup Basin, Canadian Arctic Archipelago; Bulletin of Canadian Petroleum Geology, v. 31, p. 246–281.

Whitham, K., Loomer, E.I., and Niblett, E.R.
1960: The latitudinal distribution of magnetic activity in Canada; Journal of Geophysical Research, v. 65, p. 3961–3974.

Wilkins, Sir Hubert
1938: Our search for the lost aviators; The National Geographic Magazine, v. 74, p. 141–172.

Appendix A
Biostratigraphic determinations

LOWER PALEOZOIC
UNDIVIDED CARBONATE UNIT OF PRINCE PATRICK PLATFORM (unit psOS)

Wilkie Point J-51 well

B.S. Norford

GSC loc. C-187746; Elfex et al., Wilkie Point J-51 at 7242.0' to 7246.0' below top of well; 2247'.0' to 2251.0' below base of Kitson Formation.

Identifications:
- echinoderm columns
- *Aulacera* sp.
- stromatoporoids
- indeterminate rugose coral
- ?*Salvadorea* sp.
- *Calapoecia* cf. *C. robusta* (Wilson)
- *Paleofavosites* sp. (32–34 mm corallites)
- *"Parafavosites"* sp. (22–23 mm corallites)
- *Sarcinula* sp.
- ?pentamerid brachiopod

Age: Late Ordovician, Ashgill or Gamachian

Remarks: The faunule resembles Ashgill faunas in the Hudsons Bay Basin, the Rocky Mountains, and northern District of Mackenzie, except for the abundance of laminar stromatoporoids and the presence of what appears to be the spondylium-bearing pedicle valve of a pentamerid brachiopod. The fossils are present as clasts and there is the possibility of mixing of some Silurian material in with the Ordovician. However, pentamerid brachiopods are known from Upper Ordovician rocks in the northeastern Brooks Range of northern Alaska (Potter and Blodgett, 1988) and thus could be expected to be present in the western Arctic Islands.

A.E.H. Pedder

GSC loc. C-206453; Elfex et al., Wilkie Point J-51 at 5913.5' below top of well; 917.5' below base of Kitson Formation.

Identifications:
- *Amphipora* sp.
- *Stromatopora* sp.
- *Favosities* sp.

Age: Late Silurian to Early Devonian probably; Eifelian possibly

Remarks: Thin sections of the very small sample show a Silurian or Early Devonian species of *Favosites* embedded in an abraded and styolite-bound clast of a very poorly preserved stromatoporoid. A few poorly preserved specimens of a small species of *Amphipora* surround the stromatoporoid clast.

MESOZOIC
PAT BAY FORMATION (ŦRPB)

Northwest of Salmon Point

Published report of E.T. Tozer in Tozer and Thorsteinsson (1964)

GSC loc. 37200; 7.5 km north of Salmon Point, about 15 m above basal unconformity with Devonian, contact covered.

Identifications:
- *Oxytoma* sp.
- *Plicatula* cf. *P. hekiensis* Nakazawa
- *Lima (Plagiostoma)* sp.
- *Gryphaea* cf. *G. arcuatiformis Kiparisova*
- *"Myophoria"* sp.
- terebratuloid and spiriferid brachiopods indet.

Age: Triassic, probably Karnian

GROSVENOR ISLAND FORMATION (JGI)

Cape Canning

T.P. Poulton

GSC loc. C-146170, C-146172; on a westerly flowing tributary situated approximately 5.5 and 6 km north-northeast of Cape Canning; UTM 457100E, 848630N and 475700E, 848700N. Lowest of three fossil assemblages, this one collected approximately one metre above base of formation, and fault repeated.

Identifications:
- *Badouxia*(?) or *Arnioceras*(?) sp.
- *Oxytoma* sp.
- *Pleurotomana* sp.

Age: Late Hettangian(?) or Early Sinemurian

GSC loc. C-163533; 76°25'19"N, 117°55'40"W; north bank of tributary situated 3.7 km northeast of Cape Canning, 10.5–11.0 m above the exposed base of formation.

Identifications:
- *Echioceras* sp.
- *Cenoceras* sp.
- *Oxytoma* sp.
- *Kolymonectes(?)* sp.
- bivalves, indet.

Age: Late Sinemurian

GSC loc. C-163534; 76°25'19"N, 117°55'40"W; same locality as previous collection, 12.5–13.0 m above the exposed base of formation.

Identifications:
- *Gleviceras(?)* sp.
- *Goniomya* sp.
- *Kolymonectes* sp.
- *Lima (Lima) parva* Milova

plant leaf sp.
bivalve, indet. same as in C-163533

Age: Sinemurian, probably Late Sinemurian

GSC loc. C-163536; 76°25'19"N, 117°55'40"W; same locality as previous collection, 15.0–15.5 above the exposed base of formation.

Identifications:
Echioceras arcticum Frebold

Age: Late Sinemurian

JAMESON BAY FORMATION (JJB)

Landing Lake area

T.P. Poulton

GSC loc. C-163560; 76°20'38"N, 119°52'28"W; faulted exposures situated 0.7 km west of the lake on the south bank of an eastward-flowing creek, 8 m above base of section; base of formation covered.

Identifications:
Dactylioceras sp.
bivalves, indet.
belemnites, indet.

Age: Early Toarcian

Published report of H. Frebold in Tozer and Thorsteinsson (1964)

GSC loc. 24642; faulted outcrops immediately east of the lake.

Identifications:
Catacoeloceras spinatum (Frebold)
Pseudolioceras aff. *P. compactile* (Simpson)
Pleuromya aff. *P. simplex* Warren

Age: Middle or Late Toarcian probably

East shore of Mould Bay

T.P. Poulton

GSC loc. C-134000; 76°14'44"N, 119°24'25"W; outlier and rubble of sandstone and conglomerate on the hilltop 1.5 km northwest of the weather station, 3 to 6 m above base of formation.

Identifications:
Dactylioceras sp. aff. *commune* (Simpson)
Pseudolioceras sp. aff. *compactile* (Simpson)
'Harpoceras' sp.
belemnites, indet.
bone fragment, indet.

Age: Early Toarcian

Station Creek

Published report of H. Frebold (1958); see also Tozer and Thorsteinsson (1964)

GSC loc. 24641; 6 km northeast of the weather station, not more than 30 m above the base of the formation.

Identifications:
Catacoeloceras spinatum (Frebold)
Pseudolioceras aff. *P. compactile* (Simpson)
Cucullaea sp.
Protocardia striatula (Phillips)
Pleuromya aff. *P. simplex* Warren

Age: Early(?) Toarcian

West of Green Bay

T.P. Poulton

GSC loc. C-163563; 76°29'25"N, 119°13'20"W; collection, 6.5 km west of Green Bay, from rubble and outcrop at 0–10 m above base of formation.

Identifications:
Pseudolioceras spp. aff. *compactile* (Simpson)

Age: Middle or Late Toarcian probably

Shore area of Green Bay

T.P. Poulton

GSC loc. C-133908; 76°33'45"N, 118°50'00"W; rubble of glauconitic sands of the Intrepid Inlet Member, 0.6 km north of the northernmost part of Green Bay, less than 10 m above base of formation. Sample site also includes ironstone concretions, silicified wood, leaf impressions and gastropods.

Identification:
Amaltheus sp.

Age: Late Pliensbachian

Cape Canning

T.P. Poulton

GSC loc. C-163544; 76°25'35"N, 117°52'04"W; section on north bank of tributary stream, 4.3 km northeast of Cape Canning, 6.5 m above base of formation in the Intrepid Inlet Member, and 7.5 m above highest ammonite bed of Grosvenor Island Formation (GSC loc. C-163536).

Identifications:
ammonite, indet., possibly a new species, with subdued ribs on flank; good specimens needing further study, with some resemblance to late Pliensbachian *Amaltheus stokesi*.
Entolium(?) sp.
Harpax sp. cf. *spinosus* (Sowerby)
Kolymonectes sp. cf. *K. staeschei* (Polubotko)
Lima (Lima) parva Milova
Camptonectes(?) sp.

Age: Sinemurian or Pliensbachian, possibly late Pliensbachian

Published report of H. Frebold in Tozer and Thorsteinsson (1964)

No GSC locality number. Lower part of cliffs south of Hiccles Cove, not more than 30 m above the base of the formation.

Identifications:
Pseudolioceras m'clintocki (Haughton)
Oxytoma jacksoni (Pompeckj)

Age: late Toarcian to early Aalenian

The Jameson Bay Formation in the general Hiccles Cove, Cape Canning and Wilkie Point area has yielded numerous localities featuring various late Pliensbachian, Toarcian and early Aalenian macrofauna as listed in Tozer and Thorsteinsson (1964), Frebold (1957) and Poulton (1994).

SANDY POINT FORMATION (JSP)

West of Green Bay

T.P. Poulton

GSC loc. C-163510; 76°28'52"N, 119°13'20"W; collection from sand and loose rubble, 7 km west of Green Bay, unknown height above base of formation.

Identifications:
Leioceras opalinum (Reinecke)
Oxytoma sp.
Corbula(?) sp.
Protocardia sp.

Age: earliest Aalenian

GSC loc. C-163511; 76°31'16"N, 119°08'28"W; collection from sand and loose rubble, on north facing hillside 5.5 km west of Green Bay, unknown height above base of formation.

Identifications:
Leioceras opalinum (Reinecke)
Phylloceras sp.
Gryphaea(?) sp.
Oxytoma septentrionalis (Haughton)
Oxytoma jacksoni(?) (Pompeckj)

Age: Early Aalenian

Hiccles Cove

Published report of H. Frebold in Tozer and Thorsteinsson (1964)

GSC loc. 24658; cliffs south of Hiccles Cove; unknown height above base of formation.

Identifications:
Leioceras opalinum (Reinecke)
Pleuromya sp.

Age: early Aalenian

McCONNELL ISLAND FORMATION (JMI)

East shore of Mould Bay

Report of H. Frebold in Tozer and Thorsteinsson (1964)

GSC loc. 24665; 5 km south of the weather station in sandstone within the lower part of the formation; not more than 20 m above the base, contact covered.

Identifications:
Cranocephalites vulgaris Spath
Arctocephalites sp. 2, indet.
Cylindroteuthis sp.
Inoceramus sp. indet.

Age: Early Bathonian

Disappointment Point

E.H. Davies and J.H. Wall

GSC loc. C-156031; 76°18'18"N, 118°53'58"W; one of several Jurassic outliers, 7.5 km west of Disappointment Point; 30 m above sub-Jurassic unconformity in the lowermost part of the formation.

Dinoflagellates:
Dictyopyxidia areolata Eisenack
Gonglyodinium sp. with rugulate ornament
Gonglyodinium erymnoteichos Fenton, Neves & Piel
Nannoceratopsis gracilis Alberti

Pollen:
Cerebropollenites macroverrucosus (Thiegart) Schulz
Chasmatosporites nelsonii Burger
Corollina torosa (Reissinger) Klaus
Protoconiferus monosaccus Pocock

Spores:
Densoisporites velatus Weyland & Krieger
Leiotriletes meckelfeldensis Doring
Retitriletes austroclavitidites (Cookson) Doring et al.
Stereisporites clavus Leschik
Todisporites major Couper

Foraminifera:
Ammodiscus sp. cf. *A. asper* (Terquem)

Age: Middle Jurassic suggested by *A.* sp. cf. *A. asper*, which is usually associated with Aalenian–Bajocian beds in the central and eastern parts of the Sverdrup Basin. The presence of *Gonglyodinium* spp. and *N. gracilis* suggests Oppel Zones D to E of Bajocian Age.

West of Green Bay

T.P. Poulton

GSC loc. C-163503; 76°31'50"N, 119°18'26"W; isolated outcrop on the north bank of a significant braided stream 6.3 km northwest of Green Bay; unknown height above base of formation.

Identifications:
Arkelloceras tozeri Frebold
Retroceramus sp.
Gryphaea(?) sp.
Camptonectes(?) sp.
belemnites, indet.

Age: Early Bajocian

Shore of Green Bay

T.P. Poulton

GSC loc. C-163513; 76°31'29"N, 118°49'47"W; shoreline section along north shore of Green Bay, 6.0 to 10.5 m above faulted base of section and 12.0–16.0 m below top of lower (sandstone) member.

Identifications:
Arkelloceras sp.
Retroceramus sp.
Camptonectes sp.

Age: Early Bajocian

GSC loc. C-163514; 76°31'29"N, 118°49'47"W; same locality as previous collection, 10.5–13.5 m above faulted base and 9.0 to 12.0 m below top of lower (sandstone) member.

Identifications:
Arkelloceras sp.
Retroceramus sp.

Age: Early Bajocian

GSC loc. C-163516; 76°31'29"N, 118°49'47"W; same locality as previous collection, 22.5–28.5 m above faulted base of section and 0 to 6 m above base of upper (shale) member.

Identification:
Cranocephalites sp.
Retroceramus sp.

Age: Late Bajocian or Early Bathonian

E.H. Davies

GSC loc. C-163518; 76°31'29"N, 118°49'47"W; same locality as previous collection, 33.5 m above faulted base of section and 11 m above base of upper (shale) member.

Dinoflagellates:
Atopodinium prostratum Drugg
Cribroperidinium spp.
Dictyopyxidia areolata Eisenack
Glomodinium zabros Davies
Gonglyodinium sp.
Hestertonia teichophera (Sarjeant) Sarjeant
Leptodinium hyalodermopse (Cookson & Eisenack) Stover & Evitt
Nanoceratopsis pellucida Deflandre

Pollen:
Alisporites bilateralis Rouse
Cerebropollenites macroverrucosus (Thiegart) Schulz
Parvisaccites radiatus Brenner
Podocarpidites herbtsii Burger

Spores:
Deltoidospora hallii Miner

Age: Oppel Zone H1, middle to late Callovian. *G. zabros* is restricted to Oppel Zone G and the lower part of Oppel Zone H.

North of Salmon Point

J.H. Wall

GSC loc. C-156106; 76°43'N, 118°33'W; coastal cliffs on the west shore of Intrepid Inlet, 23.5 km north of Salmon Point; collected in the upper (shale) member within 10 m of the upper contact of the formation.

Foraminifera:
Bathysiphon sp.
Ammodiscus cheradospirus Loeblich and Tappan, incomplete - one
Glomospira sp. - one
Lituotuba sp. - two
Haplophragmoides sp. cf. *H. kirki* Wickenden - one
H. spp., mostly small, nondescript, poorly preserved - dominant
Recurvoides spp., small

Age: Middle Jurassic indicated on general appearance but assemblage lacks the diagnostic species present in the McConnell Island Formation on central and western Axel Heiberg Island for stage determination and confirmation of the rock unit at this locality. The microfauna here (especially the occurrence of *H.* cf. *H. kirki*) is, however, broadly similar to that obtained from outcrops designated McConnell Island Formation in the Green Bay area and at Marie Heights on Melville Island.

Hiccles Cove

Report of H. Frebold in Tozer and Thorsteinsson (1964)

GSC loc. 24661, 35324; coastal cliff section south of Hiccles Cove; unknown height above base of formation in the lower (sandstone) member.

Identifications:
Arkelloceras tozeri Frebold
A. mclearni Frebold
Zetoceras thorsteinssoni Frebold
Inoceramus lucifer Eichwald

Age: Early Bajocian

J.H. Wall

GSC loc. C-156012; 76°33'N, 117°55'W; coastal cliff section south of Hiccles Cove, 39.0 m above base formation in the upper (shale) member.

Foraminifera:
Bathysiphon sp.
Ammodiscus cheradospirus Loeblich and Tappan
A. sp. ex gr. *A. baticus* Dain and *francisi* (Wall) - one

Glomospira pattoni Tappan
"Haplophragmoides" barrowensis Tappan - one
H. sp.
Recurvoides sp.
Trochammina sp. - one
Riyadhella sibirica (Myatliuk) - fairly prominent

Age: Middle Jurassic, Bathonian indicated largely on basis of *R. sibirica*. The general composition of the microfauna is similar to that present in the Bathonian portion of the McConnell Island Formation in outcrop on central and western Axel Heiberg Island.

Moore Bay

T.P. Poulton

GSC loc. C-163567; 77°11'43"N, 116°20'10"W; north bank isolated outcrop in the lower part of the formation, on a major stream, 2.4 km northwest of outlet on Moore Bay.

Identifications:
Pleuromya sp.
Oxytoma sp.
Corbula(?) sp.
Meleagrinella(?) sp.
Propeamussium sp.
Inoceramus(?) sp.

Age: middle Toarcian to early Bajocian

HICCLES COVE FORMATION (JHC)

West shore of Mould Bay

T.P. Poulton

GSC loc. C-163558; 76°04'51"N, 119°35'08"W; coastal low cliff exposure, 13 km due west of Manson Point on the west side of Mould Bay; 5 m above base of section and not more than 10 m above covered base of formation.

Identification:
Arcticoceras(?) sp.
Pleuromya sp.
gastropod, indet.
belemnites, indet.

Age: Late Bathonian probably, possibly late Middle Bathonian

J.H. Wall

GSC loc. C-163559; same locality as previous collection, 6.0–8.0 m above base of formation.

Foraminifera:
Reophax sp. - one
Nodosaria sp. cf. *N. orthostoecha* Loeblich and Tappan, incomplete - one
N. spp. - two or more detached single chambers
Astacolus spp.
Lenticulina spp. - dominant
Marginulinopsis sp. - one
Planularia spp.
Pseudonodoria sp. - two
Vaginulina sp. - one to two
Vaginulinopsis sp. - two

Bivalvia (Pelecypoda):
many shell fragments

Age: Middle Jurassic indicated on basis of general appearance of foraminiferal assemblage. Stage indeterminate.

E.H. Davies

GSC loc. C-163559; same locality and sample as for previous collection.

Dinoflagellates:
Grandispora spp. (reworked Paleozoic)
Nannoceratopsis pellucida Deflandre

Pollen:
Cerebropollenites macroverrucosus (Thiegart) Schulz
Palaeospongisporis sp. cf. *P. europaensis* (reworked Triassic)
Perinopollenites elatoides Couper
Verrucosisaccus sp. (reworked Triassic)

Spores:
Deltoidospora hallii Miner

Age: Bathonian to early Kimmeridgian, zone not assigned. Contains reworked Triassic species.

Landing Lake area

E.H. Davies and J.H. Wall

GSC loc. C-163561; 76°20'38"N, 119°52'28"W; faulted exposures situated 0.7 km west of the lake on the south bank of an eastward-flowing creek; at the base of the formation, 14 m above the sub-Jurassic unconformity.

Dinoflagellates:
Dichadogonyaulax sellwoodii (Sarjeant) Stover & Evitt
Dictyopyxidia areolata Eisenack
Glomodinium tripartitum (Johnson & Hills) Davies
Nannoceratopsis cf. *N. pelluida* Deflandre
Pareodinia ceratophora Deflandre

Miospores:
Alisporites bilateralis Rouse
Cerebropollenites macroverrucosus (Thiegart) Schulz
Perinopollenites elatoides Couper

Spores:
Deltoidospora hallii Miner
Leiotriletes meckelfeldensis Doring
Retitriletes austroclavitidites (Couper) Doring et al.
Saxosporis variabilis Doring
Sestrosporites pseudoalveolatus (Couper) Dettmann
Stereisporites clavus Leschik

Foraminifera (rare):
Haplophragmoides? sp. - one to two fragments

Reophax or *Ammobaculites* (incomplete) sp.- a two-chambered fragment

Age: Oppel-zone G2, early Callovian. The sparse foraminiferal assemblage is inadequate for confirmation of the age.

Environment: Marine, shallow, possibly marginal and brackish.

Head of Mould Bay

J.H. Wall

GSC loc. C-198995; 76°24'10"N, 119°31'30"W; section located 5.2 km north of head of Mould Bay; 5 m above base of formation and 11 m above sub-Jurassic unconformity.

Foraminifera:
Astacolus sp. cf. *A. hybridus* (Terquem) - one
A. lokossovensis Kosyreva - one
Citharina sp. - one
Dentalina sp. - fragments
Lenticulina subpolonica Gerke and Scharovskaya - fair development
L. spp. - prominent
Marginulinopsis suprajurensis Gerke and Scharovskaya
Pseudonodosaria sp., damaged - one
Guttulina tatarensis Myatliuk - two

Bivalvia (Pelecypoda):
shell fragments

Age: Middle Jurassic, Callovian stage indicated on basis of broad similarity to assemblages of this age in Arctic Russia, the central Sverdrup Basin and the upper part of the Hiccles Cove Formation from western Sproule Peninsula on Melville Island.

E.H. Davies

GSC loc. C-198996; same locality as previous collection; 12 m above base of formation.

Dinoflagellates:
Ellipsoidictyum cinctum Klement
Ellipsoidictyum reticulatum (Valensi) Lentin & Williams
Escharisphaeridia rudis Davies
Glomodinium zabros Davies
Mendicodinium groenlandicum (Pocock & Sarjeant) Davey

Algae and miscellanea:
chyrsophyte? cyst sp. A
Lecaniella foveolata Singh
Micrhystridium fragile Deflandre
foraminiferal liners

Pollen:
Alisporites sp.
Callialasporites monoalasporus Dev
Callialasporites turbatus, Schulz '67
Cedripites canadensis Pocock
Cerebropollenites findlaterensis Pocock
Cerebropollenites macroverrucosus (Thiegart) Schulz
Concentrisporites sulcatus
Corollina findlaterensis Pocock
Corollina torosa (Reissinger) Klaus
Exesipollenites scabratus Norris
Inaperturopollenites sp. - granulate
Perinopollenites sp.
Phyllocladites inchoatus (Pierce) Norris
Pityosporites divulgaris (Bolkhovitina) Pocock
Platysaccus lopsiensis (Maljavkina) Pocock
Podocarpidites granulosus Pocock
Vitreisporites pallidus (Reissinger) Nelsson

Spores:
Acanthotriletes variespinosus Pocock
Aequitriradites sp. indet.
Baculatisporites comaumensis (Cookson) Potoniae
Converrucosisporites cf. *C. cameroni* (De Jersey) Playford & Dettmann
Deltoidospora hallii Miner
Densosporites anulatus (Loose) Smith & Buterworth (Reworked Mississippian)
Distcyclosporis sp. with rugulate ornament
Leiotriletes meckelfeldensis Doring
Lycopodiumspotires sp.
Osmundacidites major Doring
Punctatisporites sp.
Rogalskisporites sp.

Age: Oppel zone H1 to H2, Callovian

Hiccles Cove

Published report of H. Frebold in Tozer and Thorsteinsson (1964)

GSC loc. 35345; coastal cliff section, 1.6 km southeast of Hiccles Cove, in the lower part of the formation; unknown height above base of formation.

Identifications:
Arcticoceras ishmae (Keyserling)
A. sp. cf. *A. ishmae* Keyserling

Age: late Bathonian

Published report of Poulton (1994) and unpublished report of H. Frebold, 1966

GSC loc. 70405-8; inland exposures 2.0 km east of Hiccles Cove; four horizons located 10 to 19 m above base of upper member.

Identifications:
Cadoceras cf. *C. bodylevskyi* Frebold
Cadoceras sp.
Costacadoceras sp.
Inoceramus sp.

Age: early Callovian

J.H. Wall

GSC loc. C-156037; 76°32'N, 117°48'W; inland cliff exposure, 5.7 km southeast of Hiccles Cove in a thin shale interval 1.0 m above base of upper member.

Foraminifera:
Astacolus spp.
Lenticulina spp.

Dentalina sp., incomplete - one
Marginulina sp. - one
Pseudonodosaria sp.
Guttulina tatarensis Myatliuk - one

Echinoidea:
spine(?) fragments

Age: Middle Jurassic, stage uncertain but Callovian indicated on basis of *G. tatarensis*.

E.H. Davies

GSC loc. C-156037; same locality and sample as previous collection.

Dinoflagellates:
Atopodinium prostratum Drugg (questionably present)
Ctenidodinium continuum Gocht (questionably present)
Dapcodinium semitabulatum (Morgenroth) Dorhofer & Davies
Dichadogonyaulax sellwoodii (Sarjeant) Stover & Evitt
Gonglyodinium erymnoteichos Fenton, Neves & Piel

Pollen:
Cerebropollenites macroverrucosus (Theigart) Schulz
Taxodiaceaepollenites hiatus (Potonie) Kemp
Triangulopsis discoidalis Doring

Spores:
Baculatisporites comaumensis (Cookson) Potonie
Camarozonosporites spp.
Deltoidospora hallii Miner
Leiotriletes meckelfeldensis Doring
Retitriletes austroclavitidites (Cookson) Doring et al.
Saxosporis sp.
Todisporites major Couper

Age: Oppel Zone G, Bathonian to early Callovian

RINGNES FORMATION (JR)

South of Landing Lake

J.H. Wall

GSC loc. C-133985; 76°09'47"N, 119°54'00"W; incised riverbank exposures, 19 km south of Landing Lake and 4.8 km west of the closest part of Mould Bay; 2.0 m above base of formation.

Foraminifera:
Ammodiscus thomsi Chamney - one
Saturnella brookeae Hedinger (=*Glomospirella* sp. 174 of Brooke and Braun as illustrated by Wall 1983, Pl. 3, fig. 27–29)
G. sp.
Haplophragmoides sp. 1 of Wall 1983
H. spp., mainly distorted specimens
Cribrostomoides sp.
Recurvoides sp. cf. *R. disputabilis* Dain *sensu lato* - two
Ammobaculites sp. ex gr. *A. alaskensis* Tappan - four possibly immature specimens
A. sp., incomplete, coarse-grained - one

Age: Late Jurassic, Oxfordian, Kimmeridgian. The microfauna corresponds best with that of the *A. thomsi* assemblage from the Ringnes Formation and overlying Awingak Formation in the Buchanan Lake area, eastern Axel Heiberg Island.

E.H. Davies

GSC loc. C-133985; same locality and sample as previous collection.

Dinoflagellates:
Ctenidodinium spp.
Escharisphaeridia pocockii (Sarjeant) Erkman & Sarjeant
Glomodinium evittii (Pocock) Davies
Gonyaulacysta dualis (Brideaux & Fisher) Stover & Evitt
Paragonyaulacysta borealis (Brideaux & Fisher) Stover & Evitt
Paragonyaulacysta capillosa (Brideaux & Fisher) Stover & Evitt - Abundant
Pareodinia ceratophora Deflandre

Pollen:
Campenia sp.
Taxodiaceaepollenites hiatus (Potonie) Kemp

Spores:
Osmundacidites wellmannii Couper

Age: Oppel Zone I, early to middle Kimmeridgian

T.P. Poulton

GSC loc. C-133984; same section as previous collection; 5.0–5.3 m above exposed base of formation.

Identifications:
Buchia sp. cf. *unschensis* (Pavlow)
Pleuromya(?) sp.
bivalves, indet.
terebratulid brachiopod, indet.

Age: Latest Volgian probably

Head of Mould Bay

E.H. Davies and J.H. Wall

GSC loc. C-199004; 76°22'50"N, 119°30'00"W; west-facing stream bank section 3.0 km north of the head of Mould Bay; 5.0 m below top of formation, base covered.

Dinoflagellates:
Mendicodinium groenlandicum (Pocock & Sarjeant) Davey
Escharisphaeridia rudis Davies
Gochteodinia villosa (Vozzhennikova) Norris
Gonyaulacysta dualis (Brideaux & Fisher) Stover & Evitt
Gonyaulacysta jurassica subsp. *longicornis* (Deflandre) Lentin & Williams
Lanterna saturnalis Brideaux & Fisher
Paragonyaulacysta borealis (Brideaux & Fisher) Stover & Evitt
Sentusidinium filiatum Davies
Sirmiodinium grossii Alberti
Tubotuberella rhombiformis Vozzhennikova

Algae and miscellanea:
Baltisphaeridium spp.

Pollen:
Alisporites bilateralis Rouse
Callialasporites infrapunctatus (Lantz) Pocock
Cedripites canadensis Pocock
Perinopollenites elatoides Couper
Podocarpidites granulosus Pocock
Taxodiaceaepollenites hiatus (Potonie) Kemp

Spores:
Baculatisporites comaumensis (Cookson) Potonie
Conbaculatisporis trichopunctatus Doring
Deltoidospora hallii Miner
Osmundacidites major Doring
Polycingulatisporites segmentatus (Stover) Singh
Todisporites major Couper
Varirugosisporites granituberosus Doring

Foraminifera:
Ammodiscus cheradospirus Tappan - one incomplete specimen
A. thomsi Chamney - fragments
Haplophragmoides sp. 1 of Wall 1983 (Pl. 2, figs. 4, 5; Pl. 3, figs. 2, 3)
H. spp. - prominent

Age: Late Jurassic, Oxfordian–Kimmeridgian based largely on presence of *A. thomsi* and general character of foraminiferal assemblage. Oppel Zone H3, late Oxfordian, based on palynomorph and dinoflagellate evidence.

Shore area of Green Bay

J.H. Wall

GSC loc. C-163539; 76°33'42"N, 118°56'55"W; stream bank section 2.7 km west of the northernmost part of Green Bay; 1.4 m above base of formation.

Foraminifera:
Saccammina sp. - one
Ammodiscus thomsi Chamney - fragments
A. sp.
Haplophragmoides sp. 1 of Wall 1983
H. spp.
Ammobaculites spp.
Trochammina sp. cf. *T. kosyrevae* Levina - one poorly preserved specimen
T. sp. ex gr. *T. oxfordiana* Scharovskaya as illustrated by Wall 1983 (pl. 3, fig. 12–14) - one

Plant material
megaspores

Age: Late Jurassic, Oxfordian–Kimmeridgian

GSC loc. C-163541; same section as previous collection; 12.0 m above base of formation.

Foraminifera:
Ammodiscus thomsi Chamney
Haplophragmoides sp. 1 of Wall 1983
H. spp.
Ammobaculites alaskensis Tappen subsp. minor Hedinger
A. sp.
Trochammina sp. ex gr. *T. elevata* Kosyreva
T. sp

Age: Late Jurassic, Oxfordian–Kimmeridgian indicated by presence of *A. thomsi* and general character of assemblage.

North of Salmon Point

E.H. Davies

GSC loc. C-156103; 76°36'N, 118°28'W; section below escarpment of Beaufort Formation, 11.0 km north of Salmon Point and 3.5 km west of Intrepid Inlet; 4 m above base of formation.

Dinoflagellates:
Chytroeisphaeridia chytroeides (Sarjeant) Downie & Sarjeant
Endoscrinium oxfordianum (Sarjeant) Courtinat - abundant
Gonyaulacysta dualis (Brideaux & Fisher) Stover & Evitt
Mendicodinium groenlandicum (Pocock & Sarjeant) Davey
Paragonyaulacysta borealis (Brideaux & Fisher) Stover & Evitt
Pareodinia ceratophora Deflandre
Rhynchodiniopsis cladophora (Deflandre) Below

Pollen:
Alisporites bilateralis Rouse
Cerebropollenites macroverrucosus (Theigart) Schulz
Taxodiaceaepollenites hiatus (Potonie) Kemp

Spores:
Baculatisporites comaumensis (Cookson) Potonie
Deltoidospora hallii Miner
Stereisporites clavus Leschik
Todisporites major Couper

Age: Lower part of Oppel Zone I, early Kimmeridgian

J.H. Wall

GSC loc. C-156104; same locality as previous collection; 5 m above base of formation.

Foraminifera:
Ammodiscus cheradospirus Loeblich and Tappan
A. thomsi Chamney
Saturnella brookeae Hedinger (=*Glomospirella* sp. 174 of Brooke and Braun as illustrated by Wall 1983, Pl. 3, figs. 27–29)
Haplophragmoides sp. 1 of Wall 1983
H. spp.
Cribrostomoides sp.
Ammobaculites alaskensis Tappan *sensu lato*
A. trachyostrachos Hedinger
Trochammina sp. ex gr. *T. oxfordiana* Scharovskaya as illustrated by Wall 1983, pl. 3, fig. 12–14
T. sp., compressed

Age: Late Jurassic, Oxfordian–Kimmeridgian, as shown by elements of the *A. thomsi* and *Glomospicella* sp. 174 assemblages of Wall (1983), which are characteristic of the Ringnes and overlying Awingak Formation in the eastern Sverdrup Basin.

North of Hiccles Cove

E. H. Davies and J.H. Wall

GSC loc. C-156028; 76°39'N, 117°40'W; inland ridge crest section, 7.5 km northeast of Hiccles Cove, 10 cm above exposed base of formation.

Dinoflagellates:
Korystocysta pachydermum (Deflandre) Woollam - questionably present

Pollen:
Callialasporites obrutus Norris
Cerebropollenites mesozoicus (Couper) Nilsson
Chasmatosporites nelsonii Burger
Inaperturopollenites sp. - granulate
Protoconiferus monosaccus Pocock
Podocarpidites canadensis Pocock
Taxodiaceaepollenites hiatus (Potonie) Kemp
Triangulopsis discoidalis Doring

Spores:
Aeqitriradities sp.
Baculatisporites comaumensis (Cookson) Potonie
Deltoidospora hallii Miner
Osmundacidites major Doring
Retitriletes austroclavitidites (Cookson) Doring et al.
Todisporites major Couper

Foraminifera:
Ammodiscus thomsi Chamney? - fragments
Haplophragmoides sp. 1 of Wall 1983 (Pl. 2, fig. 4, 5; Pl. 3, fig. 2, 3) - poorly preserved
H. sp.-spp., distorted
Trochammina spp. - similar to Ringnes forms from the eastern Sproule Peninsula, Melville Island (GSC loc. 87 HBB-60, C-133962)

Age: Late Jurassic, Oxfordian–Kimmeridgian suggested by the meagre foraminiferal assemblage. Oppel zones H to I, Oxfordian to early Kimmeridgian, based on microflora.

Island in Satellite Bay

E.H. Davies

GSC loc. C-163507; 77°26'22"N, 117°16'18"W; grab sample from isolated island outcrop, unknown height above base of formation. Locality is within a substantial inlier enveloped by Beaufort Formation, which is exposed on all of the surrounding shores of Satellite Bay.

Dinoflagellates:
Canningia minor Cookson & Hughes
Dictyopyxidia areolata Eisenack
Escharisphaeridia rudis Davies
Gonyaulacysta dualis (Brideaux & Fisher) Stover & Evitt
Korystocysta pachydermum (Deflandrei) Woollam
Leptodinium hyalodermopse (Cookson & Eisenack) Stover & Evitt
Paragonyaulacysta capillosa (Brideaux & Fisher) Stover & Evitt
Pareodinia ceratophora Deflandre
Sirmiodinium grossii Alberti

Pollen
Cerebropollenites macroverrucosus (Theigart) Schulz
Taxodiaceaepollenites hiatus (Potonie) Kemp

Spores:
Klukisporites pseudoreticulatus Couper
Rogalskisporites sp.

Age: Lower part of Oppel Zone I based on occurrence of *K. pachydermum*, early Kimmeridgian.

AWINGAK FORMATION (JA)

Giants Causeway

E.H. Davies

GSC loc. C-163556; 75°44'40"N, 121°13'48"W; faulted outlier, 1.6 km east of Giants Causeway collected in the basal part of the formation less than 10 m above the covered sub-Jurassic unconformity.

Dinoflagellates:
Meiourogonyaulax callomonii Sarjeant

Miospores:
Alisporites bilateralis Rouse
Cerebropollenites macroverrucosus (Theigart) Schulz
Cycadopites spp.
Exesipollenites tumulus Balme
Pityosporites divulgaris (Maljavkina) Pocock
Podocarpidites potomacensis Brenner

Spores:
Cicatricosisporites mohrioides Delcourt & Sprumont
Deltoidospora hallii Miner
Laevigatosporites ovatus Wilson & Webster
Osmundacidites major Doring
Osmundacidites wellmannii Couper
Retitriletes austroclavitidites (Cookson) Doring et al.
Stereisporites clavus Leschik
Tuberositriletes grossetuberculatus Doring

Age: Oppel Zone I, early to middle Kimmeridgian

Cape Cam

T.P. Poulton

GSC loc. C-163555; 75°51'54"N, 120°21'23"W; isolated outcrop situated 6.3 km north of Cape Cam, at 10 to 15 m above covered base of formation.

Identifications:
Mclearnia sp.
Buchia(?) sp.
Modiolus sp.
Corbula(?) sp.
Astarte(?) sp.
bivalves, indet.
serpulid casts, indet.

Age: Volgian probably

Cape Frederick

T.P. Poulton

GSC loc. C-163552; 75°53'05"N, 119°55'00"W; small faulted outlier, 6 km west of Cape Frederick, 4 m above basal unconformity with Devonian.

Identifications:
Buchia fischeriana(?) (d'Orbigny)
Arctotis sp. aff. *anabarensis* (Petrova)
Canadotis canadensis(?) Jeletzky and Poulton
Oxytoma aucta Zakharov
Chlamys(?) sp.
Camptonectes(?) sp.
ostreiid(?) bivalve, indet.
bivalve, indet.
terebratulid brachiopod(?) sp.

Age: Volgian

E.H. Davies and J.H. Wall

GSC loc. C-163551; same locality as previous collection, 5 m above basal unconformity with Devonian.

Foraminifera:
Ammodiscus sp. cf. *A. orbis* Lalicker
Haplophragmoides sp. 1 of Wall 1983
H. sp. 2 of Wall 1983
H. or *Cribrostomoides* spp., including very large specimens
Ammobaculites alaskensis Tappan subsp. *alaskensis* Hedinger
A. spp.
Trochammina sp. cf. *T. taboryensis* Levina
T. sp.
Verneuilinoides sp.
Nodosaria sp., elongate, three-chambered - one complete and one fragment
Grillina praenodulosa (Dain) - two poorly preserved
Astacolus siberensis Kosyreva - two or more
Lenticulina spp.
Marginulinopsis striatocostata (Reuss)
M. sp., smooth - one
Planularia sp. cf. *P. adulta* Putrya - one
Saracenaria sp.-spp. - three incomplete specimens
polymorphininid indeterminate - one pyritic cast
Spirillina? sp., mostly pyritized - one

Bivalvia (Pelecypoda):
juvenile specimens and fragments of larger forms

Gastropoda:
low and moderately spired conchs

Pisces:
teeth, scale and bone fragments

Echininoidea:
spine and plate(?) fragments

Dinoflagellates:
Lanterna spp.
Paragonyaulacysta borealis (Brideaux & Fisher) Stover
Paragonyaulacysta capillosa (Brideaux & Fisher) Stover - questionably present

Pollen:
Araucariacites punctatus (Nelson) Cornet & Traverse
Cedripites canadensis Pocock
Cerebropollenites macroverrucosus (Theigart) Schulz
Perinopollenites elatoides Couper
Taxodiaceaepollenites hiatus (Potonie) Kemp

Spores:
Cicatricosisporites sp.
Clavatitriletes spp.
Deltoidospora hallii Miner
Retitriletes austroclavitidites (Cookson) Doring et al.
Osmundacidites major Doring

Age: Late Jurassic, Kimmeridgian–Volgian, indicated by foraminiferal assemblage. Oppel zone I to J, Kimmeridgian based on palynomorph and dinoflagellate assemblage.

T.P. Poulton

GSC loc. C-133996; 75°54'20"N, 119°46'04"W; small faulted outlier, 2.5 km northwest of Cape Frederick, not more than 10 m above basal unconformity with Devonian.

Identifications:
Mclearnia sp.
Pleuromya sp.
Arctotis (Canadarctotis) rugosa Jeletzky and Poulton
Oxytoma sp.
Buchia sp.
bivalves, indet.
rhynchonellid brachiopod, indet.

Age: Early Volgian probably

East of Walker Inlet

E.H. Davies and J.H. Wall

GSC loc. C-163520; 76°09'19"N, 120°08'38"W; low-relief inland section, 18.0 km east of the north end of Walker Inlet and 21.2 km southwest of Landing Lake; 38.0 m above base of formation and 7.0 m below upper contact with Isachsen Formation.

Dinoflagellates:
Canningia ringnesiorum Manum & Cookson
Gonyaulacysta helicoidea (Eisenack & Cookson) Sarjeant
Sirmiodinium grossii Alberti

Miospores:
Alisporites bilaterealis Rouse
Callialasporites dampieri (Balme) Dev
Callialasporites monoalasporus Dev
Callialasporites turbatus (Balme) Schulz
Cerebropollenites macroverrucosus (Thiegart) Schulz
Laricoidites magnus (Potonie) Potonie, Thompson & Thiegart
Parvisaccites radiatus Brenner
Perinopollenites elatoides Couper

Spores:
Baculatisporites comaumensis (Cookson) Potonie
Cicatricosisporites mohrioides Delcourt & Sprumont
Cicatricosisporites sp.
Cyathidites australis Couper
Klukisporites areolatus Singh

Kraeuselisporites sp.
Retitriletes austroclavitidites (Cookson) Doring et al.
Taurocusporites reduncus Stover
Tuberositriletes grossetuberculatus Doring

Foraminifera:
Ammodiscus sp., small
Haplophragmoides sp. 1 of Wall 1983
H. spp.
Ammobaculites sp. - two
Trochammina sp. cf. *T. topagorukensis* Tappan - poorly preserved
T. spp.

Age: Late Jurassic suggested by general appearance of foraminiferal microfauna. Oppel zone I to J, Kimmeridgian, based on palynomorph and dinoflagellate assemblage.

East shore of Mould Bay

Published report of J.A. Jeletzky in Tozer and Thorsteinsson (1964)

GSC loc. 24818; coastal exposures 4.6 km north of the weather station.

Identifications:
Buchia piochii Gabb s. lato
B. fischeri (d'Orbigny)
Aucellina n. sp. aff. *A. schmidti* Sokolow
Pteria sp.
Ostrea sp.
pectinid indet.
belemnites indet.

Age: late Volgian

DEER BAY FORMATION (JK$_D$)

North of Jameson Bay

Published report of J.A. Jeletzky in Tozer and Thorsteinsson (1964)

GSC loc. 37199; 10 km northwest of "The Redoubt" in the uppermost part of the formation.

Identifications:
Buchia keyserlingi (d'Orbigny)
B. sp. aff *B. crassa* (Pavlow)
B. sp. cf. *B. bulloides* (Lahusen)

Age: late Valanginian

E.H. Davies and J.H. Wall

GSC loc. C-133956; 76°52'40"N, 117°29'20"W; isolated exposure situated 10.2 km northeast of the head of Intrepid Inlet; shale interval in the uppermost 12 m of the formation.

Dinoflagellates:
Acanthaulax spp.
Caddasphaera halosa
Cleistosphaeridium spp.
Gonyaulacysta dualis (Brideaux & Fisher) Stover & Evitt
Gonyaulacysta helicoidea (Eisenack & Cookson) Sarjeant
Paragonyaulacysta borealis (Brideaux & Fisher) Stover & Evitt
Pareodinia ceratophora Delfandre
Sirmiodinium grossii Alberti
Tubotuberella rhombiformis Vozzhennikova
Wanaea fimbriata Sarjeant- questionably present

Pollen:
Alisporites bilateralis Rouse
Araucariacites punctatus (Nilsson) Cornet & Traverse
Cerebropollenites mesozoicus (Couper) Nilsson

Spores:
Cicatricosisporites mohrioides Delcourt & Sprumont

Foraminifera:
Ammodiscus sp. cf. *A. orbis* Lalicker
A. sp.
Lituotuba sp.
Haplophragmoides and *Cribrostomoides* spp. - mainly large distorted specimens probably referable to species from the Deer Bay Fm. illustrated by Wall (1983, Pl. 4, fig. 34–40)
Ammobaculites spp. - two spp. with total of three specimens
Trochammina sp. cf. *T. rosacea* Zaspelova as illustrated by Wall (1983, Pl. 5, fig. 18–20)
Gaudryina sp. 1 of Wall (1983, Pl. 4, fig. 8) - two
Orientalia sp. 2 of Wall (1983, Pl. 4, fig. 12–14)
Globulina sp. ex gr. *G. alexandrae* Dain - two pyritic casts
Glandulopleurostomella sp. - one

Age: Late Jurassic–Early Cretaceous foraminiferal assemblage. Oppel Zone I, early to middle Kimmeridgian, based on palynomorph and dinoflagellate assemblage.

ISACHSEN FORMATION (K$_I$)

Landing Lake area

E.H. Davies

GSC loc. C-199006; 76°23'40"N, 119°37'30"W; ridge-crest section below escarpment of Beaufort Formation, 7.0 km northeast of Landing Lake and 5.2 km northwest of head of Mould Bay; about 22 m above base of formation.

Pollen:
Alisporites microsaccus (Couper) Pocock
Alisporites bilateralis Rouse
Cedripites canadensis Pocock
Parvisaccites amplus Brenner
Phyllocladites inchoatus (Pierce) Norris
Taxodiaceaepollenites hiatus (Potonie) Kremp

Spores:
Stereisporites antiquasporites (Wilson & Webster) Dettmann

Age: Lower Cretaceous, tentatively Barremian to Albian, zone undetermined

Head of Mould Bay

E.H. Davies

GSC loc. C-198967; 76°22'45"N, 119°19'00"W; hillside section, 5.7 km northeast of the head of Mould Bay; about 25 m above faulted base of section, covered base of formation.

Dinoflagellates:
- *Canningia ringnesiorum* Manum & Cookson
- *Egmontodinium* sp.
- *Subtilisphaera terrula* (Davey) Lentin & Williams

Algae and miscellanea:
- *Schizosporis reticulatus* Cookson & Dettmann

Pollen:
- *Alisporites microsaccus* (Couper) Pocock
- *Alisporites bilateralis* Rouse
- *Callialasporites monoalasporus* Dev
- *Cedripites canadensis* Pocock
- *Cerebropollenites macroverrucosus* (Thiegart) Doring et al.
- *Chasmatosporites major* Nilsson
- *Clavatipollenites minutus* Brenner
- *Corollina itunensis* (Pocock) Cornet & Traverse
- *Corollina vignollensis* Reyre et al.
- *Laricoidites magnus* (Potonie) Potonie, Thompson & Thiegart
- *Perinopollenites elatoides* Couper
- *Phyllocladites inchoatus* (Pierce) Norris
- *Podocarpidites* sp.
- *Podocarpidites canadensis* Pocock
- *Taxodiaceaepollenites hiatus* (Potonie) Kremp

Spores:
- *Retitriletes austroclavitidites* (Cookson) Doring et al.
- *Baculatisporites comaumensis* (Cookson) Potonie
- *Camarozonosporites* spp.
- *Cicatricosisporites* spp.
- *Deltoidospora hallii* Miner
- *Foraminisporis wonthaggiensis* (Cookson & Dettmann) Dettmann
- *Multiporipollenites* sp.
- *Osmundacidites major* Doring
- *Pluricellaesporites* spp.
- Stereisporites antiquasporites (Wilson & Webster) Dettmann

Age: Barremian, zone undefined, approximately equivalent to Zone C1 of Banerjee and Davies (1986)

East shore of Mould Bay

E.H. Davies

GSC loc. C-198965; 76°18'00"N, 119°15'00"W; ridge-crest outcrops in drainage basin of Station Creek, 7.2 km northeast of the weather station; about 300 m above base of formation.

Dinoflagellates:
- *Holmwoodinium* sp. cf. *H. granorugulate*
- *Holmwoodinium notatum* Batten

Algae and miscellanea:
- *Pterospermella helios* Sarjeant

Pollen:
- *Alisporites bilateralis* Rouse
- *Araucariacites australis* Cookson
- *Callialasporites monoalasporus* Dev
- *Cedripites canadensis* Pocock - abundant
- *Cerebropollenites mesozoicus* Couper
- *Corollina torosa* (Reissinger) Klaus - abundant
- *Coronatispora valdensis* (Couper) Dettmann
- *Exesipollenites* sp. - perinate
- *Exesipollenites tumulus* Balme
- *Monosulcites* sp. cf. *M. scabratus* Brenner
- *Podocarpidites potomacensis* Brenner
- *Taxodiaceaepollenites hiatus* (Potonie) Kremp - abundant

Spores:
- *Aequitriradites spinulosus* (Cookson & Dettmann) Cookson & Dettmann
- *Baculatisporites comaumensis* (Cookson) Potonie
- *Cicatricosisporites mohrioides* Delcourt & Sprumont
- *Deltoidospora hallii* Miner
- *Foraminisporia dailyi* Dettmann
- *Gleicheniidites senonicus* Ross
- *Leiotriletes meckelfeldensis* Doring
- *Pilosisporites crassangularis* (Ivanova) Dorhofer
- *Stereisporites antiquasporites* (Wilson & Webster) Dettmann - abundant

Age: Barremian, zone undefined, approximately equivalent to Zone C1 of Banerjee and Davies (1986)

GSC loc. C-198964; 76°17'30"N, 119°14'00"W; low hilltop outcrops in the drainage basin of Station Creek, 6.4 km northwest of the weather station; in shale intercalated with conglomerate from highest beds in the Isachsen at about 350 m above base of formation.

Dinoflagellates:
- *Breedoxiella caperata* (Brideaux) Norris
- *Canningia ringnesiorum* Manum & Cookson
- *Subtilisphaera perlucida* (Alberti) Jain & Millipied

Algae and miscellanea:
- No taxa observed

Pollen:
- *Alisporites bilateralis* Rouse
- *Alisporites grandis* (Cookson) Dettmann
- *Callialasporites trilobatus* (Balme) Dev
- *Cedripites canadensis* Pocock
- *Cerebropollenites mesozoicus* Couper
- *Corollina torosa* (Reissinger) Klaus
- *Exesipollenites* sp. perinate
- *Exesipollenites tumulus* Balme
- *Laricoidits magnus* (Potonie) Potonie, Thompson & Thiegart
- *Perinopollenites elatoides* Couper
- *Podocarpidites epistriatus* Brenner
- *Podocarpidites granulosus* Pocock
- *Podocarpidites potomacensis* Brenner
- *Taxodiaceaepollenites hiatus* (Potonie) Kremp - abundant

Spores:
- *Aeqitriradities* sp.
- *Aequitriradites verrucosus* (Cookson & Dettmann) Cookson & Dettmann
- *Baculatisporites comaumensis* (Cookson) Potonie
- *Cicatricosisporites microstriatus* Jardine & Magloire
- *Cicatricosisporites minor* (Bolkovitina) Pocock
- *Cicatricosisporites mohrioides* Delcourt & Sprumont
- *Deltoidospora hallii* Miner

Gleicheniidites senonicus Ross
Impardecispora apiverrucata (Couper) Venkatackala, Kar & Raza
Interlobites triangularis (Brenner) Phillips & Felix
Leiotriletes equiexinus (Couper) Doring
Osmundacidites major Doring
Osmundacidites wellmannii Couper
Stereisporites antiquasporites (Wilson & Webster) Dettmann
Tigrisporites scurrundus Norris
Triretilobata purverulentus (Verbitskaya) Dettmann

Age: Barremian to Aptian, zone undefined, approximately equivalent to Zone C2 of Banerjee and Davies (1986)

CHRISTOPHER FORMATION (Kc)

West of Walker Inlet

J.H. Wall

GSC loc. C-133991; 76°12'22"N, 120°07'27"W; outcrop immediately beneath methogenic carbonate mound, 15.0 km east of the head of Walker Inlet and 15.8 km southwest of Landing Lake; about 30.0 m above base of formation.

Foraminifera:
Ammodiscus crenulatus Chamney
Glomospira sp.
Haplophragmoides sp.
Pseudobolivina rayi (Tappan)
Lenticulina sp. - fragments
Vaginulinopsis sp. - two incomplete specimens
Discorbis norrisi Mellon and Wall
Conorbina? sp. B of Stelck *et al.* 1956 - dominant
Quadrimorphina albertensis Mellon and Wall - two small specimens

Ostracoda:
genera indeterminate - three free valves representing two genera

Bivalvia (Pelecypoda):
shell fragments

Age: Early Cretaceous, Early Albian indicated by dominant calcareous component associated with the *Q. albertensis* assemblage from the lower part of the Christopher Formation in the eastern Sverdrup Basin

J.A. Jeletzky

GSC loc. C-133992; 76°08'00"N, 120°03'09"W; collection from methogenic carbonate mound, 22.2 km south of Landing Lake and 7 km west of the closest part of Mould Bay; estimated 125 m above base of formation.

Identifications:
Grammatodon (Cosmetodon) ex. aff. *bojarkensis* Sanin 1984
Grammatodon (Cosmetodon) n. sp. indet. (rare)
Nucula (Nuculoma) cf. or aff. *N. (N.) variabilis* (Sowerby 1830) (rare)
Indeterminate taxodont pelecypods (?more than one genus)
Taimyrothyris ex gr. *T. humilis* Dagis 1968 (a terebratulid brachiopod; numerous to very numerous)
Serpula (s. lato) sp. indet. (worm tubes; mass occurrence; these irregularly twisted tubes fill the sample's matrix)
Spirorbis sp. indet. (gastropod-like coiled worm tubes; fairly common)

Age: The worm tubes appear to be related specifically to the congeneric tubes described and figured by Imlay (USGS Prof. Paper 335, Pl. I, fig. 11–11, 23, 26) from the Albian rocks of Northern Alaska. However, the taxodont pelecypods and brachiopods appear to be related to the early Early Cretaceous (i.e., Berriasian–Valanginian) species recently described by Sanin (Acad. Nauk SSSR, Sibirskoye Otdelenie, Trudy Instituta Geologii i Geofiziki, No. 310, 1976), Sanin, Zakharov, and Shurygin (ibid., No. 585, 1984), and Dagis (ibid., No. 41, 1968). No particular biochronological significance should, however, be ascribed to these affinites of macrofossils of the lot C-133992. First of all, closely similar and possibly specifically identical nuculid and grammatodontid pelecypods occur also in the Early Albian lot C-33731 discussed earlier in this report. Furthermore, the time ranges of all the species and genera concerned remain very poorly understood in North Siberia and northern Alaska. All these taxa appear to be long ranging and facies bound. Finally, none of the Prince Patrick Island taxa is specifically identical with their North Siberian and North Alaskan analogues. Consequently the lot C-133992 can only be dated as of a general Early Cretaceous (i.e., Berriasian to Albian) age. There is nothing in it, however, to contradict the assignment of the lot C-133992 to the Albian and ?Aptian Christopher Formation proposed by the collector in its label.

Head of Mould Bay

E.H. Davies and J.H. Wall

GSC loc. C-198997; 76°25'25"N, 119°33'30"W; isolated outcrop 7.5 km north of the head of Mould Bay, unknown height above base of formation.

Dinoflagellates:
Apteodinium maculatum McIntyre & Brideaux - derived
Astrocysta cretacea (Pocock) Davey
Breedoxiella caperata (Brideaux) Norris
Cleistosphaeridium aciculare Davey
Cribroperidinium spp.
Cyclonephelium distinctum Deflandre & Cookson
Cyclonephelium paucispinum Davey
Diconidinium sp. - abundant
Dingodinium cerviculum Cookson & Eisenack
Ellipsoidictyum imperfectum (Brideaux & McIntyre) Lentin & Williams
Gonyaulacysta hyalodermospsis sensu Brideaux & McIntyre 1975
Gonyaulacysta jurassica (Deflandre) Norris & Sarjeant - derived Jurassic
Holmwoodinium notatum Batten
Imbatodinium jaegeri (Alberti) Dorhofer & Davies
Odontochitina operculata (Wetzel) Deflandre
Oligosphaeridium vasiformis (Neale & Sarjeant) Davey & Williams
Oligosphaeridium fenestratum Duxbury
Ovoidinium scabrosum (Cookson & Eisenack) Davey
Paragonyaulacysta borealis (Brideaux & Fisher) Stover & Evitt - derived
Spongodinium sp.
Vesperopsis sp. A, B and M '75

Algae and miscellanea:

Baltisphaeridium spp.
Sigmapollis sp.

Pollen:
Alisporites bilateralis Rouse - abundant
Alisporites grandis Dettmann
Cerebropollenites macroverrucosus (Thiegart) Doring - abundant
Ephedripites sp.
Monosulcites scabratus Brenner
Perinopollenites elatoides Couper
Pinuspollenites spp.
Podocarpidites canadensis Pocock
Vitreisporites pallidus (Reissinger) Nilsson

Spores:
Cicatricosisporites delicatus Phillips & Felix
Cicatricosisporites mohrioides Delcoourt & Sprumont
Deltoidospora hallii Miner
Gleicheniidites senonicus Ross
Kuyliporites lunaris Cookson & Dettmann
Osmundacidites wellmannii Couper
Pluricellaesporites spp.
Stereisporites antiquasporites - abundant

Foraminifera:
Hippocrepina barksdalei (Tappan)
H. sp.
Ammodiscus crenulatus Chamney
Miliammina sp., small, poorly preserved
Haplophragmoides spp., poorly preserved
Trochammina sp., small, very thin - one
Uvigerinammina sp. cf. *U. manitobensis* (Wickenden) - a later portion probably referable to this species
U. sp. indet. - an incomplete specimen referable to either *U. manitobensis* or *U. athabascensis* (Mellon and Wall)

Age: Early Cretaceous, Albian, foraminiferal assemblage. The palynomorph and dinoflagellate assemblage is equivalent to the *Vesperopsis mayii* Zone for the Mesozoic of the Beaufort Mackenzie-Northern Alaska area (Bujak and Davies *in* Turner, 1994), Early to Middle Albian. Sample also contains reworked Jurassic microflora.

North of Jameson Bay

J.H. Wall

GSC loc. C-163566; 76°56'00"N, 116°47'20"W; escarpment section on the east side of one of several outliers, 27.5 km northeast of the head of Intrepid Inlet and 27.3 km west of Cape Hemphill; 3 m above exposed base of formation.

Foraminifera:
Saccammina lathrami Tappan
Haplophragmoides spp.
Pseudobolivina rayi (Tappan) Sliter 1981 (=*Siphotextularia? rayi* Tappan 1962)

Age: Early Cretaceous, Early to Middle Albian, *P. rayi* is recorded by Sliter (1981) from both the lower and upper units of the Christopher Formation in outcrop sections on the Ringnes islands.

Catherine Point on Eglinton Island

J.H. Wall

GSC loc. C-133951; 75°47'30"N, 118°05'00"W; inland hillside section, 7.0 km northwest of Catherine Point; 10 m above exposed base of formation.

Foraminifera:
Kechenotiske sp.
Saccammina lathrami Tappan - circular and flask-shaped specimens
Haplophragmoides sp. cf. *H. sluzari* Mellon and Wall - common
Trochammina sp.-spp., indistinct
Uvigerinammina athabascensis (Mellon and Wall) - common

Age: Early Cretaceous, late Early Albian indicated on the basis of strong occurrence of *U. athabascensis*, a key component of the *Quadrimorphina albertensis* assemblage, coincident with the lower part of the Chistopher Formation in the eastern Sverdrup basin (Wall, 1983, p. 262).

Cape Nares on Eglinton Island

E.H. Davies and J.H. Wall

GSC loc. C-198988; 75°40'30"N, 119°06'45"W; streambank section 10.7 km northeast of Cape Nares; 20 cm below exposed top of formation.

Dinoflagellates:
Astrocysta cretacea (Pocock) Davey
Batiacasphaera sp.
Chichaouadinium sp.
Cleistosphaeridium huguontionii (Valensi) Davey
Ellipsoidictyum imperfectum (Brideaux & McIntyre) Lentin & Williams
Eurydinium sp.
Fromea fragilis (Cookson & Eisenack) Stover & Evitt
Gardodinium eisenackii Alberti
Gonyaulacysta spp.
Imbatodinium jaegeri (Alberti) Dorhofer & Davies
Leptodinium hyalodermopsis sensu Brideaux & McIntyre 1975
Nummus monoculatus Morgan
Odontochitina costata Alberti
Odontochitina operculata (Wetzel) Deflandre & Cookson
Oligosphaeridium vasiformis (Neale & Sarjeant) Davey & Williams
Oligosphaeridium complex (White) Davey & Williams
Senoniasphaera microreticulata Mrideaux & McIntyre
Vesperopsis sp. A, sensu Brideaux & McIntyre 1975

Algae and miscellanea:
Micrhystridium sp. A, sensu Brideaux & McIntyre 1975 - abundant
Veryhachium spp.

Pollen:
Araucariacites australis (Cookson) - abundant
Cedripites canadensis Pocock
Cedripites cretacea Pocock - abundant
Cerebropollenites mesozoicus (Couper) Nilsson
Clavatipollenites minutus Brenner
Ephedripites virginiaensis Brenner
Monosulcites scabratus Brenner
Perinopollenites elatoides Couper

Pinuspollenites spp.
Podocarpidites granulosus Pocock
Taxodiaceaepollenites hiatus (Potonie) Kremp - dominant
Vitreisporites pallidus (Riessinger) Nilsson

Spores:
Cicatricosisporites australiensis (Cookson) Potonie
Concavissimisporites punctatus (Delcourt & Sprumont) Brenner
Dictyophyllidites harrisii Couper
Gleicheniidites senonicus Ross - abundant
Osmundacidites wellmannii Couper
Retitriletes austroclavitidites (Cookson) Doring et al.
Stereisporites antiquasporites (Wilson & Webster) Dettmann - abundant
Tigrisporites scurrundus Norris
Trilobosporites humilis Delcourt & Sprumont

Foraminifera:
Hippocrepina barksdalei (Tappan) - one
Ammodiscus crenulatus Chamney - two
Miliammina manitobensis Wickenden - two
M. sp. - one
Haplophragmoides sp.-spp., indistinct
Ammobaculites sp. - one
Trochammina sp., poorly preserved
Uvigerinammina manitobensis (Wickenden)
Verneuilinoides borealis Tappan?, poorly preserved - one

Age: Early Cretaceous, Middle to possibly early Late Albian. The microfauna most closely matches that of the *V. borealis* assemblage from the upper part of the Christopher Formation in the eastern Sverdrup Basin. The microflora are equivalent to the *Vesperopsis mayii* Zone for the Mesozoic of the Beaufort Mackenzie-Northern Alaska area (Bujak and Davies *in* Turner, 1994), Early to Middle Albian.

HASSEL FORMATION (K_H)

Plauchut and Jutard (1976) have reported Late Albian microflora from the Hassel Formation of Eglinton Island, and similarities to the microfloral assemblage in the same formation on Banks Island.

KANGUK FORMATION (K_K)

Cape Nares on Eglinton Island

E.H. Davies

GSC loc. C-198984; 75°40'30"N, 119°06'45"W; streambank section 10.7 km northeast of Cape Nares; 50 cm above exposed base of formation.

Dinoflagellates:
Achomosphaera ramulifera (Deflandre) Evitt
Cleistosphaeridium aciculare Davey
Cleistosphaeridium huguontionii (Valensi) Davey
Epelidosphaera sp.
Eurydinium eyrensis (Cookson & Eisenack) Stover Evitt
Eurydinium globosum (Davey)
Eurydinium glomeratum (Davey) Stover & Evitt
Eurydinium sp.
Isabelidinium acuminatum (Cookson & Eisenack) Stiver Eveit
Isabelidinium magnum (Davey) Stover & Evitt

Algae and miscellanea:
Palambages spp.
Spheripollenites sp. - abundant

Pollen:
Alisporites bilateralis Rouse
Cedripites cretacea Pocock
Piceaepollenites spp.
Pinuspollenites spp.
Taxodiaceaepollenites hiatus (Potonie) Kremp - dominant

Spores:
Gleicheniidites senonicus Ross

Age: Equivalent to the *Isabelidinium magnum* Zone for the Mesozoic of the Beaufort Mackenzie-Northern Alaska area (Bujak and Davies *in* Turner, 1994?), Cenomanian to Turonian

Published report of J.A. Jeletzky in Tozer and Thorsteinsson (1964)

GSC loc. 37188; collection from 10 km east of Cape Nares, about 60 m below the top of the lower (shale) member of the Kanguk Formation.

Identifications:
Inoceramus sp. cf. *I. cardissoides* Goldfuss *sensu lato*
Oxytoma sp. cf. *O. camselli* McLearn

Age: mid-Late Cretaceous (Santonian to early Campanian)

J.H. Wall

GSC loc. C-156057; 75°38'N, 119°22'W; coastal hillside section 3.4 km northeast of Cape Nares; 99 m below top of lower (shale) member, about 135 m above base of formation.

Foraminifera:
Reophax sp.-spp.., may include incomplete specimens of *Ammobaculites*
Haplophragmoides howardense Stelck and Wall
H. sp.-spp., nondescript - dominant
Trochamminoides sp.,
Ammobaculites sp., fairly wide, moderately grainy - common
Textularia sp., low chambers, flaring test
Pseudobolivina rollaensis (Stelck and Wall) - common
Dorothia smokyensis Wall(?), poorly preserved

Age: Late Cretaceous, probably correlative with the *D. smokyensis* assemblage of Late Turonian to Early Campanian age, as reported by Wall (1983, p. 264) from the Kanguk Formation in the eastern Sverdrup Basin.

GSC loc. C-156070; same section as previous collection; 7 m below top of lower (shale) member.

Foraminifera:
Haplophragmoides howardense Stelck and Wall
H. howardense manifestum Stelck and Wall
H. sp.-spp.
Trochamminoides sp.
Pseudobolivina rollaensis Stelck and Wall(?), one incomplete specimen
Trochammina ribstonensis Wickenden - two
T. sp., small - two

Verneuilinoides bearpawensis (Wickenden)
Dorothia smokyensis Wall

Radiolaria:
Spongodiscus (Spongodiscus) spp.

Porifera:
porous, generally cylindrical or subcylindrical, noncalcareous fragments

Age: Late Cretaceous, probably in the upper range of the *D. smokyensis* assemblage, that is, early Campanian, due to presence of *T. ribstonensis*

GSC loc. C-156077; same section as previous collection; 2 m above top of Eglinton Member of Kanguk Formation.

Foraminifera:
Bathysiphon sp.
Saccammina sp., coarse-grained
Ammodiscus sp.
Haplophragmoides rota Nauss
H. sp. cf. *H. rota*, large
Verneuilinoides bearpawensis (Wickenden) - poorly preserved

Porifera:
siliceous spicules

Age: Late Cretaceous, probably early Campanian

Appendix B
Magnetic compass operation at high latitudes: Examples from Prince Patrick Island (L.R. Newitt)

Introduction

The magnetic compass is a simple and convenient tool for navigation and orientation. However, users should be aware of several factors that can adversely affect the operation of a compass and lead to mis-orientation errors. These include localized magnetic anomalies, slow changes in the direction of the magnetic field (secular variation), and the variability of the magnetic field due to solar activity. Some of these phenomena have been discussed by Newitt (1991). A discussion of the secular variation of magnetic declination is given by Dawson and Newitt (1984). An interesting example of the extent to which a local magnetic anomaly can affect magnetic declination is given by Newitt and Dawson (1980).

In the high Arctic regions, the potential for compass errors increases substantially. There are two reasons for this. First, the horizontal force of the magnetic field (H), which directs a compass needle, diminishes as one approaches the magnetic pole, which was located, in 1994, at 78.3°, 104.0°W (Newitt and Barton, 1996). (Preliminary results of a survey carried out in May, 2001, indicate that the North Magnetic Pole has undergone a significant change in position since 1994 and is now located near 81°N, 108°W.) As a rule of thumb, a compass becomes erratic when H is less than 6000 nannoteslas (nT), and becomes useless when H is less than 3000 nT, as is the case over much of the high Arctic (Fig. B-1). Nevertheless, experience (C. Harrison, pers. comm.; S.-A. Jober, pers. comm.) and laboratory experiments have shown that well-constructed compasses can be used successfully in regions of low H (~ 2000 nT). Second, the variability of declination, associated with magnetic disturbances, greatly increases in the high Arctic. In part this is geometric. When H is very small, even a relatively small magnetic disturbance, expressed in nanoteslas, results in a large

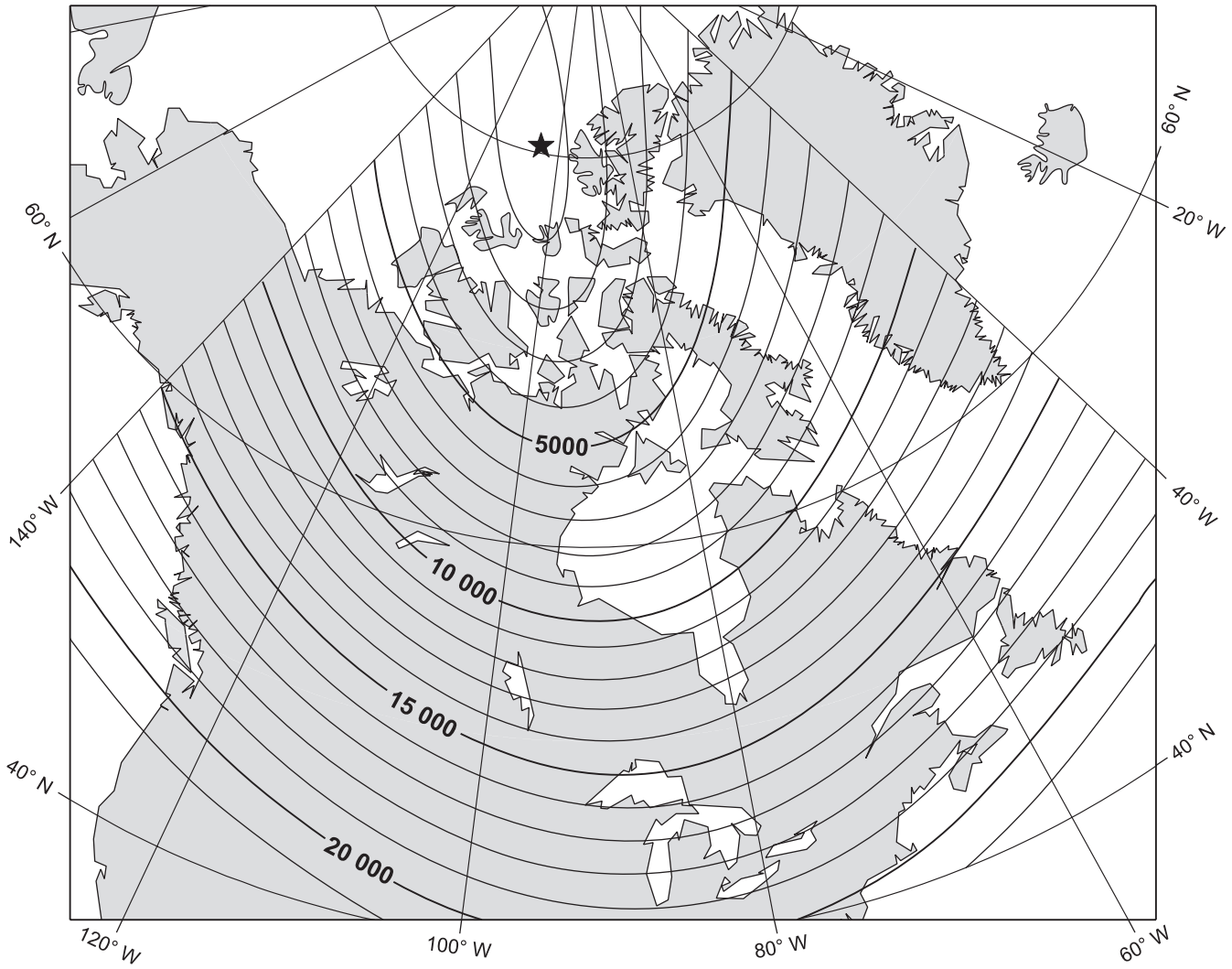

Figure B-1. *Horizontal intensity of the magnetic field in Canada for 2001; contour interval is 1000 nT. Position of the North Magnetic Pole is denoted by a ★.*

angular variation. The size of a fluctuation in declination will double with each factor of two decrease in H. However, the frequency and intensity of magnetic disturbances are also greater in the Arctic than in southern Canada, and their characteristics are different. We will look at some of these factors as they apply to the region of Prince Patrick Island.

Magnetic declination and secular variation

The angle between the magnetic meridian and the geographic meridian is called magnetic declination (or sometimes variation, especially by mariners). The magnetic field, including declination, constantly changes with time. It is therefore common practice to produce, every five years, both global and regional mathematical models of the magnetic field from which declination can be calculated. Charts of declination, based on these models, are also published. One of the most popular global models is the International Geomagnetic Reference Field (IGRF), produced under the auspices of the International Association of Geomagnetism and Aeronomy. The latest version is for year 2000 (Mandea et al., 2000). A model for Canada, referred to as the Canadian Geomagnetic Reference Field, is also available for 2000 (production is similar to that described by Haines and Newitt, 1997, for the 1995 model). The CGRF provides more detail and greater accuracy over Canada than does a global model.

An examination of charts derived from the IGRF or CGRF, such as the 2000 magnetic declination chart for Canada (Newitt, 2000) shows that the gradient of magnetic declination is not uniform. In southern Canada, it varies from 1.25° per 100 km in Manitoba to 0.625° per 100 km in British Columbia. The gradient also becomes much greater as one approaches the North Magnetic Pole. This is evident in Figure B-2, which shows lines of equal magnetic declination (and annual change) in the Prince Patrick Island region. The gradient in parts of the region exceeds 3° per 100 km; in other words, one-degree contour lines are only about 33 km apart. From a practical point of view, this means that a compass user must know where he or she is, and use the appropriate declination value for that location. A single value cannot be assumed for a large survey area in regions near the Magnetic Pole.

A second point to note is the extremely large value of annual change; declination is decreasing by more than 2° per year in area shown in the eastern part of the figure. The obvious impact of this is that published declination values become outdated very rapidly. Although annual change values are also published on maps to correct the declination, they become unreliable after a few years because the magnetic field does not change in a linear manner. This can be seen in Figure B-3, which shows the secular change at Mould Bay Magnetic Observatory on Prince Patrick Island, from 1966 to 1997. Ignoring for the moment the rapid variations, which I will discuss later, it can be seen that the declination has been decreasing, and that the rate of decrease has gone from approximately 10' a year in the later 1960s to more than 80' a year by 1997.

Variability of declination associated with magnetic disturbances

The secular variation of the magnetic field, like the main magnetic field itself, originates in the Earth's outer core. However, the magnetic field is subject to higher frequency, or transient, variations, with periods ranging from years to milliseconds, that are of solar origin. Most of these variations result from highly complex interactions between the Earth's magnetosphere and ionosphere and the continuous stream of charged particles (solar wind) emanating from the Sun. I will use the term "magnetic disturbance" to describe the results of these interactions on the Earth's magnetic field. The morphology of these transient variations differs over different regions of the Earth – the equatorial zone, mid-latitude region, auroral zone, and polar cap; the last three regions are present in Canada. From the point of view of the compass user, the effects of magnetic disturbance on declination are normally unimportant at mid-latitudes. Newitt (1991) showed that variations greater than 2° occur less than 10 per cent of the time anywhere south of the auroral zone. However, this is not the case in the polar cap. For example, on Prince Patrick Island, variations in excess of 2° occur more than 75 per cent of the time.

The morphology, distribution, and frequency of magnetic disturbances in Canada have been investigated by many authors (see, for example, Whitham et al, 1960; Loomer and Whitham, 1963; Loomer and Jansen van Beek, 1969; Loomer, 1979; Newitt and Walker, 1986, 1990). However, none of these authors looked at the subject from the point of view of magnetic declination. I shall do so in the following paragraphs. All the examples presented are based on data recorded at Mould Bay Magnetic Observatory, which, until its closure in 1997, was one of 14 observatories operated by the Geomagnetism Program of the Geological Survey of Canada, Natural Resources Canada. Mould Bay commenced operation in 1962, and between 1985 and 1997 values of the north, east, and vertical components of the magnetic field were recorded digitally at one-minute intervals. Data from all Canadian magnetic observatories are routinely archived and are available in a variety of formats.

Magnetic declination in the polar cap shows a distinct seasonal variation, as is evident in Figure B-3. Although there is year-to-year variability, an average seasonal variation can be computed. This is shown in Figure B-4, which was compiled from monthly mean values of magnetic declination for the time interval from 1966 to 1994. The effect of the secular variation has been removed. There is a distinct decrease in the average magnetic declination of almost 0.5° during the summer months from the "undisturbed" level, which occurs during mid-winter, when solar radiation is at a minimum.

The seasonal variation, however, is almost overwhelmed when the day-to-day variability of declination is considered. Figure B-5 is a plot of daily mean values of declination for the year 1993. Although there are instances when the daily mean declination value varies by only a fraction of a degree from one day to the next, there are also occasions when the declination changes by up to 2°.

Of course the magnetic field does not remain constant over a day. In fact, the largest changes in declination occur over time intervals of less than 24 hours. This is illustrated in Figure B-6, which shows magnetic field variations at Mould Bay on three days – a magnetically quiet day, an unsettled day, and a disturbed day. Truly quiet days are rare in the polar cap, and normally occur only in the winter months. Disturbed days, on the other hand, are frequent in the summer months. This is illustrated in a different manner in Figure B-7, which is based on an analysis of Mould Bay hourly range values (the change in declination over a one hour time interval). The average hourly range shows a clear maximum of about 4° in the summer, compared to 1.5° in winter.

Although declination varies extremely rapidly on the unsettled and disturbed days plotted in Figure B-6 (changes of several degrees occur in less than one hour on the disturbed day, and of more than a dozen degrees over the course of a few hours), a regular diurnal change is also evident. This is shown more clearly in Figure B-8, which is based on an analysis of hourly mean values.

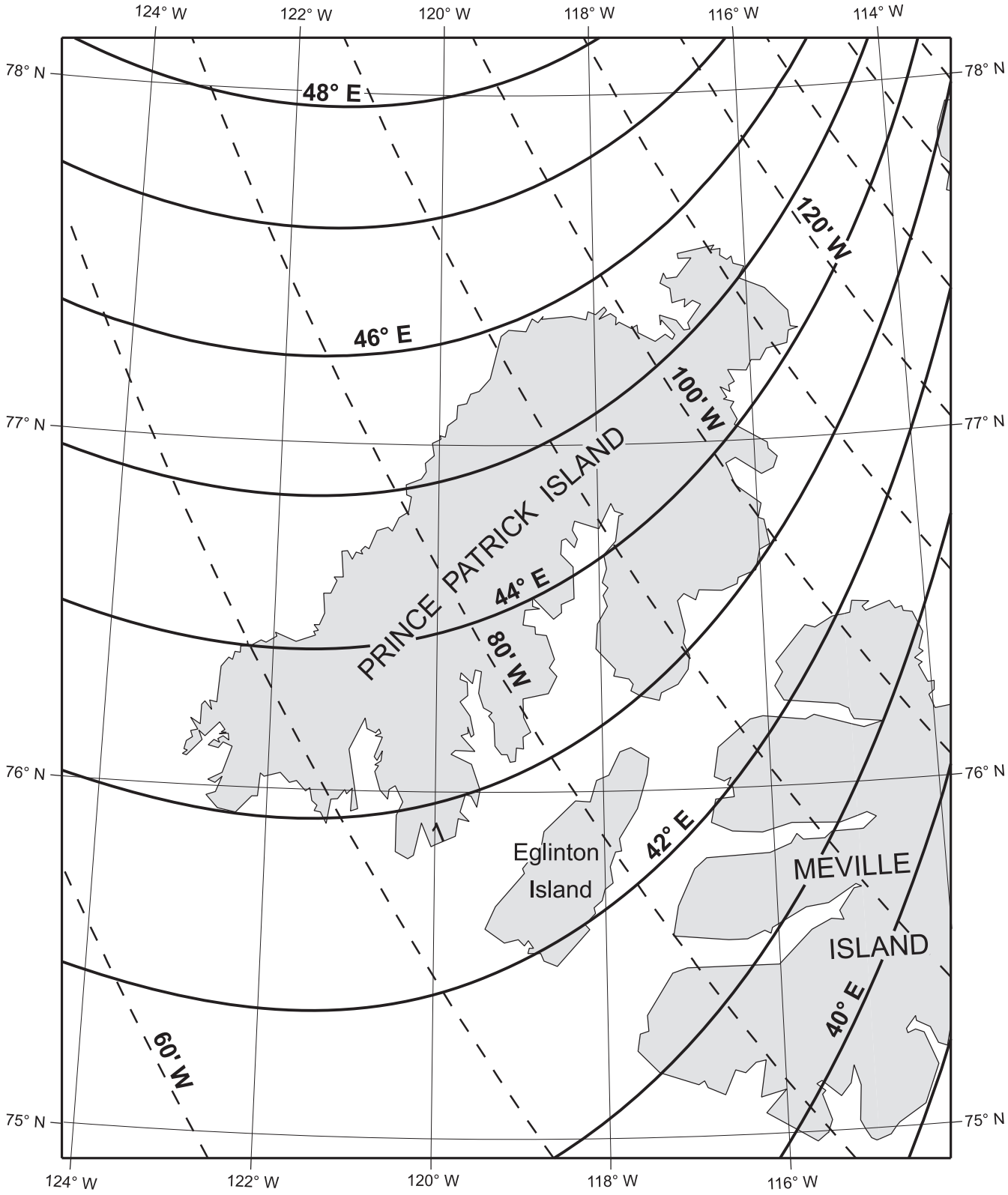

Figure B-2. *Magnetic declination for 2000, in degrees (solid lines), and annual change, in minutes per year (dashed lines) for the Prince Patrick Island region.*

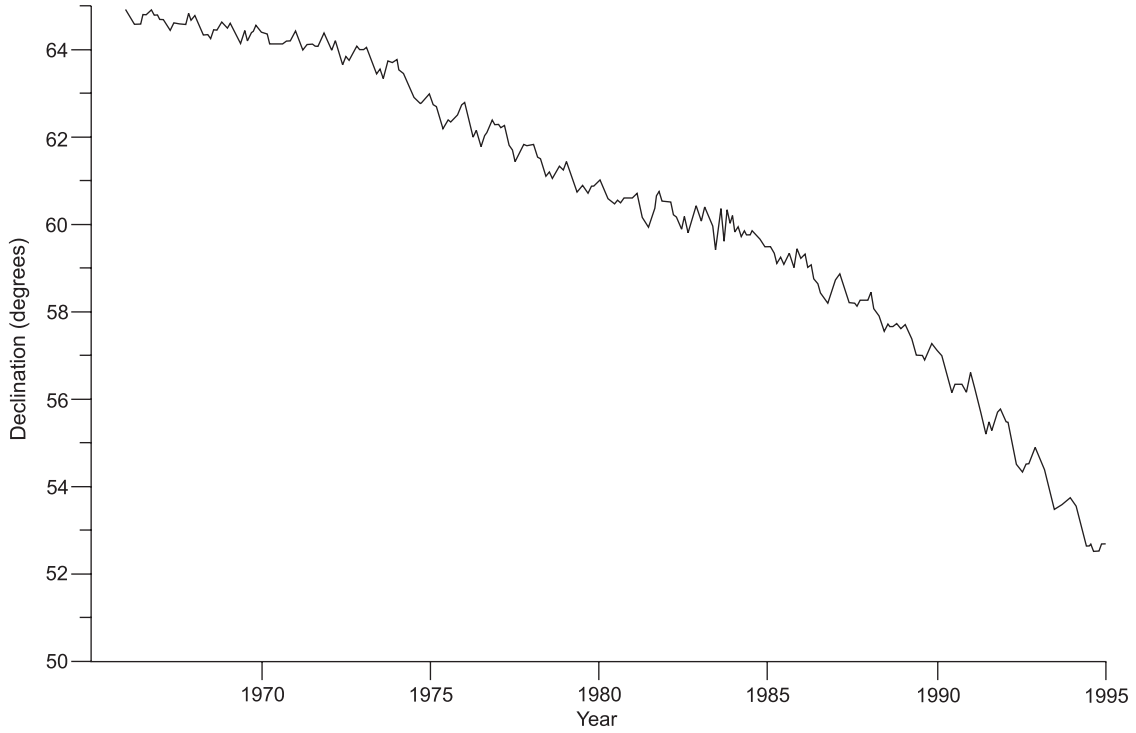

Figure B-3. *Secular change of declination at Mould Bay from 1966 to 1997, based on monthly mean values recorded at the Magnetic Observatory. A seasonal variation modulates the general downward trend.*

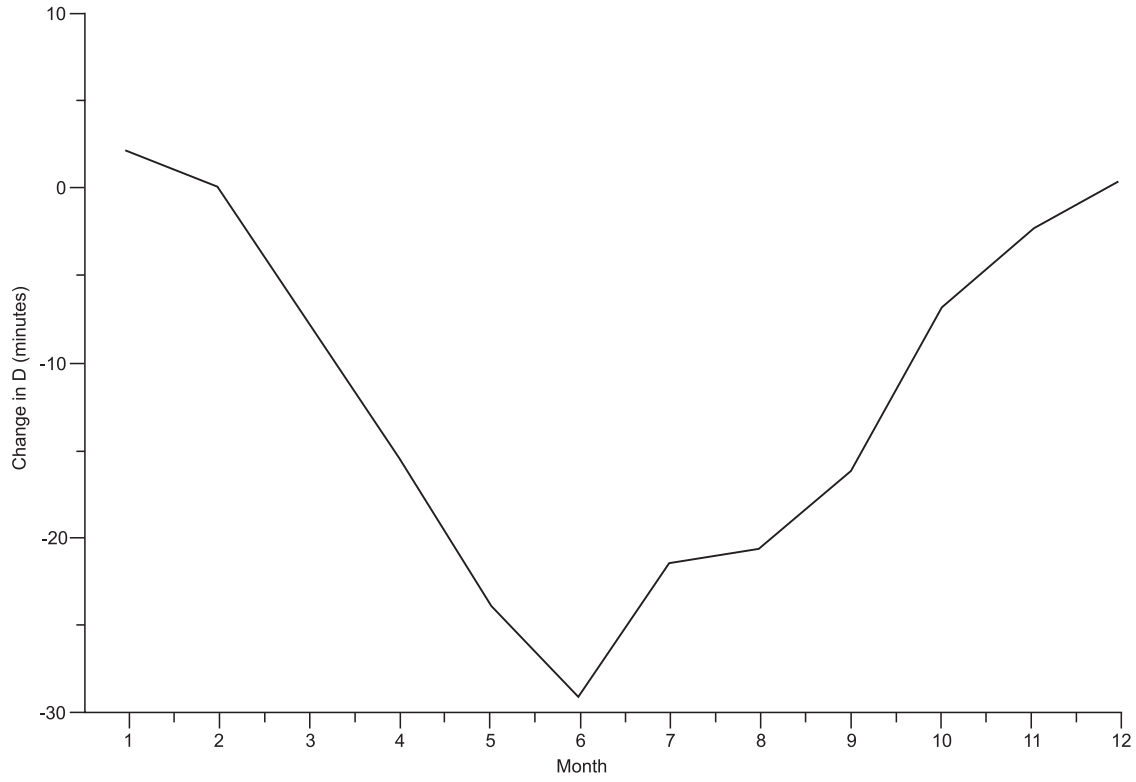

Figure B-4. *Seasonal variation of declination at Mould Bay Magnetic Observatory, computed from monthly mean values for the years 1966 to 1994. The effect of secular variation has been removed, and the curve is plotted relative to the average winter value of declination, when the effects of solar radiation are at a minimum.*

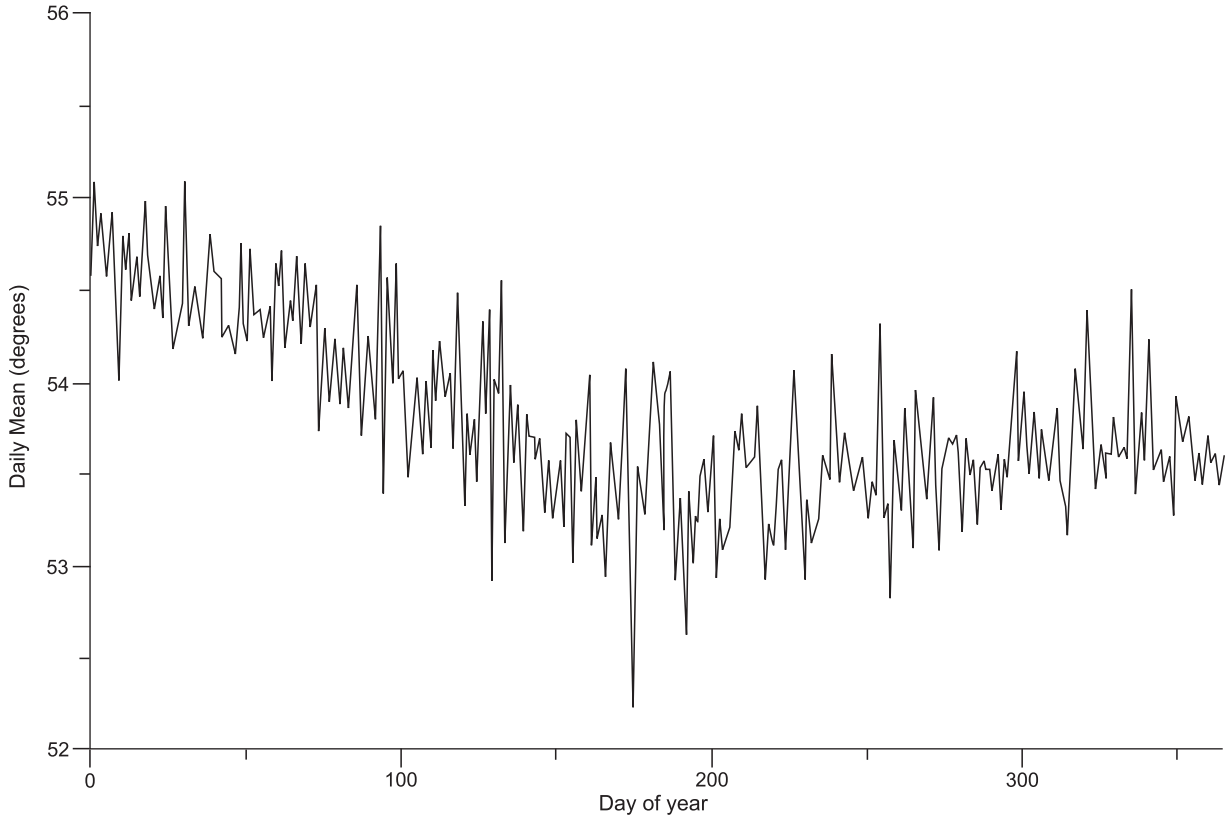

Figure B-5. *The variability of declination from day to day, shown by plotting Mould Bay daily mean values for 1993.*

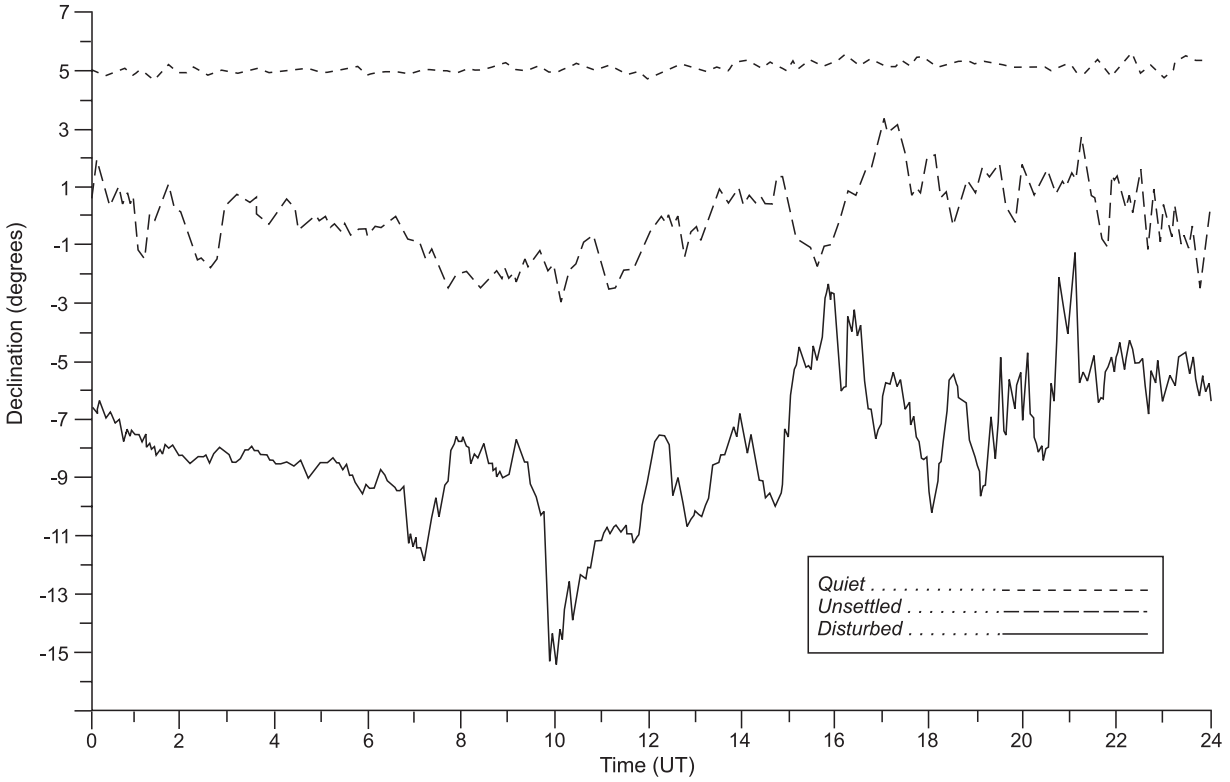

Figure B-6. *Plots of magnetic declination at Mould Bay on a magnetically quiet day (December 9, 1993), an unsettled day (June 27, 1993), and a disturbed day (March 11, 1993). Plots are derived from one minute values of magnetic declination recorded at the Magnetic Observatory. Values of declination in these plots are relative, having been adjusted to prevent overlap.*

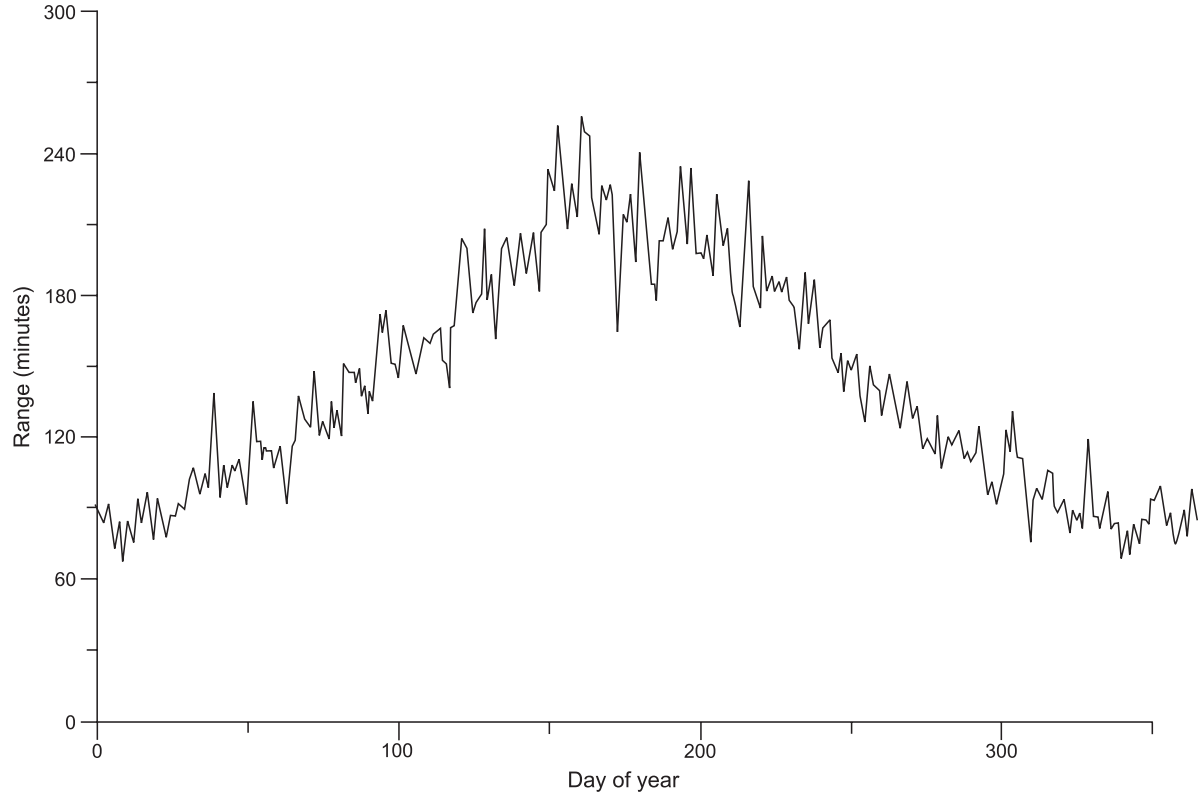

Figure B-7. *Magnetic declination plot at Mould Bay showing greater variability during the summer months due to increased magnetic disturbance during the summer. The plot is based on hourly range values recorded at Mould Bay for the years 1966 to 1994.*

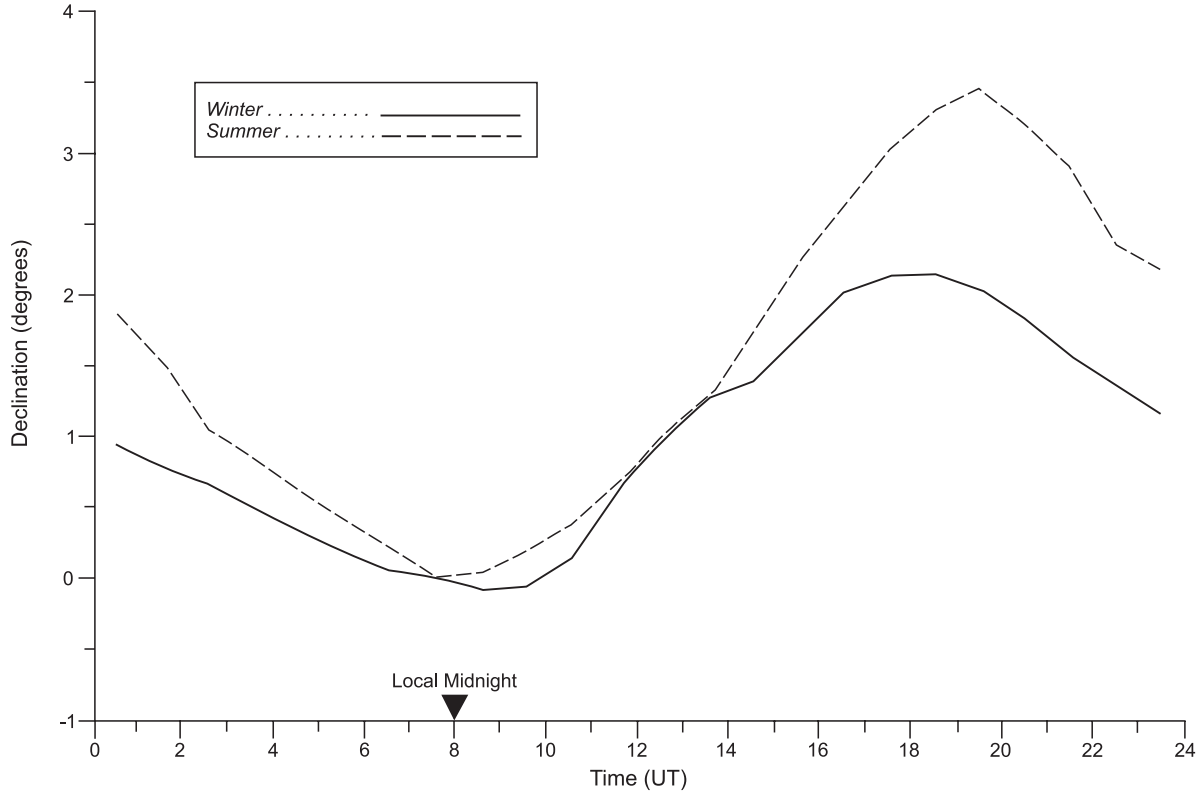

Figure B-8. *Daily variation of declination at Mould Bay during the winter (solid line), and during the summer (dashed line). Winter is defined as November, December January; summer is defined as May, June, July. Plots are derived from hourly mean values from the years 1966 to 1994. Plots are relative to the average night-time level of magnetic declination, when the magnetic field is less disturbed by solar radiation.*

The winter (November, December, January) and summer (May, June, July) seasons have been analyzed separately. The declination is near its "undisturbed" level near local midnight (8 UT at Mould Bay), and increases steadily to reach a maximum near local noon. The maximum is about 2° in winter, but is almost 3.5° in summer. In other words, a compass needle will point, on the average, 3.5° too far to the east at local noon in the summer.

The high-frequency variability of declination also shows a diurnal pattern, as seen in Figure B-9. This diagram is based on an analysis of Mould Bay hourly ranges. It can be seen that ranges are smallest (about 1.5°) just before midnight, and reach a maximum in the early afternoon of over 4°. Combining this fact with the seasonal change presented in Figure B-7 indicates that the variability would reach several degrees on average.

Magnetic anomalies

Magnetic field models, such as the IGRF and the CGRF, give values of magnetic declination that are smoothed. The actual value at a location may differ from the model value as a result of the presence of magnetic minerals in the crust. The magnitude and extent of these magnetic anomalies depends on the local geology, so it is impossible to come up with a general rule of thumb that will enable a user to judge their effects on a compass. An examination of aeromagnetic map sheets, if they are available, will indicate whether anomalies are a potential problem, but the total force values given on these charts cannot, in general, be converted to degrees.

One well-studied magnetic anomaly, for which both total force and magnetic declination measurements have been made, is Kingston Harbour (Dawson and Newitt, 1984). The anomaly is known to be caused by a gabbro intrusive with a 15 per cent concentration of magnetite and a 0.5 per cent concentration of ilmenite. Aeromagnetic measurements show a total force anomaly of 13 000 nT. Measurements made on board ship and on the ice show that this results in anomalous declination values in excess of 16°. A compass needle would point too far to the east on the west flank of the total force anomaly, and too far to the west on the east flank. A similar anomaly in the high Arctic, where H is much smaller, would likely cause a much larger effect in declination.

Bringing a metal object close to a compass will produce an effect similar to that of a magnetic anomaly. The effects of several common objects, at different distances and for different values of H, are given in Table B-1. These effects were measured in an ambient field of 17000 nT, and were scaled to an H value of 3000 nT. The table should be used only as a guideline. The actual effect of an object will depend on its exact composition, orientation and position relative to the compass needle.

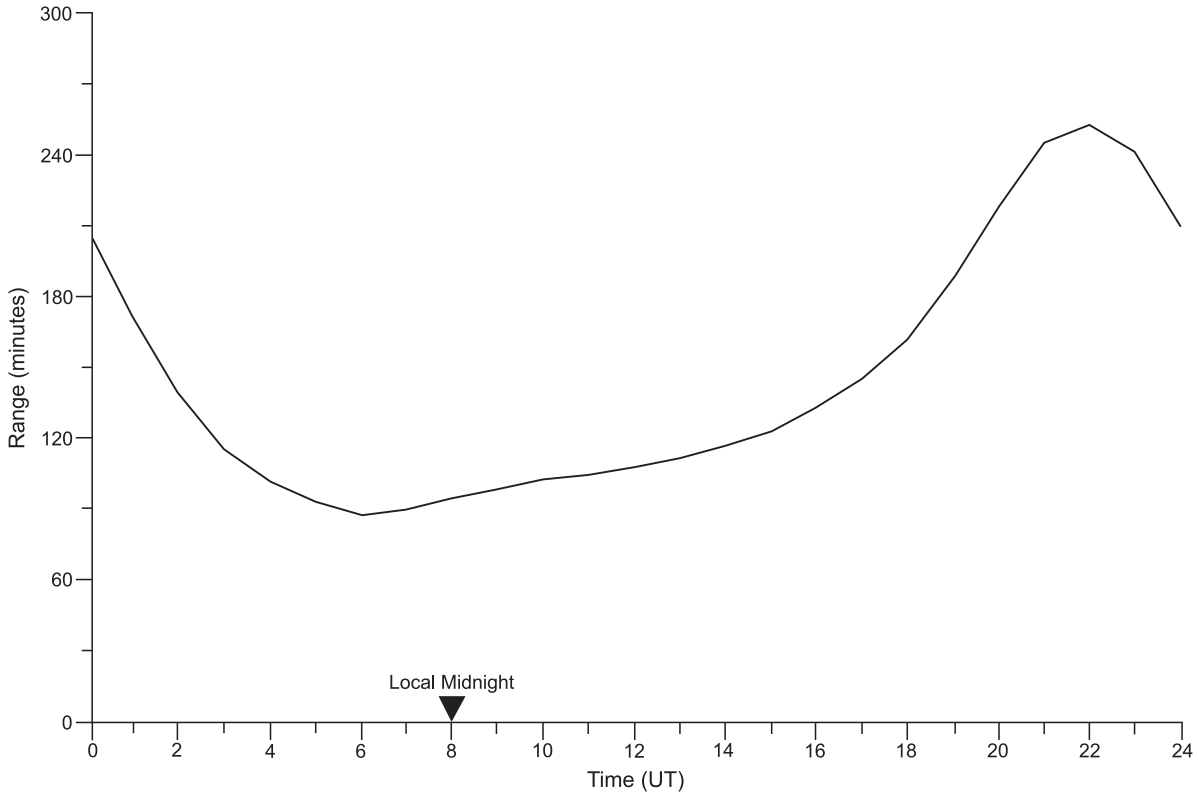

Figure B-9. *Magnetic declination plot at Mould Bay showing greater variability during the early afternoon than during the period near midnight. The plot is based on hourly range values from Mould Bay for the years 1966 to 1994.*

Conclusions

Use of a magnetic compass in the high Arctic regions is complicated by the very dynamic nature of the Earth's magnetic field. The steep magnetic gradient found near the magnetic pole causes rapid changes of declination over short distances. Large temporal variations of a secular, seasonal, daily and irregular nature are present. These may be summarized as follows for the Prince Patrick Island region:

- A large secular decrease in declination, amounting to approximately 80' a year in the mid-1990s.

- A seasonal decrease in the average declination of approximately 0.5° during the summer months.

- A seasonal increase in the variability of declination during the summer months, up to 4° per hour.

- A diurnal increase in the average magnetic declination of about 3.5° near local noon.

- A diurnal increase in the variability of declination in the early afternoon, up to about 4° per hour.

Provided these factors are taken into account, a compass remains a valuable tool for traversing, and for determining orientation and strike of geological features.

Table B-1. Effect of Common Objects on a Magnetic Compass as measured in an ambient field of 17 000 nT and scaled to 3000 nT

	H = 17000 nT			H = 3000 nT		
Object	1.0 m	0.5m	0.25m	1.0m	0.5m	0.25m
Keys	0	0	0	0	0	<0.25
Steel-toe boots	0	<0.25	<0.25	<0.25	<0.25	0.75
Jackknife	0	<0.25	0.50	<0.25	0.25	2.50
Hammer	0	<0.25	0.50	<0.25	0.50	2.75
Flashlight (on)	0	<0.25	0.75	<0.25	0.50	4.00
30-m steel tape	0	<0.25	0.75	<0.25	0.50	4.50
Screwdriver	0	<0.25	0.75	<0.25	0.50	4.75
Rifle	0	0.25	1.00	<0.25	1.75	5.00
Shovel	<0.25	0.50	1.50	0.50	3.00	9.25

This is a Windows®-based autostart disk. If the autostart is not working, go to the CD-ROM root directory and double-click on the autoplay.exe file. If you read this CD-ROM with a Mac® or UNIX® operating system, the autostart will not work.

PDF files containing the full Bulletin contents are located in the \PDF folder on this CD.

Recommended minimum hardware/software:

PC	-	Pentium® processor with Windows® 95
MAC	-	Mac® OS 7
UNIX	-	SunOS™ 4.1.3
Monitor	-	17" colour monitor, video resolution of 1280 x 1024
RAM	-	16 MB
VRAM	-	2 MB

Adobe® Acrobat® Reader® v. 5.1 is required to view the contents of this CD-ROM. It is included on the CD-ROM in the \APPS directory.

Ceci est un disque à lancement automatique pour les systèmes d'exploitation Windows®. Si le lancement automatique ne fonctionne pas, allez au répertoire principal du CD-ROM et cliquez deux fois sur le fichier autoplay.exe. Si vous lisez ce disque à l'aide d'un système d'exploitation Mac® ou UNIX®, le lancement automatique ne fonctionnera pas.

Des fichiers PDF renfermant le contenu intégral du bulletin sont situés dans le dossier \PDF sur ce disque.

Configuration minimale recommandée :

PC	-	processeur Pentium® avec Windows® 95
MAC	-	Mac® OS 7
UNIX	-	SunOS™ 4.1.3
Moniteur	-	moniteur couleur de 17 po, avec résolution vidéo de 1280 x 1024
RAM	-	16 Mo
VRAM	-	2 Mo

Le logiciel Acrobat® Reader® v. 5.1 d'Adobe® est requis pour visionner le contenu de ce CD-ROM. Il est fourni sur le disque dans le répertoire \APPS.